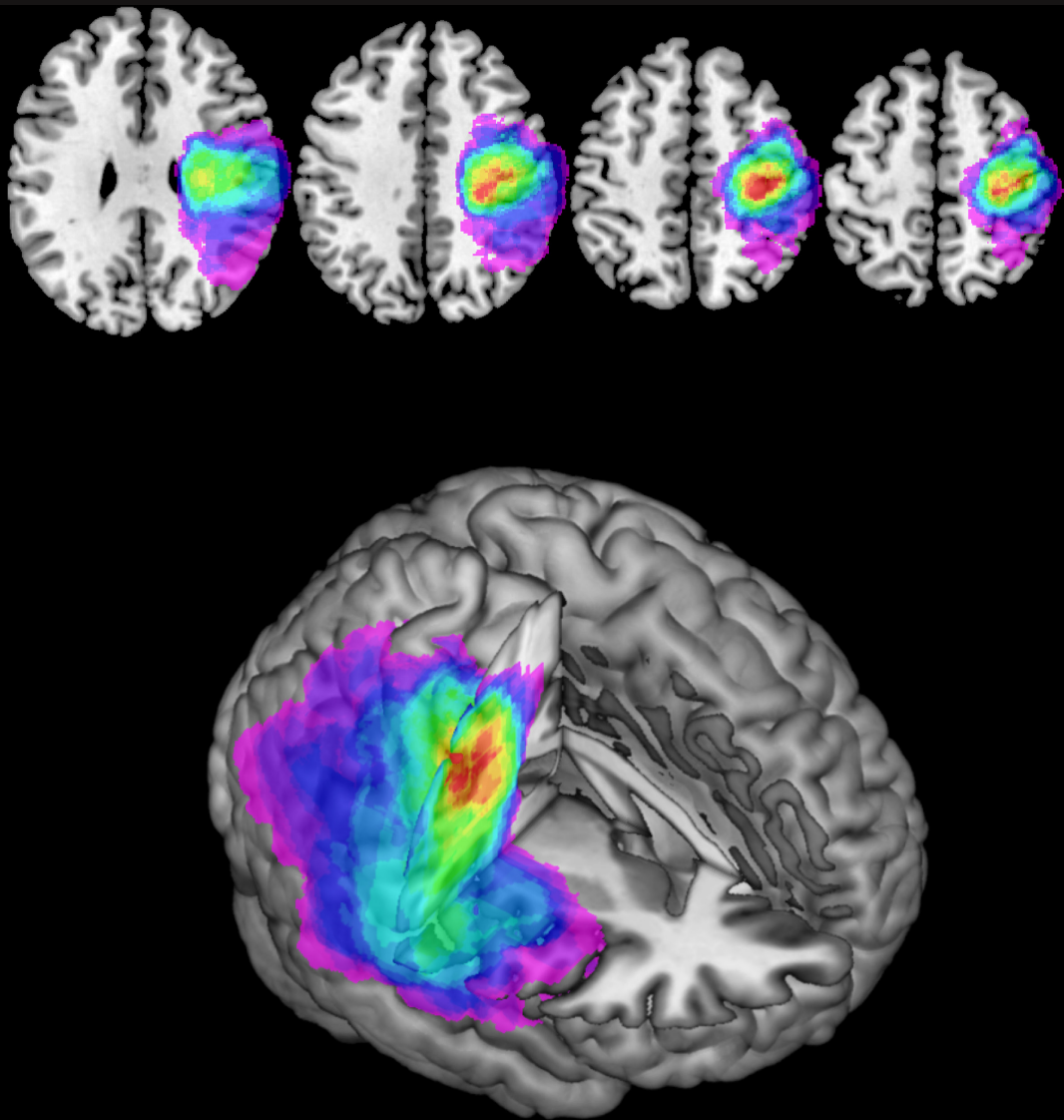


PRINCIPLES UNDERLYING POST-STROKE RECOVERY OF UPPER EXTREMITY SENSORIMOTOR FUNCTION – A NEUROIMAGING PERSPECTIVE

EDITED BY : Bruno J. Weder, Roland Wiest and Rüdiger J. Seitz
PUBLISHED IN: Frontiers in Neurology





frontiers

Frontiers Copyright Statement

© Copyright 2007-2016 Frontiers Media SA. All rights reserved.

All content included on this site, such as text, graphics, logos, button icons, images, video/audio clips, downloads, data compilations and software, is the property of or is licensed to Frontiers Media SA ("Frontiers") or its licensees and/or subcontractors. The copyright in the text of individual articles is the property of their respective authors, subject to a license granted to Frontiers.

The compilation of articles constituting this e-book, wherever published, as well as the compilation of all other content on this site, is the exclusive property of Frontiers. For the conditions for downloading and copying of e-books from Frontiers' website, please see the Terms for Website Use. If purchasing Frontiers e-books from other websites or sources, the conditions of the website concerned apply.

Images and graphics not forming part of user-contributed materials may not be downloaded or copied without permission.

Individual articles may be downloaded and reproduced in accordance with the principles of the CC-BY licence subject to any copyright or other notices. They may not be re-sold as an e-book.

As author or other contributor you grant a CC-BY licence to others to reproduce your articles, including any graphics and third-party materials supplied by you, in accordance with the Conditions for Website Use and subject to any copyright notices which you include in connection with your articles and materials.

All copyright, and all rights therein, are protected by national and international copyright laws.

The above represents a summary only. For the full conditions see the Conditions for Authors and the Conditions for Website Use.

ISSN 1664-8714

ISBN 978-2-88919-767-5

DOI 10.3389/978-2-88919-767-5

About Frontiers

Frontiers is more than just an open-access publisher of scholarly articles: it is a pioneering approach to the world of academia, radically improving the way scholarly research is managed. The grand vision of Frontiers is a world where all people have an equal opportunity to seek, share and generate knowledge. Frontiers provides immediate and permanent online open access to all its publications, but this alone is not enough to realize our grand goals.

Frontiers Journal Series

The Frontiers Journal Series is a multi-tier and interdisciplinary set of open-access, online journals, promising a paradigm shift from the current review, selection and dissemination processes in academic publishing. All Frontiers journals are driven by researchers for researchers; therefore, they constitute a service to the scholarly community. At the same time, the Frontiers Journal Series operates on a revolutionary invention, the tiered publishing system, initially addressing specific communities of scholars, and gradually climbing up to broader public understanding, thus serving the interests of the lay society, too.

Dedication to quality

Each Frontiers article is a landmark of the highest quality, thanks to genuinely collaborative interactions between authors and review editors, who include some of the world's best academicians. Research must be certified by peers before entering a stream of knowledge that may eventually reach the public - and shape society; therefore, Frontiers only applies the most rigorous and unbiased reviews.

Frontiers revolutionizes research publishing by freely delivering the most outstanding research, evaluated with no bias from both the academic and social point of view.

By applying the most advanced information technologies, Frontiers is catapulting scholarly publishing into a new generation.

What are Frontiers Research Topics?

Frontiers Research Topics are very popular trademarks of the Frontiers Journals Series: they are collections of at least ten articles, all centered on a particular subject. With their unique mix of varied contributions from Original Research to Review Articles, Frontiers Research Topics unify the most influential researchers, the latest key findings and historical advances in a hot research area! Find out more on how to host your own Frontiers Research Topic or contribute to one as an author by contacting the Frontiers Editorial Office: researchtopics@frontiersin.org

PRINCIPLES UNDERLYING POST-STROKE RECOVERY OF UPPER EXTREMITY SENSORIMOTOR FUNCTION – A NEUROIMAGING PERSPECTIVE

Topic Editors:

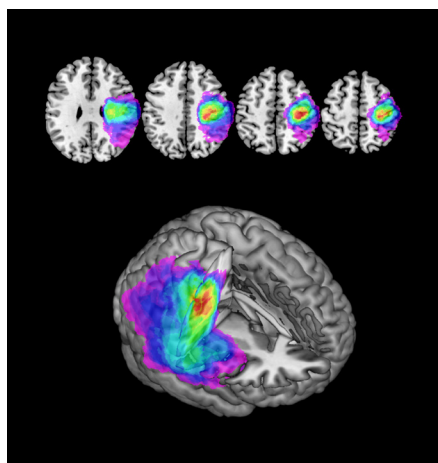
Bruno J. Weder, University Hospital Bern & Kantonsspital St. Gallen, Switzerland

Roland Wiest, University Hospital Bern, Switzerland

Rüdiger J. Seitz, Heinrich-Heine-University Düsseldorf, Germany & University of Melbourne, Australia

Neuroimaging post-stroke has the potential to uncover underlying principles of disturbed hand function and recovery characterizing defined patient groups, including their long term course as well as individual variations. The methods comprise functional magnetic resonance imaging (MRI) measuring task related activation as well as resting state. Functional MRI may be complemented by arterial spin labeling (ASL) MRI to investigate slowly varying blood flow and associated changes in brain function. For structural MRI robust and accurate computational anatomical methods like voxel-based morphometry and surface based techniques are available. The investigation of the connectivity among brain regions and disruption after stroke is facilitated by diffusion tensor imaging (DTI). Intra- and interhemispheric coherence may be studied by electromagnetic techniques such as electroencephalography and transcranial magnetic stimulation.

Consecutive phases of stroke recovery (acute, subacute, early chronic and late chronic stages) are each distinguished by intrinsic processes. The site and size of lesions entail partially different functional implications. New strategies to establish functional specificity of a lesion site include calculating contrast images between patients exhibiting a specific disorder and control subjects without the disorder. Large-size lesions often imply poor cerebral blood flow which impedes recovery significantly and possibly interferes with BOLD response of functional MRI. Thus, depending on the site and size of the infarct lesion the patterns of recovery will vary. These include recovery *sensu stricto* in the perilesional area, intrinsic compensatory mechanisms using alternative cortical and subcortical pathways, or behavioral compensatory strategies e.g. by using the non-affected limb. In this context, behavioral and neuroimaging measures should be developed and employed to delineate aspects of learning during recovery. Of special interest in recovery of hand paresis is the interplay between sensory and motor areas in the



This image shows lesion overlap maps for patients in the acute phase after a cortical sensorimotor (MI/SI) stroke, confirmed on diffusion-weighted MRI, exhibiting contralateral hand paresis or plegia as common denominator (upper half). The corresponding three-dimensional rendering with a vertical cut through the maximum overlap of the complete cohort is added in the lower half. The image relates to the paper of Abela E, Missimer J, Wiest R, Federspiel A, Hess C, Sturzenegger M, Weder B (2012) (Lesions to Primary Sensory and Posterior Parietal Cortices Impair Recovery from Hand Paresis after Stroke. *PLoS ONE* 7(2): e31275. doi:10.1371/journal.pone.0031275).

posterior parietal cortex involved during reaching and fine motor skills as well as the interaction with the contralesional hemisphere. The dominant disability should be characterized, from the level of elementary to hierarchically higher processes such as neglect, apraxia and motor planning.

In summary, this Research Topic covers new trends in state of the art neuroimaging of stroke during recovery from upper limb paresis. Integration of behavioral and neuroimaging findings in probabilistic brain atlases will further advance knowledge about stroke recovery.

Citation: Weder, B. J., Wiest, R., Seitz, R. J., eds. (2016). *Principles Underlying Post-Stroke Recovery of Upper Extremity Sensorimotor Function – A Neuroimaging Perspective*. Lausanne: Frontiers Media. doi: 10.3389/978-2-88919-767-5

Table of Contents

- 05 Editorial: Principles Underlying Post-Stroke recovery of Upper Extremity Sensorimotor Function – a Neuroimaging Perspective**
Bruno J. Weder, Roland Wiest and Rüdiger J. Seitz
- 07 Recovery Potential After Acute Stroke**
Rüdiger J. Seitz and Geoffrey A. Donnan
- 20 A review of transcranial magnetic stimulation and multimodal neuroimaging to characterize post-stroke neuroplasticity**
Angela M. Auriat, Jason L. Neva, Sue Peters, Jennifer K. Ferris and Lara A. Boyd
- 40 The Virtual Brain: modeling biological correlates of recovery after chronic stroke**
Maria Inez Falcon, Jeffrey D. Riley, Viktor Jirsa, Anthony R. McIntosh, Ahmed D. Shereen, E. Elinor Chen and Ana Solodkin
- 53 Role of the contralesional hemisphere in post-stroke recovery of upper extremity motor function**
Cathrin M. Buetefisch
- 63 Motor Recovery After Subcortical Stroke Depends on Modulation of Extant Motor Networks**
Nikhil Sharma and Jean-Claude Baron
- 73 A thalamic-fronto-parietal structural covariance network emerging in the course of recovery from hand paresis after ischemic stroke**
Eugenio Abela, John H. Missimer, Andrea Federspiel, Andrea Seiler, Christian Walter Hess, Matthias Sturzenegger, Roland Wiest and Bruno J. Weder
- 87 Improvement in touch sensation after stroke is associated with resting functional connectivity changes**
Louise C. Bannister, Sheila G. Crewther, Maria Gavrilescu and Leeanne M. Carey
- 102 Determinants of concurrent motor and language recovery during intensive therapy in chronic stroke patients: four single-case studies**
Annika Primaßin, Nina Scholtes, Stefan Heim, Walter Huber, Martina Neuschäfer, Ferdinand Binkofski and Cornelius J. Werner
- 113 The Right Supramarginal Gyrus Is Important for Proprioception in Healthy and Stroke-Affected Participants: A Functional MRI Study**
Ettie Ben-Shabat, Thomas A. Matyas, Gaby S. Pell, Amy Brodtmann and Leeanne M. Carey
- 127 Supplementary motor complex and disturbed motor control – a retrospective clinical and lesion analysis of patients after anterior cerebral artery stroke**
Florian Brugger, Marian Galovic, Bruno J. Weder and Georg Kägi
- 139 Multi-modal imaging of neural correlates of motor speed performance in the trail making test**
Julia A. Camilleri, Andrew T. Reid, Veronika I. Müller, Christian Grefkes, Katrin Amunts and Simon B. Eickhoff



Editorial: Principles Underlying Post-Stroke Recovery of Upper Extremity Sensorimotor Function – A Neuroimaging Perspective

Bruno J. Weder^{1,2*}, Roland Wiest¹ and Rüdiger J. Seitz^{3,4}

¹Support Center for Advanced Neuroimaging (SCAN), Institute for Diagnostic and Interventional Neuroradiology, University Hospital Inselspital, University of Bern, Bern, Switzerland, ²Department of Neurology, Kantonsspital St. Gallen, St. Gallen, Switzerland, ³Department of Neurology, Centre of Neurology and Neuropsychiatry, LVR-Klinikum Düsseldorf, Heinrich-Heine-University Düsseldorf, Düsseldorf, Germany, ⁴Florey Institute of Neuroscience and Mental Health, University of Melbourne, Parkville, VIC, Australia

Keywords: stroke recovery, multimodal neuroimaging, computational biophysical modeling, motor control, motor imagery, somatosensory disorders, perilesional plasticity, network reorganization

The Editorial on the Research Topic

Principles Underlying Post-Stroke Recovery of Upper Extremity Sensorimotor Function – A Neuroimaging Perspective

A substantial proportion of stroke survivors suffer from long-term sensorimotor deficits of the contralesional arm and hand (1). Neuroimaging, using a diversity of methods, has the potential to uncover underlying principles of functional disabilities and recovery characterizing patient groups as well as individual variability (2–6). The present issue aims at (i) revealing the physiological mechanisms and the long-term course of stroke recovery with respect to site and size of lesions, (ii) correlating behavioral deficits and electrophysiological parameters with imaging patterns, (iii) delineating neural networks involved, and (iv) identifying sites where interventions enhance the recovery process.

Seitz and Donnan give an overview of mechanisms and disease-related limitations in post-stroke recovery. They address two informative subsections delineating time courses of the recovery process and state-of-the-art of neurorehabilitative training to improve the stroke-induced neurological deficit.

Auriat et al. complete this clinical perspective with an overview on the use of transcranial magnetic stimulation and multimodal neuroimaging to estimate functional resources post-stroke. They provide a review of data from studies utilizing DTI, MRS, fMRI, EEG, and brain stimulation techniques, focusing on TMS and its combination with uni- and multimodal neuroimaging methods with respect to their benefits and limitations.

Falcon et al. used “The Virtual Brain (TVB),” an open source platform based on local biophysical models. Using this platform, they simulated individuals’ brain activity linking structural data directly to a TVB model. Correlating TVB parameters with graph analysis metrics, they obtained evidence for a shift of global to local dynamics in chronic stroke patients.

Bueteffisch reviews the role of an intact contralesional motor cortex (M1) in post-stroke recovery of upper extremity motor function. The impact of the contralesional M1, on the lesioned motor cortex, seems to be promoting activity in the acute and inhibiting it in the chronic stage. Supportive evidence comes from animal studies, including changes in neurotransmitter systems, dendritic growth, and synapse formation. Thus, the contralesional M1 may represent a treatment target during rehabilitation.

OPEN ACCESS

Edited and Reviewed by:

Scott E. Kashner,
University of Pennsylvania, USA

*Correspondence:

Bruno J. Weder
bruno.weder@insel.ch

Specialty section:

This article was submitted to Stroke,
a section of the journal
Frontiers in Neurology

Received: 06 December 2015

Accepted: 09 December 2015

Published: 23 December 2015

Citation:

Weder BJ, Wiest R and Seitz RJ
(2015) Editorial: Principles Underlying
Post-Stroke Recovery of Upper
Extremity Sensorimotor Function – A
Neuroimaging Perspective.
Front. Neurol. 6:267.
doi: 10.3389/fneur.2015.00267

Sharma and Baron report an fMRI study of a finger-thumb opposition sequence in chronic, well-recovered subcortical stroke patients. Using independent component analysis, they could show that recovery of motor function involved pre-existing cortical networks contributing to recovery in a differentiated manner.

The study of Abela et al. complements these investigations of functional networks associated with recovery in the case of cortical sensorimotor stroke. The structural covariance network in patients recovering from hand paresis encompassed (i) a cortico-striato-thalamic loop involved in motor execution and (ii) higher order sensorimotor cortices affected by the stroke lesions. The network emerged in the early chronic stage post-stroke was related to gray matter volume increases in the ipsilesional medio-dorsal thalamus, and its expression depend on an interaction of recovered hand function and the lesion size.

Bannister et al. report about neuroimaging evidence for the significance of the contralesional hemisphere in the recovery process after hemispheric supratentorial ischemic stroke, thus supplementing the review of Buetefisch. They followed the time course of touch sensation in the upper extremity using resting state – fMRI to explore functional connectivity. Improvement of touch sensation was related to changes in the contralesional hemisphere and cerebellum: (1) an increase in connectivity strength between the secondary somatosensory area seed and both inferior parietal cortex and middle temporal gyrus as well as the thalamus seed and cerebellum and (2) a decrease in connectivity strength between SI seed and the cerebellum.

Primaßin et al. dealt with four exemplary cases in which motor and language domains were affected differently. They focused on dissociative outcomes after 7 weeks of rehabilitative treatment following the predominant failure at baseline. Primarily, precise location of the lesions in the corticospinal tract and/or fasciculus arcuatus, respectively, turned out to be critical for recovery. Motor and language improvement seemed to occur together, rather than to compete for recovery resources.

Ben-Shabat et al. investigated changes in human proprioception, its specific brain activation, laterality, and changes following stroke. Brain activation involved the supramarginal gyrus (SMG) and dorsal premotor cortex (PMd) with a prominent lateralization in the former. Lateralization was diminished in three patients exhibiting proprioceptive deficits post-stroke and a common lesion within the thalamus. The findings underline the role of SMG and dPM in spatial processing and motor control.

Brugger et al. investigated the intriguing role of supplementary motor complex (SMC) and disturbed motor control, a retrospective clinical and lesion analysis of 10 patients presenting anterior cerebral artery stroke. In the very acute phase, alien hand syndrome (AHS) dominated accompanied by failed conscious awareness of motor intention and a missing sense of agency while performing externally triggered movements. In the follow-up, motor signs specifically related to AHS, i.e., disturbed self-initiated movements, grasping, and intermanual conflict, were mainly related to lesions of the pre-supplementary motor area and medial cingulate cortex.

Camilleri et al. studied the neural substrate underlying the performance of the trail making test (TMT) that is often used in the follow-up of stroke. In healthy volunteers, they found that performance in terms of motor speed to be related to the local brain volume of a region in the lower bank of the left inferior sulcus. Conjunction analysis of four connectivity approaches has shown this area to represent a constituent of the so-called multiple demand network, highlighting the TMT as related rather to executive than primary motor function.

In summary, the neurological deficits, recovery mechanisms, and the prognosis for recovery after stroke are hot spots of clinical neurology and systems neuroscience research. Multimodal imaging, applied neurophysiology, and careful neurobehavioral *in vivo* correlations have opened new vistas on the pathophysiological mechanisms underlying post-stroke recovery of upper extremity sensorimotor deficits paving new avenues for future research.

REFERENCES

- Go AS, Mozaffarian D, Roger VL, Benjamin EJ, Berry JD, Borden WB, et al. Heart disease and stroke statistics-2013 update: a report from the American Heart Association. *Circulation* (2013) **127**(1):e6–245. doi:10.1161/CIR.0b013e318282ab8f
- Rehme AK, Eickhoff SB, Rottschy C, Fink GR, Grefkes C. Activation likelihood estimation meta-analysis of motor-related neural activity after stroke. *Neuroimage* (2012) **59**:2771–82. doi:10.1016/j.neuroimage.2011.10.023
- Ward NS, Brown MM, Thompson AJ, Frackowiak RSJ. Neural correlates of outcome after stroke: a cross-sectional fMRI study. *Brain* (2003) **126**(Pt 6):1430–48. doi:10.1093/brain/awg145
- Schaechter JD, Perdue KL. Enhanced cortical activation in the contralesional hemisphere of chronic stroke patients in response to motor skill challenge. *Cereb Cortex* (2008) **18**:638–47. doi:10.1093/cercor/bhm096
- Thiel A, Vahdat S. Structural and resting-state brain connectivity of motor networks after stroke. *Stroke* (2014) **46**(1):296–301. doi:10.1161/STROKEAHA.114.006307

- Abela E, Seiler A, Missimer JH, Federspiel A, Hess CW, Sturzenegger M, et al. Grey matter volumetric changes related to recovery from hand paresis after cortical sensorimotor stroke. *Brain Struct Funct* (2015) **220**(5):2533–50. doi:10.1007/s00429-014-0804-y

Conflict of Interest Statement: The authors declare that the research was conducted in the absence of any commercial or financial relationships that could be construed as a potential conflict of interest.

Copyright © 2015 Weder, Wiest and Seitz. This is an open-access article distributed under the terms of the Creative Commons Attribution License (CC BY). The use, distribution or reproduction in other forums is permitted, provided the original author(s) or licensor are credited and that the original publication in this journal is cited, in accordance with accepted academic practice. No use, distribution or reproduction is permitted which does not comply with these terms.



Recovery Potential After Acute Stroke

Rüdiger J. Seitz^{1,2,3*} and Geoffrey A. Donnan³

¹ Department of Neurology, Centre of Neurology and Neuropsychiatry, LVR-Klinikum Düsseldorf, Heinrich-Heine-University Düsseldorf, Düsseldorf, Germany, ² Biomedical Research Centre, Heinrich-Heine-University Düsseldorf, Düsseldorf, Germany, ³ Florey Institute of Neuroscience and Mental Health, University of Melbourne, Parkville, VIC, Australia

In acute stroke, the major factor for recovery is the early use of thrombolysis aimed at arterial recanalization and reperfusion of ischemic brain tissue. Subsequently, neurorehabilitative training critically improves clinical recovery due to augmentation of postlesional plasticity. Neuroimaging and electrophysiology studies have revealed that the location and volume of the stroke lesion, the affection of nerve fiber tracts, as well as functional and structural changes in the perilesional tissue and in large-scale bihemispheric networks are relevant biomarkers of post-stroke recovery. However, associated disorders, such as mood disorders, epilepsy, and neurodegenerative diseases, may induce secondary cerebral changes or aggravate the functional deficits and, thereby, compromise the potential for recovery.

OPEN ACCESS

Edited by:

Brian Silver,
Alpert Medical School of Brown
University, USA

Reviewed by:

Bin Jiang,
Beijing Neurosurgical Institute, China
Roshini Prakash,
University of California
Los Angeles, USA

*Correspondence:

Rüdiger J. Seitz
seitz@neurologie.uni-duesseldorf.de

Specialty section:

This article was submitted to Stroke,
a section of the journal
Frontiers in Neurology

Received: 27 April 2015

Accepted: 26 October 2015

Published: 11 November 2015

Citation:

Seitz RJ and Donnan GA (2015)
Recovery Potential After
Acute Stroke.
Front. Neurol. 6:238.
doi: 10.3389/fneur.2015.00238

Keywords: cerebral ischemia, infarct location, thrombolysis, recovery, perilesional plasticity, network reorganization, stroke associated disturbances, neurorehabilitative training

INTRODUCTION

Stroke is one of the leading causes of persistent disability in Western countries (1). It induces acute deficits of motion, sensation, cognition, and emotion. In the majority of patients, stroke results from an interruption of cerebral blood supply and subsequent ischemic brain damage, while >25% of patients suffer from intracranial hemorrhage (2, 3). Recovery from stroke is a multifaceted process depending on different mechanisms that become operational at different phases after the acute insult ranging from hours to many months (4). Importantly, intravenous and intra-arterial thrombolyses have opened new avenues to substantially reverse the amount of brain damage and the neurological deficit after stroke (5–8). Furthermore, neuroscience-based strategies in neurorehabilitation have improved the fate of stroke patients. Specifically, training approaches including very early mobilization, antigravity support for walking, basic arm training, and arm ability training can be tailored to the neurological deficits to optimally engage the residual capacities of the patients (9–11). From a technical point of view, neuroimaging and neurophysiological methods have offered means to investigate the recovery potential of stroke patients already in the acute stage of stroke (12–14). In particular, these non-invasive neuroscientific measures substantiate clinical observations and have opened new insights into the neuroscientific basis of recovery mechanisms from stroke. More recently, the recovery potential after stroke has been studied by using multivariate analyses in which epidemiological factors have also been taken into account (15). We address here the mechanisms of post-stroke recovery including postlesional plasticity and disease-related limitations of the recovery potential in acute ischemic stroke.

MECHANISMS OF POST-STROKE RECOVERY

Dynamics of Cerebral Ischemia

A sudden interruption of arterial blood supply leads to disturbances of neural function and the clinical appearance of neurological or neuropsychological deficits. In the most severe cases, ischemia is so severe that structural brain damage and the formation of ischemic brain infarction occur (**Figure 1**). The cessation of cerebral blood circulation induces an immediate suppression of cerebral electrical activity with peri-infarct depolarization leading to repeated episodes of metabolic stress (16, 17). There is good evidence from animal experiments that ischemic damage of neurons and brain tissue occurs in proportion to the reduction of regional cerebral blood flow (rCBF) (16). Thus, the acute occlusion of a cerebral artery, the thereby caused local depression of rCBF, and its subsequent electrical, metabolic, and ionic changes are critical factors determining the extent of a cerebral ischemic infarct (18). Imaging and neurophysiological studies in humans have shown that, similar to animal experiments, spreading depression occurs in severe ischemic stroke leading to progressive infarct expansion (19, 20).

After occlusion of a cerebral artery, an area of impaired perfusion surrounds an area with a complete cessation of perfusion whose extent is determined by the compensatory recruitment of arterial collaterals. In the area of misery perfusion, the so-called penumbra, the extraction of oxygen from blood into brain tissue is enhanced as was shown in stroke patients by multiparametric imaging with positron emission tomography (21, 22). The advent of magnetic resonance imaging (MRI) has allowed a spatial dimension to be introduced. It has been shown that the area of impaired perfusion typically exceeds the area of reduced extracellular water diffusion, thus signifying virtually reversible brain tissue damage due to ischemia (23–25). In fact, there is a good correspondence between the area with enhanced oxygen extraction and the perfusion–diffusion mismatch area in acute stroke (26, 27).

The area of reduced brain perfusion undergoes a dynamic lesion transformation within the first 24 h after onset of ischemia

(28–30). In a persisting arterial occlusion, the infarct lesion expands up to 24 h (31, 32). Beyond the acute time window of about 24 h, secondary changes including an early phase with vasogenic edema and a later phase with inflammatory infiltration evolve (33–35). Lymphocytes and macrophages have been shown to accumulate in the perivascular vicinity ~6 days after a cerebral infarction and are heterogeneously distributed within the infarct area (36). Due to their immunological competence, these cells are suited to augment the infarct lesion raising the interesting notion that immunosuppression may have a beneficial affect in acute stroke (37).

Reversal of Cerebral Ischemia

In acute ischemic stroke, intravenous thrombolysis is targeted toward the rescue of brain tissue by early recanalization of the occluded cerebral artery. It has been shown to be effective up to 4.5 h with maximal efficacy within the first 90 min after symptom onset (5, 6, 38). The beneficial role of early recanalization was demonstrated by functional brain imaging (39–42) and monitoring with transcranial Doppler sonography (43, 44). More recently, neuroradiological interventions with intra-arterial thrombolysis and/or thrombectomy have been shown to be at least as effective as intravenous thrombolysis even in distal carotid or proximal middle cerebral artery (MCA) occlusion (8). By multiparametric MRI, it became evident that brain tissue at the risk of ischemic damage can be salvaged by tissue reperfusion (**Figure 1**). Important factors determining the extent of a brain infarct are the severity and duration of ischemia, the dimension and composition of the causal arterial emboli, the anatomy and the vascular changes of the cerebral arteries, and the presence of diabetic hyperglycemia (29, 41, 45–47). In failed reperfusion, severe edema formation will develop that can hardly be limited pharmacologically. Thus, to rescue patients from malignant brain swelling after stroke craniectomy has been advocated as a symptomatic therapy which is a life-saving action but does not reduce the neurological deficit in patients older than 60 years (48).

Brain infarcts may result from cardiac or artery to artery embolism, from thrombotic occlusion of the small penetrating arteries complicating vessel hyalinosis or microatheroma (49, 50). While infarcts in the territory of the posterior cerebral artery (PCA) are typically embolic in origin affecting the entire supply area of the PCA (51), infarcts in the anterior cerebral artery (ACA) territory are usually of atherosclerotic origin and more variable in lesion pattern and neurological deficit (52). The situation is most complex in the MCA territory because of the arborization of the MCA, the large territory supplied by the artery, and the widespread anastomoses of the leptomeningeal arterial branches fed from the ACA or PCA. The poorer these collaterals are due to arterosclerotic changes in the intracranial arteries, the more severe is the initial ischemic event and the resulting stroke lesion (41, 53, 54).

The location and the volume of the cerebral infarct determine the neurological deficit in an individual patient as shown for sensorimotor as well as cognitive and emotional functions (55–61). Large brain infarcts involving subcortical white matter may affect multiple brain systems which may result in complex neurological syndromes, such as apraxia, neglect,

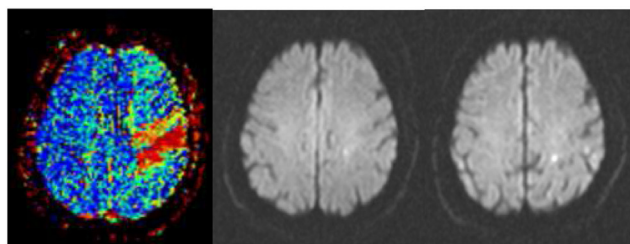


FIGURE 1 | Successful thrombolysis. (Left) Severe perfusion deficit in the precentral gyrus (red) as assessed in a time-to-peak map before thrombolysis. (Middle) Point-like abnormality in diffusion-weighted imaging at the same time signifying the perfusion–diffusion mismatch. (Right) Two small lesions in diffusion-weighted imaging 24 h after intravenous thrombolysis accompanied by complete recovery from hemiparesis.

and Gerstman's syndrome (62–64). In such patients, measures of fiber tract damage or cortical activations have been found to predict the degree of recovery (55, 65–68). Similar observations have also been made for language, somatosensory and visual functions (69–72).

Residual Brain Infarct Lesions After Thrombolysis

The successful recanalizing therapy is of fundamental importance for the topography and volume of the resulting ischemic infarct lesion (73, 74). This was taken into consideration in developing a refined classification of ischemic brain infarcts (75). It should be stated, however, that the functional prognosis of ischemic stroke is worse than that in cerebral hemorrhage in stroke survivors (76). This most likely reflects the structural damage of brain tissue in ischemic stroke, while in cerebral hemorrhage recovery can occur largely upon absorption of the hematoma. Accordingly, territorial Type I infarcts depend on the size of the emboli and the location of the arterial occlusion (**Table 1**). Distal arterial branch occlusion gives rise to small infarcts entirely limited to the cerebral cortex, while proximal arterial branch occlusions result in larger infarcts involving the cerebral cortex and the underlying

white matter (77, 78). In MCA stroke, these territorial infarcts do not destroy the entire motor and somatosensory representation areas, nor the complete descending motor cortical output or afferent sensory input tracts (55, 79, 80). This allows sufficient recovery potential associated with perilesional reorganization in the adjacent cerebral tissue in response to various neurorehabilitative approaches.

Ischemic lesions of large parts of or the entire striatocapsular region typically result from an embolic occlusion of the MCA stem (81) (**Table 1**). If reperfusion is achieved early, only the deep perforating arteries and the arteries that supply the insular cortex may remain obstructed causing infarcts of the lentiform nucleus and insula (82). However, when collaterals are insufficient due to arteriosclerotic changes in multiple cerebral arteries (41, 53, 54), the infarct lesions become larger involving to a larger extent also the hemispheric white matter. This causes hemispatial neglect and conduction aphasia due to cortico-cortical and cortico-subcortical disconnections (62, 83, 84).

Small-sized, lacunar-type, infarcts (Type III infarcts) result from an occlusion of the small penetrating cerebral arteries or even arterioles. They typically occur in the anterior choroidal artery, the deep perforating lenticular MCA branches, the thalamic branches of the PCA, or in brainstem structures and the pons (85, 86). In spite of their small spatial dimension, but due to their strategic location, they cause well-defined neurological syndromes, such as pure motor and pure sensory stroke (**Table 1**). These infarcts have a limited recovery potential as predicted by a loss of motor-evoked potentials and asymmetry of water diffusivity on MR imaging (55, 87, 88). The crucial role of the white matter for functional outcome becomes apparent from the observation that small infarcts in the precentral gyrus allow for profound motor recovery, whereas infarcts of similar volume in the periventricular white matter or the internal capsule may induce a severe and persistent hemiparesis (89, 90). Interestingly, white matter damage in stroke was found in a large genome-wide association study to be related to a mutation in chromosome 17 (91).

Patients with a chronic occlusion of extracranial cerebral arteries resulting from dissection or long-standing cerebrovascular disease constitute Type IV infarcts (**Table 1**). These patients may become symptomatic with transient ischemic attacks due to small embolic or hemodynamically induced watershed infarcts in cerebral white matter (92, 93). In these patients, blood flow depression induces a reactive vasodilatation of the intracranial blood vessels resulting in a severe delay in cerebral brain perfusion in the presence of an enhanced cerebral blood volume (94, 95).

Perilesional Plasticity

Ischemia and reperfusion evoke a large number of biochemical, metabolic, and immunological processes that evolve sequentially as identified in animal experiments (96). In addition, there are rapid changes in the expression of genes, neurotransmitters, such as glutamate and GABA, as well as neurotrophic mediators implicated as molecular substrates related to perilesional reorganization (21, 97–101). These biochemical changes are accompanied on the microscopical level by the growing of axons

TABLE 1 | Classification of ischemic brain infarcts.

Type	Infarct location	Pathogenesis	Response to thrombolysis
I	Territorial	Occlusion of cerebral artery branch	
I.1	Cortical	Distal branch	Early
I.2	Cortico-subcortical	Proximal branch	Limited
II	Striatocapsular	Occlusion of MCA stem	
II.1	±Insula	Infarct core	Early
II.2	+Periventricular white matter	Large lesion	Limited
III		Lacunar hyalinosis of arterioles	Limited
III.1	Fiber tracts		
III.2	Internal capsule (anterior choroidal artery)		
III.3	Basal ganglia, lateral thalamus		
III.4	Medial and anterior thalamus (perforating branches of posterior cerebral artery)		
IV		Chronic hemodynamic deficit + downstream emboli	
IV.1	Cortico-subcortical	Extracranial artery occlusion ± intracranial large artery occlusion ± accompanied by reactive vasodilation	Limited
IV.2	Arterial borderzone	Extracranial artery occlusion	

Adapted from Seitz and Donnan (75).

and formation of new synapses in the perilesional vicinity and in remote locations in functionally related areas in the affected and contralesional “non-affected” hemisphere (102, 103). In particular, they occur when animals recover in an enriched environment or are subjected to dedicated training (104, 105).

Non-invasive brain stimulation techniques have provided means to explore changes of cortical excitability following stroke in humans. There are different technical approaches that allow to enhance or to suppress brain activity (106). By these methods, diagnostic and therapeutic goals were aimed for as summarized in **Table 2**. For example, using paired-pulse TMS, it was found that within the first 7 days after a brain infarct, there is an enhanced cortical excitability in the cortex adjacent to the brain lesion (107–109). In fact, the sites of residual motor representation move into the region of maximal cortical disinhibition (110). Also, fMRI activation areas related to finger movements were found to remap to spared more dorsal locations of the motor cortex (111, 112). Notably, an enhanced excitability was propagated to the contralesional hemisphere (14, 107–109, 113). It decreased in the patients who showed a good recovery within the 90 days, while it persisted in those patients with poor recovery (114). In keeping with these observations, functional MRI performed ~2 days after stroke revealed an area in the ipsilesional postcentral gyrus and posterior cingulate gyrus that correlated with motor recovery ~3 months after stroke (115). Conversely, recovery of hand function was associated with progressively lateralized activation of the affected sensorimotor cortex (116–118).

Non-invasive electrical anodal stimulation of the affected motor cortex was found to augment motor skill acquisition due to improved consolidation but not due to long-term retention of the task (120). In contrast, application of 1-Hz repetitive TMS (rTMS) that downregulates the contralesional motor cortex improved the kinematics of finger and grasp movements in the affected hand (121). This was accompanied by an overactivity in the contralesional motor and premotor cortical areas predicting improvement in movement kinematics. One may wonder if long-term retention of the induced effects can be achieved by longer lasting stimulation or by the combination of voluntary action and direct brain stimulation preferentially in the acute phase after stroke. The combination of electrical stimulation of finger extensor muscles and training over 2–3 weeks did not result in a greater improvement of dexterity of the affected hand as assessed with the Jebson test than each intervention alone (122). Subjects with an intact motor cortex showed a greater improvement than

those who had damage of the motor cortex. Similarly, in chronic stroke-induced aphasia rTMS over the left inferior frontal gyrus resulted in an increase of reaction time or error rate in a semantic task suggesting restoration of a perilesional tissue in the left hemisphere after stroke (123, 124). Given the human postlesional changes of cortical excitability it may be intriguing to rebalance the interhemispheric rivalry by direct cortical stimulation or peripheral stimulation (125–128). An even greater effect was observed when bihemispheric direct cortical stimulation was used to activate the affected motor cortex and to inhibit the contralesional motor cortex (129). Cortical stimulation in association with motor training also improved motor performance (128, 130–132). Along the same line, combining peripheral nerve stimulation to the affected hand with anodal direct current stimulation of the affected motor cortex in chronic stroke facilitates motor performance beyond levels reached with either intervention alone (133).

Infarct Induced Damage to Cortico-Cortical and Cortico-Subcortical Connections

Corticospinal fibers are key factors for the recovery of motor function after stroke as demonstrated with different imaging modalities as well as electrophysiological measures (55, 87, 134–136). In non-human primates, the cortico-reticulo-spinal and cortico-rubro-spinal tracts are known to mediate motor functions in case of corticospinal tract lesions (137, 138), since these tracts have been described as functionally redundant in healthy animals (139). In humans, however the corticospinal tract is of key relevance for motor recovery (**Figure 2**). In fact, the integrity of the corticospinal tract determines the movement related motor cortex activation (65, 87). When there are no motor evoked potentials and there is poor recovery in chronic patients, the fractional anisotropy of the posterior part of the internal capsule as assessed by diffusion tensor imaging was altered in the affected hemisphere (68, 87). Notably, these patients had bilateral fMRI activations in relation to finger movements, while in the patients with a lower asymmetry, there was an activation lateralized to the affected hemisphere.

There are not only changes in the efferent motor fiber tracts but also in the cortico-cortical and probably also cortico-subcortical fiber tract systems during recovery. In fact, the intracortical excitability as assessed with TMS was increased in motor cortex of

TABLE 2 | Techniques, actions, and effects of non-invasive stimulation of the human brain.

Transcranial magnetic stimulation (TMS)				Transcranial electrical stimulation		
				Neuromodulatory effects		
Single pulse TMS	Paired-pulse TMS	Repetitive TMS	Patterned rTMS	Direct current stimulation tDCS	Alternating current stimulation	Random noise stimulation
	Intracortical (single coil)	1 Hz TMS (inhibitory)	Continuous theta-burst stimulation (inhibitory)	Cathodal tDCS		
	Cortico-cortical (two coils)	>4 Hz TMS (excitatory)	Intermittent theta-burst stimulation (excitatory)	Anodal tDCS		

After Liew et al. (119).

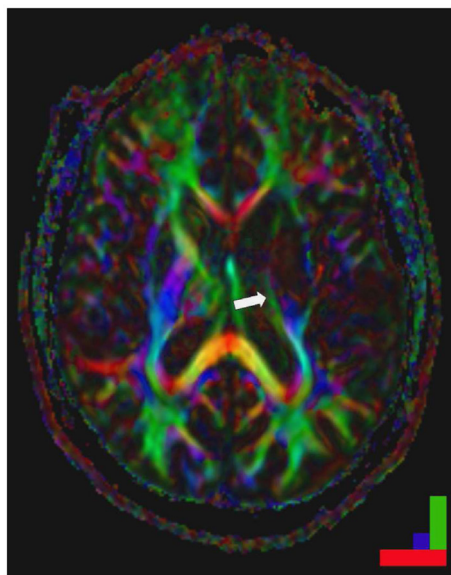


FIGURE 2 | Striatocapsular stroke (Type II.1) in a patient with persistent hemiplegia. Note the small but complete destruction of the posterior limb of the internal capsule (arrow). Color bar: green fronto-occipital diffusion, red right-left diffusion, blue dorso-ventral diffusion. By permission of Oxford University Press (URL www.oup.com), Free permission Author reusing own material, p. 82 fig: 6.4 (left part) from "Stroke Rehabilitation" edited by Carey and Leeanne (140).

both hemispheres both in subcortical and cortical infarcts (108, 114, 141, 142). Conversely, ipsilesional MEPs were more easily elicited from proximal muscles in stroke patients than in healthy subjects (143–145). Moreover, motor cortical connectivity was shown by diffusion tensor imaging to be enhanced after stroke (146). Additionally, orientation uncertainty and greater white matter complexity correlated with functional outcome and were possibly triggered by functional demands (146, 147). In addition, it was found recently that the pyramidal tract splits up in the pons forming a ventral and a dorsal tract. When both tracts are affected, patients have a poor recovery, while continuity of the projections in the dorsal portion was characterized by good recovery (136). In addition, in chronic stroke patients, DTI-derived measures of transcallosal motor fibers as well as ipsilesional corticospinal tracts pyramidal tract and alternate fiber tract determine the therapeutic response to rehabilitation. The more the diffusivity profiles resembled those observed in healthy subjects, the greater a patient's potential for functional recovery (88). These findings accord with the evidence from functional imaging suggesting that the concerted action of both cerebral hemispheres is required for recovery. This corresponds well to the observation that even patients with an excellent recovery may show a bilateral activation pattern (148, 149). This abnormal activity involved premotor cortical areas and was largely reminiscent of activity patterns in learning but are essentially transient in nature (84, 115, 149). Notably, tiny activation areas in contralesional motor cortex were related to mirror movements that frequently occur initially after stroke (150).

Network types of neuroimaging data analysis have revealed that there is a pathological interhemispheric interaction between the ipsi- and contralesional motor cortex as well as between the ipsilesional supplementary motor area (SMA) and contralesional motor cortex in patients with a single infarct lesion (151, 152). In unilateral movements of the affected hand, there was an inhibitory influence from the contralesional to the ipsilesional motor cortex which correlated with the degree of motor impairment (152). In bimanual movements, the interaction of the ipsilesional SMA and the contralesional motor cortex was reduced, and this correlated with impaired bimanual performance. This can be related to the observation that there was less activation in contralesional motor cortex when the motor task did not require working memory demands and no change when the task required online visual feedback monitoring (153). Furthermore, connectivity strength of the prefrontal cortex to the premotor cortex was enhanced in relation to motor imagery highlighting its role for higher order planning of movement (154).

DISEASE-RELATED LIMITATIONS OF THE RECOVERY POTENTIAL

Associated Diseases

It has been known for 30 years that patients with acute stroke may develop cognitive impairment and mood disorders which may aggravate their clinical conditions (155, 156). However, only recently it was shown in a large database of stroke patients subjected to systemic thrombolysis that the pre-existing functional impairment may reduce the patients' response to thrombolysis and the survival rate (157). In a prospective, open label study of 192 patients (68 ± 13 years, 50% males) subjected to intravenous thrombolysis the patients was found to improve ($P < 0.0001$), while 18% deceased within 100 days (158). This was predicted by older age (76 ± 10 years, $P < 0.05$) and more severe affection on admission ($P < 0.0001$). Also, these patients more frequently had atrial fibrillation ($P < 0.03$) than the surviving patients. Furthermore, it was found that stroke patients with a severe pre-stroke disability have a virtually 50% risk of deceasing. It seems that women are particularly liable of depression after stroke and that this is related to a greater stroke severity (159). Of note are patients with migraine that to a large proportion suffer from small vessel disease (160) or hemorrhagic stroke (161). This is of great functional relevance since white matter disease due to small vessel disease enhances the risk of depression, physical disability, and a reduction of quality of life (162). Furthermore, there is evidence from a huge meta-analysis that ischemic stroke is associated with the presence and subsequent development of dementia, particularly in recurring ischemic stroke (163). In addition, dementia was found to be associated with increased lethality (164). Interestingly, small vessel disease is the most frequent vascular abnormality in patients with Parkinson's disease (165, 166). These vascular changes seem to predispose patients with Parkinson's disease to cerebrovascular accidents (167). Arteriosclerosis was found to be of particular relevance for Parkinsonian gait, while macroscopical infarcts seem to result in rigidity (168). Moreover, infarcts induce epileptic seizures (169), which may mimic stroke as in

Todd's paresis and impair recovery due to reduced consciousness. Beyond that stroke may induce changes of affect including alexithymia (58) or depression (170). The latter was found to be most severe in chronic obstructive pulmonary disease, smoking, and in patients with poor socioeconomic status. Also the increasing lesion load with recurrent strokes in the elderly may predispose to depression (171) and death (172). Thus, there is an intimate interaction of stroke and comorbidities the latter of which impair the recovery potential of stroke patients. Deeper insight into the pathophysiology of these interactions is required to counteract these detrimental effects and to enhance the recovery potential of the multimorbid stroke patients.

Functional Deficits in Brain Infarcts

The neurological deficit has two expressions. There is the impairment to perform actions on command which is usually assessed in clinical examinations. And there is the decrease in spontaneous motor activity which may be functionally relevant (Figure 3). In a prospective study of 25 patients (63 ± 10 years) with acute MCA stroke and seven control patients without neurological disease (61 ± 14 years), movement activity was measured continuously

for 4 days in both arms using Actiwatches (Cambridge Research Instruments, UK). Stroke patients with an initial decline in arm movement activity showed no increase in movement activity in either arm over 4 days after stroke, while other patients improved steadily after admission. The impairment continued to be different among the two groups 3 months after stroke (173). Stroke severity, location and treatment, as well as arterial blood pressure and body temperature were not different among the groups. But, in the non-recovering patients, the C-reactive protein was elevated and related to a low number of waking hours. These results support the notion that in the acute stage after MCA stroke, there are patients with a secondary decline in general motor activity and an enhanced sleep demand which was related to systemic inflammation.

Moreover, recordings with the electroencephalogram (EEG) revealed that stroke patients may exhibit focal slow wave activity (SWA) as well as focal epileptic changes in the affected hemisphere (175–177). Focal SWA (1–4 Hz) has been reported to predict poor recovery from stroke (178–180) but can last even for years (181). Notably, EEG recordings have revealed that, in addition to their neurological deficit, stroke patients also have

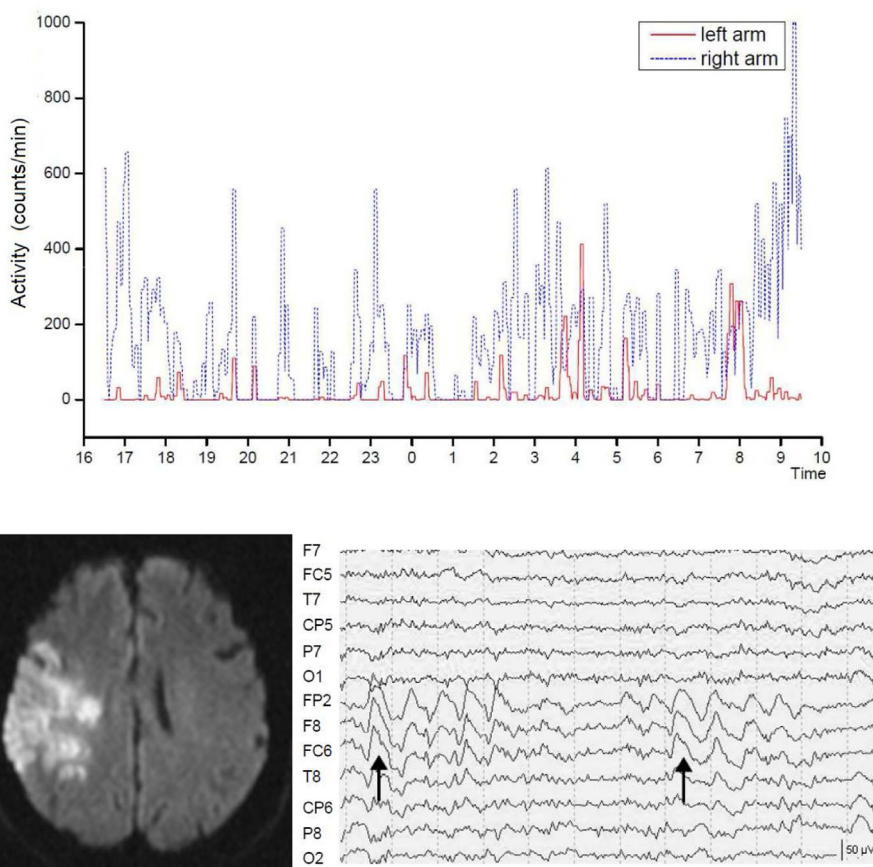


FIGURE 3 | Severely reduced spontaneous movement activity in the affected left arm in right hemispheric brain infarct. Shown is the recording time between 4 p.m. until 10 a.m. the following day. The intermittent slow wave activity in electroencephalographic recordings predicted poor motor recovery. Dotted lines indicate seconds. From Ruan and Seitz (174).

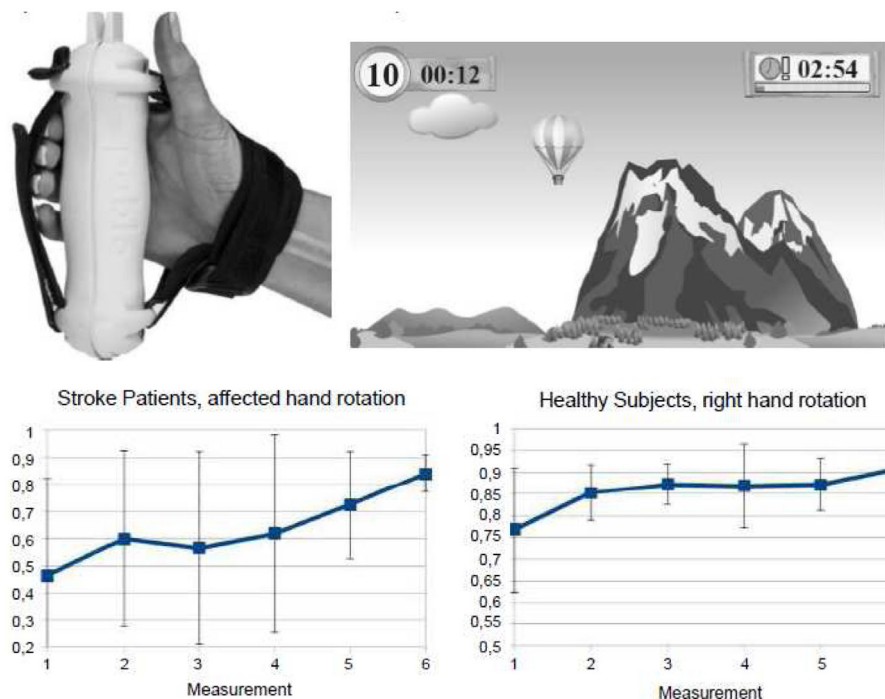


FIGURE 4 | Gaming-based training scenario using the commercially available hand hold PABLO®-device. Hand movements are measured by acceleration and force sensors and thereby steer objects in virtual reality games. Training on consecutive days enlarged the angle of hand rotations and decreased the heterogeneity of movement execution both in healthy subjects and stroke patients. From Seitz et al. (213).

an abnormal sleep architecture (182, 183). It is unclear, however, what the functional impact of SWA is on spontaneous movement activity of the affected side after stroke. In fact, stroke patients with similar infarcts concerning lesion location and volume may show recovery patterns of the formal neurological assessment that are not reflected by the spontaneous movement activity of the affected limbs (184, 185). In acute stroke patients (68 ± 8 years) and age-matched controls (68 ± 12 years), movement activity was measured continuously and synchronously with the EEG for 24 h in both arms using actiwatches (174). The stroke patients had lower total sleep time ($P = 0.031$), sleep efficiency ($P = 0.019$), percent non-rapid eye movement sleep ($P = 0.034$), and percent sleep stage N2 ($P = 0.003$) and showed reduced spontaneous movement activity in the affected arm during wakefulness. Stroke patients with abnormal focal SWA showed less spontaneous arm movement activity than those without SWA, while there were no differences in the sleep parameters (Figure 3). These findings accord with earlier observations by Bassetti and Aldrich (175) supporting the notion that sleep architecture is impaired in stroke patients leading to sleep fragmentation, increased wakefulness, and increased REM latency (186). Furthermore, the stroke patients with SWAs enjoyed a limited recovery as assessed with the NIHSS. Thus, focal SWA is a marker of profound brain pathology.

Times-Lines for Post-Stroke Recovery

The neurological deficits can regress substantially in the early period after ischemic stroke following acute stroke treatment

with arterial recanalization and effective reperfusion. The relatively early recovery in patients with small cortical lesions steadily evolves over weeks and levels out over the subsequent months (112, 187, 188). In contrast, the processes of cerebral reorganization are slow and may need many months to complete. In the acute phase of stroke, it is difficult to predict the degree of ultimate recovery, since there is a large heterogeneity of recovery over the first 3 months after stroke (12). Prediction becomes progressively better the more specific and differentiated the physiological assessment measures are and the longer the time since stroke (70, 189, 190). For example, the neurological state by day 4 predicts the long-term neurological outcome (188, 191). The recovery of activities of daily living usually develop within 26 weeks after the stroke insult and is often accompanied by compensatory hand use (192, 193).

Neurorehabilitative Training

There are numerous reports about rehabilitative approaches to improve the neurological deficit following stroke (4, 13). Notably, patients older than 65 years benefit as much as younger patients from intensive rehabilitation (190, 194), while younger patients typically improve more on mobility, balance, walking, and grip strength (195). The intensity of the training rather than the type of training appears to determine long-term improvement of motor function (113, 196–198). While passive training of wrist movements was reported to be clinically effective and associated with change in cortical activation (199), volitional control of finger and thumb extensions was found to play an important role

for successful hand shaping and grasping of objects (147, 214). Importantly, repetitive training of the affected arm resulted in an increase of activation in the sensorimotor cortex related to hand movements which initially persisted for weeks after training completion and then decreased in magnitude in relation to the functional gain (200, 201). In contrast, mirror therapy was found to improve the neurological status immediately after the intervention and to be effective even at long-term follow-up (202, 203).

Training of the affected limb as well as training targeting the non-affected limb has been proposed to be effective. For example, use of bilateral synergies has been reported to improve the motor capacity of the paretic arm (204). It was described that active-passive bilateral arm therapy can produce sustained improvements in upper limb motor function in chronic stroke patients. This was paralleled by an enhanced ipsilesional motor cortex excitability and an increased transcallosal inhibition from ipsilesional to contralesional motor cortex (205). Conversely, the concept of “learned non-use” was implemented in new approaches of rehabilitative strategies in chronic patients with brain infarction (206, 207). This therapy has been shown to be successful even when applied in the chronic state to moderately affected patients (65, 208, 209). This beneficial effect of constraint-induced movement therapy is likely to be composed of focusing the patient’s attention to the affected side and imposing repetitive training. It was shown

to result in improved motor function and enhanced activation in the partially damaged sensorimotor cortex and other gray matter areas including the hippocampus (210).

Recently, computer-based training approaches employing virtual reality scenarios have been developed for neurorehabilitative training purposes, since it was assumed that they engage the patients emotionally and thereby enhance their inclination to embrace rehabilitation training activities. For example, the rehabilitation gaming system (RGS) is a flexible, virtual reality-based device for rehabilitation of neurological patients (211). In fact, it was shown to effectively improve arm function in acute and chronic stroke patients. Furthermore, it was shown by fMRI that the RGS engages human mirror neuron mechanisms that underly visuomotor coordination (212). Similarly, the handheld multifunctional PABLO^R-device was applied for the training of visuomotor-tracking paradigms. It was observed that training of the right dominant hand improved visuomotor coordination of hand rotation movements in both hands in healthy subjects. Notably, it was successful only in the trained hand in stroke patients (Figure 4). Since these gaming applications capitalize on the positive affect of the patients and engage brain structures known to be related to emotional processing (212), these approaches point into new avenues of post-stroke rehabilitation opening new frames for the recovery potential after stroke.

REFERENCES

- Bejot Y, Benatru I, Rouaud O, Fromont A, Besancenot JP, Moreau T, et al. Epidemiology of stroke in Europe: geographic and environmental differences. *J Neurol Sci* (2007) **262**:85–8. doi:10.1016/j.jns.2007.06.025
- Intiso D, Stampatore P, Zarrelli MM, Guerra GL, Arpaia G, Simone P, et al. Incidence of first-ever ischemic and hemorrhagic stroke in a well-defined community of southern Italy, 1993–1995. *Eur J Neurol* (2003) **10**:559–65. doi:10.1046/j.1468-1331.2003.00648.x
- Shiber JR, Fontane E, Adewale A. Stroke registry: hemorrhagic vs. ischemic strokes. *Am J Emerg Med* (2010) **28**:331–3. doi:10.1016/j.ajem.2008.10.026
- Carey LM, Seitz RJ. Functional neuroimaging in stroke recovery and neurorehabilitation: conceptual issues and perspectives. *Int J Stroke* (2007) **2**:245–64. doi:10.1111/j.1747-4949.2007.00164.x
- Hacke W, Donnan G, Fieschi C, Kaste M, von Kummer R, Broderick JP, et al. Association of outcome with early stroke treatment: pooled analysis of ATLANTIS, ECASS, and NINDS rt-PA stroke trials. *Lancet* (2004) **363**:768–74. doi:10.1016/S0140-6736(04)15692-4
- Hacke W, Kaste M, Bluhmki E, Brozman M, Dávalos A, Guidetti D, et al. Thrombolysis with alteplase 3 to 4.5 hours after acute ischemic stroke. *N Engl J Med* (2008) **359**:1317–29. doi:10.1056/NEJMoa0804656
- Donnan GA, Baron JC, Ma M, Davis SM. Penumbra selection of patients for trials of acute stroke therapy. *Lancet Neurol* (2009) **8**:261–9. doi:10.1016/S1474-4422(09)70041-9
- Berkhemer OA, Fransen PS, Beumer D, van den Berg LA, Lingsma HF, Yoo AJ, et al. A randomized trial of intraarterial treatment for acute ischemic stroke. *N Engl J Med* (2015) **372**:11–20. doi:10.1056/NEJMoa1411587
- Cumming TB, Thrift AG, Collier JM, Donnan G, Bernhardt J. An early mobilization protocol successfully delivers more and earlier therapy to acute stroke patients: further results from phase II of AVERT. *Stroke* (2011) **42**:153–8. doi:10.1161/STROKEAHA.110.594598
- Hesse S. Treadmill training with partial body weight support after stroke: a review. *NeuroRehabilitation* (2008) **23**:55–65.
- Platz T, van Kaick S, Mehrholz J, Leidner O, Eickhoff C, Pohl M. Best conventional therapy versus modular impairment-oriented training for arm paresis after stroke: a single-blind, multicenter randomized controlled trial. *Neurorehabil Neural Repair* (2009) **23**:706–16. doi:10.1177/1545968309335974
- Cramer SC. Repairing the human brain after stroke: I. Mechanisms of spontaneous recovery. *Ann Neurol* (2008) **63**:272–87. doi:10.1002/ana.21393
- Cramer SC. Repairing the human brain after stroke: II. Restorative therapies. *Ann Neurol* (2008) **63**:549–60. doi:10.1002/ana.21412
- Wittenberg GF, Chen R, Ishii K, Bushara KO, Eckloff S, Croarkin E, et al. Constraint-induced therapy in stroke: magnetic-stimulation motor maps and cerebral activation. *Neurorehabil Neural Repair* (2003) **17**:48–57.
- Haselbach D, Renggli A, Carda S, Croquelois A. Determinants of neurological functional recovery potential after stroke in young adults. *Cerebrovasc Dis Extra* (2014) **4**:77–83. doi:10.1159/000360218
- Hossmann KA. Viability thresholds and the penumbra of focal ischemia. *Ann Neurol* (1994) **36**:557–65. doi:10.1002/ana.410360404
- Heiss WD, Huber M, Fink GR, Herholz K, Pietrzyk U, Wagner R, et al. Progressive derangement of perinfarct viable tissue in ischemic stroke. *J Cereb Blood Flow Metab* (1992) **12**:193–203. doi:10.1038/jcbfm.1992.29
- Dirnagl U, Iadecola C, Moskowitz MA. Pathobiology of ischaemic stroke: an integrated view. *Trends Neurosci* (1999) **22**:391–7. doi:10.1016/S0166-2236(99)01401-0
- Dohmen C, Sakowitz OW, Fabricius M, Bosche B, Reithmeier T, Ernestus RI, et al. Spreading depolarizations occur in human ischemic stroke with high incidence. *Ann Neurol* (2008) **63**:720–8. doi:10.1002/ana.21390
- Dreier JP, Major S, Manning A, Woitzik J, Drenckhahn C, Steinbrink J, et al. Cortical spreading ischaemia is a novel process involved in ischaemic damage in patients with aneurysmal subarachnoid haemorrhage. *Brain* (2009) **132**:1866–81. doi:10.1093/brain/awp102
- Heiss WD, Sobesky J, Smekal UV, Kracht LW, Lehnhardt FG, Thiel A, et al. Probability of cortical infarction predicted by flumazenil binding and diffusion-weighted imaging signal intensity: a comparative positron emission tomography/magnetic resonance imaging study in early ischemic stroke. *Stroke* (2004) **35**:1892–8. doi:10.1161/01.STR.0000134746.93535.9b
- Moustafa RP, Baron JC. Pathophysiology of ischaemic stroke: insights from imaging, and implications for therapy and drug discovery. *Br J Pharmacol* (2008) **153**(Suppl 1):S44–54. doi:10.1038/sj.bjp.0707530
- Neumann-Haefelin T, Wittsack H-J, Wenserski F, Siebler M, Seitz RJ, Mödder U, et al. Diffusion- and perfusion-weighted MRI. The DWI/PWI mismatch region in acute stroke. *Stroke* (1999) **30**:1591–7.

24. Rother J, Schellinger PD, Gass A, Siebler M, Villringer A, Fiebach JB, et al. Effect of intravenous thrombolysis on MRI parameters and functional outcome in acute stroke <6 hours. *Stroke* (2002) **33**:2438–45. doi:10.1161/01.STR.0000030109.12281.23
25. Olivot JM, Mlynash M, Thijs VN, Kemp S, Lansberg MG, Wechsler L, et al. Relationships between infarct growth, clinical outcome, and early recanalization in diffusion and perfusion imaging for understanding stroke evolution (DEFUSE). *Stroke* (2008) **39**:2257–63. doi:10.1161/STROKEAHA.107.511535
26. Sobesky J, Zaro Weber O, Lehnhardt FG, Hesselmann V, Thiel A, Dohmen C, et al. Which time-to-peak threshold best identifies penumbral flow? A comparison of perfusion-weighted magnetic resonance imaging and positron emission tomography in acute ischemic stroke. *Stroke* (2004) **35**:2843–7. doi:10.1161/01.STR.0000147043.29399.f6
27. Sobesky J, Zaro Weber O, Lehnhardt FG, Hesselmann V, Neveling M, Jacobs A, et al. Does the mismatch match the penumbra? magnetic resonance imaging and positron emission tomography in early ischemic stroke. *Stroke* (2005) **36**:980–5. doi:10.1161/01.STR.0000160751.79241.a3
28. Beaulieu C, de Crespigny A, Tong DC, Moseley ME, Albers GW, Marks MP. Longitudinal magnetic resonance imaging study of perfusion and diffusion in stroke: evolution of lesion volume and correlation with clinical outcome. *Ann Neurol* (1999) **46**:568–78. doi:10.1002/1531-8249(199910)46:4<568::AID-ANA4>3.0.CO;2-R
29. Röhl L, Ostergaard L, Simonsen CZ, Vestergaard-Poulsen P, Andersen G, Sakoh M, et al. Viability thresholds of ischemic penumbra of hyperacute stroke defined by perfusion-weighted MRI and apparent diffusion coefficient. *Stroke* (2001) **32**:1140–6. doi:10.1161/01.STR.32.5.1140
30. Wittsack HJ, Ritzl A, Fink GR, Wenserski F, Siebler M, Seitz RJ, et al. MR imaging in acute stroke: diffusion-weighted and perfusion imaging parameters for predicting infarct size. *Radiology* (2002) **222**:397–403. doi:10.1148/radiol.2222001731
31. Lee LJ, Kidwell CS, Alger J, Starkman S, Saver JL. Impact on stroke subtype diagnosis of early diffusion-weighted magnetic resonance imaging and magnetic resonance angiography. *Stroke* (2000) **31**:1081–9. doi:10.1161/01.STR.31.5.1081
32. Li F, Liu KF, Silva MD, Omae T, Sotak CH, Fenstermacher JD, et al. Transient and permanent resolution of ischemic lesions on diffusion-weighted imaging after brief periods of focal ischemia in rats: correlation with histopathology. *Stroke* (2000) **31**:946–54. doi:10.1161/01.STR.31.4.946
33. Saleh A, Schroeter M, Jonkmanns C, Hartung HP, Mödder U, Jander S. In vivo MRI of brain inflammation in human ischaemic stroke. *Brain* (2004) **127**:1670–7. doi:10.1093/brain/awh191
34. Schroeter M, Saleh A, Wiedermann D, Hoehn M, Jander S. Histochemical detection of ultrasmall superparamagnetic iron oxide (USPIO) contrast medium uptake in experimental brain ischemia. *Magn Reson Med* (2004) **52**:403–6. doi:10.1002/mrm.20142
35. Price CJ, Wang D, Menon DK, Guadagno JV, Cleij M, Fryer T, et al. Intrinsic activated microglia map to the peri-infarct zone in the subacute phase of ischemic stroke. *Stroke* (2006) **37**:1749–53. doi:10.1161/01.STR.0000226980.95389.0b
36. Saleh A, Schroeter M, Ringelstein A, Hartung HP, Siebler M, Mödder U, et al. Iron oxide particle-enhanced MRI suggests variability of brain inflammation at early stages after ischemic stroke. *Stroke* (2007) **38**:2733–7. doi:10.1161/STROKEAHA.107.481788
37. McCombe PA, Read SJ. Immune and inflammatory responses to stroke: good or bad? *Int J Stroke* (2008) **3**:254–65. doi:10.1111/j.1747-4949.2008.00222.x
38. Merino JG, Latour LL, An L, Hsia AW, Kang DW, Warach S. Reperfusion half-life: a novel pharmacodynamic measure of thrombolytic activity. *Stroke* (2008) **39**:2148–50. doi:10.1161/STROKEAHA.107.510818
39. Heiss WD, Grond M, Thiel A, von Stockhausen HM, Rudolf J, Ghaemi M, et al. Tissue at risk of infarction rescued by early reperfusion: a positron emission tomography study in systemic recombinant tissue plasminogen activator thrombolysis of acute stroke. *J Cereb Blood Flow Metab* (1998) **18**:1298–307. doi:10.1097/00004647-199812000-00004
40. Kidwell CS, Saver JL, Starkman S, Duckwiler G, Jahan R, Vespa P, et al. Late secondary ischemic injury in patients receiving intraarterial thrombolysis. *Ann Neurol* (2002) **52**:698–703. doi:10.1002/ana.10380
41. Seitz RJ, Meisel S, Weller P, Junghans U, Wittsack H-J, Siebler M. The initial ischemic event: PWI and ADC for stroke evolution. *Radiology* (2005) **237**:1020–8. doi:10.1148/radiol.2373041435
42. Ogata T, Nagakane Y, Christensen S, Ma H, Campbell BC, Churilov L, et al. A topographic study of the evolution of the MR DWI/PWI mismatch pattern and its clinical impact: a study by the EPITHET and DEFUSE investigators. *Stroke* (2011) **42**:1596–601. doi:10.1161/STROKEAHA.110.609016
43. Alexandrov AV, Demchuk AM, Felberg RA, Christou I, Barber PA, Burgin WS, et al. High rate of complete recanalization and dramatic clinical recovery during tPA infusion when continuously monitored with 2-MHz transcranial doppler monitoring. *Stroke* (2000) **31**:610–4. doi:10.1161/01.STR.31.3.610
44. Alexandrov AV, Burgin WS, Demchuk AM, El Mitwalli A, Grotta JC. Speed of intracranial clot lysis with intravenous tissue plasminogen activator therapy: sonographic classification and short-term improvement. *Circulation* (2001) **103**:2897–902. doi:10.1161/01.CIR.103.24.2897
45. Parsons MW, Barber PA, Desmond PM, Baird TA, Darby DG, Byrnes G, et al. Acute hyperglycemia adversely affects stroke outcome: a magnetic resonance imaging and spectroscopy study. *Ann Neurol* (2002) **52**:20–8. doi:10.1002/ana.10241
46. Hillis AE, Gold L, Kannan V, Cloutman L, Kleinman JT, Newhart M, et al. Site of the ischemic penumbra as a predictor of potential for recovery of functions. *Neurology* (2008) **71**:184–9. doi:10.1212/01.wnl.0000317091.17339.98
47. Almekhlafi MA, Hu WY, Hill MD, Auer RN. Calcification and endothelialisation of thrombi in acute stroke. *Ann Neurol* (2008) **64**:344–52. doi:10.1002/ana.21404
48. Arac A, Blanchard V, Lee M, Steinberg GK. Assessment of outcome following decompressive craniectomy for malignant middle cerebral artery infarction in patients older than 60 years of age. *Neurosurg Focus* (2009) **26**(6):E3. doi:10.3171/2009.3.FOCUS0958
49. Thrift AG, Dewey HM, MacDonnell RA, McNeil JJ, Donnan GA. Incidence of the major stroke subtypes: initial findings from the North East Melbourne Stroke Incidence Study (NEMESIS). *Stroke* (2001) **32**:1732–8. doi:10.1161/01.STR.32.8.1732
50. Dewey HM, Sturm J, Donnan GA, MacDonnell RA, McNeill JJ, Thrift AG. Incidence and outcome of subtypes of ischaemic stroke: initial results from the North East Melbourne Stroke Incidence Study (NEMESIS). *Cerebrovasc Dis* (2003) **15**:133–9. doi:10.1159/000067142
51. Finelli PF. Neuroimaging in acute posterior cerebral artery infarction. *Neurologist* (2008) **14**:170–80. doi:10.1097/NRL.0b013e3181627679
52. Kang SY, Kim JS. Anterior cerebral artery infarction. Stroke mechanism and clinical-imaging study in 100 patients. *Neurology* (2008) **70**:2386–93. doi:10.1212/01.wnl.0000314686.94007.d0
53. Bang OY, Saver JL, Buck BH, Alger JR, Starkman S, Ovbiagele B, et al. Impact of collateral flow on tissue fate in acute ischaemic stroke. *J Neurol Neurosurg Psychiatry* (2008) **79**:625–9. doi:10.1136/jnnp.2007.132100
54. Liebeskind DS, Cotsonis GA, Saver JL, Lynn MJ, Turan TN, Cloft HJ, et al. Collaterals dramatically alter stroke risk in intracranial atherosclerosis. *Ann Neurol* (2011) **69**:963–74. doi:10.1002/ana.22354
55. Binkofski F, Seitz RJ, Arnold S, Claßen J, Benecke R, Freund H-J. Thalamic metabolism and integrity of the pyramidal tract determine motor recovery in stroke. *Ann Neurol* (1996) **39**:460–70. doi:10.1002/ana.410390408
56. Kim JS. Predominant involvement of a particular group of fingers due to small, cortical infarction. *Neurology* (2001) **56**:1677–82. doi:10.1212/WNL.56.12.1677
57. Binkofski F, Seitz RJ. Modulation of the BOLD-response in early recovery from sensorimotor stroke. *Neurology* (2004) **63**:1223–9. doi:10.1212/01.WNL.0000140468.92212.BE
58. Schäfer R, Popp K, Jörgens S, Lindenberg R, Franz M, Seitz RJ. Alexithymia-like disorder in right anterior cingulate infarction. *Neurocase* (2007) **13**:201–8. doi:10.1080/1354790701494964
59. Barton JJ. Structure and function in acquired prosopagnosia: lessons from a series of 10 patients with brain damage. *J Neuropsychol* (2008) **2**:197–225. doi:10.1348/174866407X214172
60. Hömke L, Amunts K, Böning L, Fretz C, Binkofski F, Zilles K, et al. Analysis of lesions in patients with unilateral tactile agnosia using cytoarchitectonic probabilistic maps. *Hum Brain Mapp* (2009) **30**:1444–56. doi:10.1002/hbm.20617
61. Burke Quinlan E, Dodakian L, See J, McKenzie A, Le V, Wojnowicz M, et al. Neural function, injury, and stroke subtype predict treatment gains after stroke. *Ann Neurol* (2015) **77**:132–45. doi:10.1002/ana.24309
62. Karnath HO, Rorden C, Ticini LF. Damage to white matter fibre tracts in acute spatial neglect. *Cereb Cortex* (2009) **19**:2331–7. doi:10.1093/cercor/bhn250

63. Pazzaglia M, Smania N, Corato E, Aglioti SM. Neural underpinnings of gesture discrimination in patients with limb apraxia. *J Neurosci* (2008) **28**:3030–41. doi:10.1523/JNEUROSCI.5748-07.2008
64. Rusconi E, Pinel P, Eger E, LeBihan D, Thirion B, Dehaene S, et al. A disconnection account of Gerstmann syndrome: functional neuroanatomy evidence. *Ann Neurol* (2009) **66**:654–62. doi:10.1002/ana.21776
65. Hamzei F, Dettmers C, Rijntjes M, Weiller C. The effect of cortico-spinal tract damage on primary sensorimotor cortex activation after rehabilitation therapy. *Exp Brain Res* (2008) **190**:329–36. doi:10.1007/s00221-008-1474-x
66. Kim YH, Kim DS, Hong JH, Park CH, Hua N, Bickart KC, et al. Corticospinal tract location in internal capsule of human brain: diffusion tensor tractography and functional MRI study. *Neuroreport* (2008) **28**:817–20. doi:10.1097/WNR.0b013e328300a086
67. Schiemanck SK, Kwakkel G, Post MW, Kappelle LJ, Prevo AJ. Impact of internal capsule lesions on outcome of motor hand function at one year post-stroke. *J Rehabil Med* (2008) **40**:96–101. doi:10.2340/16501977-0130
68. Schaechter JD, Fricker ZP, Perdue KL, Helmer KG, Vangel MG, Greve DN, et al. Microstructural status of ipsilesional and contralesional corticospinal tract correlates with motor skill in chronic stroke patients. *Hum Brain Mapp* (2009) **30**:3461–74. doi:10.1002/hbm.20770
69. Vitali P, Abutalebi J, Tettamanti M, Danna M, Ansaldi AI, Perani D, et al. Training-induced brain remapping in chronic aphasia: a pilot study. *Neurorehabil Neural Repair* (2007) **21**:152–60. doi:10.1177/1545968306294735
70. Connell LA, Lincoln NB, Radford KA. Somatosensory impairment after stroke: frequency of different deficits and their recovery. *Clin Rehabil* (2008) **22**:758–67. doi:10.1177/0269215508090674
71. Poggel DA, Mueller I, Kasten E, Sabel BA. Multifactorial predictors and outcome variables of vision restoration training in patients with post-geniculate visual field loss. *Restor Neurol Neurosci* (2008) **26**:321–39.
72. Brodtmann A, Puce A, Darby D, Donnan G. Serial functional imaging poststroke reveals visual cortex reorganization. *Neurorehabil Neural Repair* (2009) **23**:150–9. doi:10.1177/1545968308321774
73. von Kummer R, Meyding-Lamadé U, Forsting M, Rosin L, Rieke K, Hacke W, et al. Sensitivity and prognostic value of early CT in occlusion of the middle cerebral artery trunk. *AJNR Am J Neuroradiol* (1994) **15**:9–15.
74. Delgado-Mederos R, Rovira A, Alvarez-Sabín J, Ribó M, Munuera J, Rubiera M, et al. Speed of tPA-induced clot lysis predicts DWI lesion evolution in acute stroke. *Stroke* (2007) **38**:955–60. doi:10.1161/01.STR.0000257977.32525.6e
75. Seitz RJ, Donnan GA. Role of neuroimaging in promoting long-term recovery from ischemic stroke. *J Magn Reson Imaging* (2010) **32**:756–72. doi:10.1002/jmri.22315
76. Paolucci S, Antonucci G, Grasso MG, Bragoni M, Coiro P, De Angelis D, et al. Functional outcome of ischemic and hemorrhagic stroke patients after inpatient rehabilitation. A matched comparison. *Stroke* (2003) **34**:2861–5. doi:10.1161/01.STR.0000102902.39759.D3
77. Bang OY, Lee PH, Heo KG, Joo US, Yoon SR, Kim SY. Stroke specific DWI lesion patterns predict prognosis after acute ischaemic stroke within the MCA territory. *J Neurol Neurosurg Psychiatry* (2005) **76**:1222–8. doi:10.1136/jnnp.2004.059998
78. Wang X, Lam WW, Fan YH, Graham CA, Rainer TH, Wong KS. Topographic patterns of small subcortical infarcts associated with MCA stenosis: a diffusion-weighted MRI study. *J Neuroimaging* (2006) **16**:266–71. doi:10.1111/j.1552-6569.2006.00027.x
79. Crafton KR, Mark AN, Cramer SC. Improved understanding of cortical injury by incorporating measures of functional anatomy. *Brain* (2003) **126**:1650–9. doi:10.1093/brain/awg159
80. Rey B, Frischknecht R, Maeder P, Clarke S. Patterns of recovery following focal hemispheric lesions: relationship between lasting deficit and damage to specialized networks. *Restor Neurol Neurosci* (2007) **25**:285–94.
81. Donnan GA, Bladin PF, Berkovic SF, Longley WA, Saling MM. The stroke syndrome of striatocapsular infarction. *Brain* (1991) **114**:51–70.
82. Seitz RJ, Sondermann V, Wittsack H-J, Siebler M. Lesion patterns in successful and failed thrombolysis in middle cerebral artery stroke. *Neuroradiology* (2009) **51**:865–71. doi:10.1007/s00234-009-0576-x
83. Stoeckel MC, Meisel S, Wittsack HJ, Seitz RJ. Pattern of cortex and white matter involvement in severe middle cerebral artery ischemia. *J Neuroimaging* (2007) **17**:131–40. doi:10.1111/j.1552-6569.2007.00102.x
84. Saur D, Lange R, Baumgaertner A, Schraknepper V, Willmes K, Rijntjes M, et al. Dynamics of language reorganization after stroke. *Brain* (2006) **129**:1371–84. doi:10.1093/brain/awl090
85. Fisher CM. Lacunar strokes and infarcts: a review. *Neurology* (1982) **32**:871–6. doi:10.1212/WNL.32.8.871
86. Boiten J, Lodder J. Lacunar infarcts. Pathogenesis and validity of the clinical syndromes. *Stroke* (1991) **22**:1374–8. doi:10.1161/01.STR.22.11.1374
87. Stinear CM, Barber PA, Smale PR, Coxon JP, Fleming MK, Byblow WD. Functional potential in chronic stroke patients depends on corticospinal tract integrity. *Brain* (2007) **130**:170–80. doi:10.1093/brain/awl333
88. Lindenberg R, Zhu LL, Rüber T, Schlaug G. Predicting functional motor potential in chronic stroke patients using diffusion tensor imaging. *Hum Brain Mapp* (2012) **33**:1040–51. doi:10.1002/hbm.21266
89. Kretschmann HJ. Localisation of the corticospinal fibres in the internal capsule in man. *J Anat* (1988) **160**:219–25.
90. Wenzelburger R, Kopper F, Frenzel A, Stolze H, Klebe S, Brossmann A, et al. Hand coordination following capsular stroke. *Brain* (2005) **128**:64–74. doi:10.1093/brain/awh317
91. Fornage M, Debette S, Bis JC, Schmidt H, Ikram MA, Dufouil C, et al. Genome-wide association studies of cerebral white matter lesion burden: the CHARGE consortium. *Ann Neurol* (2011) **69**:928–39. doi:10.1002/ana.22403
92. Surikova I, Meisel S, Siebler M, Wittsack H-J, Seitz RJ. Significance of the perfusion-diffusion mismatch area in chronic cerebral ischemia. *J Magn Reson Imaging* (2006) **24**:771–8. doi:10.1002/jmri.20686
93. Blondin D, Seitz RJ, Rusch O, Janssen H, Andersen K, Wittsack HJ, et al. Clinical impact of MRI perfusion disturbances and normal diffusion in acute stroke patients. *Eur J Radiol* (2009) **71**:1–10. doi:10.1016/j.ejrad.2008.04.003
94. Kurada S, Houkin K. Moyamoya disease: current concepts and future perspectives. *Lancet Neurol* (2008) **7**:1056–66. doi:10.1016/S1474-4422(08)70240-0
95. Lee J-I, Jander S, Oberhuber A, Schelzig H, Hänggi D, Turowski B, et al. Stroke in patients with occlusion of the internal carotid artery: options for treatment. *Expert Rev Neurother* (2014) **14**(10):1153–67. doi:10.1586/14737175.2014.955477
96. Taoufik E, Probert L. Ischemic neuronal damage. *Curr Pharm Des* (2008) **14**:3565–73. doi:10.2174/138161208786848748
97. Witte OW, Bidmon H-J, Schiene K, Redecker C, Hagemann G. Functional differentiation of multiple perilesional zones after focal cerebral ischemia. *J Cereb Blood Flow Metab* (2000) **20**:1149–65. doi:10.1097/00004647-200008000-00001
98. Redecker C, Luhmann HJ, Hagemann G, Fritschy JM, Witte OW. Differential downregulation of GABAA receptor subunits in widespread brain regions in the freeze-lesion model of focal cortical malformations. *J Neurosci* (2000) **20**:5045–53.
99. Carmichael ST, Wei L, Rovainen CM, Woolsey TA. Growth-associated gene expression after stroke: evidence for a growth-promoting region in the peri-infarct cortex. *Exp Neurol* (2005) **193**:291–311. doi:10.1016/j.expneurol.2005.01.004
100. Centonze D, Rossi S, Tortiglione A, Picconi B, Prosperetti C, De Chiara V, et al. Synaptic plasticity during recovery from permanent occlusion of the middle cerebral artery. *Neurobiol Dis* (2007) **27**:44–53. doi:10.1016/j.nbd.2007.03.012
101. Guadagno JV, Jones PS, Aigbirhio FI, Wang D, Fryer TD, Day DJ, et al. Selective neuronal loss in rescued penumbra relates to initial hypoperfusion. *Brain* (2008) **131**:2666–78. doi:10.1093/brain/awn175
102. Frost SB, Barbay S, Friel KM, Plautz EJ, Nudo RJ. Reorganization of remote cortical regions after ischemic brain injury: a potential substrate for stroke recovery. *J Neurophysiol* (2003) **89**:3205–14. doi:10.1152/jn.01143.2002
103. Dancause N, Barbay S, Frost SB, Plautz EJ, Chen D, Zoubina EV, et al. Extensive cortical rewiring after brain injury. *J Neurosci* (2005) **25**:10167–79. doi:10.1523/JNEUROSCI.3256-05.2005
104. Nudo R, Wise B, SiFuentes F, Milliken G. Neural substrates for the effects of rehabilitative training on motor recovery after ischemic infarct. *Science* (1996) **272**:1791–4. doi:10.1126/science.272.5269.1791
105. Biernaskie J, Corbett D. Enriched rehabilitative training promotes improved forelimb motor function and enhanced dendritic growth after focal ischemic injury. *J Neurosci* (2001) **21**:5272–80.
106. Liew SL, Santarnecchi E, Buch ER, Cohen LG. Non-invasive brain stimulation in neurorehabilitation: local and distant effects for motor recovery. *Front Hum Neurosci* (2014) **27**(8):378. doi:10.3389/fnhum.2014.00378

107. Cincinelli P, Pascualetti P, Zaccagnini M, Traversa R, Oliveri M, Rossini PM. Interhemispheric asymmetries of motor cortex excitability in the postacute stroke stage: a paired-pulse transcranial magnetic stimulation study. *Stroke* (2003) **34**:2653–8. doi:10.1161/01.STR.0000092122.96722.72
108. Bütefisch CM, Wessling M, Netz J, Seitz RJ, Hömberg V. Excitability and of ipsi- and contralesional motor cortices and their relationship in stroke patients. *Neurorehabil Neural Repair* (2008) **22**:4–21. doi:10.1177/1545968307301769
109. Manganotti P, Acler M, Zanette GP, Smania N, Fiaschi A. Motor cortical disinhibition during early and late recovery after stroke. *Neurorehabil Neural Repair* (2008) **22**:396–403. doi:10.1177/1545968307313505
110. Liepert J, Haevernick K, Weiller C, Barzel A. The surround inhibition determines therapy-induced cortical reorganization. *Neuroimage* (2006) **32**:1216–20. doi:10.1016/j.neuroimage.2006.05.028
111. Hamzei F, Knab R, Weiller C, Röther J. The influence of extra- and intracranial artery disease on the BOLD signal in fMRI. *Neuroimage* (2003) **20**:1393–9. doi:10.1016/S1053-8119(03)00384-7
112. Jaillard A, Martin CD, Garambois K, Lebas JF, Hommel M. Vicarious function within the human primary motor cortex? A longitudinal fMRI stroke study. *Brain* (2005) **128**:1122–38. doi:10.1093/brain/awh456
113. Boake C, Noser EA, Ro T, Baraniuk S, Gaber M, Johnson R, et al. Constraint-induced movement therapy during early stroke rehabilitation. *Neurorehabil Neural Repair* (2008) **21**:14–24. doi:10.1177/1545968306291858
114. Bütefisch CM, Netz J, Wessling M, Seitz RJ, Hömberg V. Remote changes in cortical excitability after stroke. *Brain* (2003) **126**:470–81. doi:10.1093/brain/awg044
115. Marshall RS, Zarahn E, Alon L, Minzer B, Lazar RM, Krakauer JW. Early imaging correlates of subsequent motor recovery after stroke. *Ann Neurol* (2009) **65**:596–602. doi:10.1002/ana.21636
116. Marshall RS, Perera GM, Lazar RM, Krakauer JW, Constantine RC, DeLaPaz RL. Evolution of cortical activation during recovery from corticospinal tract infarction. *Stroke* (2000) **31**:656–61. doi:10.1161/01.STR.31.3.656
117. Nhan H, Barquist K, Bell K, Esselman P, Odderson I, Cramer S. Brain function early after stroke in relation to subsequent recovery. *J Cereb Blood Flow Metab* (2004) **24**:756–63. doi:10.1097/01.WCB.0000122744.72175.9C
118. Askam T, Indredavik B, Vangberg T, Haberg A. Motor network changes associated with successful motor skill relearning after acute ischemic stroke: a longitudinal functional magnetic resonance imaging study. *Neurorehabil Neural Repair* (2009) **23**:295–304. doi:10.1177/1545968308322840
119. Liew SL, Santarnecchi E, Buch ER, Cohen LG. Non-invasive brain stimulation in neurorehabilitation: local and distant effects for motor recovery. *Front Hum Neurosci* (2014) **8**:378. doi:10.3389/fnhum.2014.00378
120. Reis J, Schambra HM, Cohen LG, Buch ER, Fritsch B, Zarahn E, et al. Noninvasive cortical stimulation enhances motor skill acquisition over multiple days through an effect on consolidation. *Proc Natl Acad Sci U S A* (2009) **106**:1590–5. doi:10.1073/pnas.0805413106
121. Nowak DA, Grefkes C, Dafotakis M, Eickhoff S, Küst J, Karbe H, et al. Effects of low-frequency repetitive transcranial magnetic stimulation of the contralesional primary motor cortex on movement kinematics and neural activity in subcortical stroke. *Arch Neurol* (2008) **65**:741–7. doi:10.1001/archneur.65.6.741
122. Bhatt E, Nagpal A, Greer KH, Grunewald TK, Steele JL, Wiemiller JW, et al. Effect of finger tracking combined with electrical stimulation on brain reorganization and hand function in subjects with stroke. *Exp Brain Res* (2007) **182**:435–47. doi:10.1007/s00221-007-1001-5
123. Winhuisen L, Thiel A, Schumacher B, Kessler J, Rudolf J, Haupt WF, et al. The right inferior frontal gyrus and poststroke aphasia: a follow-up investigation. *Stroke* (2007) **38**:1286–92. doi:10.1161/01.STR.0000259632.04324.6c
124. Marangolo P, Rizzi C, Peran P, Piras F, Sabatini U. Parallel recovery in a bilingual aphasic: a neurolinguistic and fMRI study. *Neuropsychology* (2009) **23**:405–9. doi:10.1037/a0014824
125. Muehlbacher W, Richards C, Ziemann U, Hallett M. Improving hand function in chronic stroke. *Arch Neurol* (2002) **59**:1278–82. doi:10.1001/archneur.59.8.1278
126. Floel A, Nagorsen U, Werhahn KJ, Ravindran S, Birbaumer N, Knecht S, et al. Influence of somatosensory input on motor function in patients with chronic stroke. *Ann Neurol* (2004) **56**:206–12. doi:10.1002/ana.20170
127. Fregni F, Boggio PS, Mansur CG, Wagner T, Ferreira MJ, Lima MC, et al. Transcranial direct current stimulation of the unaffected hemisphere in stroke patients. *Neuroreport* (2005) **16**:1551–5. doi:10.1097/01.wnr.0000177010.44602.5e
128. Hummel F, Celnik P, Giraux P, Floel A, Wu WH, Gerloff C, et al. Effects of non-invasive cortical stimulation on skilled motor function in chronic stroke. *Brain* (2005) **128**:490–9. doi:10.1093/brain/awh369
129. Lindenberg R, Renga V, Zhu LL, Nair D, Schlaug G. Bihemispheric brain stimulation facilitates motor recovery in chronic stroke patients. *Neurology* (2010) **75**:2176–84. doi:10.1212/WNL.0b013e318202013a
130. Nair DG, Hutchinson S, Fregni F, Alexander M, Pascual-Leone A, Schlaug G. Imaging correlates of motor recovery from cerebral infarction and their physiological significance in well-recovered patients. *Neuroimage* (2007) **34**:253–63. doi:10.1016/j.neuroimage.2006.09.010
131. Talelli P, Greenwood RJ, Rothwell JC. Exploring theta burst stimulation as an intervention to improve motor recovery in chronic stroke. *Clin Neurophysiol* (2007) **118**:333–42. doi:10.1016/j.clinph.2006.10.014
132. Khedr EM, Abdel-Fadeil MR, Farghali A, Qaid M. Role of 1 and 3 Hz repetitive transcranial magnetic stimulation on motor function recovery after acute ischaemic stroke. *Eur J Neurol* (2009) **16**:1323–30. doi:10.1111/j.1468-1331.2009.02746.x
133. Celnik P, Paik NJ, Vandermeeren Y, Dimyan M, Cohen LG. Effects of combined peripheral nerve stimulation and brain polarization on performance of a motor sequence task after chronic stroke. *Stroke* (2009) **40**:1764–71. doi:10.1161/STROKEAHA.108.540500
134. Fries W, Danek A, Witt TN. Motor responses after transcranial electrical stimulation of cerebral hemispheres with a degenerated pyramidal tract. *Ann Neurol* (1991) **29**:646–50. doi:10.1002/ana.410290612
135. Schaechter JD, Perdue KL, Wang R. Structural damage to the corticospinal tract correlates with bilateral sensorimotor cortex reorganization in stroke patients. *Neuroimage* (2008) **39**:1370–82. doi:10.1016/j.neuroimage.2007.09.071
136. Lindenberg R, Renga V, Zhu LL, Betzler F, Alsop D, Schlaug G. Structural integrity of corticospinal motor fibres predict motor impairment in chronic stroke. *Neurology* (2010) **74**:280–7. doi:10.1212/WNL.0b013e3181ccc6d9
137. Canedo A. Primary motor cortex influences on the descending and ascending systems. *Prog Neurobiol* (1997) **51**:287–335. doi:10.1016/S0301-0082(96)00058-5
138. Lang CE, Schieber MH. Reduced muscle selectivity during individuated finger movements in humans after damage to the motor cortex or corticospinal tract. *J Neurophysiol* (2004) **91**:1722–33. doi:10.1152/jn.00805.2003
139. Kennedy RR. Corticospinal, rubrospinal and rubro-olivary projections: a unifying hypothesis. *Trends Neurosci* (1990) **13**:474–9. doi:10.1016/0166-2236(90)90079-P
140. Carey LM, Abbott DF, Harvey MR, Puce A, Seitz RJ, Donnan GA. Relationship between touch impairment and brain activation after lesions of subcortical and cortical somatosensory regions. *Neurorehabil Neural Repair* (2011) **25**:443–57. doi:10.1177/1545968310395777
141. Liepert J, Storch P, Fritsch A, Weiller C. Motor cortex disinhibition in acute stroke. *Clin Neurophysiol* (2000) **111**:671–6. doi:10.1016/S1388-2457(99)00312-0
142. Hummel FC, Steven B, Hoppe J, Heise K, Thomalla G, Cohen LG, et al. Deficient intracortical inhibition (SICI) during movement preparation after chronic stroke. *Neurology* (2009) **19**:1766–72. doi:10.1212/WNL.0b013e3181a609c5
143. Lewis GN, Perreault EJ. Side of lesion influences bilateral activation in chronic, post-stroke hemiparesis. *Clin Neurophysiol* (2007) **118**:2050–62. doi:10.1016/j.clinph.2007.08.027
144. Misawa S, Kuwabara S, Matsuda S, Honma K, Ono J, Hattori T. The ipsilateral cortico-spinal tract is activated after hemiparetic stroke. *Eur J Neurol* (2008) **15**:706–11. doi:10.1111/j.1468-1331.2008.02168.x
145. Schwerin S, Dewald JPA, Haztl M, Jovanovich S, Nickeas M, MacKinnon C. Ipsilateral versus contralateral cortical motor projections to a shoulder adductor in chronic hemiparetic stroke: implications for the expression of arm synergies. *Exp Brain Res* (2008) **185**:509–19. doi:10.1007/s00221-007-1169-8
146. Pannek K, Chalk JB, Finnigan S, Rose SE. Dynamic corticospinal white matter connectivity changes during stroke recovery: a diffusion tensor probabilistic tractography study. *J Magn Reson Imaging* (2009) **29**:529–36. doi:10.1002/jmri.21627
147. Lang CE, Dejong SL, Beebe JA. Recovery of thumb and finger extension and its relation to grasp performance after stroke. *J Neurophysiol* (2009) **102**:451–9. doi:10.1152/jn.91310.2008
148. Foltys H, Krings T, Meister IG, Sparing R, Boroojerdi B, Thron A, et al. Motor representation in patients rapidly recovering after stroke: a functional magnetic resonance imaging and transcranial magnetic stimulation study. *Clin Neurophysiol* (2003) **114**:2404–2015. doi:10.1016/S1388-2457(03)00263-3

149. Bütefisch CM, Kleiser R, Körber B, Müller K, Wittsack HJ, Hömberg V, et al. Recruitment of contralesional motor cortex in stroke patients with recovery of hand function. *Neurology* (2005) **64**:1067–9. doi:10.1212/01.WNL.0000154603.48446.36
150. Nelles G, Cramer S, Schaechter J, Kaplan J, Finklestein S. Quantitative assessment of mirror movements after stroke. *Stroke* (1998) **29**:1182–7. doi:10.1161/01.STR.29.6.1182
151. Seitz RJ, Knorr U, Azari NP, Herzog H, Freund H-J. Recruitment of a visuo-motor network in stroke recovery. *Restor Neurol Neurosci* (1999) **14**:25–33.
152. Grefkes C, Nowak DA, Eickhoff SB, Dafotakis M, Küst J, Karbe H, et al. Cortical connectivity after subcortical stroke assessed with functional magnetic resonance imaging. *Ann Neurol* (2008) **63**:236–46. doi:10.1002/ana.21228
153. Kimberley TJ, Lewis SM, Strand C, Rice BD, Hall S, Slivnik P. Neural substrates of cognitive load changes during a motor task in subjects with stroke. *J Neurol Phys Ther* (2008) **32**:110–7. doi:10.1097/NPT.0b013e318183d716
154. Sharma N, Baron JC, Rowe JB. Motor imagery after stroke: relating outcome to motor network connectivity. *Ann Neurol* (2009) **66**:604–16. doi:10.1002/ana.21810
155. Ebrahim S, Nouri F, Barer D. Cognitive impairment after stroke. *Age Ageing* (1985) **14**:345–8. doi:10.1093/ageing/14.6.345
156. Robinson RG, Starr LB, Lipsey JR, Rao K, Price TR. A two-year longitudinal study of poststroke mood disorders. In-hospital prognostic factors associated with six-month outcome. *J Nerv Ment Dis* (1985) **173**:221–6. doi:10.1097/00005053-198504000-00003
157. Karlinski M, Kobayashi A, Czlonkowska A, Mikulik R, Vaclavik D, Brozman M, et al. Role of preexisting disability in patients treated with intravenous thrombolysis for ischemic stroke. *Stroke* (2014) **45**:770–5. doi:10.1161/STROKEAHA.113.003744
158. Seitz RJ, Sukienik J, Siebler M. Outcome after systemic thrombolysis is predicted by age and stroke severity – an open label experience with rtPA and tirofiban. *Neurol Int* (2012) **4**:e9,35–39. doi:10.4081/ni.2012.e9
159. Aron AW, Staff I, Fortunato G, McCullough LD. Prestroke living situation and depression contribute to initial stroke severity and stroke recovery. *J Stroke Cerebrovasc Dis* (2015) **24**(2):492–9. doi:10.1016/j.jstrokecerebrovasdis.2014.09.024
160. Guidetti D, Rota E, Morelli N, Immovilli P. Migraine and stroke: “vascular” comorbidity. *Front Neurol* (2014) **5**:193. doi:10.3389/fneur.2014.00193
161. Sacco S, Ornello R, Ripa P, Pistoia F, Carolei A. Migraine and hemorrhagic stroke. A meta-analysis. *Stroke* (2013) **44**:3032–8. doi:10.1161/STROKEAHA.113.002465
162. Brookes RL, Herbert V, Andrew J, Lawrence AJ, Morris RG, Markus HS. Depression in small-vessel disease relates to white matter ultrastructural damage, not disability. *Neurology* (2014) **83**:1417–23. doi:10.1212/WNL.0000000000000882
163. Pendlebury ST, Rothwell PM. Risk of recurrent stroke, other vascular events and dementia after transient ischaemic attack and stroke. *Cerebrovasc Dis* (2009) **27**(Suppl 3):1–11. doi:10.1159/000209260
164. Oksala NK, Jokinen H, Melkas S, Oksala A, Pohjasvaara T, Hietanen M, et al. Cognitive impairment predicts poststroke death in long-term follow-up. *J Neurol Neurosurg Psychiatry* (2009) **80**:1230–5. doi:10.1136/jnnp.2009.174573
165. Patel M, Coutinho C, Emsley HCA. Prevalence of radiological and clinical cerebrovascular disease in idiopathic Parkinson's disease. *Clin Neurol Neurosurg* (2011) **113**:830–4. doi:10.1016/j.clineuro.2011.05.014
166. de Laat KF, van Norden AG, Gons RA, van Uden IW, Zwiers MP, Bloem BR, et al. Cerebral white matter lesions and lacunar infarcts contribute to the presence of mild Parkinsonian signs. *Stroke* (2012) **43**:2574–9. doi:10.1161/STROKEAHA.112.657130
167. Huang Y-P, Chen L-S, Ming-Fang Yen M-F, Fann C-Y, Chiu Y-H, Chen H-H, et al. Parkinson's disease is related to an increased risk of ischemic stroke – a population-based propensity score-matched follow-up study. *PLoS One* (2013) **8**:e68314. doi:10.1371/journal.pone.0068314
168. Buchman AS, Leurgans SE, Nag S, Bennett DA, Schneider JA. Cerebrovascular disease pathology and Parkinsonian signs in old age. *Stroke* (2011) **42**:3183–9. doi:10.1161/STROKEAHA.111.623462
169. Chang C-S, Liao C-H, Lin C-C, Lane H-Y, Sung F-C, Kao C-H. Patients with epilepsy are at an increased risk of subsequent stroke: a population-based cohort study. *Seizure* (2014) **23**:377–81. doi:10.1016/j.seizure.2014.02.007
170. Broomfield NM, Terence J, Quinn TJ, Abdul-Rahim AH, Walters MR, Evans JJ. Depression and anxiety symptoms post-stroke/TIA: prevalence and associations in cross-sectional data from a regional stroke registry. *BMC Neurol* (2014) **14**:198. doi:10.1186/s12883-014-0198-8
171. Hornsten C, Lövheim H, Gustafson Y. The association between stroke, depression, and 5-year mortality among very old people. *Stroke* (2013) **44**:2587–9. doi:10.1161/STROKEAHA.113.002202
172. Wu H-C, Chou FH-C, Tsai K-Y, Su C-Y, Shen S-P, Chung T-C. The incidence and relative risk of stroke among patients with bipolar disorder: a seven-year follow-up study. *PLoS One* (2013) **8**:e73037. doi:10.1371/journal.pone.0073037
173. Seitz RJ, Hildebold T, Simeria K. Spontaneous arm movement activity assessed with accelerometry is a marker for early recovery after stroke. *J Neurol* (2011) **258**:457–63. doi:10.1007/s00415-010-5778-y
174. Ruan J, Seitz RJ. Impaired sleep and reduced spontaneous movement activity in acute stroke: an exploratory study. *J Neuro Clin* (2014) **1**:8.
175. Bassetti CL, Aldrich MS. Sleep electroencephalogram changes in acute hemispheric stroke. *Sleep Med* (2001) **2**:185–94. doi:10.1016/S1389-9457(00)00071-X
176. Luu P, Tucker DM, Englander R, Lockfeld A, Lutsep H, Oken B. Localizing acute stroke-related EEG changes: assessing the effects of spatial undersampling. *J Clin Neurophysiol* (2001) **18**:302–17. doi:10.1097/00004691-200107000-00002
177. Vock J, Achermann P, Bischof M, Milanova M, Müller C, Nirkko A, et al. Evolution of sleep and sleep EEG after hemispheric stroke. *J Sleep Res* (2002) **11**:331–8. doi:10.1046/j.1365-2869.2002.00316.x
178. Cyril C, Urbain MT, Calvet P, Martinez VL. The clinical significance of periodic lateralized epileptiform discharges in acute ischemic stroke. *J Stroke Cerebrovasc Dis* (2000) **9**:298–302. doi:10.1053/jscd.2000.18734
179. Hensel S, Rockstroh B, Berg P, Elbert T, Schönle PW. Left-hemispheric abnormal EEG activity in relation to impairment and recovery in aphasic patients. *Psychophysiology* (2004) **41**:394–400. doi:10.1111/j.1469-8986.2004.00164.x
180. Burghaus L, Hilker R, Dohmen C, Bosche B, Winhuisen L, Galldiks N, et al. Early electroencephalography in acute ischemic stroke: prediction of a malignant course? *Clin Neurol Neurosurg* (2007) **109**:45–9. doi:10.1016/j.clineuro.2006.06.003
181. Airboix A, Comes E, García-Eroles L, Massons JB, Oliveres M, Balcells M. Prognostic value of very early seizures for in-hospital mortality in atherothrombotic infarction. *Eur Neurol* (2003) **50**:78–84. doi:10.1159/000072503
182. Reith J, Jørgensen HS, Nakayama H, Raaschou HO, Olsen TS. Seizures in acute stroke: predictors and prognostic significance. The Copenhagen Stroke Study. *Stroke* (1997) **28**:1585–9. doi:10.1161/01.STR.28.8.1585
183. Jordan KG. Emergency EEG and continuous EEG monitoring in acute ischemic stroke. *J Clin Neurophysiol* (2004) **21**:341–52.
184. Binkofski F, Seitz RJ, Hackländer T, Pawelec D, Mau J, Freund H-J. The recovery of motor functions following hemiparetic stroke: a clinical and MR-morphometric study. *Cerebrovasc Dis* (2001) **11**:273–81. doi:10.1159/000047650
185. Meinzer M, Ebert T, Wienbruch C, Djundja D, Barthel B, Rockstroh B. Intensive language training enhances brain plasticity in chronic aphasia. *BMC Biol* (2004) **2**:20. doi:10.1186/1741-7007-2-20
186. Cheung VH, Gray L, Karunanithi M. Review of accelerometry for determining daily activity among elderly patients. *Arch Phys Med Rehabil* (2011) **92**:998–1014. doi:10.1016/j.apmr.2010.12.040
187. Duncan PW, Lai SM, Keighley J. Defining post-stroke recovery: implications for design and interpretation of drug trials. *Neuropharmacology* (2000) **39**:835–41. doi:10.1016/S0028-3908(00)00003-4
188. Kwakkel G, Kollen BJ, van der Grond J, Prevo AJ. Probability of regaining dexterity in the flaccid upper limb: impact of severity of paresis and time since onset in acute stroke. *Stroke* (2003) **34**:2181–6. doi:10.1161/01.STR.0000087172.16305.CD
189. Beebe JA, Lang CE. Active range of motion predicts upper extremity function 3 months after stroke. *Stroke* (2009) **40**:1772–92. doi:10.1161/STROKEAHA.108.536763
190. Krebs HI, Volpe B, Hogan N. A working model of stroke recovery from rehabilitation robotics practitioners. *J Neuroeng Rehabil* (2009) **2009**(25):6. doi:10.1186/1743-0003-6-6
191. Sprigg N, Gray LJ, Bath PM, Lindstrom E, Boysen G, De Deyn PP, et al. Early recovery and functional outcome are related with causal stroke subtype: data from the tinzaparin in acute ischemic stroke trial. *J Stroke Cerebrovasc Dis* (2004) **16**:180–4. doi:10.1016/j.jstrokecerebrovasdis.2007.02.003

192. Schepers P, Ketelaar M, Visser-Meily AJ, de Groot V, Twisk JW, Lindeman E. Functional recovery differs between ischaemic and haemorrhagic stroke patients. *J Rehabil Med* (2008) **40**:487–9. doi:10.2340/16501977-0198
193. Welmer AK, Holmqvist LW, Sommerfeld DK. Limited fine hand use after stroke and its association with other disabilities. *J Rehabil Med* (2008) **40**:603–8. doi:10.2340/16501977-0218
194. Baztán JJ, Gálvez CP, Soccoro A. Recovery of functional impairment after acute illness and mortality: one-year follow-up study. *Gerontology* (2009) **55**:269–74. doi:10.1159/000193068
195. Gosselin S, Desrosiers J, Corriveau H, Hébert R, Rochette A, Provencher V, et al. Outcomes during and after inpatient rehabilitation: comparison between adults and older adults. *J Rehabil Med* (2008) **40**:55–60. doi:10.2340/16501977-0144
196. Kwakkel G, Wagenaar RC, Twisk JW, Lankhorst GJ, Koetsier JC. Intensity of leg and arm training after primary middle-cerebral-artery stroke: a randomised trial. *Lancet* (1999) **354**:191–6. doi:10.1016/S0140-6736(98)09477-X
197. Takahashi CD, Der-Yeghian L, Le V, Motiwala RR, Cramer SC. Robot-based hand motor therapy after stroke. *Brain* (2008) **131**:425–37. doi:10.1093/brain/awm311
198. Luft AR, Macko RF, Forrester LW, Villagra F, Ivey F, Sorkin JD, et al. Treadmill exercise activates subcortical neural networks and improves walking after stroke: a randomized controlled trial. *Stroke* (2008) **39**:3341–50. doi:10.1161/STROKEAHA.108.527531
199. Lindberg PG, Schmitz C, Engardt M, Forssberg H, Borg J. Use-dependent up- and down-regulation of sensorimotor brain circuits in stroke patients. *Neurorehabil Neural Repair* (2007) **21**:315–26. doi:10.1177/1545968306296965
200. Dong Y, Winstein CJ, Albestegui-DuBois R, Dobkin BH. Evolution of fMRI activation in the perilesional primary motor cortex and cerebellum with rehabilitation training-related motor gains after stroke: a pilot study. *Neurorehabil Neural Repair* (2007) **21**:412–28. doi:10.1177/1545968306298598
201. Mintzopoulos D, Khanicheh A, Konstant AA, Astrakas LG, Singhal AB, Moskowitz MA, et al. Functional MRI of rehabilitation in chronic stroke patients using novel MR-compatible hand robotics. *Open Neuroimage J* (2008) **2**:94–101. doi:10.2174/1874440000802010094
202. Yavuzer G, Selles R, Sezer N, Sütbeyaz S, Bussmann JB, Köseoglu F, et al. Mirror therapy improves hand function in subacute stroke: a randomized controlled trial. *Arch Phys Med Rehabil* (2008) **89**:393–8. doi:10.1016/j.apmr.2007.08.162
203. Dohle C, Püllen J, Nakaten A, Küst J, Rietz C, Karbe H. Mirror therapy promotes recovery from severe hemiparesis: a randomized controlled trial. *Neurorehabil Neural Repair* (2009) **23**:209–17. doi:10.1177/1545968308324786
204. Mudie MH, Matyas TA. Responses of the densely hemiplegic upper extremity to bilateral training. *Neurorehabil Neural Repair* (2001) **15**:129–40. doi:10.1177/154596830101500206
205. Perez MA, Cohen LG. Mechanisms underlying functional changes in the primary motor cortex ipsilateral to an active hand. *J Neurosci* (2008) **28**:5631–40. doi:10.1523/JNEUROSCI.0093-08.2008
206. Wolf SL, LeCraw DE, Barton LA, Jann BB. Forced use of hemiplegic upper extremities to reverse the effect of learned nonuse among chronic stroke and head-injured patients. *Exp Neurol* (1989) **104**:125–32. doi:10.1016/S0014-4886(89)80005-6
207. Taub E, Uswatte G, Pidikiti R. Constraint-induced movement therapy: a new family of techniques with broad application to physical rehabilitation – a clinical review. *J Rehabil Res Dev* (1999) **36**:237–51.
208. Liepert J, Miltner WH, Bauder H, Sommer M, Dettmers C, Taub E, et al. Motor cortex plasticity during constraint-induced movement therapy in stroke patients. *Neurosci Lett* (1998) **250**:5–8. doi:10.1016/S0304-3940(98)00386-3
209. Sawaki L, Butler AJ, Leng X, Wassenaar PA, Mohammad YM, Blanton S, et al. Constraint-induced movement therapy results in increased motor map area in subjects 3 to 9 months after stroke. *Neurorehabil Neural Repair* (2008) **22**:505–13. doi:10.1177/1545968308317531
210. Gauthier LV, Taub E, Perkins C, Ortmann M, Mark UW, Uswatte G. Remodelling the brain: plastic structural brain changes produced by different motor therapies after stroke. *Stroke* (2008) **39**:1520–5. doi:10.1161/STROKEAHA.107.502229
211. Cameirao MS, Bermudez IBS, Duarte E, Verschure PF. Virtual reality based rehabilitation speeds up functional recovery of the upper extremities after stroke: a randomized controlled pilot study in the acute phase of stroke using the rehabilitation gaming system. *Restor Neurol Neurosci* (2011) **29**:287–98. doi:10.3233/RNN-2011-0599
212. Prochnow D, Bermúdez i Badia S, Schmidt J, Duff A, Brunheim S, Kleiser R, et al. An fMRI study of visuomotor processing in a virtual reality based paradigm: rehabilitation gaming system. *Eur J Neurosci* (2013) **37**:1441–7. doi:10.1111/ejn.12157
213. Seitz RJ, Kammerzell A, Samartzi M. Monitoring of visuomotor coordination in healthy subjects and patients with stroke and Parkinson's disease: an application study using the PABLO-device. *Int J Neurorehabil* (2014) **1**:113. doi:10.4172/ijn.1000113
214. Ertelt D, Small S, Solodkin A, Dettmers C, McNamara A, Binkofski F, et al. Action observation has a positive impact on rehabilitation of motor deficits after stroke. *Neuroimage* (2007) **36**(Suppl 2):T164–73. doi:10.1016/j.neuroimage.2007.03.043

Conflict of Interest Statement: The authors declare that the research was conducted in the absence of any commercial or financial relationships that could be construed as a potential conflict of interest.

Copyright © 2015 Seitz and Donnan. This is an open-access article distributed under the terms of the Creative Commons Attribution License (CC BY). The use, distribution or reproduction in other forums is permitted, provided the original author(s) or licensor are credited and that the original publication in this journal is cited, in accordance with accepted academic practice. No use, distribution or reproduction is permitted which does not comply with these terms.



A review of transcranial magnetic stimulation and multimodal neuroimaging to characterize post-stroke neuroplasticity

Angela M. Auriat¹, Jason L. Neva¹, Sue Peters¹, Jennifer K. Ferris² and Lara A. Boyd^{1,2*}

¹ Department of Physical Therapy, Faculty of Medicine, University of British Columbia, Vancouver, BC, Canada, ² Graduate Program in Neuroscience, Faculty of Medicine, University of British Columbia, Vancouver, BC, Canada

OPEN ACCESS

Edited by:

Roland Wiest,
University of Bern, Switzerland

Reviewed by:

Bin Jiang,
Beijing Neurosurgical Institute, China
Gian Marco De Marchis,
University Hospital Basel, Switzerland
Roland Beisteiner,
Medical University of Vienna, Austria

*Correspondence:

Lara A. Boyd
lara.boyd@ubc.ca

Specialty section:

This article was submitted to Stroke,
a section of the journal
Frontiers in Neurology

Received: 01 June 2015

Accepted: 12 October 2015

Published: 29 October 2015

Citation:

Auriat AM, Neva JL, Peters S,
Ferris JK and Boyd LA (2015)
A review of transcranial magnetic
stimulation and multimodal
neuroimaging to characterize
post-stroke neuroplasticity.
Front. Neurol. 6:226.
doi: 10.3389/fneur.2015.00226

Following stroke, the brain undergoes various stages of recovery where the central nervous system can reorganize neural circuitry (neuroplasticity) both spontaneously and with the aid of behavioral rehabilitation and non-invasive brain stimulation. Multiple neuroimaging techniques can characterize common structural and functional stroke-related deficits, and importantly, help predict recovery of function. Diffusion tensor imaging (DTI) typically reveals increased overall diffusivity throughout the brain following stroke, and is capable of indexing the extent of white matter damage. Magnetic resonance spectroscopy (MRS) provides an index of metabolic changes in surviving neural tissue after stroke, serving as a marker of brain function. The neural correlates of altered brain activity after stroke have been demonstrated by abnormal activation of sensorimotor cortices during task performance, and at rest, using functional magnetic resonance imaging (fMRI). Electroencephalography (EEG) has been used to characterize motor dysfunction in terms of increased cortical amplitude in the sensorimotor regions when performing upper limb movement, indicating abnormally increased cognitive effort and planning in individuals with stroke. Transcranial magnetic stimulation (TMS) work reveals changes in ipsilesional and contralesional cortical excitability in the sensorimotor cortices. The severity of motor deficits indexed using TMS has been linked to the magnitude of activity imbalance between the sensorimotor cortices. In this paper, we will provide a narrative review of data from studies utilizing DTI, MRS, fMRI, EEG, and brain stimulation techniques focusing on TMS and its combination with uni- and multimodal neuroimaging methods to assess recovery after stroke. Approaches that delineate the best measures with which to predict or positively alter outcomes will be highlighted.

Keywords: multimodal neuroimaging, stroke, sensorimotor recovery, diffusion tensor imaging, magnetic resonance spectroscopy, functional MRI, electroencephalography, transcranial magnetic stimulation

INTRODUCTION

Recent advances in stroke treatment have stressed early intervention, greatly reducing the risk of mortality after stroke (1). Yet, development of treatments aimed at improving function after stroke has failed to keep pace, in part because rehabilitation specialists do not yet understand how to best help the brain recover from stroke. The importance of this issue is underscored by work from the Boyd Lab showing a *clinically meaningful decline* in population-based quality of life for Canadians with stroke from 1998 to 2005 (2). In this work, declines in health-related quality of life in the Canadian population were associated with increases in the proportion of individuals with impaired motor function post-stroke. Together the high incidence, increased survival rates, and decreased quality of life following stroke demonstrate a critical need for improved understanding of brain recovery after stroke.

Many have attempted to define the neural mechanisms of post-stroke impairment and recovery in the hope that understanding these processes will improve rehabilitation interventions and enhance function (Figure 1, Part I). Since the development of neuroimaging techniques, such as magnetic resonance imaging (MRI) and functional MRI (fMRI), it is possible to identify both structural and functional brain changes, termed neuroplasticity, as individuals with stroke re-learn motor skills. In addition, the use of transcranial magnetic stimulation (TMS) allows cortical excitability to be temporarily enhanced or reduced, which enables researchers to experimentally test the influence of specific brain regions on motor learning and recovery from stroke. To date, numerous studies show neuroplastic change after stroke by documenting recovery of function that is independent of spontaneous change associated with acute recovery (3, 4). Our work (3, 5–9) and that of others (10–12) clearly shows that motor learning and capacity for neuroplastic change (13, 14) are preserved, even during the chronic stage after stroke. Experience-dependent neuroplasticity likely explains a portion of the change associated with motor learning after stroke in this work (15), yet despite these advances in knowledge, no clear pattern of motor-related brain activation has emerged that fully explains how the brain compensates for stroke-related damage during motor learning.

In part, our failure to grasp how the damaged brain learns stems from an incomplete understanding of the relationships between behavior and brain function. Key to improving functional recovery after stroke is more fully understanding and mapping experience-dependent neuroplasticity (17), which demonstrates that the functional organization of the motor system can be modified by use. Technological advances have enabled detailed structural assessment of the brain with volumetric analysis of white and gray matter, the indexing of white matter connectivity using diffusion imaging, quantifying metabolic changes with magnetic resonance spectroscopy (MRS), mapping of brain activity with fMRI and electroencephalography (EEG), and assessing experience-dependent neuroplasticity through the manipulation of cortical excitability using repetitive TMS (rTMS). In this review, we highlight the use of these neuroimaging techniques to map the neuroplasticity of motor learning and sensorimotor recovery, as well as the advances in knowledge that have been stimulated

from their use. In combination, the knowledge gained from these approaches is contributing significantly to the genesis of novel, evidence-based interventions designed to promote functional recovery after stroke.

NEUROIMAGING

Structural Imaging Volumetric Analysis

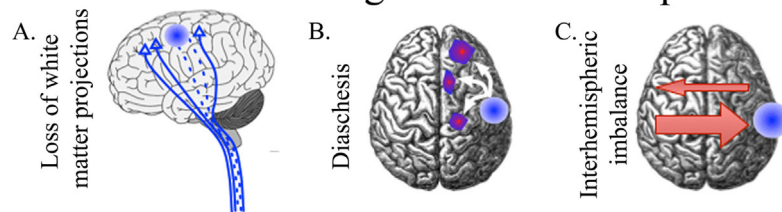
It has long been recognized that lesion location rather than size explains the bulk of neurological deficits after stroke (18). For instance, the degree damage to the cortical spinal tract (CST) rather than lesion volume correlates with motor ability after stroke (19). However, stroke-related damage also has effects on regions remote from the site of injury (20). The time point of assessment is important because of delayed atrophy in areas remote from the stroke (21). Advances in volumetric analysis of MRI have allowed for the automated quantification of brain volumes after segmentation into gray and white matter (22, 23) often using only an anatomical T1 scan (Figure 1, Section IIA). The quality of the scan influences the precision of segmentation and having additional scans, such as fluid-attenuated inversion recovery (FLAIR), T2, or proton density (PD), can improve accuracy and identification of subtle lesions (23). Unfortunately, difficulties arise when using these methods to quantify brains with a neurological pathology (24, 25). Caution must be taken to ensure programs designed to use anatomical landmarks to segment and quantify brain volumes are functioning as expected with analysis of chronic post-stroke brains, where landmarks may shift or be non-existent due to direct damage or atrophy. Recently, our group has utilized the FreeSurfer-based image analysis package (26, 27) for volumetric segmentation in chronic stroke and found that segmentation was unaffected by small subcortical lesions (24). However, participants with more extensive damage had to be excluded from the analysis due to segmentation errors. Alternative segmentation programs or using more extensive manual edits will allow for the inclusion of participants with larger lesions.

Volumetric analysis may be a valuable predictor of responders to post-stroke interventions (23, 28). Future use of volumetric analysis in rehabilitation studies will likely provide more useful information on the influence of structural integrity on post-stroke recovery. However, extreme caution and manual review/intervention of computerized assessments must be used to ensure accurate quantification of post-stroke brains (24, 25).

Diffusion-Weighted Imaging

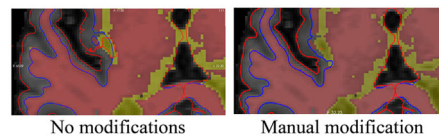
Diffusion-weighted magnetic resonance imaging (DW-MRI) non-invasively provides information on white matter pathways in the human brain. Based on its ability to determine water diffusion characteristics, DW-MRI has been extensively used to identify the orientation and integrity of white matter after stroke, and to relate these measures to motor function [see Ref. (28) for review]. Brain regions, such as the corpus callosum (CC) (29, 30) and the corticospinal tract (CST) (29, 31–33), have been repeatedly studied and related to both motor function and functional potential (30, 31, 33). DW-MRI has been touted as a

I Factors contributing to functional impairment

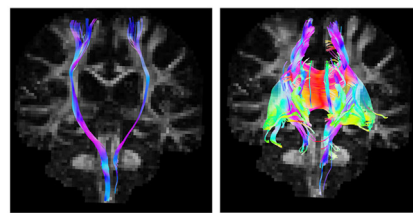


II Assessment Tools

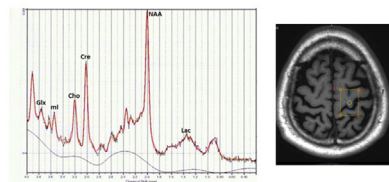
Structural Imaging



A. Volumetric Analysis

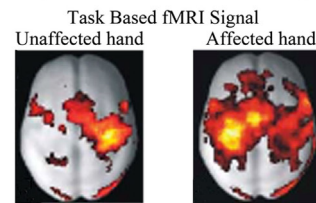


B. Diffusion Tensor Imaging

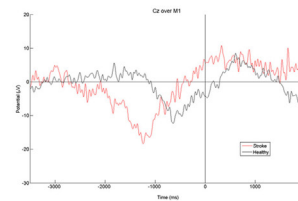


C. Magnetic Resonance Spectroscopy

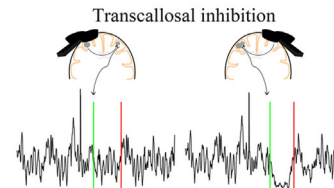
Functional Imaging



D. Functional BOLD MRI



E. Electroencephalography



F. Transcranial Magnetic Stimulation

FIGURE 1 | A summary of our current understanding of factors that contribute to post-stroke impairment (I) and the assessment tools available for quantifying these changes (II). Loss of white matter projections is illustrated as a decreased number of CST projections (IA). Diaschisis, a remote functional depression, can impact intra- and interhemispheric areas (IB). A focal lesion can disrupt the mutual balanced inhibition between hemispheres. Damage from stroke disrupts the balance by decreasing the inhibition of the contralesional hemisphere, which results in increased inhibition of the injured hemisphere (IC). FreeSurfer-based volumetric analysis, using structural T1s, can be manually modified to correct for errors in the automated segmentation of injured brains (IIA). Identification of CST and CC in an individual with chronic stroke utilizing tractography of diffusion-weighted images (IIB). The axial brain image identifies the voxel placement in the hand knob of an individual with chronic stroke, the resulting spectra quantifies multiple neurotransmitters (IIC). BOLD signal during movements of the unaffected and affected hand in individuals with left-sided subcortical stroke; modified, with permission, from Grefkes et al. (16) (IID). EEG trace from an electrode located at Cz (over primary motor cortex) in an individual with chronic stroke and a healthy control as they take a step (time 0) (IIE). Transcallosal inhibition evoked from stimulation over ipsilesional and contralesional primary motor cortex (IIF). Ipsilesional stimulation failed to produce an observable iSP in the ipsilateral (to the TMS pulse) limb, whereas contralesional stimulation evoked a quantifiable iSP in the ipsilateral (to the TMS pulse) limb. iSP occurs in the time between the green (onset) and red (offset) lines. CST, cortical spinal tract; CC, corpus callosum; fMRI, functional MRI; BOLD, blood oxygen level dependent; iSP, ipsilateral silent period; TMS, transcranial magnetic stimulation.

promising tool for rehabilitation planning and prognosis after stroke (31), and may predict neural changes after motor learning. Importantly, preliminary studies have demonstrated that the integrity of CST (24, 34) and CC (35) influences the efficacy of rTMS, suggesting that DW-MRI can provide valuable information when selecting rTMS protocols and predicting the efficacy of an intervention.

The motion of water molecules is restricted based on its location and in white matter movement of water is restricted across the tracts, with a relatively greater freedom of movement parallel to the white matter fibers. It is this basic principle, which allows for DW-MRI to identify the diffusion characteristics of white matter and predict specific white matter pathways. Several diffusion-based measures have been related to post-stroke outcome,

primarily, fractional anisotropy (FA), apparent diffusion coefficient (ADC), axial diffusivity (AD), radial diffusivity (RD), number of tracts, and tract volume. FA is the most commonly reported DW-MRI measure, and indicates the degree of directionality within the tissue microstructure, which is determined by tissue features, such as axons, myelin, and microtubules. FA ranges from 0 (completely isotropic) to 1 (completely anisotropic); therefore, higher FA indicates greater directionality (36, 37). ADC, AD, and RD are all based on the eigenvalues of the apparent diffusion tensor [λ_1 , λ_2 , and λ_3 (38)]. AD is an indicator of water diffusion along the parallel, principal, direction of axonal water diffusion [$AD = \lambda_1$ (38)]. RD is an index of water diffusion perpendicular to the principal direction of water [$RD = \lambda_2 + \lambda_3/2$ (38)]. ADC is the mean value of eigenvalues of the apparent diffusion tensor [$ADC = \lambda_1 + \lambda_2 + \lambda_3/3$ (38)]. Tractography methods allow for the visualization of fiber architecture and also allow for the identification of fiber number and volume in pathways of interest to stroke recovery (Figure 1, Section IIB).

Although the reproducibility of tractography has been established in a stroke population (39, 40), different analysis methods can affect the interpretation of results (41). At present, no “gold standard” method for fiber tractography exists for *in vivo* application (42–44). For example, our group has recently found that diffusion tensor imaging (DTI) and constrained spherical deconvolution (CSD) methods produce significantly different results when applied to individuals with chronic stroke (41). Although DTI is the most commonly applied method of tractography analysis in stroke research, CSD analysis provided a stronger relationship between CST and CC white matter characteristics, and post-stroke outcome. Additionally, DTI-based tractography often fails to reconstruct fibers projecting to the lateral aspect of the cortex (41, 42). Lateral projections of the CST play a significant role in motor recovery after stroke (45), specifically fine motor control of the hand (46). The failure of DTI to detect these lateral projections likely hinders correlations between CST and CC diffusion measures and motor function. If DW-MRI tractography is to become a feasible tool for assessing prognosis, functional potential, or rehabilitation strategies, it is important that this technique be as sensitive and specific to actual white matter fiber architecture as possible. Inability to detect an intact CST or an under-estimation of the projection of fiber populations may undermine patients’ expected potential for recovery resulting in minimized rehabilitation efforts. Additional studies are needed to identify optimized tractography strategies for identifying the fiber projections important for stroke recovery.

In addition to tractography, several strategies are utilized to interpret the microstructural white matter information provided from DW-MRI. Many studies use a FA map to place a region of interest (ROI) over a section of white matter (29), or use tract-based spatial statistics (TBSS) to isolate specific regions of change (47). Each of these methods has been able to correlate FA and/or diffusion measures of the CST with sensorimotor function and impairment following stroke (29, 32, 48). Lindenberg et al. found a correlation between fiber number asymmetry (ipsilesional – contralesional/ipsilesional + contralesional) and motor outcome in chronic stroke (32). Cho et al. used DTI

tractography to classify CST integrity after corona radiata infarct (49) and intra-cerebral hemorrhage (50), and found a relationship between tract involvement and functional outcome. ADC of the CST appears to be elevated in the chronic stage of stroke (51, 52), and has been related to functional outcomes (28, 52). AD and RD have been less frequently reported after stroke. Nonetheless, studies in individuals with acute stroke found AD of the CST to be related to motor outcomes (53, 54). One study found increased RD in several regions, including the posterior CC, in acute stroke patients compared to controls; however, increased AD occurred only in the corona radiata (55). These results are consistent with the work by Lindenberg et al., who assessed individuals with chronic stroke in comparison to controls (30). Recent work has shown that ADC, AD, and RD are elevated in the ipsilesional CST and are related to motor outcome in individuals with chronic stroke (41).

Several studies have assessed the relationship between DW-MRI-based diffusion measures of the CC and post-stroke outcome. Recently, Takenobu et al. used a combination of voxel-based statistical tractography and a deterministic ROI-based approach to determine callosal FA in acute ischemic stroke patients (47). A significant positive correlation between FA values within a ROI placed in the callosal midbody and motor impairment was reported. Lindenberg and colleagues employed a probabilistic tractography method, identifying white matter tracts passing through contralesional primary motor cortex, and found that several DTI-based outcomes were related to baseline motor function and improvements in motor function after a 5-day intervention combining non-invasive brain stimulation and motor practice (30). Specifically, transcallosal FA was negatively correlated with baseline motor function, and both AD and RD were positively correlated with change in function between pre- and post-intervention assessments.

Together these findings indicate multiple measures of white matter microstructure of the CST and CC correlate with stroke outcome. It remains to be seen which diffusion measure(s) and method(s) will provide the most reliable indication of CST and CC function. Populations with stroke tend to have heterogeneous characteristics, such as, varied time since stroke onset, wide range of functional and cognitive impairments, and differences in lesion size and location. The contribution of these factors to white matter microstructure have not been comprehensively explored, and should be evaluated in future work to enhance the use of DW-MRI to predict stroke outcome and the response to interventions.

Magnetic Resonance Spectroscopy

Magnetic resonance spectroscopy allows for the non-invasive measurement of metabolites *in vivo*, within a defined region of tissue. ^1H MRS uses resonance signals from hydrogen protons to quantify cerebral metabolites, which have different identifiable resonance signals (or peaks) in a static magnetic field, measured in parts per million (ppm). Thus, the magnitude of the peak resonance at the chemical shift point for each metabolite can be measured and a spectral map computed, providing information on the presence and concentration of metabolites within the target tissue [see Ref. (56) for review] (Figure 1, Section IIC).

The process of acquiring MRS data (shimming, water suppression, and phasing curve fitting) has now been automated and is available in programs, such as linear combination (LC) model (57) or magnetic resonance user interface (MRUI) (58).

The number of metabolites that can be differentiated in the MRS spectrum depends on the field strength of the MRI scanner (59, 60). With a 3T MRI, it is normally possible to obtain reliable peaks for six different metabolites: *N*-acetylaspartate (NAA), myo-inositol (mI), choline, creatine, glutamate, and lactate. Signals from the different peaks overlap making detection of less-abundant metabolites, such as gamma-aminobutyric acid (GABA), difficult without specific optimization of the MRS procedure that involves editing the spectra to obtain the GABA peak at the cost of losing information from other observable peaks (61). The physiological roles of the five identifiable metabolites are still under examination. The physiological role of NAA in the CNS is unclear; however, it is considered a marker of viable neurons. Lowered levels of NAA may indicate neural loss or death (62). mI is a cerebral osmolyte and occurs in astrocytes. It is considered a marker of glial cells and elevated mI is often considered a sign of gliosis or cytotoxic edema (63). mI is elevated in spared neural tissue in chronic stroke (64, 65). Choline represents the sum of four choline-containing compounds in the CNS, all of which are contained in cellular membranes; choline is considered a marker of cell membrane integrity. Elevated choline levels may indicate increased cell membrane turnover or demyelination (62, 66). Creatine also represents the sum of creatine-containing compounds, creatine and phosphocreatine, both of which are cellular energy reserves and are markers of energy metabolism in the brain (62). Creatine and choline levels are commonly believed to be stable across the brain and are often used to normalize levels of other cerebral metabolites; however, this may not be an appropriate approach in neuropathological conditions, such as stroke, as choline and creatine levels may be unstable after cerebral infarct (67). Glutamate represents the sum of glutamate and its precursor glutamine; it is not possible to differentiate these two compounds at 3T field strength (59). Glutamate is the principle excitatory neurotransmitter in the CNS and levels of glutamate may be of particular interest in indexing changes related to *N*-methyl-D-aspartate receptor (NMDAR)-mediated neuroplasticity, or glutamate excitotoxicity post-stroke.

Magnetic resonance spectroscopy has significant potential to act as an index of metabolic changes in surviving neural tissue after stroke (68). Thus, MRS has primarily been useful as a marker of neuronal loss or to indicate altered metabolic processes in penumbral tissue following infarction. NAA levels are reduced in areas of cerebral infarct (69), consistent with neural death, and appear to reduce further from acute to chronic stroke, perhaps indicating neuronal loss by diaschisis (70). Combining lactate peaks with NAA data provides useful predictive information about the viability of peri-infarct tissue in acute stroke (71–73). MRS has been less utilized in evaluating sensorimotor outcomes in chronic stroke, though analyses of spared ipsilesional tissue have provided interesting insights into neural adaptations in motor networks following distal infarct. In individuals with subcortical stroke, there is lower NAA and higher mI in spared ipsilesional primary motor cortex (M1) (65, 74); this is consistent

with neuronal stress or atrophy as result of an infarct to the motor network. Lower NAA and higher mI have also been reported in the ipsilesional supplementary motor area (SMA) and premotor cortex, respectively (64). NAA levels in M1 and non-primary motor areas positively correlate to motor function in several reports (64, 74–76) suggesting motor outcomes after stroke rely in part on the integrity of surviving neural tissue. There have been fewer reports on neurotransmitter levels and functional outcomes after stroke. Cirstea et al. report levels of glutamate in ipsilesional M1 correlate with motor impairment, with higher levels of glutamate relating to better motor function, though glutamate was not significantly reduced in ipsilesional M1 compared to contralesional M1 (65). A recent study from Blicher et al., using optimized MRS protocols for detection of GABA, reveals GABA is reduced in ipsilesional M1 after stroke (77). Further, Blicher et al. report improvements in motor function in response to constraint-induced therapy (CIT) related to individual differences in GABA levels, with higher baseline GABA in ipsilesional M1 relating to greater improvements in motor function after CIT (77). Future studies linking MRS measures to functional outcomes are needed, particularly in relation to glutamate's potential role in motor adaptation after stroke. MRS provides significant potential benefit as a modality to link observations of changes in neural activity post-stroke from fMRI or TMS imaging with changes in metabolic function.

Magnetic resonance spectroscopy could also be a valuable tool to advance our understanding of the neurochemical effects of rTMS, and may be used as a predictive measure to identify responders from non-responders. It is thought that rTMS does not change NAA levels, instead it shifts neuronal metabolism and neurotransmitter levels (78). Studies examining the effects of rTMS on MRS measures have, thus far, largely been conducted on high-frequency rTMS over the dorsolateral prefrontal cortex (DLPFC) in the treatment of depression. These studies have begun to examine individual variability in pre-stimulation metabolite levels and how these relate to treatment response. Participants who responded to high-frequency rTMS over DLPFC for treatment of depression showed lower baseline levels of glutamate prior to rTMS stimulation, and greater increases in cortical glutamate in response to rTMS (79, 80), while non-responders showed a decrease in glutamate levels in response to stimulation (80). Therefore, response to rTMS appears to rely in part on baseline levels of glutamate in target brain regions. These studies were conducted on rTMS for depression, with different stimulation targets and network effects than rTMS for sensorimotor recovery. However, they highlight the potential value of MRS as an index of treatment response to stimulation for stroke patients.

There is scant research to date on MRS response to rTMS over sensorimotor regions as it relates to stroke recovery. To our knowledge, only one such study has been conducted, by Stagg et al., using GABA-optimized MRS in examination of the effects of continuous theta burst stimulation (cTBS) to M1 (81). The authors report cTBS, which has inhibitory effects on cortical circuitry, increases GABA levels without affecting glutamate levels in M1 (81). Individual baselines in GABA levels relate to improvement gains on upper limb motor function (77), and a study in healthy adults demonstrated that individuals with greater reductions in GABA levels after transcranial direct-current stimulation (tDCS)

showed improved motor learning and greater M1 activation in fMRI (82). It remains to be seen whether individuals with differing levels of baseline GABA following stroke show differing responses to rTMS protocols, this is an avenue that should be examined in future research. Not only would future MRS work expand our understanding of the neurobiological actions of rTMS, but it also could allow for improved understanding of baseline neurochemical characteristics that predict response to rTMS protocols, and thus more targeted individualized treatment approaches in stroke rehabilitation.

Functional Imaging

Functional MRI

Functional MRI measures changes in blood movement in the brain over time. This signal is the blood oxygen level dependent (BOLD) signal. The BOLD signal is an indirect measure of neural activity and reflects the amount of deoxyhemoglobin in a tissue. The amount of deoxyhemoglobin depends on the local rate of metabolism of oxygen, the volume of blood in the region, and the amount of blood flow in a region (83). As neural activity increases in a brain region, local oxygen metabolism, blood volume, and blood flow all increase together (83). When MRI measures the BOLD signal, there is a time delay between the neural event and the signal measurement. The “fast response” occurs 2–3 s after an event with the main BOLD signal recorded ~5 s later. In the literature, the BOLD signal is sometimes described as a “hemodynamic response.”

Measurement of BOLD signal can occur as the study participant is performing a task (**Figure 1**, Section IID), or while “resting” – the participant is typically asked to think of nothing in particular but to remain awake (84). After collecting the study data, it can be processed and analyzed in very similar ways. The difference is that some analysis techniques are designed for use with certain experiment types (i.e., for resting state). Resting-state fMRI is defined as the spontaneous low-frequency (<0.1 Hz) BOLD fluctuations with spatio-temporal correlations in networks (85). What the BOLD signal fluctuations mean is not yet clear, but increasing evidence suggests it does have a neural basis (85).

In the past, stroke rehabilitative research using neuroimaging focused on the analysis of local lesion-specific activity and subsequent impairments (86, 87). Limitations in computation and mathematical modeling restricted study to isolated brain regions, though clinically the effects of an isolated stroke can demonstrate large sensorimotor and cognitive effects in remote areas (88). Recent advancements in technological and scientific knowledge have allowed for broader study of brain activity upstream and downstream from the stroke lesion, namely network analysis. Network analysis allows for the study of potential widespread changes in neural activity after a focal lesion. Analyzing patterns of network activity can inform researchers and clinicians of the effect a lesion has on the output of brain activity and may indicate whether certain “compensatory” network patterns are better than others for producing functional motor performance. A recent review of network analysis demonstrated altered activity both adjacent to and distant from a stroke lesion, affecting both hemispheres, and a pattern of change in network activity linked

with motor impairments and recovery (89). Reorganization in the lesioned hemisphere includes interactions between the fronto-parietal regions and the primary motor cortex, which may suggest greater cortical control is needed for motor performance of the paretic upper extremity (89). These studies underline the ability of network analysis to determine connectivity patterns after a stroke, and its potential for determining the effectiveness of current rehabilitative therapies. If network analysis can link certain patterns of early post-stroke activity with better prognosis, it may have a role in informing the direction of future therapies.

Brain network activity after a stroke is commonly studied with task-based fMRI. The challenges with using fMRI in individuals after a stroke, is that the post-stroke motor impairments can make motor performance difficult often resulting in movement synergies (90), mirror movements (91), and head motion during an fMRI scan (92). If during an fMRI study, participants produce head movement beyond a few millimeters, move in synergies or produce mirror movements, the scan may be rendered useless. People who have sustained a severe stroke with resulting severe motor impairments are often not studied with task-based fMRI, as motor performance of even simple tasks are frequently not possible without assistance, though some studies attempt to overcome this limitation by studying passive movements (93, 94). Even those who have sustained a mild or moderate stroke may have difficulty performing common functional tasks, such as individuated finger movements, so researchers are limited to studying basic and simple motor tasks, limiting generalizability to other motor tasks. Imaging the brain during rest allows for the study of individuals with a wide range of post-stroke motor impairments, and permits the examination of network activity without the need for task performance. For these reasons, resting-state imaging is an attractive method for studying stroke network activity.

Resting-State fMRI

Resting-state fMRI can characterize functional deficits after a stroke and provide important predictive evidence that links brain behavior with functional sensorimotor recovery of the upper limb. After a cortical stroke, participants demonstrate increased network activity in the ipsilesional fronto-parietal cortex, bilateral thalamus and cerebellum, while contralesional M1 and occipital cortical activity are decreased compared with healthy controls (95). Furthermore, the functional connectivity of the ipsilesional M1 with the contralesional thalamus, SMA, and middle frontal gyrus during the acute stroke phase positively correlate with motor recovery after 6 months (95), suggesting that changes in upper extremity motor impairment can be predicted by alterations in resting-state activity. Recently, participants with impaired upper extremity function received 12 weeks of training with shoulder and elbow robotic rehabilitation (96). Resting-state fMRI and upper extremity motor impairment was assessed before and after training. Decreased impairment could be predicted from functional connectivity changes measured by resting-state fMRI. Resting-state fMRI can reveal disrupted functional connections within hours of stroke as well as during recovery. Individuals with ischemic stroke were scanned within 24 h, 1 week, and 3 months post-stroke (97). Within hours after

stroke, lower connectivity was found in individuals with motor deficits. Interestingly, connectivity was restored 1 week later in those with recovered hand function. However, residual decreased subcortical connectivity remained 3 months later, even in those individuals without remaining hand motor impairment. These findings indicate that though motor function improves for some individuals after stroke, resting-state fMRI may remain altered. Resting-state fMRI also allows for the analysis of multiple networks simultaneously. Recent work has proposed that disrupted whole brain connectivity in both the sensorimotor and dorsal attention network is closely linked with functional impairment more than the intra-hemispheric connectivity (98).

Task-Based fMRI

Task-based fMRI can inform the capacity of individuals to recover after stroke, specifically with regard to motor function and learning. fMRI studies have found that paretic hand movement early after stroke is linked to widespread bilateral activity within the motor system, with greater bilateral activity found in individuals with greater motor impairment (99). Research directed at understanding the function of this bilateral pattern of activity suggests that the surviving brain regions influence distant regions during movement (99). It is now known that brain regions that survive the initial stroke influence one another during movement, and that multiple brain regions and pathways participate in reorganization and functional recovery, such as the CST, brainstem pathways, interhemispheric connections (100). The contralesional hemisphere also provides support for paretic hand movements (100). Task-specific practice in individuals with chronic stroke facilitated motor learning and reduced the volume of contralesional cortical activity while using the paretic arm (101). Performing the learned task altered cortical activation by producing a more normalized contralateral pattern of brain activation, which suggests task-specific motor learning may be an important stimulant for neuroplastic change and can remediate maladaptive patterns of brain activity after stroke. Our group has found motor learning and overall improvements in motor control are associated with increased response in the prefrontal-based attentional network in individuals with chronic stroke (14). Additionally, evidence of plasticity is also noted for movement of the non-paretic arm; this activity is related to alterations in neural activation in areas anatomically and functionally connected to the lesion, implying an extensive bilateral network is involved (102).

Electroencephalography

Electroencephalography uses surface electrodes placed on the scalp to detect fluctuating electrical voltages, which result from the small electrical currents generated by active neurons (103). EEG recordings are mainly generated by pyramidal neurons in cortical layers III, V, and VI, with summation of cortical activity producing a voltage field that can be recorded on the scalp (103). EEG is used for diagnosis, prognosis, treatment monitoring, and clinical management in acute ischemic stroke (104). Additionally, in chronic stroke, the EEG signal can identify subtle changes in the brain that cannot be detected by clinical measures; further, quantification of the EEG signal before and after rehabilitation

interventions can assess neuroplasticity both locally surrounding the lesion and within whole brain networks (105).

For EEG, resting-state activity can provide valuable predictive information regarding network activity after a stroke, but has limitations with regard to spatially localizing the sources, or regions of interest, within the network. Stroke can affect the synchrony of electrical oscillations in neural networks and these changes in network coherence can be associated with neurological deficits. In individuals with sub-acute stroke, functional connectivity of resting-state EEG correlated with motor performance. Individuals with stroke presented with disrupted alpha band connectivity where the spatial distribution of alpha activity reflected the pattern of motor and cognitive deficits of the individual participant (106). Even 1 month after stroke, measures of delta and alpha power were correlated with stroke severity scores (107). Focal brain lesions affect functional brain networks. In individuals 3 months after ischemic stroke, the synchrony of alpha band oscillations decreased between affected brain regions with the rest of the brain and this decrease was related to cognitive and motor deficits (108). Resting-state EEG can measure the synchronization of neuronal firing, and this can occur in the form of phase coupling or amplitude correlation. Behavioral performance after a stroke can be predicted by two distinct resting-state EEG coupling patterns: (1) amplitude of beta activity between homologous regions and (2) the lagged phase synchronization in EEG alpha activity from one brain region to rest of the cortex (109). A disruption of these coupling patterns is found to be associated with neurological deficits in individuals with stroke (109). Robot-aided rehabilitation programs are a relatively new and promising therapy, promoting brain plasticity and supporting improvements in upper extremity motor control. In a pilot study of seven individuals with stroke, 12 weeks of robotic rehabilitation decreased upper limb impairment and changed brain connectivity as indicated by altered coherence in the high beta band (24–33 Hz) (110). These studies demonstrate the ability of EEG to provide information about the patterns of impairment and recovery after stroke.

Transcranial Magnetic Stimulation

Transcranial magnetic stimulation is a useful way to non-invasively measure and modulate cortical excitability. TMS activates neurons in the cortex under the coil, which at high enough intensities transsynaptically depolarizes corticospinal output neurons. The corticospinal volleys activated by TMS reach the target muscle and can be recorded by surface electromyography (EMG) (111). Multiple single and paired-pulse techniques can be used to index neuroplasticity, providing useful information about how stroke and subsequent interventions modify brain function (see **Figure 2** for overview).

Single Pulse

Motor Thresholds In order to account for individual responses to TMS across individuals, a standardized motor threshold value is determined. Resting motor threshold is most commonly defined as the lowest percent of stimulator output that is required to produce a motor-evoked potential (MEP) with a peak-to-peak amplitude of 50 μ V on five out of 10 trials while the individual is at rest (112). Similarly, active motor threshold is defined as the

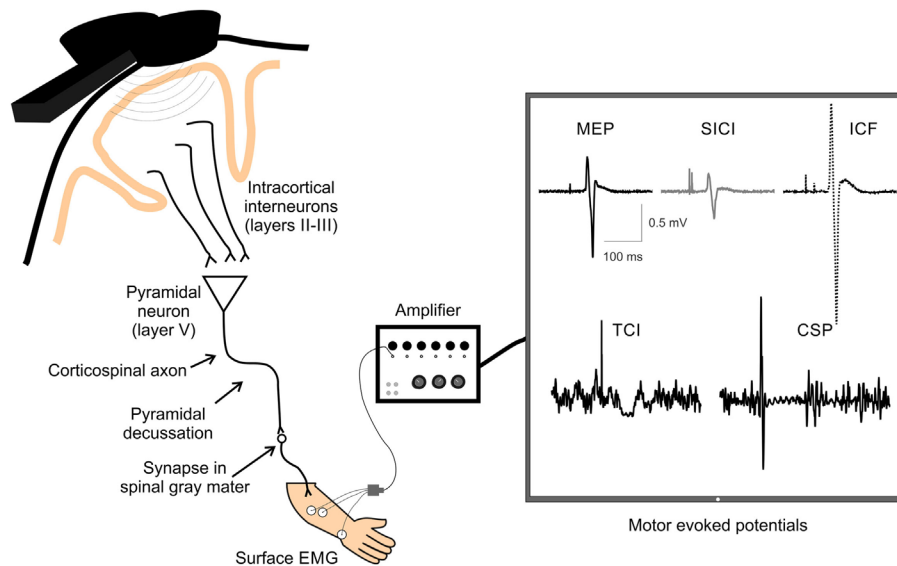


FIGURE 2 | A schematic of TMS-evoked measures of single and paired-pulse corticospinal excitability. Examples of TMS-evoked measures of corticospinal excitability recorded by surface electrodes over the extensor carpi radialis (ECR) muscle. Displayed are examples of motor-evoked potential (MEP), short-interval intracortical inhibition (SICI), intracortical facilitation (ICF), transcallosal inhibition (TCI), and cortical silent period (CSP). TMS, transcranial magnetic stimulation; EMG, electromyography.

lowest percent of stimulator output that is required to produce an MEP with a peak-to-peak amplitude of 200 μ V on five out of 10 trials while the individual maintains a light background contraction (113). Threshold values are often used to determine the stimulation intensity to use in the assessment and modulation of cortical excitability with TMS techniques.

MEP Input–Output Curves Motor-evoked potential input–output (IO) curves utilize single-pulse TMS over a range of intensities to measure the increase in excitability within the corticospinal system in response to increased stimulus intensity, as indexed by MEP amplitude (114, 115). The linear slope of the curve (115) or area under the curve (116) produced by increasing stimulator intensity is quantified as a representation of the ability of the excitability of the M1 representation to be up-regulated, and the strength of the corticospinal connections. MEP IO curves can be measured while the participant is at rest, or during a sustained contraction. Resting MEP IO curves activate lower threshold neurons, while active MEP IO curves utilize the voluntary contraction to activate higher threshold neurons, thus stimulating unique neuronal pools, which may have different functional significance (117).

M1 Cortical Mapping Single-pulse TMS can also be utilized to probe the excitability of M1 in terms of quantifying the distribution and amplitudes of MEPs in the target muscle(s). TMS mapping of M1 follows the principles of motor homunculus (118) where stimulation of different motor regions produces systematic responses in the corresponding peripheral musculature. The amplitudes and distribution of MEPs when different scalp sites are systematically stimulated can be analyzed and displayed as

topographical maps showing the greatest activity produced from a corresponding scalp location over M1. Mapping the M1 representation of particular muscles is used to understand the healthy and pathological cortex, as well as to map change in neuronal representation of muscle groups over time or following an intervention (119–129).

Silent Period When single-pulse TMS is applied while holding a slight contraction in the contralateral limb, a cortical silent period (CSP) is produced, which presents a prolonged reduction in EMG activity following the MEP (130–132). The CSP originates largely from activation of inhibitory cortical and spinal interneurons, and there is evidence that the latter half of the CSP is associated with GABA_B-like activity at the cortical level (133). Therefore, single-pulse TMS can be indicative not only of motor cortical excitability, or increases in corticospinal tract excitability in response to increasing stimulator output, but also inhibitory circuit activity within the corticospinal system.

Transcallosal inhibition (TCI), important in interhemispheric communication, can be quantified via an ipsilateral silent period (iSP) derived from single-pulse TMS (134, 135). Specifically, during a sustained unilateral muscle contraction, a single TMS pulse over the ipsilateral M1 is delivered to evoke a reduction in the background EMG activity in the ipsilateral muscle, known as the iSP. Since the iSP is diminished or absent in patients with lesions of the corpus callosum (135, 136), it is likely a result of inhibition via transcallosal projections.

Paired Pulse

Intracortical Inhibition and Facilitation The excitation of M1 pyramidal neurons that ultimately translates into corticospinal

output to target muscles is also influenced by intracortical circuitry within the motor cortex. Inhibitory intracortical circuitry within M1 influences corticospinal output, and can be quantified using TMS. Specifically, short-interval intracortical inhibition (SICI) and long-interval intracortical inhibition (LICI), quantify inhibitory circuitry. SICI is produced when two TMS pulses (a subthreshold conditioning stimulus followed by a suprathreshold test stimulus) are administered over M1 with an interstimulus interval (ISI) of 1–6 ms and results in a decreased MEP amplitude than that elicited by a single TMS pulse alone (137). Intracortical facilitation (ICF), from 10 to 15 ms after the stimulation, measures the facilitatory circuits in M1. The protocol for measuring ICF is identical to that with SICI (subthreshold conditioning stimulus and suprathreshold test stimulus), with only the ISI differing. At longer ISIs of 50–200 ms, there is again a period where inhibition is produced due to paired-pulse TMS called LICI (138, 139). Unlike SICI, LICI is evoked with two identical suprathreshold pulses. SICI is likely mediated by GABA-A (140) and LICI by GABA-B (133, 141–143) receptor-mediated circuitry, due to the differences in the time course of activation of the respective circuitry (**Figure 1**, Section IIF). ICF appears to be mediated by different neural circuitry than SICI (144), and glutamate may play a role in mediating ICF (145). Assessing these inhibitory and facilitatory circuits is an important component of understanding how neuroplastic change may be mediated and underlies associated behavioral changes, functional improvement, and assessment of neurological injury (i.e., stroke).

Short-Afferent Inhibition and Long-Afferent Inhibition Measures of short (SAI) and long-afferent inhibition (LAI) use single-pulse TMS in conjunction with peripheral nerve stimulation to examine the integration of sensory information into the motor output system. Specifically, an electrical stimulation is delivered at the contralateral median nerve prior to a TMS pulse delivered over M1 while the participant is at rest, which results in a reduced MEP relative to a single pulse alone. SAI applies this technique with an ISI of 20 ms and LAI utilizes an ISI of 200 ms (130, 146–150). SAI provides only enough time for activation of the primary somatosensory cortex and secondary somatosensory cortex, whereas LAI is long enough to ensure activation of primary somatosensory cortex, bilateral secondary somatosensory cortex, and contralateral posterior parietal cortex (130). While the mechanisms underlying both SAI and LAI have not been described, they provide information on the impact of peripheral nerve stimulation on M1 excitability, which is an important component to consider when studying sensorimotor integration in regards to neuroplasticity and neurological injury.

TMS Assessment of Cortical Excitability and Connectivity in Stroke Several methods of TMS assessment have shown that there is altered brain excitability and connectivity during all phases post-stroke (acute, sub-acute, and chronic). In approximately the first week after stroke, the ability to elicit MEPs in the paretic limb after single-pulse stimulation over the ipsilesional hemisphere predicts good recovery (151–156). A lack of elicited MEPs in the paretic limb along with increased MEP amplitudes in the non-paretic limb after contralesional stimulation predicts

poor motor recovery (31, 157), although this is not always the case (151, 158, 159). The appearance of MEPs where there were none before and improvement of TMS measures of corticospinal integrity during the first few months of recovery (160–162), both correlate with better functional outcome. An imbalance of motor cortex excitability (decrease lesioned cortex excitability and overly increased excitability of contralesional cortex) occurs following severe stroke and a restoration of balance is associated with functional recovery (151, 157, 162, 163). Several studies utilizing motor cortical mapping have shown that there are a decreased number of excitable scalp sites over the ipsilesional compared to contralesional cortex (160, 164–168), which has been suggested to indicate a hemispheric imbalance between the cortices that accompanies motor impairment of the more affected limb.

After stroke, measures of intracortical inhibition and excitation within the ipsilesional hemisphere are altered. There is increased inhibition as measured by a prolonged CSP after subcortical stroke (169). Conversely, SICI and LICI are suppressed (158, 170, 171), and ICF remains within normal ranges (172–174). Recent reports have shown that SAI is reduced in the acute phase of stroke, where increased suppression of SAI has been correlated with better motor function 6 months after stroke (175). In the contralesional hemisphere, motor thresholds and MEP amplitudes remain generally normal (151, 162, 173, 176–181), but SICI is suppressed in some (158, 172, 173, 177).

The connectivity between hemispheres is also altered following stroke, showing asymmetric transcallosal interactions. Several studies show that ipsilesional M1 generates less TCI than usual (177, 182), and contralesional M1 continues to demonstrate normal, or even increased, levels of interhemispheric inhibition (IHI) (183, 184). The net result is increased inhibition acting on ipsilesional M1 (183) that can depress ipsilesional M1 excitability. These changes may interfere with neuroplasticity in ipsilesional cortex (4, 185, 186), as increased IHI from contralesional M1 onto ipsilesional M1 reduces excitability in neurons that survived the stroke (177, 187) and is associated with more severe functional deficits (183, 184). Additionally, work from our group with chronic stroke participants has found increased TCI from the ipsilesional to contralesional M1 while maintaining a contraction, suggesting greater inhibitory signals sent from the ipsilesional to contralesional M1 (188). Further, we have recently shown that contralesional TCI was negatively correlated with hemiparetic arm function and impairment, demonstrating decreased inhibition from the contralesional to ipsilesional hemisphere is associated with greater impairment (189). Therefore, bilateral alterations in cortical excitability and circuitry are associated with the degree of motor impairment and post-stroke recovery.

Modulation of Cortical Excitability with Repetitive TMS

Repetitive TMS can be applied in specific patterns to uniquely modulate cortical excitability; the effects of rTMS may last for periods of time exceeding that of stimulus application, from minutes to an hour beyond stimulation (190–192). Therefore, rTMS can be used to index neuroplasticity or enhance cortical excitability before a behavioral intervention, such as skilled motor practice (193, 194).

Repetitive TMS, when applied in specific patterns, can excite or inhibit a local cortical region for a short duration. rTMS can be applied at low frequencies of under 1 Hz that suppresses excitability in the targeted area, or at high frequencies over 1 Hz, which transiently excites the targeted area for ~15 min (195). Similarly, theta burst stimulation (TBS) uses a 5-Hz stimulation pattern, with triplets of 20 Hz stimulation, to inhibit or facilitate cortical excitability if the TBS is applied continuously (inhibitory cTBS), or intermittently (facilitatory iTBS), respectively (190). The effects of cTBS and iTBS can last up to 60 min post-stimulation (190, 191). Importantly, the specific effects of cTBS and iTBS show substantial inter-individual variability, which likely depends upon which interneuron populations are activated by the TMS pulse (196). rTMS protocols, like TBS, have been shown to modulate cortical excitability, and at times behavior, when applied over motor-related areas, such as M1 (190), contralateral M1 (197, 198), the SMA (199), the dorsal premotor cortex (PMd) (200), the primary somatosensory cortex (S1) (194), area 5 (201), as well as non-motor areas, such as the cerebellum (202) and the DLPFC (203). Not only does rTMS modulate cortical activity directly below the magnetic coil, but activity in remote cortical and subcortical regions can be modified by application of rTMS over a single cortical target (204). Specifically, changes in MRI activity can be detected in M1/S1, SMA, PMd, cingulate motor area, the putamen, and thalamus after rTMS over left hemisphere M1 or S1 (204). These methods for modulating cortical excitability are thought to mimic early stages of long-term potentiation (LTP) or long-term depression (LTD)-like mechanisms, and are proposed to be dependent upon NMDA receptors (205). Due to the ability to modulate cortical excitability in motor and non-motor-related cortical areas beyond the time of stimulation itself (206), rTMS has been utilized by researchers to develop protocols to test whether the application of stimulation alone, or in conjunction with other behavior and therapy can further rehabilitation from neurological impairment, such as stroke.

Repetitive Brain Stimulation as an Intervention After Stroke

Since rTMS is known to modulate cortical excitability in local and remote regions to the areas stimulated, it has been suggested to be a viable therapeutic approach to aid in the recovery of motor function after stroke (207), yet there is accumulating evidence that the response to rTMS is inconsistent and variable (34, 193, 194). When targeting stimulation over M1, rTMS has been delivered in isolation (34, 208–210) and in combination with rehabilitation training (193, 194, 211, 212) in individuals with stroke. Since the effects of rTMS can outlast the period of stimulation itself (190, 206), the prevailing thought is that the aftereffects may be capitalized on by pairing it with skilled motor practice and/or rehabilitation training to promote neuroplastic change (193, 194, 213).

Theoretically, rTMS can be used to increase cortical excitability in the ipsilesional cortex by directly applying excitatory rTMS over the ipsilesional hemisphere (Figure 3) or by applying inhibitory rTMS over the contralesional to potentially decrease abnormally increased inhibition to the lesioned M1 (Figure 4). This manipulation of cortical excitability is supported by observations of imbalanced IHI after stroke (214). Impaired motor

performance following stroke is often attributed to a disruption in IHI where an overactive contralesional area suppresses the activity of the lesioned hemisphere.

Repetitive Brain Stimulation as an Intervention After Stroke: Ipsilesional Stimulation

Studies have shown promising preliminary findings using high-frequency excitatory (>1 Hz) rTMS applied over the ipsilesional hemisphere. One study showed that 3-Hz rTMS over the ipsilesional hemisphere for 10 days combined with passive limb manipulation, which gradually increased to active manipulation of the paretic limb, resulted in improvements in function and recovery of MEPs in certain individuals, with no relationships between improvements in function and MEP increases (215). Another study demonstrated increases in MEPs and improvements in a sequential finger motor task when 10-Hz rTMS was applied over the ipsilesional M1, and that cortical excitability was associated with improvements in motor learning (216). Similarly, improvements in motor skill learning have been shown when 5-Hz rTMS is applied over ipsilesional S1 (193) and this improvement is dependent on the white matter volume in the somatosensory cortex in the lesioned hemisphere (24). Although variable depending on stroke location, individuals with subcortical stroke only showed improved movement kinematics after 10-Hz rTMS over ipsilesional M1, whereas hand dexterity actually deteriorated in the majority of those with cortical stroke (217). This study also found that rTMS reduced activation of contralesional cortex for those with subcortical stroke, and caused bilateral activation of primary motor and sensory areas in those with cortical stroke (217). The authors concluded that it is likely that the extent and location of stroke may determine the beneficial response to ipsilesional excitatory rTMS. Studies have also reported little effects of applying excitatory rTMS over the ipsilesional cortex. Talelli and colleagues used iTBS over ipsilesional M1 followed by intensive physiotherapy of the paretic upper limb for 10 days that did not show any significant improvements (212). Another study combined 20-Hz rTMS over ipsilesional M1 with CIMT in chronic stroke for 2 weeks, finding that no additional improvements beyond that of CIMT alone were observed except slightly lower motor thresholds (218). However, it could be that the pairing of excitatory rTMS over the index finger muscle representation in M1 followed by reaching, grasping and other gross arm movements contributed the lack of positive effects in the above two studies. A recent study suggested that 10-Hz rTMS applied over ipsilesional M1 delivered 5 days per week for 2 weeks enhanced motor function of the paretic limb only in those with subcortical stroke and those who presented with MEPs immediately after the intervention and at a 2-week follow-up (219).

Repetitive Brain Stimulation as an Intervention After Stroke: Contralesional Stimulation

An alternative to directly enhance ipsilesional M1 excitability by applying excitatory rTMS over the lesioned hemisphere is to deliver inhibitory rTMS over contralesional M1. This approach potentially releases contralesional IHI and indirectly enhances ipsilesional M1 excitability. Some studies

Ipsilesional excitatory rTMS

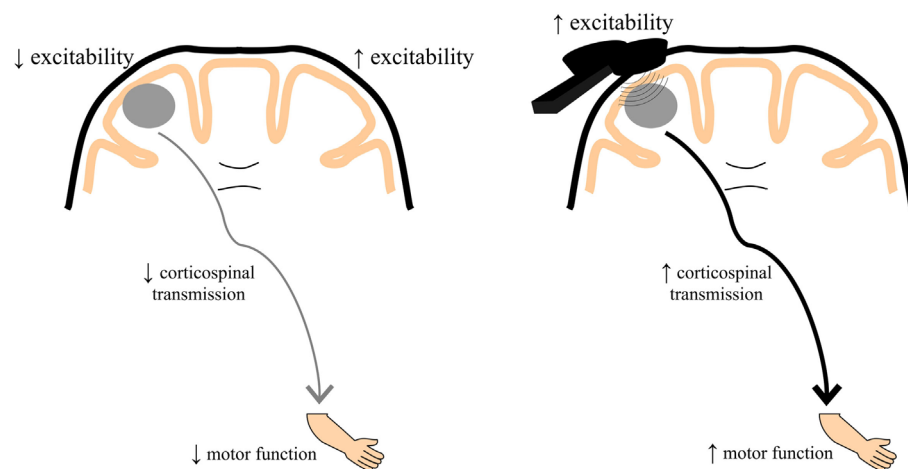


FIGURE 3 | A schematic of the theoretical effects of excitatory rTMS over the ipsilesional cortex. Decreased ipsilesional cortical excitability may contribute to decreased corticospinal transmission resulting in diminished motor function of the paretic upper limb. Ipsilesional excitatory rTMS may increase the excitability of the damaged cortex, thereby contributing to enhanced corticospinal transmission potentially leading to better motor function of the paretic upper limb. rTMS, repetitive transcranial magnetic stimulation.

Contralesional inhibitory rTMS

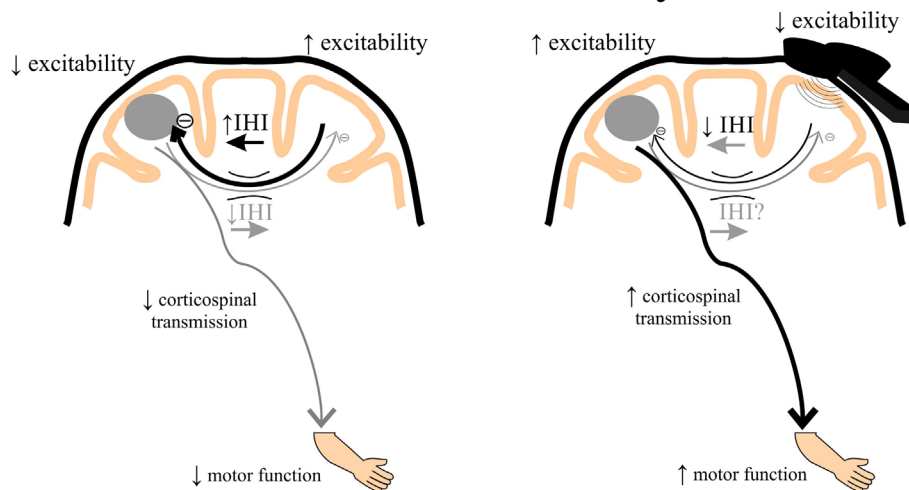


FIGURE 4 | A schematic of the theoretical effects of inhibitory rTMS over the contralesional cortex. Increased interhemispheric inhibition (IHI) from the contralesional to ipsilesional cortex via the corpus callosum may contribute to decreased ipsilesional corticospinal excitability and diminished motor function of the paretic upper limb. Contralesional inhibitory rTMS may suppress contralesional to ipsilesional IHI and assist in improving ipsilesional corticospinal transmission, potentially leading to better motor function of the paretic upper limb. rTMS, repetitive transcranial magnetic stimulation.

demonstrate that low-frequency inhibitory (<1 Hz) rTMS or cTBS applied over the contralesional hemisphere improves hand function (209, 210), reach-to-grasp movements (220), motor learning (194), and brief improvements in hand dexterity, which was associated with a reduction in TCI to the ipsilesional M1 (221).

Other studies have investigated functional brain activation changes following rTMS in stroke. One study showed a significant increase in the peri-infarct fMRI-related activity in the ipsilesional M1 after 6-Hz low-frequency rTMS over the contralesional M1 (208). Another study demonstrated improved motor performance of the paretic hand following 1-Hz rTMS

over the contralesional M1 that was associated with a decrease in over-activation of contralesional M1 activation during paretic hand movements (222). Additionally, connectivity between SMA and M1 within the ipsilesional hemisphere was enhanced after inhibitory rTMS over contralesional M1 (222). Recently, it was shown that 10 sessions of 1-Hz rTMS over contralesional M1 showed a change in contralesional plasticity (35), and that mild improvements in motor ability was associated with more normal transcallosal white matter. These data suggest that the condition of callosal white matter may influence the impact of contralesional rTMS on recovery of motor function after stroke (35).

Variability in Response and Application of rTMS in Stroke

Overall, the reported effects of rTMS in individuals with stroke are moderate (223) but inconsistent (24, 34, 193, 194, 224). Varied effects are noted regardless of what type of rTMS is employed (34, 193, 194) and irrespective of the targeted brain region (34, 193, 194, 216, 225). Further, research to date has suggested that varied responses to rTMS are not explained by simple demographic factors, such as age, sex, or stroke severity (24, 34). There are several potential reasons for this variability, such as stroke location and extent (217, 226), post-stroke duration (219, 225), presence of MEPs (31, 219, 227), hemispheric dominance pre-stroke (228), callosal (33, 189, 229) and corticospinal structural integrity (24, 34, 189), cortical target location for rTMS (193, 219, 224), brain-derived neurotrophic factor genotype (230), different interneuron populations activated by TMS (196), and combination with a well-controlled motor learning task or individualized physical therapy. Despite its broad use, a comprehensive understanding of the physiologic effects of rTMS on the brain is lacking. Further, there is no consensus on which brain region to stimulate, whether it is somatosensory (193) or motor execution (194, 216) or preparation (231) areas, and if stimulation should be applied over the ipsilesional or contralesional hemisphere (194).

Although rTMS demonstrates great potential to enhance post-stroke recovery future work is needed to address the issue of response variability. With a greater understanding of the factors driving response variability, we will be better able to target rehabilitation to the individual.

MULTIMODAL ASSESSMENTS

Multimodal Neuroimaging: Combined TMS, MRI, and EEG Assessment After Stroke

Few studies have utilized multiple methods of neuroimaging in order to predict motor function and impairment due to stroke (188, 189, 229, 232, 233). Studies have shown that those with decreased MEP amplitudes also have a weaker paretic hand, with greater activation in the ipsilesional M1 as recorded by task-based fMRI (234). A study using TMS to assess corticospinal integrity via single-pulse assessment of MEPs and fMRI during isometric hand gripping determined that in patients with less corticospinal excitability, there was an associated increase in activation of contralesional premotor and cerebellar areas (232). The suggestion from these combined methods is that other

non-primary motor cortical areas may be playing a functionally relevant role in controlling force production in more severely affected individuals with stroke. A combined paired-pulse dual coil TMS and fMRI study showed that both TMS and fMRI neurophysiological function in the contralesional PMd was associated with the degree of impairment (233). Specifically, a lack of inhibition from contralesional PMd to ipsilesional M1 measured by paired-pulse TMS and greater activation of PMd during hand-grip was correlated with the level of clinical impairment. The authors suggested that contralesional PMd may support recovery in ipsilesional M1 (233).

Stinear and colleagues have demonstrated through DTI and TMS that weak or absent MEPs evoked ipsilesionally and greater asymmetry in FA of the posterior limb of the internal capsule are predictive of poor motor recovery (227). Recent work from our lab has demonstrated the utility of combined TMS and MRI measures to predict motor function (188). Specifically, bilateral hand dexterity was found to correlate with resting motor threshold and precentral gyral thickness. Those with higher resting motor thresholds and decreased precentral gyral thickness presented with decreased bilateral hand dexterity. Furthermore, increased levels of TCI were associated with greater midcallosal white matter volume (188). In another study, we demonstrated that altered microstructure of transcallosal fiber tracts in anterior sub-regions were associated with TCI and upper extremity impairment in chronic stroke (189). Specifically, anterior transcallosal tract FA and TCI from the non-lesioned to lesioned M1 predicted a unique amount of variance in upper limb impairment. Those with less FA in anterior sub-regions of the corpus callosum and less TCI were those presenting with greater upper limb impairment (189). Another recent study combined fMRI, DTI, and TMS in the assessment of hemispheric balance between ipsilesional and contralesional cortices (229). Task-based fMRI lateralization to the ipsilesional hemisphere was associated with better TCI and stronger ipsilesional motor-related area output via DWI tractography. These studies demonstrate the usefulness of combining multiple methods of neuroimaging along with measures of TMS in order to more comprehensively assess and predict motor function and impairment. Utilizing multimodal neuroimaging can be used in future investigations to aid in identifying optimal biomarkers of stroke recovery and to predict response to rehabilitation in order to maximize treatment outcomes.

A novel multimodal neuroimaging approach combines TMS with EEG. TMS and EEG may be used in combination in real-time in order to directly characterize local and distributed cortical activity, providing a rich source of temporally specific data to determine causal mechanisms of cortical responses to TMS in humans *in vivo* (235–238). Another advantage of this approach is the ability to stimulate any cortical regions and record the evoked activity using EEG, subverting the need to record peripheral responses via surface EMG, which can prove difficult in the ipsilesional hemisphere. Although this has not been utilized in stroke, the combined technique of TMS-EEG may provide new insights into cortico-cortical connectivity in sensorimotor recovery after stroke due to spontaneous recovery and with interventions (behavioral, stimulation, pharmacological, etc.) not able to be captured before.

Multimodal Neuroimaging: TMS and MRI Assessment of rTMS-Based Interventions After Stroke

Very few studies have utilized multimodal neuroimaging with TMS to identify the underlying neurobiology of sensorimotor recovery from stroke (31, 188, 189, 227, 229, 233), and research is scarce in the investigation of an intervention using multimodal imaging with rTMS (24, 35). These studies have demonstrated the usefulness of combining imaging of cortical and subcortical structures with neurophysiological data acquired from TMS in order to better predict aspects of upper limb motor recovery and the potential response to rTMS (24, 34, 35). Carey et al. demonstrated that those with greater structural integrity of the posterior limb internal capsule of the ipsilesional hemisphere demonstrate greater response to contralesional rTMS and the behavioral improvements associated with rTMS (34). Transcallosal FA was shown to correlate with the degree of behavioral improvements due to contralesional rTMS, indicating the DTI-derived measures may aid in individually tailored interventions when considering using contralesional rTMS to potentially induce transcallosal neuroplasticity (35). Recently, we have shown that increased ipsilesional S1 white matter volume was associated with the degree of skill learning improvement when 5-Hz rTMS was applied over S1 before motor skill practice (24). These studies suggest that data acquired from structural and functional imaging may be used to categorize those who respond to rTMS in order to personalize application in a rehabilitation setting.

THE FUTURE OF MULTIMODAL NEUROIMAGING FOR PERSONALIZED THERAPY

Recently, there have been several models proposed to categorize individuals for personalized treatment based on multi-neuroimaging methods (227, 239). The “predicting recovery potential (PREP) algorithm” has been introduced and suggested that patients who present with an ipsilesional MEP have the best prognosis for recovery, and intensive unilateral therapy of the paretic limb is recommended. However, those who do not present with an ipsilesional MEP are divided into two categories: (1) low asymmetry in FA of the corticospinal tract (greater integrity of the ipsilesional corticospinal tract), with a prognosis of limited functional improvement and (2) high asymmetry in FA of the corticospinal tract (less integrity of the ipsilesional corticospinal tract) with the poorest prognosis for functional improvement. Those with low corticospinal tract asymmetry are recommended to receive “primed” ipsilesional brain stimulation and augmented training of the paretic upper limb. However, if there is an absence of an MEP after stimulating the ipsilesional M1 with a relatively high hemispheric asymmetry of FA, the recommendation of therapeutic intervention is modified to include stimulation of the contralesional M1 along with augmented bilateral therapy to engage the contralesional and ipsilesional cortices (31, 227). Di Pino and colleagues (239) similarly have suggested a bimodal balance-recovery model that

proposes a personalized application of rTMS (or other types of non-invasive brain stimulation) depending on structural reserve of the central nervous system, along with clinical and neurophysiological data from multiple imaging sources. This bimodal balance-recovery model attempts to account for the possibility of interhemispheric competition and the fact that the contralesional hemisphere may serve to support recovery of function after stroke (239).

These studies suggest that a combination of neuroimaging methods will likely benefit in the assessment of stroke-related damage and personalized treatment strategies, particularly when using rTMS (or other types of non-invasive brain stimulation) for individuals following stroke. However, there will always be a risk of mislabeling participants, resulting in a substandard care. For this reason, we must continue to utilize new technologies to broaden our understanding of stroke recovery, improving both diagnostic abilities and interventions. For instance, in an individual who does not present with an ipsilesional MEP perhaps simultaneous TMS-EEG could be used to test if cortical activity is evoked by ipsilesional TMS, making it possible to narrow down the site of impairment. This could be very useful information, giving a more accurate prognosis and identifying the ideal pathway to target for recovery. As advancements in neuroimaging continue to impact research in stroke recovery, personalized therapy will become more reliable and utilized, and new interventions will become possible.

TABLE 1 | Cost/availability are ranked relative to the other imaging methods.

Method	Benefits	Limitations	Cost/availability
Volumetric analysis	Quantification of brain volumes from basic (T1) structural scans	Limited accuracy in individuals with lesions	\$\$/+++
DW-MRI	Assesses microstructural characteristics of white matter	Tractography results are variable across methods and sensitive to movement	\$\$\$/+
MRS	Quantification of neurotransmitter levels in defined area	Requires technical expertise and expensive coil for acquisition	\$\$\$/+
fMRI	Identifies patterns of brain activation at high spatial resolution	Poor temporal resolution and is limited to participants who can complete task	\$\$\$/+
Resting-state fMRI	Not dependent on task completion	Sensitive to movement	\$\$\$/+
TMS	Assessment and modulation of cortical excitability and plasticity	Requires specialized equipment and trained personnel	\$\$/+
EEG	Provides information on functional integrity of cortex and has high temporal resolution	Poor spatial resolution and is limited to cortical activity	\$/+++

Increasing price is associated with more \$ signs, and greater availability is indicated by more + signs.

DW-MRI, diffusion-weighted MRI; MRS, magnetic resonance spectroscopy; fMRI, functional MRI; EEG, electroencephalography; TMS, transcranial magnetic stimulation.

CONCLUSION

The information provided above strongly suggests the potential for multimodal imaging in future neuroplasticity and rehabilitation studies after stroke. Structural and functional imaging and physiological assessments have all provided important insights into both the pathology of stroke and mechanisms underlying neurological recovery. **Table 1** lists the major benefits/limitations of each imaging method covered in this review. Additionally, we have also highlighted the potential of non-invasive brain stimulation as an important therapeutic approach. Although many studies have found rTMS improves recovery an increasing number are failing to find benefit. Numerous technical factors affect rTMS interventions, including the site targeted, type of stimulation, and number of stimulation sessions. However, the variability in response to rTMS also highlights the importance of understanding individual

differences in response, which likely depend on a variety of biological factors, such as, age, time after stroke, lesion size, and location, which in turn impact patterns of functional and structural connectivity. Advances in neuroimaging are improving the ability to predict the patterns of structural and functional connectivity best suited to specific interventions. In the near future, novel-individualized interventions will be able to optimize recovery after stroke.

ACKNOWLEDGMENTS

LB is a Canada Research Chair and receives support from the Michael Smith Foundation for Health Research (MSFHR; CI-SCH-01796). AA receives support from the Canadian Institutes of Health Research (CIHR; MFE199421) and MSFHR (5515). JF receives support from MSFHR. CIHR provided support to JF and SP.

REFERENCES

1. The GUSTO Investigators. An international randomized trial comparing four thrombolytic strategies for acute myocardial infarction. *N Engl J Med* (1993) **329**:673–82. doi:10.1056/NEJM199309023291001
2. Edwards JD, Koehoorn M, Boyd LA, Levy AR. Is health-related quality of life improving after stroke? A comparison of health utilities indices among Canadians with stroke between 1996 and 2005. *Stroke* (2010) **41**:996–1000. doi:10.1161/STROKEAHA.109.576678
3. Boyd LA, Winstein CJ. Impact of explicit information on implicit motor-sequence learning following middle cerebral artery stroke. *Phys Ther* (2003) **83**(11):976–89.
4. Taub E, Miller NE, Novack TA, Cook EW, Fleming WC, Nepomuceno CS, et al. Technique to improve chronic motor deficit after stroke. *Arch Phys Med Rehabil* (1993) **74**:347–54.
5. Boyd LA, Winstein CJ. Providing explicit information disrupts implicit motor learning after basal ganglia stroke. *Learn Mem* (2004) **11**:388–96. doi:10.1101/lm.80104
6. Boyd LA, Winstein CJ. Cerebellar stroke impairs temporal but not spatial accuracy during implicit motor learning. *Neurorehabil Neural Repair* (2004) **18**:134–43. doi:10.1177/0888439004269072
7. Boyd LA, Quaney BM, Pohl PS, Winstein CJ. Learning implicitly: effects of task and severity after stroke. *Neurorehabil Neural Repair* (2006) **21**:444–54. doi:10.1177/1545968307300438
8. Boyd LA, Edwards JD, Siengsukon CS, Vidoni ED, Wessel BD, Linsdell MA. Motor sequence chunking is impaired by basal ganglia stroke. *Neurobiol Learn Mem* (2009) **92**:35–44. doi:10.1016/j.nlm.2009.02.009
9. Vidoni ED, Boyd LA. Preserved motor learning after stroke is related to the degree of proprioceptive deficit. *Behav Brain Funct* (2009) **5**:36. doi:10.1186/1744-9081-5-36
10. Pohl PS, Winstein CJ. Practice effects on the less-affected upper extremity after stroke. *Arch Phys Med Rehabil* (1999) **80**:668–75. doi:10.1016/S0003-9993(99)90170-3
11. Winstein CJ, Merians AS, Sullivan KJ. Motor learning after unilateral brain damage. *Neuropsychologia* (1999) **37**:975–87. doi:10.1016/S0028-3932(98)00145-6
12. Velicki MR, Winstein CJ, Pohl PS. Impaired direction and extent specification of aimed arm movements in humans with stroke-related brain damage. *Exp Brain Res* (2000) **130**:362–74. doi:10.1007/s002219900262
13. Boyd LA, Vidoni ED, Daly JJ. Answering the call: the influence of neuroimaging and electrophysiological evidence on rehabilitation. *Phys Ther* (2007) **87**:684–703. doi:10.2522/ptj.20060164
14. Meehan SK, Randhawa B, Wessel B, Boyd LA. Implicit sequence-specific motor learning after subcortical stroke is associated with increased prefrontal brain activations: an {fMRI} study. *Hum Brain Mapp* (2011) **32**:290–303. doi:10.1002/hbm.21019
15. Nudo RJ, Milliken GW, Jenkins WM, Merzenich MM. Use-dependent alterations of movement representations in primary motor cortex of adult squirrel monkeys. *J Neurosci* (1996) **16**:785–807.
16. Grefkes C, Nowak DA, Eickhoff SB, Dafotakis M, Kust J, Karbe H, et al. Cortical connectivity after subcortical stroke assessed with functional magnetic resonance imaging. *Annals of neurology* (2008) **63**:236–46. doi:10.1002/ana.21228
17. Nudo RJ, Wise BM, SiFuentes F, Milliken GW. Neural substrates for the effects of rehabilitative training on motor recovery after ischemic infarct. *Science* (1996) **272**:1791–4. doi:10.1126/science.272.5269.1791
18. Alexander LD, Black SE, Gao F, Szilagyi G, Danells CJ, McIlroy WE. Correlating lesion size and location to deficits after ischemic stroke: the influence of accounting for altered peri-necrotic tissue and incidental silent infarcts. *Behav Brain Funct* (2010) **6**:6. doi:10.1186/1744-9081-6-6
19. Sterr A, Dean PJ, Szameitat AJ, Conforto AB, Shen S. Corticospinal tract integrity and lesion volume play different roles in chronic hemiparesis and its improvement through motor practice. *Neurorehabil Neural Repair* (2014) **28**:335–43. doi:10.1177/1545968313510972
20. Carrera E, Tononi G. Diaschisis: past, present, future. *Brain* (2014) **137**(Pt 9):2408–22. doi:10.1093/brain/awu101
21. Kraemer M, Schormann T, Hagemann G. Delayed shrinkage of the brain after ischemic stroke: preliminary observations with {voxel-guided} morphometry. *J Neuroimaging* (2004) **14**(3):265–72. doi:10.1111/j.1552-6569.2004.tb00249.x
22. Dade LA, Gao FQ, Kovacevic N, Roy P, Rockel C, CM O, et al. Semiautomatic brain region extraction: a method of parcellating brain regions from structural magnetic resonance images. *Neuroimage* (2004) **22**:1492–502. doi:10.1016/j.neuroimage.2004.03.023
23. Ramirez J, Scott CJ, McNeely AA, Berezuk C, Gao F, Szilagyi GM, et al. Lesion explorer: a video-guided, standardized protocol for accurate and reliable {MRI-derived} volumetrics in Alzheimer's disease and normal elderly. *J Vis Exp* (2013) (86):e50887:1–12. doi:10.3791/50887
24. Brodie SM, Borich MR, Boyd LA. Impact of 5-Hz rTMS over the primary sensory cortex is related to white matter volume in individuals with chronic stroke. *Eur J Neurosci* (2014) **40**:3405–12. doi:10.1111/ejn.12717
25. Naama L-C, Ramirez J, Lobaugh NJ, Black SE. Misclassified tissue volumes in Alzheimer disease patients with white matter hyperintensities: importance of lesion segmentation procedures for volumetric analysis. *Stroke* (2008) **39**:1134–41. doi:10.1161/STROKEAHA.107.498196
26. Dale AM, Fischl B, Sereno MI. Cortical surface-based analysis. I. Segmentation and surface reconstruction. *Neuroimage* (1999) **9**:179–94. doi:10.1006/nimg.1998.0395
27. Fischl B, Salat DH, Busa E, Albert M, Dieterich M, Haselgrove C, et al. Whole brain segmentation: automated labeling of neuroanatomical structures in the human brain. *Neuron* (2002) **33**:341–55. doi:10.1016/S0896-6273(02)00569-X

28. Jang SH. Prediction of motor outcome for hemiparetic stroke patients using diffusion tensor imaging?: a review. *NeuroRehabilitation* (2010) **27**:367–72. doi:10.3233/NRE-2010-0621
29. Borich MR, Mang C, Boyd LA. Both projection and commissural pathways are disrupted in individuals with chronic stroke: investigating microstructural white matter correlates of motor recovery. *BMC Neurosci* (2012) **13**:107. doi:10.1186/1471-2202-13-107
30. Lindenberg R, Zhu LL, Rüber T, Schlaug G. Predicting functional motor potential in chronic stroke patients using diffusion tensor imaging. *Hum Brain Mapp* (2012) **33**:1040–51. doi:10.1002/hbm.21266
31. Stinear CM, Barber PA, Smale PR, Coxon JP, Fleming MK, Byblow WD. Functional potential in chronic stroke patients depends on corticospinal tract integrity. *Brain* (2007) **130**:170–80. doi:10.1093/brain/awl333
32. Lindenberg R, Renga V, Zhu LL, Betzler F, Alsop D, Schlaug G. Structural integrity of corticospinal motor fibers predicts motor impairment in chronic stroke. *Neurology* (2010) **74**:280–7. doi:10.1212/WNL.0b013e3181ccc6d9
33. Borich MR, Brown KE, Boyd LA. Motor skill learning is associated with diffusion characteristics of white matter in individuals with chronic stroke. *J Neurol Phys Ther* (2014) **37**:1–10. doi:10.1097/NPT.0b013e3182a3d353
34. Carey JR, Deng H, Gillick BT, Cassidy JM, Anderson DC, Zhang L, et al. Serial treatments of primed low-frequency rTMS in stroke: characteristics of responders vs. nonresponders. *Restor Neurol Neurosci* (2014) **32**:323–35. doi:10.3233/RNN-130358
35. Demirtas-tatlidede A, Alonso-alonso M, Shetty RP, Ronen I, Alvaro P-L, Fregni F. Long-term effects of contralesional {rTMS} in severe stroke: safety, cortical excitability, and relationship with transcallosal motor fibers. *NeuroRehabilitation* (2014) **36**:51–9. doi:10.3233/NRE-141191
36. Basser PJ, Pierpaoli C. Microstructural and physiological features of tissues elucidated by quantitative-diffusion-tensor MRI. *J Magn Reson* (1996) **111**:209–19. doi:10.1006/jmrb.1996.0086
37. Assaf Y, Pasternak O. Diffusion tensor imaging (DTI)-based white matter mapping in brain research: a review. *J Mol Neurosci* (2008) **34**:51–61. doi:10.1007/s12031-007-0029-0
38. Basser P. Inferring microstructural features and the physiological state of tissues from diffusion-weighted images. *NMR Biomed* (1995) **8**:333–44. doi:10.1002/nbm.1940080707
39. Borich MR, Wadden KP, Boyd LA. Establishing the reproducibility of two approaches to quantify white matter tract integrity in stroke. *Neuroimage* (2012) **59**:2393–400. doi:10.1016/j.neuroimage.2011.09.009
40. Danielian L, Iwata N, Thomasson D, Floeter M. Reliability of fiber tracking measurements in diffusion tensor imaging for longitudinal study. *Neuroimage* (2011) **49**:1572–80. doi:10.1016/j.neuroimage.2009.08.062. Reliability
41. Auriat AM, Borich MR, Snow NJ, Wadden KP, Boyd LA. Comparing a diffusion tensor and non-tensor approach to white matter fiber tractography in chronic stroke. *Neuroimage Clin* (2015) **7**:771–81. doi:10.1016/j.nicl.2015.03.007
42. Farquharson S, Tournier JD, Calamante F, Fabiny G, Schneider-Kolsky M, Jackson GD, et al. White matter fiber tractography: why we need to move beyond DTI. *J Neurosurg* (2013) **118**:1367–77. doi:10.3171/2013.2.JNS.121294
43. Tournier J-D, Mori S, Leemans A. Diffusion tensor imaging and beyond. *Magn Reson Med* (2011) **65**:1532–56. doi:10.1002/mrm.22924
44. Jones DK. Studying connections in the living human brain with diffusion MRI. *Cortex* (2008) **44**:936–52. doi:10.1016/j.cortex.2008.05.002
45. Hallett M, Wassermann E, Cohen L, Chmielowska J, Gerloff C. Cortical mechanisms of recovery of function after stroke. *NeuroRehabilitation* (1998) **10**:131–42. doi:10.3233/NRE-1998-10205
46. Davidoff R. The pyramidal tract. *Neurology* (1990) **40**:332–9. doi:10.1212/WNL.40.2.332
47. Takenobu Y, Hayashi T, Moriaki H, Nagatsuka K, Naritomi H, Fukuyama H. Motor recovery and microstructural change in rubro-spinal tract in subcortical stroke. *Neuroimage Clin* (2014) **4**:201–8. doi:10.1016/j.nicl.2013.12.003
48. Schaechter JD, Fricker ZP, Perdue KL, Helmer KG, Vangel MG, Greve DN, et al. Microstructural status of ipsilesional and contralesional corticospinal tract correlates with motor skill in chronic stroke patients. *Hum Brain Mapp* (2009) **30**:3461–74. doi:10.1002/hbm.20770
49. Cho SH, Kim DG, Kim DS, Kim YH, Lee CH, Jang SH. Motor outcome according to the integrity of the corticospinal tract determined by diffusion tensor tractography in the early stage of corona radiata infarct. *Neurosci Lett* (2007) **426**:123–7. doi:10.1016/j.neulet.2007.08.049
50. Cho SH, Kim SH, Choi BY, Cho SH, Kang JH, Lee CH, et al. Motor outcome according to diffusion tensor tractography findings in the early stage of intracerebral hemorrhage. *Neurosci Lett* (2007) **421**:142–6. doi:10.1016/j.neulet.2007.04.052
51. Schlaug G, Siewert B, Benfield A, Edelman R, Warach S. Time course of the apparent diffusion coefficient (ADC) abnormality in human stroke. *Neurology* (1997) **49**:113–9. doi:10.1212/WNL.49.1.113
52. Schwamm LH, Koroshetz WJ, Sorensen AG, Wang B, Copen WA, Budzik R, et al. Time course of lesion development in patients with acute stroke: serial diffusion- and hemodynamic-weighted magnetic resonance imaging. *Stroke* (1998) **29**:2268–76. doi:10.1161/01.STR.29.11.2268
53. Grassel D, Ringer T, Fitzek C, Fitzek S, Kohl M, Kaiser W, et al. Wallerian degeneration of pyramidal tract after paramedian pons infarct. *Cerebrovasc Dis* (2010) **30**:380–8. doi:10.1159/000319573
54. Groisser BN, Copen WA, Singhal AB, Hirai KK, Schaechter JD. Corticospinal tract diffusion abnormalities early after stroke predict motor outcome. *Neurorehabil Neural Repair* (2014) **28**(8):751–60. doi:10.1177/1545968314521896
55. Bozzali M, Mastrospasqua C, Cercignani M, Giuliotti G, Bonni S, Caltagirone C, et al. Microstructural damage of the posterior corpus callosum contributes to the clinical severity of neglect. *PLoS One* (2012) **7**:e48079. doi:10.1371/journal.pone.0048079
56. Gujar SK, Maheshwari S, Bjorkman-Burtscher I, Sundgren PC. Magnetic resonance spectroscopy. *J Neuroophthalmol* (2005) **25**:217–26. doi:10.1089/ars.2010.3453
57. Naressi A, Couturier C, Devos JM, Janssen M, Mangeat C, De Beer R, et al. Java-based graphical user interface for the MRUI quantitation package. *MAGMA* (2001) **12**:141–52. doi:10.1016/S1352-8661(01)00111-9
58. Provencher SW. Estimation of metabolite concentrations from localized in vivo proton NMR spectra. *Magn Reson Med* (1993) **30**:672–9. doi:10.1002/mrm.1910300604
59. Gruetter R, Weisdorf SA, Rajanayagan V, Terpstra M, Merkle H, Truwit CL, et al. Resolution improvements in in vivo 1H NMR spectra with increased magnetic field strength. *J Magn Reson* (1998) **135**:260–4. doi:10.1006/jmre.1998.1542
60. Paiva FF, Otaduy MCG, Souza RO, Moll J, Bramati IE, et al. Comparison of human brain metabolite levels using 1H MRS at 1.5T and 3.0T. *Dement Neuropsychol* (2013) **7**:216–20.
61. Puts N, Edden R. In vivo magnetic spectroscopy of GABA: a methodological review. *Prog Nucl Magn Reson Spectrosc* (2012) **60**:1–26. doi:10.1016/j.pnmrs.2011.06.001. In
62. Castillo M, Kwok L, Mukherji SK. Clinical applications of proton MR spectroscopy. *AJNR Am J Neuroradiol* (1996) **17**:1–15.
63. Kim JP, Lentz MR, Westmoreland SV, Greco JB, Ratai EM, Halpern E, et al. Relationships between astrogliosis and 1H MR spectroscopic measures of brain choline/creatine and myo-inositol/creatine in a primate model. *AJNR Am J Neuroradiol* (2005) **26**(4):752–9.
64. Cirstea CM, Nudo RJ, Craciunas SC, Popescu EA, Choi I-Y, Lee P, et al. Neuronal-glial alterations in non-primary motor areas in chronic subcortical stroke. *Brain Res* (2012) **1463**:75–84. doi:10.1016/j.brainres.2012.04.052
65. Cirstea CM, Brooks WM, Craciunas SC, Popescu EA, Choi I-Y, Lee P, et al. Primary motor cortex in stroke: a functional MRI-guided proton MR spectroscopic study. *Stroke* (2011) **42**:1004–9. doi:10.1161/STROKEAHA.110.601047
66. Tran T, Ross B, Lin A. Magnetic resonance spectroscopy in neurological diagnosis. *Neurol Clin* (2009) **27**:21–60. doi:10.1016/j.ncl.2008.09.007
67. Maniega SM, Cvorovic V, Armitage PA, Marshall I, Bastin ME, Wardlaw JM. Choline and creatine are not reliable denominators for calculating metabolite ratios in acute ischemic stroke. *Stroke* (2008) **39**:2467–9. doi:10.1161/STROKEAHA.107.507020
68. Novotny EJ, Fulbright RK, Pearl PL, Gibson KM, Rothman DL. Magnetic resonance spectroscopy of neurotransmitters in human brain. *Ann Neurol* (2003) **54**(Suppl 6):S25–31. doi:10.1002/ana.10697
69. Gideon P, Henriksen O, Sperling B, Christiansen P, Olsen TS, Jørgensen HS, et al. Early time course of N-acetylaspartate, creatine and phosphocreatine, and compounds containing choline in the brain after acute stroke. A proton magnetic resonance spectroscopy study. *Stroke* (1992) **23**:1566–72. doi:10.1161/01.STR.23.11.1566

70. Gideon P, Sperling B, Arlien-Søborg P, Olsen TS, Henriksen O. Long-term follow-up of cerebral infarction patients with proton magnetic resonance spectroscopy. *Stroke* (1994) **25**:967–73. doi:10.1161/01.STR.25.5.967
71. Bivard A, Krishnamurthy V, Stanwell P, Yassi N, Spratt NJ, Nilsson M, et al. Spectroscopy of reperfused tissue after stroke reveals heightened metabolism in patients with good clinical outcomes. *J Cereb Blood Flow Metab* (2014) **34**:1944–50. doi:10.1038/jcbfm.2014.166
72. Parsons MW, Li T, Barber PA, Yang Q, Darby DG, Desmond PM, et al. Combined 1H MR spectroscopy and diffusion-weighted MRI improves the prediction of stroke outcome. *Neurology* (2000) **55**:498–506. doi:10.1212/WNL.55.4.498
73. Dani KA, An L, Henning EC, Shen J, Warach S. Multivoxel MR spectroscopy in acute ischemic stroke: comparison to the stroke protocol MRI. *Stroke* (2012) **43**:2962–7. doi:10.1161/STROKEAHA.112.656058
74. Craciunas SC, Brooks WM, Nudo RJ, Popescu EA, Choi I-YY, Lee P, et al. Motor and premotor cortices in subcortical stroke: proton magnetic resonance spectroscopy measures and arm motor impairment. *Neurorehabil Neural Repair* (2013) **27**(5):411–20. doi:10.1177/1545968312469835
75. Kobayashi M, Takayama H, Suga S, Mihara B. Longitudinal changes of metabolites in frontal lobes after hemorrhagic stroke of basal ganglia: a proton magnetic resonance spectroscopy study. *Stroke* (2001) **32**:2237–45. doi:10.1161/hs1001.096621
76. Federico F, Simone IL, Lucivero V, Giannini P, Laddomada G, Mezzapesa DM, et al. Prognostic value of proton magnetic resonance spectroscopy in ischemic stroke. *Arch Neurol* (1998) **55**(4):489–94. doi:10.1001/archneur.55.4.489
77. Blicher JU, Near J, Naess-Schmidt E, Stagg CJ, Johansen-Berg H, Nielsen JF, et al. GABA levels are decreased after stroke and GABA changes during rehabilitation correlate with motor improvement. *Neurorehabil Neural Repair* (2015) **29**:278–86. doi:10.1177/1545968314543652
78. Liebetanz D, Fauser S, Michaelis T, Czéh B, Watanabe T, Paulus W, et al. Safety aspects of chronic low-frequency transcranial magnetic stimulation based on localized proton magnetic resonance spectroscopy and histology of the rat brain. *J Psychiatr Res* (2003) **37**:277–86. doi:10.1016/S0022-3956(03)00017-7
79. Luborzewski A, Schubert F, Seifert F, Danker-Hopfe H, Brakemeier EL, Schlattmann P, et al. Metabolic alterations in the dorsolateral prefrontal cortex after treatment with high-frequency repetitive transcranial magnetic stimulation in patients with unipolar major depression. *J Psychiatr Res* (2007) **41**:606–15. doi:10.1016/j.jpsychires.2006.02.003
80. Yang X-R, Kirton A, Wilkes TC, Pradhan S, Liu I, Jaworska N, et al. Glutamate alterations associated with transcranial magnetic stimulation in youth depression: a case series. *J ECT* (2014) **1**–6. doi:10.1097/YCT.0000000000000094
81. Stagg CJ, Wylezinska M, Matthews PM, Johansen-Berg H, Jezzard P, Rothwell JC, et al. Neurochemical effects of theta burst stimulation as assessed by magnetic resonance spectroscopy. *J Neurophysiol* (2009) **101**:2872–7. doi:10.1152/jn.91060.2008
82. Stagg CJ, Bachtir V, Johansen-Berg H. The role of GABA in human motor learning. *Curr Biol* (2011) **21**:480–4. doi:10.1016/j.cub.2011.01.069
83. Norris DG. Principles of magnetic resonance assessment of brain function. *J Magn Reson Imaging* (2006) **23**:794–807. doi:10.1002/jmri.20587
84. Fox MD, Greicius M. Clinical applications of resting state functional connectivity. *Front Syst Neurosci* (2010) **4**:19. doi:10.3389/fnsys.2010.00019
85. Auer D. Spontaneous low-frequency blood oxygenation level-dependent fluctuations and functional connectivity analysis of the “resting” brain. *Magn Reson Imaging* (2008) **26**:1055–64. doi:10.1016/j.mri.2008.05.008
86. Lundgren J, Flodström K, Sjögren K, Liljequist B, Fugl-Meyer AR. Site of brain lesion and functional capacity in rehabilitated hemiplegics. *Scand J Rehabil Med* (1982) **14**:141–3.
87. Miyai I, Blau AD, Reding MJ, Volpe BT. Patients with stroke confined to basal ganglia have diminished response to rehabilitation efforts. *Neurology* (1997) **48**:95–101. doi:10.1212/WNL.48.1.95
88. Ju Y, Hussain M, Asmaro K, Zhao X, Liu L, Li J, et al. Clinical and imaging characteristics of isolated pontine infarcts: a one-year follow-up study. *Neurol Res* (2013) **35**:498–504. doi:10.1179/1743132813Y.0000000207
89. Rehme AK, Grefkes C. Cerebral network disorders after stroke: evidence from imaging-based connectivity analyses of active and resting brain states in humans. *J Physiol* (2012) **591**:17–31. doi:10.1113/jphysiol.2012.243469
90. Roh J, Rymer WZ, Perreault EJ, Yoo SB, Beer RF. Alterations in upper limb muscle synergy structure in chronic stroke survivors. *J Neurophysiol* (2013) **109**:768–81. doi:10.1152/jn.00670.2012
91. Lee MY, Choi JH, Park RJ, Kwon YH, Chang JS, Lee J, et al. Clinical characteristics and brain activation patterns of mirror movements in patients with corona radiata infarct. *Eur Neurol* (2010) **64**:15–20. doi:10.1159/000313979
92. Seto E, Sela G, McIlroy WE, Black SE, Staines WR, Bronskill MJ, et al. Quantifying head motion associated with motor tasks used in fMRI. *Neuroimage* (2001) **14**:284–97. doi:10.1006/nimg.2001.0829
93. Jung T, Kim JY, Seo JH, Jin SU, Joong Lee H, Lee S, et al. Combined information from resting-state functional connectivity and passive movements with functional magnetic resonance imaging differentiate fast late-onset motor recovery from progressive recovery in hemiplegic stroke patients: a pilot study. *J Rehabil Med* (2013) **45**:546–52. doi:10.2340/16501977-1165
94. Sun L, Yin D, Zhu Y, Fan M, Zang L, Wu Y, et al. Cortical reorganization after motor imagery training in chronic stroke patients with severe motor impairment: a longitudinal fMRI study. *Neuroradiology* (2013) **55**:913–25. doi:10.1007/s00234-013-1188-z
95. Park C, Chang WH, Ohn SH, Kim ST, Bang OY, Pascual-Leone A, et al. Longitudinal changes of resting-state functional connectivity during motor recovery after stroke. *Stroke* (2011) **42**:1357–62. doi:10.1161/STROKEAHA.110.596155
96. Varkuti B, Guan C, Pan Y, Phua KS, Ang KK, Kuah CWK, et al. Resting state changes in functional connectivity correlate with movement recovery for BCI and robot-assisted upper-extremity training after stroke. *Neurorehabil Neural Repair* (2012) **27**(1):53–62. doi:10.1177/1545968312445910
97. Golestani A-MM, Tymchuk S, Demchuk A, Goodyear BG, Group V-2 S. Longitudinal evaluation of resting-state {fMRI} after acute stroke with hemiparesis. *Neurorehabil Neural Repair* (2013) **27**:153–63. doi:10.1177/1545968312457827
98. Carter AR, Shulman GL, Corbetta M. Why use a connectivity-based approach to study stroke and recovery of function? *Neuroimage* (2012) **62**:2271–80. doi:10.1016/j.neuroimage.2012.02.070
99. Ward N. Assessment of cortical reorganisation for hand function after stroke. *J Physiol* (2011) **589**:5625–32. doi:10.1113/jphysiol.2011.220939
100. Grefkes C, Ward NS. Cortical reorganization after stroke: how much and how functional? *Neuroscientist* (2014) **20**:56–70. doi:10.1177/1073858413491147
101. Boyd LA, Vidoni ED, Wessel BD. Motor learning after stroke: is skill acquisition a prerequisite for contralesional neuroplastic change? *Neurosci Lett* (2010) **482**:21–5. doi:10.1016/j.neulet.2010.06.082
102. Hanlon CA, Buffington AL, McKeown MJ. New brain networks are active after right {MCA} stroke when moving the ipsilesional arm. *Neurology* (2005) **64**:114–20. doi:10.1212/01.WNL.0000148726.45458.A9
103. Olejniczak P. Neurophysiologic basis of EEG. *J Clin Neurophysiol* (2006) **23**:186–9. doi:10.1097/01.wnp.0000220079.61973.6c
104. Jordan KG. Emergency EEG and continuous EEG monitoring in acute ischemic stroke. *J Clin Neurophysiol* (2004) **21**(5):341–52.
105. Giaquinto S, Cobianchi A, Macera F, Nolfi G. EEG recordings in the course of recovery from stroke. *Stroke* (1994) **25**:2204–9. doi:10.1161/01.STR.25.11.2204
106. Dubovik S, Pignat JM, Ptak R, Aboulafia T, Allet L, Gillibert N, et al. The behavioral significance of coherent resting-state oscillations after stroke. *Neuroimage* (2012) **61**:249–57. doi:10.1016/j.neuroimage.2012.03.024
107. Finnigan SP, Walsh M, Rose SE, Chalk JB. Quantitative EEG indices of sub-acute ischaemic stroke correlate with clinical outcomes. *Clin Neurophysiol* (2007) **118**:2525–32. doi:10.1016/j.clinph.2007.07.021
108. Dubovik S, Ptak R, Aboulafia T, Magnin C, Gillibert N, Allet L, et al. EEG alpha band synchrony predicts cognitive and motor performance in patients with ischemic stroke. *Behav Neurol* (2013) **26**(3):187–9. doi:10.3233/BEN-2012-129007
109. Guggisberg AG. Two intrinsic coupling types for resting-state integration in the human brain. *Brain Topogr* (2015) **28**:318–29. doi:10.1007/s10548-014-0394-2
110. Pellegrino G, Pellegrino G, Tombini M, Assenza G, Bravi M, Sterzi S, et al. Inter-hemispheric coupling changes associate with motor improvements after robotic stroke rehabilitation. *Restor Neurol Neurosci* (2012) **30**:497–510. doi:10.3233/RNN-2012-120227
111. Di Lazzaro V, Ziemann U. The contribution of transcranial magnetic stimulation in the functional evaluation of microcircuits in human motor cortex. *Front Neural Circuits* (2013) **7**:18. doi:10.3389/fncir.2013.00018
112. Rossini P, Barker A, Berardelli A, Caramia M, Caruso G, Cracco R, et al. Non-invasive electrical and magnetic stimulation of the brain, spinal

- cord and roots: basic principles and procedures for routine clinical application. Report. *Electroencephalogr Clin Neurophysiol* (1994) **91**:79–92. doi:10.1016/0013-4694(94)90029-9
113. Rothwell JC, Hallett M, Berardelli A, Eisen A, Rossini P, Paulus W. Magnetic stimulation: motor evoked potentials. The international federation of clinical neurophysiology. *Electroencephalogr Clin Neurophysiol Suppl* (1999) **52**:97–103.
 114. Devanne H, Lavoie BA, Capaday C. Input-output properties and gain changes in the human corticospinal pathway. *Exp Brain Res* (1997) **114**:329–38. doi:10.1007/PL00005641
 115. Ridding MC, Rothwell JC. Stimulus/response curves as a method of measuring motor cortical excitability in man. *Electroencephalogr Clin Neurophysiol* (1997) **105**:340–4. doi:10.1016/S0924-980X(97)00041-6
 116. Singh AM, Neva JL, Staines WR. Acute exercise enhances the response to paired associative stimulation-induced plasticity in the primary motor cortex. *Exp Brain Res* (2014) **232**(11):3675–85. doi:10.1007/s00221-014-4049-z
 117. Hess CW, Mills KR, Murray NM. Responses in small hand muscles from magnetic stimulation of the human brain. *J Physiol* (1987) **388**:397–419. doi:10.1113/jphysiol.1987.sp016621
 118. Penfield W, Rasmussen T. *The Cerebral Cortex of Man. A Clinical Study of Localization of Function*. New York, NY: The Macmillan Company (1950).
 119. Levy WJ, Amassian VE, Schmid UD, Jungreis C. Mapping of motor cortex gyral sites non-invasively by transcranial magnetic stimulation in normal subjects and patients. *Electroencephalogr Clin Neurophysiol* (1991) **43**:51–75.
 120. Wassermann EM, McShane LM, Hallett M, Cohen LG. Noninvasive mapping of muscle representations in human motor cortex. *Electroencephalogr Clin Neurophysiol* (1992) **85**:1–8. doi:10.1016/0168-5597(92)90094-R
 121. Wilson SA, Thickbroom GW, Mastaglia FL. Transcranial magnetic stimulation mapping of the motor cortex in normal subjects: the representation of two intrinsic hand muscles. *J Neurol Sci* (1993) **18**:134–44. doi:10.1016/0022-510X(93)90102-5
 122. Mortifee P, Stewart H, Schulzer M, Eisen A. Reliability of transcranial magnetic stimulation for mapping the human motor cortex. *Electroencephalogr Clin Neurophysiol* (1994) **93**:131–7. doi:10.1016/0168-5597(94)90076-0
 123. Thickbroom GW, Sammut R, Mastaglia FL. Magnetic stimulation mapping of motor cortex: factors contributing to map area. *Electroencephalogr Clin Neurophysiol* (1998) **109**:79–84. doi:10.1016/S0924-980X(98)00006-X
 124. Thickbroom GW, Byrnes ML, Mastaglia FL. A model of the effect of MEP amplitude variation on the accuracy of TMS mapping. *Clin Neurophysiol* (1999) **110**:941–3. doi:10.1016/S1388-2457(98)00080-7
 125. Thickbroom G, Byrnes M, Archer S, Kermode A, Mastaglia F. Corticomotor organisation and motor function in multiple sclerosis. *J Neurol* (2005) **252**:765–71. doi:10.1007/s00415-005-0728-9
 126. Pearce AJ, Thickbroom GW, Byrnes ML, Mastaglia FL. Functional reorganisation of the corticomotor projection to the hand in skilled racquet players. *Exp Brain Res* (2000) **130**:238–43. doi:10.1007/s002219900236
 127. Thielscher A, Kammer T. Linking physics with physiology in TMS: a sphere field model to determine the cortical stimulation site in TMS. *Neuroimage* (2002) **17**:1117–30. doi:10.1006/nimg.2002.1282
 128. Uy J, Ridding MC, Miles TS. Stability of maps of human motor cortex made with transcranial magnetic stimulation. *Brain Topogr* (2002) **14**:293–7. doi:10.1023/A:1015752711146
 129. Kleim JA, Kleim ED, Cramer SC. Systematic assessment of training-induced changes in corticospinal output to hand using frameless stereotaxic transcranial magnetic stimulation. *Nat Protoc* (2007) **2**:1675–84. doi:10.1038/nprot.2007.206
 130. Chen R, Lozano AM, Ashby P. Mechanism of the silent period following transcranial magnetic stimulation. Evidence from epidural recordings. *Exp Brain Res* (1999) **128**:539–42. doi:10.1007/s002210050878
 131. Fuhr P, Agostino R, Hallett M. Spinal motor neuron excitability during the silent period after cortical stimulation. *Electroencephalogr Clin Neurophysiol* (1991) **81**:257–62. doi:10.1016/0168-5597(91)90011-L
 132. Ingulleri M, Berardelli A, Caucchi G, Manfredi M. Silent period evoked by transcranial stimulation of the human cortex and cervicomedullary junction. *J Physiol* (1993) **466**:521–34.
 133. Werhahn K, Kunesch E, Noschtar S, Benecke R, Classen J. Differential effects on motorcortical inhibition induced by blockade of GABA uptake in humans. *J Physiol* (1999) **517**:591–7. doi:10.1111/j.1469-7793.1999.05911.x
 134. Ferbert A, Priori A, Rothwell J, Day B, Colebatch JG, Marsden C. Interhemispheric inhibition of the human motor cortex. *J Physiol* (1992) **453**:525–46. doi:10.1113/jphysiol.1992.sp019243
 135. Meyer B, Rörich S, Von Einsiedel H, Kruggel F, Weindl A. Inhibitory and excitatory interhemispheric transfers between motor cortical areas in normal humans and patients with abnormalities of the corpus callosum. *Brain* (1995) **118**:429–40. doi:10.1093/brain/118.2.429
 136. Meyer BU, Rörich S, Woiciechowsky C. Topography of fibers in the human corpus callosum mediating interhemispheric inhibition between the motor cortices. *Ann Neurol* (1998) **43**:360–9. doi:10.1002/ana.410430314
 137. Kujirai T, Caramia MD, Rothwell JC, Day BJ, Thompson PD, Ferbert A, et al. Corticocortical inhibition in the human motor cortex. *J Physiol* (1993) **471**:501–19. doi:10.1113/jphysiol.1993.sp019912
 138. Valls-Sole J, Pascual-Leone A, Wassermann EM, Hallett M. Human motor evoked responses to paired transcranial magnetic stimulation. *Electroencephalogr Clin Neurophysiol* (1992) **85**:355–64. doi:10.1016/0168-5597(92)90048-G
 139. Wassermann EM, Samii A, Mercuri B, Ikoma K, Oddo D, Grill SE, et al. Responses to paired transcranial magnetic stimuli in resting, active, recently activated muscle. *Exp Brain Res* (1996) **109**:158–63. doi:10.1007/BF00228638
 140. Ziemann U, Rothwell JC, Ridding MC. Interaction between intracortical inhibition and facilitation in human motor cortex. *J Physiol* (1996) **496**:873–81. doi:10.1113/jphysiol.1996.sp021734
 141. Roick H, Von Giesen H, Benecke R, von Giesen HJ. On the origin of the postexcitatory inhibition seen after transcranial magnetic brain stimulation in awake human subjects. *Exp Brain Res* (1993) **94**:489–98. doi:10.1007/BF00230207
 142. Siebner HR, Willech F, Peller M, Auer C, Boecker H, Conrad B, et al. Imaging brain activation induced by long trains of repetitive transcranial magnetic stimulation. *Neuroreport* (1998) **9**:943–8. doi:10.1097/00001756-199803300-00033
 143. McDonnell MN, Orekhov Y, Ziemann U. The role of GABA B receptors in intracortical inhibition in the human motor cortex. *Exp Brain Res* (2006) **173**:86–93. doi:10.1007/s00221-006-0365-2
 144. Chen R, Tam A, Bütefisch C, Corwell B, Ziemann U, Rothwell JC, et al. Intracortical inhibition and facilitation in different representations of the human motor cortex. *J Neurophysiol* (1998) **80**:2870–81.
 145. Ziemann U, Chen R, Cohen LG, Hallett M. Dextromethorphan decreases the excitability of the human motor cortex. *Neurology* (1998) **51**:1320–4. doi:10.1212/WNL.51.5.1320
 146. Chen R. Interactions between inhibitory and excitatory circuits in the human motor cortex. *Exp Brain Res* (2004) **154**:1–10. doi:10.1007/s00221-003-1684-1
 147. Manganotti P, Zanette G, Bonato C, Tinazzi M, Polo A, Fiaschi A. Crossed and direct effects of digital nerves stimulation on motor evoked potential: a study with magnetic brain stimulation. *Electroencephalogr Clin Neurophysiol* (1997) **105**:280–9. doi:10.1016/S0924-980X(97)00018-0
 148. Tokimura H, Ridding MC, Tokimura Y, Amassian VE, Rothwell JC. Short latency facilitation between pairs of threshold magnetic stimuli applied to human motor cortex. *Electroencephalogr Clin Neurophysiol* (1996) **101**:263–72. doi:10.1016/0924-980X(96)95664-7
 149. Sailer A, Molnar GF, Cunic DI, Chen R. Effects of peripheral sensory input on cortical inhibition in humans. *J Physiol* (2002) **544**:617–29. doi:10.1113/jphysiol.2002.028670
 150. Sailer A, Molnar GF, Paradiso G, Gunraj CA, Lang AE, Chen R. Short and long latency afferent inhibition in Parkinson's disease. *Brain* (2003) **126**:1883–94. doi:10.1093/brain/awg183
 151. Delvaux V, Alagona G, Gérard P, De Pasqua V, Pennisi G, de Noordhout AM. Post-stroke reorganization of hand motor area: a 1-year prospective follow-up with focal transcranial magnetic stimulation. *Clin Neurophysiol* (2003) **114**:1217–25. doi:10.1016/S1388-2457(03)00070-1
 152. Heald A, Bates D, Cartlidge N, French J, Miller S. Longitudinal study of central motor conduction time following stroke. 2. Central motor conduction measured within 72 h after stroke as a predictor of functional outcome at 12 months. *Brain* (1993) **116**:1371–85. doi:10.1093/brain/116.6.1371
 153. Catano A, Houa M, Caroyer J, Ducarne H, Noel P. Magnetic transcranial stimulation in non-haemorrhagic sylvian strokes: interest of facilitation for early functional prognosis. *Electroencephalogr Clin Neurophysiol* (1995) **97**:349–54. doi:10.1016/0924-980X(95)00127-7

154. D'Olhaberriague L, Gamissans JME, Marrugat J, Valls A, Ley CO, Seoane JL. Transcranial magnetic stimulation as a prognostic tool in stroke. *J Neurol Sci* (1997) **147**:73–80. doi:10.1016/S0022-510X(96)05312-9
155. Escudero JV, Sancho J, Bautista D, Escudero M, López-Trigo J. Prognostic value of motor evoked potential obtained by transcranial magnetic brain stimulation in motor function recovery in patients with acute ischemic stroke. *Stroke* (1998) **29**:1854–9. doi:10.1161/01.STR.29.9.1854
156. Hendricks HT, Pasman JW, Merx JL, van Limbeek J, Zwarts MJ. Analysis of recovery processes after stroke by means of transcranial magnetic stimulation. *J Clin Neurophysiol* (2003) **20**:188–95. doi:10.1097/00004691-200305000-00004
157. Trompetto C, Assini A, Buccolieri A, Marchese R, Abbruzzese G. Motor recovery following stroke: a transcranial magnetic stimulation study. *Clin Neurophysiol* (2000) **111**:1860–7. doi:10.1016/S1388-2457(00)00419-3
158. Manganotti P, Patuzzo S, Cortese F, Palermo A, Smania N, Fiaschi A. Motor disinhibition in affected and unaffected hemisphere in the early period of recovery after stroke. *Clin Neurophysiol* (2002) **113**:936–43. doi:10.1016/S1388-2457(02)00062-7
159. Pennisi G, Alagona G, Rapisarda G, Nicoletti F, Costanzo E, Ferri R, et al. Transcranial magnetic stimulation after pure motor stroke. *Clin Neurophysiol* (2002) **113**:1536–43. doi:10.1016/S1388-2457(02)00255-9
160. Traversa R, Cicinelli P, Bassi A, Rossini P, Bernardi G. Mapping of motor cortical reorganization after stroke a brain stimulation study with focal magnetic pulses. *Stroke* (1997) **28**(1):110–7. doi:10.1161/01.STR.28.1.110
161. Traversa R, Cicinelli P, Oliveri M, Giuseppina Palmieri M, Maddalena Filippi M, Pasqualetti P, et al. Neurophysiological follow-up of motor cortical output in stroke patients. *Clin Neurophysiol* (2000) **111**:1695–703. doi:10.1016/S1388-2457(00)00373-4
162. Traversa R, Cicinelli P, Pasqualetti P, Filippi M, Rossini PM. Follow-up of interhemispheric differences of motor evoked potentials from the “affected” and “unaffected” hemispheres in human stroke. *Brain Res* (1998) **803**:1–8. doi:10.1016/S0006-8993(98)00505-8
163. Cicinelli P, Traversa R, Rossini PM. Post-stroke reorganization of brain motor output to the hand: a 2-4 month follow-up with focal magnetic transcranial stimulation. *Electroencephalogr Clin Neurophysiol* (1997) **105**:438–50. doi:10.1016/S0924-980X(97)00052-0
164. Liepert J, Miltner WH, Bauder H, Sommer M, Dettmers C, Taub E, et al. Motor cortex plasticity during constraint-induced movement therapy in stroke patients. *Neurosci Lett* (1998) **250**:5–8. doi:10.1016/S0304-3940(98)00386-3
165. Liepert J, Bauder H, Miltner WH, Taub E, Weiller C. Treatment-induced cortical reorganization after stroke in humans. *Stroke* (2000) **31**(6):1210–6. doi:10.1161/01.STR.31.6.1210
166. Sawaki L, Butler AJ, Leng X, Wassenaar PA, Mohammad YM, Blanton S, et al. Constraint-induced movement therapy results in increased motor map area in subjects 3 to 9 months after stroke. *Neurorehabil Neural Repair* (2008) **22**:505–13. doi:10.1177/1545968308317531
167. Ro T, Noser E, Boake C, Johnson R, Gaber M, Speroni A, et al. Functional reorganization and recovery after constraint-induced movement therapy in subacute stroke: case reports. *Neurocase* (2006) **12**:50–60. doi:10.1080/13554790500493415
168. Traversa R, Cicinelli P, Filippi M, Oliveri M, Palmieri MG, Pasqualetti P, et al. A method to monitor motor cortical excitability in human stroke through motor evoked potentials. *Brain Res Brain Res Protoc* (1999) **4**:44–8. doi:10.1016/S1385-299X(98)00063-4
169. Ahonen J, Jehkonen M, Dastidar P, Molnar G, Hakkinen V. Cortical silent period evoked by transcranial magnetic stimulation in ischemic stroke. *Electroencephalogr Clin Neurophysiol* (1998) **109**:224–9. doi:10.1016/S0924-980X(98)00014-9
170. Liepert J, Storch P, Fritsch A, Weiller C. Motor cortex disinhibition in acute stroke. *Clin Neurophysiol* (2000) **111**:671–6. doi:10.1016/S1388-2457(99)00312-0
171. Liepert J, Restemeyer C, Kucinski T, Zittel S, Weiller C. Motor strokes: the lesion location determines motor excitability changes. *Stroke* (2005) **36**:2648–53. doi:10.1161/01.STR.0000189629.10603.02
172. Liepert J, Hamzei F, Weiller C. Motor cortex disinhibition of the unaffected hemisphere after acute stroke. *Muscle Nerve* (2000) **23**:1761–3. doi:10.1002/1097-4598(200011)23:11<1761::AID-MUS14>3.0.CO;2-M
173. Bütefisch CM, Netz J, Weßling M, Seitz RJ, Hömberg V. Remote changes in cortical excitability after stroke. *Brain* (2003) **126**:470–81. doi:10.1093/brain/awg044
174. Swayne OB, Rothwell JC, Ward NS, Greenwood RJ. Stages of motor output reorganization after hemispheric stroke suggested by longitudinal studies of cortical physiology. *Cereb Cortex* (2008) **18**:1909–22. doi:10.1093/cercor/bhm218
175. Di Lazzaro V, Profice P, Pilato F, Capone F, Ranieri F, Florio L, et al. The level of cortical afferent inhibition in acute stroke correlates with long-term functional recovery in humans. *Stroke* (2012) **43**:250–2. doi:10.1161/STROKEAHA.111.631085
176. Pennisi G, Rapisarda G, Bella R, Calabrese V, Maertens De Noordhout A, Delwaide PJ. Absence of response to early transcranial magnetic stimulation in ischemic stroke patients: prognostic value for hand motor recovery. *Stroke* (1999) **30**:2666–70. doi:10.1161/01.STR.30.12.2666
177. Shimizu T, Hosaki A, Hino T, Sato M, Komori T, Hirai S, et al. Motor cortical disinhibition in the unaffected hemisphere after unilateral cortical stroke. *Brain* (2002) **125**:1896–907. doi:10.1093/brain/awf183
178. Fridman EA, Hanakawa T, Chung M, Hummel F, Leiguarda RC, Cohen LG. Reorganization of the human ipsilesional premotor cortex after stroke. *Brain* (2004) **127**:747–58. doi:10.1093/brain/awh082
179. Catano A, Houa M, Caroyer JM, Ducarne H, Noël P. Magnetic transcranial stimulation in acute stroke: early excitation threshold and functional prognosis. *Electroencephalogr Clin Neurophysiol* (1996) **101**:233–9. doi:10.1016/0924-980X(96)95656-8
180. Byrnes ML, Thickbroom GW, Phillips BA, Mastaglia FL. Long-term changes in motor cortical organisation after recovery from subcortical stroke. *Brain Res* (2001) **889**:278–87. doi:10.1016/S0006-8993(00)03089-4
181. Foltys H, Krings T, Meister IG, Sparing R, Boroojerdi B, Thron A, et al. Motor representation in patients rapidly recovering after stroke: a functional magnetic resonance imaging and transcranial magnetic stimulation study. *Clin Neurophysiol* (2003) **114**:2404–15. doi:10.1016/S1388-2457(03)00263-3
182. Boroojerdi B, Diefenbach K, Ferbert A. Transcallosal inhibition in cortical and subcortical cerebral vascular lesions. *J Neurol Sci* (1996) **144**:160–70. doi:10.1016/S0022-510X(96)00222-5
183. Murase N, Duque J, Mazzocchio R, Cohen LG. Influence of interhemispheric interactions on motor function in chronic stroke. *Ann Neurol* (2004) **55**:400–9. doi:10.1002/ana.10848
184. Duque J, Hummel F, Celnik P, Murase N, Mazzocchio R, Cohen LG. Transcallosal inhibition in chronic subcortical stroke. *Neuroimage* (2005) **28**:940–6. doi:10.1016/j.neuroimage.2005.06.033
185. Taub E, Uswatte G, King DK, Morris D, Crago JE, Chatterjee A. A placebo-controlled trial of constraint-induced movement therapy for upper extremity after stroke. *Stroke* (2006) **37**:1045–9. doi:10.1161/01.STR.0000206463.66461.97
186. Carey JR, Fregni F, Pascual-Leone A. rTMS combined with motor learning training in healthy subjects. *Restor Neurol Neurosci* (2006) **24**(3):191–9.
187. Bütefisch CM, Wessling M, Netz J, Seitz RJ, Homberg V. Relationship between interhemispheric inhibition and motor cortex excitability in subacute stroke patients. *Neurorehabil Neural Repair* (2008) **22**:4–21. doi:10.1177/1545968307301769
188. Borich M, Neva J, Boyd L. Evaluation of differences in brain neurophysiology and morphometry associated with hand function in individuals with chronic stroke. *Restor Neurol Neurosci* (2015) **33**:31–42. doi:10.3233/RNN-140425
189. Mang CS, Borich MR, Brodie SM, Boyd LA. Diffusion imaging and transcranial magnetic stimulation assessment of transcallosal pathways in chronic stroke. *Clin Neurophysiol* (2015) **126**(10):1959–71. doi:10.1016/j.clinph.2014.12.018
190. Huang YZ, Edwards MJ, Rounis E, Bhatia KP, Rothwell JC. Theta burst stimulation of the human motor cortex. *Neuron* (2005) **45**:201–6. doi:10.1016/j.neuron.2004.12.033
191. Huang YZ, Rothwell JC, Lu CS, Wang J, Weng YH, Lai SC, et al. The effect of continuous theta burst stimulation over premotor cortex on circuits in primary motor cortex and spinal cord. *Clin Neurophysiol* (2009) **120**:796–801. doi:10.1016/j.clinph.2009.01.003
192. Pascual-Leone A, Valls-Sole J, Wassermann EM, Hallett M, Valls-Solé J. Responses to rapid-rate transcranial magnetic stimulation of the human motor cortex. *Brain* (1994) **117**:847–58. doi:10.1093/brain/117.4.847
193. Brodie SM, Meehan SK, Borich MR, Boyd LA. 5 Hz repetitive transcranial magnetic stimulation over the ipsilesional sensory cortex enhances motor

- learning after stroke. *Front Hum Neurosci* (2014) **8**:143. doi:10.3389/fnhum.2014.00143
194. Meehan SK, Dao E, Lindsell MA, Boyd LA. Continuous theta burst stimulation over the contralesional sensory and motor cortex enhances motor learning post-stroke. *Neurosci Lett* (2011) **500**:26–30. doi:10.1016/j.neulet.2011.05.237
 195. Pascual-Leone A, Tommas JM, Keenan J, Canete C, Catala MD. Study and modulation of human cortical excitability with transcranial magnetic stimulation. *J Clin Neurophysiol* (1998) **15**:333–43. doi:10.1097/00004691-199807000-00005
 196. Hamada M, Murase N, Hasan A, Balaratnam M, Rothwell JC. The role of interneuron networks in driving human motor cortical plasticity. *Cereb Cortex* (2013) **23**:1593–605. doi:10.1093/cercor/bhs147
 197. Suppa A, Ortu E, Zafar N, Deriu F, Paulus W, Berardelli A, et al. Theta burst stimulation induces after-effects on contralateral primary motor cortex excitability in humans. *J Physiol* (2008) **18**:4489–500. doi:10.1113/jphysiol.2008.156596
 198. Neva JL, Vesia M, Singh AM, Staines WR. Modulation of left primary motor cortex excitability after bimanual training and intermittent theta burst stimulation to left dorsal premotor cortex. *Behav Brain Res* (2014) **261**:289–96. doi:10.1016/j.bbr.2013.12.029
 199. Legon W, Dionne JK, Staines WR. Continuous theta burst stimulation of the supplementary motor area: effect upon perception and somatosensory and motor evoked potentials. *Brain Stimul* (2013) **6**:877–83. doi:10.1016/j.brs.2013.04.007
 200. Stinear CM, Barber PA, Coxon JP, Verryt TS, Acharya PP, Byblow WD. Repetitive stimulation of premotor cortex affects primary motor cortex excitability and movement preparation. *Brain Stimul* (2009) **2**:152–62. doi:10.1016/j.brs.2009.01.001
 201. Premji A, Rai N, Nelson A. Area 5 influences excitability within the primary motor cortex in humans. *PLoS One* (2011) **6**:e20023. doi:10.1371/journal.pone.0020023
 202. Arasanz CP, Staines WR, Roy EA, Schweizer TA. The cerebellum and its role in word generation: a cTBS study. *Cortex* (2012) **48**:718–24. doi:10.1016/j.cortex.2011.02.021
 203. Bolton DA, Staines WR. Transient inhibition of the dorsolateral prefrontal cortex disrupts attention-based modulation of tactile stimuli at early stages of somatosensory processing. *Neuropsychologia* (2011) **49**:1928–37. doi:10.1016/j.neuropsychologia.2011.03.020
 204. Bestmann S, Baudewig J, Siebner HR, Rothwell JC, Frahm J. Functional MRI of the immediate impact of transcranial magnetic stimulation on cortical and subcortical motor circuits. *Eur J Neurosci* (2004) **19**:1950–62. doi:10.1111/j.1460-9568.2004.03277.x
 205. Huang YZ, Rothwell JC, Edwards MJ, Chen RS. Effect of physiological activity on an NMDA-dependent form of cortical plasticity in human. *Cereb Cortex* (2008) **18**:563–70. doi:10.1093/cercor/bhm087
 206. Chen R, Yung D, Li J. Organization of ipsilateral excitatory and inhibitory pathways in the human motor cortex. *J Neurophysiol* (2003) **89**:1256–64. doi:10.1152/jn.00950.2002
 207. Corti M, Patten C, Triggs W. Repetitive transcranial magnetic stimulation of motor cortex after stroke. *Am J Phys Med Rehabil* (2012) **91**:254–70. doi:10.1097/PHM.0b013e318228bf0c
 208. Carey JR, Anderson DC, Gillick BT, Whitford M, Pascual-Leone A. 6-Hz primed low-frequency rTMS to contralesional M1 in two cases with middle cerebral artery stroke. *Neurosci Lett* (2010) **469**:338–42. doi:10.1016/j.neulet.2009.12.023
 209. Boggio PS, Alonso-Alonso M, Mansur CG, Rigonatti SP, Schlaug G, Pascual-Leone A, et al. Hand function improvement with low-frequency repetitive transcranial magnetic stimulation of the unaffected hemisphere in a severe case of stroke. *Am J Phys Med Rehabil* (2006) **85**:927–30. doi:10.1097/01.phm.0000242635.88129.38
 210. Fregni F, Boggio PS, Valle AC, Rocha RR, Duarte J, Ferreira MJL, et al. A sham-controlled trial of a 5-day course of repetitive transcranial magnetic stimulation of the unaffected hemisphere in stroke patients. *Stroke* (2006) **37**:2115–22. doi:10.1161/01.STR.0000231390.58967.6b
 211. Seniow J, Bilik M, Lesniak M, Waldowski K, Iwanski S, Czlonkowska A. Transcranial magnetic stimulation combined with physiotherapy in rehabilitation of poststroke hemiparesis: a randomized, double-blind, placebo-controlled study. *Neurorehabil Neural Repair* (2012) **26**:1072–9. doi:10.1177/1545968312445635
 212. Talelli P, Wallace A, Dileone M, Hoad D, Cheeran B, Oliver R, et al. Theta burst stimulation in the rehabilitation of the upper limb: a semirandomized, placebo-controlled trial in chronic stroke patients. *Neurorehabil Neural Repair* (2012) **26**:976–87. doi:10.1177/1545968312437940
 213. Cohen L, Ziemann U, Chen R, Classen J, Hallett M, Gerloff C, et al. Studies of neuroplasticity with transcranial magnetic stimulation. *J Clin Neurophysiol* (1998) **15**:305–24. doi:10.1097/00004691-199807000-00003
 214. Grefkes C, Fink GR. Connectivity-based approaches in stroke and recovery of function. *Lancet Neurol* (2014) **13**:206–16. doi:10.1016/S1474-4422(13)70264-3
 215. Khedr EM. Therapeutic trial of repetitive transcranial magnetic stimulation after acute ischemic stroke. *Neurology* (2005) **65**(3):466–8. doi:10.1212/01.wnl.0000173067.84247.36
 216. Kim Y-H, You SH, Ko M-H, Park J-W, Lee KH, Jang SH, et al. Repetitive transcranial magnetic stimulation-induced corticomotor excitability and associated motor skill acquisition in chronic stroke. *Stroke* (2006) **37**:1471–6. doi:10.1161/01.STR.0000221233.55497.51
 217. Ameli M, Grefkes C, Kemper F, Riegg FP, Rehme AK, Karbe H, et al. Differential effects of high-frequency repetitive transcranial magnetic stimulation over ipsilesional primary motor cortex in cortical and subcortical middle cerebral artery stroke. *Ann Neurol* (2009) **66**:298–309. doi:10.1002/ana.21725
 218. Malcolm MP, Triggs WJ, Light KE, Gonzalez LJ, Wu S, Reid K, et al. Repetitive transcranial magnetic stimulation as an adjunct to constraint-induced therapy: an exploratory randomized controlled trial. *Am J Phys Med Rehabil* (2007) **86**:707–15. doi:10.1097/PHM.0b013e31813e0de0.Repetitive
 219. Lee JH, Kim SB, Lee KW, Kim MA, Lee SJ, Choi SJ. Factors associated with upper extremity motor recovery after repetitive transcranial magnetic stimulation in stroke patients. *Ann Rehabil Med* (2015) **39**:268–76. doi:10.5535/arm.2015.39.2.268
 220. Tretriluxana J, Kantak S, Tretriluxana S, Wu AD, Fisher BE. Low frequency repetitive transcranial magnetic stimulation to the non-lesioned hemisphere improves paretic arm reach-to-grasp performance after chronic stroke. *Disabil Rehabil Assist Technol* (2013) **8**:121–4. doi:10.3109/17483107.2012.737136
 221. Takeuchi N, Chuma T, Matsuo Y, Watanabe I, Ikoma K. Repetitive transcranial magnetic stimulation of contralesional primary motor cortex improves hand function after stroke. *Stroke* (2005) **36**:2681–6. doi:10.1161/01.STR.0000189658.51972.34
 222. Grefkes C, Nowak DA, Wang LE, Dafotakis M, Eickhoff SB, Fink GR. Modulating cortical connectivity in stroke patients by rTMS assessed with fMRI and dynamic causal modeling. *Neuroimage* (2010) **50**:233–42. doi:10.1016/j.neuroimage.2009.12.029
 223. Hsu WY, Cheng CH, Liao KK, Lee IH, Lin YY. Effects of repetitive transcranial magnetic stimulation on motor functions in patients with stroke: a meta-analysis. *Stroke* (2012) **43**:1849–57. doi:10.1161/STROKEAHA.111.649756
 224. Bolognini N, Pascual-Leone A, Fregni F. Using non-invasive brain stimulation to augment motor training-induced plasticity. *J Neuroeng Rehabil* (2009) **6**:8. doi:10.1186/1743-0003-6-8
 225. Rose DK, Patten C, McGuirk TE, Lu X, Triggs WJ. Does inhibitory repetitive transcranial magnetic stimulation augment functional task practice to improve arm recovery in chronic stroke? *Stroke Res Treat* (2014) **2014**:1–10. doi:10.1155/2014/305236
 226. Emara T, El Nahas N, Elkader HA, Ashour S, El Etrebi A. MRI can predict the response to therapeutic repetitive transcranial magnetic stimulation (rTMS) in stroke patients. *J Vasc Interv Neurol* (2009) **2**(2):163–8.
 227. Stinear CM, Barber PA, Petoe M, Anwar S, Byblow WD. The {PREP} algorithm predicts potential for upper limb recovery after stroke. *Brain* (2012) **135**:2527–35. doi:10.1093/brain/awb146
 228. Lüdemann-Podubecká J, Bösl K, Theilig S, Wiederer R, Nowak DA. The effectiveness of 1Hz rTMS over the primary motor area of the unaffected hemisphere to improve hand function after stroke depends on hemispheric dominance. *Brain Stimul* (2015) **8**(4):823–30. doi:10.1016/j.brs.2015.02.004
 229. Cunningham DA, Machado A, Janini D, Varnerin N, Bonnett C, Yue G, et al. The assessment of inter-hemispheric imbalance using imaging and

- non-invasive brain stimulation in patients with chronic stroke. *Arch Phys Med Rehabil* (2014) **96**(4 Suppl):S94–103. doi:10.1016/j.apmr.2014.07.419
230. Uhm KE, Kim Y-H, Yoon KJ, Hwang JM, Chang WH. BDNF genotype influence the efficacy of rTMS in stroke patients. *Neurosci Lett* (2015) **594**:117–21. doi:10.1016/j.neulet.2015.03.053
 231. Plow EB, Cunningham DA, Varnerin N, Machado A. Rethinking stimulation of the brain in stroke rehabilitation: why higher motor areas might be better alternatives for patients with greater impairments. *Neuroscientist* (2014) **21**(3):225–40. doi:10.1177/1073858414537381
 232. Ward NS, Newton JM, Swayne OB, Lee L, Frackowiak RS, Thompson AJ, et al. The relationship between brain activity and peak grip force is modulated by corticospinal system integrity after subcortical stroke. *Eur J Neurosci* (2007) **25**:1865–73. doi:10.1111/j.1460-9568.2007.05434.x
 233. Bestmann S, Swayne O, Blankenburg F, Ruff CC, Teo J, Weiskopf N, et al. The role of contralesional dorsal premotor cortex after stroke as studied with concurrent TMS-fMRI. *J Neurosci* (2010) **30**:11926–37. doi:10.1523/JNEUROSCI.5642-09.2010
 234. Lotze M, Beutling W, Loibl M, Domin M, Platz T, Schminke U, et al. Contralesional motor cortex activation depends on ipsilesional corticospinal tract integrity in well-recovered subcortical stroke patients. *Neurorehabil Neural Repair* (2012) **26**:594–603. doi:10.1177/1545968311427706
 235. Borich MR, Brown KE, Lakhani B, Boyd LA. Applications of electroencephalography to characterize brain activity. *J Neurol Phys Ther* (2015) **39**:43–51. doi:10.1097/NPT.0000000000000072
 236. Ilmoniemi RJ, Kicić D. Methodology for combined TMS and EEG. *Brain Topogr* (2010) **22**:233–48. doi:10.1007/s10548-009-0123-4
 237. Komssi S, Kahkonen S, Ilmoniemi RJ, Kähkönen S. The effect of stimulus intensity on brain responses evoked by transcranial magnetic stimulation. *Hum Brain Mapp* (2004) **21**:154–64. doi:10.1002/hbm.10159
 238. Kicić D, Lioumis P, Ilmoniemi RJ, Nikulin VV. Bilateral changes in excitability of sensorimotor cortices during unilateral movement: combined electroencephalographic and transcranial magnetic stimulation study. *Neuroscience* (2008) **152**:1119–29. doi:10.1016/j.neuroscience.2008.01.043
 239. Di Pino G, Pellegrino G, Assenza G, Capone F, Ferreri F, Formica D, et al. Modulation of brain plasticity in stroke: a novel model for neurorehabilitation. *Nat Rev Neurol* (2014) **10**:597–608. doi:10.1038/nrneurol.2014.162

Conflict of Interest Statement: The authors declare that the research was conducted in the absence of any commercial or financial relationships that could be construed as a potential conflict of interest.

Copyright © 2015 Auriat, Neva, Peters, Ferris and Boyd. This is an open-access article distributed under the terms of the Creative Commons Attribution License (CC BY). The use, distribution or reproduction in other forums is permitted, provided the original author(s) or licensor are credited and that the original publication in this journal is cited, in accordance with accepted academic practice. No use, distribution or reproduction is permitted which does not comply with these terms.



The Virtual Brain: modeling biological correlates of recovery after chronic stroke

Maria Inez Falcon¹, Jeffrey D. Riley^{1,2}, Viktor Jirsa^{3,4}, Anthony R. McIntosh⁵, Ahmed D. Shereen¹, E. Elinor Chen¹ and Ana Solodkin^{1,2*}

¹ Department of Anatomy and Neurobiology, University of California Irvine School of Medicine, Irvine, CA, USA, ² Department of Neurology, University of California Irvine School of Medicine, Irvine, CA, USA, ³ Institut de Neurosciences des Systèmes, Faculté de Médecine, Aix-Marseille Université, Marseille, France, ⁴ INSERM UMR1106, Aix-Marseille Université, Marseille, France, ⁵ Rotman Research Institute, Baycrest Health Sciences, University of Toronto, Toronto, ON, Canada

OPEN ACCESS

Edited by:

Rüdiger Jürgen Seitz,
University Hospital Düsseldorf,
Germany

Reviewed by:

Ferdinand Binkowski,
RWTH Aachen University, Germany
Cornelius Weiller,
Universität Freiburg, Germany

*Correspondence:

Ana Solodkin
solodkin@uci.edu

Specialty section:

This article was submitted to Stroke,
a section of the
journal Frontiers in Neurology

Received: 09 April 2015

Accepted: 16 October 2015

Published: 02 November 2015

Citation:

Falcon MI, Riley JD, Jirsa V,
McIntosh AR, Shereen AD, Chen EE
and Solodkin A (2015) The Virtual
Brain: modeling biological correlates
of recovery after chronic stroke.
Front. Neurol. 6:228.
doi: 10.3389/fneur.2015.00228

There currently remains considerable variability in stroke survivor recovery. To address this, developing individualized treatment has become an important goal in stroke treatment. As a first step, it is necessary to determine brain dynamics associated with stroke and recovery. While recent methods have made strides in this direction, we still lack physiological biomarkers. The Virtual Brain (TVB) is a novel application for modeling brain dynamics that simulates an individual's brain activity by integrating their own neuroimaging data with local biophysical models. Here, we give a detailed description of the TVB modeling process and explore model parameters associated with stroke. In order to establish a parallel between this new type of modeling and those currently in use, in this work we establish an association between a specific TVB parameter (long-range coupling) that increases after stroke with metrics derived from graph analysis. We used TVB to simulate the individual BOLD signals for 20 patients with stroke and 10 healthy controls. We performed graph analysis on their structural connectivity matrices calculating degree centrality, betweenness centrality, and global efficiency. Linear regression analysis demonstrated that long-range coupling is negatively correlated with global efficiency ($P = 0.038$), but is not correlated with degree centrality or betweenness centrality. Our results suggest that the larger influence of local dynamics seen through the long-range coupling parameter is closely associated with a decreased efficiency of the system. We thus propose that the increase in the long-range parameter in TVB (indicating a bias toward local over global dynamics) is deleterious because it reduces communication as suggested by the decrease in efficiency. The new model platform TVB hence provides a novel perspective to understanding biophysical parameters responsible for global brain dynamics after stroke, allowing the design of focused therapeutic interventions.

Keywords: stroke, brain dynamics, graph theory, computational biophysical modeling, connectome, brain networks, imaging, MRI

INTRODUCTION

Heterogeneity of functional outcomes following stroke remains a major limitation to stroke rehabilitation. While the majority of stroke survivors suffer from motor impairment, particularly in the upper extremities (1), the degree and type of this impairment and the level of recovery following rehabilitation are highly variable (2). The functional basis for variation in patient deficits is still poorly understood, and there is no consensus on a theoretical or empirical framework for linking brain injury to functional deficits (3). In order to address this issue, recent approaches in stroke rehabilitation have aimed at the development and the optimization of individualized treatments that maximize long-term functional gains (4, 5).

To this end, different theoretical approaches have been used. The most general method has probed stratification measures based on patient demographics, behavioral outcomes, affective states, brain function, and lesion characteristics (4–6). None have been shown as a reliable biomarker. Particularly noticeably has been the presence of an inconsistent relationship between brain lesion and the resulting functional deficits (6), likely due to the inherent complexity of damage in a highly interconnected brain.

Researchers have thus turned to network analysis to understand stroke (7–9). In this approach, one of the goals is to explain the observed variations after stroke and predict recovery. Interestingly, the initial efforts with network analysis focused on alterations to specific pathways as the key links to understand behavior (8, 10). For example, while some functional connectivity studies showed that lesions within the motor areas can cause dysfunction of remote brain regions (11–13), others showed a relationship between improved motor function and strengthening interhemispheric and intrahemispheric connectivity involving the primary motor cortex (14). An important issue in interpreting such relationships is that the changes may reflect either the abnormal functioning of a damaged network or the formation of a different network that results in new behavioral patterns.

Furthermore, while these initial studies have been an important development, their main limitation is that they assume stable, localized changes within specific sub-networks, obliterating global changes, with the consequence that these potential biomarkers have been very adequate as descriptors at the group level but not in individual patients (15).

Recently, the neuroimaging community has begun to focus on connectomics, or the mapping of all connections at the whole-brain level. These connectomes, derived from structural [diffusion tensor imaging (DTI)] or functional outputs (fMRI and EEG), have recently been termed “big data,” referring to datasets that require the generation of large amounts of multimodal imaging data, (including raw, preprocessed, and intermediate data), for a high number of subjects (16). These initiatives span normal function [Human Connectome Project (17), CONNECT (18), Brainnetome (19), development [National Institutes of Health (NIH) Pediatric Database] and brain disorders such as Alzheimer’s disease (Alzheimer’s Disease Neuroimaging Initiative)].

In order to help interpret such large datasets, graph theory is increasingly used to distinguish inherent patterns that likely correlate with brain networks at the whole-brain level. Using

connectomics and graph theory, specific brain regions can be understood as nodes (20), and lesions can be understood as damage to nodes and/or the connections among them. With these methods, stroke has been shown to produce changes in both structural and functional network connectivity, particularly related to the organization of “hubs,” or highly interconnected nodes (21, 22). Graph theory provides an assessment of the changes at an organizational level. However, this approach still suffers from some limitations, mainly the inability to determine dynamical changes in a constantly changing brain and the lack of concrete biophysical substrates for understanding those dynamics. Consequently, according to Smith et al., one of the major challenges in the field of functional connectomics “will be to enable application of biologically interpretable models using large numbers of nodes in a robust and practical way” (9).

In other words, although tackling questions about brain network dynamics in both healthy and stroke populations requires a great deal of data, simply collecting more data is not itself an answer. While these efforts provide the necessary empirical foundation, they lack a computational and theoretical framework with quantitative tools to link these multiple datasets to “reconstruct” the brain and provide the link between these data and the brain function of individuals.

In this context, novel theoretical perspectives have been proposed based upon the nature of the brain as a large-scale network (3, 23–25). The implementation of the framework has been significantly accelerated by The Virtual Brain (TVB), a novel large-scale neural modeling platform (26–28). TVB uses neuroimaging data to parameterize a model and because individual data is used, the individual person’s brain can become a “virtual brain.”

The Virtual Brain (thevirtualbrain.org) was developed as a platform for modeling the dynamics of large-scale neural systems (3, 29). TVB integrates structural long-range connectivity generated from empirical DTI data with mesoscopic, or local level models [at each node or region of interest (ROI)]. By combining these two scales (global connectivity with local dynamics), TVB is able to predict and simulate an individual’s brain activity, essentially modeling a virtual representation of their brain. TVB thus lies at the intersection of experimental and theoretical neurosciences, making it well positioned to provide a link between population and individual datasets.

The models available in TVB integrate the anatomical connectivity between parts of the brain (provided by DTI) and the dynamics of local neural populations (embedded in the platform). Using these models, TVB has the flexibility to generate simulated data ranging from local field potentials to EEG and fMRI BOLD signals, allowing for a multimodal link between simulated and empirical data. The scalable architecture of TVB allows us to include neurophysiological information (e.g., receptor distributions and ion channels) adding another level of detail and bringing the model’s behavior closer to the real brain. Spatiotemporal motifs as present in empirical EEG/fMRI data can be reproduced to a large degree (29, 30). Because biophysical parameters are invisible to brain-imaging devices, TVB acts as a “computational microscope” that allows the inference of internal states and processes of the large-scale model.

The Virtual Brain therefore serves as a powerful research tool that has the potential to utilize big data and to develop and test advanced theories of brain dynamics. The individualization of TVB allows the creation of one model per person and systematically assesses the modeled biophysical parameters related to individual differences. The natural extension of this approach goes further into clinical applications, deriving parameters that both relate to biophysics and predict clinical outcome, making TVB an ideal tool for addressing limitations in stroke research.

The objective of this manuscript is twofold:

- (1) To give a thorough overview of the modeling method employed using TVB as it pertains to stroke, with the goal of providing details for those interested in using it in the context of stroke.
- (2) To provide a link between one of the TVB parameters (long-range coupling) to current whole-brain analytical approaches based on graph analysis.

MATERIALS AND METHODS

Subjects

Twenty individuals with ischemic stroke in the middle cerebral artery territory (41.13 ± 23.78 months postonset) and 10 age-matched controls were recruited for the study. Demographics for all stroke subjects are shown in **Table 1**.

Imaging Acquisitions

Magnetic resonance images were collected using a 3-T Philips scanner and an eight-channel SENSE head coil for signal reception and body coil transmitter for signal excitation. The following sequences were used:

1. High-resolution anatomical images (T1-w): three-dimensional (3D) Magnetization Prepared Rapid Gradient Echo sequence, FOV = 250×250 , resolution = $1 \text{ mm} \times 1 \text{ mm} \times 1 \text{ mm}$, SENSE reduction factor = 1.5, TR/TE = 7.4/3.4 ms, flip angle = 8, sagittal orientation, and number of slices = 301 covering the whole brain.
2. Diffusion Tensor Imaging (DTI): FOV = 224×224 , TR/TE = 13,030/55, 72 slices, slice thickness = 2 mm, resolution = $0.875 \times 0.875 \times 2$, $b = 1,000 \text{ s/mm}^2$ (and $b = 0$), 32 diffusion directions.
3. Functional imaging acquisition at rest (rsfMRI): whole brain (37 slices), single-shot echo-planar MR (EPI), slice thickness = 4.0 mm, FOV = 230×230 , voxel size = $2.8 \text{ mm} \times 2.8 \text{ mm}$, TR/TE = 2,000/20 ms, and duration = 5 min.

Resting State fMRI Preprocessing

Resting state fMRI (rsfMRI) preprocessing analysis was performed using AFNI functions (31) and included the following steps:

1. Motion correction using a six-parameter 3D registration of functional and anatomical data sets (32).
2. Three-dimensional spatial registration to a reference acquisition from the first fMRI run.
3. Registration of functional images to the anatomical volume.
4. Despiking of the time series.
5. Mean normalization of the time series.
6. Inspection and censoring of time points occurring during excessive motion ($>1 \text{ mm}$) (33).
7. Regression of cerebrospinal fluid and white matter signals to remove slow drifts in the fMRI signal.

TABLE 1 | Demographics and stroke characteristics of the stroke cohort.

Subject	Age	Sex	Handedness	Affected hemisphere	Affected hand	Stroke location	Stroke volume (mm ³)
1	41	F	Right	Right	ND	Cort	22,495.0
2	54	F	Right	Left	D	Cort/subcort	49,078.0
3	57	M	Right	Left	D	Cort/subcort	17,411.0
4	57	M	Right	Left	D	Cort/subcort	38,703.0
5	54	F	Right	Left	D	Subcort	27,677.0
6	50	M	Right	Right	ND	Subcort	3,570.0
7	23	M	Right	Left	D	Subcort	560.0
8	55	F	Right	Right	ND	Cort	6,781.0
9	68	M	Right	Left	D	Subcort	1,988.3
10	56	F	Right	Left	D	Subcort	6,239.7
11	46	M	Right	Left	D	Subcort	325.0
12	56	F	Left	Right	D	Cort/subcort	60,669.0
13	37	M	Right	Left	D	Cort/subcort	83,406.2
14	62	M	Right	Left	D	Subcort	22,154.8
15	57	M	Right	Right	ND	Cort/subcort	25,392.0
16	66	M	Right	Left	ND	Cort/subcort	19,927.0
17	61	M	Right	Left	D	Subcort	978.0
18	74	M	Right	Left	D	Cort/subcort	63,642.0
19	67	F	Right	Right	ND	Subcort	588.0
20	74	F	Right	Left	D	Cort/subcort	44,892.0

D, dominant hemisphere; ND, non-dominant; Cort, cortical; subcort, subcortical.

Preprocessing: Structural Connectivity Brain Parcelation

Parcellating image data that contain lesions with the use of semiautomated schemes produce inaccurate results due to the absence of tissue and consequent mechanical deformation. We therefore developed The Virtual Brain transplant (VBT). This method effectively replaces the lesion produced by the cortical stroke with T1-w images of brain tissue from the contralesional hemisphere from the same subject (34). This method allows us to use a semiautomated parcelation scheme subsequent to the transplant. The VBT process consisted of the following steps (Figure 1):

1. Lesion segmentation by hand.
2. The high-resolution anatomical T1-w brain images and lesion masks were uploaded to a transplantation pipeline, which dissected the MRI brain tissue from the non-lesioned hemisphere homologous to the lesion, and transplanted it into the lesioned hemisphere at the site of the lesion, filling in the missing portions of the brain.
3. After the initial transplant was done, manual corrections in the interface between the native and transplanted T1-w images were performed.
4. The brain was segmented into 83 cortical and subcortical regions using the Lausanne 2008 (Freesurfer) parcelation scheme within the Connectome Mapper Toolkit (35, 36).

T1-w to DTI Alignment

The T1-w anatomical image was then aligned to a reference $b = 0$ s/mm² DTI image, using a six degrees of freedom linear transformation with FSL's FLIRT function (37). This transformation was also applied to the Freesurfer parcelations.

DTI Tractography

We performed the following steps:

1. DWI was aligned to the same reference $b = 0$ s/mm² image used to align the corrected T1-w via VBT to DTI. Distortions caused by eddy currents and head motion were corrected using the FSL eddy current correction (12 degrees of freedom linear transformation), and the diffusion gradient vectors rotated accordingly (38). That is, the T1-w images with the "transplanted masks" are used to supply the region of interest landmarks for tractography but do not directly impact the tractography algorithm as the transplant is not performed in the DWI space.
2. The diffusion-weighted images were resampled to 2mm isotropic resolution (39).
3. White matter deterministic tractography of DTI data was performed in Trackvis software (39) using the FACT algorithm (40). Threshold values of a maximum of 60° turning angle and a minimum of 0.20 fractional anisotropy (FA) were used as stopping criteria for the tracking algorithm. These thresholds take into account the decrease in signal in regions with the lesion. The FA threshold is particularly useful in

terminating tracks before they enter regions containing the lesion. These regions, filled with CSF, have FA values close to zero. Therefore white matter pathways ordinarily connecting two ROIs will not be tracked if the ROI is completely lesioned, despite appearing intact in the transplanted T1-w image from which the parcelation is made. If a parcelation is partially compromised by the lesion then white matter pathways will also be partially tracked as reflected by a lesser number of streamlines.

Generation of Structural Connectivity Matrices

Using the Connectome Mapper Toolkit, two connectivity metrics were extracted for each pathway in order to generate two structural connectivity matrices that quantify connectivity between all pairs of the cortical regions for each subject:

1. Weights, defined as $FA \times \text{number of streamlines}$ in the pathway (note that per the white matter deterministic tractography of DTI data, pathways connecting regions impacted by the lesion will show a decreased number of streamlines and potentially altered FA). This metric reflects the maximum rate of transmission of information through edges (41). The number of streamlines in the pathway was assessed using the deterministic FACT algorithm.
2. Lengths of the individual tracts, defined in millimeters, were derived after smoothing the tractography with a B-Spline filter (39).

These matrices are symmetrical, as connections using DTI are considered unidirectional (30).

Modeling with TVB

Modeling with TVB involves three initial steps, namely the import of individual structural connectivity matrices (obtained as described earlier), the selection of a biophysical local model, and the choice of relevant biophysical parameter values. TVB has several types of local models available, each one taking into account different biophysical parameters. Hence, whereas some are focused on field potentials [Stefanescu–Jirsa two dimensional (2D) and Stefanescu–Jirsa 3D (SJ3D)], others are focused on firing rates (Wilson–Cowan, Brunel–Wang, and Jansen–Rit) or are phenomenological (Generic 2D, Kuramoto, and Epileptor). In our previous efforts, since we simulated the BOLD response, the mesoscopic model used was the SJ3D, one of the more complex and refined models in the repertoire of TVB.

The reasoning behind this choice was not only the obvious relationship between the BOLD response and local field potentials (42–44) but the additional fact that the BOLD signal has poor time resolution and the model does not rely heavily on synaptic delays. Concretely, the SJ3D model is a reduced form of the Hindmarsh–Rose model (43), which forecasts individual neuronal behavior. The SJ3D model predicts local dynamics using six differential equations that include variables representing *physiological properties* such as neuron membrane potentials, transport of ions across the membrane through fast and slow ion channels, and the dynamic coupling of excitatory and inhibitory neuronal populations.

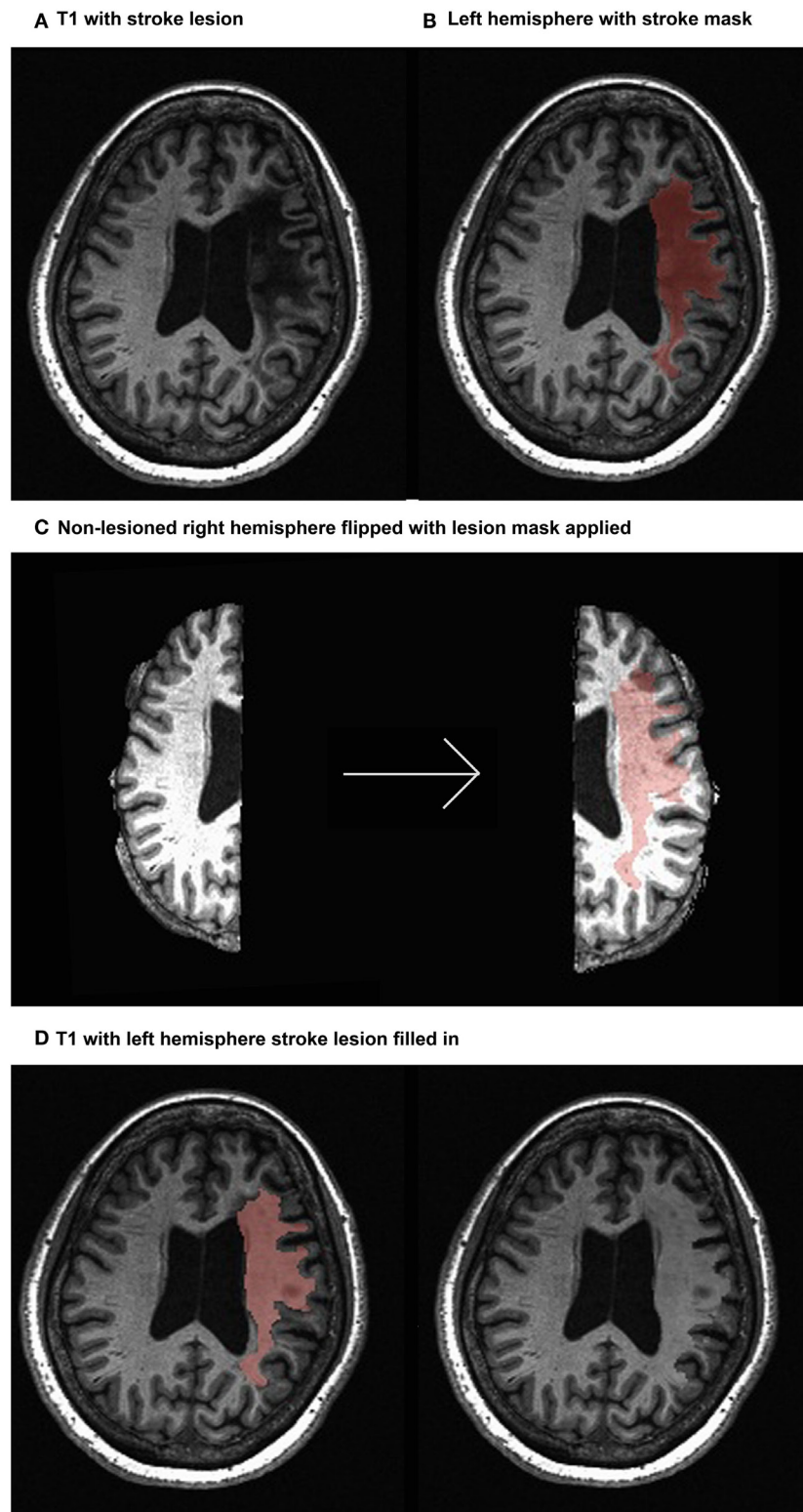


FIGURE 1 | Virtual brain transplant method. Virtual brain transplant is done in stroke cases with cortical damage with the goal of being able to parcellate the brain. This graphic representation summarizes the process of replacing the damaged portion of the brain with the homologous non-stroke tissue. **(A)** T1-w image showing the lesion (left hemisphere) of one subject. **(B)** Close-up of the left hemisphere, demarcating the lesion mask in red. **(C)** Segregation of the right and left hemispheres (left) and after the right hemisphere has been flipped having the lesion mask applied (right). **(D)** Depiction of the tissue from the right hemisphere applied to the lesion in the left hemisphere (left) and the resulting transplanted brain volume (right).

The sequential steps for modeling in TVB are as follows (graphical depiction can be found in **Figure 2**):

1. Importing the two metrics derived from individualized SC matrices [weights ($FA \times \text{number of fibers}$) and lengths] representing connections between regions, along with the T1-w structural data providing individual brain topology.
2. Parameter space exploration: the goal of this process is the optimization of the model parameters. When applying TVB methodology to stroke, one can classify the numerous parameters included in the modeling into two categories: global parameters that will model brain dynamics between nodes, and local parameters that will describe brain dynamics within nodes. In the first category, the two main parameters to optimize are conduction velocity and long-range coupling. Likewise the biophysical parameters within the SJ3D model to be used are those providing the coupling between excitatory and inhibitory populations within the local regions: K_{11} (excitatory on excitatory), K_{12} (excitatory on inhibitory), and K_{21} (inhibitory on excitatory). This exploration systematically explores the entire range of available values for each parameter and identifies the value with the highest overall distribution of variance (**Figure 3**) as the optimal parameter value to be used on each individual for the actual signal simulation. The order of optimization can be done as follows:
 - a. Long-range coupling and conduction velocity: starting ranges are 0.001–0.1 global coupling and 1–100 conduction velocity.
 - b. K_{12} and K_{21} : starting ranges are 0–1.0 for both. K_{12} is optimized first, and the identified value is then used when optimizing K_{21} .
 - c. K_{11} : starting range is 0–1.0.
3. Simulating the BOLD response: based on the values obtained in the parameter exploration, simulation of the BOLD time series should reflect the same duration (4 min) and sampling rate ($TR = 2$ s) of the empirical MRI acquisition. Noise is added to each node. The noise to be used is white with Gaussian amplitude (mean = 0, standard deviation = 1). Numerical integration of the system is performed using stochastic Heun's method (45), with an integration step size of 0.0122 ms.
4. Validating the simulated brain signals: this is done by comparing the simulated and empirical time series in terms of their amplitude, frequency, and phase.
 - a. Amplitude: the range is calculated by identifying the highest and lowest peaks present in the time series across all regions. The overall mean is calculated by averaging the mean amplitude per region across all regions. Mean amplitudes should be similar. An example is shown in **Figure 4A**.
 - b. Frequency is computed via fast Fourier transforms of the time series with Matlab's "fft" function with an fs of 0.5 Hz

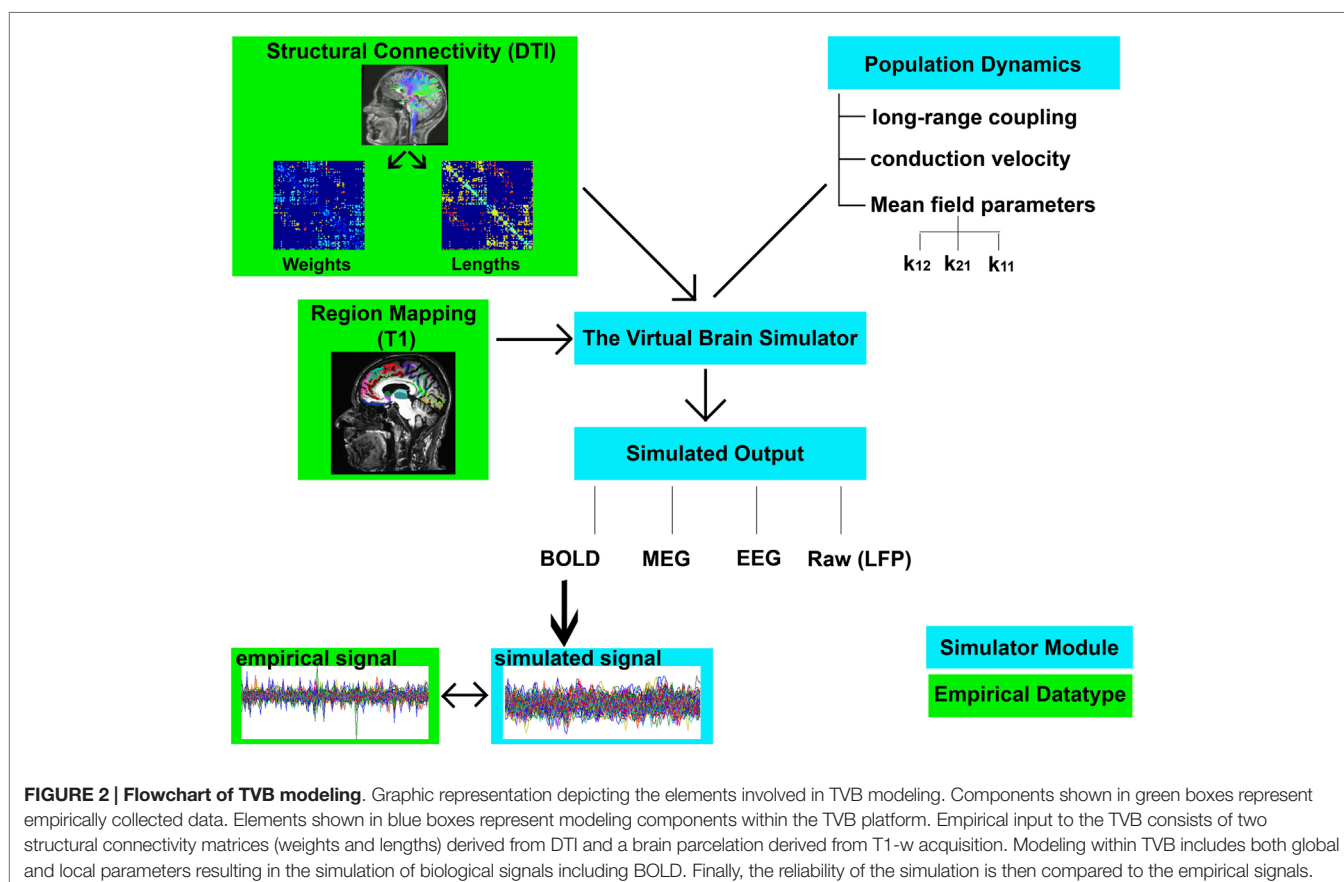


FIGURE 2 | Flowchart of TVB modeling. Graphic representation depicting the elements involved in TVB modeling. Components shown in green boxes represent empirically collected data. Elements shown in blue boxes represent modeling components within the TVB platform. Empirical input to the TVB consists of two structural connectivity matrices (weights and lengths) derived from DTI and a brain parcellation derived from T1-w acquisition. Modeling within TVB includes both global and local parameters resulting in the simulation of biological signals including BOLD. Finally, the reliability of the simulation is then compared to the empirical signals.

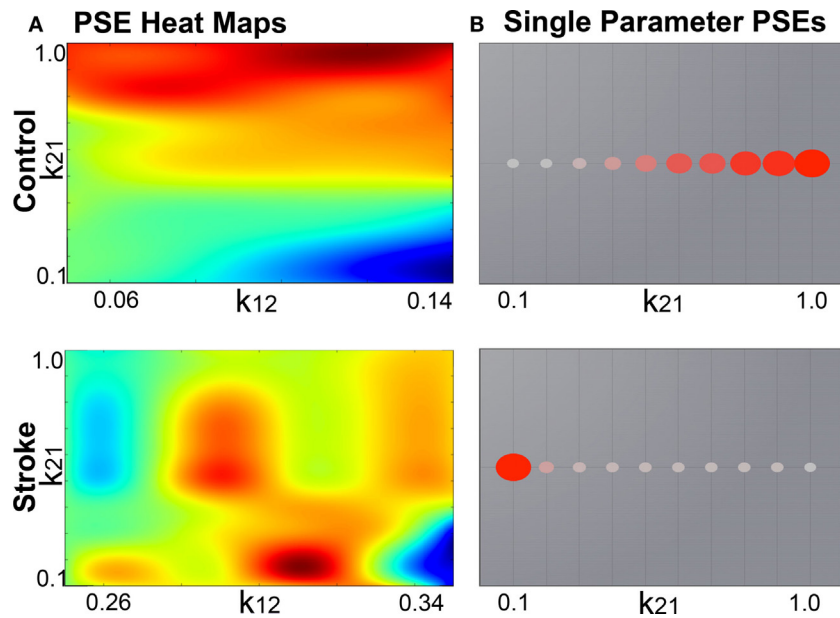


FIGURE 3 | Example global parameter space explorations in healthy and stroke cases. This figure represents the two viewing options for multiple parameter or single parameter explorations. **(A)** Parameter explorations of the K_{12} and K_{21} variables (coupling between inhibitory and excitatory populations) in one healthy control (top) and one stroke case (bottom). Heat maps depict the distribution of system variance, with hotter colors indicating values of parameters that yield higher variance. High resolution of heat maps allows for identification of precise parameter values related to high variance. **(B)** Parameter exploration of the K_{21} variable alone, after optimization has been completed. Colored circles depict degree of variance at each value of K_{21} .

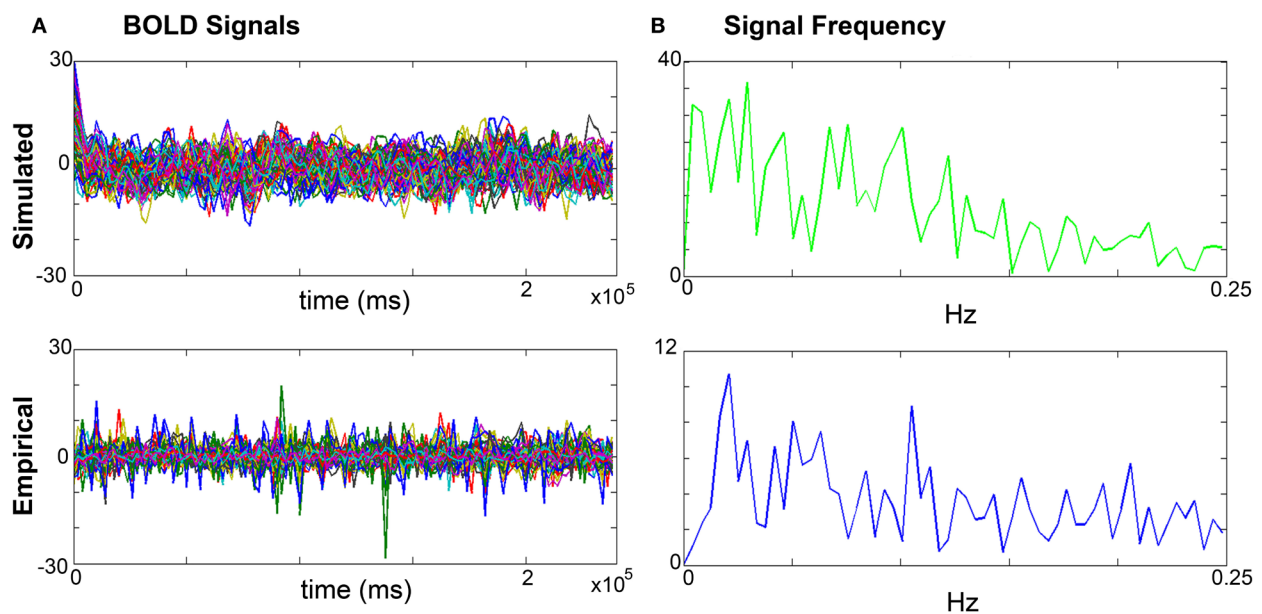


FIGURE 4 | Comparisons of simulated and empirical signals: amplitude and frequency. **(A)** BOLD time series: example of a simulated (top) and empirical (bottom) time series. Note the similarity of amplitudes as indicated by the maxima and minima. **(B)** Frequency: example frequency distribution graphs for primary motor cortex (M1) of the simulated (top) and empirical (bottom) time series where both signals have similar profiles and peaks.

to determine the range, profile, and peak frequencies. The maximum frequency for simulated signals should be around 0.25 Hz that coincides with the empirical BOLD responses. An example is shown in **Figure 4B**.

c. Phase can be done by calculating the pair-wise covariance of the time series for each region for each subject (30) using the “corr” function in Matlab, which results in a functional connectivity matrix for each subject. In order to smooth the

data, one can average all matrices from groups of interest to obtain a group control matrix and then calculate the pairwise linear correlation coefficient between the simulated functional connectivity matrix for each individual to the group (**Figure 5**). Results from this analysis should reveal similar phases between empirical and simulated signals. Significance of the correlation can be achieved via Fisher Z-transformation.

Comparison Between Healthy Controls and Stroke

We found an increase in long-range coupling in the stroke group compared to healthy controls. The meaning of long-range coupling is not intuitive, especially when compared to other parameters more closely linked to biophysical features, such as conduction velocity, channel dynamics, and the coupling between excitatory and inhibitory neuronal populations. The long-range coupling function is applied to the activity propagated between brain region regions by the structural pathways before it enters the local dynamic equations of the model. Its primary purpose is to rescale the incoming activity to a level appropriate to model. At a more intuitive level this parameter describes the balance between the global and the local dynamics. In other words, an increase in long-range coupling suggests a preponderance of local over long-range brain dynamics.

In order to put this parameter in the context of current network analytical approaches, in this study we determined the relationship between the modeled long-range coupling in stroke cases with structural network metrics derived from graph analysis including degree centrality, betweenness centrality, and global efficiency.

Graph Analysis

Graph Analysis Metrics

Based on the deterministic tractography performed for each individual subject, a binary adjacency matrix A_{ij} was generated

whose elements represent the connections (edges) between nodes i and j (46–48). From these matrices, three measures of functional integration were obtained: average degree centrality, average betweenness centrality, and global efficiency as others have done (49–51), using the NetworkX software (52) [mathematical notation adapted from (20)]:

1. Average degree centrality is the number of nodes adjacent to node i , averaged across all nodes in the graph (53):

$$k_{av} = \frac{1}{n} \sum_{i \in N} k_i = \frac{1}{n} \sum_{i, j \in N} a_{ij}$$

where n is the number of nodes in the graph, and N is the set of those nodes; k_i is the degree centrality for node i , and a_{ij} equals 1 when nodes i and j are the nearest neighbors and zero otherwise. This is the simplest measure of centrality and is commonly used to discriminate between well-connected nodes (hubs) and less well-connected nodes (51).

2. Average betweenness centrality refers to the fraction of shortest paths between any pair of nodes in the network that travel through a given node averaged across all nodes (54):

$$b_{av} = \frac{1}{n} \sum_{i \in N} b_i = \frac{1}{n} \sum_{i \in N} \frac{2}{(n-1)(n-2)} \sum_{\substack{h, j \in N \\ h \neq i, j \neq i}} \frac{p_{hj}(i)}{p_{hj}}$$

where b_i is the betweenness centrality for node i ; p_{hj} is the number of shortest paths between nodes h and j , and $p_{hj}(i)$ is the number of shortest paths between h and j that pass through node i . This is the oldest and most commonly used measure of centrality (51) where “shortest” refers to the path between two nodes that contains the least number of intermediate nodes.

3. Global efficiency is the average of the inverse of the shortest path length between all nodes (minimum number of edges traversed to connect one node to another) (21, 53):

$$E = \frac{1}{n} \sum_{i \in N} E_i = \frac{1}{n} \sum_{i \in N} \frac{\sum_{j \in N, j \neq i} d_{ij}^{-1}}{n-1}$$

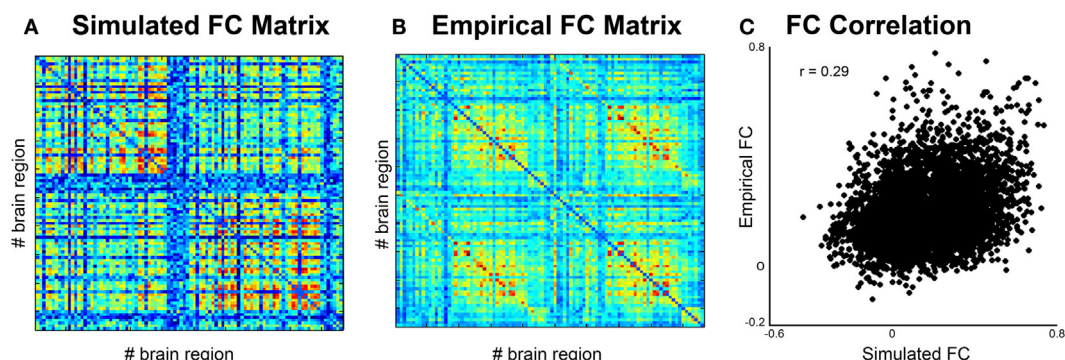


FIGURE 5 | Comparison of simulated and empirical signals: phase. (A) Functional connectivity matrix from simulated data modeled from one subject. (B) Average functional connectivity matrix from empirical data from all healthy subjects. (C) Correlation of functional connectivity between simulated (x-axis) and empirical (y-axis) time series.

where d_{ij}^{-1} is the inverse of the shortest path length between nodes i and j . For binary matrices, a network where each node has a direct connection to all other nodes in the graph has maximal global efficiency, equal to 1, while a partially disconnected network has lower global efficiency (49).

Comparison of Graph Analysis Metrics Between Groups

To test for differences in degree centrality, betweenness centrality, and global efficiency between healthy and stroke cases, we used the Wilcoxon-rank sum test. Significance threshold was set to $P = 0.017$ (Bonferroni correction). A simple linear regression analysis was used to correlate TVB long-range coupling (independent variable) with graph analysis metrics (dependent variables).

RESULTS

Comparison of Graph Analysis Metrics Between Stroke Cases and Healthy Controls

Results from the Wilcoxon-rank sum test showed no significant differences between healthy controls and stroke cases in degree centrality ($P = 0.11$), betweenness centrality ($P = 0.86$), or global efficiency ($P = 0.0822$). However, the distributions of each graph analysis metric between the two groups showed differences (Figure 6). Specifically, global efficiency showed a trend toward lower values in stroke cases compared to controls ($P = 0.04$) but not degree centrality ($P = 0.22$) nor betweenness centrality ($P = 0.95$). While there was not a statistical difference in distribution of

degree centrality between healthy and stroke populations, a large amount of subjects showed lower values of degree centrality.

Correlation Between Long-Range Coupling and Graph Analysis Metrics

Linear regression analysis showed that the only graph analysis metric associated with the TVB long-range coupling parameter was global efficiency (Figure 7). That is, higher values of global coupling were correlated with lower values of global efficiency ($t = -2.19$, $P = 0.038$). There was no significant correlation between global coupling and degree centrality ($P = 0.7$) or betweenness centrality ($P = 0.6$).

DISCUSSION

We have demonstrated that TVB can be a novel tool for identifying biophysical biomarkers of stroke recovery, showing that (1) the parameters associated with TVB modeling directly link structural imaging data to biophysical processes associated with brain dynamics; (2) the models are individualized, as they are based on the specific structural connectome from each person; and (3) TVB parameters can be correlated with other metrics not currently associated with biological parameters (i.e., graph analysis metrics). Importantly, this study harnessed the relationship between TVB and graph analysis, wherein the latter supplies an additional description of changes in relationships between different brain regions, while TVB supplies the neurobiological mechanisms responsible for them. The outlined steps using TVB offer a unique method, providing a new dimension to the study of stroke.

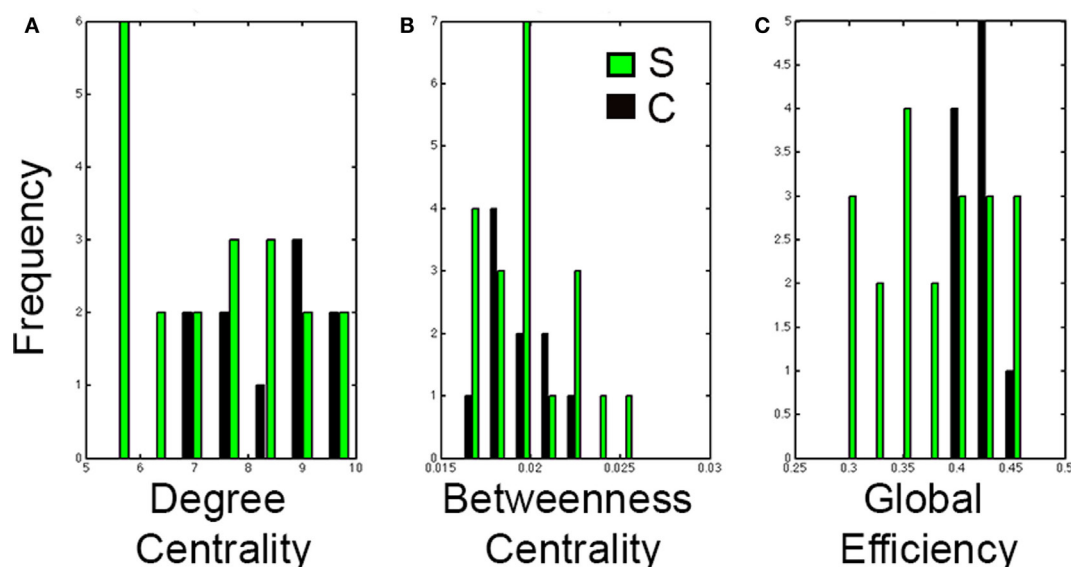
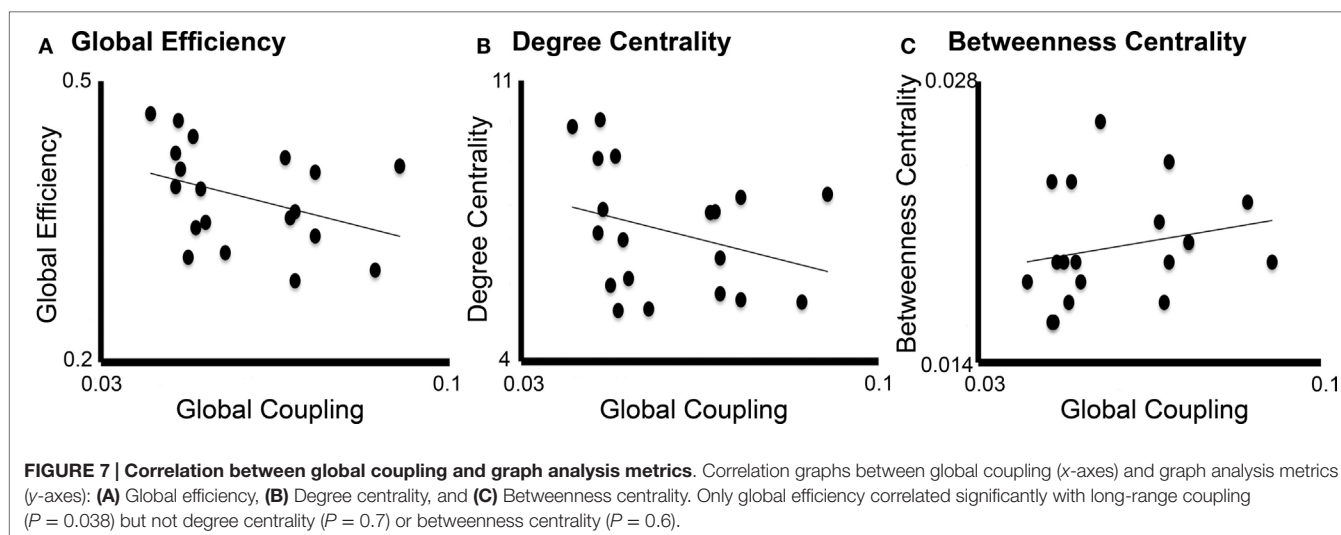


FIGURE 6 | Distributions of graph analysis metrics in control and stroke cases. Distribution graphs comparing the control (black) and stroke (green) cases for (A) Degree centrality, (B) Betweenness centrality, and (C) Global efficiency. Note that distributions in stroke shift to the left for global efficiency but not for degree centrality nor for betweenness centrality.



TVB Integrates Macroscopic and Mesoscopic Levels to Predict Brain Dynamics

There is currently no way to directly measure the local parameters modeled in TVB in humans, whereas global measures derived from imaging data have been used as potential biomarkers of stroke recovery (6, 55), the parameters considered within TVB at the local level represent a dimension reduction derived from processes at the cellular or even molecular levels. That is, the mesoscopic level represents the transitional state between the macro- and microscales (56). Thus, these parameters better inform us of underlying brain mechanism responsible for brain dynamics that current imaging analyses are unable to access, such as dynamics between excitatory and inhibitory neuronal populations and ion channel properties. In this way, TVB can assist to generate hypotheses associated with basic mechanisms that are responsible for the changes in brain dynamics associated with stroke.

In this context, it is important to mention that TVB can have wide applicability in the clinical setting because the input required for its operation can be minimal. In ideal circumstances, the experimental data needed are T1-w, fMRI (EEG or MEG), and DTI. However, some of these categories may not be necessary when only physiological data are available (e.g., EEG) without anatomical or connectivity data. In these cases, TVB platform includes normalized anatomical data (a parcellated cortical surface based on the MNI atlas) and a theoretical structural connectome based on the CocoMac database (3, 57). For stroke cases, while it is preferable to have anatomical data, it is still possible to run accurate simulations by manually modifying this provided structural connectome to exemplify the individual lesions.

The Resulting TVB Models are Individualized

There is large consensus on the importance of individualized medicine as one of the means to improve medical care. In this

sense, a central feature of TVB is its direct focus on individual subjects' brain dynamics. The structural connectivity matrix of each individual drives the modeling producing the individualized simulated brain activity, whereas the applicability of previous studies has been at the group level (15). By generating reliable simulations, the system provides a window into the state of bio-physical parameters associated with it in each person and hence enables the development of customized, individualized therapies and treatments.

There are a myriad of stroke therapies currently under investigation, including constraint-induced motor therapy (58–60), action observation therapy (61, 62), neurostimulation (e.g., transcranial magnetic stimulation and transcranial direct-current stimulation) (63, 64), robotic therapy (65, 66), and cellular-based (e.g., stem cell) therapies (67), that have shown limited degrees of effectiveness, due perhaps to the fact that they are not specifically targeting brain mechanisms responsible for individual dysfunction. This is a reflection of the paucity in our understanding of basic mechanisms generating individual brain dynamics. Having new hypotheses applicable to each patient will enable us to generate new therapeutic interventions that specifically target the elements producing particular brain states. Furthermore, the more we learn about basic processes based on animal studies for instance, the more we can modify current TVB local models and hence, obtain more sophisticated simulations.

TVB Parameters can be Related to Other Network Metrics

An additional feature of parameters derived from TVB is that they can be contrasted with other measures. Our results showed a trend toward decreased global efficiency in stroke that measures the network's capacity for communication, with greater efficiency indicating better overall communication (20, 49). In other words, network communication is impaired after stroke. Interestingly,

degree centrality and betweenness centrality after stroke were not different from healthy controls probably due to the large variance of stroke size.

The negative correlation between global efficiency and the modeled long-range coupling provides unique insight into the network structure of the brain following stroke. We have previously observed increased long-range coupling after stroke, intuitively indicating a higher influence of local dynamics on brain activity than long-range dynamics. In this context, it is important to remember that the global model is derived from the structural connections between nodes, and hence, one would expect that shorter (direct) paths that originate from damaged nodes should be compromised. The graph analysis results suggest that the post-stroke connectivity between nodes is done through less efficient, longer paths (20). Therefore, decreased global efficiency and increased long-range coupling after stroke suggest a breakdown in the ability to transfer information between regions, weighting the activity toward local dynamics. Our findings thus highlight the global impact of stroke, despite its relatively focal damage. This novel finding in stroke is consistent with studies in other neurological diseases, such as schizophrenia, where imbalances between local and global dynamics, specifically a breakdown of local structure and a shift toward global dynamics have been suggested (68).

Limitations

The Virtual Brain as any modeling approach is laden with limitations. Among them:

1. The fact that TVB simulations depend on structural connectivity assumes the structural matrices having reasonable reliability. This is very relevant in stroke because the damage can produce mechanical distortions of tissue. In our case, we have used TVB transplant to minimize these issues. Additionally, there are many definitions of “weights” of connections (69, 70) although novel approaches promise at least high intraindividual reliability in the reconstruction (71). In our case, we used a surrogate measure reflecting the “number of fibers per pathway.” This is the reason why we normalized the number of streamlines between nodes by the FA of the particular pathway.
2. The weights of connections are currently based on the size (number of streamlines) of the pathways, yet the particular features of the synaptic connections are not taken into consideration. For example, the penetrance of a smaller pathway could be larger than a bigger pathway if the former establishes the synaptic contact with more proximal versus distal dendrites. This type of information is available for other species but is not yet known in humans.

Future Directions and Clinical Impact

The ability of generating a virtual brain from any individual opens up an interesting venue for therapeutics. Once a hypothesis is

derived from the biophysical parameters affected by the stroke, the effects on brain dynamics can be tested within the TVB platform by modifying the parameters for an individual case. In this way, TVB can be used as a test for potential therapeutic interventions before they are tested in animal models or individual patients.

The Virtual Brain thus has the potential to revolutionize stroke treatment in the future, by allowing for:

1. The application to “big data.” While the current study used a smaller sample size, once we have parameter changes, future studies can more readily utilize TVB in a large number of patients.
2. The ability to study longitudinal brain changes in stroke, from acute and sub-acute to chronic stroke. Because of the predictive potential of TVB, the inclusion of patients at early stages can provide the identification of powerful biomarkers for recovery.
3. The individualization of treatment with minimal input: one single MRI scan including the anatomical scan, DTI, and resting state fMRI.
4. The ability to perform whole-brain modeling, integrating the particular intercommunication between nodes (DTI derived) to local biophysical models associated with concrete basic functional parameters.
5. The opportunity to identify tangible targets for treatment that are testable within the application itself.
6. An open source platform: it is possible to add new, more sophisticated mesoscopic and microscopic models via the open source nature of TVB. Therefore, new developments on basic physiological knowledge can be easily integrated in the future.
7. Allowing the simulation of resting state brain activity, as was done in this study, but also of evoked responses through a built-in feature that allows for the stimulation of brain areas, with features determined by the modeler.

AUTHOR CONTRIBUTIONS

All authors had full access to all data in the study and take responsibility for the integrity of the data and the accuracy of the data analysis. Study concept and design: AS, VJ, and MF. Analysis and interpretation of data: AS, MF, JR, VJ, EC, ADS, and AM. Drafting of the manuscript: MF, AS, VJ, and ADS. Critical revision of the manuscript for important intellectual content: AS, VJ, JR, and AM. Statistical analysis: EC. Obtained funding: AS, VJ, and AM. Study supervision: AS and VJ.

ACKNOWLEDGMENTS

This work was supported by the James McDonnell Foundation (NRG Group) and the NIH (NIH RO1-NS-54942).

REFERENCES

- Nichols-Larsen DS, Clark PC, Zeringue A, Greenspan A, Blanton S. Factors influencing stroke survivors' quality of life during subacute recovery. *Stroke* (2005) **36**(7):1480–4. doi:10.1161/01.STR.0000170706.13595.4f
- Reinkensmeyer DJ, Guigon E, Maier MA. A computational model of use-dependent motor recovery following a stroke: optimizing corticospinal activations via reinforcement learning can explain residual capacity and other strength recovery dynamics. *Neural Netw* (2012) **29–30**:60–9. doi:10.1016/j.neunet.2012.02.002
- Jirsa VK, Sporns O, Breakspear M, Deco G, McIntosh AR. Towards The Virtual Brain: network modeling of the intact and the damaged brain. *Arch Ital Biol* (2010) **148**:189–205.
- Cramer SC. Stratifying patients with stroke in trials that target brain repair. *Stroke* (2010) **41**(10 Suppl):S114–6. doi:10.1161/STROKEAHA.110.595165
- Munshi A, Sharma V. Genetic signatures in the treatment of stroke. *Curr Pharm Des* (2015) **21**(3):343–54. doi:10.2174/1381612820666140826113502
- Burke E, Cramer SC. Biomarkers and predictors of restorative therapy effects after stroke. *Curr Neurol Neurosci Rep* (2013) **13**(2):329. doi:10.1007/s11910-012-0329-9
- Baldassarre A, Ramsey L, Hacker CL, Callejas A, Astafiev SV, Metcalf NV, et al. Large-scale changes in network interactions as a physiological signature of spatial neglect. *Brain* (2014) **137**(Pt 12):3267–83. doi:10.1093/brain/awu297
- Carter AR, Shulman GL, Corbetta M. Why use a connectivity-based approach to study stroke and recovery of function? *Neuroimage* (2012) **62**(4):2271–80. doi:10.1016/j.neuroimage.2012.02.070
- Smith SM, Vidaurre D, Beckmann CF, Glasser MF, Jenkinson M, Miller KL, et al. Functional connectomics from resting-state fMRI. *Trends Cogn Sci* (2013) **17**(12):666–82. doi:10.1016/j.tics.2013.09.016
- Ward NS. Neural correlates of outcome after stroke: a cross-sectional fMRI study. *Brain* (2003) **126**(6):1430–48. doi:10.1093/brain/awg145
- Carter AR, Astafiev SV, Lang CE, Connor LT, Rengachary J, Strube MJ, et al. Resting interhemispheric functional magnetic resonance imaging connectivity predicts performance after stroke. *Ann Neurol* (2010) **67**(3):365–75. doi:10.1002/ana.21905
- Rehme AK, Grefkes C. Cerebral network disorders after stroke: evidence from imaging-based connectivity analyses of active and resting brain states in humans. *J Physiol* (2013) **591**(Pt 1):17–31. doi:10.1113/jphysiol.2012.243469
- Wang L, Yu C, Chen H, Qin W, He Y, Fan F, et al. Dynamic functional reorganization of the motor execution network after stroke. *Brain* (2010) **133**(Pt 4):1224–38. doi:10.1093/brain/awq043
- Grefkes C, Ward NS. Cortical reorganization after stroke: how much and how functional? *Neuroscientist* (2013) **20**(1):56–70. doi:10.1177/1073858413491147
- Mueller S, Keeser D, Samson AC, Kirsch V, Blautzik J, Grothe M, et al. Convergent findings of altered functional and structural brain connectivity in individuals with high functioning autism: a multimodal MRI study. *PLoS One* (2013) **8**(6):e67329. doi:10.1371/journal.pone.0067329
- Poldrack RA, Gorgolewski KJ. Making big data open: data sharing in neuroimaging. *Nat Neurosci* (2014) **17**(11):1510–7. doi:10.1038/nn.3818
- Sotiropoulos SN, Jbabdi S, Xu J, Andersson JL, Moeller S, Auerbach EJ, et al. Advances in diffusion MRI acquisition and processing in the human connectome project. *Neuroimage* (2013) **80**:125–43. doi:10.1016/j.neuroimage.2013.05.057
- Assaf Y, Alexander DC, Jones DK, Bazzi A, Behrens TEJ, Clark CA, et al. The CONNECT project: combining macro- and micro-structure. *Neuroimage* (2013) **80**:273–82. doi:10.1016/j.neuroimage.2013.05.055
- Jiang T. Brainnetome: a new -ome to understand the brain and its disorders. *Neuroimage* (2013) **80**:263–72. doi:10.1016/j.neuroimage.2013.04.002
- Rubinov M, Sporns O. Complex network measures of brain connectivity: uses and interpretations. *Neuroimage* (2010) **52**(3):1059–69. doi:10.1016/j.neuroimage.2009.10.003
- Crossley NA, Mechelli A, Scott J, Carletti F, Fox PT, McGuire P, et al. The hubs of the human connectome are generally implicated in the anatomy of brain disorders. *Brain* (2014) **137**(Pt 8):2382–95. doi:10.1093/brain/awu132
- Sporns O. Towards network substrates of brain disorders. *Brain* (2014) **137**:2117–8. doi:10.1093/brain/awu132
- Ghosh A, Rho Y, McIntosh AR, Kötter R, Jirsa VK. Cortical network dynamics with time delays reveals functional connectivity in the resting brain. *Cogn Neurodyn* (2008) **2**:115–20. doi:10.1007/s11571-008-9044-2
- Deco G, Jirsa VK, McIntosh AR. Emerging concepts for the dynamical organization of resting-state activity in the brain. *Nat Rev Neurosci* (2011) **12**:43–56. doi:10.1038/nrn2961
- Deco G, Jirsa VK, McIntosh AR. Resting brains never rest: computational insights into potential cognitive architectures. *Trends Neurosci* (2013) **36**:268–74. doi:10.1016/j.tins.2013.03.001
- Sanz Leon P, Knock SA, Woodman MM, Domide L, Mersmann J, McIntosh AR, et al. The Virtual Brain: a simulator of primate brain network dynamics. *Front Neuroinform* (2013) **7**:10. doi:10.3389/fninf.2013.00010
- Sanz-Leon P, Knock SA, Spiegler A, Jirsa VK. Mathematical framework for large-scale brain network modeling in The Virtual Brain. *Neuroimage* (2015) **111**:385–430. doi:10.1016/j.neuroimage.2015.01.002
- Woodman MM, Pezard L, Domide L, Knock SA, Sanz-Leon P, Mersmann J, et al. Integrating neuroinformatics tools in The Virtual Brain. *Front Neuroinform* (2014) **8**:36. doi:10.3389/fninf.2014.00036
- Ritter P, Schirner M, McIntosh AR, Jirsa V. The Virtual Brain integrates computational modelling and multimodal neuroimaging. *Brain Connect* (2013) **49**:1–65. doi:10.1089/brain.2012.0120
- Ritter P, Schirner M, McIntosh AR, Jirsa VK. The Virtual Brain integrates computational modeling and multimodal neuroimaging. *Brain Connect* (2013) **3**(2):121–45. doi:10.1089/brain.2012.0120
- Cox RW. AFNI: software for analysis and visualization of functional magnetic resonance neuroimages. *Comput Biomed Res* (1996) **29**(3):162–73. doi:10.1006/cbmr.1996.0014
- Cox RW, Jesmanowicz A. Real-time 3D image registration for functional MRI. *Magn Reson Med* (1999) **42**(6):1014–8. doi:10.1002/(SICI)1522-2594(199912)42:6<1014::AID-MRM4>3.0.CO;2-F
- Johnstone T, Ores Walsh KS, Greischar LL, Alexander AL, Fox AS, Davidson RJ, et al. Motion correction and the use of motion covariates in multiple-subject fMRI analysis. *Hum Brain Mapp* (2006) **27**(10):779–88. doi:10.1002/hbm.20219
- Solodkin A, Hasson U, Siugzdaitis R, Schiel M, Chen EE, Kotter R, et al. Virtual brain transplantation (VBT): a method for accurate image registration and parcellation in large cortical stroke. *Arch Ital Biol* (2010) **148**(3):219–41. doi:10.4449/aib.v148i3.1221
- Fischl B, Sereno MI, Dale AM. Cortical surface-based analysis. II: inflation, flattening, and a surface-based coordinate system. *Neuroimage* (1999) **9**(2):195–207. doi:10.1006/nimg.1998.0396
- Gerhard S, Daducci A, Lemkaddem A, Meuli R, Thiran J-P, Hagmann P. The connectome viewer toolkit: an open source framework to manage, analyze, and visualize connectomes. *Front Neuroinformatics* (2011) **5**:3. doi:10.3389/fninf.2011.00003
- Jenkinson M, Bannister P, Brady M, Smith S. Improved optimization for the robust and accurate linear registration and motion correction of brain images. *Neuroimage* (2002) **17**(2):825–41. doi:10.1006/nimg.2002.1132
- Leemans A, Jones DK. The B-matrix must be rotated when correcting for subject motion in DTI data. *Magn Reson Med* (2009) **61**(6):1336–49. doi:10.1002/mrm.21890
- Wedeer VJ, Wang RP, Schmahmann JD, Benner T, Tseng WYI, Dai G, et al. Diffusion spectrum magnetic resonance imaging (DSI) tractography of crossing fibers. *Neuroimage* (2008) **41**(4):1267–77. doi:10.1016/j.neuroimage.2008.03.036
- Mori S, van Zijl PCM. Fiber tracking: principles and strategies – a technical review. *NMR Biomed* (2002) **15**(7–8):468–80. doi:10.1002/nbm.781
- Zalesky A, Fornito A. A DTI-derived measure of cortico-cortical connectivity. *IEEE Trans Med Imaging* (2009) **28**(7):1023–36. doi:10.1109/TMI.2008.2012113
- Sotero RC, Trujillo-Barreto NJ. Biophysical model for integrating neuronal activity, EEG, fMRI and metabolism. *Neuroimage* (2008) **39**(1):290–309. doi:10.1016/j.neuroimage.2007.08.001
- Stefanescu RA, Jirsa VK. A low dimensional description of globally coupled heterogeneous neural networks of excitatory and inhibitory neurons. *PLoS Comput Biol* (2008) **4**(11):e1000219. doi:10.1371/journal.pcbi.1000219

44. Turner R. Techniques for imaging neuroscience. *Br Med Bull* (2003) **65**(1):3–20. doi:10.1093/bmb/65.1.3
45. Manella R. Quasisymplectic integrators for stochastic differential equations. *Phys Rev E* (2004) **69**(4):041107. doi:10.1103/PhysRevE.69.041107
46. Drakesmith M, Caeyenberghs K, Dutt A, Zammit S, Evans CJ, Reichenberg A, et al. Schizophrenia-like topological changes in the structural connectome of individuals with subclinical psychotic experiences. *Hum Brain Mapp* (2015) **36**(7):2629–43. doi:10.1002/hbm.22796
47. Shu N, Liu Y, Li K, Duan Y, Wang J, Yu C, et al. Diffusion tensor tractography reveals disrupted topological efficiency in white matter structural networks in multiple sclerosis. *Cereb Cortex* (2011) **21**(11):2565–77. doi:10.1093/cercor/bhr039
48. Zhang R, Wei Q, Kang Z, Zalesky A, Li M, Xu Y, et al. Disrupted brain anatomical connectivity in medication-naïve patients with first-episode schizophrenia. *Brain Struct Funct* (2015) **220**(2):1145–59. doi:10.1007/s00429-014-0706-z
49. Achard S, Bullmore E. Efficiency and cost of economical brain functional networks. *PLoS Comput Biol* (2007) **3**(2):e17. doi:10.1371/journal.pcbi.0030017
50. Betzel RF, Byrge L, He Y, Goñi J, Zuo X-N, Sporns O. Changes in structural and functional connectivity among resting-state networks across the human lifespan. *Neuroimage* (2014) **102**(Pt 2):345–57. doi:10.1016/j.neuroimage.2014.07.067
51. Bullmore ET, Bassett DS. Brain graphs: graphical models of the human brain connectome. *Annu Rev Clin Psychol* (2011) **7**:113–40. doi:10.1146/annurev-clinpsy-040510-143934
52. Schult D, Swart P. Exploring network structure, dynamics, and function using NetworkX. *Proceedings of the 7th Python in Science* (2008). Available from <http://permalink.lanl.gov/object/tr?what=info:lanl-repo/lareport/LA-UR-08-05495>
53. Bullmore E, Sporns O. Complex brain networks: graph theoretical analysis of structural and functional systems. *Nat Rev Neurosci* (2009) **10**(3):186–98. doi:10.1038/nrn2575
54. Sporns O, Honey CJ, Kötter R. Identification and classification of hubs in brain networks. *PLoS One* (2007) **2**(10):e1049. doi:10.1371/journal.pone.0001049
55. Milot M-H, Cramer SC. Biomarkers of recovery after stroke. *Curr Opin Neurol* (2008) **21**(6):654–9. doi:10.1097/WCO.0b013e3283186f96.Biomarkers
56. Mitra PP. The circuit architecture of whole brains at the mesoscopic scale. *Neuron* (2014) **83**(6):1273–83. doi:10.1016/j.neuron.2014.08.055
57. Kötter R. Online retrieval, processing, and visualization of primate connectivity data from the CoCoMac database. *Neuroinformatics* (2004) **2**(2):127–44. doi:10.1385/NI.2.2:127
58. Kitago T, Liang J, Huang VS, Hayes S, Simon P, Tenteromano L, et al. Improvement after constraint-induced movement therapy: recovery of normal motor control or task-specific compensation? *Neurorehabil Neural Repair* (2013) **27**(2):99–109. doi:10.1177/1545968312452631
59. Wolf SL, Winstein CJ, Miller JP, Taub E, Uswatte G, Morris D, et al. Effect of constraint-induced movement therapy on upper extremity function 3 to 9 months after stroke: the EXCITE randomized clinical trial. *JAMA* (2006) **296**(17):2095–104. doi:10.1001/jama.296.17.2095
60. Wolf SL, Winstein CJ, Miller JP, Thompson PA, Taub E, Uswatte G, et al. NIH public access. *Lancet Neurol* (2008) **7**(1):33–40. doi:10.1016/S1474-4422(07)70294-6
61. Ertelt D, Small S, Solodkin A, Dettmers C, McNamara A, Binkofski F, et al. Action observation has a positive impact on rehabilitation of motor deficits after stroke. *Neuroimage* (2007) **36**(Suppl 2):T164–73. doi:10.1016/j.neuroimage.2007.03.043
62. Small SL, Buccino G, Solodkin A. Brain repair after stroke—a novel neurological model. *Nat Rev Neurol* (2013) **9**(12):698–707. doi:10.1038/nrneuro.2013.222
63. Agosta S, Herpich F, Miceli G, Ferraro F, Battelli L. Contralesional rTMS relieves visual extinction in chronic stroke. *Neuropsychologia* (2014) **62**:269–76. doi:10.1016/j.neuropsychologia.2014.07.026
64. De Aguiar V, Paolazzi CL, Miceli G. tDCS in post-stroke aphasia: the role of stimulation parameters, behavioral treatment and patient characteristics. *Cortex* (2014) **63C**:296–316. doi:10.1016/j.cortex.2014.08.015
65. Rosati G, Oscari F, Reinkensmeyer DJ, Secoli R, Avanzini F, Spagnol S, et al. Improving robotics for neurorehabilitation: enhancing engagement, performance, and learning with auditory feedback. *IEEE International Conference on Rehabilitation Robotics: [Proceedings]*. Zurich (2011).
66. Taheri H, Rowe J, Gardner D. Robot-assisted guitar hero for finger rehabilitation after stroke. *Conf Proc IEEE Eng Med Biol Soc* (2012) **2012**:3911–7. doi:10.1109/EMBC.2012.6346822
67. Tang Y-H, Ma Y-Y, Zhang Z-J, Wang Y-T, Yang G-Y. Opportunities and challenges: stem cell-based therapy for the treatment of ischemic stroke. *CNS Neurosci Ther* (2015) **21**(4):337–47. doi:10.1111/cns.12386
68. Van den Berg D, Gong P, Breakspear M, van Leeuwen C. Fragmentation: loss of global coherence or breakdown of modularity in functional brain architecture? *Front Syst Neurosci* (2012) **6**:20. doi:10.3389/fnsys.2012.00020
69. Hagmann P, Cammoun L, Gigandet X, Meuli R, Honey CJ, Wedeen VJ, et al. Mapping the structural core of human cerebral cortex. *PLoS Biol* (2008) **6**(7):e159. doi:10.1371/journal.pbio.0060159
70. Lohse C, Bassett DS, Lim KO, Carlson JM. Resolving anatomical and functional structure in human brain organization: identifying mesoscale organization in weighted network representations. *PLoS Comput Biol* (2014) **10**(10):e1003712. doi:10.1371/journal.pcbi.1003712
71. Besson P, Lopes R, Leclerc X, Derambure P, Tyvaert L. Intra-subject reliability of the high-resolution whole-brain structural connectome. *Neuroimage* (2014) **102**(Pt 2):283–93. doi:10.1016/j.neuroimage.2014.07.064

Conflict of Interest Statement: The authors declare that the research was conducted in the absence of any commercial or financial relationships that could be construed as a potential conflict of interest.

Copyright © 2015 Falcon, Riley, Jirsa, McIntosh, Shereen, Chen and Solodkin. This is an open-access article distributed under the terms of the Creative Commons Attribution License (CC BY). The use, distribution or reproduction in other forums is permitted, provided the original author(s) or licensor are credited and that the original publication in this journal is cited, in accordance with accepted academic practice. No use, distribution or reproduction is permitted which does not comply with these terms.



Role of the contralesional hemisphere in post-stroke recovery of upper extremity motor function

Cathrin M. Bueteftsch^{1,2*}

¹ Emory University, Atlanta, GA, USA, ² Georgia Institute of Technology, Atlanta, GA, USA

OPEN ACCESS

Edited by:

Rüdiger Jürgen Seitz,
LVR-Klinikum Düsseldorf University,
Germany

Reviewed by:

Mustapha Ezzeddine,
University of Minnesota, USA
Qing Hao,
Johns Hopkins University, USA

*Correspondence:

Cathrin M. Bueteftsch
cathrin.m.bueteftsch@emory.edu

Specialty section:

This article was submitted to Stroke,
a section of the journal
Frontiers in Neurology

Received: 16 May 2015

Accepted: 22 September 2015

Published: 16 October 2015

Citation:

Bueteftsch CM (2015) Role of the
contralesional hemisphere in
post-stroke recovery of upper
extremity motor function.
Front. Neurol. 6:214.
doi: 10.3389/fneur.2015.00214

Identification of optimal treatment strategies to improve recovery is limited by the incomplete understanding of the neurobiological principles of recovery. Motor cortex (M1) reorganization of the lesioned hemisphere (ipsilesional M1) plays a major role in post-stroke motor recovery and is a primary target for rehabilitation therapy. Reorganization of M1 in the hemisphere contralateral to the stroke (contralesional M1) may, however, serve as an additional source of cortical reorganization and related recovery. The extent and outcome of such reorganization depends on many factors, including lesion size and time since stroke. In the chronic phase post-stroke, contralesional M1 seems to interfere with motor function of the paretic limb in a subset of patients, possibly through abnormally increased inhibition of lesioned M1 by the contralesional M1. In such patients, decreasing contralesional M1 excitability by cortical stimulation results in improved performance of the paretic limb. However, emerging evidence suggests a potentially supportive role of contralesional M1. After infarction of M1 or its corticospinal projections, there is abnormally increased excitatory neural activity and activation in contralesional M1 that correlates with favorable motor recovery. Decreasing contralesional M1 excitability in these patients may result in deterioration of paretic limb performance. In animal stroke models, reorganizational changes in contralesional M1 depend on the lesion size and rehabilitation treatment and include long-term changes in neurotransmitter systems, dendritic growth, and synapse formation. While there is, therefore, some evidence that activity in contralesional M1 will impact the extent of motor function of the paretic limb in the subacute and chronic phase post-stroke and may serve as a new target for rehabilitation treatment strategies, the precise factors that specifically influence its role in the recovery process remain to be defined.

Keywords: transcranial magnetic stimulation, motor cortex reorganization, neurorehabilitation of motor function, motor stroke recovery, functional magnetic resonance image

Introduction

With the introduction of relatively sophisticated neuroimaging techniques, such as positron emission tomography (PET) and functional and structural magnetic resonance imaging (MRI), and novel electrophysiological techniques, such as transcranial magnetic stimulation (TMS), studying the underlying mechanisms of motor recovery after stroke in humans have become increasingly feasible. In 1991, Chollet et al. (1) reported for the first time the activation of bilateral sensorimotor cortices in stroke patients moving their affected hand and suggested that ipsilateral motor projection may play

a role in recovery. This claim was further substantiated in 1993 by Carr et al. (2) who used TMS of the primary motor cortex (M1) to probe the functional integrity of the corticospinal tract (CST) after stroke. He reported that, in patients with poor motor outcome, TMS applied to the motor cortex of the hemisphere affected by stroke (ipsilesional M1) did not produce detectable motor-evoked potentials (MEPs), indicating disrupted function of the CST. However, when TMS was applied to the motor cortex of the hemisphere spared by the stroke (contralesional M1), MEPs were detected in both the hands. These findings suggested abnormal corticospinal projections from the contralesional M1 to muscles of the affected hand (see below for more detailed discussion).

In the following years, the role of the contralesional M1 in motor recovery after stroke and its potential as new target for rehabilitation efforts have been a topic of intense research efforts in humans and animal stroke models (3–5). As this field moved forward, it became apparent that several factors may impact the role of contralesional M1 in the control of the paretic hand movements and that even in healthy intact brain the ipsilateral M1 (corresponding to the contralesional M1 in paretic hand movements) is active in the control of strictly unilateral hand movement (6–11). In the context of the incomplete understanding of the ipsilateral M1 in motor control, the interpretation of findings pertaining to the role of contralesional M1 (corresponding to the ipsilateral M1 in intact human) in motor recovery after stroke remains problematic.

In this review, the evidence for contralesional M1 activity in recovery of hand function after stroke will be discussed. In the first part of this review, I will summarize the advances in our understanding of motor control of hand movements as they pertain to a better understanding of contralesional M1 function in motor recovery of hand movements. There is emerging evidence that ipsilateral M1 (corresponding to contralesional M1 in stroke patients) is active even in healthy subjects, depending on age and motor task demands (11–14). Motor task-dependent activity of ipsilateral M1 and the interaction between M1s may contribute to the contradicting data in contralesional M1 in stroke patients, where stroke-related motor impairment impacts the demand of a given motor task. In the second part of the review, I will discuss data available from animal stroke models and humans after stroke pertaining to the role of contralesional M1 reorganization in post-stroke recovery. Finally, I will discuss in which way neurorehabilitation science can leverage on the knowledge of contralesional M1 reorganization to develop new and effective rehabilitation treatment strategies.

Ipsilateral M1 and Interhemispheric Interaction in the Control of Hand Movements in Intact Man

The Contribution of Ipsilateral M1 and its Corticospinal Connections in the Control of Hand Movements

In fMRI studies of unilateral hand motor performance in intact man, strictly contralateral M1 activation was demonstrated by some investigators (15, 16) while bilateral M1 activation was

observed by others (6, 11, 17–19). Increased ipsilateral M1 was demonstrated in tasks with higher accuracy or complexity demands (6–8, 11, 17, 20). However, the interpretation of these neuroimaging data was limited by measuring qualitatively different movements where the tasks were not being matched for their kinematics (e.g., force, amplitude, and frequency) and by lacking the verification of a strictly unilateral execution of the motor task during the acquisition of imaging data. Measuring unilateral performance is important as without it, the presence of bilateral upper extremity activity with increasing difficulty of the task referred to as “mirror movements” cannot be ruled out and may contribute to observed bilateral M1 activation. In our recent study of healthy middle-aged people ($n = 13$, 10 females, age 55.4 ± 10.9 years), subjects performed a pointing task with a joy stick. By decreasing the size of the target, the demand on accuracy was parametrically increased while participating muscle groups and movement kinematic were kept the same. Unilateral performance was verified with electromyographic (EMG) recording from upper extremity muscles. As illustrated in **Figure 1**, performance of the pointing task (collapsed across different target sizes) resulted in extensive activation of bilateral sensorimotor cortex in the precentral and postcentral gyri/sulci (**Figure 1**, red). This contrasts with activation arising from the qualitatively different finger tapping task (**Figure 1**, green/yellow), which resulted in activation restricted to contralateral sensorimotor areas and the corresponding ipsilateral cerebellum. Of note is that ipsilateral M1 activation in the pointing task is largely anterior to the activation arising from the tapping task executed by the contralateral hand.

While there is evidence for ipsilateral corticospinal projections in humans, evidence for the control of the hand movements via ipsilateral corticospinal connections is weak. In intact humans, stimulation of M1 using TMS elicits MEPs in ipsilateral hand muscles but these are difficult to obtain and require high stimulation intensity and pre-innervations of the target muscle (21). In non-human primates, recording of ipsilateral M1 neurons during upper limb movements demonstrate that cells in iM1 are modulated by the task but that the timing of this activity is best correlated with weak muscle activity in the contralateral non-moving arm (22). Alternatively, task-related effects in the ipsilateral M1 could be mediated by corticoreticulospinal connections. In contrast to corticospinal connection, corticoreticulospinal projections are bilateral and are thought to be involved in the execution of selective finger movements (23). The involvement of this pathway is supported by TMS-derived evidence of longer latencies of MEPs elicited in the ipsilateral hand muscles (21). One could also argue that this M1 area may be concerned with the integration of afferent input from other motor areas. Recent evidence of bilateral M1 projections from posterior parietal (24, 25) and dorsal premotor areas, likely conveying some task-related information such as visuospatial and motor planning information, support a more indirect effect and the notion that M1 functions at a higher level in motor control by integrating afferent information and then generating a descending motor command that defines the spatiotemporal form of the movement (26). A higher level role for M1 in motor control is also supported by the results of a recent repetitive TMS (rTMS)

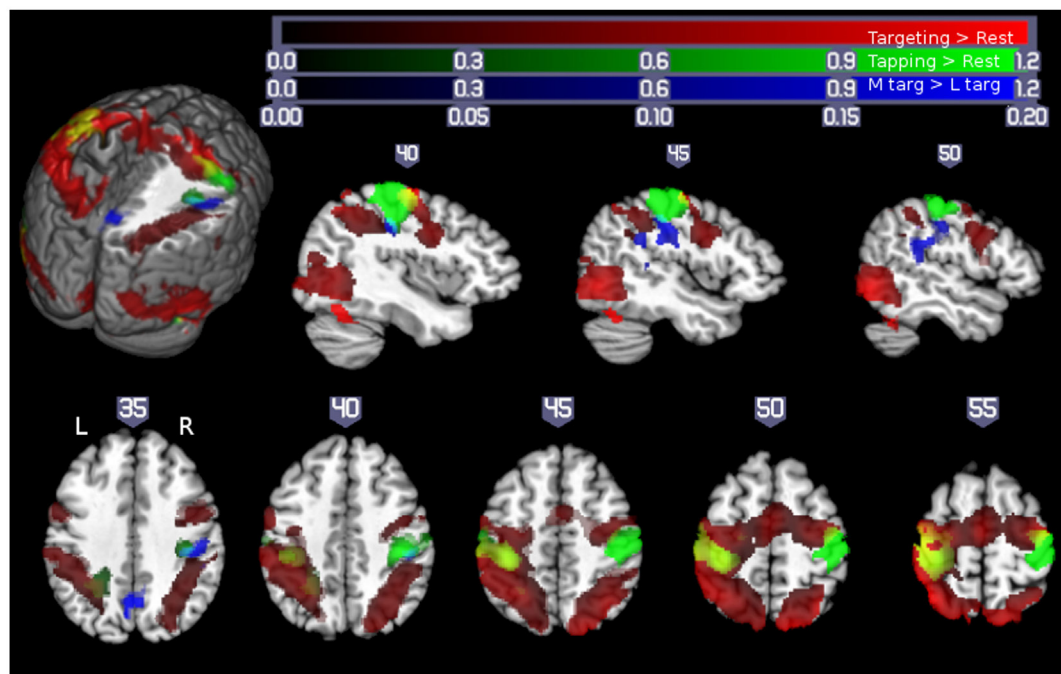


FIGURE 1 | Motor demand-dependent activation of motor cortices using a pointing task: pointing and finger tapping tasks related brain activation: Activity related to the pointing task (collapsed across XL, L, and M targets) is indicated in red. Activation related to right- and left-handed finger tapping is indicated in green, with overlap between finger tapping and pointing task performance shown in yellow. Note that while there was extensive bilateral activation for the pointing task, M1 activation in the finger tapping tasks was only seen contralateral to the performing hand, so that the left hemisphere is solely due to right-handed finger tapping (with left hemisphere yellow areas show overlap between right-handed finger tapping and right-handed pointing task performance) and the right hemisphere activity is solely due to left-handed finger tapping (yellow colors in the right hemisphere show overlap between activity due to the right-handed targeting task and left-handed finger tapping task, outlined with a yellow border for ease of visualization). Significant activation related to increasing motor demand (M targets > L targets) is indicated in blue (overlap between this region and left-handed finger tapping shown in cyan, outlined for clarity). All activations are shown overlaid on the Colin27 template in standard space, thresholded at a corrected $p < 0.05$ (uncorrected threshold $p < 0.005$ and cluster size $> 2360 \text{ mm}^3$). Increased color intensity corresponds to higher estimates of percent signal change. Cuts in the three-dimensional rendering are shown at $x = 0$, $y = -15$, and $z = 35$. The right hemisphere is depicted in the upper panel. The right (R) and left (L) side of the brain are indicated in the lower panel. Numerical labels above each slice show slice coordinates in the x dimension (sagittal sections) or z dimension (axial sections) (11).

study where low-frequency rTMS applied to left M1 improved performance in both hands for the task with the highest demand on precision while performance remained unchanged for the tasks with lower demands (14).

Interhemispheric Interaction in the Control of Hand Movements in Intact Humans

In addition to the corticospinal projections and ipsilateral corticocortico connections, motor areas of the two hemispheres are interconnected to each other and interact in the execution of motor tasks. Improved performance after transiently inhibiting the ipsilateral M1 by means of low-frequency rTMS (14, 27, 28) could indicate that there may be a need for suppression of task performance related ipsilateral M1 excitatory activity. Because the relationship between the two primary motor cortices is impacted by stroke (4, 5, 29) and topic of great interest in neuromodulation treatment approaches targeting the contralesional M1 (3), this topic will be reviewed for the intact brain.

The main structure connecting the motor areas is the corpus callosum. Connections between primary motor areas are less

abundant than premotor areas and primarily excitatory [for detailed review, see Ref. (5)]. Interhemispheric inhibition (IHI) can be demonstrated with TMS by applying a conditioning stimulus (CS) to one M1 and a test stimulus (TS) to the homotopic area of the other M1 (30) (Figure 2). The CS inhibits the size of the MEP produced by the TS. The amount of inhibition is expressed as a percentage of the mean MEP amplitude evoked by a single TS. While resting IHI is measured with the subject at rest, active IHI is measured during movement preparation. In healthy subjects executing a hand motor task, the inhibitory effect of one M1 on the other M1 decreases (31) depending on the movement kinematics (32, 33). In a study by Talelli et al. (20), a relationship between resting IHI and task-related ipsilateral M1 activity as measured by fMRI was demonstrated. Specifically, peak forces for a hand grip were positively correlated with increases in ipsilateral M1-blood oxygenation level-dependent (BOLD) response when IHI between motor cortices was weak. This positive correlation changed to a negative correlation when IHI was strong. This would indicate that activity in ipsilateral M1 is controlled to some extent by the inhibitory effect of the contralateral M1.

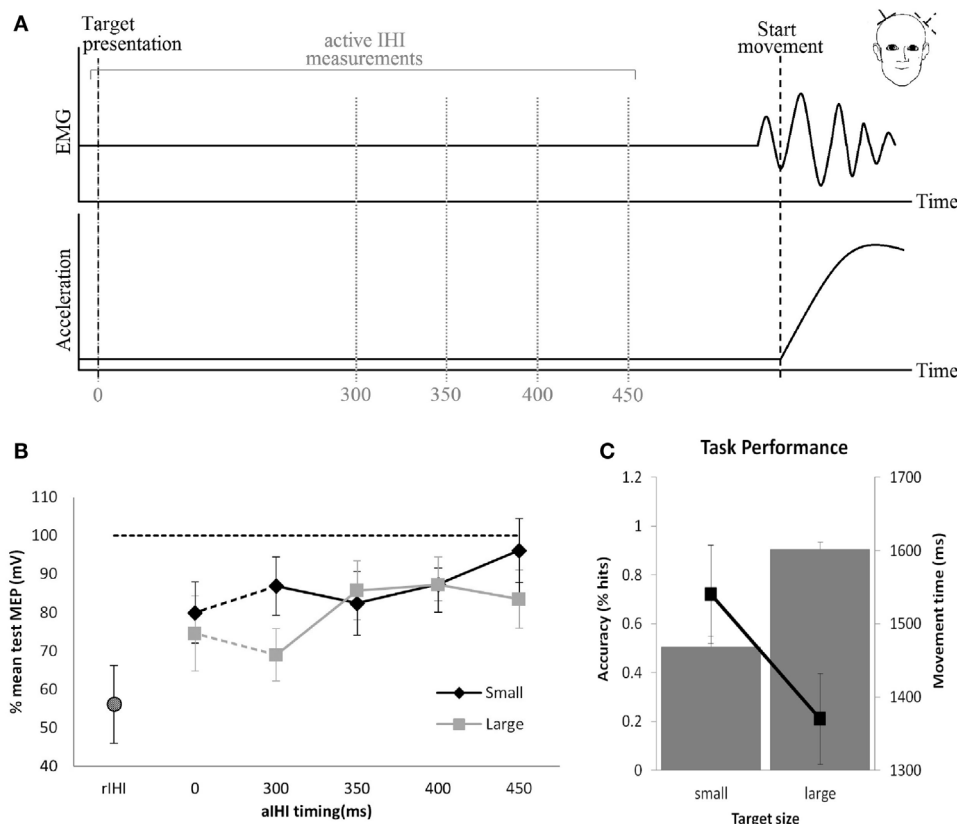


FIGURE 2 | Resting and active interhemispheric inhibition (IHI): (A) IHI can be demonstrated by applying a conditioning stimulus to M1, which inhibits the size of the motor-evoked potential (MEP) produced by the test stimulus applied to the homotopic area of the opposite M1. These measures are obtained during rest (resting IHI, rIHI) or in the pre-movement period during preparation of a movement (active IHI). **(B)** During rest, there is significant rIHI (round symbol) from one M1 on the other M1. Active IHI (rectangular symbol) decreases immediately prior to the movement onset depending on kinematics of the movement **(B,C)**. **(B,C)** Pointing to a large target with less demand on accuracy (square) results in less reduction of active IHI compared to pointing at a small target (diamond) with high demand on accuracy (33).

Contralesional M1 Reorganization in Post-Stroke Recovery

Reorganization of Contralesional M1 in the Post-Stroke Recovery Period (fMRI Evidence)

In task-related functional imaging studies of stroke patients, the activation of contralesional motor areas (corresponding to ipsilateral motor areas in healthy subjects) have been consistently reported (34). Cross-sectional studies of stroke patients moving the affected hand revealed a shift from an initially (abnormal) bilateral activation of motor areas in the subacute stroke patients (1, 9, 16, 35–40) toward a more normal unilateral activation pattern of ipsilesional motor areas in chronic stroke patients (40). Importantly, in a longitudinal study of stroke patients, this activation shift to the ipsilesional hemisphere was associated with good recovery, whereas persistence of the bilateral activation pattern was associated with poor outcome (40). On the basis of these studies, it was concluded that greater involvement of contralesional M1 predicted poorer motor outcome. (34, 40). However, in several studies, mirror movements of the non-affected hand were reported during the performance with the affected hand during imaging (34). This raised the possibility

that some contralesional M1 activity is, in fact, related to mirror movements of the non-affected hand (41, 42). As mirror movements and coactivation of the non-affected hand are seen more frequently in patients with poor motor outcome (41, 43), the presence of these movements may have confounded the findings of increased contralesional M1 activation in patients with poor outcome.

In our own fMRI study of subacute stroke patients with excellent recovery, strictly unilateral performance resulted in activation of bilateral motor cortices (16). In this study, eight stroke patients underwent fMRI of the brain to test M1 activity related to the performance of a non-sequential finger opposition task with their paretic hand. EMG activity of bilateral arm muscles was recorded during the scanning. All patients showed excellent recovery. Their results were compared to age-matched normal volunteers. While overt mirror movements were absent in all patients, three patients showed substantial EMG activity of the non-affected arm when performing the task with the affected hand. Their data were excluded from further analysis. As demonstrated in **Figure 3**, in the remaining five patients with strictly unilateral performance, bilateral activation of premotor and primary motor cortices was evident. In contrast, the age-matched controls showed a strictly

unilateral activation of the corresponding contralateral M1. These results support the notion that activation in contralesional M1 most likely reflects a reorganizational process in these patients. However, based on the findings in healthy subjects, where ipsilateral M1 is activated as the task becomes more demanding, increased activity could also be explained by a relatively higher demand on motor skill in stroke patients when compared to healthy controls (i.e., because of the compromised hand function due to stroke, the execution of the task is more challenging for the patient compared to the controls). Schaechter and Perdue (44) studied chronic stroke patients with good recovery of hand function and demonstrated that cortical activation during performance of the unskilled and skilled movement was increased in the patients relative to controls in the contralesional primary sensorimotor cortex. These findings suggest that in the chronic phase after stroke the neuronal substrate supporting affected hand function includes contralesional M1. The question whether this abnormal contralesional M1 activity is related to recovery-related regenerative responses as demonstrated for the subacute stroke patients or whether these changes reflect degenerative responses to the stroke remains to be determined as both processes are to some extent activity dependent, interact and impact similar circuitries (4).

Mechanisms Underlying Reorganization of Contralesional M1 in the Post-Stroke Recovery Period

The interpretation of task-related fMRI results is limited by the fact that changes in inhibitory and excitatory activity cannot be distinguished and the functional relevance of these changes in M1 activity is unclear. Specifically, task-related increases in BOLD in

contralesional M1 could result from increases of inhibitory or excitatory activity or any combination of these.

In rodent stroke models, functional and structural reorganizational changes in contralesional M1 have been reported [for detailed review, see Ref. (4, 5)]. Briefly, in these models, small focal cortical lesions led to long-lasting changes in contralesional M1, such as down-regulation of GABA_A-receptor function (45, 46) and up-regulation of NMDA-receptor function (47, 48), both mechanisms operating in increases of synaptic efficacy such as long-term potentiation (LTP). In contrast to human studies (see below), excitability in contralesional M1 was transiently increased but returned to the original values within hours. Similarly, representation of the rodent forelimb expanded in the contralesional M1 but returned to normal dimensions over the following days [for review, see Ref. (5)]. From a structural perspective, increase in neuropil volume (49), use-dependent dendritic growth followed by dendritic pruning, synapse formation, and changes in the specific structure of synaptic connections have been described (49–51).

In humans, increased intracortical excitability of contralesional M1 has been demonstrated in subacute and chronic stroke patients (29, 52–54) when explored with the paired pulse TMS technique. In this paradigm, a suprathreshold TS is preceded by a subthreshold CS at an interstimulus interval (ISI) of 2 ms. In the M1 of healthy subjects, CS inhibits the MEP produced by the subsequent TS, referred to as short interval intracortical inhibition (55). This effect is mediated by GABA_A-receptors (56) and arises in close proximity to the stimulated area (57). By varying the intensity of CS, the effects mediated by inhibitory and excitatory networks can be separated in more detail (29, 54) (**Figures 4A,B**). In a study of subacute stroke patients, the inhibitory effect of CS at

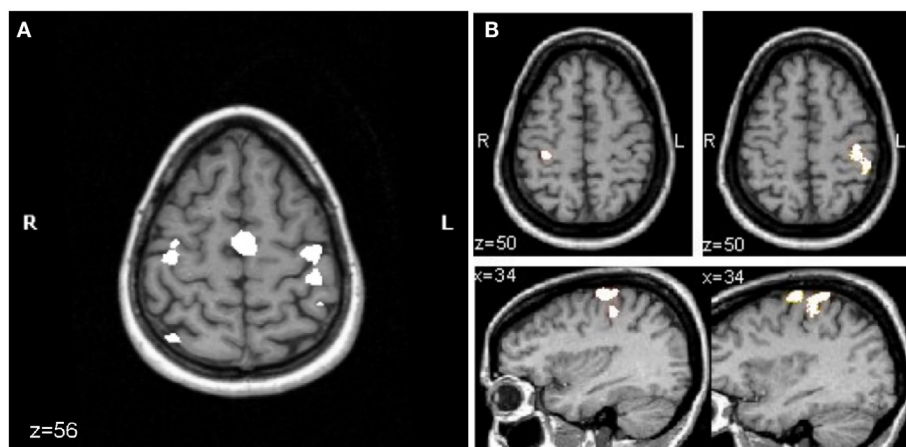


FIGURE 3 | Mean fMRI activation map of the performance of a finger sequence with the affected hand in patients ($n = 5$) (A) and with either hand in the age-matched control group ($n = 9$) (B). For both groups, the activation map is superimposed on the T1-weighted MRI of the same healthy control subject. (A) In patients, right in the axial slice of brain ($z = 56$) corresponds to the lesioned hemisphere and left to the contralesional hemisphere. Activation of contralesional precentral gyrus is evident (corrected $p < 0.05$). (B) For the control group performing the finger sequence with the left (lower left image, corrected $p = 0.05$) or right (lower right image, uncorrected $p < 5.8e-12$) hand, there was activation in the precentral gyrus of the hemisphere that is contralateral to the performing hand. Initially, the significance level was set as low as corrected $p = 0.05$ to pick up any activity in the motor cortex ipsilateral to the moving hand (shown for left hand movement, lower left image). At this significance level, massive activation was seen in the pre- and postcentral gyrus contralaterally when moving the right hand. To separate clusters of activity in pre- and postcentral gyrus, the significance level was increased until the two clusters became distinct (uncorrected $p < 5.8e-12$, lower right panel) (16).

low intensity was similar to values found in healthy age-matched controls while the inhibitory effect was abnormally reduced at higher intensities. This may indicate that the balance of excitatory and inhibitory activity in neuronal circuits was shifted toward excitatory activity (29, 54). Alternatively, abnormal function of the high threshold GABAergic inhibitory interneurons may result in a decreased inhibitory effect of CS at higher intensities. These findings suggest that regulation of excitatory and inhibitory neurotransmitter systems may play a role early in the reorganization process in contralesional M1 (48, 58) and may support functional recovery early after stroke. This notion is supported by the finding in patients in the subacute phase of stroke involving M1 or its corticospinal projections where a close association between increased excitability of contralesional M1 and good recovery of hand function was demonstrated (54). However, whether these findings hold up and can be applied to patients with other lesion locations has to be determined in larger longitudinal studies.

Relationship Between Contralesional M1 and Ipsilesional M1 (Interhemispheric Inhibition) in the Post-Stroke Recovery Period

As described for the intact brain, the two motor cortices inhibit each other through connections via the corpus callosum (5). In addition to the discussed mechanisms underlying contralesional M1 reorganization, stroke-related changes in the inhibitory drive between motor cortices could play an important role in reorganizational changes of contralesional M1. While increased contralesional M1 excitability was demonstrated in multiple studies (29, 31, 53, 54, 59), very few studies have examined the relationship between increased contralesional M1 excitability and resting IHI. It was concluded that loss of inhibitory drive of the lesioned M1 on the contralesional M1 through interhemispheric connections may contribute to the reorganizational processes observed for this motor cortex. Increases in contralesional M1 excitability may result in an excessive inhibitory effect on the ipsilesional M1, which may interfere with its reorganization and related recovery (31, 53, 59). In our study of 23 subacute stroke patients with documented ongoing recovery of motor function, contralesional M1 excitability was increased as demonstrated by paired pulse TMS technique (29) (see above for detailed description of the methods). Resting IHI from ipsilesional M1 on contralesional M1 was reduced in both cortical and subcortical location of the stroke while IHI from contralesional M1 on ipsilesional M1 was normal (Figures 4C,D). In patients with cortical stroke, there was an inverse correlation between inhibitory effect from contralesional on ipsilesional M1 and contralesional M1 excitability. This relationship was not seen in patients with subcortical stroke. This would indicate that in subacute patients recovering from stroke, the demonstrated increased contralesional M1 excitability is not causally related to abnormally reduced IHI from ipsilesional M1 on contralesional M1. Further, because IHI of the contralesional on ipsilesional M1 was normal and measures of contralesional M1 excitability were increased, there was no evidence in this study to support the hypothesis that an abnormally increased contralesional M1 excitability results in abnormally increased IHI of contralesional on ipsilesional M1 with subsequently decreased activity or excitability of ipsilesional M1 in this patient population.

However, when IHI was measured in the pre-movement interval (active IHI, see above for details of the methods) contralesional on the ipsilesional M1 was abnormally increased in chronic stroke patients when compared to healthy age-matched controls (31). The role of abnormally increased active IHI and the relationship between abnormal active IHI, measures of M1 excitability, and recovery of hand function in stroke needs to be determined in more detail and is currently a topic of active investigations.

There is some evidence regarding the relationship between the ipsi- and contralesional M1 in rodent stroke models. Specifically, an ischemic lesion of M1 leads to partial denervation of the contralesional M1, which has a tendency to sprout into the perilesional neuronal tissue of ipsilesional M1 (60, 61). Moreover, learning a new motor skill with the non-affected limb reduces spontaneous recovery and limits rehabilitation-related functional improvements of the affected limb (62–64). These findings underscore the importance of interhemispheric connections between and ipsi- and contralesional M1 and their potential involvement in mediating reorganizational effects on the ipsilesional M1.

Factors that Determine the Role of Contralesional M1 in the Post-Stroke Recovery Period

The factors that determine involvement of contralesional M1 are currently not known. In non-human primate stroke models, progressively larger M1 hand lesions were associated with a proportional expansion of ipsilesional ventral premotor (PMv) (65, 66) and supplementary motor area (SMA) (67) hand representation.

In rodent stroke models, reorganizational changes in contralesional M1 depend on the lesion size (68) and rehabilitation treatment (64, 69) and include long-term changes in neurotransmitter systems, dendritic growth, and synapse formation (45, 46, 50, 51, 70, 71). Inhibiting the contralesional hemisphere in rats that recovered from large ischemic infarcts generates more behavioral deficits of the impaired forelimb in comparison to control animals (72).

In humans, Schaechter and Perdue (44) demonstrated in chronic stroke patients a linear relationship between abnormally increased affected hand movement-related contralesional M1 activity and extend of CST damage. Further, the observed differential effect on contralesional M1 excitability and the relationship between contralesional M1 excitability and IHI (Figure 4) (29) supports the notion that location of the stroke seems to impact reorganizational processes. These differential remote effects of the lesion are also consistent with the findings that contralesional M1 seems to support function in a subset of patients after stroke (18) but may interfere with recovery or affected hand function in others (73, 74).

Interventions in Stroke Rehabilitation Treatment Targeting Contralesional M1

Several reports have demonstrated that non-invasive cortical stimulation can enhance functional reorganization, motor cortical excitability, and the beneficial effects of motor training on performance (75–80). Either ipsi- or contralesional M1 are target of these interventional approaches (3). In this

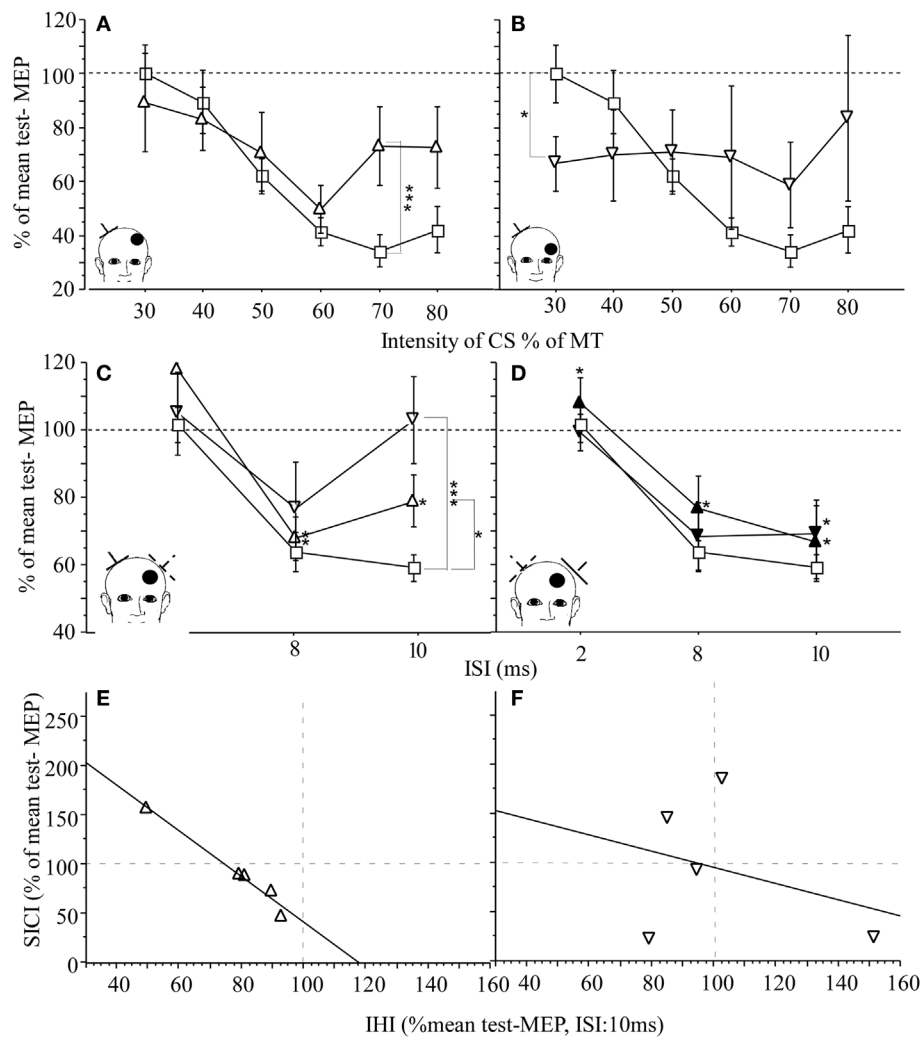


FIGURE 4 | M1 excitability and IHI in patients with subacute stroke ($n = 23$) and healthy age-matched controls ($n = 20$): EMG was recorded from the first dorsal interosseus muscle (FDI). (A,B) Effect of lesion location on SICI in patients. Control (square) and contralesional M1 of patients with cortical [open triangle (A)] and subcortical location of infarction [open inverted triangle (C)]. IHI of the lesioned M1 on the contralesional M1 is reduced in patients with cortical (open triangle) or subcortical infarction (open inverted triangle) when compared to healthy controls (square). (D) IHI from contralesional M1 on the lesioned M1 was intact for cortical infarction (black triangle) and subcortical infarction (black inverted triangle). The conditioned MEP amplitude is expressed as percentage of the mean test-MEP. (E,F) Relationship between M1 excitability, SICI (CS at 80% MT), and IHI in patients with cortical infarction (triangle) and subcortical infarction (inverted triangle). For each patient (each point represents one subject), SICI of the contralesional M1 was plotted against IHI from lesioned on the contralesional M1 (open symbols). Regression was calculated. For cortical location of the infarction, there was an inverse linear relationship between SICI of the contralesional M1 and IHI from lesioned on the contralesional M1 [(E) $r^2 = 0.972$, $p = 0.002$]. Although there is a similar trend in the subcortical group (F), the relationship was more variable [(F) $r^2 = 0.105$, $p = \text{ns}$]. The insert indicates the position of the coil for application of CS (dotted lines) and the TS (solid lines). The location of the lesion is indicated by the bullet. CS = intensity of conditioning stimulus, MT = motor threshold. The scattered lines indicate the cutoff between facilitation (>100) and inhibition (<100). Mean \pm SE. * $p < 0.05$, ** $p < 0.02$, and * $p < 0.01$ (29).**

review, I will focus on non-invasive cortical stimulation targeting the contralesional M1.

Down-regulation of excitability in one motor cortex influences corticomotor excitability in the opposite motor cortex. Several reports of studies in healthy subjects have now demonstrated that 1 Hz rTMS applied to M1 of one hemisphere results in increased corticomotor excitability in the opposite M1 (81, 82) and improved performance in the corresponding hand (14, 83) depending on the level of motor demand (14). As discussed

in the previous sections, although the extent to which the contralesional M1 contributes to motor recovery is not known, many currently employed rTMS protocols are designed with the assumption that following stroke, ipsilesional M1 is hypoactive while contralesional M1 is hyperactive and should be inhibited (3, 80). Accordingly, stimulation of contralesional M1 has been used to inhibit its hyperactivity (3, 74, 78, 84–86). Meta-analyses on the effectiveness of repetitive transcranial magnetic stimulation (rTMS) or transcranial direct current stimulation (tDCS)

in stroke rehabilitation therapy do not agree on the available evidence to either support or reject it (87–90).

Summary

Taken together, there is evidence from human and animal studies that activity in contralesional M1 will impact motor function of the paretic limb differently in different patients. However, currently employed treatment strategies are geared toward inhibiting its function. There is a great need to identify the precise factors

that specifically influence the role of contralesional M1 in the recovery process. A better understanding of those factors is critical to the development of effective therapies tailored to its specific role in the recovery process to improve outcome post stroke.

Acknowledgments

CB was supported by NINDS (R56NS070879, R01NS060830, and 1R01NS090677-01A1) and NICHD (R21HD067906 and 1R01NS090677-01A1).

References

- Chollet F, Dipiero V, Wise RJ, Brooks DJ, Dolan RJ, Frackowiak RS. The functional anatomy of motor recovery after stroke in humans: a study with positron emission tomography. *Ann Neurol* (1991) **29**:63–71. doi:10.1002/ana.410290112
- Carr LJ, Harrison LM, Evans AL, Stephens JA. Patterns of central motor reorganization in hemiplegic cerebral palsy. *Brain* (1993) **116**(Pt 5):1223–47. doi:10.1093/brain/116.5.1223
- Hummel F, Celnik P, Pascual-Leone A, Fregni F, Byblow WD, Bueteefisch CM, et al. Controversy: noninvasive and invasive cortical stimulation show efficacy in treating stroke patients. *Brain Stimul* (2008) **1**:370–82. doi:10.1016/j.brs.2008.09.003
- Jones TA, Allred RP, Jefferson SC, Kerr AL, Woodie DA, Cheng SY, et al. Motor system plasticity in stroke models: intrinsically use-dependent, unreliably useful. *Stroke* (2013) **44**:S104–6. doi:10.1161/STROKEAHA.111.000037
- Dancuse N, Touvykine B, Mansoori BK. Inhibition of the contralesional hemisphere after stroke: reviewing a few of the building blocks with a focus on animal models. *Prog Brain Res* (2015) **218**:361–87. doi:10.1016/b.pbr.2015.01.002
- Winstein CJ, Grafton ST, Pohl PS. Motor task difficulty and brain activity: investigation of goal-directed reciprocal aiming using positron emission tomography. *J Neurophysiol* (1997) **77**:1581–94.
- Seidler RD, Noll DC, Thiers G. Feedforward and feedback processes in motor control. *Neuroimage* (2004) **22**:1775–83. doi:10.1016/j.neuroimage.2004.05.003
- Verstynen T, Diedrichsen J, Albert N, Aparicio P, Ivry RB. Ipsilateral motor cortex activity during unimanual hand movements relates to task complexity. *J Neurophysiol* (2005) **93**:1209–22. doi:10.1152/jn.00720.2004
- Nair DG, Hutchinson S, Fregni F, Alexander M, Pascual-Leone A, Schlaug G. Imaging correlates of motor recovery from cerebral infarction and their physiological significance in well-recovered patients. *Neuroimage* (2007) **34**:253–63. doi:10.1016/j.neuroimage.2006.09.010
- Verstynen T, Ivry RB. Network dynamics mediating ipsilateral motor cortex activity during unimanual actions. *J Cogn Neurosci* (2011) **23**:2468–80. doi:10.1162/jocn.2011.21612
- Bueteefisch CM, Pirog Revell K, Shuster L, Hines B, Parsons M. Motor demand dependent activation of ipsilateral motor cortex. *J Neurophysiol* (2014) **112**(4):999–1009. doi:10.1152/jn.00110.2014
- Chen R, Cohen LG, Hallett M. Role of the ipsilateral motor cortex in voluntary movement. *Can J Neurol Sci* (1997) **24**:284–91.
- Tallesi P, Waddingham W, Ewas A, Rothwell JC, Ward NS. The effect of age on task-related modulation of interhemispheric balance. *Exp Brain Res* (2008) **186**:59–66. doi:10.1007/s00221-007-1205-8
- Bueteefisch CM, Hines B, Shuster L, Pergami P, Mathes A. Motor demand-dependent improvement in accuracy following low-frequency transcranial magnetic stimulation of left motor cortex. *J Neurophysiol* (2011) **106**:1614–21. doi:10.1152/jn.00048.2011
- Catalan MJ, Honda M, Weeks RA, Cohen LG, Hallett M. The functional neuroanatomy of simple and complex sequential finger movements: a PET study. *Brain* (1998) **121**(Pt 2):253–64. doi:10.1093/brain/121.2.253
- Bueteefisch CM, Kleiser R, Korber B, Muller K, Wittsack HJ, Homberg V, et al. Recruitment of contralesional motor cortex in stroke patients with recovery of hand function. *Neurology* (2005) **64**:1067–9. doi:10.1212/01.WNL.0000154603.48446.36
- Hummel F, Kirsammer R, Gerloff C. Ipsilateral cortical activation during finger sequences of increasing complexity: representation of movement difficulty or memory load? *Clin Neurophysiol* (2003) **114**:605–13. doi:10.1016/S1388-2457(02)00417-0
- Lotze M, Markert J, Sauseng P, Hoppe J, Plewnia C, Gerloff C. The role of multiple contralesional motor areas for complex hand movements after internal capsular lesion. *J Neurosci* (2006) **26**:6096–102. doi:10.1523/JNEUROSCI.4564-05.2006
- Diedrichsen J, Wiestler T, Krakauer JW. Two distinct ipsilateral cortical representations for individuated finger movements. *Cereb Cortex* (2012) **23**(6):1362–77. doi:10.1093/cercor/bhs120
- Tallesi P, Ewas A, Waddingham W, Rothwell JC, Ward NS. Neural correlates of age-related changes in cortical neurophysiology. *Neuroimage* (2008) **40**:1772–81. doi:10.1016/j.neuroimage.2008.01.039
- Ziemann U, Ishii K, Borgheresi A, Yaseen Z, Battaglia F, Hallett M, et al. Dissociation of the pathways mediating ipsilateral and contralateral motor-evoked potentials in human hand and arm muscles. *J Physiol* (1999) **518**(Pt 3):895–906. doi:10.1111/j.1469-7793.1999.0895p.x
- Soteropoulos DS, Edgley SA, Baker SN. Lack of evidence for direct corticospinal contributions to control of the ipsilateral forelimb in monkey. *J Neurosci* (2011) **31**:11208–19. doi:10.1523/JNEUROSCI.0257-11.2011
- Soteropoulos DS, Williams ER, Baker SN. Cells in the monkey ponto-medullary reticular formation modulate their activity with slow finger movements. *J Physiol* (2012) **590**:4011–27. doi:10.1113/jphysiol.2011.225169
- Koch G, Fernandez Del Olmo M, Cheeran B, Schippling S, Caltagirone C, Driver J, et al. Functional interplay between posterior parietal and ipsilateral motor cortex revealed by twin-coil transcranial magnetic stimulation during reach planning toward contralateral space. *J Neurosci* (2008) **28**:5944–53. doi:10.1523/JNEUROSCI.0957-08.2008
- Koch G, Ruge D, Cheeran B, Fernandez Del Olmo M, Pecchioli C, Marconi B, et al. TMS activation of interhemispheric pathways between the posterior parietal cortex and the contralateral motor cortex. *J Physiol* (2009) **587**:4281–92. doi:10.1113/jphysiol.2009.174086
- Kalaska JF. From intention to action: motor cortex and the control of reaching movements. *Adv Exp Med Biol* (2009) **629**:139–78. doi:10.1007/978-0-387-77064-2_8
- Kobayashi M, Hutchinson S, Schlaug G, Pascual-Leone A. Ipsilateral motor cortex activation on functional magnetic resonance imaging during unilateral hand movements is related to interhemispheric interactions. *Neuroimage* (2003) **20**:2259–70. doi:10.1016/S1053-8119(03)00220-9
- Dafotakis M, Grefkes C, Wang L, Fink GR, Nowak DA. The effects of 1 Hz rTMS over the hand area of M1 on movement kinematics of the ipsilateral hand. *J Neural Transm* (2008) **115**:1269–74. doi:10.1007/s00702-008-0064-1
- Bueteefisch CM, Wessling M, Netz J, Seitz RJ, Homberg V. Relationship between interhemispheric inhibition and motor cortex excitability in subacute stroke patients. *Neurorehabil Neural Repair* (2008) **22**:4–21. doi:10.1177/1545968307301769
- Ferbert A, Priori A, Rothwell JC, Day BL, Colebatch JG, Marsden CD. Interhemispheric inhibition of the human motor cortex. *J Physiol* (1992) **453**:525–46. doi:10.1113/jphysiol.1992.sp019243
- Murase N, Duque J, Mazzocchio R, Cohen LG. Influence of interhemispheric interactions on motor function in chronic stroke. *Ann Neurol* (2004) **55**:400–9. doi:10.1002/ana.10848
- Duque J, Mazzocchio R, Dambrosia J, Murase N, Olivier E, Cohen LG. Kinematically specific interhemispheric inhibition operating in the process

- of generation of a voluntary movement. *Cereb Cortex* (2005) **15**:588–93. doi:10.1093/cercor/bbh160
33. Wischniewski M, Kowalski G, Belagaje S, Bueteifisch C. *Task Dependent Modulation of Interhemispheric Inhibition*. Washington, DC: SFN (2014).
34. Calautti C, Baron JC. Functional neuroimaging studies of motor recovery after stroke in adults: a review. *Stroke* (2003) **34**:1553–66. doi:10.1161/01.STR.0000071761.36075.A6
35. Weiller C, Chollet F, Friston KJ, Wise RJ, Frackowiak RS. Functional reorganization of the brain in recovery from striatocapsular infarction in man. *Ann Neurol* (1992) **31**:463–72. doi:10.1002/ana.410310502
36. Cramer SC, Nelles G, Benson RR, Kaplan JD, Parker RA, Kwong KK, et al. A functional MRI study of subjects recovered from hemiparetic stroke. *Stroke* (1997) **28**:2518–27. doi:10.1161/01.STR.28.12.2518
37. Cao Y, Dolhaberiague L, Vikingstad EM, Levine SR, Welch KM. Pilot study of functional MRI to assess cerebral activation of motor function after poststroke hemiparesis. *Stroke* (1998) **29**:112–22. doi:10.1161/01.STR.29.1.112
38. Johansen-Berg H, Rushworth MF, Bogdanovic MD, Kischka U, Wimalaratna S, Matthews PM. The role of ipsilateral premotor cortex in hand movement after stroke. *Proc Natl Acad Sci U S A* (2002) **99**:14518–23. doi:10.1073/pnas.222536799
39. Small SL, Hlustik P, Noll DC, Genovese C, Solodkin A. Cerebellar hemispheric activation ipsilateral to the paretic hand correlates with functional recovery after stroke. *Brain* (2002) **125**:1544–57. doi:10.1093/brain/awf148
40. Ward NS, Brown MM, Thompson AJ, Frackowiak RS. Neural correlates of motor recovery after stroke: a longitudinal fMRI study. *Brain* (2003) **126**:2476–96. doi:10.1093/brain/awg145
41. Kim YH, Jang SH, Chang Y, Byun WM, Son S, Ahn SH. Bilateral primary sensori-motor cortex activation of post-stroke mirror movements: an fMRI study. *Neuroreport* (2003) **14**:1329–32. doi:10.1097/01.wnr.0000078702.79393.9b
42. Wittenberg GF, Chen R, Ishii K, Bushara KO, Eckloff S, Croarkin E, et al. Constraint-induced therapy in stroke: magnetic-stimulation motor maps and cerebral activation. *Neurorehabil Neural Repair* (2003) **17**:48–57. doi:10.1177/0888439002250456
43. Nelles G, Cramer SC, Schaechter JD, Kaplan JD, Finklestein SP. Quantitative assessment of mirror movements after stroke. *Stroke* (1998) **29**:1182–7. doi:10.1161/01.STR.29.6.1182
44. Schaechter JD, Perdue KL. Enhanced cortical activation in the contralesional hemisphere of chronic stroke patients in response to motor skill challenge. *Cereb Cortex* (2008) **18**:638–47. doi:10.1093/cercor/bhm096
45. Buchkremer-Ratzmann I, August M, Hagemann G, Witte OW. Electrophysiological transcallosal diaschisis after cortical photothrombosis in rat brain. *Stroke* (1996) **27**:1105–9. doi:10.1161/01.STR.27.6.1105
46. Neumann-Haefelin T, Witte OW. Perinfarct and remote excitability changes after transient middle cerebral artery occlusion. *J Cereb Blood Flow Metab* (2000) **20**:45–52. doi:10.1097/00004647-200001000-00008
47. Qu M, Buchkremer-Ratzmann I, Schiene K, Schroeter M, Witte OW, Zilles K. Bihemispheric reduction of GABA_A receptor binding following focal cortical photothrombotic lesions in the rat brain. *Brain Res* (1998) **813**:374–80. doi:10.1016/S0006-8993(98)01063-4
48. Witte OW. Lesion-induced plasticity as a potential mechanism for recovery and rehabilitative training. *Curr Opin Neurol* (1998) **11**:655–62. doi:10.1097/00019052-199812000-00008
49. Hsu JE, Jones TA. Time-sensitive enhancement of motor learning with the less-affected forelimb after unilateral sensorimotor cortex lesions in rats. *Eur J Neurosci* (2005) **22**:2069–80. doi:10.1111/j.1460-9568.2005.04370.x
50. Jones TA, Schallert T. Use-dependent growth of pyramidal neurons after neocortical damage. *J Neurosci* (1994) **14**:2140–52.
51. Jones TA, Kleim JA, Greenough WT. Synaptogenesis and dendritic growth in the cortex opposite unilateral sensorimotor cortex damage in adult rats: a quantitative electron microscopic examination. *Brain Res* (1996) **733**:142–8. doi:10.1016/0006-8993(96)00792-5
52. Liepert J, Hamzei F, Weiller C. Motor cortex disinhibition of the unaffected hemisphere after acute stroke. *Muscle Nerve* (2000) **23**:1761–3. doi:10.1002/1097-4598(200011)23:11<1761::AID-MUS14>3.0.CO;2-M
53. Shimizu T, Hosaki A, Hino T, Sato M, Komori T, Hirai S, et al. Motor cortical disinhibition in the unaffected hemisphere after unilateral cortical stroke. *Brain* (2002) **125**:1896–907. doi:10.1093/brain/awf183
54. Bueteifisch CM, Netz J, Wessling M, Seitz RJ, Homberg V. Remote changes in cortical excitability after stroke. *Brain* (2003) **126**:470–81. doi:10.1093/brain/awg044
55. Kujirai T, Caramia MD, Rothwell JC, Day BL, Thompson PD, Ferbert A, et al. Corticocortical inhibition in human motor cortex. *J Physiol* (1993) **471**:501–19. doi:10.1113/jphysiol.1993.sp019912
56. Ziemann U, Lonnecker S, Steinhoff BJ, Paulus W. The effect of lorazepam on the motor cortical excitability in man. *Exp Brain Res* (1996) **109**:127–35. doi:10.1007/BF00228633
57. Di Lazzaro V, Restuccia D, Oliviero A, Profice P, Ferrara L, Insola A, et al. Magnetic transcranial stimulation at intensities below active motor threshold activates intracortical inhibitory circuits. *Exp Brain Res* (1998) **119**:265–8. doi:10.1007/s002210050341
58. Nudo JR. Recovery after damage to motor cortical areas. *Curr Opin Neurobiol* (1999) **9**:740–7. doi:10.1016/S0959-4388(99)00027-6
59. Borojerdi B, Diefenbach K, Ferbert A. Transcallosal inhibition in cortical and subcortical cerebral vascular lesions. *J Neurol Sci* (1996) **144**:160–70. doi:10.1016/S0022-510X(96)00222-5
60. Carmichael ST, Wei L, Rovainen CM, Woolsey TA. New patterns of intracortical projections after focal cortical stroke. *Neurobiol Dis* (2001) **8**:910–22. doi:10.1006/nbdi.2001.0425
61. Liu Z, Zhang RL, Li Y, Cui Y, Chopp M. Remodeling of the corticospinal innervation and spontaneous behavioral recovery after ischemic stroke in adult mice. *Stroke* (2009) **40**:2546–51. doi:10.1161/STROKEAHA.109.547265
62. Allred RP, Maldonado MA, Hsu JE, Jones TA. Training the “less-affected” forelimb after unilateral cortical infarcts interferes with functional recovery of the impaired forelimb in rats. *Restor Neurol Neurosci* (2005) **23**:297–302.
63. Allred RP, Jones TA. Maladaptive effects of learning with the less-affected forelimb after focal cortical infarcts in rats. *Exp Neurol* (2008) **210**:172–81. doi:10.1016/j.expneurol.2007.10.010
64. Allred RP, Cappellini CH, Jones TA. The “good” limb makes the “bad” limb worse: experience-dependent interhemispheric disruption of functional outcome after cortical infarcts in rats. *Behav Neurosci* (2010) **124**:124–32. doi:10.1037/a0018457
65. Frost SB, Barbay S, Friel KM, Plautz EJ, Nudo RJ. Reorganization of remote cortical regions after ischemic brain injury: a potential substrate for stroke recovery. *J Neurophysiol* (2003) **89**:3205–14. doi:10.1152/jn.01143.2002
66. Dancause N, Barbay S, Frost SB, Zoubina EV, Plautz EJ, Mahnken JD, et al. Effects of small ischemic lesions in the primary motor cortex on neurophysiological organization in ventral premotor cortex. *J Neurophysiol* (2006) **96**:3506–11. doi:10.1152/jn.00792.2006
67. Eisner-Janowicz I, Barbay S, Hoover E, Stowe AM, Frost SB, Plautz EJ, et al. Early and late changes in the distal forelimb representation of the supplementary motor area after injury to frontal motor areas in the squirrel monkey. *J Neurophysiol* (2008) **100**:1498–512. doi:10.1152/jn.90447.2008
68. Kim SY, Jones TA. Lesion size-dependent synaptic and astrocytic responses in cortex contralateral to infarcts in middle-aged rats. *Synapse* (2010) **64**:659–71. doi:10.1002/syn.20777
69. Jones TA, Jefferson SC. Reflections of experience-expectant development in repair of the adult damaged brain. *Dev Psychobiol* (2011) **53**:466–75. doi:10.1002/dev.20557
70. Qü M, Mittmann T, Luhmann HJ, Schleicher A, Zilles K. Long-term changes of ionotropic glutamate and GABA receptors after unilateral permanent focal cerebral ischemia in the mouse brain. *Neuroscience* (1998) **85**:29–43. doi:10.1016/S0306-4522(97)00656-8
71. Witte OW, Bidmon HJ, Schiene K, Redeker C, Hagemann G. Functional differentiation of multiple perilesional zones after focal cerebral ischemia. *J Cereb Blood Flow Metab* (2000) **20**:1149–65. doi:10.1097/00004647-200008000-00001
72. Biernaskie J, Szymanska A, Windle V, Corbett D. Bi-hemispheric contribution to functional motor recovery of the affected forelimb following focal ischemic brain injury in rats. *Eur J Neurosci* (2005) **21**:989–99. doi:10.1111/j.1460-9568.2005.03899.x
73. Mansur CG, Fregni F, Boggio PS, Riberto M, Gallucci-Neto J, Santos CM, et al. A sham stimulation-controlled trial of rTMS of the unaffected hemisphere in stroke patients. *Neurology* (2005) **64**:1802–4. doi:10.1212/01.WNL.0000161839.38079.92
74. Fregni F, Boggio PS, Valle AC, Rocha RR, Duarte J, Ferreira MJ, et al. A sham-controlled trial of a 5-day course of repetitive transcranial magnetic

- stimulation of the unaffected hemisphere in stroke patients. *Stroke* (2006) **37**:2115–22. doi:10.1161/01.STR.0000231390.58967.6b
75. Muellbacher W, Ziemann U, Boroojerdi B, Hallett M. Effects of low-frequency transcranial magnetic stimulation on motor excitability and basic motor behavior. *Clin Neurophysiol* (2000) **111**:1002–7. doi:10.1016/S1388-2457(00)00284-4
 76. Bütefisch CM, Khurana V, Kopylev L, Cohen LG. Enhancing encoding of a motor memory in the primary motor cortex by cortical stimulation. *J Neurophysiol* (2004) **91**:2110–6. doi:10.1152/jn.01038.2003
 77. Hummel F, Celnik P, Giraux P, Floel A, Wu WH, Gerloff C, et al. Effects of non-invasive cortical stimulation on skilled motor function in chronic stroke. *Brain* (2005) **128**:490–9. doi:10.1093/brain/awh369
 78. Hummel F, Cohen LG. Improvement of motor function with noninvasive cortical stimulation in a patient with chronic stroke. *Neurorehabil Neural Repair* (2005) **19**:14–9. doi:10.1177/1545968304272698
 79. Khedr EM, Ahmed MA, Fathy N, Rothwell JC. Therapeutic trial of repetitive transcranial magnetic stimulation after acute ischemic stroke. *Neurology* (2005) **65**:466–8. doi:10.1212/01.wnl.0000173067.84247.36
 80. Dancause N, Nudo RJ. Shaping plasticity to enhance recovery after injury. *Prog Brain Res* (2011) **192**:273–95. doi:10.1016/B978-0-444-53355-5.00015-4
 81. Plewnia C, Lotze M, Gerloff C. Disinhibition of the contralateral motor cortex by low-frequency rTMS. *Neuroreport* (2003) **14**:609–12. doi:10.1097/00001756-200303240-00017
 82. Schambra HM, Sawaki L, Cohen LG. Modulation of excitability of human motor cortex (M1) by 1 Hz transcranial magnetic stimulation of the contralateral M1. *Clin Neurophysiol* (2003) **114**:130–3. doi:10.1016/S1388-2457(02)00342-5
 83. Kobayashi M, Hutchinson S, Theoret H, Schlaug G, Pascual-Leone A. Repetitive TMS of the motor cortex improves ipsilateral sequential simple finger movements. *Neurology* (2004) **62**:91–8. doi:10.1212/WNL.62.1.91
 84. Takeuchi N, Chuma T, Matsuo Y, Watanabe I, Ikoma K. Repetitive transcranial magnetic stimulation of contralesional primary motor cortex improves hand function after stroke. *Stroke* (2005) **36**:2681–6. doi:10.1161/01.STR.0000189658.51972.34
 85. Dafotakis M, Grefkes C, Eickhoff SB, Karbe H, Fink GR, Nowak DA. Effects of rTMS on grip force control following subcortical stroke. *Exp Neurol* (2008) **211**:407–12. doi:10.1016/j.expneurol.2008.02.018
 86. Nowak DA, Grefkes C, Dafotakis M, Eickhoff S, Kust J, Karbe H, et al. Effects of low-frequency repetitive transcranial magnetic stimulation of the contralesional primary motor cortex on movement kinematics and neural activity in subcortical stroke. *Arch Neurol* (2008) **65**:741–7. doi:10.1001/archneur.65.6.741
 87. Adeyemo BO, Simis M, Macea DD, Fregni F. Systematic review of parameters of stimulation, clinical trial design characteristics, and motor outcomes in non-invasive brain stimulation in stroke. *Front Psychiatry* (2012) **3**:88. doi:10.3389/fpsy.2012.00088
 88. Hsu WY, Cheng CH, Liao KK, Lee IH, Lin YY. Effects of repetitive transcranial magnetic stimulation on motor functions in patients with stroke: a meta-analysis. *Stroke* (2012) **43**:1849–57. doi:10.1161/STROKEAHA.111.649756
 89. Elsner B, Kugler J, Pohl M, Mehrholz J. Transcranial direct current stimulation (tDCS) for improving function and activities of daily living in patients after stroke. *Cochrane Database Syst Rev* (2013) **11**:CD009645. doi:10.1002/14651858.CD009645.pub2
 90. Hao Z, Wang D, Zeng Y, Liu M. Repetitive transcranial magnetic stimulation for improving function after stroke. *Cochrane Database Syst Rev* (2013) **5**:CD008862. doi:10.1002/14651858.CD008862.pub2

Conflict of Interest Statement: The author declares that the research was conducted in the absence of any commercial or financial relationships that could be construed as a potential conflict of interest.

Copyright © 2015 Bütefisch. This is an open-access article distributed under the terms of the Creative Commons Attribution License (CC BY). The use, distribution or reproduction in other forums is permitted, provided the original author(s) or licensor are credited and that the original publication in this journal is cited, in accordance with accepted academic practice. No use, distribution or reproduction is permitted which does not comply with these terms.



Motor Recovery After Subcortical Stroke Depends on Modulation of Extant Motor Networks

Nikhil Sharma^{1,2,3*} and Jean-Claude Baron^{1,4}

¹ Stroke Research Group, Department of Clinical Neurosciences, University of Cambridge, Cambridge, UK, ² MRC Unit for Lifelong Health and Ageing, University College London, London, UK, ³ The National Hospital for Neurology and Neurosurgery, London, UK, ⁴ INSERM U894, Centre Hospitalier Sainte-Anne, Sorbonne Paris Cité, Paris, France

Introduction: Stroke is the leading cause of long-term disability. Functional imaging studies report widespread changes in movement-related cortical networks after stroke. Whether these are a result of stroke-specific cognitive processes or reflect modulation of existing movement-related networks is unknown. Understanding this distinction is critical in establishing more effective restorative therapies after stroke. Using multivariate analysis (tensor-independent component analysis – TICA), we map the neural networks involved during motor imagery (MI) and executed movement (EM) in subcortical stroke patients and age-matched controls.

Methods: Twenty subcortical stroke patients and 17 age-matched controls were recruited. They were screened for their ability to carry out MI (Chaotic MI Assessment). The fMRI task was a right-hand finger-thumb opposition sequence (auditory-paced 1 Hz; 2, 3, 4, 5, 2...). Two separate runs were acquired (MI and rest and EM and rest; block design). There was no distinction between groups or tasks until the last stage of analysis, which allowed TICA to identify independent components (ICs) that were common or distinct to each group or task with no prior assumptions.

Results: TICA defined 28 ICs. ICs representing artifacts were excluded. ICs were only included if the subject scores were significant (for either EM or MI). Seven ICs remained that involved the primary and secondary motor networks. All ICs were shared between the stroke and age-matched controls. Five ICs were common to both tasks and three were exclusive to EM. Two ICs were related to motor recovery and one with time since stroke onset, but all were shared with age-matched controls. No IC was exclusive to stroke patients.

Conclusion: We report that the cortical networks in stroke patients that relate to recovery of motor function represent modulation of existing cortical networks present in age-matched controls. The absence of cortical networks specific to stroke patients suggests that motor adaptation and other potential confounders (e.g., effort and additional muscle use) are not responsible for the changes in the cortical networks reported after stroke. This highlights that recovery of motor function after subcortical stroke involves preexisting cortical networks that could help identify more effective restorative therapies.

Keywords: motor imagery, functional imaging, fMRI, mental imagery, brain mapping

OPEN ACCESS

Edited by:

Bruno J. Weder,
University of Bern, Switzerland

Reviewed by:

Maarten G. Lansberg,
Stanford University, USA
Andreas Charidimou,
Harvard Medical School, USA and
University College London, UK

*Correspondence:

Nikhil Sharma
nikhil.sharma@ucl.ac.uk

Specialty section:

This article was submitted to Stroke,
a section of the journal
Frontiers in Neurology

Received: 04 August 2015

Accepted: 19 October 2015

Published: 16 November 2015

Citation:

Sharma N and Baron J-C (2015)
Motor Recovery After Subcortical
Stroke Depends on Modulation of
Extant Motor Networks.
Front. Neurol. 6:230.
doi: 10.3389/fneur.2015.00230

INTRODUCTION

Stroke remains a leading cause of long-term disability and carries a significant social and economic cost (1, 2). After stroke, functional imaging studies of movement report widespread changes in activation of the cortical networks (3–8). The precise cognitive processes that determine these changes remain unclear. In this study, we used a data-led method to explore if the changes in movement-related networks are a result of processes specific to stroke patients (i.e., use of additional muscles) or whether they represent modulation of extant movement-related networks. Understanding this distinction in neuroplasticity is likely to help establish the driver of fMRI changes reported after stroke and help establish the most effective restorative therapies for patients (9–11).

Using a variety of tasks, numerous groups have reported changes in movement-related networks – importantly these remote changes relate to the recovery of motor performance. Movement-related fMRI activation in the ipsilesional primary motor cortex is associated with better recovery (4, 7, 8, 12, 13). Indeed it is on this model that many restorative intervention studies are based (14) changes in movement-related networks are being used to predict response to therapies (15). Yet it is possible that the changes in movement-related networks may represent an epiphenomenon of the increased difficulty involved in carrying out the task after a stroke (6).

There are several caveats when considering comparisons of patients with healthy volunteers (6). For instance, the kinematics of movements, EMG patterns, motor strategies (adaptation versus relearning), and whether movement involved different body parts in different subjects have not been monitored consistently in the MRI. In other words, it is possible that the differences reported represent a composite of cognitive processes specific to stroke patients that may not be directly related to the recovery process as such.

Understanding whether there are networks specific to stroke patients will greatly aid the understanding of the recovery process after stroke. It may allow a more targeted approach to rehabilitation as it could identify the most appropriate training programs. We explored the extent to which the widely described changes in motor networks after stroke are a result of specific processes (i.e., motor adaptation or use of different muscle) or whether they represent modulation of extant motor performance. There are two key aspects to our study.

First, to remove any biases produced by subtle differences in motor performance, we studied both motor imagery (MI) and executed movement (EM). MI is intrinsically linked to the motor system and can be used to study the motor system without actual movement (16–19). In stroke patients with normal activations during EM, we have reported abnormal hemispheric lateralization during MI that related to recovery of motor function. In other words, by studying MI as well as EM, we are able to identify aspects of task-dependent activation that relate to motor execution and those more “upstream” (20).

Second, we use a data-led approach using tensor-independent component analysis (TICA) (21). Using TICA, we examine

the cortical networks that are common to stroke patients and aged-matched controls or exclusive to either. Unlike the conventional mass univariate approach, TICA is a powerful data-led approach that explores similarities as well as differences in cortical networks. Importantly, both tasks (MI and EM) from both groups (stroke and aged-matched controls) are considered the same. We are able to use a “blinded task” during the production of the independent components (ICs) as they have the same temporal profile. In other words, we make no prior assumptions as to the extent of overlap, if any, between the task-related networks in stroke patients and controls or between the MI and EM. If the widely reported changes in movement-dependent networks are related to a stroke-specific cognitive process, then this analytic approach will likely produce separate components.

We hypothesize that in recovered subcortical stroke patients, the task-related motor networks identified for both EM and MI are shared with the age-matched controls. In keeping with our reports from healthy volunteers, we expect to find networks related exclusively to EM and others that are shared with MI. Finally, we expect that in stroke patients, the task-related networks would correlate with measures of motor recovery.

MATERIALS AND METHODS

Subjects

Twenty subcortical stroke patients were recruited (six females; mean age, 66 ± 8.8 years). Inclusion criteria were the following: (i) first-ever ischemic or hemorrhagic stroke with initial motor deficit lasting at least 2 weeks; (ii) ability to perform the motor activation task; and (iii) right-handedness. They had no past medical history of any neurological, psychiatric, or musculoskeletal disorders and were not taking regular medication. Seventeen age-matched control subjects (nine males) aged 40 years (mean, 57.6 ± 8.5 years) were recruited through local advertisement. Subjects had no history of medical disorders and were not taking regular medication. All subjects were right handed as assessed by the Edinburgh scale (22) and gave written consent in accordance with the Declaration of Helsinki, and the protocol was approved by the Cambridge Regional Ethics Committee.

All subjects underwent assessment with the Chaotic Motor Imagery Assessment (CMIA). They were excluded if unable to perform MI adequately. Chaotic Motor Imagery is defined as an inability to perform MI accurately or, if having preserved accuracy, the demonstration of temporal uncoupling (23). The full-assessment is described in detail in Ref. (24). Briefly, the assessment has three components performed in order. Where appropriate, subjects were given specific instructions to perform first-person kinesthetic MI. They were instructed not to view the scene from the third person and not to count or assign numbers or tones to each finger.

The stroke patients were assessed with the NIH Stroke Scale (NIHSS), the Action Research Arm Test (ARAT), Stroke Impact Score (SIS), and the Motricity Index. Thumb to index finger tapping over 15 s (TIT ratio) (25) and mirror synkinesia were measured. Transcranial Doppler was used to assess vasomotor reactivity and was preserved in all.

Functional MRI

Motor (Imagery) Paradigm

The fMRI task was a block design (20, 26) of a right-hand finger-thumb opposition sequence (paced at 1 Hz; sequence 2, 3, 4, 5, 2...) and rest. There were two separate runs acquired (MI and rest and EM and rest). Subjects were instructed to keep their eyes closed throughout the session. We used bilateral fiber-optic gloves (Fifth Dimension Technologies, SA) to monitor finger movements and exclude inappropriate movement. The gloves were also used to confirm the performance of MI – after each MI block (24). Post MR subjects rated the vividness of MI performance on a seven-point scale.

Data Acquisition

A 3-T Brucker MRI scanner was used to acquire both T2-weighted and proton density anatomical images and T2*-weighted MRI transverse echo-planar images sensitive to the BOLD signal for fMRI (64 × 64 × 23; FOV 20 × 20 × 115; 23 slices 4 mm, TR = 1.5 s, TE 30 ms, voxel size 4 × 4 × 4).

Image Analysis

Analysis was carried out using TICA (21) as implemented in MELODIC (Multivariate Exploratory Linear Decomposition into Independent Components) Version 3.09, part of FSL (FMRIB's Software Library, www.fmrib.ox.ac.uk/fsl). Only the affected hand in stroke patients was assessed. Where necessary images were flipped, the hand studied was always contralateral to the left hemisphere matching the right-hand tasks of the age-matched controls. Contralateral is therefore ipsilesional in stroke patients.

The first 12 volumes were discarded to allow for T1 equilibration effects. Preprocessing involved masking of non-brain voxels, voxel-wise de-meaning of the data, and normalization of the voxel-wise variance. Subject movement was less than 2 mm.

The preprocessed data were whitened and projected into a multidimensional subspace using probabilistic principal component analysis where the number of dimensions was estimated using the Laplace approximation to the Bayesian evidence of the model order (27). The whitened observations were decomposed into sets of vectors which describe signal variation across the temporal domain (time courses), the session/subject domain, and the spatial domain (maps) by optimizing for non-Gaussian spatial source distributions using a fixed-point iteration technique (28). Estimated component maps were divided by the standard deviation of the residual noise and thresholded by fitting a mixture model to the histogram of intensity values. The time course of each IC was then entered into a general linear model of the convolved block design of Task versus Rest.

An IC was considered to be involved in MI or EM if a one-way *t*-test found the subject scores to be significantly different from zero across subjects. When an IC was significantly involved in both tasks, then a paired *t*-test ($p < 0.05$ corrected for multiple comparisons) was performed on the subject score for each task. In the stroke group, the subject scores of each remaining component were correlated (Spearman $p < 0.05$ corrected for multiple comparisons) with the impairment scores.

RESULTS

Behavioral Results

Four control subjects and eight stroke patients were excluded because of chaotic motor imagery. Twelve stroke patients remained [eight left hemisphere; four females; for full demographic details see Sharma et al. (24)]. There was no difference in score between the stroke group and control subjects.

All subjects suppressed movement and all were compliant during the fMRI task. Median post-MRI MI vividness score was 6 (range, 4–7).

fMRI Data

No distinction was made between tasks until the final stage of processing. As 25 subjects performed two tasks, MI and EM, 50 “blinded” tasks were processed. As no distinction was made between imagery and EM during the generation of the ICs, we use the term “blinded.”

A subject score for each IC is produced that includes the effect size for the 50 blinded tasks (13 controls subjects, EM and MI, 12 stroke patients) for the associated spatiotemporal process shown in the spatial map.

Twenty-eight ICs were defined by TICA. ICs that identified artifact recognized by previously published patterns and high frequency were excluded by visual inspection. ICs driven by outliers or were not significant across either task were also excluded. Therefore, only components in which the subject scores were significantly different from zero (for either the stroke or control group for either task) were included.

Seven ICs remained. Each component was significantly involved in both the stroke group and the control group. As hypothesized, some ICs were shared between EM and MI (subject scores significantly greater than zero for both tasks in both groups) and some were exclusive to EM (subject score greater than zero for EM only in both groups).

Figures 1 and 2 show the whole brain activations and deactivations, the time course (BOLD), subject scores, and percentage of total variance explained. **Table 1** summarizes the areas involved [labeled using the Jülich Atlas (29)].

Independent Components (IC 1, 2, 4, 5, 8) Shared by Executed Movement and Motor Imagery

Five components (IC 1, 2, 4, 5, 8; **Figures 1 and 2**) were significantly involved in both age-matched controls and stroke patients and were common to both EM and MI (subject scores > 0 for both tasks in both groups). Together these five ICs explained 33% of the total explained variance. All of the components significantly correlated with the active blocks of the task.

In three of the components (IC1, 2, 5), the subjects score was greater during EM than during MI in the age-matched controls only – no such difference was found in the stroke group. IC1 involved activation of the contralateral motor areas and bilateral involvement of premotor and parietal areas. More specifically, there was contralateral activation of BA4a, SMA, BA3b, and

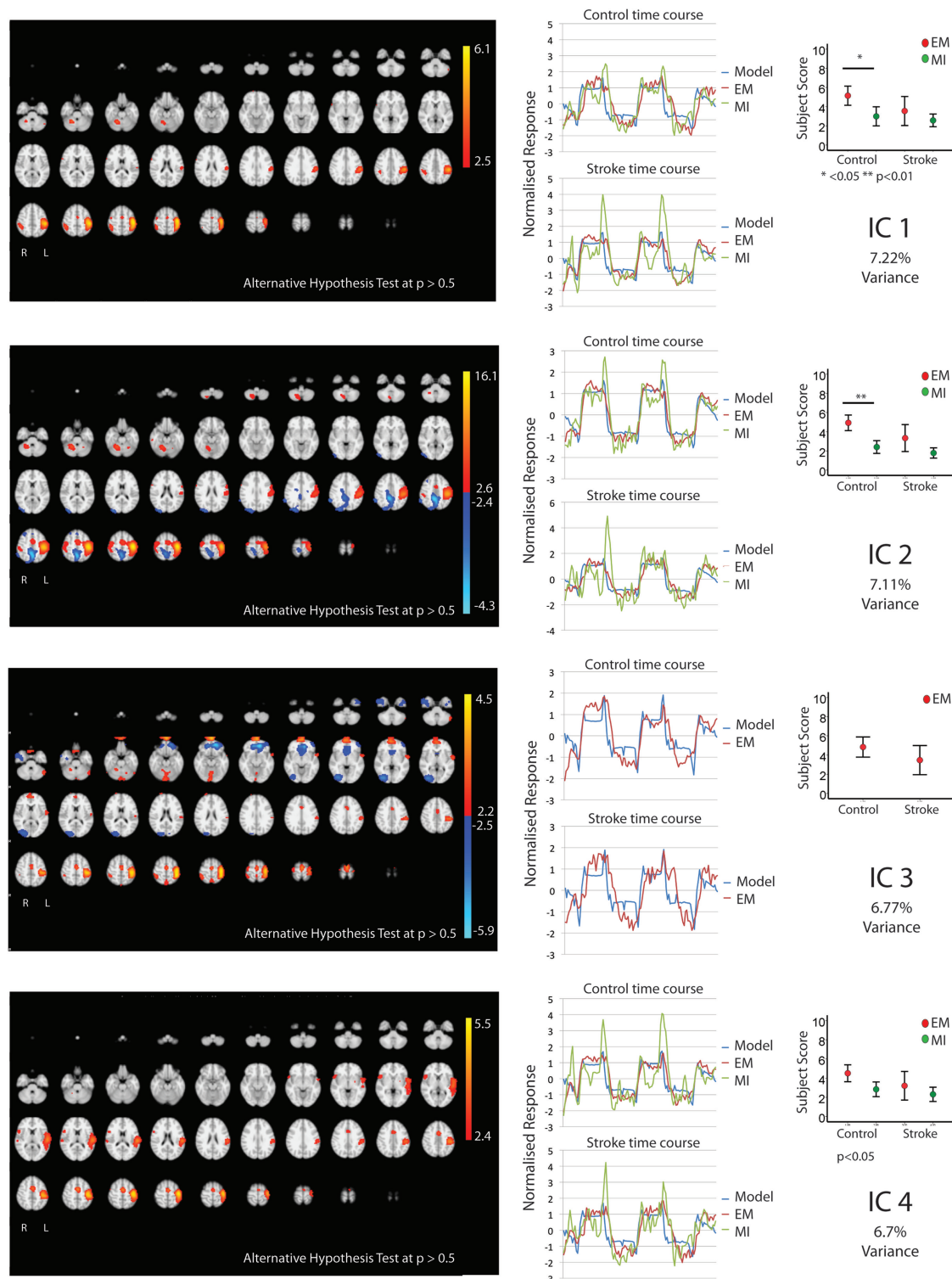


FIGURE 1 | The figures show the involvement of each IC across the whole brain with a standard threshold of $p > 0.5$ (alternative hypothesis test) and the variance it accounts for out of the total explained variance. In four stroke patients, the images were flipped so that the left hemisphere is always contralateral to executed movement/motor imagery. The left hemisphere equates to the ipsilesional hemisphere. The scales show the transformed z-score, orange is activation, and blue is deactivation. The normalized time course response is shown for each task and the full model fit (full model fit = blue, executed movement = red, and motor imagery = green). The mean subject scores with standard error bars are shown for each task and differences highlighted (executed movement = red, motor imagery = green). The time course and subject score for each task are shown.

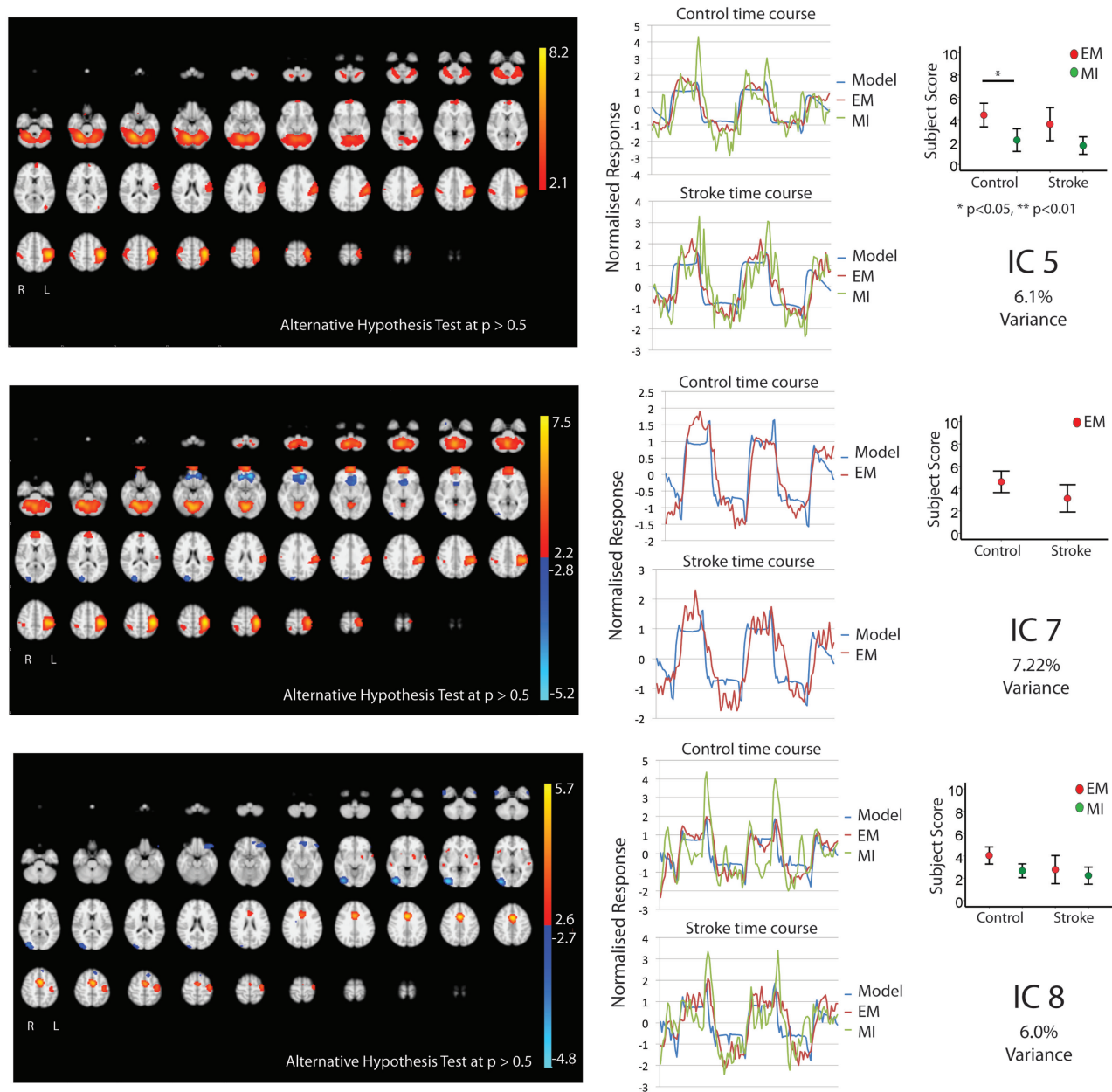


FIGURE 2 | The figures show the involvement of each IC across the whole brain with a standard threshold of $p > 0.5$ (alternative hypothesis test) and the variance it accounts for out of the total explained variance. In four stroke patients, the images were flipped so that the left hemisphere is always contralateral to executed movement/motor imagery. The left hemisphere equates to the ipsilesional hemisphere. The scales show the transformed z-score, orange is activation, and blue is deactivation. The normalized time course response is shown for each task and the full model fit (full model fit = blue, executed movement = red, and motor imagery = green). The mean subject scores with standard error bars are shown for each task and differences highlighted (executed movement = red, motor imagery = green). The time course and subject score for each task are shown.

parietal areas [IPC(PFo)]. There was bilateral activation of PMd, both SI and SII, and parietal areas (hIP2,3 and 7PC). There was ipsilateral activation of the parietal areas [hIP1, IPC (Pft)] and cerebellum.

Similarly IC 2 predominantly showed contralateral activation of BA4, parietal lobe [IPC (Pfo)], and bilateral activation of PMd, SI, SII, parietal lobe (hIP2), and contralateral cerebellum. However, in a different topographical location

(more dorsal), there was a small degree of deactivation of the contralateral BA4a and ipsilateral parietal lobe [IPC (Pfm)].

Independent component 4 was exclusively contralateral. While sensory motor areas (BA4, SMA, PMd, SI, SII, BA3a,3b) and parietal areas [both SPL(7PC) & IPC(Pfop)] were involved, it was the only IC to involve BA44. Notably there was no cerebellar activation.

TABLE 1 | Regions activated or deactivated in each independent component.

	Activated in both executed movement and motor imagery										Executed movement only			
	IC1		IC2		IC4		IC5		IC8		IC3		IC7	
	Left	Right	Left	Right	Left	Right	Left	Right	Left	Right	Left	Right	Left	Right
BA44					↑									
BA4	↑		↑ ^a	↓	↑		↑		↑		↑		↑	
Pre-SMA														
SMA	↑				↑				↑	↑	↑	↑		
PMd	↑	↑	↑	↑	↑			↑	↑		↑	↑	↑	
Area 1	↑	↑	↑	↑	↑		↑	↑			↑	↑	↑	
Area 2	↑	↑	↑	↑	↑		↑	↑	↑		↑	↑		↑
3a			↑		↑				↑		↑		↑	
3b	↑		↑	↑	↑		↑		↑		↑	↑	↑	↑
hIP1		↑												
hIP2	↑	↑	↑	↑			↑					↑		↑
hIP3	↑	↑						↑					↑	
SPL(7A)													↑	
SPL(7PC)	↑	↑	↑		↑		↑				↑	↑		
IPC(PFop)	↑		↑		↑						↑		↑	↑
IPC(PFt)		↑						↑			↑			↑
IPC(PFm)				↓										
IPC(Pga)														
IPC(PF)														
Thal_premotor														
Thal_motor														
Thal_Somatosensory														
Caudate														
TE														
CB		↑		↑			↑	↑			↑	↑	↑	↑

^aSmall area of deactivation in a more dorsal area.

Independent component 5 shared many features of IC1 and IC2, with involvement of primary and secondary motor areas as well as parietal areas. More specifically, there was contralateral activation of BA4, BA3b, parietal areas [SPL(7PC)], bilateral activation of SI, SII, and cerebellum, and ipsilateral parietal areas [IPC(PFt)]. Notably, it was the only component with only ipsilateral involvement of PMd and parietal area (hIP3).

Independent component 8 was similar to IC4 with predominantly contralateral activation (except for SMA). This involved BA4a, BA3a. In contrast, it was the only component with contralateral PMd, SII activation.

Independent Components Involved During Executed Movement Only (IC 3, 7)

Two components, IC 3 and 7, were involved during EM only explaining 6.77 and 7.22% of total variance, respectively. IC3 involved activation of the contralateral BA4, BA3a, and IPC, with bilateral activation of SMA, PMd, S1&2, BA3b, parietal area (SPL), and cerebellum. There was ipsilateral activation of parietal area (hIP2). IC7 activated the contralateral BA4, PMd, S1, BA3a, and parietal areas [HIP3 SPL (7A)], with bilateral involvement of BA3b, parietal area [IPC (PFop)], and cerebellum. There was ipsilateral activation of SII, hIP2, and parietal area [IPC (Pft)].

Relationship of Motor Imagery and Executed Movement ICs in Stroke Patients to Motor Performance and Time Since Stroke (IC 1, 3, 7)

In the stroke group, there were two ICs (1 and 3) that related to motor performance. While IC 3 was exclusive to EM, it is notable that IC1 – a component common to both EM and MI – is also related to motor performance.

As there was no significant difference between the IC1 subject scores for each task, both tasks were explored together. There was a significant positive correlation between this combined IC1 subject score and the Motricity (Arm) scores ($p = 0.581$; $p < 0.05$), i.e., the greater the activity within this network the better the recovery. The same overall pattern of correlation was mirrored with SIS ($p = 0.501$; $p < 0.05$) and Motor Activity Log ($p = 0.540$; $p < 0.05$).

Independent component 3 (EM only) was positively correlated with SIS ($p = 0.648$; $p < 0.05$). In other words, greater activation of IC3 was associated with better recovery.

Finally, IC7 was negatively correlated with time since stroke ($p = 0.592$; $p < 0.05$), i.e., this activation within this network reduced with time since stroke.

Figure 3 summarizes these findings.

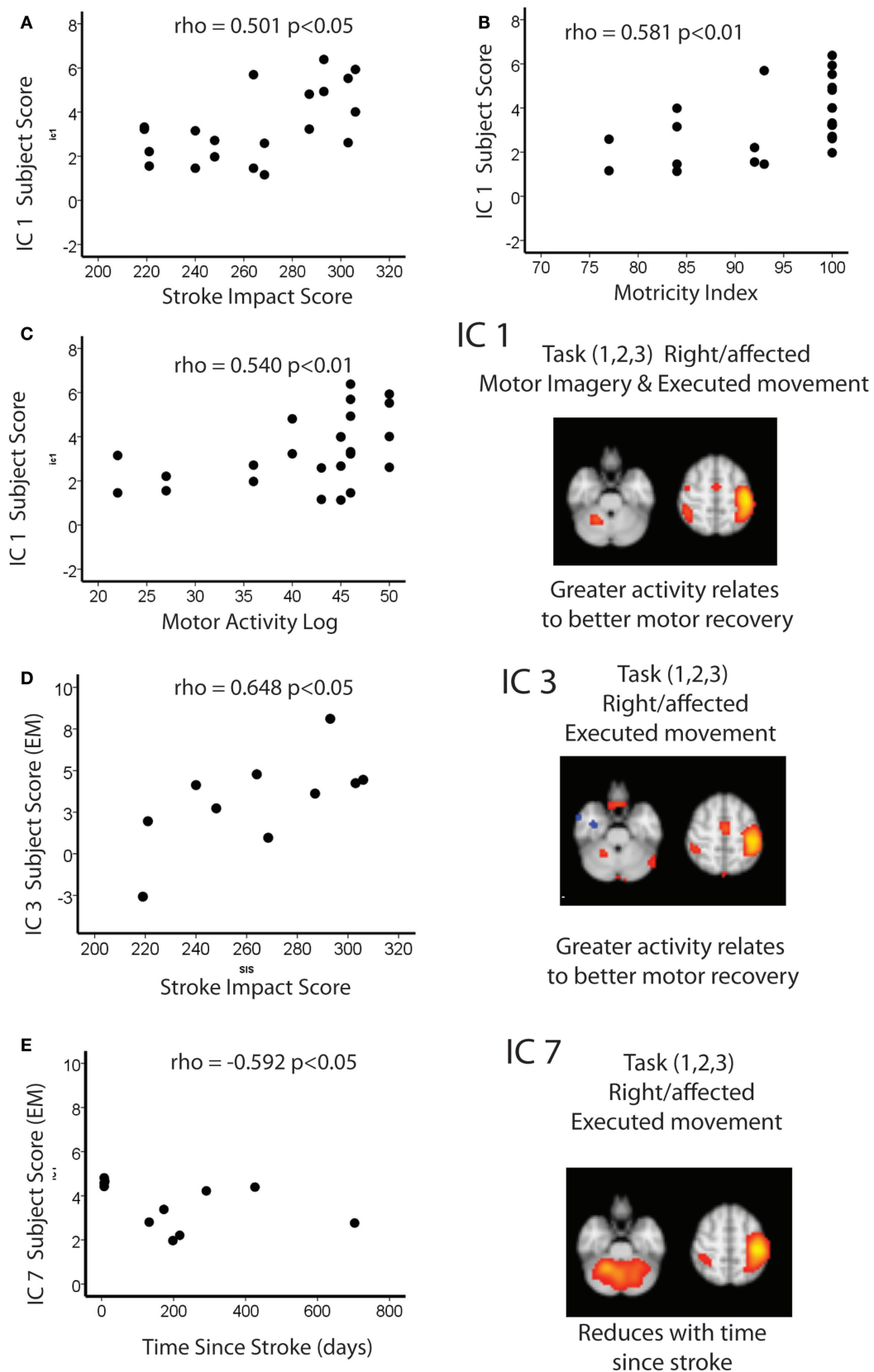


FIGURE 3 | Spearman correlations between IC1 and (A) stroke impact score (B) motricity index and (C) motor activity log. Spearman correlations between IC3 and (D) stroke impact score and (E) time since stroke.

DISCUSSION

We report that the cortical networks that relate to recovery of function are not specific to stroke but instead represent modulation of existing networks. As expected, most cortical networks were shared between EM and MI (accounting 33.13% of the total explained variance), with only two networks that were exclusively found during EM (accounting for 13.99% of the explained variance). The absence of any cortical networks specific to stroke patients suggests that the changes in cortical networks reported after stroke are not a result of a subtle biases exclusive to stroke patients – this may have included a motor behavior like adaptation (adjusting movement to new demands) or other potential confounders such as effort or attention. This work emphasizes that recovery of motor function involves preexisting cortical networks that may help identify more effective restorative therapies for stroke patients.

This study further extends the close similarities between MI and EM. We report that the first IC (IC1 accounting for 7.22% of the total explained variance) was involved in both groups and in both tasks (EM and MI). It involved activation of the contralateral motor areas and bilateral involvement of premotor and parietal areas. The involvement of the motor cortex – an area pivotal to motor learning (30) – strengthens the rationale for using MI training after stroke. We found that greater involvement of IC1 was associated with better recovery of motor performance after stroke. As this IC is shared between tasks, it suggests that a key aspect of the recovery process occurs “upstream” from motor execution. Importantly, this network is shared with age-matched controls, implying that it is not exclusive to stroke.

Consistent with our previous findings in healthy volunteers (31), we report two networks that are exclusive to motor execution (IC 3 and 7 explaining 6.77 and 7.22% of total variance, respectively). The areas common to both are the contralateral primary and secondary motor areas (although IC7 was largely bilateral with marked cerebellar involvement). This is likely explained by the differences between EM and imagery. First, EM involves discharge via the corticospinal tract (CST) that we have previously suggested dominates the movement-related activation (6). Second, the resultant movement produces afferent sensory feedback to the motor system.

We postulate that the IC3 is responsible for the discharge via the CST, given the near exclusive activation of the primary motor cortex. In support of this view, greater subject score of this network is associated with better recovery of motor performance (as assessed with the SIS). This is consistent with the findings from transcranial magnetic stimulation (TMS) studies that suggest that preservation of the CST is associated with a better recovery of motor performance after stroke (32–34).

It is likely that IC7 is related to the sensory feedback during motor execution, given the significant bilateral cerebellar activation. We found that this network reduces with time since stroke, similar to other reports that use network analysis of resting-state fMRI (35). Remarkably, both of these movement-related networks are shared with age-matched controls, again consistent

with the idea that recovery of motor performance after subcortical stroke involves modulation of extant networks rather than stroke-specific networks.

The interactions between the primary motor cortices are the foundation for numerous interventions after stroke (4, 14, 15, 25). These interventions can include but are not limited to TMS [see Cramer et al. (7) for an overview]. Overall, there is growing support for this model (13, 36). In addition to the contralateral motor cortex activation, we identify an area of deactivation within the more dorsal aspect of the ipsilateral/contralateral motor cortex (IC2). While there are complex interactions between the motor cortices during movement, the topographical distributions of these areas, i.e., away from the “hand area” make interpretation difficult. Of course, the model previously suggested (4, 14, 15, 25) is an oversimplification and fails to capture the existence of multiple cortical networks that are involved in the recovery process. It may also apply to certain stages and degrees of recovery only. Importantly, future work needs to address the effect of interventions like TMS and tDCS on multiple cortical networks (37, 38) as their effects may be more nuanced than simply increases or decreases activation. This highlights the importance of selecting the most appropriate training that should be combined with TMS or tDCS (39).

This study has a number of limitations. The patients included were relatively well recovered and whether similar results would be found in a more severely affected group is unknown. We studied only subcortical stroke. It is feasible that our findings may not apply to cortical strokes. We studied both right- and left-hemisphere strokes in right handers and flipped the MR images to one side in order to carry out the TICA on a meaningful sample size. Again, we cannot rule out that findings for dominant and non-dominant hemisphere stroke may differ. We excluded stroke patients who were performing chaotic motor imagery, and it is therefore possible that these patients may have used alternative cognitive processes that could have been interpreted as being stroke specific – though one would not expect these networks to relate to the recovery of motor performance as such. Although TICA can examine cortical networks that are shared between tasks, it has limitations (40). By considering EM and MI together in TICA analysis, we must assume that the tasks have the same temporal profile. It is entirely possible that this approach has overlooked cortical networks that have different temporal profiles – this limits the use of TICA-based fMRI as a biomarker for patient selection. However, if that was the case, then one would expect those areas to have been highlighted by earlier mass univariate fMRI studies.

CONCLUSION

In summary, we find that in our sample of well-recovered subcortical stroke patients, cortical networks associated with recovery of motor performance include some cognitive processes upstream from actual movement while others are exclusively dependent on execution. Importantly, all of these networks were

present in age-matched controls, suggesting that recovery of motor performance after stroke requires existing cortical motor networks rather than recruiting additional areas. These results also imply that the models of motor recovery after stroke [suggested by Ward and Cohen (14)] should be updated to consider movement as a combination of distinct cortical networks, each of which may have a separate contribution to recovery. Finally, we need to explore how each of these networks is affected by non-invasive stimulation to fully exploit their therapeutic potential.

REFERENCES

- Lozano R, Naghavi M, Foreman K, Lim S, Shibuya K, Aboyans V, et al. Global and regional mortality from 235 causes of death for 20 age groups in 1990 and 2010: a systematic analysis for the global burden of disease study 2010. *Lancet* (2012) **380**(9859):2095–128. doi:10.1016/S0140-6736(12)61728-0
- Murray CJL, Vos T, Lozano R, Naghavi M, Flaxman AD, Michaud C, et al. Disability-adjusted life years (DALYs) for 291 diseases and injuries in 21 regions, 1990–2010: a systematic analysis for the global burden of disease study 2010. *Lancet* (2012) **380**(9859):2197–223. doi:10.1016/S0140-6736(12)61689-4
- Calautti C, Leroy F, Guinestre JY, Baron JC. Dynamics of motor network overactivation after striatocapsular stroke: a longitudinal PET study using a fixed-performance paradigm. *Stroke* (2001) **32**(11):2534–42. doi:10.1161/hsl101.097401
- Calautti C, Baron JC. Functional neuroimaging studies of motor recovery after stroke in adults: a review. *Stroke* (2003) **34**(6):1553–66. doi:10.1161/01.STR.0000071761.36075.A6
- Cramer SC. Functional imaging in stroke recovery. *Stroke* (2004) **35**(11 Suppl 1):2695–8. doi:10.1161/01.STR.0000143326.36847.b0
- Sharma N, Cohen LG. Recovery of motor function after stroke. *Dev Psychobiol* (2012) **54**(3):254–62. doi:10.1002/dev.20508
- Cramer SC, Sur M, Dobkin BH, O'Brien C, Sanger TD, Trojanowski JQ, et al. Harnessing neuroplasticity for clinical applications. *Brain* (2011) **134**(Pt 6):1591–609. doi:10.1093/brain/awr039
- Grefkes C, Ward NS. Cortical reorganization after stroke: how much and how functional? *Neuroscientist* (2014) **20**(1):56–70. doi:10.1177/1073858413491147
- Fregni F, Pascual-Leone A. Hand motor recovery after stroke: tuning the orchestra to improve hand motor function. *Cogn Behav Neurol* (2006) **19**(1):21–33. doi:10.1097/00146965-200603000-00003
- Hummel FC, Cohen LG. Non-invasive brain stimulation: a new strategy to improve neurorehabilitation after stroke? *Lancet Neurol* (2006) **5**(8):708–12. doi:10.1016/S1474-4422(06)70525-7
- Cramer SC. Repairing the human brain after stroke. II. Restorative therapies. *Ann Neurol* (2008) **63**(5):549–60. doi:10.1002/ana.21412
- Grefkes C, Nowak DA, Eickhoff SB, Dafotakis M, Küst J, Karbe H, et al. Cortical connectivity after subcortical stroke assessed with functional magnetic resonance imaging. *Ann Neurol* (2008) **63**(2):236–46. doi:10.1002/ana.21228
- Calautti C, Jones PS, Naccarato M, Sharma N, Day DJ, Bullmore ET, et al. The relationship between motor deficit and primary motor cortex hemispheric activation balance after stroke: longitudinal fMRI study. *J Neurol Neurosurg Psychiatry* (2010) **81**(7):788–92. doi:10.1136/jnnp.2009.190512
- Ward NS, Cohen LG. Mechanisms underlying recovery of motor function after stroke. *Arch Neurol* (2004) **61**(12):1844–8. doi:10.1001/archneur.61.12.1844
- Burke Quinlan E, Dodakian L, See J, McKenzie A, Le V, Wojnowicz M, et al. Neural function, injury, and stroke subtype predict treatment gains after stroke. *Ann Neurol* (2015) **77**(1):132–45. doi:10.1002/ana.24309
- Jeannerod M, Decety J. Mental motor imagery: a window into the representational stages of action. *Curr Opin Neurobiol* (1995) **5**(6):727–32. doi:10.1016/0959-4388(95)80099-9
- Parsons LM, Fox PT, Downs JH, Glass T, Hirsch TB, Martin CC, et al. Use of implicit motor imagery for visual shape discrimination as revealed by PET. *Nature* (1995) **375**(6526):54–8. doi:10.1038/375054a0
- Guillot A, Collet C, Nguyen VA, Malouin F, Richards C, Doyon J. Functional neuroanatomical networks associated with expertise in motor imagery. *Neuroimage* (2008) **41**(4):1471–83. doi:10.1016/j.neuroimage.2008.03.042

ACKNOWLEDGMENTS

This work was supported by The Stroke Association (TSA 2003/10) and the Medical Research Council (MRC G0001219). NS was supported by a Brain Entry Scholarship, The Stroke Association (TSA 2003/10), and Sackler Fellowship. The authors thank Dr. E. A. Warburton and Mr. P. S. Jones for support. The help of Diana Day and the Wolfson Brain Imaging Centre radiographers is gratefully acknowledged.

- Sharma N. Motor imagery after stroke: where next? *Imaging Med* (2012) **4**(1):129–36. doi:10.2217/iim.11.77
- Sharma N, Simmons LH, Jones PS, Day DJ, Carpenter TA, Pomeroy VM, et al. Motor imagery after subcortical stroke: a functional magnetic resonance imaging study. *Stroke* (2009) **40**(4):1315–24. doi:10.1161/STROKEAHA.108.525766
- Beckmann CF, Smith SM. Tensorial extensions of independent component analysis for multisubject fMRI analysis. *Neuroimage* (2005) **25**(1):294–311. doi:10.1016/j.neuroimage.2004.10.043
- Oldfield RC. The assessment and analysis of handedness: the Edinburgh inventory. *Neuropsychologia* (1971) **9**(1):97–113. doi:10.1016/0028-3932(71)90067-4
- Sharma N, Pomeroy VM, Baron J-C. Motor imagery: a backdoor to the motor system after stroke? *Stroke* (2006) **37**(7):1941–52. doi:10.1161/01.STR.0000226902.43357.fc
- Sharma N, Baron J-C, Rowe JB. Motor imagery after stroke: relating outcome to motor network connectivity. *Ann Neurol* (2009) **66**(5):604–16. doi:10.1002/ana.21810
- Calautti C, Naccarato M, Jones PS, Sharma N, Day DD, Carpenter AT, et al. The relationship between motor deficit and hemisphere activation balance after stroke: a 3T fMRI study. *Neuroimage* (2007) **34**(1):322–31. doi:10.1016/j.neuroimage.2006.08.026
- Sharma N, Jones PS, Carpenter TA, Baron J-C. Mapping the involvement of BA 4a and 4p during motor imagery. *Neuroimage* (2008) **41**(1):92–9. doi:10.1016/j.neuroimage.2008.02.009
- Smith SM, Jenkinson M, Woolrich MW, Beckmann CF, Behrens TEJ, Johansen-Berg H, et al. Advances in functional and structural MR image analysis and implementation as FSL. *Neuroimage* (2004) **23**(Suppl 1):S208–19. doi:10.1016/j.neuroimage.2004.07.051
- Hyvärinen A. Fast and robust fixed-point algorithms for independent component analysis. *IEEE Trans Neural Netw* (1999) **10**(3):626–34. doi:10.1109/72.761722
- Eickhoff S, Stephan K, Mohlberg H, Grefkes C, Fink G, Amunts K, et al. A new SPM toolbox for combining probabilistic cytoarchitectonic maps and functional imaging data. *Neuroimage* (2005) **25**(4):1325–35. doi:10.1016/j.neuroimage.2004.12.034
- Muellbacher W, Ziemann U, Wissel J, Dang N, Kofler M, Facchini S, et al. Early consolidation in human primary motor cortex. *Nature* (2002) **415**(6872):640–4. doi:10.1038/nature712
- Sharma N, Baron J-C. Does motor imagery share neural networks with executed movement: a multivariate fMRI analysis. *Front Hum Neurosci* (2013) **7**:564. doi:10.3389/fnhum.2013.00564
- Ward NS, Newton JM, Swayne OBC, Lee L, Thompson AJ, Greenwood RJ, et al. Motor system activation after subcortical stroke depends on corticospinal system integrity. *Brain* (2006) **129**(Pt 3):809–19. doi:10.1093/brain/awl002
- Stinear CM, Barber PA, Smale PR, Coxon JP, Fleming MK, Byblow WD. Functional potential in chronic stroke patients depends on corticospinal tract integrity. *Brain* (2007) **130**(1):170–80. doi:10.1093/brain/awl333
- Perez MA, Cohen LG. The corticospinal system and transcranial magnetic stimulation in stroke. *Top Stroke Rehabil* (2009) **16**(4):254–69. doi:10.1310/tsr1604-254
- Wang L, Yu C, Chen H, Qin W, He Y, Fan F, et al. Dynamic functional reorganization of the motor execution network after stroke. *Brain* (2010) **133**(Pt 4):1224–38. doi:10.1093/brain/awq043
- Lefebvre S, Dricot L, Laloux P, Gradkowski W, Desfontaines P, Evrard F, et al. Neural substrates underlying stimulation-enhanced motor skill learning after stroke. *Brain* (2015) **138**(Pt 1):149–63. doi:10.1093/brain/awu336

37. Hao Z, Wang D, Zeng Y, Liu M. Repetitive transcranial magnetic stimulation for improving function after stroke. *Cochrane Database Syst Rev* (2013) 5:CD008862. doi:10.1002/14651858.CD008862.pub2
38. Le Q, Qu Y, Tao Y, Zhu S. Effects of repetitive transcranial magnetic stimulation on hand function recovery and excitability of the motor cortex after stroke: a meta-analysis. *Am J Phys Med Rehabil* (2014) 93(5):422–30. doi:10.1097/PHM.000000000000027
39. Reis J, Robertson E, Krakauer JW, Rothwell J, Marshall L, Gerloff C, et al. Consensus: “can tDCS and TMS enhance motor learning and memory formation?”. *Brain Stimul* (2008) 1(4):363–9. doi:10.1016/j.brs.2008.08.001
40. Helwig NE, Hong S. A critique of tensor probabilistic independent component analysis: implications and recommendations for multi-subject fMRI data analysis. *J Neurosci Methods* (2013) 213(2):263–73. doi:10.1016/j.jneumeth.2012.12.009

Conflict of Interest Statement: The authors declare that the research was conducted in the absence of any commercial or financial relationships that could be construed as a potential conflict of interest. The Review Editor Andreas Charidimou declares that, despite being previously affiliated to the same institution as Nikhil Sharma, and despite having collaborated on publications (not related to the current topic) in the last 2 years with Jean-Claude Baron, the review process was handled objectively.

Copyright © 2015 Sharma and Baron. This is an open-access article distributed under the terms of the Creative Commons Attribution License (CC BY). The use, distribution or reproduction in other forums is permitted, provided the original author(s) or licensor are credited and that the original publication in this journal is cited, in accordance with accepted academic practice. No use, distribution or reproduction is permitted which does not comply with these terms.



A thalamic-fronto-parietal structural covariance network emerging in the course of recovery from hand paresis after ischemic stroke

Eugenio Abela¹, John H. Missimer², Andrea Federspiel³, Andrea Seiler^{1,4}, Christian Walter Hess⁴, Matthias Sturzenegger⁴, Roland Wiest¹ and Bruno J. Weder^{1,5*}

¹Support Center for Advanced Neuroimaging (SCAN), Institute for Diagnostic and Interventional Neuroradiology, University Hospital Inselspital, University of Bern, Bern, Switzerland, ²Laboratory of Biomolecular Research, Paul Scherrer Institute, Villigen, Switzerland, ³Department of Psychiatric Neurophysiology, University Hospital of Psychiatry, University of Bern, Bern, Switzerland, ⁴Department of Neurology, University Hospital Inselspital, University of Bern, Bern, Switzerland, ⁵Department of Neurology, Kantonsspital St. Gallen, St. Gallen, Switzerland

OPEN ACCESS

Edited by:

Jean-Claude Baron,
University of Cambridge, UK

Reviewed by:

Martin Lotze,
University of Greifswald, Germany
Emmanuel Carrera,
University of Geneva, Switzerland
Christian Gerloff,
University Medical Center Hamburg-
Eppendorf, Germany

*Correspondence:

Bruno J. Weder,
Support Center for Advanced
Neuroimaging (SCAN), Institute for
Diagnostic and Interventional
Neuroradiology, University Hospital
Inselspital, University of Bern, Bern
3010, Switzerland
bruno.weder@insel.ch

Specialty section:

This article was submitted to Stroke,
a section of the journal
Frontiers in Neurology

Received: 13 May 2015

Accepted: 17 September 2015

Published: 13 October 2015

Citation:

Abela E, Missimer JH, Federspiel A,
Seiler A, Hess CW, Sturzenegger M,
Wiest R and Weder BJ (2015) A
thalamic-fronto-parietal structural
covariance network emerging in the
course of recovery from hand paresis
after ischemic stroke.
Front. Neurol. 6:211.
doi: 10.3389/fneur.2015.00211

Aim: To describe structural covariance networks of gray matter volume (GMV) change in 28 patients with first-ever stroke to the primary sensorimotor cortices, and to investigate their relationship to hand function recovery and local GMV change.

Methods: Tensor-based morphometry maps derived from high-resolution structural images were subject to principal component analyses to identify the networks. We calculated correlations between network expression and local GMV change, sensorimotor hand function and lesion volume. To verify which of the structural covariance networks of GMV change have a significant relationship to hand function, we performed an additional multivariate regression approach.

Results: Expression of the second network, explaining 9.1% of variance, correlated with GMV increase in the medio-dorsal (md) thalamus and hand motor skill. Patients with positive expression coefficients were distinguished by significantly higher GMV increase of this structure during stroke recovery. Significant nodes of this network were located in md thalamus, dorsolateral prefrontal cortex, and higher order sensorimotor cortices. Parameter of hand function had a unique relationship to the network and depended on an interaction between network expression and lesion volume. Inversely, network expression is limited in patients with large lesion volumes.

Conclusion: Chronic phase of sensorimotor cortical stroke has been characterized by a large scale co-varying structural network in the ipsilesional hemisphere associated specifically with sensorimotor hand skill. Its expression is related to GMV increase of md thalamus, one constituent of the network, and correlated with the cortico-striato-thalamic loop involved in control of motor execution and higher order sensorimotor cortices. A close relation between expression of this network with degree of recovery might indicate reduced compensatory resources in the impaired subgroup.

Keywords: stroke recovery, structural covariance network, fronto-parietal network, thalamocortical loop, tensor-based morphometry

Introduction

As both cross-sectional and a few longitudinal observational studies have demonstrated, behavioral recovery from hemiparesis after ischemic stroke shows marked between-subject variability (1, 2). This variability is thought to be determined not only by general demographic or clinical factors – such as age, gender or medical comorbidities – but also by neurobiological processes prompted by damage to critical nodes of functional and structural brain networks (3, 4). Activation studies using functional MRI (fMRI) have contributed considerably in the past to current knowledge of these processes (5–7); moreover, resting state fMRI and structural MRI have provided complementary insights in recent years (8). The improved understanding of stroke provided by neuroimaging could impact neurorehabilitative therapies (9–11).

Activation studies performed with fMRI have shown that successfully recovered subjects show almost normal cerebral patterns, exhibiting change during recovery from attention demanding controlled processing of motor performance in the subacute stage to more fluent and automatic processing in the late chronic stage (12). This suggests recovery at the synaptic and/or neuronal level in the perilesional zone. In contrast, individuals presenting impaired recovery retain ineffective motor patterns and may not regain fully the specific motor function (13, 14); they, thus, possibly require cognitive control and concentrated effort to maintain motor execution (15). Accordingly, volitional and emotional effort are means to enhance output in a diseased, low-efficient motor system, as indicated by the enhanced activation of motor networks observed in fMRI-studies of patients with chronic motor impairment (12). An additional aspect of the recovery process evidenced by studies at varying stages post-stroke is the influence of the contralesional hemisphere, functionally rather supporting motor activity in the early acute phase and mainly inhibiting it in the chronic stage (16, 17).

In the following, we utilize structural MRI to study stroke recovery in a patient cohort of 28 patients selected for first cortical sensorimotor stroke and associated initial hand paresis or plegia. The analysis employs a relatively new method, tensor-based morphometry (TBM), to quantify gray matter volume (GMV) changes during recovery (18, 19). While indicating structural neuronal plasticity, the changes cannot be assigned *in vivo* to a specific mechanism, e.g., axon sprouting, dendritic branching or synaptogenesis (20). Requiring high-resolution MRI [3D modified driven equilibrium Fourier transform (3D-MDEFT)] imaging, TBM evaluates the transformations relating one acquisition to a second in a single subject. In our longitudinal study, the first acquisition was performed after 3 months in the subacute phase and the second after 9 months in the chronic phase. In all patients, initial diffusion-weighted MR images (21) delineated impacted critical brain lesions. High-resolution T1 (3D-MDEFT)-MRIs were acquired in 28 patients 3 and 9 months after stroke (22). An example of multimodal imaging in a wider sense (23), the acquisition protocols provided two non-redundant data sets from the same MR instrument in the same study population: bright tissue contrast for lesion delineation in the acute phase and GMV changes derived from the high-resolution T1 images by TBM analysis.

Accompanying the imaging was an array of clinical, motor and sensory assessments performed regularly during the 9-month study. Of the behavioral assessments, picking small objects (PSO), a lateralized motor skill requiring a particular precision grip, showed the greatest variance over the 9-month trial period (21). Response feature analysis (RFA) using Akaike's information criterion applied to the 9-month recovery trajectories of the individual patient tests partitioned the patient cohort into three subgroups showing fast linear, slow exponential or impaired recovery (24). A multivariate analysis, principal component analysis (PCA), of the PSO task confirmed the partitioning among the 28 patients and characterized each patient's expression of the principal recovery trajectory by a single coefficient (22). This expression coefficient served as correlate to identify the neural pattern, represented as a principal component image of a PCA of the 28 TBM images, most closely associated with recovery. We have shown previously in the context of PET regional cerebral blood flow (CBF) images that PCA provides a powerful tool for elucidating disease-related abnormalities and post-lesional reorganization of neural networks in the human brain (25).

A previous mass-univariate analysis of these TBM images yielded three findings: (i) most striking, impaired patients with chronic disturbed hand motor skills showed the most prominent GMV increase in the ipsilesional medio-dorsal (md) thalamus, including also the head of the caudate nucleus; (ii) all patients evidenced GMV decreases within the contralesional anterior cerebellum at a location typical of cerebellar diaschisis after sensorimotor cortical stroke; and (iii) patients showing fast recovery exhibited a slight GMV increase in the perilesional premotor cortex (PMC). These results stimulated several questions: Does the significant GMV increase of md thalamus in these patients represent an isolated, local effect or does it implicate an extended gray matter network involved in recovery after a sensorimotor cortical stroke? Does the extended network show a structural covariance pattern that discriminates among classes of recovery process? How does the network relate to the initial lesion pattern?

These questions led to the hypotheses examined in the current study: the prominent GMV changes in the md thalamus relate to the dorsolateral prefrontal circuit of Alexander et al. (26) as proposed in our previous paper and may have access to the dysfunctional sensorimotor network post-stroke (22). A posited distributed neuronal network including the md thalamus is specifically related to sensorimotor hand skill. This network manifests a structural covariance pattern that may distinguish among patient subgroups according to recovery class. The structural covariance pattern shows a correlation with the initial lesion pattern.

Participants and Methods

Patients and Healthy Controls

We prospectively recruited patients at two comprehensive stroke centers (Departments of Neurology, University Hospital Bern and Kantonsspital St. Gallen, Switzerland) from January 01, 2008 through July 31, 2010. Inclusion criteria were (1) first-ever stroke, (2) clinically significant contralesional sensorimotor hand function impairment as leading symptom, and (3) inclusion of the pre- and/or post-central gyri within the ischemic

lesion confirmed on acute diffusion-weighted (DWI) and fluid attenuated inversion recovery (FLAIR) MRI scans. Patients were excluded if they presented (1) aphasia or cognitive deficits that precluded understanding the study purposes or task instructions, (2) prior cerebrovascular events, (3) occlusion or stenosis >70% of the carotid arteries in MR-angiography, (4) purely subcortical stroke, and (5) other medical conditions interfering with task performance. We recruited 36 patients, seven of which dropped out (three withdrew consent, two were too frail for repeated testing, one was shown to have no cortical stroke after enrollment, one was lost to follow-up). The final sample consisted of 29 patients (five female). As a control group for the analyses of behavioral and clinical data, we recruited 22 healthy older adults (11 female) from the local community. Groups were matched for age (unpaired two-tailed t -test: $t(49) = 3.4$, $p < 0.12$) and handedness according to the Edinburgh Handedness Questionnaire (unpaired two-tailed t -test: $t(49) = 0.36$, $p < 0.30$). The study received ethical approval from both research centers [Ethikkommission des Kantons St. Gallen (EKSG), Kantonsspital St. Gallen, 9007 St. Gallen and Kantonale Ethikkommission Bern (KEK), 3010 Bern, Switzerland]. All participants gave written informed consent before enrollment according to the Declaration of Helsinki. The same cohort was used for our previous publications (21, 22, 27).

Data Acquisition Study Timeline

We performed a baseline examination within the first 2 weeks after stroke (median 5 days, range 1–18 days) with extended measurements of clinical and behavioral data (see below). The same measurements were taken 3 months (91 days, 80–121 days) and 9 months (277 days, 154–303 days) after stroke. During each of these two visits, we acquired high-resolution anatomical imaging data. Patients were additionally seen at monthly intervals in-between these examinations to evaluate recovery of dexterous hand function.

Clinical and Behavioral Data

Clinical stroke severity was assessed using the National Institutes of Health Stroke Scale (NIHSS) (28). Hand motor function was assessed with two outcome variables, grip force and dexterity. Grip force was measured by hand dynamometry (HD) with a Jamar Dynamometer (29, 30). Dexterous hand function was measured using the modified Jebsen Taylor Test (JTT), a standardized quantitative assessment that consists of five timed subtests that simulate everyday activities (31). For our current analysis, we relied on data from the JTT subtest “PSO”, which consists of picking six common objects (two paper clips, two bottle caps, two coins) and dropping them into an empty can as fast as possible. As previously shown by our group, PSO explains by far most of the longitudinal variance in JTT scores and allows accurate classification of patient subgroups (see Supplementary Material for details) (21). The two motor tasks measure complementary aspects of hand motor function. Behaviorally, HD is performed with a simple power grip using the whole hand, whereas PSO necessitates precision grip characterized by opposition of the thumb against one or two fingers (32); and furthermore a proper coupling of grasping and lifting phases of objects performing this task which has been shown to be specifically vulnerable in the case

of lesioned dorsolateral PMC (33). Neuroanatomically, each grip form is controlled by different components of the sensorimotor network: power grips are mainly controlled by the primary sensorimotor cortices, whereas precision grip control includes the premotor and posterior parietal cortices (34, 35). As a measure of sensorimotor integration, we included a tactile object recognition (TOR) task, which consisted in discriminating 30 everyday objects with either hand (36). This task was administered at the same time as the NIH evaluation. Further details on measurement procedures can be found in the Supplementary Material.

Imaging Data

All patients underwent acute phase imaging at admission according to local stroke imaging protocols. This included a diffusion-weighted imaging (DWI) scan and T1-weighted (T1w) anatomical image. At 3 and 9 months after stroke, each patient underwent high-resolution T1w imaging using a 3D-MDEFT with following imaging parameters (37): repetition time $TR = 7.92$ ms, echo time $TE = 2.48$ ms, flip angle = 16° , inversion with symmetric timing (inversion time 910 ms), $256 \times 224 \times 176$ matrix points with a non-cubic field of view (FOV) of $256 \text{ mm} \times 224 \text{ mm} \times 176 \text{ mm}$, yielding a nominal isotropic resolution of 1 mm^3 (i.e., $1 \text{ mm} \times 1 \text{ mm} \times 1 \text{ mm}$), fat saturation, 12 min total acquisition time. Identical prescription of MR images was achieved by use of the Siemens auto-align sequence that automatically sets up consistent slice orientation based on a standard MRI atlas.

Data Analysis Synopsis

Longitudinal clinical and behavioral data were analyzed with a variant of RFA (24). This is a technique that uses summary measures to simplify analysis of serial measurements [cf. Ref. (24) for clinical examples]. As described below and in Ref. (21), we proceed in two levels: at the single-subject level, we summarize each patient's z -transformed longitudinal data using linear and non-linear curve fitting. At the group level, we then calculate a PCA of these curves to derive a number that summarizes each patient's recovery relative to the whole cohort. The analysis of structural high-resolution imaging data was performed similarly. At the single-subject level, we calculated TBM maps that encode (longitudinal) local GMV change between 3 and 9 months after stroke, as previously described (22). At the group level, we again calculated a PCA to identify regions with co-varying GMV change across time. In analogy to previous work analyzing structural covariance in the human brain, we refer to these maps as *longitudinal structural covariance networks* (38, 39).

Response Feature Analysis of Clinical and Behavioral Data

First, each patient's PSO task data were transformed to z -scores using the mean and SD of a healthy control group of 22 age-matched subjects; normal performance was defined as $z \leq 0 \pm 2.5$ units. Then, each patient's recovery trajectory was identified by fitting a set of linear and exponential models to the z -scores, and the best fitting model was selected using Akaike's information criterion. Patients were classified in three recovery subgroups according to their recovery model: fast (linear recovery trajectory), slow (exponential recovery

trajectory converging to $z \geq -2.5$) and impaired recovery (exponential recovery trajectory converging to $z < -2.5$). The principal component analyses of the PSO and TOR task, and NIH evaluation were performed with Matlab program, *princomp* (The Mathworks, Inc., Natick, MA, USA). The PSO task yielded ten principal component time courses and variances (one per visit); the TOR task and NIH evaluation, three time courses and variances. Each produced 36 patient expression coefficients (or “scores”). The Kaiser–Guttman criterion was used to select salient principal components (40). Missing data, arising when patient did not show or could not perform task, were replaced by means over all patients at the time point of the missing data; 10 out of 280 planned visits yielded missing data. The present study uses the expression coefficients of the subset of 28 patients for which TBM images were acquired.

Lesion Mapping

Lesions were manually traced on DWI images using MRICron,¹ as described in Ref. (21). Lesion volumes were calculated by summing all voxels within the resultant binary lesion masks. The latter were used to exclude lesioned voxels during normalization of all images into the stereotaxic Montreal Neurological Institute (MNI) space (see below). Additionally, we built summary lesion maps for each recovery subgroup, which we thresholded at >20% lesion density for comparison with structural data (see below).

Tensor-Based Morphometry

Tensor-based morphometry maps were calculated as described in Ref. (22) using SPM8 (version 4667²) running on MATLAB (R2009a, MathWorks, Natick, MA, USA). Briefly, we first realigned 3D-MDEFT images from both acquisition time points to correct for position differences. We next used segmentation with cost-function masking to derive gray matter tissue partitions (41, 42). We then calculated in each subject the Jacobian determinants (first derivatives) of high-dimensional deformation fields that transform voxel-by-voxel the T1w image from month 3 onto the T1w image from month 9. Multiplication of the first derivatives with the matter segmentation from month 3 results in a map that encodes matter volume expansion or contraction per voxel across time. These maps were transformed into the stereotaxic MNI space using normalization parameters derived from segmentation. Normalized GMV change maps were finally smoothed with a 12 mm × 12 mm × 12 mm isotropic 3D Gaussian kernel, motivated by previous studies that show a reduction of false positives for this kernel size in voxel-based morphometry studies (43). These smoothed maps were entered in the covariance analysis as described below. Based on our previous study, we used an unbiased region of interest analysis to extract local GMV changes from ipsilesional thalamus, ipsilesional dorsal PMC and contralesional cerebellum (22).

Structural Covariance Using Principal Component Analysis

The PCA of the TBM images was performed on a subset of 28 patients representing the volume changes between months 3 and

9 (of the 29 patients retained for the study 1 had to be excluded because of MR motion artifacts). PCA was executed on the images data using in house software written in MATLAB based on the algorithm described by Alexander et al. and Moeller et al. (44, 45). Extracerebral voxels were excluded from the analysis using a mask derived from the gray matter component yielded by segmentation of the anatomical image volume into gray matter, white matter and cerebrospinal fluid followed by the calculation of residual matrices for each of the 28 scans. From matrices whose rows corresponded to the 28 scans and columns to the 132407 relevant voxels in a single image volume were subtracted from each element (i) the mean of voxel values of its column and (ii) the mean of voxel values of its row, and (iii) added to each element the grand mean of all voxel values in the original matrices. The row, column, and grand means of the resulting residual matrices vanish. Using the singular value decomposition implemented in Matlab, each residual matrix was then decomposed into 28 components. Each component consisted of an image volume, i.e., eigenimage, a temporal expression coefficient, i.e., eigenvariate, and an eigenvalue. The squared eigenvalue is proportional to the fraction of variance described by each component; the subject expression coefficients describe the amount that each scan contributes to the component; and the component image displays the degree to which the voxels co-vary in the component in the course from months 3 to 9. The subject expression coefficients and voxel values of a principal component are orthonormal and range between -1 and 1 ; the orthogonality reflects the lack of statistical correlation among the principal components. Significant clusters were delineated by applying a height threshold at the first and ninety-ninth percentile of voxel values and an extent threshold of 32 voxels (corresponding to the minimal resolution element of the TBM maps). These clusters were localized using the Jülich cytoarchitectonic probabilistic atlas (SPM Anatomy toolbox, Version 1.8, made available through the Human Brain Mapping division at the Forschungszentrum Jülich at http://www.fz-juelich.de/inm/inm-1/DE/Forschung/_docs/SPMANatomyToolbox/SPMANatomyToolbox_node.html). Furthermore, we calculated the overlap between each network cluster and subgroup lesion density maps.

Statistical Analysis

We used median and range for descriptive statistics. We first assessed the relationship of structural covariance component expression, clinical and structural variables, e.g., lesion volume and regional GMV change, using Pearson's correlation coefficient in order to identify the network related to hand function recovery. Next, we assessed differences with respect to subgroups in network expression and behavioral variables. To do so, we first applied the Shapiro–Wilk test and inspected Q–Q plots for each variable to assess deviations from normality. We used then non-parametric tests to compare scalar variables where appropriate, i.e., the Kruskal–Wallis one-way analysis of variance by ranks to assess differences in the central tendency among any of the three subgroups, and the Mann–Whitney *U* test to compare pairs of subgroups against each other. Finally, we used robust (multiple) regression within the framework of the general linear model to test the relationship of network expression, clinical and structural

¹<https://www.nitrc.org/projects/mricron>

²<http://www.fil.ion.ucl.ac.uk/spm/software/spm8/>

variables to hand function recovery and their interaction across the whole patient cohort. The criterion for significance was set at $p < 0.05$, Bonferroni corrected for multiple comparisons.

Results

Clinical and Behavioral Data

Clinical characteristics of the patient cohort are summarized in **Table 1**. Representative sections of each subjects' ischemic lesion can be found in Figure S1 in Supplementary Material. The behavioral data was incorporated in two principal component analyses. The first principal components of PSO and NIH assessments were chosen for further analysis because they explained the greatest fractions of variance, 70 and 90%, respectively, of the corresponding PCAs. RFA of the PSO task indicated that eight patients showed normal motor performance at baseline (subgroup "fast recovery"), ten patients exponential recovery that converged to normal motor performance ("slow recovery") and eight whose recovery trajectories followed exponential recovery curves that did not reach normal performance ("impaired recovery") (21).

Selection of Longitudinal Structural Covariance Networks

Table 2 characterizes three principal components of the TBM images (structural covariance networks) that correlated with clinical and behavioral variables across the whole patient cohort. The first component ($PC1_{TBM}$) correlated with GMV reduction in the cerebellum contralateral to the affected hemisphere. The second component ($PC2_{TBM}$) correlated with lesion size, GMV volume increase in the md thalamus, clinical ($PC1_{NIHSS}$ expression) and hand function specific recovery ($PC1_{PSO}$ expression). The fourth principal component correlated exclusively with $PC1_{NIHSS}$ expression. None of the other PCs surviving the Kaiser–Guttman criterion correlated with any of the external variables.

Thalamocortical Network Related To Hand Function Recovery Effects Across the Patient Cohort

Since the second structural covariance network $PC2_{TBM}$ correlated with our specific measure of hand function recovery, we focused further analysis on its critical clusters (or nodes, **Figure 1A**). Clusters that co-varied with the thalamus fell within the first percentile of voxel values, and were labeled as "positive" clusters since the thalamus showed gray matter increase. These clusters (ordered by size) included insular and peri-insular cortex, dorsolateral prefrontal and ventral premotor cortices, thalamus, posterior parietal cortices and two smaller clusters in the temporal and occipital cortex. A single cluster fell within the ninety-ninth percentile and included pre- and post-central cortex. **Table 3** summarizes localization, statistics and functional correlates of all clusters that survived thresholding ($PC1_{TBM}$ and $PC4_{TBM}$, are summarized in Tables S1 and S2 in Supplementary Material, respectively). Functional interpretation was done in the context of motor hand function, based on current literature. The expression of this network had a strong correlation with thalamic GMV change across the whole cohort (**Figure 2A**).

Effects Within Patient Subgroups

Having identified a structural network related to hand function recovery (**Table 4**), we next analyzed its relationship to lesion topography within recovery subgroups. Lesion analyses are summarized in **Figure 1B**. Projection of subgroup lesion density maps onto $PC2_{TBM}$ clusters showed that the thalamic cluster was spared across all subgroups, but that the other clusters showed varied involvement. A detailed volumetric analysis (**Table 5**) showed that only a small fraction of each lesion density map affected network clusters (median and range 0.95%, 0–6.7%), indicating that GMV density changes occurred either in perilesional or more distant areas. When analyzing the percentage of each cluster affected by the lesion, there were notable differences: lesions in the fast recovery subgroup affected mostly the parietal-opercular and insular cluster (Cluster 1+), whereas lesions in the impaired subgroup affected mostly the ventral premotor cortex and intraparietal sulcus (IPS) (Cluster 3+ and 4+). The slow recovery subgroup showed no clear lesion profile. Affection of the pre/post-central cluster (Cluster 1–) increased across subgroups.

We further compared the patients subgroups presenting normal motor performance after 9 months (fast and slow recovery) with the subgroup that did not achieve normal performance (impaired recovery). As expected from the RFA, the latter group yielded the highest expression coefficients in $PC1_{NIHSS}$ ($p < 0.01$) and specifically in $PC1_{PSO}$ ($p < 0.0001$). This group had also the largest GMV expansion in the medio-dorsal thalamus and the highest lesion volumes (both $p < 0.05$). **Figure 2** shows the relationship between $PC2_{TBM}$ expression and thalamic GMV change (panel A) and hand skill recovery as reflected by PSO (panel B), respectively. Considering all individuals, GMV change correlated with expression coefficients of the structural covariance network of $PC2_{TBM}$ ($R = 0.72$ and $p < 0.5$ after correction for multiple comparisons). $PC2_{TBM}$ expression could also distinguish between subgroups: When dividing patients into subgroups with positive versus negative network expression coefficients (without regard to recovery subgroup assignments), we found that the positive subgroup has significantly higher thalamus GMV change (median 1.35% with range 0.83–1.79%), whereas the negative subgroup shows no significant change (median 0% with range 0.04–0.04%, Mann–Whitney U test $p < 0.001$).

However, only the impaired recovery subgroup showed a linear relationship between the expression of structural covariance network of $PC2_{TBM}$ and recovery (**Figure 2B**): the slope estimate (and SE) was 53.1 ± 22.7 ; adjusted $R = 0.74$ with $p < 0.05$. Note that one patient of this subgroup showed a negative $PC1_{PSO}$ expression score. Inspection of the raw data indicated that this particular subject showed a secondary deterioration of skilled hand function during the last 2 months of the study, after an initially favorable course. Removal of this outlier did not change results. A few individuals of the recovered subgroups exhibited high GMV changes in the medio-dorsal thalamus, representing exceptions to the group trend.

Multivariate Linear Regression

To further test the specificity of the association between $PC2_{TBM}$ and hand function recovery, we calculated a multivariate linear

TABLE 1 | Descriptive statistics of clinical and demographic data of stroke patients at baseline, month 3 and month 9.

No.	Id	Age	Gender	Side	Etiology	NIH B	NIH M3	NIH M9	mRS B	mRS M3	mRS M9	HD B	HD M3	HD M9	PSO B	PSO M3	PSO M9	TOR B	TOR M3	TOR M9
1	p01	77	M	L	UN	4	2	1	2	1	1	31	40	41	9.7	7.9	5.7	30	30	30
2	p02	50	M	R	OC	7	1	0	4	1	0	6	54	63	0.0	6.0	6.2	25	28	30
3	p03	78	M	R	LAD	5	5	3	3	2	2	15	17	42	13.5	11.1	9.1	28	29	27
4	p05	80	M	L	LAD	2	3	1	2	1	1	42	42	37	10.6	6.5	8.4	30	30	30
5	p06	53	F	R	LAD	6	3	3	3	2	1	11	9	19	29.9	10.1	14.9	0	0	0
6	p07	78	F	R	CE	4	2	2	2	1	1	18	21	21	14.0	7.5	7.1	0	12	24
7	p09	70	F	R	CE	3	2	0	2	1	0	21	31	34	9.1	8.5	6.0	29	30	30
8	p11	41	F	L	LAD	3	2	0	1	0	0	32	37	39	5.6	4.0	5.11	24	30	30
9	p12	54	M	R	UN	4	2	1	3	1	0	14	33	38	8.5	5.5	5.2	30	30	30
10	p15	54	M	L	LAD	6	4	1	3	1	1	10	24	33	38.8	13.1	11.1	0	6	10
11	p16	73	M	R	OC	4	2	0	2	1	0	51	55	55	7.3	4.9	5.3	26	29	30
12	p17	58	M	L	CE	4	2	0	3	0	0	20	39	48	11.5	4.3	4.7	30	29	30
13	p20	70	M	L	CE	6	4	2	3	1	1	24	35	42	12.9	9.7	9.3	0	6	10
14	p24	74	M	R	CE	4	1	0	1	0	0	34	49	50	14.3	6.9	5.1	28	30	30
15	p25	49	M	R	CE	3	2	1	2	1	0	49	59	67	12.3	5.3	5.9	0	6	10
16	p26	44	M	L	CE	3	1	0	1	0	0	9	33	50	11.5	6.0	5.1	30	30	30
17	p30	63	M	L	CE	4	1	1	3	0	0	43	41	45	10.6	6.3	6.3	30	30	30
18	p31	63	M	L	UN	5	0	0	2	0	0	30	48	44	5.3	4.2	4.7	30	30	30
19	p33	75	M	R	LAD	3	2	2	2	1	1	3	14	22	0.0	18.8	11.5	12	28	30
20	p35	78	M	L	LAD	5	3	2	3	1	1	23	48	40	10.1	6.8	6.1	30	30	30
21	p36	60	M	L	CE	4	1	1	3	1	1	31	40	41	18.2	8.0	6.6	30	30	30
22	p37	75	M	R	OC	4	2	1	2	1	1	0	27	32	0.0	8.6	10.4	4	23	25
23	p38	77	M	L	LAD	5	2	2	3	1	1	10	21	23	26.9	10.9	8.3	29	30	30
24	p41	51	M	R	CE	2	1	0	2	1	1	36	41	52	7.1	5.1	4.8	30	30	30
25	p42	64	M	R	LAD	1	0	0	2	0	0	14	33	35	18.9	7.1	7.4	29	30	30
26	p43	82	M	L	LAD	3	3	2	2	2	1	17	10	18	16.8	21.4	13.9	20	22	25
27	p44	67	M	R	UN	11	10	9	4	3	3	15	15	41	52.3	45.1	12.3	3	4	2
28	p45	53	M	R	LAD	11	9	4	5	3	2	0	10	17	0.0	45.5	19.9	0	1	3
Median		65.5	24 M	13 L	11 LAD,	4	2	1	2	1	1	20	35	41	11.0	7.3	6.5	28	29	30
Range		41, 82	4 F	15 R	10 CE, 4 UN, 3 OC	1, 11	0, 10	0, 9	1, 4	0, 3	0, 3	0, 51	9, 59	17, 67	0.0, 52.3	4.0, 45.5	4.7, 19.9	0, 30	0, 30	0, 30
Median (z)												−1.3	−0.2	0.4	−5.0	−1.2	−0.4	0.6	0.6	0.6
Range (z)												−2.8, 1.3	−2.3, 1.9	1.6, 2.6	−38.9, 0.5	−33.2, 1.6	−11.7, 1.0	−7.5, 0.6	−6.5, 0.6	−4.5, 0.6

M, male; F, female. Etiology is classified according to the Trial of ORG 10172 in acute stroke treatment (TOAST): LAD, large artery disease; CE, cardioembolism; OC, other determined cause; UN, undetermined cause. NIH, National Institutes of Health Stroke Scale; mRS, modified Rankin Scale; HD, hand dynamometry (in kilograms); PSO, picking small objects task (in seconds); TOR, tactile object recognition (in numbers of recognized objects); z, z-scores using mean and standard deviation of healthy controls for each task.

TABLE 2 | Correlation of longitudinal structural covariance networks across all patients (n = 28).

Component	Variance (%)	Parameters with significant correlations ^a	Values of parameters ^b	Correlation coefficient (r)
PC1 _{TBM}	19.9	GMV change ant. cerebellum	−0.2 (−1.3, 0.6) %	−0.57
PC2 _{TBM}	9.1	Lesion volume	9.0 (0.6, 141.7) cc	0.61
		PC1 _{NIHSS} expression	−3.65 to 11.9	0.61
		PC1 _{PSO} expression	−20.99 to 64.26	0.51
		GMV change md Thalamus	0.4 (−0.6, 4.0) cc	0.72
PC4 _{TBM}	8.1	PC1 _{NIHSS} expression	0 (−3.65, 11.9)	0.54
Cumulative Variance	37.1			

NIHSS score, National Institute of Health Stroke Scale-score; PSO, picking small objects, MI primary motor cortex, SI primary sensory cortex.
^aSignificant correlations after correction for eight multiple comparisons: $0.05/8 = 0.006$ yields significant entries. This probability corresponds to a correlation coefficient of 0.466.
^bValues of parameters are indicated as median, including range, expression coefficients are indicated as range due to normalization (median of 0).

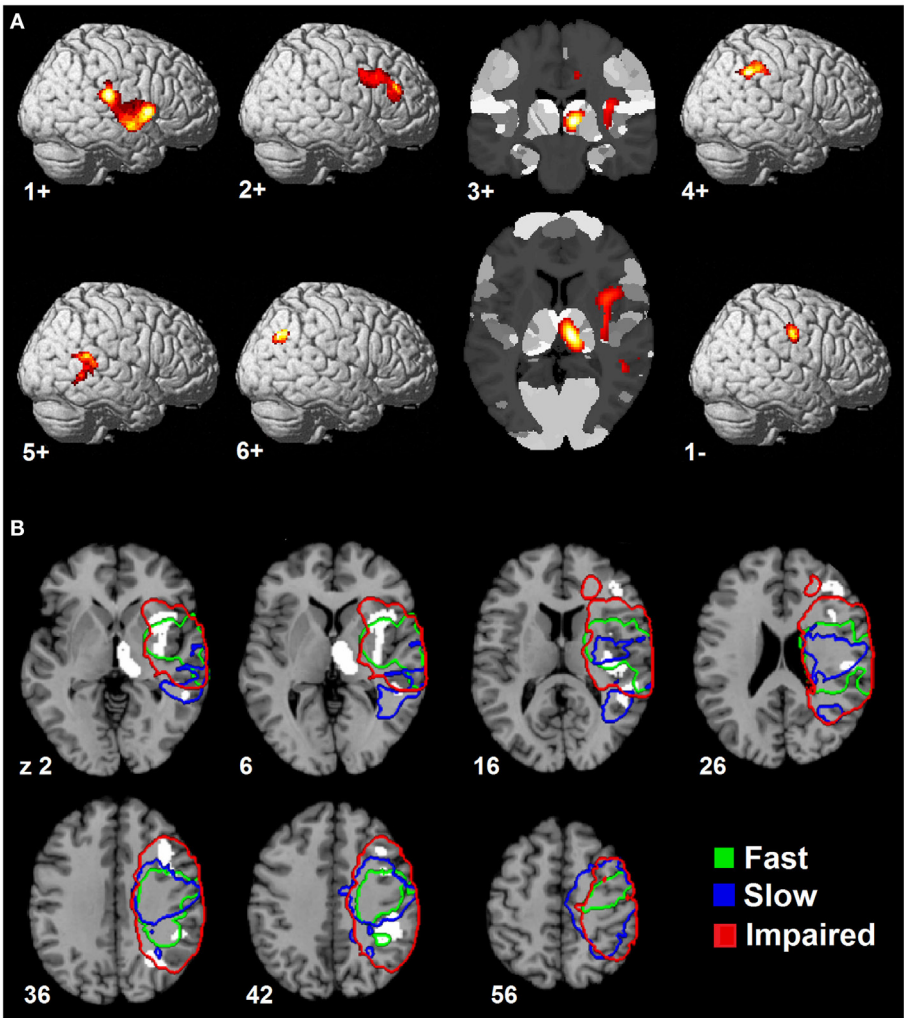
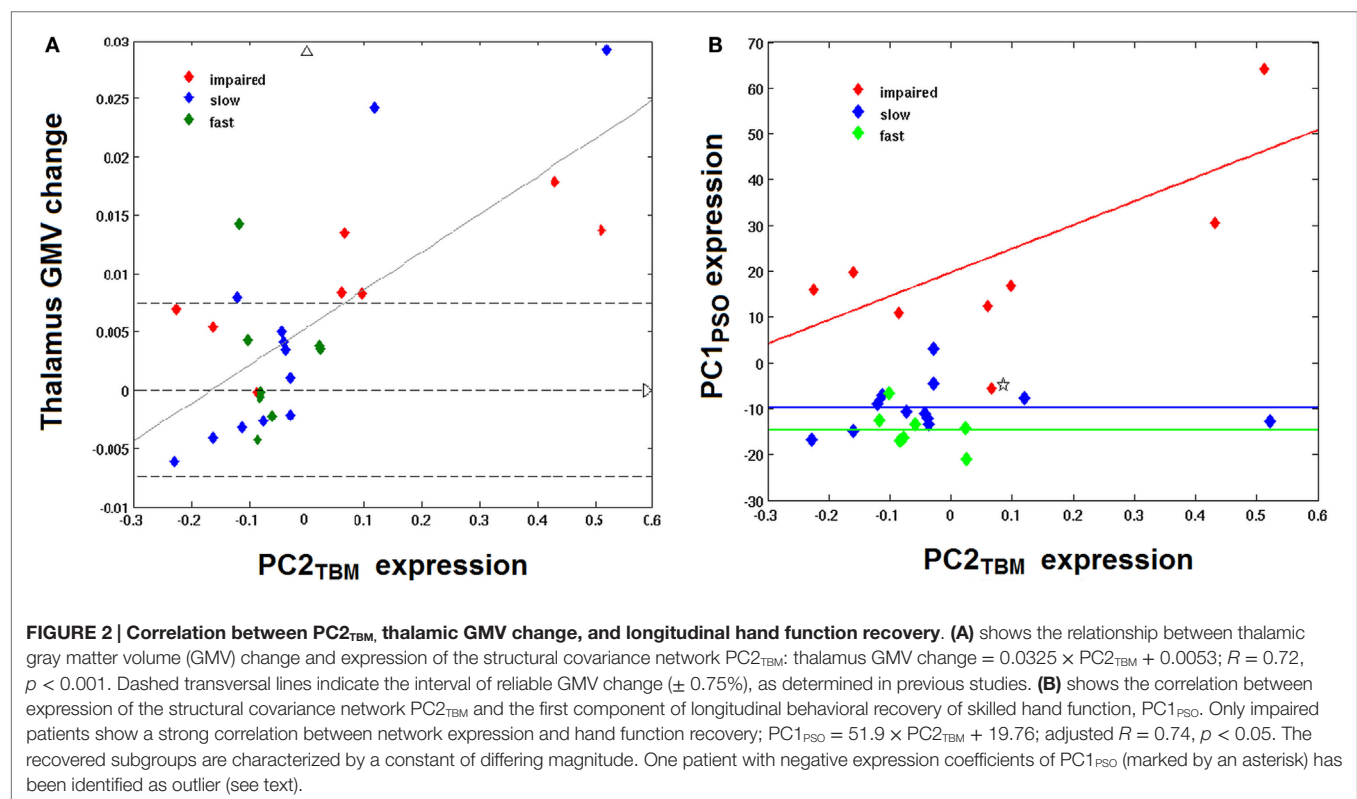


FIGURE 1 | Spatial topography of longitudinal structural covariance network correlating with hand function recovery. (A) shows the six largest clusters of supra-threshold voxels for the second principal component (PC2_{TBM}) projected onto a standard three dimensional brain and onto a cytoarchitectonic atlas (cluster 3+) in MNI space. Clusters are labeled according to their (positive or negative) correlation with gray matter volume expansion in the medio-dorsal thalamus. The threshold for positive clusters corresponds to the first percentile of voxel values (absolute value 0.0064), the threshold for the negative cluster to the ninety-ninth percentile (absolute value 0.0095). **(B)** shows the spatial relationship between the covariance network clusters and lesion maps of patient subgroups. Color-coded contours define areas with ≥20% lesion probability in each subgroup. Size, localization, cytoarchitectonic assignment, and functional correlates of the individual clusters are summarized in **Table 3**.

TABLE 3 | Clusters of the longitudinal structural covariance network (PC2_{TBM}) related to hand function recovery: size, localization, cytoarchitectonic assignment, and functional correlates.

Cluster	Size (n vox.)	MNI (max.)	Anatomical area	Cytoarchitectonic area	Functional correlate (references in brackets)
First-percentile voxels (height threshold: 0.0064, extension threshold: 32 voxels)					
1+	1362	38/–28/16	R. parietal operculum	OP1, OP2, OP3	Tactile working memory, stimulus discrimination and perceptual learning (41–44)
			R. insula	Ig1, Ig2	Multisensory processing (36, 50–53)
		54/–26/28	R. inferior parietal lobule	PFcm, PFop, PFt	Action observation and imitation (47–49)
2+	653	43/26/26	R. DLPFC (dorsal-posterior part)	n.a.	Action execution and working memory (34, 35)
		40/10/34	R. ventral premotor cortex	n.a.	Motor hand skill related to intrinsic objects properties (83)
3+	502	10/–20/6	R. thalamus	Thal: prefrontal Thal: temporal Thal: parietal	MD nucleus to prefrontal cortex (33–35) MD nucleus to temporal lobe (33–35) LP/Pu complex to parietal lobe (33–35)
4+	408	42/–38/42	R. intraparietal sulcus R. post-central gyrus R. inferior parietal lobule	hlp1, hlp2, hlp3 BA2 PFt, PFm	Spatial attention, visuomotor transformation (57, 66–68) Primary somatosensory information processing (56) For PFt see above; for PFm non-spatial attention (49)
5+	271	52/–48/2	R. superior (and middle temporal) gyrus	n.a.	Spatial awareness (69)
6+	158	30/–62/36	R. middle occipital gyrus	n.a.	Spatial processing of tactile stimuli (70)
Ninety-ninth-percentile voxels (height threshold: 0.0095, extension threshold: 32 voxels)					
1–	179	54/–14/38	Pre- and post-central gyrus	BA 4p, 3b, 1, 2	Voluntary and passive finger motion (BA 4p) (71) Somatosensory information perception (3b) and processing (1, 2, 73)



regression of PC1_{PSO} onto covariance network expression, age, volume, and thalamic GMV change: it showed significant effects of the model intercept ($p = 0.036$), PC2_{TBM} expression ($p = 0.048$) and lesion volume ($p = 0.037$). The significant intercept indicated

residual variance not modeled by our predictors. We, therefore, investigated a reduced model that included PC1_{PSO} as dependent variable, and only the significant predictors from the first model, i.e., PC2_{TBM} expression, lesion volume and their interaction

TABLE 4 | Clinical and structural variables across recovery subgroups.

	Fast recovery <i>n</i> = 8	Slow recovery <i>n</i> = 12	Impaired recovery <i>n</i> = 8	Kruskal–Wallis, <i>p</i>	Mann–Whitney, impaired versus recovered <i>p</i> (2-tailed)
Network of gmV change between months 3 and 9					
PC2 _{TBM} expression coeff.	−0.079 (−0.117, 0.025)	−0.04 (−0.23, 0.52)	0.06 (−0.22, 0.51)	0.55	n.a.
Parameters tested for correlation					
Age	63 (41, 73)	75 (49, 80)	68.5 (53, 82)	0.31	n.a.
Lesion size (cc) ^a	7.80 (0.76, 75.52)	3.48 (0.57, 70.39)	42.84 (2.72, 141.71)	0.08	<0.05
PC1 (NIH) expression coeff. ^a	−2.18 (−3.07, 0.61)	−1.31 (−3.65, 2.12)	1.33 (−1.40, 11.90)	<0.01	<0.01
PC1 (PSO) expression coeff. ^a	−15.3 (−21.0, 6.7)	−10.8 (−16.8, 3.1)	16.5 (−5.6, 64.3)	<0.0001	<0.0001
PC1 (TOR) expression coeff.	13.9 (−0.45, 14.3)	13.9 (11.0, 14.3)	−29.3 (−34.3, 13.7)	<0.001	<0.001
GMV premotor area	0.0043 (−0.0010, 0.0092)	0.0017 (−0.0013, 0.0078)	0.0011 (−0.0020, 0.0083)	0.69	n.a.
GMV thalamus ^a	0.0017 (−0.0043, 0.0143)	0.0023 (−0.0061, 0.0292)	0.0083 (−0.0002, 0.0179)	0.06	<0.05
GMV cerebellum	−0.0019 (−0.0130, 0.0031)	−0.0029 (−0.0089, 0.0060)	−0.0012 (−0.0121, 0.0051)	0.43	n.a.

All values are given as median (range).

NIH, National Institutes of Health Stroke Scale; PSO, picking small objects; PC1, first principal component of longitudinal data of corresponding clinical or behavioral variable; PC2_{TBM}, second principal component of tensor-based morphometry data; GMV, gray matter volume.

^aSignificant correlations after correction for multiple comparisons: at a nominal alpha level of 0.05 and eight correlations, a *p*-value of 0.05/8 = 0.006 yields significant entries. This probability corresponds to a correlation coefficient of 0.466.

TABLE 5 | Overlap between subgroup lesion density maps and longitudinal structural covariance network related to hand function recovery.

	Cluster 1+ pOP	Cluster 2+ vPMC	Cluster 3+ Thal	Cluster 4+ IPS	Cluster 5+ STG	Cluster 6+ MOG	Cluster 1+– PCG
Raw volume (cc)	10.9	5.2	4.0	3.3	2.2	1.3	1.4
Fast	105.7	0.3	0	1.0	0.3	0	0.3
Slow	113.9	0.5	0	1.0	1.0	0.2	0.6
Impaired	239.7	3.3	0	3.3	1.1	0.9	1.4
Percent of lesion on cluster							
Fast	6.7	0.3	0	0.9	0.3	0	0.3
Slow	1.6	0.4	0	0.9	0.9	0.2	0.5
Impaired	3.6	1.4	0	1.4	0.5	0.4	0.6
Percent of cluster affected							
Fast	61.5	5.8	0	30.3	13.6	0	21.4
Slow	14.7	9.4	0	29.7	46.4	17.7	44.3
Impaired	33.0	62.7	0	98.8	51.4	69.2	100.0

Cluster labels correspond to **Table 3**, additionally including main anatomical region within each cluster. Volumes are calculated for subgroup density maps in **Figure 1B** and each cluster separately.

pOP, parietal operculum; vPMC, ventral premotor cortex; Thal, thalamus; IPS, inferior parietal sulcus; STG, superior temporal gyrus; MOG, middle occipital gyrus; PCG, pre- and post-central gyri.

(PC2_{TBM} expression × lesion volume) as independent variables. The interaction term significantly predicted PC1_{PSO} scores ($\beta = 1.1$, $t(24) = 3.83$, $p < 0.001$) over and above the other variables (both $p > 0.1$). The interaction term explained a significant portion of variance in hand function recovery ($R^2 = 0.639$, $F(3, 24) = 14.18$, $p < 1.6 \times 10^{-5}$). Full model parameters are summarized in the Table S3 in Supplementary Material.

Discussion

In this study, we have identified structural covariance networks deduced from GMV changes during the recovery of patients suffering from hand paresis after ischemic sensorimotor stroke. These networks correspond to the first, second, and fourth

principal components determined from a PCA of TBM images and explained 19.9, 9.1, and 8.1% of the variance, respectively. Implied by the correlation of its expression coefficients with GMV-decrease in the anterior cerebellum contralateral to pre- and post-central infarction in all patients, the first component PC1_{TBM} appears to reflect a neuronal network caused by diaschisis from sensorimotor cortex (46). The second component PC2_{TBM}, associated with a specific manual skill, i.e., precision grip, as implied by its correlation with PC1_{PSO} represents a neuronal network involving GMV-increase in the md thalamus. Finally, the correlation of the fourth component expression coefficients with the NIHSS scores summarized in PC1_{NIHSS} suggests that the corresponding network reflects general neurological deficit. A third behavioral parameter of sensory information processing, TOR,

showed no significant correlation with a principal component, although a deficit persisted in the impaired subgroup.

Finally, a multivariate linear regression approach verified (i) the unique relationship of $PC1_{PSO}$ to the structural covariance network of $PC2_{TBM}$; and furthermore, that this relationship is related specifically to the network expression but not to a single constituent, e.g., md thalamus. Since $PC2_{TBM}$ relates directly to hand function recovery and thus to our study aim, we will discuss this network in more detail in the following.

Associations of the Structural Covariance Network With External Variables

This study represents important progress following our recent paper on “Gray matter volumetric changes related to recovery from hand paresis after cortical sensorimotor stroke” (9) as it relates the most prominent finding of gray matter increase in the md thalamus in patients after a first-ever stroke to a large distributed structural covariance network including a cortico-striato-thalamic loop and diverse sensorimotor cortices.

Irrespective of the clinical and behavioral course, this $PC2_{TBM}$ network distinguishes clearly within the study cohort since the subgroup with positive expression coefficients is associated with large GMV increases in the md thalamus between months 3 and 9, while the subgroup with negative expression coefficients did not exhibit a recognizable GMV change. The GMV increases in the former subgroup exceed the measurement uncertainty and are consistent with the few comparable studies, e.g., in the paper of Gauthier et al. (32). As **Table 2** shows, the neural network represented by $PC2_{TBM}$ is significantly related to the recovery of motor hand skill in the patient cohort; however, only the impaired recovery subgroup shows a strong linear regression, while the fast and slow recovery groups show little correlation with $PC1_{PSO}$ (**Figure 2B**). A multivariate linear regression positing the dependence of $PC1_{PSO}$ on the three salient principal components as well as on age, lesion volume, and GMV change in the thalamus showed significant effects only in $PC2_{TBM}$ and lesion volume. A refined analysis showed a significant interaction between these two variables, and revealed that the interaction was the only significant explanatory variable. The fast and slow recovery groups indicated an inverse relationship between $PC2_{TBM}$ and lesion volume; the greater lesion volumes were accompanied by smaller component expression coefficients, and vice versa. In contrast, the members of the impaired group exhibiting the largest interaction expressed most strongly $PC1_{PSO}$.

Network Topography and Suggested Functions

The salient regions of the second principal component $PC2_{TBM}$ are summarized in **Table 3**; the regions characterized by voxel intensities of the first percentile contain the thalamic cluster. Using a probabilistic atlas of white matter connections, we found that this thalamic cluster was located on regions of the md thalamus that are preferentially connected to prefrontal, temporal and parietal cortex (33, 34). These three cortical regions were also found in the set of regions belonging to the first percentile, underscoring the importance of the thalamic gray matter increase. The implicated md thalamus and dorsolateral prefrontal cortex are constituents

of the subcortico-cortical, dorsolateral prefrontal loop (35). The involvement of this dorsolateral prefrontal-striato-thalamic loop suggests a compensatory mechanism to maintain motor execution by cognitive control once the primary (more automatic) sensorimotor network of hand motor skill is dysfunctional (47).

Both parts of posterior medial thalamus and dorsal-posterior subarea of the dorsolateral prefrontal cortex are interconnected with the posterior parietal cortex (PPC) (48), which our previous VLSM studies (8) have shown to be seriously affected in the impaired subgroup.

Densely interconnected structures of ventral PMC, PPC, SII and posterior insula are represented in the component image of $PC2_{TBM}$, representing possible sub-networks engaged in higher order sensorimotor information processing and spatial awareness (see below). In the PPC locally functional processed information, e.g., space and action perception, is transmitted via feedback loops to ventral PMC (34, 49, 50). The areas co-varying positively with the thalamus represent a complex neuronal network consisting of functional and dysfunctional nodes. The functional nodes outside of the lesions comprise the dorsolateral prefrontal loop for motor execution (26), whereas the dysfunctional nodes include various higher order sensorimotor cortices within the lesions. Performance of sensorimotor hand skill, especially in the impaired recovery group, is related to lesion size and extension into network nodes in ventral PMC, PPC, SII, and posterior insula.

A remarkable feature of the structural covariance pattern is the appearance of the parietal operculum subarea OP1 in the absence of OP4. OP4 plays a role mainly in basal sensorimotor integration processes, e.g., incorporating sensory feedback into motor actions which are the basis for information processing during tactile exploration (51, 52). The involved OP1 seems to support more complex information processing demanded during tactile working memory, stimulus discrimination, and perceptual learning (53–56). These differing functional roles are reflected by the distinct connectivity profiles of the areas: OP4 is connected to fronto-parietal areas, while OP1 is connected predominantly to the inferior parietal cortex (IPC) (57). In a three-region model in humans, the rostral IPC, including PFcm, PFop, PFt, has been shown to be involved in reaching and grasping (58). The very rostral part (PFop) seems to be activated specifically during observation of tool use. Moreover, meta-analyses indicated the participation of PFt in action observation and imitation networks (59–61). In humans somatosensory activation of the posterior insula has been observed during simple stimulation paradigms, e.g., estimation of the roughness of gratings and TOR, suggesting a role in somatosensory processing (62–65). Multisensory processing in the posterior insula has also been observed in primate experiments with responses also to auditory, baroreceptive and painful stimuli (66, 67).

As has been shown in primates, while area 2 is activated by fine grained proprioceptive sensory information obtained by transitive finger movements (68), specific neuron populations within anterior IPS (AIP) are activated by grasping and manipulation of 3-D objects as well as by visual fixation of objects (69). Analogously, in humans area 2 is involved in the perception

of geometrical and texture characteristics like edge length and roughness. This function contrasts to the putative human homologue of the IPS, which responds to shape perception, including somatosensory discrimination, visuo-tactile matching, and, together with premotor cortices, skilled motor manipulation of 3-D objects (50, 70–73). The human IPS has been characterized using cytoarchitectonical techniques (74, 75). Functional connectivity analyses have shown these sub-areas along the IPS to be distinguished by distinct connections (76). The AIP ROIs (hIP1 and hIP2) connect mainly to frontal attentional regions, whereas posterior IPS (hIP3) connects mainly to posterior occipital regions. Analog connections have been shown in macaque anatomical studies, e.g., the strong connections between the AIP and ventral PMC and the posterior IPS (CIP) to visual cortices (77). This explains also visuomotor coordination via the AIP and the implication of the posterior IPS in peripersonal visual representations (78–80). Karnath et al. found that in patients free of lesions in visual as well as subcortical structures, the critical site for spatial awareness was located in the superior temporal gyrus (BA 22 and 42) (81). Using fMRI it could be shown that the right middle occipital gyrus processes spatial rather than non-spatial auditory and tactile stimuli (82). In a review, Rizzolatti et al. conclude that the ventral PMC executes both motor and cognitive functions: motor functions comprise hand actions related to intrinsic object properties and head and arm actions related to spatial locations, whereas cognitive functions include space perception, action understanding and imitation (83). In the context of our study the observation of Ehrsson et al. is of importance as they found that precision grip showed more extending activations compared to power grip, involving ventral PMC in both hemispheres (35).

Of the salient regions of the second principal component PC2_{TBM}, a single cortical cluster contains voxels belonging to the ninety-ninth percentile, which presumably characterizes fast and slow recovered individuals. It includes a sub-network within pre- and post-central gyrus, ventral to the center of gravity of the lesion in the slowly recovering subjects as described in our previous paper (21). The isolated involvement of 4p, but not of 4a, substantiates the double representation of the motor system in the precentral gyrus, the former activated in simple motor tasks, whereas the latter responds to more complex and self-initiated tasks (84). In activation studies of healthy individuals, voluntary and passive finger motion stimulated areas 4p and 3a, simple sensory stimulation areas 3b, 1 and 2 and complex sensory stimulation area 4a (85).

Limitations

This study comprises a detailed evaluation and discussion of structural covariance networks associated with hand motor skill. At the outset, the number and composition of recovery subgroups in the patient cohort was unknown. Thus, the number of patients in each subgroup is relatively small. Larger cohorts would be desirable to assign subjects reliably to subgroups characterized by distinct patterns of structural reorganization associated with varying degrees of recovery. Besides subgroup specific patterns,

especially in the subgroup with slow but complete recovery, the assessment of idiosyncratic aspects, e.g., exceptions to the involvement of the dorsolateral prefrontal-striato-thalamic loop, is another challenge. Meeting it would necessitate detailed protocols, including a comprehensive neuro-rehabilitation program, reporting of targeting interventions and physiological measures of movement efforts versus efficiency of motor activity. As the existence of the subgroup with fast complete recovery indicates, an earlier begins after stroke of the study might help to assess structural plasticity in the first 3 months when most recovery occurs. The incomplete gender matching must also be taken into consideration, because women have been shown to perform dexterity tasks (nine-hole peg test) faster than men depending on age, and upper limb kinesthetic asymmetries in contralateral reproduction of elbow movements, elicited by tendon vibration, were prevalent in males (86, 87).

Conclusion

As posited in Section “Introduction”, our study confirms that the md thalamus, distinguished by significant gray matter increase after first-ever stroke, is a constituent of an extensive structural covariance network encompassing (i) a cortico-striato-thalamic loop involved in motor execution and (ii) higher order sensorimotor cortices affected to varying degrees in the study cohort. Positive expression coefficients of the network are associated with significant GMV increases in the md thalamus in contrast to negative expression coefficients. This brain structural covariance pattern reflects a specific structural covariance network related to recovery of motor hand skill and may distinguish among patient subgroups according to recovery class. The surrogate marker for motor hand skill, PSO, depends on an interaction between the expression of the network and lesion volume. Related to this condition, the impaired group exhibiting the largest interaction expressed most strong PC1_{PSO} and inversely were limited in the expression of the structural covariance network of PC2_{TBM}. To conclude, our application of tensor-based morphology has shown it to be a powerful method for studying gray matter changes after stroke; it is capable of revealing both local changes and in associated extensive neural networks. Regarding its future use application, TBM will be potentially of interest in the study of targeted treatment effects in the long-term.

Acknowledgments

We are indebted to our patients and their caregivers for generously supporting our study. We thank our neuroradiological technicians for help with image acquisition and data management. This work was funded by a Swiss National Foundation grant (SNF 3200B0-118018).

Supplementary Material

The Supplementary Material for this article can be found online at <http://journal.frontiersin.org/article/10.3389/fneur.2015.00211>

References

- Kwakkel G, Kollen BJ, van der Grond J, Prevo AJH. Probability of regaining dexterity in the flaccid upper limb: impact of severity of paresis and time since onset in acute stroke. *Stroke* (2003) **34**(9):2181–6. doi:10.1161/01.STR.0000087172.16305.CD
- Kwakkel G, Kollen B, Lindeman E. Understanding the pattern of functional recovery after stroke: facts and theories. *Restor Neurol Neurosci* (2004) **22**(3–5):281–99. doi:10.1177/1545968308317972
- Cramer SC. Repairing the human brain after stroke: I. Mechanisms of spontaneous recovery. *Ann Neurol* (2008) **63**(3):272–87. doi:10.1002/ana.21393
- Krakauer JW. Arm function after stroke: from physiology to recovery. *Semin Neurol* (2005) **25**:384–95. doi:10.1055/s-2005-923533
- Rehme AK, Eickhoff SB, Rottschy C, Fink GR, Grefkes C. Activation likelihood estimation meta-analysis of motor-related neural activity after stroke. *Neuroimage* (2012) **59**:2771–82. doi:10.1016/j.neuroimage.2011.10.023
- Ward NS, Brown MM, Thompson AJ, Frackowiak RSJ. Neural correlates of outcome after stroke: a cross-sectional fMRI study. *Brain* (2003) **126**(Pt 6):1430–48. doi:10.1093/brain/awg145
- Schaechter JD, Perdue KL. Enhanced cortical activation in the contralesional hemisphere of chronic stroke patients in response to motor skill challenge. *Cereb Cortex* (2008) **18**:638–47. doi:10.1093/cercor/bhm096
- Thiel A, Vahdat S. Structural and resting-state brain connectivity of motor networks after stroke. *Stroke* (2014) **46**(1):296–301. doi:10.1161/STROKEAHA.114.006307
- Grefkes C, Fink GR. Connectivity-based approaches in stroke and recovery of function. *Lancet Neurol* (2014) **13**(2):206–16. doi:10.1016/S1474-4422(13)70264-3
- Silasi G, Murphy THH. Stroke and the connectome: how connectivity guides therapeutic intervention. *Neuron* (2014) **83**(6):1354–68. doi:10.1016/j.neuron.2014.08.052
- Dijkhuizen RM, Zaharchuk G, Otte WM. Assessment and modulation of resting-state neural networks after stroke. *Curr Opin Neurol* (2014) **27**(6):637–43. doi:10.1097/WCO.0000000000000150
- Ward NS, Brown MM, Thompson AJ, Frackowiak RSJ. Neural correlates of motor recovery after stroke: a longitudinal fMRI study. *Brain* (2003) **126**(Pt 11):2476–96. doi:10.1093/brain/awg145
- Kitago T, Liang J, Huang VS, Hayes S, Simon P, Tenteromano L, et al. Improvement after constraint-induced movement therapy: recovery of normal motor control or task-specific compensation? *Neurorehabil Neural Repair* (2012) **27**(2):99–109. doi:10.1177/1545968312452631
- Raghavan P, Petra E, Krakauer JW, Gordon AM. Patterns of impairment in digit independence after subcortical stroke. *J Neurophysiol* (2006) **95**:369–78. doi:10.1152/jn.00873.2005
- Mochizuki G, Hoque T, Mraz R, Macintosh BJ, Graham SJ, Black SE, et al. Challenging the brain: exploring the link between effort and cortical activation. *Brain Res* (2009) **1301**:9–19. doi:10.1016/j.brainres.2009.09.005
- Grefkes C, Fink GR. Reorganization of cerebral networks after stroke: new insights from neuroimaging with connectivity approaches. *Brain* (2011) **134**(Pt 5):1264–76. doi:10.1093/brain/awr033
- Takeuchi N, Izumi S-I. Maladaptive plasticity for motor recovery after stroke: mechanisms and approaches. *Neural Plast* (2012) **2012**:359728. doi:10.1155/2012/359728
- Leow AD, Klunder AD, Jack CR, Toga AW, Dale AM, Bernstein MA, et al. Longitudinal stability of MRI for mapping brain change using tensor-based morphometry. *Neuroimage* (2006) **31**(2):627–40. doi:10.1016/j.neuroimage.2005.12.013
- Ashburner J, Csernansky JG, Davatzikos C, Fox NC, Frisoni GB, Thompson PM. Computer-assisted imaging to assess brain structure in healthy and diseased brains. *Lancet Neurol* (2003) **2**(2):79–88. doi:10.1016/S1474-4422(03)00304-1
- Zatorre RJ, Fields RD, Johansen-Berg H. Plasticity in gray and white: neuroimaging changes in brain structure during learning. *Nat Neurosci* (2012) **15**(4):528–36. doi:10.1038/nn.3045
- Abela E, Missimer J, Wiest R, Federspiel A, Hess C, Sturzenegger M, et al. Lesions to primary sensory and posterior parietal cortices impair recovery from hand paresis after stroke. *PLoS One* (2012) **7**(2):e31275. doi:10.1371/journal.pone.0031275
- Abela E, Seiler A, Missimer JH, Federspiel A, Hess CW, Sturzenegger M, et al. Grey matter volumetric changes related to recovery from hand paresis after cortical sensorimotor stroke. *Brain Struct Funct* (2014). doi:10.1007/s00429-014-0804-y
- Uludağ K, Roebroeck A. General overview on the merits of multimodal neuroimaging data fusion. *Neuroimage* (2014) **102**:3–10. doi:10.1016/j.neuroimage.2014.05.018
- Matthews JN, Altman DG, Campbell MJ, Royston P. Analysis of serial measurements in medical research. *BMJ* (1990) **300**(6719):230–5. doi:10.1136/bmj.300.6725.680-a
- Seitz RJ, Knorr U, Azari NP, Weder B. Cerebral networks in sensorimotor disturbances. *Brain Res Bull* (2001) **54**(3):299–305. doi:10.1016/S0361-9230(00)00438-X
- Alexander GE, DeLong MR, Strick PL. Parallel organization of functionally segregated circuits linking basal ganglia and cortex. *Annu Rev Neurosci* (1986) **9**:357–81. doi:10.1146/annurev.ne.09.030186.002041
- Wiest R, Abela E, Missimer J, Schroth G, Hess CW, Sturzenegger M, et al. Interhemispheric cerebral blood flow balance during recovery of motor hand function after ischemic stroke-A longitudinal MRI study using arterial spin labeling perfusion. *PLoS One* (2014) **9**(9):e106327. doi:10.1371/journal.pone.0106327
- Brott T, Adams HP, Olinger CP, Marler JR, Barsan WG, Biller J, et al. Measurements of acute cerebral infarction: a clinical examination scale. *Stroke* (1989) **20**(7):864–70. doi:10.1161/01.STR.20.7.871
- Mathiowetz V, Weber K, Volland G, Kashman N. Reliability and validity of grip and pinch strength evaluations. *J Hand Surg Am* (1984) **9**(2):222–6. doi:10.1016/S0363-5023(84)80146-X
- Mathiowetz V, Kashman N, Volland G, Weber K, Dowe M, Rogers S. Grip and pinch strength: normative data for adults. *Arch Phys Med Rehabil* (1985) **66**:69–74.
- Jebsen RH, Taylor N, Trieschmann RB, Trotter MJ, Howard LA. An objective and standardized test of hand function. *Arch Phys Med Rehabil* (1969) **50**:311–9.
- Castiello U. The neuroscience of grasping. *Nat Rev Neurosci* (2005) **6**(9):726–36. doi:10.1038/nrn1775
- Davare M, Andres M, Cosnard G, Thonnard J-L, Olivier E. Dissociating the role of ventral and dorsal premotor cortex in precision grasping. *J Neurosci* (2006) **26**(8):2260–8. doi:10.1523/JNEUROSCI.3386-05.2006
- Stoeckel MC, Weder B, Binkofski F, Choi H-J, Amunts K, Pieperhoff P, et al. Left and right superior parietal lobule in tactile object discrimination. *Eur J Neurosci* (2004) **19**(4):1067–72. doi:10.1111/j.0953-816X.2004.03185.x
- Ehrsson HH, Fagergren E, Forssberg H. Differential fronto-parietal activation depending on force used in a precision grip task: an fMRI study. *J Neurophysiol* (2001) **85**(6):2613–2623.
- Bohlhalter S, Fretz C, Weder B. Hierarchical versus parallel processing in tactile object recognition: a behavioural-neuroanatomical study of aperceptive tactile agnosia. *Brain* (2002) **125**(Pt 11):2537–48. doi:10.1093/brain/awf245
- Deichmann R, Schwarzbauer C, Turner R. Optimisation of the 3D MDEFT sequence for anatomical brain imaging: technical implications at 1.5 and 3 T. *Neuroimage* (2004) **21**(2):757–67. doi:10.1016/j.neuroimage.2003.09.062
- Mechelli A, Friston KJ, Frackowiak RS, Price CJ. Structural covariance in the human cortex. *J Neurosci* (2005) **25**(36):8303–10. doi:10.1523/JNEUROSCI.0357-05.2005
- Alexander-Bloch A, Giedd JN, Bullmore E. Imaging structural co-variance between human brain regions. *Nat Rev Neurosci* (2013) **14**(5):322–36. doi:10.1038/nrn3465
- Guttman L. Some necessary conditions for common-factor analysis. *Psychometrika* (1954) **19**(2):149–61. doi:10.1007/BF02289162
- Ashburner J, Friston KJ. Unified segmentation. *Neuroimage* (2005) **26**(3):839–51. doi:10.1016/j.neuroimage.2005.02.018
- Andersen SM, Rapcsak SZ, Beeson PM. Cost function masking during normalization of brains with focal lesions: still a necessity? *Neuroimage* (2010) **53**(1):78–84. doi:10.1016/j.neuroimage.2010.06.003
- Salmund CH, Ashburner J, Vargha-Khadem F, Connelly A, Gadian DG, Friston KJ. Distributional assumptions in voxel-based morphometry. *Neuroimage* (2002) **17**(2):1027–30. doi:10.1006/nimg.2002.1153

44. Alexander GE, Bergfield KL, Chen K, Reiman EM, Hanson KD, Lin L, et al. Gray matter network associated with risk for Alzheimer's disease in young to middle-aged adults. *Neurobiol Aging* (2012) 33(12):2723–32. doi:10.1016/j.neurobiolaging.2012.01.014
45. Moeller JR, Ishikawa T, Dhawan V, Spetsieris P, Mandel F, Alexander GE, et al. The metabolic topography of normal aging. *J Cereb Blood Flow Metab* (1996) 16(3):385–98. doi:10.1097/00004647-199605000-00005
46. Komaba Y, Mishina M, Utsumi K, Katayama Y, Kobayashi S, Mori O. Crossed cerebellar diaschisis in patients with cortical infarction: logistic regression analysis to control for confounding effects. *Stroke* (2004) 35(2):472–6. doi:10.1161/01.STR.0000109771.56160.F5
47. McFarland NR, Haber SN. Thalamic relay nuclei of the basal ganglia form both reciprocal and nonreciprocal cortical connections, linking multiple frontal cortical areas. *J Neurosci* (2002) 22(18):8117–32. doi:10.22/18/8117[pil]
48. Behrens TEJ, Johansen-Berg H, Woolrich MW, Smith SM, Wheeler-Kingshott CAM, Boulby PA, et al. Non-invasive mapping of connections between human thalamus and cortex using diffusion imaging. *Nat Neurosci* (2003) 6(7):750–7. doi:10.1038/nn1075
49. Vandenberghe R, Gillebert CR. Dissociations between spatial-attentional processes within parietal cortex: insights from hybrid spatial cueing and change detection paradigms. *Front Hum Neurosci* (2013) 7:366. doi:10.3389/fnhum.2013.00366
50. Stoeckel MC, Weder B, Binkofski F, Buccino G, Shah NJ, Seitz RJ. A fronto-parietal circuit for tactile object discrimination. *Neuroimage* (2003) 19(3):1103–14. doi:10.1016/S1053-8119(03)00182-4
51. Rizzolatti G, Wolpert DM. Motor systems. *Curr Opin Neurobiol* (2005) 15(6):623–5. doi:10.1016/j.conb.2005.10.018
52. Halsband U, Lange RK. Motor learning in man: a review of functional and clinical studies. *J Physiol Paris* (2006) 99(4–6):414–24. doi:10.1016/j.jphysparis.2006.03.007
53. Romo R, Hernández A, Salinas E, Brody CD, Zainos A, Lemus L, et al. From sensation to action. *Behav Brain Res* (2002) 135(1–2):105–18. doi:10.1016/S0166-4328(02)00161-4
54. Torquati K, Pizzella V, Della Penna S, Franciotti R, Babiloni C, Rossini PM, et al. Comparison between SI and SII responses as a function of stimulus intensity. *Neuroreport* (2002) 13(6):813–9. doi:10.1097/00001756-200205070-00016
55. Pleger B, Foerster AF, Ragert P, Dinse HR, Schwenkreis P, Malin JP, et al. Functional imaging of perceptual learning in human primary and secondary somatosensory cortex. *Neuron* (2003) 40(3):643–53. doi:10.1016/S0896-6273(03)00677-9
56. Burton H, Sinclair RJ, McLaren DG. Cortical network for vibrotactile attention: a fMRI study. *Hum Brain Mapp* (2008) 29(2):207–21. doi:10.1002/hbm.20384
57. Eickhoff SB, Jbabdi S, Caspers S, Laird AR, Fox PT, Zilles K, et al. Anatomical and functional connectivity of cytoarchitectonic areas within the human parietal operculum. *J Neurosci* (2010) 30(18):6409–21. doi:10.1523/JNEUROSCI.5664-09.2010
58. Peeters R, Simone L, Nelissen K, Fabbri-Destro M, Vanduffel W, Rizzolatti G, et al. The representation of tool use in humans and monkeys: common and uniquely human features. *J Neurosci* (2009) 29(37):11523–39. doi:10.1523/JNEUROSCI.2040-09.2009
59. Molenberghs P, Cunnington R, Mattingley JB. Is the mirror neuron system involved in imitation? A short review and meta-analysis. *Neurosci Biobehav Rev* (2009) 33(7):975–80. doi:10.1016/j.neubiorev.2009.03.010
60. Van Overwalle F, Baetens K. Understanding others' actions and goals by mirror and mentalizing systems: a meta-analysis. *Neuroimage* (2009) 48(3):564–84. doi:10.1016/j.neuroimage.2009.06.009
61. Caspers S, Eickhoff SB, Geyer S, Scheperjans F, Mohlberg H, Zilles K, et al. The human inferior parietal lobule in stereotaxic space. *Brain Struct Funct* (2008) 212(6):481–95. doi:10.1007/s00429-008-0195-z
62. Gelman PA, Krauss BR, Szevenyi NM, Apkarian AV. Fingertip representation in the human somatosensory cortex: an fMRI study. *Neuroimage* (1998) 7(4 Pt 1):261–83. doi:10.1006/nimg.1998.0341
63. Deuchert M, Ruben J, Schwiemann J, Meyer R, Thees S, Krause T, et al. Event-related fMRI of the somatosensory system using electrical finger stimulation. *Neuroreport* (2002) 13(3):365–9. doi:10.1097/00001756-200203040-00023
64. Reed CL, Shoham S, Halgren E. Neural substrates of tactile object recognition: an fMRI study. *Hum Brain Mapp* (2004) 21(4):236–46. doi:10.1002/hbm.10162
65. Kitada R, Hashimoto T, Kochiyama T, Kito T, Okada T, Matsumura M, et al. Tactile estimation of the roughness of gratings yields a graded response in the human brain: an fMRI study. *Neuroimage* (2005) 25(1):90–100. doi:10.1016/j.neuroimage.2004.11.026
66. Zhang ZH, Dougherty PM, Oppenheimer SM. Monkey insular cortex neurons respond to baroreceptive and somatosensory convergent inputs. *Neuroscience* (1999) 94(2):351–60. doi:10.1016/S0306-4522(99)00339-5
67. Coq J-O, Qi H, Collins CE, Kaas JH. Anatomical and functional organization of somatosensory areas of the lateral fissure of the New World titi monkey (*Callicebus moloch*). *J Comp Neurol* (2004) 476(4):363–87. doi:10.1002/cne.20237
68. Jones EG, Coulter JD, Hendry SH. Intracortical connectivity of architectonic fields in the somatic sensory, motor and parietal cortex of monkeys. *J Comp Neurol* (1978) 181(2):291–347. doi:10.1002/cne.901810206
69. Hikosaka O, Tanaka M, Sakamoto M, Iwamura Y. Deficits in manipulative behaviors induced by local injections of muscimol in the first somatosensory cortex of the conscious monkey. *Brain Res* (1985) 325(1–2):375–80. doi:10.1016/0006-8993(85)90344-0
70. Hartmann S, Missimer JH, Stoeckel C, Abela E, Shah J, Seitz RJ, et al. Functional connectivity in tactile object discrimination: a principal component analysis of an event related fMRI-study. *PLoS One* (2008) 3(12):e3831. doi:10.1371/journal.pone.0003831
71. Hömke L, Amunts K, Böniß L, Fretz C, Binkofski F, Zilles K, et al. Analysis of lesions in patients with unilateral tactile agnosia using cytoarchitectonic probabilistic maps. *Hum Brain Mapp* (2009) 30(5):1444–56. doi:10.1002/hbm.20617
72. Grefkes C, Weiss PH, Zilles K, Fink GR. Crossmodal processing of object features in human anterior intraparietal cortex: an fMRI study implies equivalencies between humans and monkeys. *Neuron* (2002) 35(1):173–84. doi:10.1016/S0896-6273(02)00741-9
73. Binkofski F, Buccino G, Posse S, Seitz RJ, Rizzolatti G, Freund H. A fronto-parietal circuit for object manipulation in man: evidence from an fMRI-study. *Eur J Neurosci* (1999) 11(9):3276–86. doi:10.1046/j.1460-9568.1999.00753.x
74. Choi H-J, Zilles K, Mohlberg H, Schleicher A, Fink GR, Armstrong E, et al. Cytoarchitectonic identification and probabilistic mapping of two distinct areas within the anterior ventral bank of the human intraparietal sulcus. *J Comp Neurol* (2006) 495(1):53–69. doi:10.1002/cne.20849
75. Scheperjans F, Eickhoff SB, Hömke L, Mohlberg H, Hermann K, Amunts K, et al. Probabilistic maps, morphometry, and variability of cytoarchitectonic areas in the human superior parietal cortex. *Cereb Cortex* (2008) 18(9):2141–57. doi:10.1093/cercor/bhm241
76. Uddin LQ, Supekar K, Amin H, Rykhlevskaia E, Nguyen DA, Greicius MD, et al. Dissociable connectivity within human angular gyrus and intraparietal sulcus: evidence from functional and structural connectivity. *Cereb Cortex* (2010) 20(11):2636–46. doi:10.1093/cercor/bhq011
77. Grefkes C, Fink GR. The functional organization of the intraparietal sulcus in humans and monkeys. *J Anat* (2005) 207(1):3–17. doi:10.1111/j.1469-7580.2005.00426.x
78. Frey SH, Vinton D, Norlund R, Grafton ST. Cortical topography of human anterior intraparietal cortex active during visually guided grasping. *Brain Res Cogn Brain Res* (2005) 23(2–3):397–405. doi:10.1016/j.cogbrainres.2004.11.010
79. Culham JC, Cavina-Pratesi C, Singhal A. The role of parietal cortex in visuomotor control: what have we learned from neuroimaging? *Neuropsychologia* (2006) 44(13):2668–84. doi:10.1016/j.neuropsychologia.2005.11.003
80. Makin TR, Holmes NP, Zohary E. Is that near my hand? Multisensory representation of peripersonal space in human intraparietal sulcus. *J Neurosci* (2007) 27(4):731–40. doi:10.1523/JNEUROSCI.3653-06.2007
81. Karnath H-O, Ferber S, Himmelbach M. Spatial awareness is a function of the temporal not the posterior parietal lobe. *Nature* (2001) 411(6840):950–3. doi:10.1038/35082075
82. Renier LA, Anurova I, De Volder AG, Carlson S, VanMeter J, Rauschecker JP. Preserved functional specialization for spatial processing in the middle

- occipital gyrus of the early blind. *Neuron* (2010) **68**(1):138–48. doi:10.1016/j.neuron.2010.09.021
83. Rizzolatti G, Rizzolatti G, Fogassi L, Fogassi L, Gallese V, Gallese V. Motor and cognitive functions of the ventral premotor cortex. *Curr Opin Neurobiol* (2002) **12**(2):149–54. doi:10.1016/S0959-4388(02)00308-2
 84. Geyer S, Ledberg A, Schleicher A, Kinomura S, Schormann T, Bürgel U, et al. Two different areas within the primary motor cortex of man. *Nature* (1996) **382**:805–7. doi:10.1038/382805a0
 85. Terumitsu M, Ikeda K, Kwee IL, Nakada T. Participation of primary motor cortex area 4a in complex sensory processing: 3.0-T fMRI study. *Neuroreport* (2009) **20**(7):679–83. doi:10.1097/WNR.0b013e32832a1820
 86. Wang Y-C, Bohannon RW, Kapellusch J, Garg A, Gershon RC. Dexterity as measured with the 9-Hole Peg Test (9-HPT) across the age span. *J Hand Ther* (2015) **28**(1):53–9. doi:10.1016/j.jht.2014.09.002
 87. Cohen NR, Pomplun M, Gold BJ, Sekuler R. Sex differences in the acquisition of complex skilled movements. *Exp Brain Res* (2010) **205**(2):183–93. doi:10.1007/s00221-010-2351-y

Conflict of Interest Statement: The authors declare that the research was conducted in the absence of any commercial or financial relationships that could be construed as a potential conflict of interest.

Copyright © 2015 Abela, Missimer, Federspiel, Seiler, Hess, Sturzenegger, Wiest and Weder. This is an open-access article distributed under the terms of the Creative Commons Attribution License (CC BY). The use, distribution or reproduction in other forums is permitted, provided the original author(s) or licensor are credited and that the original publication in this journal is cited, in accordance with accepted academic practice. No use, distribution or reproduction is permitted which does not comply with these terms.

Improvement in touch sensation after stroke is associated with resting functional connectivity changes

Louise C. Bannister^{1,2,3}, Sheila G. Crewther², Maria Gavrilescu^{1,4} and Leeanne M. Carey^{1,3,5*}

¹Neurorehabilitation and Recovery, Stroke Division, Florey Institute of Neuroscience and Mental Health, Melbourne, VIC, Australia, ²School of Psychology and Public Health, College of Science, Health and Engineering, La Trobe University, Melbourne, VIC, Australia, ³Occupational Therapy, School of Allied Health, College of Science, Health and Engineering, La Trobe University, Melbourne, VIC, Australia, ⁴Defence Science and Technology Organisation, Melbourne, VIC, Australia, ⁵Florey Department of Neuroscience and Mental Health, The University of Melbourne, Melbourne, VIC, Australia

OPEN ACCESS

Edited by:

Bruno J. Weder,
University of Bern, Switzerland

Reviewed by:

Michael Brainin,
Donau-Universität Krems, Austria
Emmanuel Carrera,
Geneva University Hospital,
Switzerland

*Correspondence:

Leeanne M. Carey,
Neurorehabilitation and Recovery,
Stroke Division, Florey Institute of
Neuroscience and Mental Health,
Melbourne Brain Centre,
245 Burgundy Street, Heidelberg,
VIC 3084, Australia
leeanne.carey@florey.edu.au

Specialty section:

This article was submitted to Stroke,
a section of the journal
Frontiers in Neurology

Received: 07 April 2015

Accepted: 07 July 2015

Published: 31 July 2015

Citation:

Bannister LC, Crewther SG,
Gavrilescu M and Carey LM (2015)
Improvement in touch sensation after
stroke is associated with resting
functional connectivity changes.
Front. Neurol. 6:165.
doi: 10.3389/fneur.2015.00165

Background: Distributed brain networks are known to be involved in facilitating behavioral improvement after stroke, yet few, if any, studies have investigated the relationship between improved touch sensation after stroke and changes in functional brain connectivity.

Objective: We aimed to identify how recovery of somatosensory function in the first 6 months after stroke was associated with functional network changes as measured using resting-state connectivity analysis of functional magnetic resonance imaging (fMRI) data.

Methods: Ten stroke survivors underwent clinical testing and resting-state fMRI scans at 1 and 6 months post-stroke. Ten age-matched healthy participants were included as controls.

Results: Patients demonstrated a wide range of severity of touch impairment 1 month post-stroke, followed by variable improvement over time. In the stroke group, significantly stronger interhemispheric functional correlations between regions of the somatosensory system, and with visual and frontal areas, were found at 6 months than at 1 month post-stroke. Clinical improvement in touch discrimination was associated with stronger correlations at 6 months between contralesional secondary somatosensory cortex (SII) and inferior parietal cortex and middle temporal gyrus, and between contralesional thalamus and cerebellum.

Conclusion: The strength of connectivity between somatosensory regions and distributed brain networks, including vision and attention networks, may change over time in stroke survivors with impaired touch discrimination. Connectivity changes from contralesional SII and contralesional thalamus are associated with improved touch sensation at 6 months post-stroke. These functional connectivity changes could represent future targets for therapy.

Keywords: stroke recovery, somatosensory disorders, neuronal plasticity, magnetic resonance imaging, tactile, intrinsic functional connectivity

Introduction

Somatosensory impairment is common after stroke, occurring in 50–80% of stroke survivors (1, 2). However, investigations of the neural correlates of clinical somatosensory improvement after stroke are scarce (3). In particular, knowledge of how brain networks are interrupted is limited, but is critical to better understand the nature of the clinical deficit and post-stroke recovery (4).

Stroke impacts not only the focal lesion site but also on remote brain regions (5, 6). Lesions have important remote effects on the function of connected neural networks that are structurally intact, i.e., physiological changes in distant but functionally related brain areas (4, 7, 8). These remote effects contribute significantly to the observed behavioral deficits and recovery potential (4, 8). Further, changes in brain networks (across both hemispheres and function-specific networks) have been shown to be important in recovery of motor and attention functions (4, 6). A significant challenge is to identify the brain networks and processes that mediate functional improvement so that rehabilitation strategies can be aimed at the appropriate targets (9).

Only a few studies have investigated changes in the brain over time in association with somatosensory recovery (3, 10–13). These studies have primarily involved identification of brain regions associated with task-related brain activation. A few studies have reported that somatosensory recovery is associated with patterns of activation in primary somatosensory (SI) cortex that resembles those seen in healthy controls. For example, return of ipsilesional SI activation has been shown to be associated with improved somatosensory perception (10–12). Staines et al. (12) found that enhanced primary somatosensory cortex activation using functional MRI in the stroke-affected hemisphere occurred in conjunction with improved touch detection in four patients with thalamocortical strokes. Likewise, Wikström et al. (10) reported that increased amplitude of early somatosensory evoked fields in the ipsilesional SI in response to median nerve stimulation was associated with recovery of two-point discrimination (the ability to discern that two nearby objects touching the skin are truly two distinct points, not one) in stroke patients.

While relative “normalization” of brain activity in primary and secondary (SII) somatosensory regions in both hemispheres seems to underlie good clinical recovery, patients with more severe impairments have been shown to recruit attention and multisensory brain regions to a greater degree than that seen in healthy controls, in order to accomplish successful task performance (3, 11, 14–17). In an early positron emission tomography (PET) study of five patients after subcortical stroke, Weder et al. (14) reported activation across bilateral sensorimotor cortex and distributed regions, such as premotor cortex and cerebellum, with worse performance on a tactile shape discrimination task found to correlate with bilateral sensorimotor cortex activation. Tecchio et al. (16) used magnetoencephalography (MEG) to study 18 patients at the acute (5 days) and post-acute (6 months) stages after stroke. They reported that excessive interhemispheric asymmetry correlated with a greater degree of clinical improvement over time in those patients who showed partial recovery. Taskin et al. (15) reported reduced activation of ipsilesional SI with preserved responsiveness of SII in six patients who had

suffered thalamic strokes. More recently, in 19 patients, a study into the relationship between touch impairment and interruption to cortical and subcortical somatosensory areas revealed that the neural correlates of touch impairment in patients with interruption to subcortical somatosensory areas (e.g., thalamus), involved a distributed network of ipsilesional SI and SII, contralesional thalamus, and attention-related frontal and occipital regions (3).

Use of task-based brain activation paradigms can be challenging for stroke patients who may have difficulty performing a given task, and inability to perform the task may impact on the validity of the results (18). Resting-state functional connectivity analysis of functional magnetic resonance imaging (fMRI) data has more recently been employed as a way of assessing activity in the brain over time and across different networks of the brain (19, 20). Resting-state functional connectivity reveals intrinsic, spontaneous networks that elucidate the functional architecture of the human brain at rest (task-independent). Functional connectivity is defined as the statistical association (or temporal correlation) among two or more anatomically distinct regions (21). Data are analyzed for coherence across the whole brain and/or in relation to particular regions of interest (ROIs). Evidence suggests that this measure is indicative of behaviorally relevant brain networks without requiring task performance (22). Consistent resting-state networks, with sharp transitions in correlation patterns, are reliably detected in individual and group data (23, 24).

In stroke patients, use of this technique has revealed disruption of functional connectivity of brain networks, even within structurally intact brain regions (6, 25, 26). Changes in functional connectivity have been described in motor recovery under resting-state and task-related conditions (27). Further, changes in functional connectivity over time have been found to occur in conjunction with behavioral change, both in healthy individuals (22) and in stroke patients (7, 25). For example, He and colleagues (25) reported that in patients with spatial neglect, dorsal attention network connectivity was disrupted early after stroke, but appeared to have improved to similar levels as controls by 9 months post-stroke, in conjunction with behavioral improvement. This supports the interpretation that different networks or areas of the brain may dynamically change and assume different roles to allow behavior to occur.

The aim of the current study was to identify longitudinal changes in functional connections of the somatosensory network in stroke patients with somatosensory impairment, and to establish if and how these correlations are associated with improvement in touch discrimination.

The importance of interhemispheric functional connectivity in behavioral performance and recovery has been highlighted from studies using resting-state fMRI (rsfMRI) with animal and human stroke populations (7, 25, 28). The most consistent finding is of changes in interhemispheric functional connectivity between homotopic areas, such as ipsilesional and contralesional primary motor cortex (7). Longitudinal changes have also been reported. Decreased interhemispheric functional connectivity of the ipsilesional sensorimotor cortex has been reported early after stroke, with return to more normal levels during the recovery process (7, 29, 30). These findings are not surprising given that

interhemispheric connections are implicated in sensory (31) and cognitive processing (32) and in models of motor and somatosensory recovery (33–37). Thus, changes in interhemispheric functional connectivity in stroke patients and associations between these changes and behavioral improvement are expected. We hypothesized that over time, stroke patients would exhibit return to a more “typical” pattern of interhemispheric functional connectivity between homologous cortical somatosensory regions, and that stronger interhemispheric resting-state functional correlations between homologous SI and SII regions at 6 months than at 1 month post-stroke would be associated with clinical improvement.

Increased connectivity with distributed networks has also been reported in recovery after stroke. First, the visual system drives human attention and planning (38, 39), and a rich history of evidence for cross-modal plasticity between the visual and somatosensory systems exists (40). Recruitment of visual areas has been reported in previous studies of motor recovery after stroke (30, 41) as well as in patients with somatosensory impairment after stroke (3). Second, greater recruitment of attention systems is known to be necessary (42) to compensate for the impairment of function-specific brain areas due to aging or injury (43, 44). In stroke patients, increased attention has been shown to be required to accomplish previously simple tasks, such as walking, and attention skills have been shown to predict outcome after stroke (42, 45). Increased activation of frontoparietal attention areas, such as inferior parietal cortex (IPC), has been reported to occur in recovering stroke patients with motor problems (46–48). Thus, greater functional connections with frontoparietal attention networks could be expected in stroke patients with somatosensory impairment. As such, we predicted that stronger thalamocortical and cortico-cortical functional correlations with frontoparietal visual attention networks at 6 months post-stroke would be associated with clinical improvement.

Materials and Methods

Participants

Ten stroke patients with impaired touch discrimination of the upper limb were assessed at 1 and 6 months post-stroke. Inclusion criteria were as follows: first episode infarct, medical stability, ability to give informed consent and comprehend simple instructions, and right-hand dominance. Exclusion criteria included the following: brain-stem infarct or hemorrhagic stroke, previous neurological dysfunction, medical history impairing hand function or precluding MRI, or evidence of neglect based on standard neuropsychological tests. We also studied 10 age-matched, right-hand dominant healthy controls (4 male, mean age 60.60 years, range 23–79 years) without any history of neurological or somatosensory impairment. The relevant university and hospital human ethics committees approved the study and written informed consent was obtained from each participant.

Demographic and Clinical Profile

Background information included age, gender, and premorbid hand dominance (49). For the stroke patients, a clinical profile

obtained within 48 h of the MRI study included the following: severity of neurological impairment, using the National Institute of Health Stroke Scale (NIHSS) (50); severity of global disability, using the Barthel Index (51); and upper limb function, using the action research arm test (ARAT) (52). Severity of somatosensory impairment was quantified across several modalities, including touch (see below); limb position sense, using the wrist position sense test (WPST) (53); tactile object recognition, using the functional tactile object recognition test (54); and temperature discrimination, using the Rolyan® hot and cold discrimination kit. Age-matched healthy controls were also assessed on measures of somatosensation.

Quantification of Touch Impairment

The primary somatosensory outcome measure was the tactile discrimination test (TDT) (55), a psychophysical measure of touch discrimination of plastic gratings using the fingertip. Participants discriminate differences in finely graded plastic texture surfaces using the method of constant stimuli and a three-alternative forced-choice design. Five surface sets, which span the Weber function of texture differences, are each presented 10 times. The test score is the probability of correct discrimination response across all stimuli presented ($n = 50$) and represents the area that subtends the psychometric function after accounting for chance. The TDT has high test–retest reliability, age-appropriate normative standards, and excellent discriminative properties (55). Touch detection of the fingertips was assessed using the Weinstein enhanced sensory test (WEST) hand monofilaments and the rapid threshold procedure (56).

Image Acquisition

Functional Imaging Sequences

Whole-brain fMRI studies were performed using a 3-T GE Horizon LX Sigma MRI scanner with quadrature head coil (GE Medical Systems, WN, USA). Five minutes of resting-state data (100 volumes) were acquired for all participants. Images were acquired in 25 axial slices spanning cerebellum to the apex of the cerebrum using a gradient-echo, echoplanar (EPI) sequence [repetition time (TR) = 3000 ms; echo time (TE) = 40 ms; flip angle = 75°; field of view (FOV) = 240 mm; 128 × 128 matrix; slice thickness = 4 mm; interslice gap = 1 mm; in-plane voxel size = 1.95 mm × 1.95 mm; bandwidth = 100]. The participants were instructed to close their eyes and perform no particular task. Participants' arms rested comfortably on their chest, but not touching each other or anything else. The data were collected immediately after performing an in-scanner somatosensory task involving perception of a plastic texture grating, the results of which have been reported elsewhere (3). The participants were monitored during the scanning session to ensure that they were awake and alert. They were debriefed after resting-state data collection and none of them reported falling asleep.

Structural Imaging Sequences

Whole-brain anatomic and angiographic images were acquired at the same session and included the following: a high-resolution 3D anatomical image, 2D T1-weighted and axial 2D T2-weighted images in the same plane as EPI, and 2D angiographic images.

Data Analysis

Pre-Processing of fMRI Data

Pre-processing for each participant's data included image conversion, slice timing correction, determination of optimum realignment target (median center-of-within-brain intensity), motion detection and realignment (rigid body with six degrees of freedom), normalization to a customized EPI brain template (see below), Gaussian smoothing (8 mm full width at half maximum), and automated creation of within-brain mask of normalized images, using Statistical Parametric Mapping, SPM2 (www.fil.ion.ucl.ac.uk) and iBrain™ software (57). Motion correction parameters were included as covariates of no interest. Data from each imaging run were scaled to a grand mean of 100. The statistical analysis of the resting-state data employed an Autoregressive AR (1) model to account for temporal autocorrelation in the data.

For group analyses, fMRI data were brought into standard space. The spatial normalization target used was a custom template, approximating the EPI template in Montreal Neurological Institute (MNI) space supplied with SPM2. The custom template was created in an iterative fashion from a larger group of participants ($N = 33$) involved in the overall study. Images of patients with right hemisphere lesions were flipped such that all infarcts were in the left hemisphere.

Pre-Processing for Connectivity Analysis

Several processing steps were used to optimally prepare the functional data for analysis of voxel-based correlations. Data were high-pass filtered (using SPM8) (www.fil.ion.ucl.ac.uk) with a high-pass cut-off of 0.01 Hz and low-pass filtered in iBrain™ (57) using a finite impulse response filter to remove the effect of high-frequency noise ($f < 0.08$ Hz) (58).

Construction of Seed Regions of Interest

To measure interregional functional connectivity of the somatosensory system, we identified functionally and anatomically defined regions of interest (ROIs) representing nodes in the somatosensory system. These ROIs for functional connectivity analysis were determined by identifying regions of maximal activation from somatosensory fMRI task-related brain activation data in healthy controls (59). Significant activation clusters were restricted to the *a priori* determined cortical ROIs, the hand regions of SI, and bilateral SII, using cytoarchitectonic maps (60). The thalamic clusters were restricted to regions of the thalamus previously reported to show high probability of connectivity to somatosensory cortex, based on a thalamic connectivity atlas (61).

Six seeds were selected, and comprised clusters in the left and right primary and secondary somatosensory cortices and left and right somatosensory ventroposterior lateral thalami. Each cortical seed ROI was approximately 100 voxels in size (voxels were $1.95 \text{ mm} \times 1.95 \text{ mm} \times 4 \text{ mm}$ in size). The cortical seed regions were constructed to make the ROIs relatively uniform in size and were anatomically verified. As the thalamic seeds were based on the thalamic atlas (61), the size was determined by that template (141 and 168 voxels). Seeds were placed on the normalized images for each individual.

rsfMRI Correlation Analysis

The first step in all rsfMRI analyses was to extract BOLD signal time courses from each of the six ROIs by averaging timecourses over voxels within each region for each individual at each time point. For each individual, to compute functional connectivity maps corresponding to a selected seed ROI, the average BOLD signal timecourse of the voxels within the ROI was correlated against all other voxels within the brain, as originally described by Biswal et al. (62). Several potential sources of spurious variance along with their temporal derivatives were included in the design matrix as confounds: (1) six parameters obtained by rigid body correction of head motion; (2) the average whole-brain signal; (3) signal from a ventricular cerebrospinal fluid (CSF) ROI; and (4) signal from a region centered in the white matter (63). Regions in the CSF and white matter were identified manually using MRIcro software (64). The regression of these factors as variables of no interest was aimed at removing fluctuations unlikely to be involved in specific regional correlations (63). The analysis was performed using Statistical Parametric Mapping, SPM8 (www.fil.ion.ucl.ac.uk), with the individual functional connectivity maps thresholded at p -value < 0.001 (uncorrected) at the voxel level.

Second Level Imaging Analysis

In the group analysis, the contrast ($\text{con}^*.img$) images from the individual analyses of each individual participant were combined in a second level, random-effects model. To test for differences in patterns of functional connectivity between the healthy and stroke groups, *between-group* differences were evaluated using two-sample t tests. To test for differences in patterns of functional connectivity within the stroke group between the 1-month and 6-month time points, *within-group* differences were evaluated using paired t tests. In order to identify how differences in functional connectivity over time might be associated with changes on clinical test scores, individual changes in TDT scores over time were included as a regressor in subsequent correlation analyses in the group-level random-effects analysis of change in functional connectivity for the stroke group. Only clusters with p -values < 0.05 (false discovery rate, FDR, corrected) are reported as significant. Anatomical localization of significant clusters was defined using the anatomy toolbox in SPM8, which is based on probabilistic cytoarchitectonic maps (60).

Lesion locations were outlined on axial slices of the 3D anatomical images obtained at 6 months post-stroke, plotted into stereotactic space, as described previously (65), and displayed on a template. The percentage overlap between lesion location and the seed regions was defined for each participant.

Results

Demographic, Lesion, and Clinical Data

Ten stroke survivors (4 male, mean age 58.96 years, range 18–79 years) were studied at approximately 1 month ($M = 4.56$, $SD = 1.58$ weeks) and 6 months ($M = 26.99$, $SD = 1.69$ weeks) post-stroke (Table 1). All were right-hand dominant with a median hand laterality quotient of 100 (49). The left hemisphere was infarcted in six patients (Figure 1). Five patients had lesions

TABLE 1 | Background and clinical characteristics and lesion details of stroke patients (*N* = 10).

ID	Age	Gender	Side of lesion	Site of lesion	Lesion volume (voxels)	Overlap with seed regions (%)	Weeks since stroke		NIHSS	
							1 month	6 months	1 month	6 months
S10	71	M	L	Lateral thalamus (vpl, vpm)	345	0	7.57	25.29	1	0
S13	71	F	L	Lateral thalamus (vpl, vpm)	253	5 – L Th	3.29	28.57	2	1
S14	56	M	L	Multiple lesions in hemispheric white matter	22,761	2 – L Th	6.14	25.86	6	6
S16	76	M	R	Posterior insula, inferior parietal lobule, adjacent hemispheric white matter	14,728	19 – R SII	6.00	30.86	1	1
S17	40	F	R	Posterior insula, inferior parietal lobule, postcentral gyrus	3998	19 – R SII	3.71	26.86	3	1
S18	79	M	L	Putamen/caudate nucleus, parietal/cortical	21,939	87 – L SII	3.86	26.00	4	1
S19	18	F	R	Thalamus (lp), hippocampus, fusiform gyrus	12,465	0	2.43	25.29	4	3
S20	55	F	L	Supramarginal gyrus, parietal operculum, superior parietal lobule, postcentral gyrus	6593	0	3.57	27.14	4	1
S21	63	F	L	Thalamus (vpl), occipital periventricular white matter, lacunar lesion in head of right caudate nucleus	10,107	10 – L Th	5.00	27.29	3	2
S22	59	F	R	Postcentral gyrus, superior parietal lobule, anterior portion	8990	10 – R SII	4.00	26.71	2	2
Median (IQR)	59.00 (55.00–71.00)	4M; 6F	6L; 4R		8990 (2435–13,597)		3.93 (3.61–5.75)	26.77 (25.89–27.25)	3.00 (2.00–4.00)	1.00 (1.00–2.00)
25th–75th										

ID, stroke identification number; NIHSS, National Institute of Health Stroke Scale, 1–4 = minor stroke, 5–15 = moderate stroke, 16–20 = moderate/severe stroke, and 21–42 = severe stroke (50); M, male; F, female; R, right; L, left; voxel size = 1.95 mm × 1.95 mm × 4 mm; vpl, ventral posterolateral nucleus; vpm, ventral posteromedial nucleus; lp, lateral posterior nucleus; Th, thalamus; SII, secondary somatosensory cortex; IQR, interquartile range.

primarily involving subcortical somatosensory structures, in particular the thalamus, and five had lesions predominantly involving cortical SI and/or SII. The percentage overlap between lesion location and our pre-defined seed regions is provided in **Table 1**. All with subcortical lesions had involvement of thalamus, often including ventral posterolateral nucleus, a region known to project somatosensory information to SI. Only three had 2–10% overlap with the thalamic seed used in analysis. Those with cortical lesions primarily had involvement of postcentral gyrus (*n* = 3) and/or secondary somatosensory regions (*n* = 5) including parietal operculum and nearby regions of the insula and supramarginal gyrus. Across patients there was no overlap between lesion site and the SI seed. Four patients had lesion locations that overlapped with the SII seed; three had 10–19% overlap and a further patient with a very large lesion had 87% overlap.

Patients presented with wide variation in severity of touch discrimination (**Table 2**), ranging from −11.58 (very severe impairment) to 79.31 (just within the normal range) on the TDT (55) at the 1-month study. Several patients performed within normal limits on the TDT at 6 months post-stroke, and in three cases at the 1-month time point. Somatosensory impairment was indicated in these patients on the basis that the TDT score for the affected hand was lower than for the “unaffected” hand, they demonstrated impairment on other clinical somatosensory tests, and/or they reported a “hyper-sensitivity” profile of *heightened* sensitivity to somatosensory stimuli.

For the stroke group, mean affected-hand score on the TDT at the 1-month time point was 35.98 ± 33.13 SD (median 35.47 percentage correct area under the curve), compared to 79.85 ± 8.11 SD (median 77.09) for healthy controls in the matched hand. TDT scores were significantly higher in the healthy control group than in the patient group (Mann–Whitney *U* = 11.00, *p* = 0.002). The stroke group demonstrated significant improvement in TDT scores with the affected hand between the 1- and 6-month time points (*Z* = −2.293, *p* = 0.022). Clinical scores and demographic and clinical information for the stroke patients are presented in **Table 1**.

Functional Connectivity During the Resting State Functional Connectivity of Stroke Patients Compared to Healthy Controls

Within the healthy control group, the SI seeds for both hemispheres showed significant functional connectivity with bilateral SI and motor (Brodmann Area, BA 4a, 6) regions (**Figure 2**). In contrast, at 1 month post-stroke the stroke group exhibited a lack of interhemispheric connectivity for both of the SI seeds, with each SI seed functionally connected only with surrounding SI and motor areas. At 6 months post-stroke, there appeared to be some return of interhemispheric SI connectivity for the stroke group (**Figure 2**). For example, the ipsilesional SI seed showed significant functional connectivity not only with surrounding SI and motor areas but also with contralesional SI, contralesional visual and motor areas, and with ipsilesional SII. Similarly, the

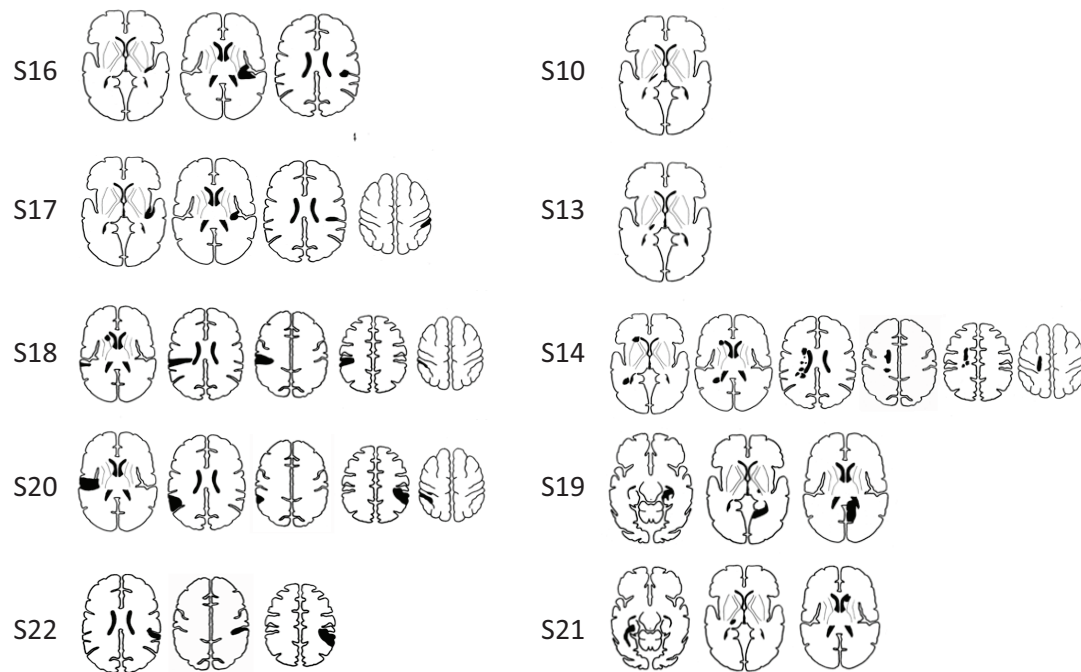


FIGURE 1 | Infarct locations for individual stroke participants. Lesions were predominantly located in cortical somatosensory regions (SI and/or SII) (images in left column), and in somatosensory areas of the thalamus (images in

right column). Infarct locations for each individual are plotted in stereotactic space. Images are displayed in neurological convention (subject's left is displayed on image left).

contralesional SI seed remained functionally connected with surrounding SI and motor regions, and showed connections not present at the 1-month time point with ipsilesional SI and SII, and contralesional middle occipital gyrus. At the 1-month time point, the healthy group exhibited significantly greater functional connectivity than the stroke group between the contralesional SI seed and a cluster in the contralesional occipital lobe and contralesional cerebellum ($MNI = 30/-56/16$; $k = 99$ voxels; $z = 4.76$).

In the healthy control group, SII seeds of each hemisphere exhibited significant functional connectivity with bilateral SII and SI, as well as with medial supplementary motor area (SMA, BA 6). The stroke group demonstrated a similar pattern of connectivity for the ipsilesional SII seed at 1 month post-stroke. For the contralesional SII seed, significantly connected clusters also extended into bilateral SI. At 6 months post-stroke, the ipsilesional SII seed showed functional connectivity only with surrounding SII and SI. The contralesional SII seed was again functionally connected with bilateral SII and contralesional SI, with additional small clusters in contralesional SMA (BA 6) and medial visual areas (BA 17, 18, commonly referred to as human V4 and V2).

In the healthy control group, thalamus seeds of each hemisphere were functionally connected to a statistically significant extent with bilateral thalami (thalamus surrounding the seed region in the same hemisphere, as well as contralateral thalamus) and SII/insula in the same hemisphere (Figure 2). At 1 month post-stroke, the patient group showed significant functional connectivity from both thalamus seeds with bilateral thalami,

although to a less extent than that seen in the healthy control group. In addition, the contralesional thalamus was functionally connected with small clusters in contralesional inferior and superior frontal gyri, and contralesional cerebellum. At 6 months, ipsilesional thalamus in stroke patients still showed significant functional connectivity with thalami in both hemispheres, whereas the contralesional thalamus was only functionally connected with surrounding contralesional thalamus and with a small cluster in the left putamen.

Longitudinal Functional Connectivity Changes in the Stroke Group

To test for differences in patterns of functional connectivity within the stroke group between the 1- and 6-month time points, within-group differences were evaluated using paired t tests (Table 3). For the contralesional SI seed, there was significantly greater functional connectivity at 1-month than at 6-month post-stroke between contralesional SI and a cluster falling in the contralesional cerebellum and hippocampus. At 6 months, there was significantly greater functional connectivity between contralesional thalamus and a cluster in ipsilesional middle cingulate cortex.

Functional Connectivity Changes Associated with Somatosensory Improvement

In subsequent correlation analyses, changes over time in clinical scores, as measured using the TDT, were included as a regressor in the group-level random-effects analysis of change in functional

TABLE 2 | Scores on somatosensory and hand function tests in the stroke group ($N = 10$).

ID	TDT - Aff (/100)		TDT - Unaff (/100)		WEST - Aff		WEST - Unaff		fTORT - Aff (/42)		Temp Aff (/10)		WPST Aff (error)		ARAT Aff (/57)	
	Initial	6 months	Initial	6 months	Initial	6 months	Initial	6 months	Initial	6 months	Initial	6 months	Initial	6 months	Initial	6 months
S10	43.10	77.59	75.37	85.22	1.1	0.2	0.135	0.035	41	40	5	9	15.40	10.90	57.0	56.0
S13	72.91	72.66	81.03	72.41	1.1	0.135	0.035	0.07	41	40	10	10	7.85	4.45	55.0	55.5
S14	30.54	47.29	67.98	81.03	102	0.07	0.07	0.07	29	40	7	9	21.75	20.30	0.0	0.0
S16	75.12	76.85	86.45	93.60	0.135	0.135	0.14	0.135	38	42	4	4	14.20	7.10	56.5	57.0
S17	8.87	40.39	52.71	77.59	300	1.1	0.035	0.035	34	42	0	2	16.65	13.90	42.0	53.5
S18	40.39	67.73	83.99	89.41	200	1.1	0.035	0.07	40	41	8	8	15.20	13.85	54.5	57.0
S19	79.31	66.99	84.73	73.64	0.035	0.035	0.07	0.035	40	42	10	10	11.15	5.35	57.0	57.0
S20	-11.58	78.57	87.93	81.53	102	0.2	0.07	0.135	40	41	0	0	17.70	12.30	49.0	57.0
S21	29.56	33.74	68.72	85.47	2	0.07	0.035	0.035	37	41	8	7	16.25	12.50	55.0	56.5
S22	-8.37	32.02	63.55	57.88	2	1.1	0.07	0.035	31	39	8	4	15.60	15.70	11.0	42.0
Median	35.47	67.36	78.20	81.28	2.00	0.17	0.07	0.05	39.0	41.0	7.5	7.5	15.50	12.40	54.75	56.25
(IQR)	(14.04–65.46)	(42.12–75.80)	(68.17–84.55)	(74.63–85.41)	(1.10–102.00)	(0.09–0.88)	(0.035–0.07)	(0.04–0.07)	(34.8–40.0)	(40.0–41.8)	(4.3–8.0)	(4.0–9.0)	(14.45–16.55)	(8.05–13.89)	(43.75–56.13)	(54.00–57.00)

TDT, tactile discrimination test (55); score is percentage correct area under the curve (2). The 95th percentile criterion for abnormality is a score <66.1. Minus values indicate scores with touch discrimination less than chance; WEST, Weinstein enhanced sensory test monofilaments touch detection score for the fingertip used in the TDT; threshold in grams pressure (59); fTORT, functional tactile object recognition test, score out of maximum 42, 5th percentile criterion of abnormality is 37 (54); Temp., Hot/cold temperature discrimination, number correct out of 10; WPST (average error), wrist position sense test, average error in degrees, 95th percentile criterion of abnormality is 9.5° average error (53); ARAT, action research arm test, score out of maximum 57 (52); IQR, interquartile range.

connectivity for the stroke group. The functional connectivity changes significantly associated with changes in TDT scores are shown in **Table 3** and **Figure 3**. Greater improvement in TDT scores was associated with greater functional connectivity at 6-month than at 1-month post-stroke between the contralesional SII seed and clusters in the contralesional IPC and contralesional middle temporal gyrus. Greater connectivity at 6-month than at 1-month post-stroke between the contralesional thalamus seed and a cluster in contralesional cerebellum was also associated with greater improvement. Greater functional connectivity at 1-month than at 6-month post-stroke between the contralesional SI seed and contralesional cerebellum was associated with greater improvement in TDT scores over time. Conversely, relative to the 6-month recovery time, greater improvement in TDT scores may be viewed as being associated with less functional connectivity at 6 months than at 1 month between the contralesional SI seed and contralesional cerebellum (**Figure 3**).

Discussion

Interhemispheric Functional Connectivity is Disrupted at 1 month After Stroke and Shows Some Recovery Toward Normal Levels at 6 months

Our findings of functional connectivity extend previous findings of changes in activation of brain regions with somatosensory impairment and add to the growing body of literature on the role of interhemispheric connectivity in stroke recovery across a range of functions. One month post-stroke, patients with impaired touch sensation and lesions predominantly located in somatosensory areas of the thalamus, and/or in cortical somatosensory regions (SI and/or SII), exhibited disruption of interhemispheric functional connectivity of homologous SI regions relative to age-matched healthy controls. At 1 month post-stroke, the stroke group only exhibited SI functional connectivity with SI within the same hemisphere; at 6 months, there was some return of interhemispheric SI connectivity.

Our finding of less interhemispheric connectivity in the stroke patients with impaired touch sensation relative to healthy controls early post-stroke is consistent with evidence of disrupted interhemispheric functional connectivity in stroke patients for other functions, such as movement and attention (7, 25, 27, 28). The disruption observed is likely to be behaviorally relevant, given that activity in both hemispheres has been shown to be important in sensory processing (31, 66) and in activation studies of somatosensory and motor recovery (33–36). Further, previous studies using rsfMRI in stroke recovery across functions have highlighted the importance of interhemispheric functional connectivity in behavioral performance and in recovery over time (7, 25, 28).

Evidence of SI interhemispheric connectivity at 6 months in stroke patients with less severe touch impairment is consistent with growing evidence from related studies. Activation studies of motor recovery indicate “return to more normal patterns” is associated with better recovery in the post-acute and chronic phase (e.g., 6 months) post-stroke (67, 68). In addition, a recent review of rsfMRI studies in motor recovery

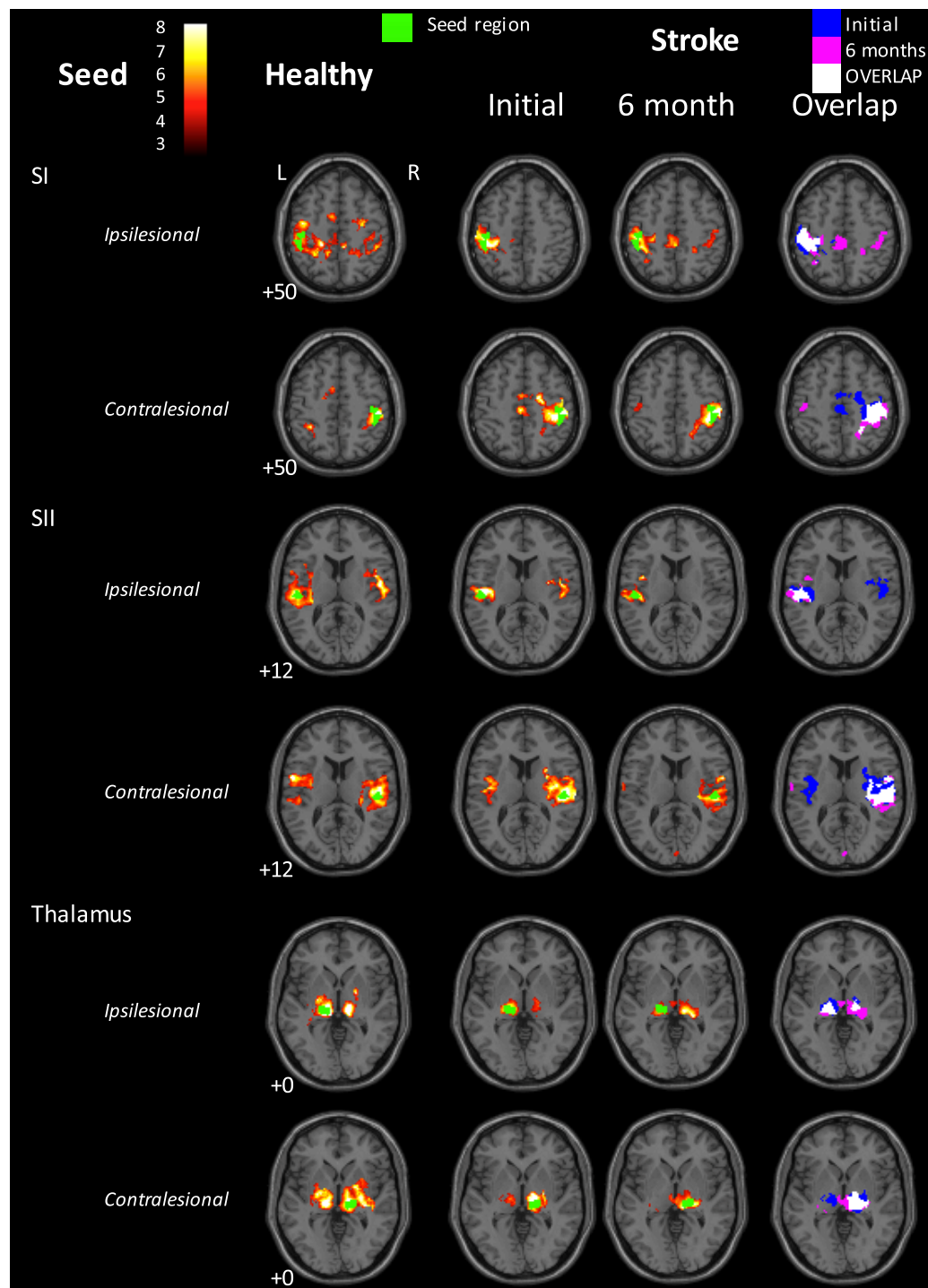


FIGURE 2 | Functional connectivity maps for the healthy control group and for the stroke group at the 1- and 6-month time points. Left three columns: group-level functional connectivity maps. Right-hand column: overlaps of binarized group-level functional connectivity maps for the stroke group at the two time points. Blue = 1-month time point; Red = 6-month time point; Yellow = overlap. The stroke group appears to show disrupted interhemispheric functional connectivity for the SI seeds at 1 month post-stroke, relative to healthy controls. Some return of interhemispheric functional connectivity can be seen at 6 months. In contrast, interhemispheric SII connectivity in the stroke group appeared greater at 1 month than at 6 months post-stroke. The seed region is indicated in green.

Images are displayed in neurological convention (subject's left is displayed on image left). The left hemisphere represents the ipsilesional hemisphere – images of patients with right hemisphere lesions were flipped such that all infarcts are represented in the left hemisphere. Healthy controls were individually matched and images flipped accordingly. Slice numbers represent axial slice position in Montreal Neurological Institute (MNI) space. Color scale represents Z-values of group functional connectivity maps. SI, primary somatosensory cortex; SII, secondary somatosensory cortex. Analyses are based on contrast maps with an individual voxel height threshold level of $p < 0.001$. Results are displayed for significant clusters with $p < 0.05$ (false discovery rate, FDR, corrected).

TABLE 3 | Functional connectivity changes in the stroke group between the 1- and 6-month time points, and changes associated with improvement in TDT scores.

Seed region	Cluster size (voxels)	Z-value	MNI maxima coordinates (x, y, z)	Cluster anatomical location of significantly correlated regions
Regions showing greater functional connectivity at 1 month				
Contralesional SI	60	4.14	14, -32, -18 12, -28, -6 6, -34, -20	Contralesional cerebellum lobules I–V, hippocampus
Regions showing greater functional connectivity at 6 months				
Contralesional thalamus	49	4.44	-16, -22, 38	Ipsilesional middle cingulate
Regions showing greater functional connectivity at 6 months than 1 month post-stroke in association with improvement in touch discrimination				
Contralesional SII	53	4.55	52, -58, 26	Contralesional IPC
	30	5.02	58, -26, -10	Contralesional middle temporal gyrus
Contralesional thalamus	35	4.27	12, -42, -40 20, -44, -34	Contralesional cerebellum lobule IX
Regions showing greater functional connectivity at 1 month than 6 months post-stroke in association with improvement in touch discrimination				
Contralesional SI	42	3.89	28, -44, -24	Contralesional cerebellum lobules V, VI

Anatomical definitions are based on the anatomy toolbox in SPM8, which is based on probabilistic cytoarchitectonic maps (60).

MNI, Montreal Neurological Institute; SI, primary somatosensory cortex; SII, secondary somatosensory cortex; IPC, inferior parietal cortex.

found that reorganization of motor networks encompasses a restoration of interhemispheric functional coherence in the resting state, particularly between the primary motor cortices (27). While we do not report a significant longitudinal change in connectivity between contralesional and ipsilesional SI, we did observe significant interhemispheric connectivity for both SI seeds at 6 months that was not present at 1 month. Together, our findings resonate with studies illustrating the role of inhibitory influences from intact hemisphere in stroke recovery (33) and highlight the need to re-establish a balance of activity across hemispheres in association with improvement (35).

Disruption and Resolution of Functional Connectivity with Occipital Visual Areas

Another key finding was the role of functional connectivity with primary visual occipital regions. At the 1-month time point, functional connectivity between contralesional SI and the occipital lobe was significantly less in the stroke group compared to the matched healthy control group. At the 6-month time point, the stroke group demonstrated functional connections with visual occipital areas that were not present at 1 month post-stroke, including between ipsilesional SI and contralesional visual areas (BA 17, 18), between contralesional SI and contralesional middle occipital gyrus, and between contralesional SII and bilateral visual areas (BA 17, 18). Together, these findings suggest a pattern of disruption of functional connections between somatosensory and visual areas at 1 month post-stroke, which showed some return after 6 months.

Supporting the suggestion of less connectivity with visual occipital regions early post-stroke is Park et al.'s (30) finding that one month after stroke, patients with motor impairment demonstrated decreased functional connectivity between primary motor regions and occipital cortex. Similarly, Carey et al. (3) reported that in a group of stroke patients with thalamic lesions studied at 1 month post-stroke, touch discrimination correlated negatively with task-related activation in occipital

regions. Connectivity with occipital regions at 6-month are also consistent with Seitz et al.'s (41) study of the functional networks related to motor recovery, which found that improved motor function after stroke was associated with involvement of distributed areas including extrastriate visual areas. Thus, there seems to be a pattern of disrupted interactions between sensorimotor and visual occipital systems around 1 month after stroke, with some resolution over time that may be clinically relevant.

Functional Connections to Frontoparietal Attention Regions

In stroke patients, functional connections to frontoparietal attention regions (69), involving middle cingulate and IPC, were significantly greater at 6 months than at 1 month post-stroke, and these differences between time points were in part associated with changes in behavioral performance. Functional connectivity between contralesional thalamus and ipsilesional middle cingulate cortex was significantly greater at 6 months than at 1 month post-stroke. Furthermore, behavioral improvement on the TDT was associated with greater functional connectivity 6 months post-stroke between contralesional SII and a cluster in contralesional IPC. In addition, the individuals who showed thalamocortical functional connectivity with frontal regions at the 1-month time point also had relatively low TDT scores, while those who showed this connectivity pattern at 6 months had better TDT scores.

Activation of distributed attention networks has been observed in previous task-based studies of stroke recovery, including in relation to somatosensory recovery (3, 36). Involvement of frontoparietal attention networks in association with behavioral outcome has been a common finding in stroke patients in the motor domain (46–48). Further, longitudinal changes in rsfMRI include changes in frontal and parietal cortices during motor recovery (30). Here, we extend this finding of functional connectivity to somatosensory recovery post-stroke. Baseline brain activity in the medial thalamus and the frontoparietal network is important

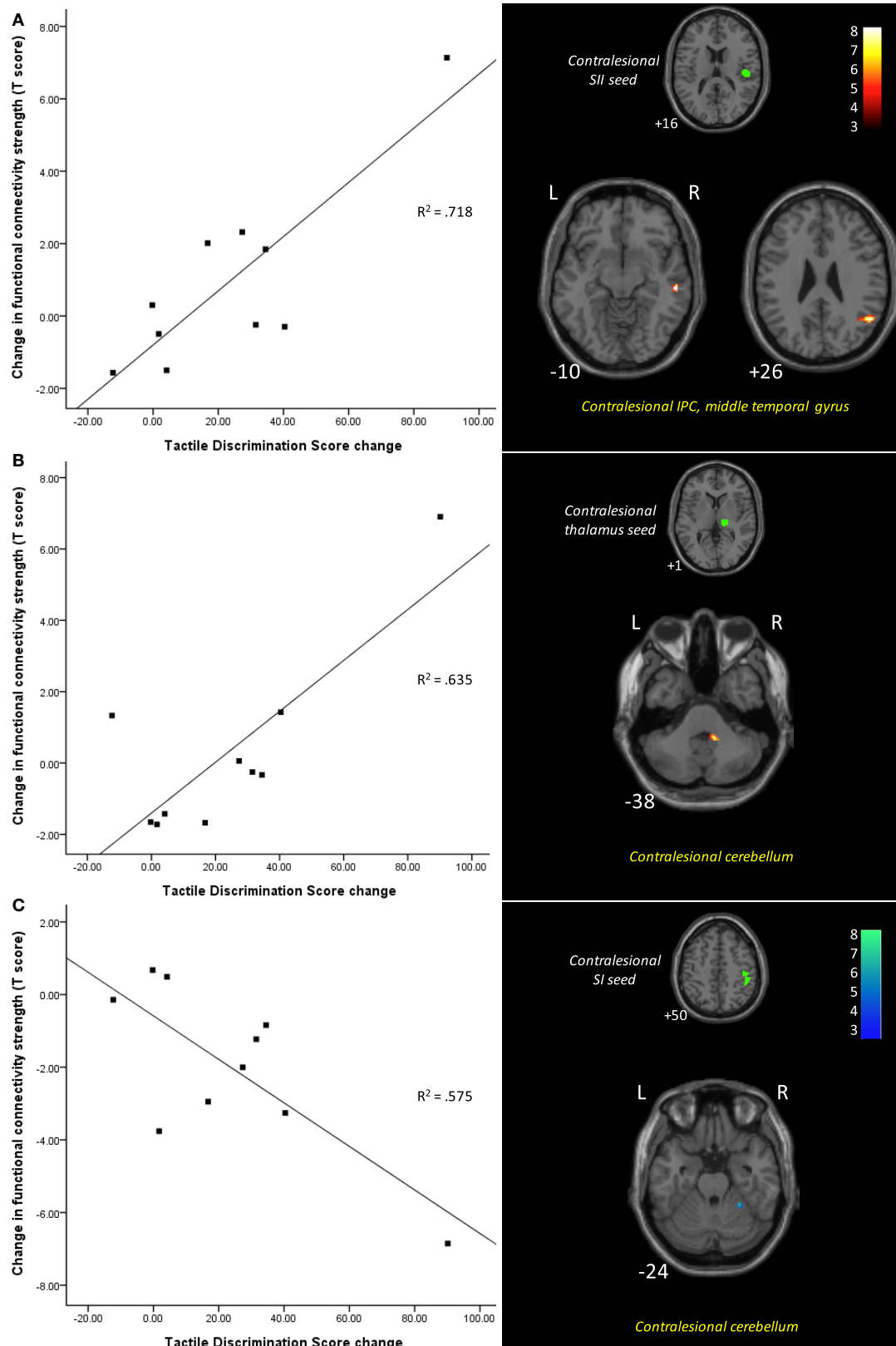


FIGURE 3 | Functional connectivity differences between 1 and 6 months post-stroke associated with changes in tactile discrimination test (TDT) scores.

(Continued)

FIGURE 3 | Continued

Scatter plots illustrate change in TDT score plotted against the difference between the two time points in connectivity strength between the seed and the cluster (shown in images on the right), for each individual. Improvement in TDT scores was associated with **(A)** greater functional connectivity at 6 months between the contralesional SII seed and clusters in the contralesional inferior parietal cortex and contralesional middle temporal gyrus; **(B)** greater functional connectivity at 6 months between the contralesional thalamus seed and a cluster in contralesional cerebellum; and **(C)** less functional connectivity at 6 months between the contralesional SI seed and contralesional cerebellum. Images are displayed in neurological convention

(subject's left is displayed on image left). The left hemisphere represents the ipsilesional hemisphere – images of patients with right hemisphere lesions were flipped such that all infarcts are represented in the left hemisphere. Slice numbers represent axial slice position in Montreal Neurological Institute (MNI) space. Color scale represents Z-values of functionally connected clusters associated with TDT score change. SI, primary somatosensory cortex; SII, secondary somatosensory cortex; IPC, inferior parietal cortex. Analyses are based on contrast maps with an individual voxel height threshold level of $p < 0.001$. Only clusters with p -values < 0.05 (false discovery rate, FDR, corrected) are reported as significant and displayed.

in perception (70) and may affect information processing following sensory impairment. In addition, focal attention involved in perception of pain, processing of reward, and error detection, has been associated with activity in medial frontal/anterior cingulate (69). Attention is essential to any perception or learning (69, 71), and has been identified as a key element of recovery from brain injury (25, 42, 45). It could be speculated that our findings reflect stroke patients' use of higher-level attention and behavioral processes to supplement previously more automatic somatosensory perceptual functions.

Involvement of Contralesional Hemisphere

Changes in functional connectivity between the 1- and 6-month time points and in association with improvement in TDT over time were all seeded within the contralesional hemisphere, i.e., contralesional SI at 1 month and contralesional thalamus and SII at 6 months. We did not find significant changes over time in connectivity from our ipsilesional seeds. Further, the regions showing relatively increased correlation were also primarily in the contralesional hemisphere, with the exception of ipsilesional middle gyrus at 6-month > 1 -month post-stroke. These findings highlight a role for change in connectivity of the “intact” contralesional hemisphere, in particular somatosensory SI, SII and thalamus regions, in individuals with impaired touch sensation post-stroke. Further, the observation that increased connectivity from these contralesional somatosensory seeds was associated with improvement in touch discrimination scores over time suggests a role for the contralesional somatosensory network in facilitating touch discrimination perception. While previous task-based fMRI studies typically show an initial increase in activation of contralesional sensorimotor cortex early followed by restoration of activation in the ipsilesional cortex, our finding suggests that disruption of the initial interhemispheric connectivity at resting state may lead to ongoing alterations in the activity (functional connectivity) of contralesional hemisphere. These relative increases in connectivity, observed both early and late, may help in achieving a more balanced interhemispheric connectivity in association with greater improvement in patients with partial recovery.

At 1-month, increased connectivity between contralesional SI and contralesional cerebellum was associated with greater improvement in touch sensation over time. In comparison, at 6 months, the relatively greater connectivity associated with better touch discrimination was between contralesional SII and IPC and contralesional thalamus and cerebellum. Interestingly, contralesional cerebellum had changed connectivity to somatosensory

seeds associated with improvement at both times, but via different nodes of the network. A role for increased connectivity between contralesional SI and cerebellum, at 1-month associated with improvement, is consistent with our observation of greater connectivity between these regions in the healthy group, compared to stroke patients, at 1-month. Longitudinal changes in rsfMRI during motor recovery have also involved bilateral thalamus and cerebellum, with involvement of cerebellum persisting over the 6-month period post onset (30). A large proportion of cerebellum maps to association areas (72). In addition, the cerebellum has connections with SI, although preferentially with the contralateral cerebrum (72). Afferent projections first synapse in the deep cerebellar nuclei and then project to a second synapse in the contralateral thalamus that in turn serves as a relay to the cerebral cortex, consistent with involvement of thalamus at 6 months. Co-observation of greater functional connectivity of contralesional thalamus with ipsilesional middle cingulate at 6 months, suggests an increased interhemispheric connectivity. Involvement of contralesional thalamus has been reported in association with touch impairment in a sample of 19 stroke survivors at 1-month post-stroke (3). Contralesional thalamus has potential to be accessed irrespective of lesion location (3), has an influence on bilateral SI via its prefrontal connections (73), and may have a role in gating of sensory information and in large-scale reorganization in the somatosensory cortex and thalamus after sensory loss (74, 75).

Limitations

The major limitation of this study was the small and heterogeneous sample of stroke patients. Replication of these preliminary findings in larger samples is required. Use of a larger sample would also allow investigation of these changes without the need to flip individual brain maps into common space. This would permit inferences about the role of lateralized frontoparietal attention networks in facilitating post-stroke behavioral improvement (8). While it is recognized that functional connectivity may be influenced by the participants recent experience (76), the sequence of acquisition was common for all participants, i.e., it was immediately preceded by a touch discrimination task. Further, our stroke findings may be interpreted with reference to healthy controls who underwent the same protocol sequence, and our longitudinal findings with reference to connectivity studies in the same individual over time.

Application of rsfMRI analyses in stroke patients presents issues that need to be considered in the interpretation of our findings. The potential impact of lesion location on pre-defined seed ROIs is an unavoidable issue. This was in part minimized through

application of individual lesion masks during the normalization phase. In addition, we quantified the percentage overlap between the lesion and seed region for each participant to monitor the presence of this potential limitation. All but one participant had <20% overlap. There was no overlap with the ipsilesional SI seed and only 10% or less overlap with the thalamic seed. The seed with most overlap was the SII seed, with 4 of 10 patients having overlap. Our major findings of change in connectivity were evident for contralesional seeds, and thus, can be interpreted with confidence. Further, lack of evidence of significant change for ipsilesional SI and thalamic seeds is unlikely explained by analysis method and seed overlap, as this was minimal. Interpretation of functional connectivity from ipsilesional SII may be impacted by overlap between lesion and seed. Although we did not find a significant change over time, we did observe significant connectivity from ipsilesional SII at 1 and 6 months, suggesting presence of lesion overlap with this seed is an unlikely explanation. A recent investigation of overlap between lesion location and seeds between stroke and healthy groups suggests that the percent of infarct-related overlap to any ROI was not related to connectivity strength in connections that included those damaged seeds (77). While this finding is based on a larger sample ($n = 32$) and multiple correlations, it does provide some support for interpretation of seed-based connectivity data in stroke patients. Finally, even if the differences in connectivity observed between stroke and healthy controls is due to impaired anatomic connections from these regions, our findings still inform us of the key functional connections involved in somatosensory impairment, the impact of lesion on the function, and the changes in functional connectivity associated with clinical improvement in touch discrimination.

Use of the BOLD signal in fMRI studies of stroke patients has been a highly debated issue given the potential impact of vascular compromise. The BOLD signal provides an indirect indication of neural activity, and changes in resting-state activity can reflect a complex combination of neural, vascular, and metabolic factors (78). Connectivity analysis methods have the advantage that they do not rely on BOLD signal stability, nor assume a common hemodynamic response function (79). However, they are not immune to issues associated with abnormal neurovascular coupling in stroke patients. Indeed, it is unclear how potential vascular latency differences between brain regions impact interpretation following stroke. For example, changes in peri-infarct regions, such as hypoperfusion and potential decoupling of the neurovascular response (80), may impact the signal. It has been suggested that differences across regions may confound studies of whole-brain connectivity (81). A few studies have therefore adjusted for non-neural vascular latency differences prior to resting-state connectivity analyses in healthy controls with only a minor impact on their findings (81). However, we should exercise caution when interpreting findings in stroke patients, particularly in locations close to the lesion border. Further, it is important to recognize that changes observed with rsfMRI may reflect an interaction between neural activity and vascular changes over 1–6 months. It should also be noted that we did not exclude patients with conditions that may impact the BOLD signal, such as leukoencephalopathy and/or carotid artery disease, and thus the impact of these conditions if present is unknown.

Implications and Future Directions

In summary, stroke patients showed changes in functional connectivity over a period of recovery under non-specific rehabilitation conditions. Further, most changes in functional connections from 1 to 6 months post-stroke were shown to relate to improvement in touch discrimination scores over time, in patients with partial recovery. There appeared to be some return of functional connections over time in patients between homologous SI regions, and between somatosensory and visual occipital areas, although not to the levels seen in age-matched controls. Change in connectivity over time and/or in association with improvement was observed in relation to contralesional somatosensory seeds, and primarily involved frontoparietal attention regions and cerebellum. Change in contralesional SI connectivity was important at 1-month in relation to improvement over time, while changes in connectivity of contralesional SII and thalamus become important at 6 months.

These changes in connectivity could represent future targets for therapy. In particular, increase in strength in connections between somatosensory regions and attention and vision regions is consistent with pre-existing connections with these networks and suggest targets for neuroscience-based rehabilitation approaches designed to access viable brain networks (36). While our findings indicate that some individuals spontaneously access these regions in association with improved performance, the potential exists for knowledge of these individual differences to guide access in other stroke survivors through therapy. For example, the effective sensory discrimination training approach described by us to achieve stimulus specific improvements in touch discrimination (82) employs training strategies to achieve cross-modal calibration of perceived texture roughness across touch and vision, as well as use of attentive exploration of textured stimuli and deliberate use of anticipation trials (36, 82). These strategies may be helpful in accessing vision and attention networks in survivors who may not otherwise make these connections.

Targeting of contralesional and distributed networks via secondary somatosensory cortex and thalamus is also suggested. Our findings first highlight the role of the contralesional hemisphere in post-stroke performance and recovery. The seed-based change in contralesional functional connectivity is consistent with structural and functional connectivity studies of sensorimotor training that suggest global network efficiency is influenced by long-range connections across hemispheres, in addition to ipsilesional integrity (83). Changes in connectivity of contralesional SII and thalamus at 6 months suggest a role for nodes that have connections within the somatosensory network and beyond. SII has strong connections with SI, thalamus, and homologous SII, as well as with frontal and parietal networks (84). SII has more dense bilateral connectivity than SI (85), is involved in tactile working memory, discrimination, and perceptual learning (86–88), and is regarded as an integration node of the somatosensory network. Enhanced SII connections with IPC and middle temporal gyrus at 6 months highlight connectivity with distributed networks. The potential exists to influence this highly connected node of the somatosensory network through rehabilitation designed to access discriminative and tactile

learning functions. The thalamus is also implicated. It has an important role in gating somatosensory input and deactivation of contralesional thalamus is associated with touch discrimination performance in stroke survivors at 1 month post-stroke (3). Involvement of thalamus is consistent with evidence from animal studies (74, 75) that gating of sensory inputs, rather than cortical representation alone, is important in recovery. In addition, increased connectivity between thalamus and cerebellum suggests short-range functional connectivity of subcortical networks (89). Thalamus and cerebellum are two of three major subcortical network hubs identified (89). Involvement of both long-range and short-range functional connectivity changes may reflect not only the individual variation in recovery and underlying mechanisms but also the potential to drive one or other through appropriately targeted therapy. While connectivity-based research is still in its infancy post-stroke, it has great potential to guide the development of scientifically informed rehabilitation interventions.

References

- Kim JS, Choi-Kwon S. Discriminative sensory dysfunction after unilateral stroke. *Stroke* (1996) 27:677–82. doi:10.1161/01.STR.27.4.677
- Carey LM, Matyas TA. Frequency of discriminative sensory loss in the hand after stroke. *J Rehabil Med* (2011) 43(3):257–63. doi:10.2340/16501977-0662
- Carey LM, Abbott DF, Harvey MR, Puce A, Seitz RJ, Donnan GA. Relationship between touch impairment and brain activation after lesions of subcortical and corticofugal somatosensory regions. *Neurorehabil Neural Repair* (2011) 25(5):443–57. doi:10.1177/1545968310395777
- Carter AR, Shulman GL, Corbetta M. Why use a connectivity-based approach to study stroke and recovery of function? *Neuroimage* (2012) 62(4):2271–80. doi:10.1016/j.neuroimage.2012.02.070
- Corbetta M, Kincade M, Lewis C, Snyder A, Sapir A. Neural basis and recovery of spatial attention deficits in spatial neglect. *Nat Neurosci* (2005) 8:1603–10. doi:10.1038/nn1574
- Carey L, Seitz R, Parsons M, Levi C, Farquharson S, Tournier J-D, et al. Beyond the lesion – neuroimaging foundations for poststroke recovery. *Future Neurol* (2013) 8(5):507–24. doi:10.2217/fnl.13.39
- Carter AR, Astafiev SV, Lang CE, Connor LT, Rengachary J, Strube MJ, et al. Resting interhemispheric functional magnetic resonance imaging connectivity predicts performance after stroke. *Ann Neurol* (2010) 67(3):365–75. doi:10.1002/ana.21905
- Corbetta M. Functional connectivity and neurological recovery. *Dev Psychobiol* (2012) 54:239–53. doi:10.1002/dev.20507
- Kolb B, Teskey GC, Gibb R. Factors influencing cerebral plasticity in the normal and injured brain. *Front Hum Neurosci* (2010) 4:204. doi:10.3389/fnhum.2010.00204
- Wikström H, Roine RO, Aronen HJ, Salonen O, Sinkkonen J, Ilmoniemi RJ, et al. Specific changes in somatosensory evoked fields during recovery from sensorimotor stroke. *Ann Neurol* (2000) 47:353–60. doi:10.1002/1531-8249(200003)47:3<353::AID-ANA11>3.3.CO;2-I
- Carey LM, Abbott DF, Puce A, Jackson GD, Syngieniotis A, Donnan GA. Reemergence of activation with poststroke somatosensory recovery: a serial fMRI case study. *Neurology* (2002) 59(5):749–52. doi:10.1212/WNL.59.5.749
- Staines WR, Black SE, Graham SJ, McLroy WE. Somatosensory gating and recovery from stroke involving the thalamus. *Stroke* (2002) 33(11):2642–51. doi:10.1161/01.STR.0000032552.40405.40
- Rossini PM, Altamura C, Ferreri F, Melgari J-M, Tecchio F, Tombini M, et al. Neuroimaging experimental studies on brain plasticity in recovery from stroke. *Eura Medicophys* (2007) 43:241–54.
- Weder B, Knorr U, Herzog H, Nebeling B, Kleinschmidt A, Huang Y, et al. Tactile exploration of shape after subcortical ischaemic infarction studied with PET. *Brain* (1994) 117(3):593–605. doi:10.1093/brain/117.3.593
- Taskin B, Jungehulsing GJ, Ruben J, Brunecker P, Krause T, Blankenburg F, et al. Preserved responsiveness of secondary somatosensory cortex in patients with thalamic stroke. *Cereb Cortex* (2006) 16(10):1431–9. doi:10.1093/cercor/bhj080
- Tecchio F, Zappasodi F, Tombini M, Oliviero A, Pasqualetti P, Vernieri F, et al. Brain plasticity in recovery from stroke: an MEG assessment. *Neuroimage* (2006) 32(3):1326–34. doi:10.1016/j.neuroimage.2006.05.004
- Tecchio F, Zappasodi F, Tombini M, Caulo M, Vernieri F, Rossini PM. Interhemispheric asymmetry of primary hand representation and recovery after stroke: a MEG study. *Neuroimage* (2007) 36(4):1057–64. doi:10.1016/j.neuroimage.2007.02.058
- Price CJ, Friston KJ. Scanning patients with tasks they can perform. *Hum Brain Mapp* (1999) 8:102–8. doi:10.1002/(SICI)1097-0193(1999)8:2/3<102::AID-HBM6>3.0.CO;2-J
- Biswal BB, Mennes M, Zuo XN, Gohel S, Kelly C, Smith SM, et al. Toward discovery science of human brain function. *Proc Natl Acad Sci U S A* (2010) 107(10):4734–9. doi:10.1073/pnas.0911855107
- Friston KJ. Functional and effective connectivity: a review. *Brain Connect* (2011) 1(1):13–36. doi:10.1089/brain.2011.0008
- Sporns O, Chialvo DR, Kaiser M, Hilgetag CC. Organization, development and function of complex brain networks. *Trends Cogn Sci* (2004) 8(9):418–25. doi:10.1016/j.tics.2004.07.008
- Lewis CM, Baldassarre A, Committeri G, Romani GL, Corbetta M. Learning sculpts the spontaneous activity of the resting human brain. *Proc Natl Acad Sci U S A* (2009) 106(41):17558–63. doi:10.1073/pnas.0902455106
- Cohen AL, Fair DA, Dosenbach NU, Miezin FM, Dierker D, Van Essen DC, et al. Defining functional areas in individual human brains using resting functional connectivity MRI. *Neuroimage* (2008) 41(1):45–57. doi:10.1016/j.neuroimage.2008.01.066
- Shirer WR, Ryali S, Rykhlevskaia E, Menon V, Greicius MD. Decoding subject-driven cognitive states with whole-brain connectivity patterns. *Cereb Cortex* (2012) 22(1):158–65. doi:10.1093/cercor/bhr099
- He BJ, Snyder AZ, Vincent JL, Epstein A, Shulman GL, Corbetta M. Breakdown of functional connectivity in frontoparietal networks underlies behavioral deficits in spatial neglect. *Neuron* (2007) 53(6):905–18. doi:10.1016/j.neuron.2007.02.013
- Nomura EM, Gratton C, Visser RM, Kayser A, Perez F, D'Esposito M. Double dissociation of two cognitive control networks in patients with focal brain lesions. *Proc Natl Acad Sci U S A* (2010) 107(26):12017–22. doi:10.1073/pnas.1002431107
- Rehme AK, Grefkes C. Cerebral network disorders after stroke: evidence from imaging-based connectivity analyses of active and resting brain states in humans. *J Physiol* (2013) 591(1):17–31. doi:10.1113/jphysiol.2012.243469

Acknowledgments

The authors thank the stroke survivors and healthy control participants who participated in the study. They would also like to thank Dr. Rüdiger Seitz who provided expertise in delineation of infarcts in **Figure 1** and Dr. David Abbott who provided assistance with preliminary analyses. The authors received financial support for the research and authorship of this article from the National Health and Medical Research Council (NHMRC) of Australia (project grant numbers 307902 and 1022694; and Career Development Award number 307905 to LC); an Australian Research Council Future Fellowship (number FT0992299 to LC); a McDonnell Foundation collaborative award (to LC); a La Trobe University Post-Graduate Research Award (to LB); a La Trobe University Post-Graduate Writing-up Award (to LB); the Austin Hospital Medical Research Foundation; the National Stroke Research Institute of Australia and by the Victorian Government's Operational Infrastructure Support Program.

28. van Meer MPA, van der Marel K, Wang K, Otte WM, El Bouazati S, Roeling TA, et al. Recovery of sensorimotor function after experimental stroke correlates with restoration of resting-state interhemispheric functional connectivity. *J Neurosci* (2010) **30**(11):3964–72. doi:10.1523/JNEUROSCI.5709-09.2010
29. Wang L, Yu CS, Chen H, Qin W, He Y, Fan FM, et al. Dynamic functional reorganization of the motor execution network after stroke. *Brain* (2010) **133**(4):1224–38. doi:10.1093/brain/awq043
30. Park C-H, Chang WH, Ohn SH, Kim ST, Bang OY, Pascual-Leone A, et al. Longitudinal changes of resting-state functional connectivity during motor recovery after stroke. *Stroke* (2011) **42**:1357–62. doi:10.1161/STROKEAHA.110.596155
31. Iwamura Y, Taoka M, Iriki A. Bilateral activity and callosal connections in the somatosensory cortex. *Neuroscientist* (2001) **7**(5):419–29. doi:10.1177/107385840100700511
32. Schulte T, Müller-Oehring EM. Contribution of callosal connections to the interhemispheric integration of visuomotor and cognitive processes. *Neuropsychol Rev* (2010) **20**(2):174–90. doi:10.1007/s11065-010-9130-1
33. Ward NS, Cohen LG. Mechanisms underlying recovery of motor function after stroke. *Arch Neurol* (2004) **61**(12):1844–8. doi:10.1001/archneur.61.12.1844
34. Seitz RJ, Bütefisch CM. Recovery from ischemic stroke: a translational research perspective for neurology. *Future Neurol* (2006) **1**:571–86. doi:10.2217/14796708.1.5.571
35. Carey LM, Seitz R. Functional neuroimaging in stroke recovery and neurorehabilitation: conceptual issues and perspectives. *Int J Stroke* (2007) **2**(4):245–64. doi:10.1111/j.1747-4949.2007.00164.x
36. Carey LM. Touch and body sensations. In: Carey LM, editor. *Stroke Rehabilitation: Insights from Neuroscience and Imaging*. New York, NY: Oxford University Press (2012). p. 157–72.
37. Grefkes C, Ward NS. Cortical reorganisation after stroke: how much and how functional? *Neuroscientist* (2014) **20**:56–70. doi:10.1177/1073858413491147
38. Corbetta M, Shulman GL. Control of goal-directed and stimulus-driven attention in the brain. *Nat Rev Neurosci* (2002) **3**:201–15. doi:10.1038/nrn755
39. Corbetta M, Patel G, Shulman GL. The reorienting system of the human brain: from environment to theory of mind. *Neuron* (2008) **58**(3):306–24. doi:10.1016/j.neuron.2008.04.017
40. Sathian K. Cross-modal plasticity in sensory systems. In: Selzer M, Clarke S, Cohen LG, Duncan PW, Gage FH, editors. *Textbook of Neural Repair and Rehabilitation: Neural Repair and Plasticity*. Cambridge, IN: Cambridge University Press (2006). p. 180–93.
41. Seitz RJ, Knorr U, Azari NP, Herzog H, Freud H-J. Visual network activation in recovery from sensorimotor stroke. *Restor Neurol Neurosci* (1999) **14**:25–33.
42. Crewther SG, Goharpy N, Bannister L, Lamp G. Goal-driven attention in recovery post-stroke. In: Carey LM, editor. *Stroke Rehabilitation: Insights from Neuroscience and Neuroimaging*. New York, NY: Oxford University Press (2012). p. 191–207.
43. Minati L, Grisoli M, Bruzzone MG. MR spectroscopy, functional MRI, and diffusion-tensor imaging in the aging brain: a conceptual review. *J Geriatr Psychiatry Neurol* (2007) **20**:3–21. doi:10.1177/0891988706297089
44. Roski C, Caspers S, Langner R, Laird AR, Fox PT, Zilles K, et al. Adult age-dependent differences in resting-state connectivity within and between visual-attention and sensorimotor networks. *Front Aging Neurosci* (2013) **5**:67. doi:10.3389/fnagi.2013.00067
45. Robertson IH, North N. Active and passive activation of left limbs: influence on visual and sensory neglect. *Neuropsychologia* (1993) **31**:293–300. doi:10.1016/0028-3932(93)90093-F
46. Johansen-Berg H, Dawes H, Guy C, Smith S, Wade DT, Matthews PM. Correlation between motor improvements and altered fMRI activity after rehabilitative therapy. *Brain* (2002) **125**:2731–42. doi:10.1093/brain/awf282
47. Loubinoux I, Carel C, Pariente J, Dechaumont S, Albucher J-F, Marque P, et al. Correlation between cerebral reorganization and motor recovery after subcortical infarcts. *Neuroimage* (2003) **20**:2166–80. doi:10.1016/j.neuroimage.2003.08.017
48. Tombari D, Loubinoux I, Pariente J, Gerdelat A, Albucher J-F, Tardy J, et al. A longitudinal fMRI study: in recovering and then in clinically stable subcortical stroke patients. *Neuroimage* (2004) **23**:827–39. doi:10.1016/j.neuroimage.2004.07.058
49. Oldfield RC. The assessment and analysis of handedness: the Edinburgh inventory. *Neuropsychologia* (1971) **9**:97–113. doi:10.1016/0028-3932(71)90067-4
50. Brott T, Adams HP, Olinger CP, Marler JR, Barsan WG, Biller J, et al. Measurements of acute cerebral infarction: a clinical examination scale. *Stroke* (1989) **20**(7):864–70. doi:10.1161/01.STR.20.7.871
51. Mahoney FI, Barthel DW. Functional evaluation – the Barthel index. *Med State Med J* (1965) **14**:61–5.
52. Van der Lee JH, De Groot V, Beckerman H, Wagenaar RC, Lankdorst GJ, Bouter LM. The intra- and interrater reliability of the action research arm test: a practical test of upper extremity function in patients with stroke. *Arch Phys Med Rehabil* (2001) **82**(1):14–9. doi:10.1053/apmr.2001.18668
53. Carey LM, Oke LE, Matyas TA. Impaired limb position sense after stroke: a quantitative test for clinical use. *Arch Phys Med Rehabil* (1996) **77**(12):1271–8. doi:10.1016/S0003-9993(96)90192-6
54. Carey LM. Loss of somatic sensation. In: Selzer M, Clarke S, Cohen L, Duncan P, Gage FH, editors. *Textbook of Neural Repair and Rehabilitation Vol II Medical Neurorehabilitation*. Cambridge, IN: Cambridge University Press (2006). p. 231–47.
55. Carey LM, Oke LE, Matyas TA. Impaired touch discrimination after stroke: a quantitative test. *Neurorehabil Neural Repair* (1997) **11**(4):219–32. doi:10.1177/154596839701100404
56. Weinstein S. *Hand instrument. The "Shirt-Pocket Portable" Nerve Tester*. Care and Use Manual. San Jose, CA: North Coast Medical Inc (1996).
57. Abbott D, Jackson G. iBrain® – Software for analysis and visualisation of functional MR images. *Neuroimage* (2001) **13**(6):S59. doi:10.1016/S1053-8119(01)91402-8
58. Cordes D, Haughton VM, Arfanakis K, Carew JD, Turski PA, Moritz CH, et al. Frequencies contributing to functional connectivity in the cerebral cortex in "resting-state" data. *AJNR Am J Neuroradiol* (2001) **22**:1326–33.
59. Carey LM, Abbott A, Harvey M, Puce A, Seitz R. Dynamic texture perception for dominant and non-dominant hands within individuals: an fMRI study in adult healthy volunteers. *Neuroimage* (2008) **41**(Suppl 1):S146. doi:10.1016/j.neuroimage.2008.04.008
60. Eickhoff SB, Stephan KE, Mohlberg H, Grefkes C, Fink GR, Amunts K, et al. A new SPM toolbox for combining probabilistic cytoarchitectonic maps and functional imaging data. *Neuroimage* (2005) **25**(4):1325–35. doi:10.1016/j.neuroimage.2004.12.034
61. Johansen-Berg H, Behrens TEJ, Sillery E, Ciccarelli O, Thompson AJ, Smith SM, et al. Functional-anatomical validation and individual variation of diffusion tractography-based segmentation of the human thalamus. *Cereb Cortex* (2005) **15**(1):31–9. doi:10.1093/cercor/bhh105
62. Biswal B, Yetkin FZ, Haughton VM, Hyde JS. Functional connectivity in the motor cortex of resting human brain using echo-planar MRI. *Magn Reson Med* (1995) **34**(4):537–41. doi:10.1002/mrm.1910340409
63. Fox MD, Snyder AZ, Vincent JL, Corbetta M, Van Essen DC, Raichle ME. The human brain is intrinsically organized into dynamic, anticorrelated functional networks. *Proc Natl Acad Sci U S A* (2005) **102**(27):9673–8. doi:10.1073/pnas.0504136102
64. Rorden C, Brett M. Stereotaxic display of brain lesions. *Behav Neurol* (2000) **12**:191–200. doi:10.1155/2000/421719
65. Seitz RJ, Hoflich P, Binkofski F, Tellmann L, Herzog H, Freund H-J. Role of the premotor cortex in recovery from middle cerebral artery infarction. *Arch Neurol* (1998) **55**(8):1081–8. doi:10.1001/archneur.55.8.1081
66. Dijkerman HC, de Haan EH. Somatosensory processes subserving perception and action. *Behav Brain Sci* (2007) **30**(2):189–201. doi:10.1017/S0140525X07001392
67. Carey LM, Abbott DE, Egan GE, O'Keefe GJ, Jackson GD, Bernhardt J, et al. Evolution of brain activation with good and poor motor recovery after stroke. *Neurorehabil Neural Repair* (2006) **20**:24–41. doi:10.1177/1545968305283053
68. Ward NS, Brown MM, Thompson AJ, Frackowiak RSJ. Neural correlates of motor recovery after stroke: a longitudinal fMRI study. *Brain* (2003) **126**:2476–96. doi:10.1093/brain/awg145
69. Petersen SE, Posner MI. The attention system of the human brain: 20 years after. *Annu Rev Neurosci* (2012) **35**:73–89. doi:10.1146/annurev-neuro-062111-150525
70. Boly M, Balteau E, Schnakers C, Degueldre C, Moonen G, Luxen A, et al. Baseline brain activity fluctuations predict somatosensory perception in humans. *Proc Natl Acad Sci U S A* (2007) **104**(29):12187–92. doi:10.1073/pnas.0611404104
71. Langner R, Eickhoff SB. Sustaining attention to simple tasks: a meta-analytic review of the neural mechanisms of vigilant attention. *Psychol Bull* (2013) **139**(4):870–900. doi:10.1037/a0030694

72. Buckner RL, Krienen FM, Castellanos A, Diaz JC, Yeo BT. The organization of the human cerebellum estimated by intrinsic functional connectivity. *J Neurophysiol* (2011) **106**:2322–45. doi:10.1152/jn.00339.2011
73. Staines WR, Graham SJ, Black SE, McIlroy WE. Task-relevant modulation of contralateral and ipsilateral primary somatosensory cortex and the role of prefrontal-cortical sensory gating systems. *Neuroimage* (2002) **15**(1):190–9. doi:10.1006/nimg.2001.0953
74. Kaas JH. Is most of neural plasticity in the thalamus cortical? *Proc Natl Acad Sci U S A* (1999) **96**(14):7622–3. doi:10.1073/pnas.96.14.7622
75. Jain N, Qi HX, Collins CE, Kaas JH. Large-scale reorganization in the somatosensory cortex and thalamus after sensory loss in macaque monkeys. *J Neurosci* (2008) **28**(43):11042–60. doi:10.1523/JNEUROSCI.2334-08.2008
76. Waites AB, Stanislavsky A, Abbott DF, Jackson GD. Effect of prior cognitive state on resting state networks measured with functional connectivity. *Hum Brain Mapp* (2005) **24**:59–68. doi:10.1002/hbm.20069
77. New AB, Robin DA, Parkinson AL, Duffy JR, McNeil MR, Piguet O, et al. Altered resting-state network connectivity in stroke patients with and without apraxia of speech. *Neuroimage Clin* (2015) **8**:429–39. doi:10.1016/j.nicl.2015.03.013
78. Liu TT. Neurovascular factors in resting-state functional MRI. *Neuroimage* (2013) **80**:339–48. doi:10.1016/j.neuroimage.2013.04.071
79. Veldsman M, Cumming T, Brodtmann A. Beyond BOLD: optimizing functional imaging in stroke populations. *Hum Brain Mapp* (2015) **36**(4):1620–36. doi:10.1002/hbm.22711
80. de Haan B, Rorden C, Karnath H-O. Abnormal perilesional BOLD signal is not correlated with stroke patients' behaviour. *Front Hum Neurosci* (2013) **7**:669. doi:10.3389/fnhum.2013.00669
81. Chang C, Thomason ME, Glover GH. Mapping and correction of vascular hemodynamic latency in the BOLD signal. *Neuroimage* (2008) **43**:90–102. doi:10.1016/j.neuroimage.2008.06.030
82. Carey LM. Sensory loss in stroke patients: effective training of tactile and proprioceptive discrimination. *Arch Phys Med Rehabil* (1993) **74**:602–11. doi:10.1016/0003-9993(93)90158-7
83. Buch ER, Modir Shanechi A, Fourkas AD, Weber C, Birbaumer N, Cohen LG. Parietofrontal integrity determines neural modulation associated with grasping imagery after stroke. *Brain* (2012) **135**:596–614. doi:10.1093/brain/awr331
84. Eickhoff SB, Jbabdi S, Caspers S, Laird AR, Fox PT, Zilles K, et al. Anatomical and functional connectivity of cytoarchitectonic areas within the human parietal operculum. *J Neurosci* (2010) **30**:6409–21. doi:10.1523/JNEUROSCI.5664-09.2010
85. Tame L, Braun C, Lingnau A, Schwarzbach J, Demarchi G, Hegner YL, et al. The contribution of primary and secondary somatosensory cortices to the representation of body parts and body sides: an fMRI adaptation study. *J Cogn Neurosci* (2012) **24**:2306–20. doi:10.1162/jocn_a_00272
86. Burton H, Sinclair RJ, Wingert JR, Dierker DL. Multiple parietal operculum subdivisions in humans: tactile activation maps. *Somatosens Mot Res* (2008) **25**:149–62. doi:10.1080/08990220802249275
87. Pleger B, Foerster AF, Ragert P, Dinse HR, Schwenkreis P, Malin J-P, et al. Functional imaging of perceptual learning in human primary and secondary somatosensory cortex. *Neuron* (2003) **40**:643–53. doi:10.1016/S0896-6273(03)00677-9
88. Romo R, Hernandez A, Zainos A, Lemus L, Brody CD. Neuronal correlates of decision-making in secondary somatosensory cortex. *Nat Neurosci* (2002) **5**:1217–25. doi:10.1038/nn950
89. Tomasi D, Volkow ND. Association between functional connectivity hubs and brain networks. *Cereb Cortex* (2011) **21**(9):2003–13. doi:10.1093/cercor/bhq268

Conflict of Interest Statement: The authors declare that the research was conducted in the absence of any commercial or financial relationships that could be construed as a potential conflict of interest.

Copyright © 2015 Bannister, Crewther, Gavrilescu and Carey. This is an open-access article distributed under the terms of the Creative Commons Attribution License (CC BY). The use, distribution or reproduction in other forums is permitted, provided the original author(s) or licensor are credited and that the original publication in this journal is cited, in accordance with accepted academic practice. No use, distribution or reproduction is permitted which does not comply with these terms.



Determinants of concurrent motor and language recovery during intensive therapy in chronic stroke patients: four single-case studies

Annika Primaßin^{1,2†}, Nina Scholtes^{1†}, Stefan Heim^{3,4,5,6}, Walter Huber¹,
Martina Neuschäfer⁷, Ferdinand Binkofski^{1,8*‡} and Cornelius J. Werner^{5‡}

¹ Section Clinical-Cognitive Sciences, Department of Neurology, Uniklinik RWTH Aachen, Aachen, Germany, ² Department of Clinical Neurophysiology, University Medical Center, Göttingen, Germany, ³ Department of Psychiatry, Psychotherapy and Psychosomatics, Medical Faculty, RWTH Aachen, Aachen, Germany, ⁴ JARA – Translational Brain Medicine, Aachen, Germany, ⁵ Department of Neurology, Medical Faculty, Uniklinik RWTH Aachen, Aachen, Germany, ⁶ Institute of Neuroscience and Medicine (INM-1), Research Centre Jülich, Jülich, Germany, ⁷ School for Physiotherapy, Uniklinik RWTH Aachen, Aachen, Germany, ⁸ Institute of Neuroscience and Medicine (INM-4), Research Centre Jülich, Jülich, Germany

OPEN ACCESS

Edited by:

Bruno J. Weder,
University of Bern, Switzerland

Reviewed by:

Jean-Marie Annoni,
University of Fribourg, Switzerland
Stephan Bohlhalter,
Neurology and Neurorehabilitation
Center, Switzerland

*Correspondence:

Ferdinand Binkofski,
Institute of Neuroscience and
Medicine (INM-4), Research Centre
Jülich, Wilhelm-Johnen-Straße,
Jülich 52425, Germany
f.binkofski@fz-juelich.de

[†]Annika Primaßin and Nina Scholtes
share first authorship.

[‡]Ferdinand Binkofski and Cornelius J.
Werner share last authorship.

Specialty section:

This article was submitted to Stroke,
a section of the
journal Frontiers in Neurology

Received: 13 May 2015

Accepted: 22 September 2015

Published: 09 October 2015

Citation:

Primaßin A, Scholtes N, Heim S,
Huber W, Neuschäfer M, Binkofski F
and Werner CJ (2015) Determinants
of concurrent motor and language
recovery during intensive therapy in
chronic stroke patients: four
single-case studies.
Front. Neurol. 6:215.
doi: 10.3389/fneur.2015.00215

Despite intensive research on mechanisms of recovery of function after stroke, surprisingly little is known about determinants of concurrent recovery of language and motor functions in single patients. The alternative hypotheses are that the two functions might either “fight for resources” or use the same mechanisms in the recovery process. Here, we present follow-up data of four exemplary patients with different base levels of motor and language abilities. We assessed functional scales and performed exact lesion analysis to examine the connection between lesion parameters and recovery potential in each domain. Results confirm that preservation of the corticospinal tracts (CSTs) is a neural predictor for good motor recovery while preservation of the arcuate fasciculus (AF) is important for a good language recovery. However, results further indicate that even patients with large lesions in CST, AF, and superior longitudinal fasciculus, respectively, are able to recover their motor/language abilities during intensive therapy. We further found some indicators of a facilitating interaction between motor and language recovery. Patients with positive improvement of motor skills after therapy also improved in language skills, while the patients with no motor improvements were not able to gain any language recovery.

Keywords: stroke, motor, language, hemiplegia, hemiparesis, aphasia, recovery

Introduction

It is a common clinical observation that in patients with both initial hemiparesis and aphasia after stroke, motor and language recovery may take different courses. Interestingly, scientific research has primarily focused on the examination of the course of recovery regarding either motor or language abilities, but only few studies addressed both. Aphasia has even been a criterion for exclusion in several studies of motor recovery (1, 2).

To our knowledge, there is only one multiple single-case study that addressed the issue of language recovery going parallel to a therapy of motor functions of the upper limb. Harnish et al. (3) examined

five stroke patients during the course of 6 weeks of motor therapy. They assessed not only the recovery of motor functions of the upper limbs and functional motor reorganization but also changes in their language abilities. The authors report that in the three subjects showing the largest motor improvements they could also observe significant language improvements. In the individual fMRI measurements, where the patients had to tap the fingers of the paretic hand within the scope of their capacities, a shift of activation to the right hemisphere during the course of motor treatment could be observed in these three patients. Harnish et al. concluded that language changes seem to co-occur with motor changes after motor therapy. Anatomical analyses of the patients' lesions were not carried out.

The finding of Harnish et al. that motor recovery can foster language recovery is very interesting for the current state of discussion about common mechanisms in motor and language processing. Especially the theory of cognitive embodiment has gained broad attention and kindled a whole line of research. In the light of embodiment theory, cognitive functions like language are grounded in the sensorimotor experiences and to the underlying systems (4, 5). For example, Hauk et al. (6) were able to show that language processing and comprehension activate motor regions, while Glenberg et al. (7) found that first- and second-grade children who manipulate images of toys on a computer screen develop improved comprehension skills in reading – a comprehension benefit was evoked by the conduction of motor tasks. There are numerous imaging studies demonstrating activation of the sensorimotor systems by listening to language with motor content [for example, see Ref. (8, 9)]. Recently anatomic correlates for common motor speech and motor (10) as well as language and motor processing (11) have been postulated on the basis of imaging data.

With the theoretical and experimental background that motor and language activity are not functionally independent, interdependencies regarding the course of recovery of these two domains can be assumed as well. These relations might result in two possible interactions between motor and language recovery processes: either competitive or additive effects may occur. Competitive rehabilitative interactions might be characterized by a “fight” for resources between the language and motor recovery capacities. In this case, a good motor recovery may limit or even prevent the course of language recovery and vice versa. The inverse assumption of an additive interaction between both domains during recovery implies that a positive course of motor recovery would influence language recovery positively, and vice versa. The results of Harnish et al. (3), which are in line with the findings concerning embodiment, seem to support the second hypothesis.

The identification of determinants of motor and language recovery after stroke is within the main stream of research on neurorehabilitation. There are several studies evaluating the role of lesion parameters as well as brain activation for complete or poor recovery for language and motor domain separately. We will briefly highlight the most relevant results in order to establish the backdrop for our study.

As to the motor domain, the lesion location is an important predictor for motor rehabilitation (12), whereas the size of the brain lesion seems to be no predictor for motor function recovery

after stroke (12–14). Shelton and Reding (15) found that the probability of recovery of the upper limbs after stroke seems to diminish in dependence of the lesion location in the following order: cortex, corona radiata, and internal capsule. The dimension of impairment of the corticospinal tract (CST) is another indicator for good rehabilitation of hand motor function after stroke; severe damage of the CST has mainly been assessed in more severely affected patients (12–15).

Similarly, in the language domain, lesion location may play an important role in sufficient language recovery. Meinzer et al. (16) found that language rehabilitation after intensive language therapy was correlated with the integrity of the left hippocampus and the surrounding white matter. Marchina et al. (17) were able to show that the extent of impairment of the left arcuate fasciculus (AF) is a predictor for language recovery. The global lesion size does not have an influence on language rehabilitation after stroke [e.g., see Ref. (16, 18)].

Functional imaging has resulted in inconsistent results for both recovery of motor [e.g., see Ref. (19–23)] and language abilities [e.g., see Ref. (24–29)]. The heterogeneity of the results in the language and motor domain can possibly be attributed to different methods and objectives that were used in previous studies as well as different types of strokes (e.g., subcortical vs. cortical). Therefore, it is hardly possible to combine the mentioned results of the two different domains for predicting recovery patterns in patients with concurrent impairments in both domains.

Therefore, neural correlates for simultaneous recovery in the language and motor domain after stroke remain unclear. The results of Harnish et al. (3), which were investigated through fMRI and behavioral measurements, give a first hint for an additive interaction between both domains during the course of rehabilitation. To our knowledge, there are no studies with the aim to explore lesion characteristics of different ways of concurrent motor and language recovery. Therefore, it remains unclear if an additive interaction between motor and language recovery processes through therapy can be linked to specific structural lesions in the brain.

The aim of the present study was to investigate systematically the determinants of language and motor recovery in four exemplary patients with different base levels of motor and language abilities. Alongside the clinical assessment of motor and language abilities, we focused on (1) the examination of lesion characteristics at pre-test and (2) possible interactions of motor and language recovery processes following the 7-week language and motor therapy phase (i.e., outcome at the post-test).

Apraxia of speech is a clinically known influence factor to the possibilities of improving language skills in aphasic patients. Furthermore, since anatomic correlates for common motor speech and motor processing have been described (10), motor speech could be considered a “link” between motor and language processing functions. Therefore, in addition to motor and language processing functions, we considered the phenomenon of apraxia of speech independently for the patients in our patient group. Since we aimed to discuss motor speech functions on a purely exploratory level, no precise hypotheses were formulated.

Over all, four hypotheses were formulated concerning both lesion characteristics and possible therapy-induced interactions:

Regarding (1), lesion characteristics, the following hypotheses were addressed:

- (i) In line with current research (12–14, 16, 18), we assume that global lesion size is not a correlate for sufficient concurrent motor and language recovery.
- (ii) We expect that patients with smaller lesions in function-specific white matter tracts for motor (CST) and language processing [AF, superior longitudinal fasciculus (SLF)] show good recovery potential in the particular domains as opposed to patients with extensive lesions to these tracts.

Regarding (2), possible interactions of motor and language recovery processes, our hypotheses are as follows:

- (iii) In line with Harnish et al. (3), we assume that patients with an increase in motor abilities after therapy phase will also show positive language recovery (i.e., an increase in language abilities at the post-test) and vice versa. This would indicate an additive interaction between motor and language domains during simultaneous motor and language therapy.
- (iv) Complementarily, we anticipate that patients who do not profit from motor therapy do not show an increase in language abilities at the post-test after therapy phase and vice versa.

Materials and Methods

Patients

Four patients suffering from subacute to chronic stroke with different base levels of motor and language skills at the beginning of the study (see **Figure 1**) were selected. The selection of patients with opposing base levels in motor and language skills was conducted in order to include previous individual recovery processes into the evaluation of the current recovery process. Clinical records documented that at the acute stage of the stroke, all patients were described as non-fluent to globally aphasic and had paresis of varying degrees, ranging from mild hemiparesis (4/5) to full hemiplegia. The different base levels resulted from the patients' individual recovery processes prior to the participation in the study.

At the beginning of the study, language skills were classified as “good” (Base: L+) or “poor” (Base: L−) according to the patients' individual profile height in the language assessment of the Aachener Aphasia Test [AAT; (30) (see **Table 1**)]. Correspondingly, the classification of “good” vs. “poor” motor skills (M+ vs. M−) was based on the raw score of the Wolf Motor Function Test [WMFT (31), see **Table 2**]. This resulted in four possible baseline profiles: Base: M+/L+, M−/L+, M+/L−, and M−/L−, denoting good functions in both motor and language domains, the dissociations between the domains, and finally the combination of both severely impaired motor and language function at the pre-test of the study.

Apart from different performance patterns in the language and motor domain, the patients had to meet the following criteria for inclusion into the study: (1) general MRI compatibility, (2) native German speakers, (3) right-handed according

to the Edinburgh Inventory of Handedness [Laterality coefficient ≥ 80 ; (32)], (4) normal or corrected-to-normal vision, (5) no hearing loss, (6) no pregnancy, (7) single stroke in the left hemisphere, (8) subacute or chronic stage of stroke (at least 6 weeks post onset), (9) clinically diagnosed aphasia or residual symptoms of aphasia and clinically diagnosed hemiparesis, and (10) no history of dementia or other CNS or psychiatric diseases.

The patients were recruited from the Aphasia Rehabilitation Ward of the Neurological Clinic, Uniklinik RWTH Aachen. Informed written consent for participating in the study was obtained from each patient prior to the participation in the study. The study was approved by the local ethics committee and conducted according to the Declaration of Helsinki. Patient characteristics are displayed in **Figure 1**.

Research Design

All patients were recruited during their 7-week stay at the Aphasia Rehabilitation Ward of the Department of Neurology, Uniklinik RWTH Aachen. A pre–post test design was used to assess both motor and language abilities prior and after the 7-week therapy phase. The pre-test took place during the first week of the treatment. Deficits were quantified using standardized assessment tests and applied by trained personnel (speech and language therapists, physiotherapists, and neurologists). Structural MRI scans were conducted in the first week of the patients' stay at the hospital. The post-test took place during the seventh (i.e., last) week of the stay at the Aphasia Rehabilitation Ward. Again, the functional language and motor scales were used to evaluate patients' development during the intensive treatment. MRI measurements were not repeated. Between pre- and post-test, the patients participated in 7 weeks of motor and language therapy (for an overview of the research design, see **Figure 2**).

Clinical Examinations

The following tests were applied:

Functional Language Scales

The “Aachener Aphasia Test” [AAT (30)], a robust and highly validated test of language in multiple domains, was conducted to assess the patients' overall linguistic abilities. Additionally, five subtests of the standard neurolinguistic test battery “Lexikon Modellorientiert” [LEMO (33)] were employed: subtest 5 – “lexical decision making,” subtest 25 – “finding synonyms,” subtest 30 – “oral naming,” and subtest 32 – “finding rhymes.”

Functional Motor Scales

The Wolf Motor Function Test [WMFT (31)] was applied to evaluate the quality and duration of the patients' arm and hand movements. In addition, the Dynamic Gait Index [DGI (34)] was conducted in order to assess gait and balance.

Additional Scale

Three subtests from the “Aachener Materialien zur Diagnostik Neurogener Sprechstörungen” [AMDNS (35)] were used in order to screen for neurogenic speech disorders: “duration of phonation,” “variability of speech intensity,” and “articulatory diadochokinesis.” These subtests were used to control the influence

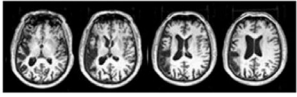
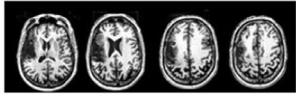
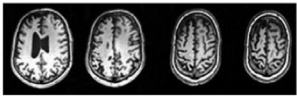
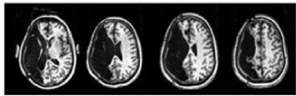
Base Levels	Language +	Language -
Motor +	Patient 1 (M+/L+; 53 y/o, m) <ul style="list-style-type: none"> – ischemic stroke, left MCA territory, 17 months p.o. – Base Level abilities: amnesic aphasia, mild apraxia of speech, mild disorder of fine motor skills – Lesion characteristics: lesion mostly covered frontal, temporal and parietal regions, the insular cortex and putamen 	Patient 3 (M+/L-; 55 y/o, m) <ul style="list-style-type: none"> – cardioembolic stroke, left MCA territory, 10 months p.o. – Base Level abilities: global aphasia, apraxia of speech, mild residual symptoms of hemiparesis – Lesion characteristics: lesion included the frontal and parietal lobe 
Motor -	Patient 2 (M-/L+; 43 y/o, m) <ul style="list-style-type: none"> – ischemic stroke, left MCA and ACA, 7 months p.o. – Base Level abilities: mild residual symptoms of aphasia, hemiparesis – Lesion characteristics: frontoparietotemporal, also including insular cortex, putamen, thalamus and caudate nucleus 	Patient 4 (M-/L-; 47 y/o, f) <ul style="list-style-type: none"> – ischemic stroke, left MCA; 31 months p.o. – Base Level abilities: global aphasia, apraxia of speech, severe hemiparesis – Lesion characteristics: spacious lesion with subsequent hemispherectomy including nearly the whole left hemisphere 

FIGURE 1 | Overview of the four patients' base levels upon inclusion into the study, including T1-weighted images of the patients' lesions, optimized for displaying the position of the lesion. Abbreviations: "+" = good; "-" = poor motor/language skills; p.o., post onset; MCA, middle cerebral artery; ACA, anterior cerebral artery.

TABLE 1 | Results of the patients in the AAT and LEMO.

Pat. (base)	AAT				LEMO					
	Profile height		LD		FS		FR		ON	
	Pre	Post	Pre	Post	Pre	Post	Pre	Post	Pre	Post
1 (M+/L+)	57.9	58.7	78	79	38	39	11	7°	19	20
2 (M-/L+)	72.5	73.3	80	80	40	40	20	20	18	18
3 (M+/L-)	41.9	43*	45	61*	34	36	10	6	–	–
4 (M-/L-)	40.9	41.3	70	74	35	37	–	–	9	9

AAT, Aachener Aphasia Test; LEMO, Lexikon Modellorientiert; Pat., patient; pre, pre-test; post, post-test; LD, Lexical Decision; FS, Finding Synonyms; FR, Finding Rhymes; ON, Oral Naming; *significant improvement [AAT: calculated with AATP; LEMO: McNemar Test, $p < 0.05$; (*)]; °, significant deterioration (McNemar Test, $p < 0.05$).

of the patients' motor speech function on motor and language ability and recovery.

In addition, subtest "Articulation" (spontaneous speech) of the AAT was considered separately, since it is specially related to motor speech functions.

Analysis of Behavioral Data

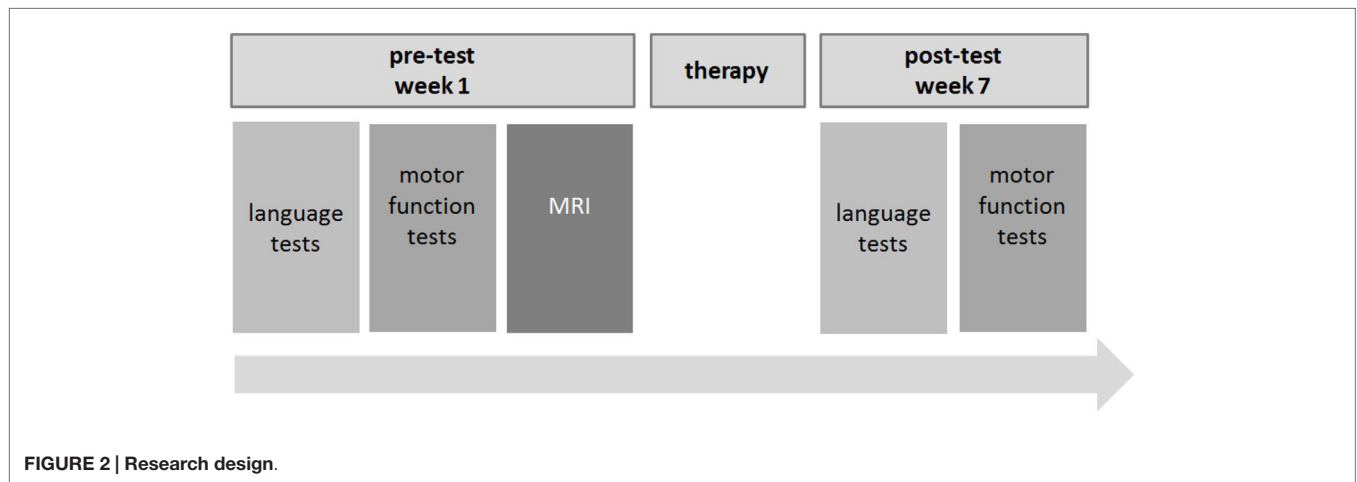
The single-case characteristics of our study put some restraints on the statistical tests that are available. For the AAT, significant improvements and deteriorations were differentiated. To test for significant changes in the patient's performance between pre- and post-test, the computer program "AATP" (36) was employed. This program automatically calculates significant changes using the psychometric single-case diagnosis (37) with $p < 0.1$, an alpha-level that is common for single cases. In reference to LEMO, significant changes between pre- and post-test were calculated

TABLE 2 | Results of the patients in WMFT and DGI.

Pat. (base)	WMFT		DGI	
	Pre	Post	Pre	Post
1 (M+/L+)	70	73	24	24
2 (M-/L+)	34	40*	20	24**
3 (M+/L-)	69	74**	21	23
4 (M-/L-)	5	5	11	13

Pat., patient; pre, pre-test; post, post-test; WMFT, Wolf Motor Function Test; DGI, Dynamic Gait Index; **significant improvement (Wilcoxon signed rank test, $p < 0.05$); *significant improvement (Wilcoxon signed rank test, $p < 0.1$).

for each subtest conducting the McNemar test ($p < 0.1$ or $p < 0.05$). Concerning the WMFT and DGI, significant changes were calculated with the Wilcoxon signed rank test ($p < 0.1$ or $p < 0.05$). In the additional scale AMDNS, only notable changes



were evaluated. They were defined as a positive or negative change of severity comparing the degrees of severity on a 4-point scale (3 = severe impairment, 0 = no impairment).

Imaging Acquisition

Structural MRI measurements (T1, FLAIR) were conducted for lesion analyses using a Philips 3T scanner at the Brain Imaging Facility at University Hospital, RWTH Aachen. All images were made using SENSE (Sensitivity Encoding) technology conducting an eight-channel phase array head coil. A three-dimensional isotropic T1-weighted sequence (MPRAGE) was performed in the sagittal plane. Acquisition parameters were: repetition time/echo time = 9.9/4.6 ms; flip angle = 8; field of view = 256 mm; matrix = 256×256 ; slice thickness = 1 mm; voxel size = $1 \text{ mm} \times 1 \text{ mm} \times 1 \text{ mm}$. Acquisition parameters for the FLAIR measurement were: repetition time/echo time = 11,000/125 ms; field of view = 224 mm; matrix = 312×157 ; slice thickness = 3 mm; voxel size = $0.72 \text{ mm} \times 1.13 \text{ mm} \times 3 \text{ mm}$.

Analysis of Imaging Data

All data were analyzed on an individual subject basis. For the analysis of lesions, all lesions were marked within the FLAIR image using MRICron (38). Afterwards, the lesion maps were normalized via FLIRT (39) and transformed into standard MNI space. Anatomical masks of interest from the atlases supplied with FSL [MNI Structural Atlas (40) and JHU White-Matter Tractography Atlas (41)] were extracted. The right hemisphere in the MNI Structural Atlas was masked out by zeroing all voxels with x -coordinates 0–45; anatomical structures of interest were already lateralized in the JHU White-Matter Tractography Atlas. No thresholding was applied. The size of each structure was determined by counting the number of non-zero voxels in each map. Then, an intersection of the patient-specific lesions (in standard space) with the respective anatomical maps was created by multiplying them with each other using FSL command line tools (fslmaths). This yielded a map representing the damage to the particular map inflicted by the patient's lesion. The size of this map was determined by counting the non-zero voxels inside this map. Afterwards, the calculation of the percentage of the entire anatomical structure affected by the lesion followed by dividing

the voxel count of the intersection by the voxel count of the anatomical map.

Lesions of the patients were analyzed according to their localization in the following cortical and subcortical structures: frontal lobe, parietal lobe, temporal lobe, occipital lobe, insula, putamen, thalamus, and caudate. Concerning white matter tracts, the lesion analysis procedure previously described was conducted for the CSTs, SLF and AF. All fiber tracts were included due to their previously described role in motor and language processing.

Results

Behavioral Data

The patients' overall behavioral outcome (changes of performance after the 7-week therapy phase) in the functional scales showed heterogeneous results both for motor and language assessments (see **Tables 1** and **2**; Tables S1–S3 in Supplementary Material).

Additional Scale

Motor speech abilities (AMDNS) showed heterogeneous results with both notable improvements and deteriorations across all patients' performances. However, none of the measured changes occurred on a significant level. An overview of the results in these tests is given in **Table 3**. As described above, subtest "Articulation" of the AAT was considered separately and showed heterogeneous results with notable improvements in Patient 1 (Base: M+/L+) and Patient 3 (Base: M+/L–), one notable deterioration [Patient 2 (Base: M–/L+)] and one stable result [Patient 4 (Base: M–/L–; see **Table 4**)].

Synoptical Analysis of Behavioral and Lesion-Related Data

As shown in **Tables 5** and **6**, all patients had lesions in the frontal and parietal lobe, as well as white matter tract injury in the SLF and AF (see also **Figures 3** and **4**). Concerning further cortical and subcortical structures, patients did not show a homogeneous pattern of their lesions. In the following tables, we demonstrate an overview of the patients' recovery outcome following the 7-week therapy phase together with the patients' lesion characteristics in

cortical and subcortical (Table 5) as well as white matter tract areas (Table 6).

Discussion

The present study explored if there are determinants for concurrent motor and language recovery during intensive therapy in four exemplary chronic stroke patients with different base levels of language and motor abilities. In particular, we examined if (1) concerning lesion characteristics (i) the global lesion size is a correlate of sufficient concurrent motor and language recovery

and if (ii) the extent of damage of the function-specific white matter tracts for motor and language is predictive for the recovery potential in the respective domains.

In the further analysis of (2) possible interactions of motor and language recovery processes, we investigated if (iii) an additive interaction between motor and language domains during simultaneous motor and language therapy occurs and if (iv) there will be a lack of interaction between both domains when there is no recovery progress in at least one domain.

The four patients had different motor and language base levels and were systematically examined in this study to evaluate the relation of their therapy outcome in both domains (i.e., recovery process that was measured from pre- to post-test) and lesion parameters. To explore predictors for (iii) concurrent motor and language recovery, various functional scales in the motor and language domain and also in the motor speech domain were applied. Concerning the lesion analysis, cortical and subcortical lesion characteristics as well as white matter tract damage were explored.

One major finding of this study is that we could detect some indicators for an additive behavior of motor and language recovery. It seems that motor and language recovery co-occur in a sense that motor recovery facilitates the possibility of a positive therapy-induced language recovery. In addition, lesion size *per se* is not determining a sufficient motor and language recovery. However, the specific lesion areas play an important role for a sufficient recovery. Another main finding was that large damage in important fiber structures for motor or language processing allows no prediction about the recovery of the fiber-induced function at a single subject level.

Lesion Characteristics

Global Lesion Size

Considering the global lesion size in our four patients, Patient 3 (Base: M+/L−) was the only participant who was able to improve significantly in both motor and language functions at the post-test. In addition, this patient had the second largest overall lesion size. In comparison, Patient 2 (Base: M−/L+), the patient showing the

TABLE 3 | Results of the patients in the AMDNS (degree of impairment).

Pat. (base)	AMDNS					
	DIA		DU		INT	
	Pre	Post	Pre	Post	Pre	Post
1 (M+/L+)	18	15	9	5	0	3
2 (M−/L+)	18	18	3	3	3	0
3 (M+/L−)	6	6	6	6	0	2
4 (M−/L−)	9	9	16	17	3	3

Cumulative dysarthria score: degree of impairment: 0 = no impairment; 3 = severe impairment. Pat., patient; pre, pre-test; post, post-test; DIA, diadochokinesis; DU, duration of phonation; INT, variability of speech intensity.

TABLE 4 | Results of the patients in the subtest “Articulation” (AAT; degree of impairment).

Pat. (base)	Articulation (AAT)	
	Pre	Post
1 (M+/L+)	3	4
2 (M−/L+)	5	4
3 (M+/L−)	2	3
4 (M−/L−)	3	3

Degree of impairment: 5 = no impairment; 1 = severe impairment (i.e., cannot be evaluated due to lack of intelligibility).

TABLE 5 | Overview of the patients’ functional recovery (post-test) in both domains, lesion volume, and percentage of damaged tissue in defined cortical and subcortical brain areas.

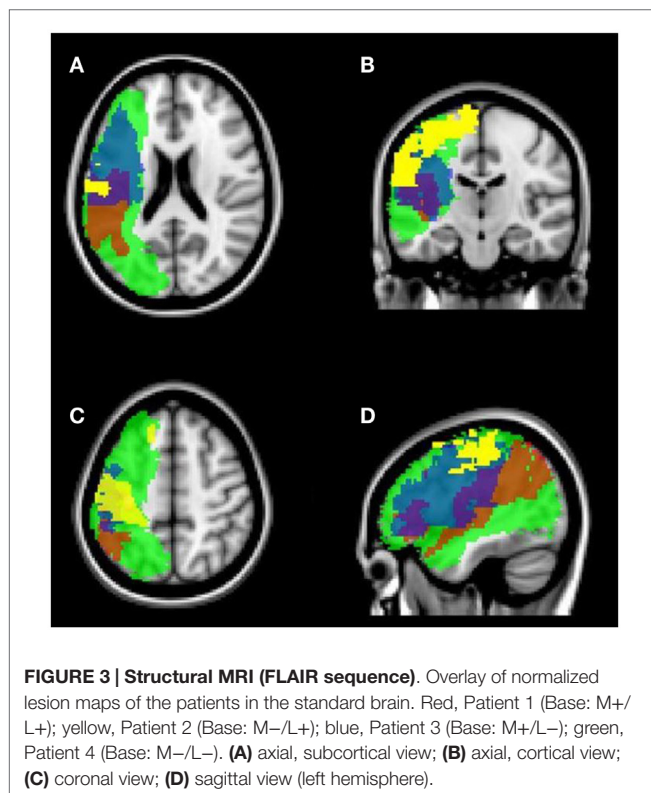
Pat. (base)	Outcome after 7-week therapy phase		Total lesion volume	Lesion volume to specific areas							
				Cortical (Lobar)				Subcortical			
	Motor recovery	Language recovery		Fro	Par	Tem	Occ	Ins	Put	Tha	Cau
1 (M+/L+)	Non-responder WMFT (o), DGI (o)	Non-responder AAT (o), LEMO−	10,325	2,403	6,368	2,409	335	1,903	437	–	–
2 (M−/L+)	Strong responder WMFT+, DGI+	Non-responder AAT (o), LEMO (o)	6,852	5,815	3,193	–	–	–	–	–	–
3 (M+/L−)	Partial responder WMFT+, DGI (o)	Strong Responder AAT+, LEMO+	14,406	8,422	4,171	1,255	–	2,764	732	23	25
4 (M−/L−)	Non-responder WMFT (o), DGI (o)	Non-responder AAT (o), LEMO (o)	50,472	18,747	16,884	9,692	7,556	3,340	1,237	87	12

+, Significant improvement; (o), no change; −, significant deterioration. Non-responder, patient showed no positive response to motor or language therapy; partial responder, partial positive response, i.e., significant improvement in one of the applied tests; strong responder, strong positive response, i.e., significant improvement in both applied tests; –, no lesion measured; Fro, frontal lobe; Par, parietal lobe; Tem, temporal lobe; Occ, occipital lobe; Ins, insula; Put, putamen; Tha, thalamus; Cau, nucleus caudate. Lesion volume was calculated within the FLAIR data (voxels).

TABLE 6 | Overview of the patients' functional recovery (post-test) in both domains, lesion volume, and percentage of damaged tissue in particular white matter tracts.

Pat. (base)	Outcome after 7-week therapy phase		Lesion volume to specific white matter tracts		
	Motor recovery	Language recovery	CST	SLF	AF
1 (M+/L+)	Non-responder WMFT (o), DGI (o)	Non-responder AAT (o), LEMO–	–	5,115	1,196
2 (M–/L+)	Strong responder WMFT+, DGI+	Non-responder AAT (o), LEMO (o)	1,057	1,916	736
3 (M+/L–)	Partial responder WMFT+, DGI (o)	Strong responder AAT+, LEMO+	568	7,188	3,944
4 (M–/L–)	Non-responder WMFT (o), DGI (o)	Non-responder AAT (o), LEMO (o)	1,643	16,462	7,458

+, Significant improvement; (o), no change; –, significant deterioration. Non-responder, patient showed no positive response to motor or language therapy; partial responder, partial positive response, i.e., significant improvement in one of the applied tests; strong responder, strong positive response, i.e., significant improvement in both applied tests; –, no lesion measured; CST, corticospinal tract; SLF, superior longitudinal fasciculus; AF, arcuate fasciculus. Lesion volume was calculated within the FLAIR data (voxels).



smallest global lesion size, was able to improve in motor but not language scales at the post-test, whereas Patient 1 (Base: M+/L+) and Patient 4 (Base: M–/L–, the patient with the largest global lesion size), did not show improvement in any scale. The fact that Patient 3 (Base: M+/L–) was able to improve on such an extensive level shows that the global lesion size cannot be the single determinant regarding recovery potential. This finding is in line with the current state of research [e.g., see Ref. (12–14, 16, 18)].

White Matter Tracts

Concerning white matter tracts, lesion characteristics seem to be less distinct. Although Patient 1 (Base: M+/L+) was the only

patient who did not show a lesion of the CST, he also did not improve in motor therapy, most possibly due to a high motor base level and a ceiling effect. Patient 3 (Base: M+/L–) showed the smallest lesion of all patients (i.e., of all patients with lesions of the CST) and was able to improve in one motor test. Whereas Patient 2 (Base: M–/L+) with the second largest lesion of the CST was a strong responder to motor therapy with improvements in both motor function tests. Patient 4 (Base: M–/L–) had the most extensive CST lesion and was a non-responder to motor therapy.

Especially the distinction between Patients 2 (Base: M–/L+) and 3 (Base: M+/L–) is of further interest: although fiber damage of the CST in Patient 2 (Base: M–/L+) was about two times larger than that in Patient 3 (Base: M+/L–), probably leading to his worse baseline profile, Patient 2 (Base: M–/L+) actually showed better abilities to recover in the motor domain than Patient 3 (Base: M+/L–; strong responder vs. partial responder, see Tables 5 and 6). This difference could be attributed to the fact that the measurable extent of the lesion in Patient 2 is primarily caused by the location of the lesion at the level of the primary motor cortex, whereas Patient 3's smaller lesion mainly affects the part of the pyramidal tract further down in the corona radiata (see Figure 4). It is possible that this specificity of the anatomical lesion site in Patient 3 leads to a higher amount of damage to fibers that are relevant to motor recovery.

In summary, among our patient group, Patient 1 (Base: M+/L+) showed no lesion of the CST and no therapy-induced improvement due to ceiling effects and an already high level of motor functions at the pre-test. Patient 2 (Base: M+/L–) showed an extensive overall lesion, however, damage was more related to cortical structures than to lesions in the CST. This patient showed good recovery potential with improvements in both motor function tests. In comparison, Patient 3 (Base: M+/L–) showed a smaller lesion, however, he only recovered to a smaller degree than Patient 2 (Base: M–/L+). His lesion location in the corona radiata probably led to a reduction in recovery potential. Last, Patient 4 (Base: M–/L–) with the most extensive lesion of the CST was not able to improve in motor therapy at all. This result is supportive to the finding that strategic lesion location, rather than

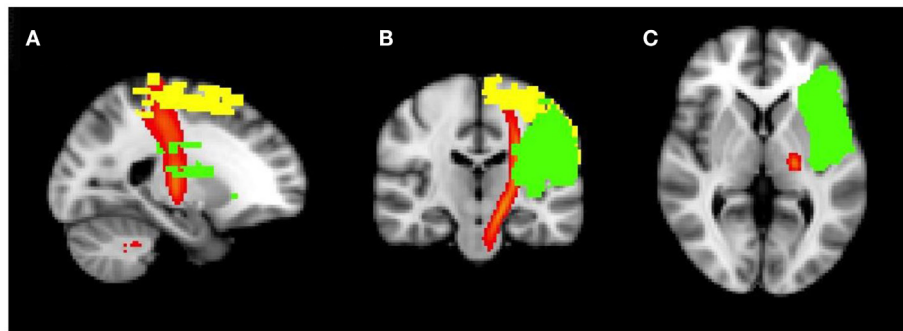


FIGURE 4 | Structural MRI (FLAIR sequence). Overlay of normalized lesion maps of patients 2 and 3 in the standard brain. Yellow, Patient 2 (Base: M-/L+); green, Patient 3 (Base: M+/L-); red, corticospinal tract. **(A)** sagittal view; **(B)** coronal view; **(C)** axial, subcortical view.

lesion volume, is an important determinant to recovery potential [e.g., see Ref. (15)].

Concerning the lesion of the AF, similar results could be found. Patient 2 (Base: M-/L+) who showed the smallest lesion of the AF did not show therapy-induced language improvement at the post-test, as well as Patient 1 (Base: M+/L+) who presented with the second smallest lesion. Patient 4 (Base: M-/L-) who showed the most spacious lesion of the AF was also not able to profit significantly from intensive therapy. Only Patient 3 (Base: M+/L-) was able to improve strongly in both language scales, although he showed the second largest lesion of the AF.

These findings seemingly point toward the assumption that the specific lesion size of the CST and/or AF does not directly influence the outcome of motor and/or language recovery. However, we feel that this assumption would be too shortsighted since at this point, the individual base levels, i.e., the level of motor and language skills that the patients presented with at the pre-test, need to be considered: regarding the lesion of the CST, we pointed out that Patient 1 (Base: M+/L+) did not show motor recovery although he did not have any lesion of the CST. However, Patient 1 already showed a comparatively high level of motor skills at the pre-test (see **Table 2**), leaving him with only small possibilities for significant improvements at the post-test. The same holds for Patient 2 (Base: M-/L+) regarding the extent of the AF lesion. As described, Patient 2 showed the smallest AF lesion of all patients but did not show language recovery. This could be attributed to possible ceiling effects. However, even after eliminating those two patients with possible ceiling effects from our considerations, in our patient group still neither the patient with the (then) smallest CST lesion [Patient 3 (Base: M+/L-)] nor the patient with the (then) smallest AF lesion [Patient 1 (M+/L+)] are the patients showing most motor and language recovery, respectively. This observation points strongly toward the conclusion, that even patients with large lesion of the CST/AF are able to recover motor/language abilities during intensive therapy.

Interactions of Motor and Language Recovery Processes

Based on the results that were published by Harnish et al. (3), we assumed that the patients with an increase in motor abilities

after the 7-week therapy phase would show positive language recovery (i.e., an increase in language abilities at the post-test), indicating that an additive interaction between motor and language domains during simultaneous motor and language therapy occurs. We also anticipated that patients who do not profit from motor therapy do not show an increase in language abilities at the post-test after therapy phase and vice versa. Regarding the data of our four patients, two of our patients, namely Patient 2 (Base: M-/L+) and Patient 3 (Base: M+/L-), were able to profit from motor therapy, leading to a significant improvement of motor functions at the post-test. Of these two patients, Patient 2 (Base: M-/L+) did not show improvements in the language domain while Patient 3 (Base: M+/L-) was a strong responder to language therapy also (see **Tables 5** and **6**). However, Patient 2 (Base: M-/L+) already showed a comparatively high level of language skills at the pre-test with a mean profile height of 72.5 in the AAT (see **Table 1**) as well as even the maximum possible raw scores at LeMo, indicating only mild residual symptoms of aphasia even at the beginning of the therapy phase.

As to Patient 1 (Base: M+/L+) and Patient 4 (Base: M-/L-), none of them were able to improve motor function skills and, in addition, none of them were able to profit from language therapy. Of the two patients, Patient 1 (Base: M+/L+) already showed a relatively high language profile at the pre-test, however, with a mean profile height of 57.9 in the AAT, he clearly could have improved significantly in that scale. Additionally, the raw scores indicate that significant improvement of the subtest “Finding Rhymes” (LeMo) would also have been possible (see **Table 1**). Therefore, the existence of ceiling effects in this patient can be excluded and the lack of positive therapy outcome has to be considered as a “real” effect.

In none of our four patients improvements in the motor or the language domains were bound to measurable deteriorations in the other domain. This lack of dissociation between the recovery processes of the two domains hints toward the assumption that a “fight for resources” could not be observed in our patient group.

In conclusion, only one patient with a positive response to motor therapy [Patient 3 (Base: M+/L-)] was able to improve significantly in language functions at the pre-test, whereas Patient 2 (Base: M-/L+), who also improved significantly in

motor functions, could not have achieved measurable improvements due to ceiling effects in the language domain but did show numerical improvements of language skills. The evident motor recovery in the case of Patient 3 (Base: M+/L−) might have been a facilitating factor for a good response to language therapy. The two patients who could not benefit from the intensive motor therapy program [Patient 1 (Base: M+/L+) and Patient 4 (Base: M−/L−)] could also not improve significantly concerning language skills. Therefore, we assume that these results are suggestive of a positive interaction operating between motor and language domains during recovery in the sense that a positive therapy-induced motor recovery is a prerequisite to the possibility of recovering language skills through language therapy. This finding is in accordance with Harnish et al. (3). Regarding the oppositional outcome (positive language therapy outcome leading to improved motor outcome), no such interactions could be observed, therefore, due to our small sample size, it is not possible to formulate a conclusion concerning the possibility of contrary recovery dynamics.

Apraxia of Speech

Interestingly, dissociations in the recovery of apraxia of speech became apparent in the additional functional Scale AMDNS and in the subtest “articulation” of the AAT.

Only Patient 1 (Base: M+/L+), who had the smallest amount of lesioned voxels in the frontal lobe (see **Table 5**), was able to improve notably in “articulatory diadochokinesis” and “duration of phonation” (AMDNS) and showed a notable improvement in the communication parameter “articulation” (AAT; see **Tables 3 and 4**). Patient 2 (Base: M−/L+), showing a larger lesion in the frontal lobe, showed stable performances regarding motor speech. Patient 3 (Base: M+/L−) and 4 (Base: M−/L−) had the highest amount of lesioned voxels in the frontal lobe and stable or inferior results in the post-test [except of a notable improvement in the communication parameter “articulation” (AAT, Patient 3)]. Patients 3 (Base: M+/L−) and 4 (Base: M−/L−) were also not able to conduct complex articulatory diadochokinesis tasks at the pre- and post-test, probably due to the severe apraxia of speech. These two patients demonstrate larger affection of the insular cortex by the lesion in comparison to Patient 2 (Base: M−/L+; no insular lesion) and Patient 1 (Base: M+/L+; see **Table 5**). The insula is associated with articulatory coding/motor programming and motor control [e.g., see Ref. (42, 43)] and its left precentral gyrus forms also an anatomical correlate for the development of apraxia of speech (44, 45). Therefore, preservation of the insula appears to be a necessary, but not exclusive predictor for motor speech recovery. Lesions in other cortical or subcortical regions may also play a role for developing recovery potential in motor speech coordination. This assumption would be in accordance with the findings of Ogar et al. (45). They pointed out that patients showing a severe apraxia of speech had larger lesions in neighboring regions like Broca’s area or basal ganglia. To conclude, the described literature and our findings suggest that the overall amount of lesioned voxels in the frontal lobe *per se* is able to predict motor speech recovery in our sample of patients. This finding has to be tested in a larger number of patients and, in addition, distinctive

subcortical parts of the frontal lobe like insular or basal ganglia should be analyzed precisely in reference to their predictive value for recovery.

Limitations

The present multiple case study provides a new approach in analyzing concurrent motor and language recovery as well as the interaction behavior between these domains during recovery. On the one hand, our findings provide some first indicators, given the fundamental research gap in this field. On the other hand, the data in this study are of limited generalizability as only single cases were examined. In addition, a more specific analysis of specific brain areas is needed. It was also not possible to control the time of onset/duration of aphasia and motor dysfunction in the patients. This is a variable of potential influence due to different restitution processes in different time intervals after stroke [e.g., restitution in the early subacute vs. chronic stage of aphasia; see Ref. (46)]. A group study would be necessary to elucidate if these first results are transferable to a larger sample of subjects.

Conclusion and Perspectives

To conclude, we show that primarily the strategic location of the lesion is a determinant of functional recovery in the motor and language domain. Another main finding was that large damage to important white matter structures for motor or language processing is not a single predictive factor for the recovery of the affected function. Regarding motor speech, the extent of damage to the frontal lobe (especially insula) seems to be a neural correlate for a good motor speech (apraxia of speech) recovery. Poor motor speech abilities, often associated with an apraxia of speech, play a special role in the recovery of language skills and are distinguished by large frontal lesions.

With respect to the interaction of the motor and language domain during recovery, first hints for additive effects were found. Those patients with good base levels in motor skills improved in language abilities. Therefore, motor and language improvement seem to co-occur, as stated before by Harnish and colleagues (3), rather than to compete for recovery resources.

Concerning the mechanisms of recovery, we were not able to find evidence for a “fight for resources,” since motor or language recovery was not associated with a loss of abilities in the other domain, respectively. But it was clearly visible that there is no prospect of recovery in the language domain if there are no resources and abilities available in the motor domain. This is indicative for an additive, synergetic recovery mechanism as described by Harnish and colleagues (3).

A further important finding was that the characteristics of the lesion (specific area, overall size) are no obligatory determinant or predictor for the success of motor or language therapy. We could show that a patient with large CST damage exhibited positive motor recovery while a patient with large AF/SLF damage improved well in the language testing.

In this study, only single cases were analyzed. A larger group study will investigate recovery mechanisms and correlates supported by a higher statistical power as well as additional fMRI measurements. The results, together with the findings in this

paper, will add to the knowledge about recovery processes in this clinically relevant patient group.

Acknowledgments

This work was supported by the START-Program of the Faculty of Medicine, RWTH Aachen University under grant number 691239, and by the Brain Imaging Facility of the Interdisciplinary

Centre for Clinical Research within the Faculty of Medicine, RWTH Aachen. We especially thank Angelika Becker, Erika Söndgen, and Georg Eder for their effort and time.

Supplementary Material

The Supplementary Material for this article can be found online at <http://journal.frontiersin.org/article/10.3389/fneur.2015.00215>

References

- Calautti C, Jones PS, Naccarato M, Sharma N, Day DJ, Bullmore ET, et al. The relationship between motor deficit and primary motor cortex hemispheric activation balance after stroke: longitudinal fMRI study. *J Neurol Neurosurg Psychiatr* (2007) **81**(7):788–92. doi:10.1136/jnnp.2009.190512
- Ward NS, Brown MM, Thompson AJ, Frackowiak RS. Neural correlates of outcome after stroke: a cross-sectional fMRI study. *Brain* (2003) **126**(Pt 6):1430–48. doi:10.1093/brain/awg145
- Harnish S, Meinzer M, Trinastic J, Fitzgerald D, Page S. Language changes coincide with motor and fMRI changes following upper extremity motor therapy for hemiparesis: a brief report. *Brain Imaging Behav* (2011) **8**(3):370–7. doi:10.1007/s11682-011-9139-y
- Borghi AM, Riggio L. Sentence comprehension and simulation of object temporary, canonical and stable affordances. *Brain Res* (2009) **1253**:117–28. doi:10.1016/j.brainres.2008.11.064
- Bersalou LW. Perceptual symbol systems. *Behav Brain Sci* (1999) **22**:577–609.
- Hauk O, Johnsrude I, Pulvermüller F. Somatotopic representation of action words in human motor and premotor cortex. *Neuron* (2004) **41**(2):301–7. doi:10.1016/S0896-6273(03)00838-9
- Glenberg AM, Goldberg AB, Zhu X. Improving early reading comprehension using embodied CAI. *Instr Sci* (2011) **39**:27–39. doi:10.1007/s11251-009-9096-7
- Jirak D, Menz MM, Buccino G, Borghi AM, Binkofski F. Grasping language – a short story on embodiment. *Conscious Cogn* (2010) **19**:711–20. doi:10.1016/j.concog.2010.06.020
- Tettamanti M, Buccino G, Saccuman MC, Gallese V, Danna M, Scifo P, et al. Listening to action-related sentences activates fronto-parietal motor circuits. *J Cogn Neurosci* (2005) **17**(2):273–81. doi:10.1162/0898929053124965
- Heim S, Amunts K, Hensel T, Grande M, Huber W, Binkofski F, et al. The role of human parietal area 7A as a link between sequencing in hand actions and in overt speech production. *Front Psychol* (2012) **3**:534. doi:10.3389/fpsyg.2012.00534
- Hoeren M, Kümmerer D, Bormann T, Beume L, Ludwig VM, Vry MS, et al. Neural bases of imitation and pantomime in acute stroke patients: distinct streams for praxis. *Brain* (2014) **137**(Pt 10):2796–810. doi:10.1093/brain/awu203
- Binkofski F, Seitz RJ, Hackländer T, Pawelec D, Mau J, Freund HJ. Recovery of motor functions following hemiparetic stroke: a clinical and magnetic resonance-morphometric study. *Cerebrovasc Dis* (2001) **11**(3):273–81. doi:10.1159/000047650
- Binkofski F, Seitz RJ, Arnold S, Classen J, Benecke R, Freund HJ. Thalamic metabolism and corticospinal tract integrity determine motor recovery in stroke. *Ann Neurol* (1996) **39**(4):460–70. doi:10.1002/ana.410390408
- Zhu LL, Lindenberg R, Alexander MP, Schlaug G. Lesion load of the corticospinal tract predicts motor impairment in chronic stroke. *Stroke* (2010) **41**(5):910–5. doi:10.1161/STROKEAHA.109.577023
- Shelton FN, Reding MJ. Effect of lesion location on upper limb motor recovery after stroke. *Stroke* (2001) **32**(1):107–12. doi:10.1161/01.STR.32.1.107
- Meinzer M, Mohammadi S, Kugel H, Schiffbauer H, Flöel A, Albers J, et al. Integrity of the hippocampus and surrounding white matter is correlated with language training success in aphasia. *Neuroimage* (2010) **53**(1):283–90. doi:10.1016/j.neuroimage.2010.06.004
- Marchina S, Zhu LL, Norton A, Zipse L, Wan CY, Schlaug G. Impairment of speech production predicted by lesion load of the left arcuate fasciculus. *Stroke* (2011) **42**(8):2251–6. doi:10.1161/STROKEAHA.110.606103
- Lazar RM, Speizer AE, Festa JR, Krakauer JW, Marshall RS. Variability in language recovery after first-time stroke. *J Neurol Neurosurg Psychiatry* (2008) **79**(5):530–4. doi:10.1136/jnnp.2007.122457
- Rehme AK, Fink GR, Cramon DY, von Grefkes C. The role of the contralateral motor cortex for motor recovery in the early days after stroke assessed with longitudinal fMRI. *Cereb Cortex* (2011) **21**(4):756–68. doi:10.1093/cercor/bhq140
- Schaechter JD, Perdue KL, Wang R. Structural damage to the corticospinal tract correlates with bilateral sensorimotor cortex reorganization in stroke patients. *Neuroimage* (2008) **39**(3):1370–82. doi:10.1016/j.neuroimage.2007.09.071
- Gerloff C, Khalaf B, Sailer A, Wassermann EM, Chen R, Matsuoka T, et al. Multimodal imaging of brain reorganization in motor areas of the contralateral hemisphere of well recovered patients after capsular stroke. *Brain* (2006) **129**(3):791–808. doi:10.1093/brain/awh713
- Grefkes C, Ward NS. Cortical reorganization after stroke: how much and how functional? *Neuroscientist* (2013) **20**(1):56–70. doi:10.1177/1073858413491147
- Stoeckel MC, Binkofski F. The role of ipsilateral primary motor cortex in movement control and recovery from brain damage. *Exp Neurol* (2010) **221**(1):13–7. doi:10.1016/j.expneurol.2009.10.021
- Rosen HJ, Petersen SE, Linenweber MR, Snyder AZ, White DA, Chapman L, et al. Neural correlates of recovery from aphasia after damage to left inferior frontal cortex. *Neurology* (2000) **55**(12):1883–94. doi:10.1212/WNL.55.12.1883
- Saur D, Ronneberger O, Kümmerer D, Mader I, Weiller C, Klöppel S. Early functional magnetic resonance imaging activations predict language outcome after stroke. *Brain* (2010) **133**(4):1252–64. doi:10.1093/brain/awq021
- Zipse L, Norton A, Marchina S, Schlaug G. When right is all that is left: plasticity of right-hemisphere tracts in a young aphasic patient. *Ann N Y Acad Sci* (2012) **1252**:237–45. doi:10.1111/j.1749-6632.2012.06454.x
- Raboyeau G, Boissezon X, de Marie N, Balduyck S, Puel M, Bezy C, et al. Right hemisphere activation in recovery from aphasia: lesion effect or function recruitment? *Neurology* (2008) **70**(4):290–8. doi:10.1212/01.wnl.0000287115.85956.87
- Saur D, Hartwigsen G. Neurobiology of language recovery after stroke: lessons from neuroimaging studies. *Arch Phys Med Rehabil* (2012) **93**(1 Suppl):S15–25. doi:10.1016/j.apmr.2011.03.036
- Brownset SLE, Warren JE, Geranmayeh F, Woodhead Z, Leech R, Wise RJS. Cognitive control and its impact on recovery from aphasic stroke. *Brain* (2014) **137**(Pt 1):242–54. doi:10.1093/brain/awt289
- Huber W, Poeck K, Weniger D, Willmes K. *Aachener Aphasia Test*. Göttingen: Hogrefe (1983).
- Wolf SL, Catlin PA, Ellis M, Archer AL, Morgan B, Piacentino A. Assessing wolf motor function test as outcome measure for research in patients after stroke. *Stroke* (2001) **32**(7):1635–9. doi:10.1161/01.STR.32.7.1635
- Oldfield RC. The assessment and analysis of handedness: the Edinburgh inventory. *Neuropsychologia* (1971) **9**(1):97–113. doi:10.1016/0028-3932(71)90067-4
- Bleser R, de Cholewa J, Stadie N, Tabatabaie S. *LEMO: Lexikon Modellorientiert*. München: Elsevier (2010).
- Shumway-Cook A, Woollacott MH. *Motor Control: Theory and Practical Applications*. Philadelphia, PA: Lippincott Williams & Wilkins (2001). 614 p.
- Schnitker R, Huber W, Pustelniak M, Weyer D, Willmes K, Bülte D. Die aachener materialien zur diagnostik neurogener sprechstörungen (AMDNS). *Neurol Rehabil* (2011) **5**:6:277.
- Guillot G, Willmes K, Kremer C. *AATP 4.0 Für Windows [Computer Program]*. Bonn: Phoenix Software GmbH (2008).
- Huber HP. *Psychometrische Einzelfalldiagnostik*. Weinheim: Beltz (1973).

38. Rorden C. *MRICron [Computer Program]. Version 7.* (2012). Available from: <http://www.mricro.com>
39. Jenkinson M, Smith SM. A global optimisation method for robust affine registration of brain images. *Med Image Anal* (2001) 5(2):143–56. doi:10.1016/S1361-8415(01)00036-6
40. Mazziotta JC, Toga AW, Evans A, Fox P, Lancaster J. A probabilistic atlas of the human brain: theory and rationale for its development. The international consortium for brain mapping (ICBM). *Neuroimage* (1995) 2(2):89–101. doi:10.1006/nimg.1995.1012
41. Oishi K, Faria A, van Zijl PC, Mori S. *MRI Atlas of Human White Matter.* London: Elsevier (2011). 257 p.
42. Petersen SE. Positron emission tomographic studies of the processing of single words. *J Cogn Neurosci* (1989) 1(2):153. doi:10.1162/jocn.1989.1.2.153
43. Ackermann H, Riecker A. The contribution of the insula to motor aspects of speech production: a review and a hypothesis. *Brain Lang* (2004) 89(2):320–8. doi:10.1016/S0093-934X(03)00347-X
44. Dronkers N. A new brain region for coordinating speech articulation. *Nature* (1996) 384(6605):159–61. doi:10.1038/384159a0
45. Ogar J, Willock S, Baldo J, Wilkins D, Ludy C, Dronkers N. Clinical and anatomical correlates of apraxia of speech. *Brain Lang* (2006) 97(3):343–50. doi:10.1016/j.bandl.2006.01.008
46. Cherney LR, Small SL. Aphasia, apraxia of speech and dysarthria. In: Harvey RL, Macko RF, Stein J, Zorowitz RD, Winstein CJ, editors. *Stroke Recovery and Rehabilitation.* New York, NY: Demos Medical Publishing (2008). p. 155–82.

Conflict of Interest Statement: The authors declare that the research was conducted in the absence of any commercial or financial relationships that could be construed as a potential conflict of interest.

Copyright © 2015 Primaßin, Scholtes, Heim, Huber, Neuschäfer, Binkofski and Werner. This is an open-access article distributed under the terms of the Creative Commons Attribution License (CC BY). The use, distribution or reproduction in other forums is permitted, provided the original author(s) or licensor are credited and that the original publication in this journal is cited, in accordance with accepted academic practice. No use, distribution or reproduction is permitted which does not comply with these terms.



The Right Supramarginal Gyrus Is Important for Proprioception in Healthy and Stroke-Affected Participants: A Functional MRI Study

Ettie Ben-Shabat^{1,2*}, Thomas A. Matyas^{1,2}, Gaby S. Pell¹, Amy Brodtmann^{1†} and Leeanne M. Carey^{1,2†}

¹Neurorehabilitation and Recovery, Stroke, Florey Institute of Neuroscience and Mental Health, Melbourne, VIC, Australia,

²Occupational Therapy, School of Allied Health, College of Science, Health and Engineering, La Trobe University, Melbourne, VIC, Australia

OPEN ACCESS

Edited by:

Roland Wiest,
University of Bern, Switzerland

Reviewed by:

Maarten G. Lansberg,
Stanford University, USA
Nobutaka Kawahara,
Yokohama City University, Japan

*Correspondence:

Ettie Ben-Shabat
ebenshabat@gmail.com

[†]Amy Brodtmann and Leeanne
M. Carey have contributed
equally to this work.

Specialty section:

This article was submitted to Stroke,
a section of the journal
Frontiers in Neurology

Received: 29 August 2015

Accepted: 12 November 2015

Published: 12 April 2015

Citation:

Ben-Shabat E, Matyas TA, Pell GS,
Brodtmann A and Carey LM (2015)
The Right Supramarginal Gyrus Is
Important for Proprioception in
Healthy and Stroke-Affected
Participants: A Functional MRI Study.
Front. Neurol. 6:248.
doi: 10.3389/fneur.2015.00248

Human proprioception is essential for motor control, yet its central processing is still debated. Previous studies of passive movements and illusory vibration have reported inconsistent activation patterns related to proprioception, particularly in high-order sensorimotor cortices. We investigated brain activation specific to proprioception, its laterality, and changes following stroke. Twelve healthy and three stroke-affected individuals with proprioceptive deficits participated. Proprioception was assessed clinically with the Wrist Position Sense Test, and participants underwent functional magnetic resonance imaging scanning. An event-related study design was used, where each proprioceptive stimulus of passive wrist movement was followed by a motor response of mirror copying with the other wrist. Left (LWP) and right (RWP) wrist proprioception were tested separately. Laterality indices (LIs) were calculated for the main cortical regions activated during proprioception. We found proprioception-related brain activation in high-order sensorimotor cortices in healthy participants especially in the supramarginal gyrus (SMG LWP $z = 4.51$, RWP $z = 4.24$) and the dorsal premotor cortex (PMd LWP $z = 4.10$, RWP $z = 3.93$). Right hemispheric dominance was observed in the SMG (LI LWP mean 0.41, SD 0.22; RWP 0.29, SD 0.20), and to a lesser degree in the PMd (LI LWP 0.34, SD 0.17; RWP 0.13, SD 0.25). In stroke-affected participants, the main difference in proprioception-related brain activation was reduced laterality in the right SMG. Our findings indicate that the SMG and PMd play a key role in proprioception probably due to their role in spatial processing and motor control, respectively. The findings from stroke-affected individuals suggest that decreased right SMG function may be associated with decreased proprioception. We recommend that clinicians pay particular attention to the assessment and rehabilitation of proprioception following right hemispheric lesions.

Keywords: proprioception, kinesthesia, upper extremity, functional laterality, stroke, magnetic resonance imaging, cerebral cortex

Abbreviations: BA, Brodmann area; fMRI, functional magnetic resonance imaging; IPL, inferior parietal lobe; LI, laterality index; LWP, left wrist proprioception; MI, primary motor cortex; PMd, dorsal premotor cortex; RWP, right wrist proprioception; SI, primary somatosensory cortex; SIMI, primary sensorimotor cortex; SII, secondary somatosensory cortex; SMA, supplementary motor area; SMG, supramarginal gyrus.

INTRODUCTION

Limb proprioception refers to knowledge of the spatial location of one's limb in the absence of vision. Proprioception is vital for motor control (1), particularly of the upper limbs (2). It is essential for the control of coordinated movements, especially small or precise movements, and for motor skill acquisition (3). Hence, proprioceptive deficits in the upper limbs are associated with decreased function (1). Despite the importance of proprioception for function, it remains unclear which brain regions beyond the primary sensorimotor cortices (SIMIs) are involved in the processing of proprioception and how this brain activation is altered following focal brain lesions associated with proprioceptive deficits.

Researchers studying brain activation during passive movements of the elbow (4, 5), wrist (6, 7), hand (8), and finger (9, 10) have identified activation in the contralateral primary somatosensory (SI) and motor (MI) cortices and the inferior parietal lobe (IPL). However, investigators disagreed on the pattern (contralateral, ipsilateral, or both) and exact location of activation [supramarginal gyrus (SMG) or the secondary somatosensory cortex (SII)]. In contrast, neurophysiological studies of primates, identified the superior parietal lobe as a key region for the processing of proprioception (11, 12). The ability of current brain imaging paradigms to investigate proprioceptive specific processing, and in particular the contribution from higher order brain regions, requires careful consideration and design.

Inconsistent proprioception-related brain activation has also been reported in high-order motor cortices including the supplementary motor area (SMA), cerebellum (6, 8), and the premotor cortex (PMC) (5, 6, 8). Variations in proprioception-related brain activation may have been due to the fact that brain imaging studies of passive movements varied in paradigm design. In some cases, the support of the moving limb was suboptimal and may have introduced significant tactile stimulation (6, 8, 10), thus generating confounding brain activation.

Proprioception-related brain activation has also been studied using illusory vibrations. This is vibration of a tendon at a frequency between 70 and 100Hz, which creates an illusion of movement (13). Early findings from illusory vibration studies emphasized activation in motor cortices including: MI, SMA, PMC, and the cingulate motor area (14, 15). Later, researchers also identified brain activation in the IPL (5, 16–18). However, as was the case with passive movements, reported activation varied in location, with reports of activation in the parietal operculum (5, 15, 17) or the SMG (16, 18). Hemispheric bias was also controversial with some researchers reporting bilateral activation (16, 18), while others report a right hemisphere dominance (15, 17).

Illusory vibrations provide different peripheral stimuli to passive movements. The stimulus is large phasic and of uniform frequency in the primary afferent fibers of the muscle spindles (19, 20). Minimal, if any, stimulation is produced in the secondary fibers of the muscle spindles and the joint receptors (19, 20). In contrast, passive movements produce multifrequency phasic and tonic stimulation of the primary afferent fibers in the muscle spindles (21). Secondary fibers of the muscle spindles and joint receptors are also stimulated (21–23). It is possible that different

peripheral stimuli were associated with differential brain activation (5). In such circumstances, brain activation during passive movements is likely to reflect the central processing of proprioception more accurately than illusory vibration.

An important limitation of both passive movement and illusory vibration brain imaging studies of proprioception is that participants were not required to provide accurate and measurable responses to the proprioceptive stimuli during scanning. Responses to proprioceptive stimuli are important for two reasons. First, by asking participants for accurate responses to proprioceptive stimuli (and monitoring the responses), examiners ensure that participants adequately engage in proprioceptive information processing. Second, the response requirement introduces a certain degree of difficulty to the proprioceptive task, which would not have been present if responses were not required. Increased task difficulty is desirable due to the associated increase in cortical activation (24, 25).

In healthy participants, findings from behavioral studies have suggested asymmetry in the accuracy of proprioception from the right and left limbs (26–28). Asymmetry in behavioral measures suggests hemispheric dominance and thus asymmetry in proprioception-related brain activation. Brain activation studies of illusory vibration stimulation confirmed right hemispheric dominance (15, 17, 18). Brain activation in the IPL and inferior frontal gyrus was found in all three studies, but the exact loci of activation and degree of laterality (i.e., right hemispheric or bilateral activation) varied. None of the brain imaging studies of passive movements investigated laterality of proprioception.

Quantitative behavioral measures of proprioception in stroke-affected individuals have shown deficits in about 50% of the participants (1, 29). Considering the adverse effect of proprioceptive deficits on function (1), it is important not only to understand the central processing of proprioception in healthy participants but also how it changes following brain lesions associated with proprioceptive deficits. This is because proprioception can be rehabilitated (30–32) with associated changes in brain activation (33) and improvement in function (34).

The current study was designed to investigate the brain-behavior relationship of proprioception. The research questions were:

- (1) Which high-order brain areas are important for early coding of natural proprioceptive stimuli?
- (2) Is proprioception-related brain activation lateralized, and if so in which areas?
- (3) How does proprioception-related brain activation in stroke-affected individuals with proprioceptive deficits differ from that of healthy participants?

To answer these questions, we designed an event-related functional magnetic resonance imaging (fMRI) study with a controlled proprioceptive stimulus and response paradigm. The study was exploratory with data-driven laterality analyses.

First, proprioceptive stimuli were delivered with maximal limb support and minimal tactile stimulation to eliminate confounding brain activation. Second, participants were required to respond accurately to each proprioceptive stimulus for optimal brain activation related to attended proprioceptive information processing.

Third, the paradigm and analyses were designed to show brain activation at the beginning of a proprioception task during the coding of proprioceptive stimuli. We hypothesized that coding proprioception would involve high-order somatosensory cortices in the parietal lobe including the IPL, the SII, and the superior parietal lobe. We also hypothesized that proprioception-related brain activation would be found in high-order motor cortices in the frontal lobe including the PMC, SMA, and cingulate motor cortex. The second hypothesis was that proprioception-related brain activation would be lateralized to the right hemisphere, particularly the high-order cortices. Finally, we hypothesized that laterality would decrease following stroke which affected proprioception.

MATERIALS AND METHODS

Participants

Twelve healthy right-handed participants (35) were recruited. Participants were aged 23.4 ± 3.3 years (seven females) and their age was restricted (18–30 years) to control for age-related variations in proprioception (36) and brain activation (37). Participants' proprioception was within the normative range (average absolute error below $11 \pm 4.8^\circ$) as verified behaviorally with the Wrist Position Sense Test (38).

Three participants with chronic strokes (CSs) and proprioceptive deficits were also recruited: CS1 45 years, male, 16 months post right hemisphere stroke, average absolute wrist position error on the Wrist Position Sense Test was $25.6 \pm 22.5^\circ$; CS2 65 years, female, 72 months post left hemisphere stroke, average absolute error $17.9 \pm 15.2^\circ$; and CS3 46 years, male, 68 months post left hemisphere stroke, average absolute error $20.8 \pm 18.4^\circ$.

Participants had no history of wrist injury, neurological injury (other than the three participants affected by stroke), psychiatric conditions, ongoing medical issues, diabetes, hearing impairments, or any of the standard contraindications to MRI scanning. The study was approved by the La Trobe University and Austin Health Human Ethics Committees, conforming to Declaration of Helsinki standards. Participants gave written informed consent prior to recruitment.

Experimental Design and Analysis Approach

Participants performed a limb position matching task in the scanner using an event-related study design. The experimental paradigm was carefully constructed to ensure that fMRI data were collected specifically during coding of proprioception and not during response generation. Care was also taken to ensure that other confounding stimuli were excluded. We used an exploratory approach to identify the parietal and frontal regions activated specifically at the beginning of the proprioceptive stimuli during coding of proprioception. Brain laterality analyses were data driven, and only regions that showed significant activation during coding of proprioception were then analyzed for laterality. *A priori* selection of specific brain regions for the laterality analyses was not possible due to the conflicting literature. Testing and analysis of right wrist proprioception and its

laterality were performed separately to that of the left wrist. No direct comparisons were made between left and right wrist data. Data of stroke-affected individuals were analyzed as case studies and no direct comparisons were made with data of healthy participants.

Experimental Paradigm

An event-related fMRI study was conducted in which participants performed a limb position matching task. The proprioceptive task was performed with eyes closed to eliminate the effect of vision on proprioception. Participants' hands were placed in splints attached to a lap-tray (wrist and splint axes were aligned), and their arms were supported on contoured foam cushions. Hand placement was designed to minimize confounding tactile stimulation or voluntary movement. The event-related design enabled temporal separation of brain activation related to proprioception from that related to motor response. A single trial was composed of two events: a proprioceptive stimulus event and a response event (see **Figure 1**). Each event was followed by a randomly varying interstimulus interval which varied between 0.5 and 12 s: 0.5–6.0 s for 70% of events, 6.0–10.0 s for 20% of events, or 10.0–12.0 s for 10% of events (i.e., jittering) (39). The purpose of the response events was to ensure participants' vigilance. Hence, the specific pattern of brain activation during response events was not relevant to the research question. The brain activation of interest took place at the beginning of the proprioceptive events, during coding of proprioception.

The investigator was visually cued to passively move the participant's hand via a lever (to minimize tactile stimulation) for a maximal duration of 3 s. In addition, the investigator was pretrained to deliver passive wrist movements at a rate of 10° a second or faster, to ensure stimulation of the main proprioceptors which are sensitive to changes in joint position, and to produce a phasic firing pattern (40). Passive movements of the wrist were presented in random order to any one of 21 predetermined positions within a 100° range of wrist flexion-extension movements. Positions were analyzed together rather than individually as the research question pertained to proprioception-related brain activation in general and not the differential processing of each position.

Response requirements were designed to ensure maximal attendance to the proprioceptive stimulus. Response events commenced with a 600 ms auditory cue of either a pink noise (random noise with an equal energy in all octaves) or a click train, and participants were allowed 3 s for their response. The pink noise cued the participant to mirror copy the wrist position with the opposite hand (70% of the events), while the click train cued participants not to copy the wrist position (30% of the events). The examiner closely monitored participants' responses during the scans and accuracy of response measurements were collected in the prescan testing. Vigilance was also monitored in the prescan testing by assessing adherence to auditory sounds that served as cues to either respond or not respond to the proprioceptive stimuli. Responses were considered non-vigilant if participants moved their response hand half way or more toward mirror copying the stimulus position when cued not to respond. Vigilance was scored as percentage

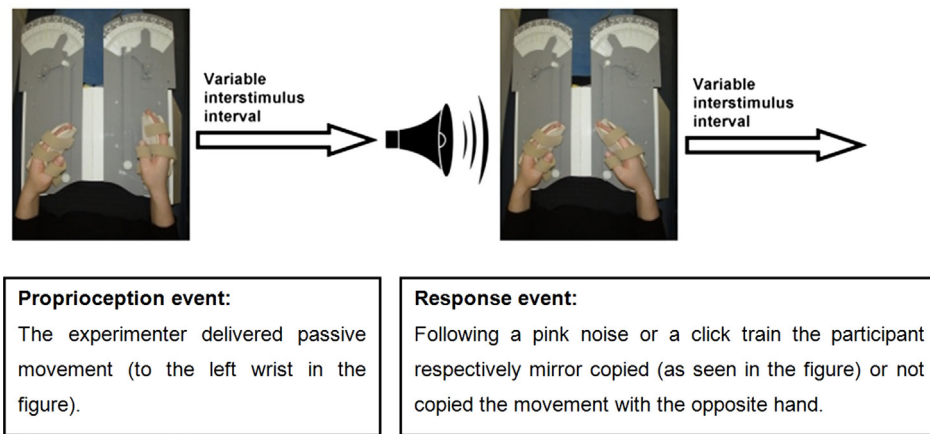


FIGURE 1 | The event-related experimental design.

of correct adherence to “do not respond” cues. Participants were first studied during left wrist proprioceptive stimuli (LWP) with right wrist responses, and then 2–6 months later during right wrist proprioceptive stimuli (RWP) and left wrist responses. The time between LWP and RWP scans was not expected to affect the results as no direct comparisons were made between the two.

Tests and Prescan Training Performed Outside the Scanner

The proprioceptive paradigm was practiced in a prescan session, 1–9 days before the scan to ensure familiarity with the task. During the prescan sessions, measurements of angular wrist displacements were taken by potentiometers attached to the wrist axes. Following familiarization, participants’ responses were measured for accuracy and vigilance.

Electromyographic recordings were taken outside the scanner only. The EMG amplifier that we used is designed to work in the electrically noisy clinical environment and therefore has an operating bandwidth of 18–370 Hz. Outside the bandwidth, signal was filtered below –3 db. Notch filter was set at 50 Hz. Rectified signal was then sampled at 10 Hz, and these samples were employed to compute the average signal for each condition: passive movements, active movements, and rest. Recordings were collected simultaneously from two channels (wrist flexors and extensors) during random 30 s blocks of passive movements, active movements, and rest. Recordings were collected over 6.5 min, and 2 s of data was trimmed from the beginning and end of each block to avoid contamination of the data. Data were then normalized in the following manner. For each participant, the median of active movement readings was multiplied by a constant that gave it the value of 100. Then all recordings from the same muscle group were multiplied by this constant. Data of all participants were then pooled, and a non-parametric Wilcoxon *T*-test was conducted to compare EMG recordings during passive and active movements. Statistically significant difference was interpreted as evidence of participants’ ability to relax their forearm muscles during passive

movements. This ensured that brain activation was not related to voluntary muscle contraction.

Data Acquisition

A scanning session contained four runs. Each run extended over 20 trials. Runs commenced with auditory instructions, which lasted for 27 s. The first 12 volumes of each run were discarded (nine volumes of instruction and three equilibration volumes). One hundred and thirty-one whole brain volumes were collected from each run. The computer program Presentation® (Version 9.70¹) was used to coordinate scanner timing with the delivery times of the visual cues to the investigator and the auditory cues to the participants. The same software served to generate log-files, which recorded event times in each run.

Data were acquired on a 3 T GE Horizon LX MRI scanner (GE Systems, Milwaukee, WI, USA). Tilted axial slices were oriented parallel to a line passing inferior to the genu of the corpus callosum and superior to the cerebellum. The tilted imaging plane served to maximize the signal from the parietal cortex. Functional scans were acquired using a T2*-weighted gradient echo echo-planar imaging sequence [imaging parameters: repetition time = 3000 ms, echo time = 40 ms, flip angle = 75°, field of view = 240 mm, matrix = 128 × 128, 25 slices, 4 mm thick, and 1 mm gap (in-plane resolution 1.875 mm × 1.875 mm)].

Anatomical axial 3D scans were acquired using a T1-weighted FSPGR imaging sequence [repetition time = 13.8 ms, echo time = 2.7 ms, inversion time = 500 ms, flip angle = 20°, field of view = 240 mm, matrix = 512 × 512, 80 slices, 2 mm thick (in-plane resolution 0.47 mm × 0.47 mm)]. Axial 2D T2-weighted image was also taken [repetition time = 3400 ms, echo time = 77 ms, inversion time = 500 ms, flip angle = 90°, field of view = 240 mm, matrix = 512 × 512, 25 slices, 4 mm thick, 1 mm gap (in-plane resolution 0.47 mm × 0.47 mm)].

¹<http://www.neurobs.com/presentation>.

Stroke Lesion Mapping

Lesion sites were identified on the non-normalized anatomical axial 3D T1 images of each stroke-affected participant. A neurologist visually mapped the lesion sites to normalized generic axial slices (41) taken from the Talairach atlas (42). A second neurologist then evaluated that the lesions were accurately mapped. While lesion mapping has a subjective element, this process minimized the risk of bias.

Data Analysis of fMRI Scans

Individual Image Processing

Data analyses were carried out using SPM 2 (Wellcome Department of Imaging Neuroscience, London, UK). Raw images were inspected for artifacts or structural abnormalities and then pre-processed: (i) correction for slice acquisition time, (ii) realignment to a target volume closest to the median value of head motion (iBrain™ Version 3² used for median image calculation), (iii) coregistration of anatomical scans to functional scans, (iv) spatial normalization into the Montreal Neurological Institute space [with masking the lesion sites for the stroke-affected participants – cost function masking (43)], and (v) spatial smoothing with a kernel size of 8 mm.

Statistical Analyses

Only the beginning of each proprioception event was modeled as the research question was related to brain activation during coding of proprioceptive stimuli. Timing of each event was entered according to time recorded in the Presentation® log-file. We used a hemodynamic response function and included an additional dispersion regressor to allow for the longer event durations in this study (up to 3 s).

It was expected that the brain regions most significantly activated during the beginning of the proprioceptive stimuli (coding of proprioception) would not be activated to the same degree during other components of each trial, namely: response generation, auditory cues, and interstimulus intervals. Therefore, contrasts were generated to identify brain activation that took place at the beginning of proprioception events above conditions of no interest (response generation, auditory cues, and interstimulus intervals). Individual data of healthy participants were analyzed using a standard unpaired *t*-test. The voxel-height threshold was set at $p < 0.001$, uncorrected for multiple comparisons. Analysis at the individual level was exploratory; therefore, a low threshold was selected to reveal trends of brain activation. The threshold used for data of stroke-affected participants was set at $p < 0.05$ corrected for multiple comparisons due to the expected bilateral brain activation (44, 45) of greater extent (44) compared to healthy participants. A high pass filter was used to remove the effect of low frequency drift on the data.

Group Analyses

Random effect analyses were used to generate *t*-contrasts for group activation maps of the LWP and RWP scans. As with individual analyses, only the beginnings of proprioception

events were modeled, and they were contrasted against all other brain activation that took place during the experiment (response events, auditory cues, and interstimulus intervals). To avoid the risks of multiple comparisons, cluster correction (minimum cluster size of 20 voxels) for multiple comparisons was used at $p < 0.05$ (contrasts entered in the analysis were at voxel-height threshold of $p < 0.001$). Anatomical loci of significant activation were identified using probabilistic maps (46) available from the SPM2 toolbox.

The probabilistic maps, however, did not specify the cytoarchitectonic probability of Brodmann area (BA) 6. Thus, using the Talairach coordinates BA 6 was divided into lateral and medial parts. The area lateral to $x = 15$ was considered as the PMC and medial to it, the SMA. The PMC was divided into superior and inferior areas. The area superior to $z = 42$ was considered as the dorsal PMC (PMd), while inferior to it was the ventral PMC (PMv). The SMA was divided into anterior and posterior parts. The area anterior to $y = 0$ was considered as pre-SMA, while posterior to it was interpreted as the SMA proper [see Figure 2, (47)].

Laterality Analyses

Laterality calculations in the form of laterality index (LI) were used to quantify the hemispheric symmetries of proprioception-related brain activation during LWP and RWP separately, and no direct comparisons were made between the two. Anatomical brain regions selected for the LI calculations (regions of interest) were the primary SI and MI (based on the literature reviewed in Section “Introduction”), and more importantly high-order somatosensory and motor cortices identified in both the LWP and RWP group analyses. Outlines for the regions of interest were defined using an independent template – the Wake Forest University PickAtlas available from the SPM2 toolbox. For BA 6, outlines of subregions were generated manually using the FSLView tool (Version 3.0), in accordance with the guidelines detailed in Section “Group Analyses.”

Laterality was determined using signal extent based on the previously described protocol (48). Signal intensity of each voxel in the region of interest was determined by the statistical parametric maps of the LWP and the RWP contrasts. The average signal intensity was then calculated for the 5% of voxels showing the highest *t*-score. The LI was calculated as: (right – left)/(right + left). Using the top 5% of voxels showing the highest *t*-score served to reduce the risk of confounding brain activation related to inhomogeneities in the magnetic field or multiple comparisons. This risk was also reduced by contrasting brain activation during proprioceptive coding with all other experimental conditions (response generation, auditory processing, and rest), rather than contrasting with rest only.

Laterality thresholding is designed to limit type I errors. Based on the literature, we selected an *a priori* threshold of $-0.2 \geq \text{LI}$ value ≥ 0.2 to indicate lateralized brain function (49). Thus, we expected that in the dominant region the area of the most significant brain activation showed at least 33% higher signal intensity compared to the homologous area. LIs were calculated for each ROI of each participant based on the individual analyses. Group LIs were reported as mean and standard deviation.

²<http://www.brain.org.au/software.html>.

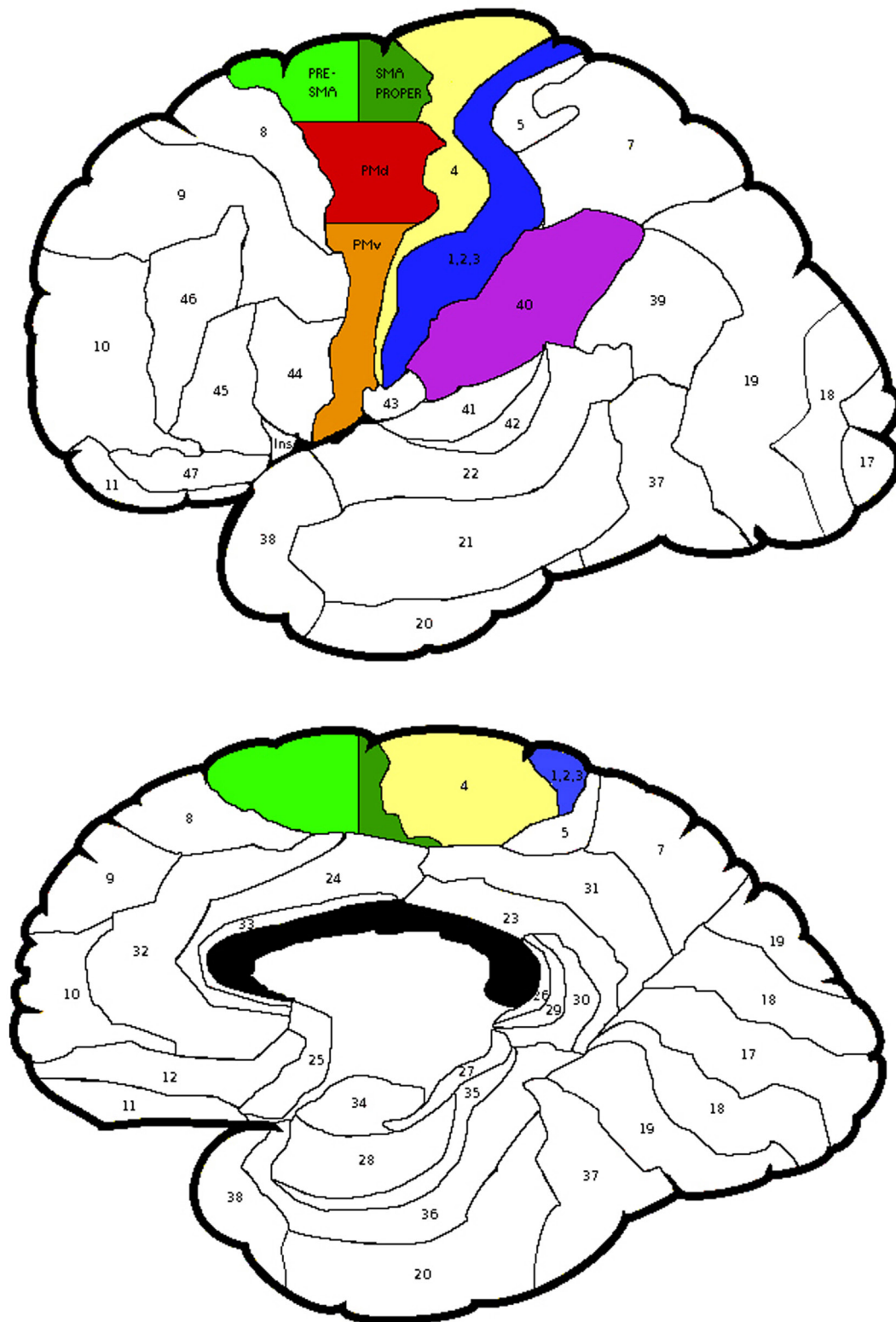


FIGURE 2 | The regions of interest selected for the laterality calculations and the subdivisions of Brodmann Area 6. Areas depicted: Brodmann Areas 1,2,3, primary somatosensory cortex; area 4, primary motor cortex; area 40, supramarginal gyrus; PMv, ventral premotor cortex; PMd, dorsal premotor cortex; subdivisions of area 6, Pre-SMA, pre-supplementary motor area and SMA proper, supplementary motor area proper.

RESULTS

Clinical and Proprioception Results

All healthy participants completed the LWP scans and six completed the RWP scans. The other six were not available to participate in the RWP study. During the prescan sessions, participants were vigilant for 96.8% of the tested trials (range: 89–100%, $SD = 4.8\%$). The mean absolute error of participants' response accuracy for the matching task performed in the scanner was 8.6° ($SD = 2.7^\circ$) for LWP and 7.5° ($SD = 0.9^\circ$) for RWP.

As with the previous studies (5), forearm muscle electromyographic recordings for healthy participants during passive movements (mean 10.73, $SD = 7.70$) were significantly lower than during active movements (116.96, 76.44) when tested with the Wilcoxon T test ($p < 0.001$).

Lesion sites of stroke-affected participants were subcortical, and the common lesion site was the thalamus (see **Figure 3**). The lesions of CS1 and CS3 extended to include the posterior limb of the internal capsule and the basal ganglia. During the prescan session, the mean absolute error of response for CS1 (LWP) was 17.9° ($SD = 9.6^\circ$), vigilance 91.7%; for CS2 (RWP) mean absolute error of response 7.5° ($SD = 7.0^\circ$), vigilance 94.4%; and for CS3 (RWP) mean absolute error of response 19.6° ($SD = 13.3^\circ$), vigilance 100%.

Cortical Areas Activated During Proprioception

Group brain activation of healthy participants during the LWP task was in the right SI cortex, particularly in BA 3a, the right SMG, PMd, MI (BA 4a and 4p), superior and middle frontal gyri, SMA proper, and the middle cingulate cortex (see **Table 1**; **Figure 4**). Group brain activation during performance of the RWP task was significant in the right SMG, the left PMd, and MI (BA 4a) (see **Table 1**; **Figure 4**).

Proprioception-related brain activation varied among stroke-affected participants; however, common areas of brain activated included the IPL, SPL, and PMd (see **Table 2**).

Laterality of Proprioception-Related Brain Activation

Laterality was investigated for the SMG and PMd, high-order somatosensory and motor cortices identified in the group analyses and for the SI and MI given their well-established role in

proprioception (see **Figure 2**). Right laterality of SMG activation was observed for both the LWP and the RWP scans (see **Figure 5**; **Table 3**). Laterality calculations for the PMd illustrated a lesser degree of laterality compared to the SMG, with contralateral activation during LWP and bilateral activation during RWP (see **Figure 5**; **Table 3**). As expected, LIs of the SI and MI showed contralateral activation (see **Figure 5**; **Table 3**). For stroke-affected participants, brain activation was bilateral in both the SMG and PMd (see **Table 3**).

DISCUSSION

We investigated the brain-behavior relationship pertaining to processing of proprioceptive stimuli at the wrist. There are three novel aspects to our study design. First, natural proprioceptive stimuli of passive movements were used, and maximal effort was made to control for confounding tactile and motor stimuli. Participants were required to provide accurate and measurable response to each proprioceptive stimulus both in and outside the scanner. Second, the event-related design with its variable inter-stimulus intervals enabled temporal isolation of brain activation related to coding proprioception. Third, stroke-affected participants with proprioceptive deficits were studied with respect to the effect of pathology on proprioception-related brain activation.

Our findings indicated that proprioception-related brain activation in high-order somatosensory and motor cortices included the SMG and PMd. The right SMG was activated during both RWP and LWP, and its activity was reduced in the presence of proprioceptive deficits. Proprioception-related brain activation in the PMd was contralateral during LWP and bilateral during RWP. Thus, a certain degree of right PMd laterality was also observed during the central processing of proprioception. These findings confirm right hemispheric dominance in the processing of proprioception, but unlike other studies highlight the key role the right SMG plays in proprioception.

High-Order Proprioception-Related Brain Activation

The findings from our study suggest that the high-order proprioception-related brain activation of both the SMG and PMd is pivotal for the central processing of proprioception. Several studies have identified proprioception-related brain activation in frontoparietal networks; however, various activation loci were

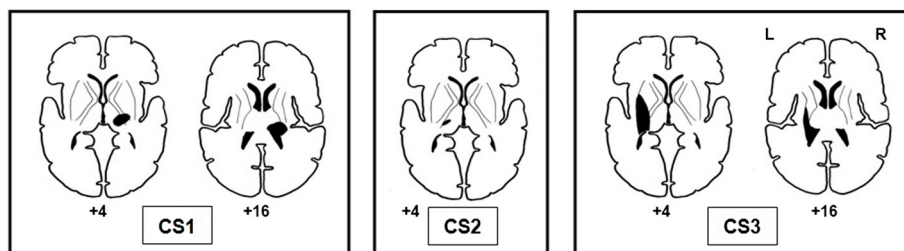


FIGURE 3 | Lesion sites of the three stroke-affected participants.

TABLE 1 | Group analyses of brain activation loci in healthy participants during proprioception.

Task	Anatomical location	BA	Cluster size	Z score	Talairach coordinates		
					x	y	z
LWP	R SI	3a	844	4.57	34	−32	45
	R SMG ^a	40		4.51	52	−40	37
	R PMd ^a	6		4.10	32	−26	69
	R MI	4a		3.96	36	−32	69
	R MI	4p		3.86	36	−22	53
	R SFG ^a	6/8		3.32	24	4	57
	R MFG	6/8	83	3.31	26	6	53
	R SMA (proper) ^a	6		3.75	16	−12	61
	R MCC ^a	6/24		3.19	10	−8	49
RWP	R SMG ^a	40	33	4.24	56	−38	29
	L PMd	6	29	3.93	−32	−26	64
	L MI ^a	4a		3.38	−36	−32	69

Clusters of proprioception-related brain activation are reported at the cluster-level threshold of $p < 0.05$ FDR corrected.

^aAnatomical locations of more than one maxima. Within each cluster (>20 voxels), only the most significant maximum is listed per anatomical location. BA, Brodmann area; L, left; LWP, left wrist proprioception; PMd, dorsal premotor cortex; R, right; RWP, right wrist proprioception; SFG, superior frontal gyrus; SI, primary somatosensory cortex; SMA, supplementary motor area; SMG, supramarginal gyrus; SPL, superior parietal lobe; MCC, middle cingulate cortex; MI, primary motor cortex; MFG, middle frontal gyrus.

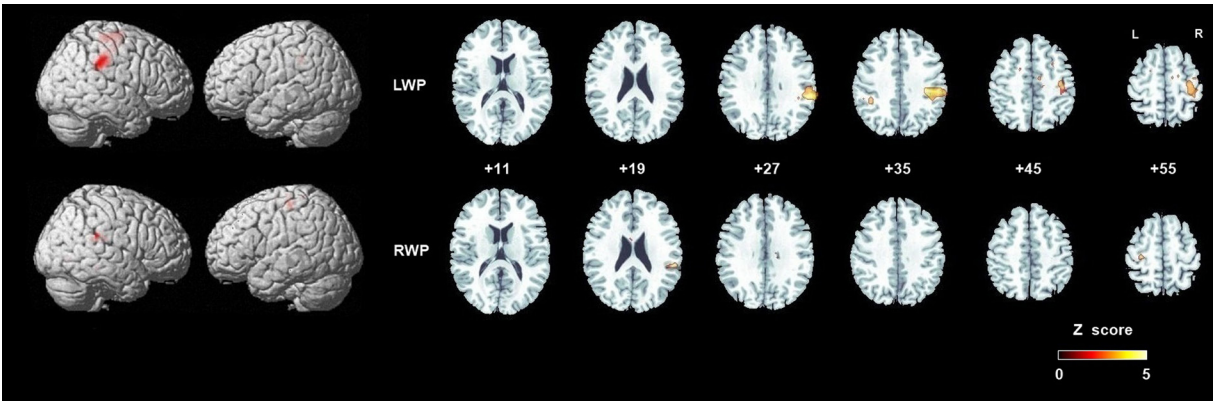


FIGURE 4 | Group analyses of brain activation in healthy participants during proprioception. Group brain activation was overlaid on a whole brain and axial sections of the Montreal Neurological Institute template. Threshold level $p < 0.05$ corrected at the cluster level. Abbreviations: LWP, left wrist proprioception; RWP, right wrist proprioception.

suggested (15, 18, 50–52). Both passive movement and illusory vibration studies identified brain activation in the IPL. Within the IPL, most studies reported proprioception-related brain activation in the parietal operculum (5, 9, 15, 17, 51, 53–55) and only a few reported brain activation in the SMG (6, 18, 56, 57). The SMG is located in the lateral aspect of the IPL whilst the parietal operculum is located medially to the SMG and in the roof of the Sylvian fissure (46). Variability across subjects in the cytoarchitectonic maps of the five areas that occupy the surface SMG has been reported (58) and may have contributed to the variable naming of regions (e.g., parietal operculum compared to SMG) in previous studies. The parietal operculum unlike the SMG is best known for its involvement in the processing of tactile stimuli (59). Tactile stimulation may have accompanied some of the passive movement stimuli in previous studies, for example, from the soles of the feet during ankle dorsiflexion (54, 55). Where tactile stimulation accompanied the proprioceptive

stimulation, it is not possible to identify which of the two stimuli generated activation in the parietal operculum.

The SMG is part of the somatosensory association cortex which has a role in interpretation of tactile sensory information as well as in perception of space and limbs location (15, 18). Previous literature suggests that frontoparietal activation in the SMG and PMC may be related to the spatial processing of stimuli around the hand (60) or the recognition of voluntary movement in the human, equivalent of the mirror neuron system (61). Such functions would rely heavily on knowledge of one's limb position. Indeed Brozzoli et al. (60) showed that the posterior parietal cortex was explicitly responsible for the hand's position sense.

Brain activation in the SMA is the commonest activation in high-order motor cortices identified in illusory vibration (15, 18) and passive movement (51, 54–56, 62, 63) studies. The SMA has been implicated in processes underlying internally guided movements (i.e., active movements). In comparison, the PMd has

TABLE 2 | Individual brain activation loci of stroke-affected participants during proprioception.

Participant and task	Anatomical location	BA	Cluster size	Z score	Talairach coordinates		
					x	y	z
CS1 LWP	L IPL ^a	40/7	272	7.44	-42	-50	53
	L Sup M Gyr ^a	6	182	7.26	-4	22	53
	L SMA (proper)	6		6.99	-4	16	61
	R ITG	37	58	7.22	58	-60	-7
	R SPL	7	111	6.99	16	-72	65
	R IPL ^a	40	149	6.96	40	-54	53
	R SMG ^a	40	126	5.94	56	-38	33
	L PMd ^a	6	87	5.91	-36	-8	65
CS2 RWP	L SPL ^a	7	458	7.26	-26	-56	73
	L SI ^a	2		7.19	-34	-40	57
	L SI ^a	1		6.64	-36	-42	73
	L IPL ^a	40	292	7.15	-54	-40	45
	L STG	41/42		5.76	-64	-42	25
	L SMG	40		5.50	-54	-48	29
	L PMd ^a	6	130	6.37	-24	-20	81
	L SMA (proper)	6		5.99	-6	-14	73
	R SMG ^a	40	80	5.74	56	-46	49
	R IPL ^a	40		5.06	58	-34	57
CS3 RWP	L PMd ^a	6	340	Inf	-32	-14	73
	L MFG	6		4.95	-24	-4	61
	R IPL ^a	40	519	Inf	32	-54	45
	R SMG ^a	40		6.50	40	-38	45
	R SPL ^a	7	421	Inf	12	-86	57
	R cuneus	18/19		Inf	12	-88	49
	L SOG	18		7.19	-10	-88	45
	L cuneus ^a	18		5.11	-6	-98	25
	L SMG ^a	40	304	Inf	-66	-38	37
	L STG	42/37		6.58	-52	-42	25
	R PMd	6	255	7.73	26	-10	69
	L IPL	40	246	7.61	-42	-56	57
	L SPL ^a	7		6.19	-38	-58	69
	L angular gyrus	39		5.46	-48	-62	45
	L ITG	37	71	7.26	-60	-56	-7
	R MOG	19	93	7.02	34	-88	33
	L calc gyrus ^a	17	55	5.48	-20	-64	9

Clusters of proprioception-related brain activation are reported at the cluster-level threshold of $p < 0.05$ FDR corrected.

^aAnatomical locations with more than one maximum. Within each cluster (>50 voxels), only the most significant maximum is listed per anatomical location. BA, Brodmann area; calc gyrus, calcarine gyrus; IPL, inferior parietal lobe; ITG, inferior temporal gyrus; L, left; LWP, left wrist proprioception; MFG, middle frontal gyrus; MOG, middle occipital gyrus; PMd, dorsal premotor cortex; PMv, ventral premotor cortex; R, right; RWP, right wrist proprioception; SI, primary sensory cortex; SMA, supplementary motor area; SMG, supramarginal gyrus; SOG, superior occipital gyrus; SPL, superior parietal lobe; STG, superior temporal gyrus; Sup M Gyr, superior medial gyrus.

been associated with externally guided movements (i.e., passive movements) (64). Given that passive movements are externally imposed, higher activation of PMd than SMA was both expected and found in our study.

Frontal activation in the PMd is important for the processing of proprioception, probably due to the tight coupling between proprioception and its use during movement. Bilateral PMd and right SMG activation was found in a brain imaging study of precision grip but not power grip (65). As proprioception is pivotal for precise motor control (3), it is likely that the frontoparietal brain activation found during precision grip included that of proprioception.

Other lines of research have also found functional association between the SMG and PMd. Anatomical studies in primates showed that proprioceptive information travels to the PMd and that extensive connections exist between the posterior parietal lobe and the PMd (66). In a brain imaging study where healthy

participants were required to integrate proprioceptive information into spatial visual or somatic sensory tasks, frontoparietal activation (especially in the right hemisphere) was found (67). Finally, lesion studies indicated that the integrity of the parietal cortex, frontal cortex, and their connections was required for recovery from spatial neglect (68).

Right Hemispheric Dominance During Proprioception

We found activation of the right SMG during both RWP and LWP, and its activity was reduced in the presence of proprioceptive deficits. Some evidence exists for left laterality of proprioception in the IPL (16, 69). Most of the evidence, however, suggests right hemispheric laterality during proprioception. Illusory vibration studies identified lateralized frontoparietal activation in the right SI (BA 2), middle frontal gyrus (BA 44, 45), parietal operculum,

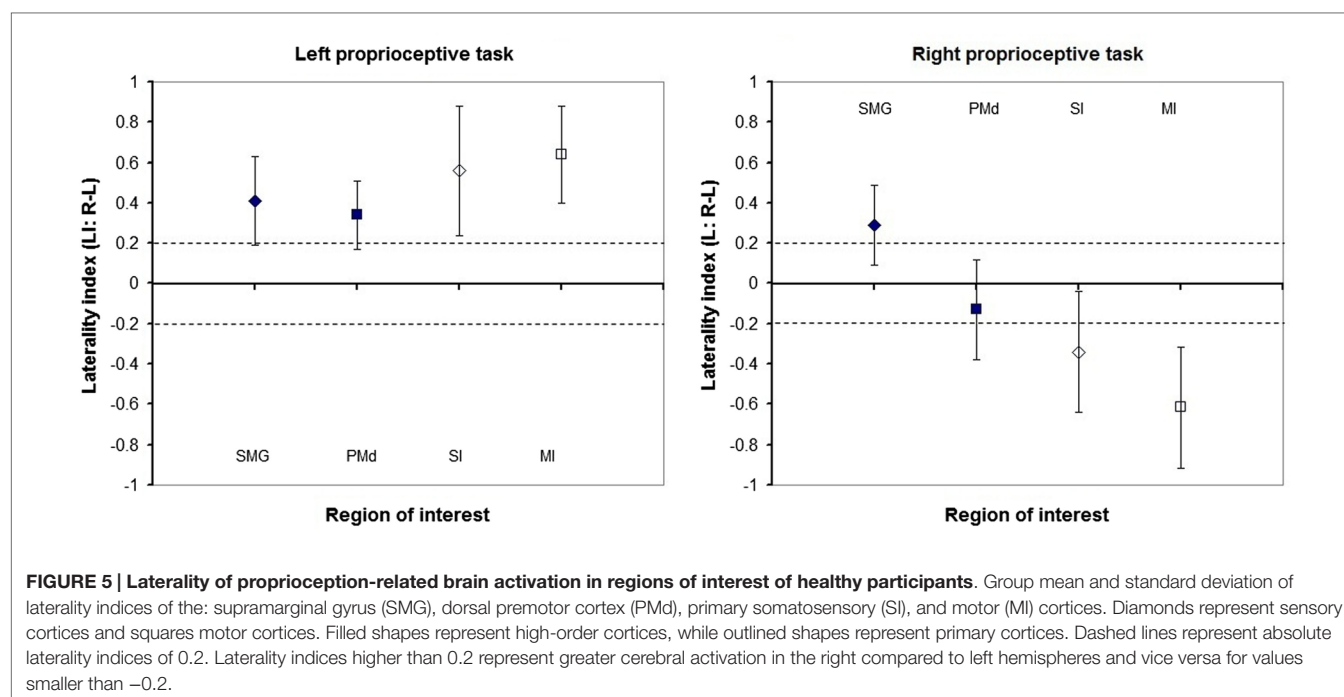


TABLE 3 | Laterality calculations of brain activation during proprioception of healthy and stroke-affected participants.

Anatomical region	Healthy				CS1 LWP LI	CS2 RWP LI	CS3 RWP LI
	LWP LI (n = 12)		RWP LI (n = 6)				
	Mean	SD	Mean	SD			
SMG	0.41	0.22	0.29	0.21	−0.18	−0.19	−0.05
PMd	0.34	0.17	−0.13	0.25	−0.06	0.02	0.18
SI	0.56	0.32	−0.34	0.30	−0.56	0.42	0.19
MI	0.64	0.24	−0.62	0.30	−0.77	0.66	0.59

Positive values indicate right hemisphere activation greater than left and vice versa for negative values. Stroke-affected participants are listed as CS1–3. LI, laterality index; LWP, left wrist proprioception; MI, primary motor cortex; PMd, dorsal premotor cortex; RWP, right wrist proprioception; SI, primary sensory cortex; SMG, supramarginal gyrus.

and insula (15, 17), with one study reporting activation in the SMG rather than the parietal operculum (18). In passive movement studies of left and right limbs, right hemispheric laterality was evident in the superior temporal gyrus and the parietal operculum for ankle movements (55) or bilateral IPL and parietal operculum for wrist movements (51). Our findings provide support for right hemispheric laterality but identify the right SMG in particular as a key region activated during proprioception. The lack of brain activation in the parietal operculum is likely due to the effort made in our study to minimize confounding tactile stimulus.

Right SMG activation during proprioception may be explained by the role that this region plays in spatial processing (70). In their important work, Stephan and colleagues (70) used identical visual stimuli to perform a simple reaction time task, a lingual task or a spatial task. They found that despite the common visual stimuli only the spatial processing task activated the right SMG and the junction of the occipital, parietal, and

temporal lobes. We regard proprioception as a spatial-processing task because it involves judgments of a limb's spatial location. If proprioception is a spatial-processing task and the right SMG is a key brain region involved in spatial processing, then this could explain the significance of right SMG activation found in our study.

Studies of participants with hemispatial neglect have also demonstrated an association with right SMG lesions (71). The diagnosis of hemispatial neglect is often made based on visuo-spatial assessment (72), which involves the extrapersonal space. Committeri et al. (73) showed that lesions in the right SMG were particularly related to impaired spatial processing in the personal space studying a large sample of participants with hemispatial neglect, although proprioception as such was not tested. Our findings raise the question of whether hemispatial neglect caused by right SMG lesions not only affects personal space in general but also affects proprioception specifically.

The Effect of Proprioceptive Deficits Poststroke on the Central Processing of Proprioception

The thalamus was the common lesion site of the three stroke-affected participants included in our study. For two of the participants (CS1 and CS3), the brain lesions extended to the internal capsule, and both displayed more severe proprioceptive deficits on behavioral testing (the Wrist Position Sense Test and the prescan behavioral measures). Similar lesion sites in the thalamus and the internal capsule were found in other studies of participants with proprioceptive deficits (74–79).

We found that SMG activation was bilateral in stroke-affected participants. This was the most significant difference observed from the proprioception-related brain activation patterns in healthy participants, where right SMG laterality was found. The findings from stroke-affected individuals with proprioceptive deficits are consistent with the significance of right SMG integrity for adequate proprioceptive function. In previous brain imaging studies of stroke-affected participants where passive movement stimuli were delivered, participants with somatosensory deficits were specifically excluded (50–52, 77, 80, 81). Our findings are therefore not comparable and are novel for stroke survivors with quantified proprioceptive deficits.

Of interest is our finding of ipsilateral brain activation in SIMI. A similar pattern of ipsilateral rather than contralateral SIMI activation has been found in stroke-affected individuals with motor deficits (82, 83). Furthermore, ipsilateral SIMI activation was found in the studies of participants with tactile deficits who performed a touch discrimination task during scans (84, 85). Our findings suggest that similar to other sensory and motor modalities, proprioceptive deficits are associated with a shift of brain activation to the ipsilateral SIMI.

Study Limitations

Sample size is the main limitation for this study. Twelve participants performed the LWP and only six of them performed the RWP. Due to the smaller RWP group size, group analyses were conducted with a threshold of 0.001 uncorrected for multiple comparisons. Such a threshold increases the risk of false positives, i.e., reporting activation that did not actually occur. To assess the effect of this risk on our results, two additional analyses were conducted. First, group analysis of the LWP was performed at a threshold of 0.05 corrected for multiple comparisons (FDR). Second, a LWP group analysis was conducted for the six participants who also performed the RWP. Results of both analyses showed the same patterns of brain activation were maintained with the same anatomical loci. To minimize the risk of false positives reported in this paper only activation under the threshold of 0.05 corrected at the cluster level was reported. Thus, the additional analyses designed to address limitations related to sample size and threshold, supported the principal proprioception-related brain activation identified in this study.

Contralateral brain activation in SI was not found during RWP. The laterality calculation showed that SI activation during RWP tended to be bilateral. In another brain imaging study of

arm proprioception, bilateral SI activation was found during right stimulation compared to contralateral activation during left stimulation (15). In our study, bilateral SI activation during RWP together with the small sample size was the likely cause for activation not reaching significance level. Thus, bilateral SI activation was under represented in our study.

Clinical Implications

The presence of laterality in proprioception-related brain activation suggests differences in the central processing of proprioception arriving from the left and right limbs. Previous behavioral studies have identified smaller absolute errors for left compared to right limb proprioception (26–28). Our findings together with those of previous brain imaging studies support right hemisphere dominance of proprioception.

Right hemisphere dominance for proprioception has clinical implications for both assessment and treatment. Particular care appears necessary when assessing proprioception in people with brain lesions affecting the right hemisphere, particularly the SMG. The question of which assessment tool to use for proprioceptive assessment is beyond the scope of this paper. However, accurate quantitative tools with normative ranges such as the Wrist Position Sense Test (38) are preferred. A relevant clinical question is the relative contribution of lesions in the right SMG and PMd to proprioceptive deficits.

People with right hemispheric lesions are more likely to require specific proprioceptive rehabilitation. Furthermore, based on the studies of recovery from spatial neglect (68), recovery from proprioceptive deficits may be a function of right SMG and or PMd integrity. A future study examining the relative effect of rehabilitation on right SMG and PMd function would be useful, as would studies on whether normalization of brain activation in these regions correlate with functional recovery.

CONCLUSION

We present a novel and innovative brain imaging study of proprioception, where participants were required to provide a direct response to each stimulus, and where response accuracy was monitored. This is the first time that laterality of proprioception-related brain activation has been directly studied with a natural proprioceptive stimulus (passive movements). This is also the first time that such stimuli have been used to examine brain activation in stroke affected individuals with proprioceptive deficits. We achieved temporal isolation of brain activation during coding of proprioceptive stimuli by using the event-related study design. This activation involved high-order somatosensory and motor cortices, namely the SMG and PMd, respectively. Laterality analyses and lesion studies indicated that the right SMG plays a key role in the processing of proprioception. The results provide a novel insight into the brain–behavior system of proprioception and how it is affected by brain lesions. These insights suggest that people with right hemispheric lesions may be more susceptible to proprioceptive deficits, particularly if the right SMG is affected. As the right SMG is commonly implicated in spatial neglect, it raises important questions of whether spatial neglect and proprioceptive deficits are different or associated

impairments, and what the relative contribution of the SMG and PMd to proprioceptive function might be. If SMG and PMd lesions affect proprioception differently, then it is possible that different treatment methods may be required to address these differential impairments.

AUTHOR CONTRIBUTIONS

EB-S contributed to conception, data collection, analysis, interpretation, and manuscript preparation. TM contributed to conception, interpretation, and critical revision of the manuscript. GP contributed to conception, analysis, and critical revision of the manuscript. AB contributed to conception, analysis, interpretation, and critical revision of the manuscript. LC contributed to conception, data collection, analysis, interpretation, and critical revision of the manuscript.

REFERENCES

- Dukelow SP, Herter TM, Bagg SD, Scott SH. The independence of deficits in position sense and visually guided reaching following stroke. *J Neuroeng Rehabil* (2012) 9:72. doi:10.1186/1743-0003-9-72
- Paschalis V, Nikolaidis MG, Giakas G, Jamurtas AZ, Koutedakis Y. Differences between arms and legs on position sense and joint reaction angle. *J Strength Cond Res* (2009) 23:1652–5. doi:10.1519/JSC.0b013e3181b4382d
- Gandevia S, Burke D. Does the nervous system depend on kinesthetic information to control natural limb movements? *Behav Brain Sci* (1992) 15:614–32.
- Weiller C, Juptner M, Fellows S, Rijntjes M, Leonhardt G, Kiebel S, et al. Brain representation of active and passive movements. *Neuroimage* (1996) 4:105–10. doi:10.1006/nimg.1996.0034
- Radovanovic S, Korotkov A, Ljubisavljevic M, Lyskov E, Thunberg J, Kataeva G, et al. Comparison of brain activity during different types of proprioceptive inputs: a positron emission tomography study. *Exp Brain Res* (2002) 143:276–85. doi:10.1007/s00221-001-0994-4
- Alary F, Doyon B, Loubinoux I, Carel C, Boulanour K, Ranjeva JP, et al. Event-related potentials elicited by passive movements in humans: characterization, source analysis, and comparison to fMRI. *Neuroimage* (1998) 8:377–90. doi:10.1006/nimg.1998.0377
- Ward NS, Newton JM, Swayne OB, Lee L, Thompson AJ, Greenwood RJ, et al. Motor system activation after subcortical stroke depends on corticospinal system integrity. *Brain* (2006) 129:809–19. doi:10.1093/brain/awl002
- Guzzetta A, Staudt M, Petacchi E, Ehlers J, Erb M, Wilke M, et al. Brain representation of active and passive hand movements in children. *Pediatr Res* (2007) 61:485–90. doi:10.1203/pdr.0b013e3180332c2e
- Mima T, Sadato N, Yazawa S, Hanakawa T, Fukuyama H, Yonekura Y, et al. Brain structures related to active and passive finger movements in man. *Brain* (1999) 122:1989–97. doi:10.1093/brain/122.10.1989
- Chang MC, Ahn SH, Cho YW, Son SM, Kwon YH, Lee MY, et al. The comparison of cortical activation patterns by active exercise, proprioceptive input, and touch stimulation in the human brain: a functional MRI study. *NeuroRehabilitation* (2009) 25:87–92. doi:10.3233/NRE-2009-0502
- Georgopoulos AP, Caminiti R, Kalaska JF. Static spatial effects in motor cortex and area 5: quantitative relations in a two-dimensional space. *Exp Brain Res* (1984) 54:446–54. doi:10.1007/BF00235470
- Mountcastle VB, Lynch JC, Georgopoulos A, Sakata H, Acuna C. Posterior parietal association cortex of the monkey: command functions for operations within extrapersonal space. *J Neurophysiol* (1975) 38:871–908.
- Goodwin GM, McCloskey DI, Matthews PB. The contribution of muscle afferents to kinaesthesia shown by vibration induced illusions of movement and by the effects of paralyzing joint afferents. *Brain* (1972) 95:705–48. doi:10.1093/brain/95.4.705

ACKNOWLEDGMENTS

The authors thank the participants for volunteering to take part in this study. We also thank Dr. Rüdiger Seitz for comments on the manuscript. Dr. EB-S was supported by a La Trobe University Post-Graduate Research Award and a grant from the National Health and Medical Research Council, Centre for Clinical Research Excellence (Neuroscience), administered by the National Stroke Research Institute, Melbourne, VIC, Australia. Dr. Leeanne Carey was supported by a National Health and Medical Research Foundation (NHMRC) Career Development Award (number 307905), an Australian Research Council Future Fellowship (number FT0992299), and a McDonnell Foundation Collaborative Award. The work was supported by NHMRC project grants 307902 and 1022694 and the Victorian Government's Operational Infrastructure Support Program. The funding sources had no role in conduct of the study or writing of the report.

- Naito E, Ehrsson H, Geyer S, Zilles K, Roland PE. Illusory arm movements activate cortical motor areas: a positron emission tomography study. *J Neurosci* (1999) 19:6134–44.
- Naito E, Roland PE, Grefkes C, Choi HJ, Eickhoff S, Geyer S, et al. Dominance of the right hemisphere and role of area 2 in human kinaesthesia. *J Neurophysiol* (2005) 93:1020–34. doi:10.1152/jn.00637.2004
- Romaiguere P, Anton JL, Roth M, Casini L, Roll JP. Motor and parietal cortical areas both underlie kinaesthesia. *Brain Res Cogn Brain Res* (2003) 16:74–82. doi:10.1016/S0926-6410(02)00221-5
- Naito E, Nakashima T, Kito T, Aramaki Y, Okada T, Sadato N. Human limb-specific and non-limb-specific brain representations during kinesthetic illusory movements of the upper and lower extremities. *Eur J Neurosci* (2007) 25:3476–87. doi:10.1111/j.1460-9568.2007.05587.x
- Goble DJ, Coxon JP, Van Impe A, Geurts M, Van Hecke W, Sunaert S, et al. The neural basis of central proprioceptive processing in older versus younger adults: an important sensory role for right putamen. *Hum Brain Mapp* (2012) 33:895–908. doi:10.1002/hbm.21257
- Jones LA. Motor illusions: what do they reveal about proprioception? *Psychol Bull* (1988) 103:72–86. doi:10.1037/0033-2909.103.1.72
- Roll JP, Vedel JP, Ribot E. Alteration of proprioceptive messages induced by tendon vibration in man: a microneurographic study. *Exp Brain Res* (1989) 76:213–22. doi:10.1007/BF00253639
- Matthews PBC. *Mammalian Muscle Receptors and Their Central Actions*. London: Edward Arnold (Publishers) Ltd (1972).
- Clark FJ, Burgess PR. Slowly adapting receptors in cat knee joint: can they signal joint angle? *J Neurophysiol* (1975) 38:1448–63.
- Grigg P, Greenspan BJ. Response of primate joint afferent neurons to mechanical stimulation of knee joint. *J Neurophysiol* (1977) 40:1–8.
- Rao SM, Bandettini PA, Binder JR, Bobholz JA, Hammeke TA, Stein EA, et al. Relationship between finger movement rate and functional magnetic resonance signal change in human primary motor cortex. *J Cereb Blood Flow Metab* (1996) 16:1250–4. doi:10.1097/00004647-199611000-00020
- Fox MD, Snyder AZ, Vincent JL, Corbetta M, Van Essen DC, Raichle ME. The human brain is intrinsically organized into dynamic, anticorrelated functional networks. *Proc Natl Acad Sci U S A* (2005) 102:9673–8. doi:10.1073/pnas.0504136102
- Roy EA, MacKenzie C. Handedness effects in kinesthetic spatial location judgements. *Cortex* (1978) 14:250–8. doi:10.1016/S0010-9452(78)80051-3
- Goble DJ, Lewis CA, Brown SH. Upper limb asymmetries in the utilization of proprioceptive feedback. *Exp Brain Res* (2006) 168:307–11. doi:10.1007/s00221-005-0280-y
- Adamo DE, Martin BJ. Position sense asymmetry. *Exp Brain Res* (2009) 192:87–95. doi:10.1007/s00221-008-1560-0
- Carey LM, Matyas TA. Frequency of discriminative sensory loss in the hand after stroke in a rehabilitation setting. *J Rehabil Med* (2011) 43:257–63. doi:10.2340/16501977-0662

30. Carey LM, Matyas TA, Oke LE. Sensory loss in stroke patients: effective training of tactile and proprioceptive discrimination. *Arch Phys Med Rehabil* (1993) 74:602–11. doi:10.1016/0003-9993(93)90158-7
31. Smania N, Montagnana B, Faccioli S, Fiaschi A, Aglioti SM. Rehabilitation of somatic sensation and related deficit of motor control in patients with pure sensory stroke. *Arch Phys Med Rehabil* (2003) 84:1692–702. doi:10.1053/S0003-9993(03)00277-6
32. Carey LM, Matyas TA. Training of somatosensory discrimination after stroke: facilitation of stimulus generalization. *Am J Phys Med Rehabil* (2005) 84:428–42. doi:10.1097/01.PHM.0000159971.12096.7F
33. Dechaumont-Palacin S, Marque P, De Boissezon X, Castel-Lacanal E, Carel C, Berry I, et al. Neural correlates of proprioceptive integration in the contralesional hemisphere of very impaired patients shortly after a subcortical stroke: an fMRI study. *Neurorehabil Neural Repair* (2008) 22:154–65. doi:10.1177/1545968307307118
34. Carey JR, Kimberley TJ, Lewis SM, Auerbach EJ, Dorsey L, Rundquist P, et al. Analysis of fMRI and finger tracking training in subjects with chronic stroke. *Brain* (2002) 125:773–88. doi:10.1093/brain/awf091
35. Oldfield RC. The assessment and analysis of handedness: the Edinburgh inventory. *Neuropsychologia* (1971) 9:97–113. doi:10.1016/0028-3932(71)90067-4
36. Adamo DE, Martin BJ, Brown SH. Age-related differences in upper limb proprioceptive acuity. *Percept Mot Skills* (2007) 104:1297–309. doi:10.2466/PMS.104.3.1297-1309
37. Huettel SA, Singerman JD, McCarthy G. The effects of aging upon the hemodynamic response measured by functional MRI. *Neuroimage* (2001) 13:161–75. doi:10.1006/nimg.2000.0675
38. Carey LM, Oke LE, Matyas TA. Impaired limb position sense after stroke: a quantitative test for clinical use. *Arch Phys Med Rehabil* (1996) 77:1271–8. doi:10.1016/S0003-9993(96)90192-6
39. Miezin FM, Maccotta L, Ollinger JM, Petersen SE, Buckner RL. Characterizing the hemodynamic response: effects of presentation rate, sampling procedure, and the possibility of ordering brain activity based on relative timing. *Neuroimage* (2000) 11:735–59. doi:10.1006/nimg.2000.0568
40. Hall LA, McCloskey DI. Detections of movements imposed on finger, elbow and shoulder joints. *J Physiol* (1983) 335:519–33. doi:10.1113/jphysiol.1983.sp014548
41. Binkofski F, Seitz RJ, Arnold S, Classen J, Benecke R, Freund HJ. Thalamic metabolism and corticospinal tract integrity determine motor recovery in stroke. *Ann Neurol* (1996) 39:460–70. doi:10.1002/ana.410390408
42. Talairach J. *Co-Planar Stereotaxic Atlas of the Human Brain: 3-Dimensional Proportional System: An Approach to Cerebral Imaging*. New York, NY: G. Thieme; Thieme Medical Publishers (1988).
43. Crinion J, Ashburner J, Leff A, Brett M, Price C, Friston K. Spatial normalization of lesioned brains: performance evaluation and impact on fMRI analyses. *Neuroimage* (2007) 37:866–75. doi:10.1016/j.neuroimage.2007.04.065
44. Hutchinson S, Kobayashi M, Horkan CM, Pascual-Leone A, Alexander MP, Schlaug G. Age-related differences in movement representation. *Neuroimage* (2002) 17:1720–8. doi:10.1006/nimg.2002.1309
45. Naccarato M, Calautti C, Jones PS, Day DJ, Carpenter TA, Baron JC. Does healthy aging affect the hemispheric activation balance during paced index-to-thumb opposition task? An fMRI study. *Neuroimage* (2006) 32:1250–6. doi:10.1016/j.neuroimage.2006.05.003
46. Eickhoff SB, Amunts K, Mohlberg H, Zilles K. The human parietal operculum. II. Stereotaxic maps and correlation with functional imaging results. *Cereb Cortex* (2006) 16:268–79. doi:10.1093/cercor/bhi106
47. Mayka MA, Corcos DM, Leurgans SE, Vaillancourt DE. Three-dimensional locations and boundaries of motor and premotor cortices as defined by functional brain imaging: a meta-analysis. *Neuroimage* (2006) 31:1453–74. doi:10.1016/j.neuroimage.2006.02.004
48. Fernandez G, De Greiff A, Von Oertzen J, Reuber M, Lun S, Klaver P, et al. Language mapping in less than 15 minutes: real-time functional MRI during routine clinical investigation. *Neuroimage* (2001) 14:585–94. doi:10.1006/nimg.2001.0854
49. Deblaere K, Boon PA, Vandemaele P, Tieleman A, Vonck K, Vingerhoets G, et al. MRI language dominance assessment in epilepsy patients at 1.0 T: region of interest analysis and comparison with intracarotid amyltal testing. *Neuroradiology* (2004) 46:413–20. doi:10.1007/s00234-004-1196-0
50. Loubinoux I, Carel C, Pariente J, Dechaumont S, Albuher JF, Marque P, et al. Correlation between cerebral reorganization and motor recovery after subcortical infarcts. *Neuroimage* (2003) 20:2166–80. doi:10.1016/j.neuroimage.2003.08.017
51. Ward NS, Brown MM, Thompson AJ, Frackowiak RS. Longitudinal changes in cerebral response to proprioceptive input in individual patients after stroke: an fMRI study. *Neurorehabil Neural Repair* (2006) 20:398–405. doi:10.1177/1545968306286322
52. Van de Winckel A, Wenderoth N, De Weerd W, Snaert S, Peeters R, Van Hecke W, et al. Frontoparietal involvement in passively guided shape and length discrimination: a comparison between subcortical stroke patients and healthy controls. *Exp Brain Res* (2012) 220:179–89. doi:10.1007/s00221-012-3128-2
53. Reddy H, Floyer A, Donaghy M, Matthews PM. Altered cortical activation with finger movement after peripheral denervation: comparison of active and passive tasks. *Exp Brain Res* (2001) 138:484–91. doi:10.1007/s002210100732
54. Sahyoun C, Floyer-Lea A, Johansen-Berg H, Matthews PM. Towards an understanding of gait control: brain activation during the anticipation, preparation and execution of foot movements. *Neuroimage* (2004) 21:568–75. doi:10.1016/j.neuroimage.2003.09.065
55. Ciccarelli O, Toosy AT, Marsden JF, Wheeler-Kingshott CM, Sahyoun C, Matthews PM, et al. Identifying brain regions for integrative sensorimotor processing with ankle movements. *Exp Brain Res* (2005) 166:31–42. doi:10.1007/s00221-005-2335-5
56. Carel C, Loubinoux I, Boulanouar K, Manelfe C, Rascol O, Celsis P, et al. Neural substrate for the effects of passive training on sensorimotor cortical representation: a study with functional magnetic resonance imaging in healthy subjects. *J Cereb Blood Flow Metab* (2000) 20:478–84. doi:10.1097/00004647-200003000-00006
57. Loubinoux I, Carel C, Alary F, Boulanouar K, Viallard G, Manelfe C, et al. Within-session and between-session reproducibility of cerebral sensorimotor activation: a test – retest effect evidenced with functional magnetic resonance imaging. *J Cereb Blood Flow Metab* (2001) 21:592–607. doi:10.1097/00004647-200105000-00014
58. Caspers S, Eickhoff SB, Geyer S, Scheperjans F, Mohlberg H, Zilles K, et al. The human inferior parietal lobule in stereotaxic space. *Brain Struct Funct* (2008) 212(6):481–95. doi:10.1007/s00429-008-0195-z
59. Rowe MJ, Turman AB, Murray GM, Zhang HQ. Parallel organization of somatosensory cortical areas I and II for tactile processing. *Clin Exp Pharmacol Physiol* (1996) 23:931–8. doi:10.1111/j.1440-1681.1996.tb01145.x
60. Brozzoli C, Gentile G, Ehrsson HH. That's near my hand! Parietal and premotor coding of hand-centered space contributes to localization and self-attribution of the hand. *J Neurosci* (2012) 32(42):14573–82. doi:10.1523/JNEUROSCI.2660-12.2012
61. Cattaneo L, Rizzolatti G. The mirror neuron system. *Arch Neurol* (2009) 66(5):557–60. doi:10.1001/archneurol.2009.41
62. Bernard RA, Goran DA, Sakai ST, Carr TH, Mcfarlane D, Nordell B, et al. Cortical activation during rhythmic hand movements performed under three types of control: an fMRI study. *Cogn Affect Behav Neurosci* (2002) 2:271–81. doi:10.3758/CABN.2.3.271
63. Thickbroom GW, Byrnes ML, Mastaglia FL. Dual representation of the hand in the cerebellum: activation with voluntary and passive finger movement. *Neuroimage* (2003) 18:670–4. doi:10.1016/S1053-8119(02)00055-1
64. Schubotz RI, von Cramon DY. Functional-anatomical concepts of human premotor cortex: evidence from fMRI and PET studies. *Neuroimage* (2003) 20(Suppl 1):S120–31. doi:10.1016/j.neuroimage.2003.09.014
65. Ehrsson HH, Fagergren A, Jonsson T, Westling G, Johansson RS, Forssberg H. Cortical activity in precision- versus power-grip tasks: an fMRI study. *J Neurophysiol* (2000) 83:528–36.
66. Wise SP, Boussaoud D, Johnson PB, Caminiti R. Premotor and parietal cortex: corticocortical connectivity and combinatorial computations. *Annu Rev Neurosci* (1997) 20:25–42. doi:10.1146/annurev.neuro.20.1.25
67. Galati G, Committeri G, Sanes JN, Pizzamiglio L. Spatial coding of visual and somatic sensory information in body-centred coordinates. *Eur J Neurosci* (2001) 14:737–46. doi:10.1046/j.0953-816x.2001.01674.x
68. Corbetta M, Kincade MJ, Lewis C, Snyder AZ, Sapir A. Neural basis and recovery of spatial attention deficits in spatial neglect. *Nat Neurosci* (2005) 8:1603–10. doi:10.1038/nn1574
69. Alary F, Simoes C, Jousmaki V, Forss N, Hari R. Cortical activation associated with passive movements of the human index finger: an MEG study. *Neuroimage* (2002) 15:691–6. doi:10.1006/nimg.2001.1010

70. Stephan KE, Marshall JC, Friston KJ, Rowe JB, Ritzl A, Zilles K, et al. Lateralized cognitive processes and lateralized task control in the human brain. *Science* (2003) **301**:384–6. doi:10.1126/science.1086025
71. Doricchi F, Tomaiuolo F. The anatomy of neglect without hemianopia: a key role for parietal-frontal disconnection? *Neuroreport* (2003) **14**:2239–43. doi:10.1097/00001756-200312020-00021
72. Halligan PW, Marshall JC, Wade DT. Visuospatial neglect: underlying factors and test sensitivity. *Lancet* (1989) **2**:908–11. doi:10.1016/S0140-6736(89)91561-4
73. Committeri G, Pitzalis S, Galati G, Patria F, Pelle G, Sabatini U, et al. Neural bases of personal and extrapersonal neglect in humans. *Brain* (2007) **130**:431–41. doi:10.1093/brain/awl265
74. Sacco RL, Bello JA, Traub R, Brust JC. Selective proprioceptive loss from a thalamic lacunar stroke. *Stroke* (1987) **18**:1160–3. doi:10.1161/01.STR.18.6.1160
75. Gutrecht JA, Zamani AA, Pandya DN. Lacunar thalamic stroke with pure cerebellar and proprioceptive deficits. *J Neurol Neurosurg Psychiatry* (1992) **55**:854–6. doi:10.1136/jnnp.55.9.854
76. Shintani S, Tsuruoka S, Shiigai T. Pure sensory stroke caused by a cerebral hemorrhage: clinical-radiologic correlations in seven patients. *Am J Neuroradiol* (2000) **21**:515–20.
77. Thiel A, Aleksic B, Klein J, Rudolf J, Heiss WD. Changes in proprioceptive systems activity during recovery from post-stroke hemiparesis. *J Rehabil Med* (2007) **39**:520–5. doi:10.2340/16501977-0089
78. Lee MY, Kim SH, Choi BY, Chang CH, Ahn SH, Jang SH. Functional MRI finding by proprioceptive input in patients with thalamic hemorrhage. *NeuroRehabilitation* (2012) **30**:131–6. doi:10.3233/NRE-2012-0736
79. Kenzie JM, Semrau JA, Findlater SE, Herter TM, Hill MD, Scott SH, et al. Anatomical correlates of proprioceptive impairments following acute stroke: a case series. *J Neurol Sci* (2014) **342**:52–61. doi:10.1016/j.jns.2014.04.025
80. Tombari D, Loubinoux I, Pariente J, Gerdelat A, Albucher JF, Tardy J, et al. A longitudinal fMRI study: in recovering and then in clinically stable sub-cortical stroke patients. *Neuroimage* (2004) **23**:827–39. doi:10.1016/j.neuroimage.2004.07.058
81. Lindberg PG, Schmitz C, Engardt M, Forssberg H, Borg J. Use-dependent up- and down-regulation of sensorimotor brain circuits in stroke patients, proprioception intact. *Neurorehabil Neural Repair* (2007) **21**:315–26. doi:10.1177/1545968306296965
82. Feydy A, Carlier R, Roby-Brami A, Bussel B, Cazalis F, Pierot L, et al. Longitudinal study of motor recovery after stroke: recruitment and focusing of brain activation. *Stroke* (2002) **33**:1610–7. doi:10.1161/01.STR.0000017100.68294.52
83. Calautti C, Baron JC. Functional neuroimaging studies of motor recovery after stroke in adults: a review. *Stroke* (2003) **34**:1553–66. doi:10.1161/01.STR.0000071761.36075.A6
84. Carey LM, Abbott DF, Puce A, Jackson GD, Syngieniotis A, Donnan GA. Reemergence of activation with poststroke somatosensory recovery: a serial fMRI case study. *Neurology* (2002) **59**:749–52. doi:10.1212/WNL.59.5.749
85. Carey LM, Abbott DF, Harvey MR, Puce A, Seitz RJ, Donnan GA. Relationship between touch impairment and brain activation after lesions of subcortical and cortical somatosensory regions. *Neurorehabil Neural Repair* (2011) **25**:443–57. doi:10.1177/1545968310395777

Conflict of Interest Statement: The authors declare that the research was conducted in the absence of any commercial or financial relationships that could be construed as a potential conflict of interest.

Copyright © 2015 Ben-Shabat, Matyas, Pell, Brodtmann and Carey. This is an open-access article distributed under the terms of the Creative Commons Attribution License (CC BY). The use, distribution or reproduction in other forums is permitted, provided the original author(s) or licensor are credited and that the original publication in this journal is cited, in accordance with accepted academic practice. No use, distribution or reproduction is permitted which does not comply with these terms.



Supplementary motor complex and disturbed motor control – a retrospective clinical and lesion analysis of patients after anterior cerebral artery stroke

Florian Brugger^{1,2}, Marian Galovic¹, Bruno J. Weder³ and Georg Kägi^{1*}

¹ Klinik für Neurologie, Kantonsspital St. Gallen, St. Gallen, Switzerland, ² Sobell Department of Motor Neuroscience and Movement Disorders, University College London, London, UK, ³ Support Center of Advanced Neuroimaging, Inselspital, Bern, Switzerland

OPEN ACCESS

Edited by:

Jean-Claude Baron,
University of Cambridge, UK

Reviewed by:

Pavel Lindberg,
Université Paris Descartes, France
Emmanuel Carrera,
University of Geneva, Switzerland
Alexandra L. Borstad,
The Ohio State University, USA

*Correspondence:

Georg Kägi,
Department of Neurology,
Kantonsspital St. Gallen,
Rorschacherstrasse 95, St. Gallen
CH-9007, Switzerland
georg.kaegi@kssg.ch

Specialty section:

This article was submitted to
Stroke, a section of the
journal *Frontiers in Neurology*

Received: 15 May 2015

Accepted: 14 September 2015

Published: 12 October 2015

Citation:

Brugger F, Galovic M, Weder BJ and
Kägi G (2015) Supplementary motor
complex and disturbed motor
control – a retrospective clinical and
lesion analysis of patients after
anterior cerebral artery stroke.
Front. Neurol. 6:209.
doi: 10.3389/fneur.2015.00209

Background: Both the supplementary motor complex (SMC), consisting of the supplementary motor area (SMA) proper, the pre-SMA, and the supplementary eye field, and the rostral cingulate cortex are supplied by the anterior cerebral artery (ACA) and are involved in higher motor control. The Bereitschaftspotential (BP) originates from the SMC and reflects cognitive preparation processes before volitional movements. ACA strokes may lead to impaired motor control in the absence of limb weakness and evoke an alien hand syndrome (AHS) in its extreme form.

Aim: To characterize the clinical spectrum of disturbed motor control after ACA strokes, including signs attributable to AHS and to identify the underlying neuroanatomical correlates.

Methods: A clinical assessment focusing on signs of disturbed motor control including intermanual conflict (i.e., bilateral hand movements directed at opposite purposes), lack of self-initiated movements, exaggerated grasping, motor perseverations, mirror movements, and gait apraxia was performed. Symptoms were grouped into (A) AHS-specific and (B) non-AHS-specific signs of upper limbs, and (C) gait apraxia. Lesion summation mapping was applied to the patients' MRI or CT scans to reveal associated lesion patterns. The BP was recorded in two patients.

Results: Ten patients with ACA strokes (nine unilateral, one bilateral; mean age: 74.2 years; median NIH-SS at admission: 13.0) were included in this case series. In the acute stage, all cases had marked difficulties to perform volitional hand movements, while movements in response to external stimuli were preserved. In the chronic stage (median follow-up: 83.5 days) initiation of voluntary movements improved, although all patients showed persistent signs of disturbed motor control. Impaired motor control is predominantly associated with damaged voxels within the SMC and the anterior and medial cingulate cortex, while lesions within the pre-SMA are specifically related to AHS. No BP was detected over the damaged hemisphere.

Conclusion: ACA strokes involving the premotor cortices, particularly the pre-SMA, are associated with AHS-specific signs. In the acute phase, motor behavior is characterized by the inability to carry out self-initiated movements. Motor control deficits may persist to a variable degree beyond the acute phase. Alterations of the BP point to an underlying SMC dysfunction in AHS.

Keywords: anterior cerebral artery, stroke, supplementary motor area, anterior cingulate cortex, Bereitschaftspotential

Introduction

Voluntary and involuntary movements are generated and controlled by a complex bihemispheric neuronal network involving the primary motor (MI) and supplementary motor complex [SMC; consisting of the supplementary motor area (SMA) proper and pre-SMA], cingulate cortex, and dorsolateral prefrontal cortex as well as a number of subcortical brain structures such as the basal ganglia and the cerebellum. Motor areas supplied by the anterior cerebral artery (ACA) involve the SMC, the anterior and middle cingulate cortex, and the rostral section of the corpus callosum. This part of the motor network is particularly involved in the generation of self-initiated (i.e., volitional), complex movement sequences, inhibition of purposeless movements triggered by external stimuli such as the grasp reflex, error control during motor performance, and motor learning (1, 2). An electrophysiological measure of voluntary control is available with the so-called Bereitschaftspotential (BP). The BP is a negative potential over the vertex emerging approximately 1 s before the onset of a voluntary movement. The early component most presumably originates from the SMA, while the later component is mainly assigned to the primary motor cortex and the lateral premotor cortex (3). The BP probably reflects cognitive processes preceding the initiation of volitional movements (4). According to recent computational frameworks for action, both conscious awareness of intention and a sense of agency characterize voluntary movements (5). By applying direct electrical stimulation to the SMC, a conscious intention of moving can be provoked underlining its role in generating volitional movements (6).

As previously mentioned, ACA strokes lead to a severe disruption of the above-mentioned motor network. The clinical spectrum of disturbed motor control after ACA strokes may encompass signs such as involuntary grasping of nearby objects, utilization behavior, and intermanual conflicts (i.e., the two hands are directed at opposite purposes) with absence of volitional movements (7). Underutilization of one body side in the absence of relevant weakness or sensory disturbances or deficits of reflexes, as it can be observed in ACA strokes, has been summarized under the term “motor neglect” (8). Apart from limb weakness, the above-mentioned motor signs have been acknowledged as characteristic features of the so-called alien hand syndrome (AHS) (9, 10). Its first description was rendered by Goldstein in 1908 who reported “a type of apraxia with the feeling of estrangement

between the patient and his hand” (11). In 1972, Brion and Jeydnak observed analogous symptoms in a patient with a corpus callosum tumor, which inspired them to coin the term “la main étrangère.” It was subsequently translated into the English term “alien hand” (12, 13).

It has turned out that the clinical picture of AHS is variable and reflects a spectrum of abnormalities in motor control rather than a homogeneous clinical entity (14). Dolado et al. proposed following hallmarks as essential for the diagnosis of an AHS: (i) a feeling of foreignness of the affected limb, (ii) failure to recognize ownership of it when visual clues are removed, (iii) autonomous motor activities that are perceived as involuntary and are different from other identifiable movement disorder, and (iv) attribution of an action to another subject due to lacking sense of agency (15). Lesions within the SMC, the cingulate cortex and the corpus callosum have often been implicated in the context of AHS (10).

Although AHS has been known for a very long time, there is no comprehensive clinical-anatomical correlation addressing impaired motor control in a larger number of ACA stroke patients. Hitherto, most of the published literature is restricted to case reports and case series [reviewed in (7, 16, 17)]. The only systematic approaches published suffer from methodological drawbacks, including definitions that are too wide apart with regard to disturbed motor control and/or the lack of using adequate imaging methods (16, 17). Therefore, the aim of this case series was to characterize the clinical spectrum of disrupted motor control, including signs attributable to AHS and to identify the main underlying neuroanatomical correlates (18). We hypothesized that an involvement of the SMC is essential for the occurrence of the AHS spectrum of disturbed motor control after ACA strokes.

Patients and Methods

Study Population

Over a period of 6 years, patients with arm paresis or plegia, after circumscribed ACA infarction were identified at our center and included in this case series. Conscious awareness of intention and sense of agency of volitional movements of the affected limb, both thought to be key features of an AHS, were the main focus of this study (5). On the basis of these two key features, clinical signs of disturbed motor control were classified into three different groups (7, 10, 13, 15–17, 19–31). Group A included AHS-specific signs, namely (A.I) lack of self-initiated movements, (A.II) exaggerated (not suppressible) grasping and groping behavior, and (A.III) presence of an intermanual conflict (i.e., the two hands are directed at opposite purposes). Group B included clinical signs, which did not necessarily reflect disturbed

Abbreviations: ACA, anterior cerebral artery; AHS, alien hand syndrome; BP, Bereitschaftspotential; MNI, Montreal National Institute; NIHSS, National Institute of Health Stroke Scale; SMA, supplementary motor area; SMC, supplementary motor cortex; SPM, statistical parametric mapping; VOI, volume of interest.

awareness of intention and sense of agency. These symptoms were thus considered as non-AHS-specific signs of disturbed motor control: (B.I) maintaining a particular limb position after a preceding complex motor task (i.e., motor perseveration), (B.II) Co-activation of the contralateral limb during volitional movements of the ipsilateral limb (i.e., mirror movements), and (B.III) any form of tremor. Group C included symptoms, which were signs beyond disturbed motor control of the upper limbs: (C.I) in this group, gait apraxia was expected (21). The study was approved by the ethics committee of the Kanton St. Gallen and was conducted according to GCP guidelines.

Epidemiological Data and Clinical Tests

Demographics and disease characteristics, including National Institute of Health Stroke Scale (NIHSS)-scores and stroke etiology according to TOAST criteria (32), were taken from the patients' records. All patients underwent a standard neurological examination. The following procedures were used to screen clinically for the aforementioned clinical signs of disturbed motor control: (A.I) *impaired self-initiated movements* were studied by observing volitional gestures and the interaction with the examiner during taking the history and the clinical assessment. Furthermore, patients were asked to voluntarily perform tasks such as virtual piano playing or typing on a keyboard. Testing of muscle strength was difficult in the acute phase due to the inability to perform voluntary movements, but weakness was excluded in the subacute stage in all cases. (A.II) *The presence of an intermanual conflict* was evaluated by antiphasic upper limb movements (i.e., windmill-like movements of both arms), transferring objects from one hand to the other or by performing bimanual tasks (e.g., putting on glasses). A marked shift or loss of phase, disturbances on performing coordinated bimanual tasks, and purposeless counteracting of upper limbs during bimanual tasks were attributed to the presence of an intermanual conflict. (A.III) *Exaggerated grasping behavior* was tested by moving objects nearby in the visual field and by asking them to suppress compulsive grasping. Patients were also observed when they released objects or when they transferred objects from one hand to the other. (B.I) *Motor perseveration* was defined as maintaining a particular hand position, which was clearly related to a preceding (complex) motor task. (B.II) *Mirror movements* were picked up during the assessment of the affected hand by observing the contralateral one and vice versa. (B.III) We also screened our patients for any form of resting, postural and action *tremor*. (C.I) *Gait apraxia* was assessed in those patients who were able to walk independently. They were asked to walk along the corridor and to turn toward and away from the affected side. Shuffling gait with high cadence and paroxysmal interruption of locomotion, with trembling of the feet in place and preserved (seemingly paradoxical) ability to increase step length and height when stepping over an object on the floor or when presenting cueing signals, were considered as signs of gait apraxia (33). Patients were asked if they had the feeling of their feet being glued on the floor.

Typical clinical signs of disturbed motor control in the context of an ACA stroke, as specified above, were documented according to a predefined protocol. In nine patients (with exception from patient P6), videos of the clinical examination as detailed

above were available for retrospective review. In P6, who explicitly declined video monitoring, symptoms were documented in detail in his hospital files. Symptom severity and persistence were rated by a neurologist in a semi-quantitative manner: clinical symptoms were considered as severe (+++), if they were permanently present and/or if they were a relevant source of impairment in the patient's ability to carry out the clinical test. Severity was considered as moderate (++), if symptoms were frequently present, but only mildly interfered with the patient's ability to carry out the clinical test. If there was just a hint of a particular sign or if the respective sign occurred only rarely, it was considered as mild (+). Absence of a particular sign was rated as "0." Notably, due to the lack of validated clinical scores, this scale has been designed for the purpose of this case series. To assess the reliability of this rating, a second blinded examiner rated the videos and the interrater reliability rate (IRR) was calculated by the means of kappa statistics. Calculations yielded a kappa coefficient of 0.83 ± 0.12 observed as proportion of maximum possible kappa thus indicating a good IRR.

Bereitschaftspotential (Readiness Potential)

The BP was recorded by using an EEG-EMG polygraphy. The EEG electrodes were placed over C3, C4, and Cz and the reference over Fpz according to the 10–20 EEG system. The ground electrode was fixed at the ear lobe. Patients were asked to keep their eyes closed and to repetitively perform briskly initiated middle finger extensions of 1-s duration in a self-paced manner, with an interval between each movement of approximately 6–7 s. Before the actual recording, they were instructed how to perform the finger movements while getting the sense for timing and movement initiation. To generate entirely self-initiated movements, they were instructed not to count or to pace the movement onset by using any other form of rhythmical encoding (e.g., by humming). They were also advised to fully shift their attention on the finger movement and to avoid falling asleep. Muscle activity was recorded from the long finger extensors by surface EMG. To avoid blinking, particularly at the time of movement initiation, we positioned two small sand bags over their eyelids. Eighty to 100 sequences of middle finger extensions were recorded from each hand. The BP was calculated offline using the ASA software (ENT Enschede, Netherlands). At least 50 artifact-free EEG epochs lasting from 2.0 s before to 1.0 s after motor onset were chosen and averaged for each limb separately. The BP was baseline corrected by averaging the epoch 1.5–2.0 s before motor onset. The amplitude at 0.25, 0.50, 0.75, 1.00, 1.25, and 1.25 s before and 0.25, 0.50, 0.75, and 1.00 s after motor onset as well at motor onset was calculated by averaging all data points acquired 50 ms before and after each respective time point (34). The results were then plotted against the grand average of the BP from 13 healthy controls.

Lesion Summation Mapping

Images were acquired within the first days after hospital submission (median 2.5 days; range 0–30). Isotropic diffusion weighted imaging (DWI) sequences and T1 sequences were acquired in a 1.5 T or a 3 T MRI scanner (T1: slice thickness 5 mm, DWI: $b = 1000 \text{ s/m}^2$, slice thickness 4 mm). We used DWI sequences for lesion analysis as they showed the best contrast for ischemic

brain tissue. In two patients, only CT scans were available. In both patients, however, the scans already showed a clearly demarcated ischemic brain lesion. Hence, they were feasible for reliably drawing lesion maps and were included for further imaging analysis.

For pre-processing of the scans, DWI and T1 sequences were first co-registered using Statistical Parametric Mapping 8 (SPM8)¹ (18, 35). According to the general agreement for working in the stereotaxic standard space, the anterior commissure was defined as the origin of the coordinate system in all scans (MNI-coordinates $x = 0, y = 0, z = 0$). The ischemic lesions were drawn manually on the DWI sequences using the freely available MRIcron software² and the drawings were put together to a 3D volume of interest (VOI). Both DWI and T1-weighted sequences were normalized to a MRI template and T1-weighted images were segmented by the means of the Clinical Toolbox running on SPM8³. The lesion maps were entered as masks in the algorithm for cost function masking to avoid distortion of the voxels within the ischemic lesion during spatial normalization. CT normalization routine integrated in the Clinical Toolbox was used analogously to normalize CT scans to a standard space template. Afterwards, all lesions were flipped to the left side to enhance power of the analysis. In the patient with a bilateral ACA infarction, the larger hemispheric volume defect was accordingly flipped to the left side.

Calculation of lesion maps was done in three steps. (1) Weighted summation (overlap) maps were calculated in SPM 8 for each clinical sign. Only VOIs from patients showing a particular sign were included in the retrospective calculation (see **Table 1**). A Kernel filter with 4 mm full-width half maximum was used to slightly smooth the summation maps. Each map was then thresholded to voxels damaged in >25% of our patients showing the respective clinical sign. (2) Summation maps for each symptom group (A, B, C) were created by using the image calculator function integrated in SPM8. The respective summation maps were calculated by summing up the summation maps of the different symptoms included in groups A and B, respectively. The summation map of group C was identical to the map for gait apraxia and therefore did not require further calculation. (3) To address the question which part of the ischemic lesions contributes to

disturbed motor control of upper limbs in general, the union set of group A and B ($A \cup B$) and the set difference of $(A \cap B) \setminus C$ were calculated. To address the question which brain section is specific for symptoms of the AHS spectrum, the set difference of $A \setminus (B \cup C)$ was calculated. Prior to calculation of all these sets, each group summation map was transferred into binary maps using the SPM8 image calculator.

In a final step, each lesion map was plotted onto the automated anatomical label (AAL) atlas using MRIcron and the involved brain areas as well as the center of gravity were identified by the respective built-in function. As the AAL does not distinguish between the pre-SMA and SMA proper, ROIs with the anterior commissural line as the border between these two areas (1, 36) were manually drawn in MRIcron and were used to determine the number of damaged voxels encompassed by each subsection.

Results

Study Populations

Information from 10 patients aged between 63 and 87 years (mean 74.2) were available. Among them were eight males and two females. Initial NIHSS ranged from 2 to 21 points (median 13.0). Seven patients were followed up from the acute stage and three patients were added after reviewing our stroke database and clinical notes from the last 2 years. All patients investigated in the acute stage had disturbed conscious awareness of intention and sense of agency. The first signs of recovery occurring within days were involuntary finger movements elicited by touching their palm. In one patient, information on these features were missing. Five patients had an ischemic lesion within the left hemispheric ACA territory, four within the right and one had large bilateral ACA infarctions. The lesion pattern ranged from circumscribed infarcts confined to the SMA to bilateral territorial infarcts within the ACA territory. According to the TOAST criteria (32), macroangiopathy was identified as a stroke etiology in 3/10 patients, cardioembolic events in 6/10, and arterial emboli secondary to aneurysm coiling in the ACA in 1/10. Detailed clinical and radiological information are summarized in **Table 1**.

Signs of Motor Control

Initially, all cases had marked difficulties to perform volitional hand movements. In the acute setting, 9/10 patients presented

¹<http://www.fil.ion.ucl.ac.uk/>

²<http://www.mccauslandcenter.sc.edu>

³<http://www.mricron.com/clinical-toolbox/>

TABLE 1 | Baseline demographic data and clinical findings.

No	Age (years)	Sex	First ever stroke	Stroke etiology	NIHSS-score
P1	83	Female	Total right-sided ACA stroke	Cardioembolism	15
P2	82	Male	Partial left-sided ACA	Cardioembolism	17
P3	74	Male	Partial left-sided ACA	Cardioembolism	21
P4	87	Female	Total right-sided ACA infarct	Cardioembolism	7
P5	63	Male	Total bilateral ACA infarct	Cardioembolism	15
P6	75	Male	Partial left-sided ACA infarct	Cardioembolism	16
P7	69	Male	Partial left-sided ACA infarct	Large artery arteriosclerosis	3
P8	70	Male	Total right-sided ACA infarct	Large artery arteriosclerosis	6
P9	65	Male	Partial left-sided ACA infarct	Stroke of other determined etiology (Secondary to aneurysma coiling)	11
P10	74	Male	Partial right-sided ACA infarct	Large artery arteriosclerosis	7
					2

Stroke etiology according to Toast criteria; ACA, anterior cerebral artery; NIHSS, National institute of health stroke scale.

TABLE 2 | Disturbed motor control.

No	I. Primary presentation		II. Motor signs at follow-up					
	AHS	Impaired self-initiated movements	Grasping	Intermanual conflict	Motor perseveration	Mirror movements	Tremor	Gait apraxia
P1	++	+++	+++	+	0	++	na	++
P2	++	+	++	++	+	+	0	+
P3	++	+	++	++	+	+	+	+
P4	++	+	0	++	+	+	0	+
P5	+	++	+++	++	+	na	++	na
P6	++	(+)	0	+	+	+	0	0
P7	na	(+)	0	++	0	0	0	0
P8	++	++	++	++	+	+	++	+
P9	++	0	++	+	0	+	+	0
P10	+	0	0	+	+	+	0	0

Primary presentation (scoring): AHS, ++; minor or transient AHS, +.

Motor signs at follow-up (scoring): severe presentation, +++; moderate presentation, ++; mild presentation, +; symptom not present, 0. na, information not available.

with an apparently severe paresis or plegia of one or both upper extremities, respectively (five right-sided, three left-sided symptoms, and one bilateral symptoms). In the subacute and chronic stage for all patients, movement initiation improved but signs of disturbed motor control such as exaggerated grasping, and disturbing movements of the affected limb persisted to a variable extent. These data are summarized in **Table 2** and relate to the last control after the ischemic stroke (median duration of follow-up: 83.5; range: 7–585 days). Lack of self-initiated movements was present in 8/10 patients, intermanual conflict in 10/10 patients, exaggerated grasping and groping behavior in 6/10 patients, motor perseveration in 8/10 patients, mirror movements in 7/9 patients, tremor in 5/10, and gait apraxia in 4/8 patients. In the patient with bilateral ACA infarcts, a reliable evaluation of mirror movements was not possible due to the severe impairment of initiating movements of both limbs.

Imaging

Table 3 summarizes the size of and the anatomical location of the weighted summation maps for each clinical sign. The total centers of gravity of the specific maps for grasping, intermanual conflict, lack of self-initiated movements, mirror movements, and motor perseveration were located in the caudal tier of the anterior cingulate cortex, whereas the center of gravity of the maps for gait apraxia and tremor were located within the white matter adjacent to the anterior cingulate cortex (MNI-coordinates: lack of self-initiated movements: $x = -11$, $y = 9$, $z = 36$; intermanual conflict $x = -3$, $y = -3$, $z = 34$; grasping: $x = -10$, $y = 10$, motor perseveration: $x = -10$, $y = 10$, $z = 34$; mirror movements: $x = -7$, $y = 0$, $z = 42$; $z = 34$; tremor: $x = -3$, $y = -2$, $z = 27$; gait apraxia: $x = -13$, $y = 16$, $z = 27$) (**Figure 1**). The combined summation map for all AHS-specific motor symptoms (i.e., group A) encompassed a total lesion volume of 99,863 voxels (corresponding to a lesion volume of 99.9 ml with a center of mass in the anterior cingulate cortex ($x = -10$, $y = 12$, $z = 35$). Similarly, the respective map for non-AHS-specific motor symptoms of the upper limbs (group B) had a lesion volume of 101,691 voxels (lesion volume: 101.7 ml) with its center of mass in the anterior cingulate cortex ($x = -11$, $y = 11$, $z = 36$) (**Figure 2**).

The union set of the maps for group A and B ($A \cap B$) had a total size of 66,132 voxels (corresponding to a total lesion volume of 66.1 ml). 4.8% of the total lesion volume was located in the SMA proper, 8.5% in the pre-SMA, 14.4% in the anterior cingulate cortex, 10.0% in the MC, 6.5% in the genu, and 5.8% in the body of the corpus callosum. The remaining 50% of the lesion volume affected various other frontal brain regions. The calculation of the set difference of $A \cap B \setminus C$ revealed a total lesion volume of 9,394 voxels (total lesion volume: 9.4 ml). 8.1% of the lesion volume was found in the SMA proper, 25.2% in the pre-SMA, 13.1% in the midcingulate cortex, and 3.0% in the body of the corpus callosum. The set difference of $A \setminus B \cup C$ encompassed 2,447 voxels (total lesion volume 2.4 ml). 0.6% of the lesion volume was located in the SMA proper, 32.3% in the pre-SMA, and 20.8% in the midcingulate cortex (**Table 4**; **Figure 3**). In between comparison showed that group A had the highest percentage of lesion load within the pre-SMA while the corpus callosum was not affected.

The Bereitschaftspotential (Readiness Potential)

The BP was recorded in two patients (P2 and P3). Both of them had a left-sided ACA infarct involving a large section of the vascular territory. Accordingly, the BP could not be detected over the contralateral hemisphere (corresponding to the electrodes C3) while performing finger movements with the affected right hand. Interestingly, a BP could not be recorded over the right hemisphere either (C4), when they performed the same task with the clinically unaffected left hand. The patients' recordings are shown in **Figure 4** (plotted against a grand average of BP recordings from 13 healthy controls).

Illustrative Cases Reflecting the Spectrum of Disturbed Motor Control in ACA Strokes

Of all cases, P1 (female, 83 years) with an ischemic lesion of the entire ACA territory, including the genu corpus callosum showed the most severe form of an intermanual conflict and exaggerated grasping. In the subacute stage, she was unable to perform bimanual tasks, e.g., putting on her glasses, as the affected limb counteracted the unaffected one. Moving objects in the nearby visual field led to compulsive grasping (magnetic hand) (**Figure 5**). After

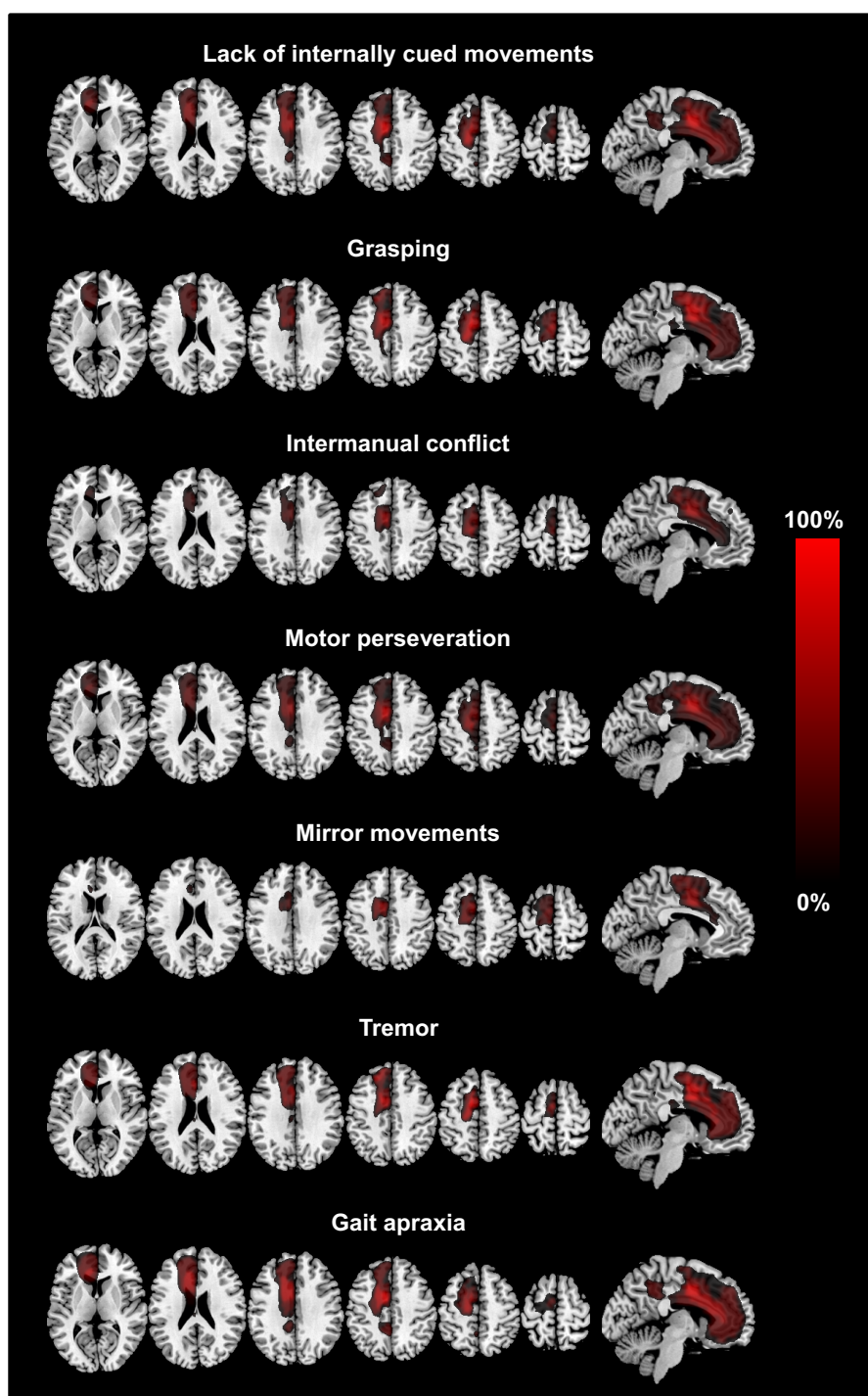


FIGURE 1 | The figure shows axial slices and a sagittal slice of a T1-standard MRI scan with the superimposed summation lesion maps for each clinical sign. Each lesion map is thresholded at voxels damaged in >25% of patients showing the respective clinical sign. The legend (provided in percentages) refers to the total number of patients showing the respective clinical sign (MNI-coordinates: z = 8, 23, 33, 43, 53, 63 and x = -6, respectively).

motor intention nor of the self-agency of their movements, thus suggesting a full-blown motor form of AHS (15, 20, 24). The dissociation between self-initiated and externally triggered movements is essential, because they are largely dependent on the medial motor system supplied by the ACA, whereas the latter

mainly rely on the lateral premotor system (supplied by the MCA) (37). A few patients presented with mild or only transient signs of AHS, as reflected by disturbed motor awareness in the acute, but not in the chronic phase. However, at the follow-up they still showed some signs of disturbed motor control as seen in the more

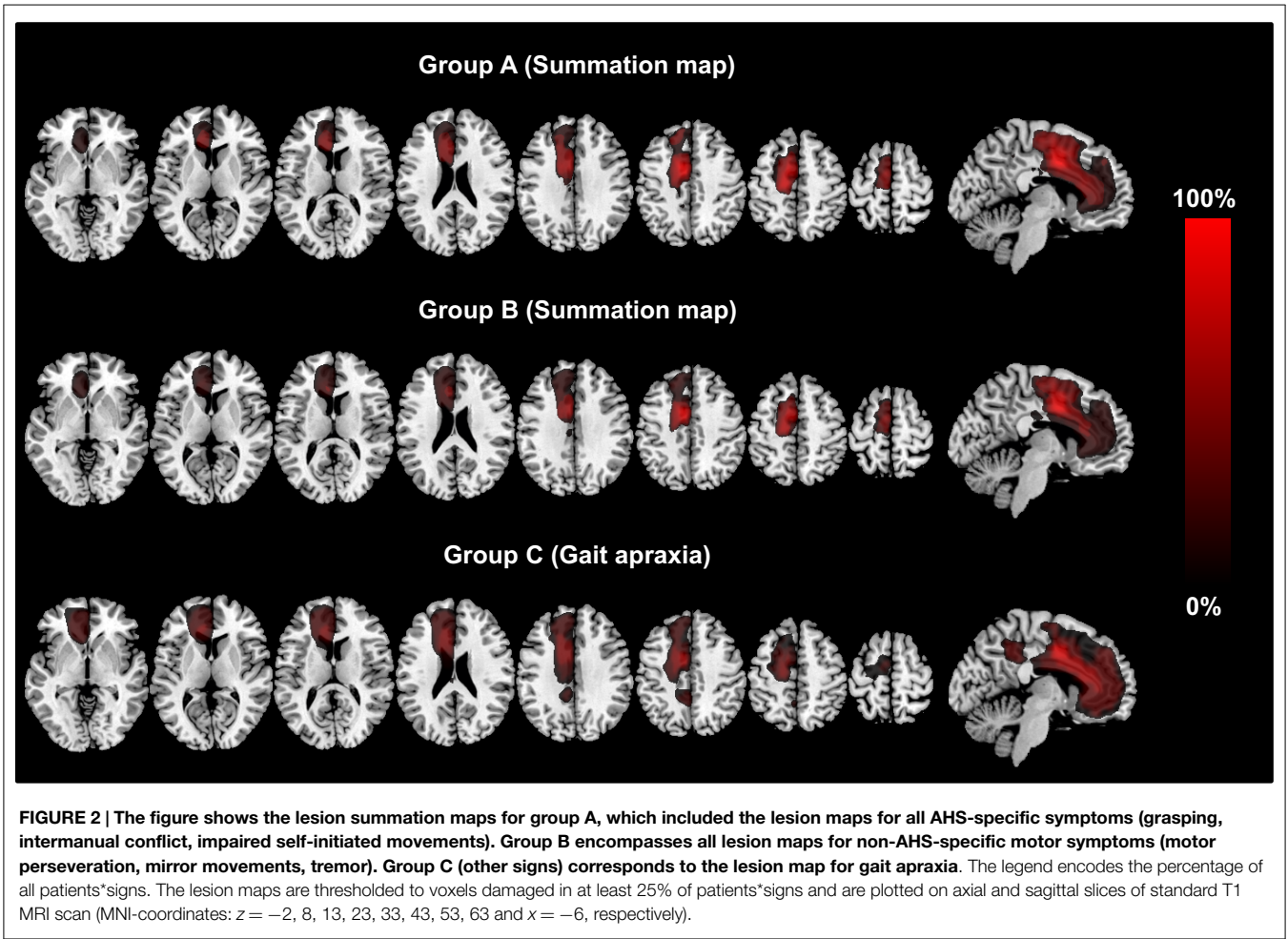


TABLE 4 | Percentage of lesion on regions of interest related to AHS associated and specific symptoms.

Total lesion volume			SMC				ACC		MCC		PCC		CC (genu)		CC (body)	
Volume			Volume (SMAp)		Volume (pre-SMA)		Volume		Volume		Volume		Volume		Volume	
Voxels	%		Voxels	%	Voxels	%	Voxels	%	Voxels	%	Voxels	%	Voxels	%	Voxels	%
AnB	66,132	100	3,162	4.8	5,599	8.5	9,551	14.4	6,622	10.0	0	0.0	4,317	6.5	3,811	5.8
AnB\C	9,394	100	763	8.1	2,364	25.2	0	0.0	1,232	13.1	0	0.0	0	0.0	279	3.0
A\B\C	2,447	100	14	0.6	791	32.3	0	0.0	505	20.6	0	0.0	0	0.0	0	0.0

The table shows the location of the intersections with regard to the involvement of various brain regions of interest. The proportion of the total lesion volume is shown for each brain regions (in voxels and in percentage of the total lesion volume). A, symptom group A; AHS, alien hand syndrome; ACC, anterior cingulate cortex; B, symptom group B; C, symptom group C; CC, corpus callosum; MCC, midcingulate cortex; n.a., not applicable; PCC posterior cingulate cortex; SMA, supplementary motor area; SMAp, SMA proper; SMC, supplementary motor cortex.

severely affected cases, though to a much milder degree. This underscores the notion that the presentation of an AHS has a wide clinical spectrum.

Moreover, we were interested whether clinical signs of AHS (as defined as lack of conscious awareness of intention and the sense of agency) and non-AHS-specific signs, commonly observed in association with AHS, are caused by different lesion patterns. We could demonstrate that both AHS-specific and non-AHS-specific

signs trace back to lesions within the SMC, and the anterior and medial cingulate cortex. This result was not entirely unexpected due to the important role of these brain areas in voluntary motor control (i.e., self-initiated movements and suppression of externally triggered motor subroutines) (1, 2). Our results are in line with a previously published retrospective analysis of 100 ACA strokes, which showed that motor disturbances were by far the most common signs (17).

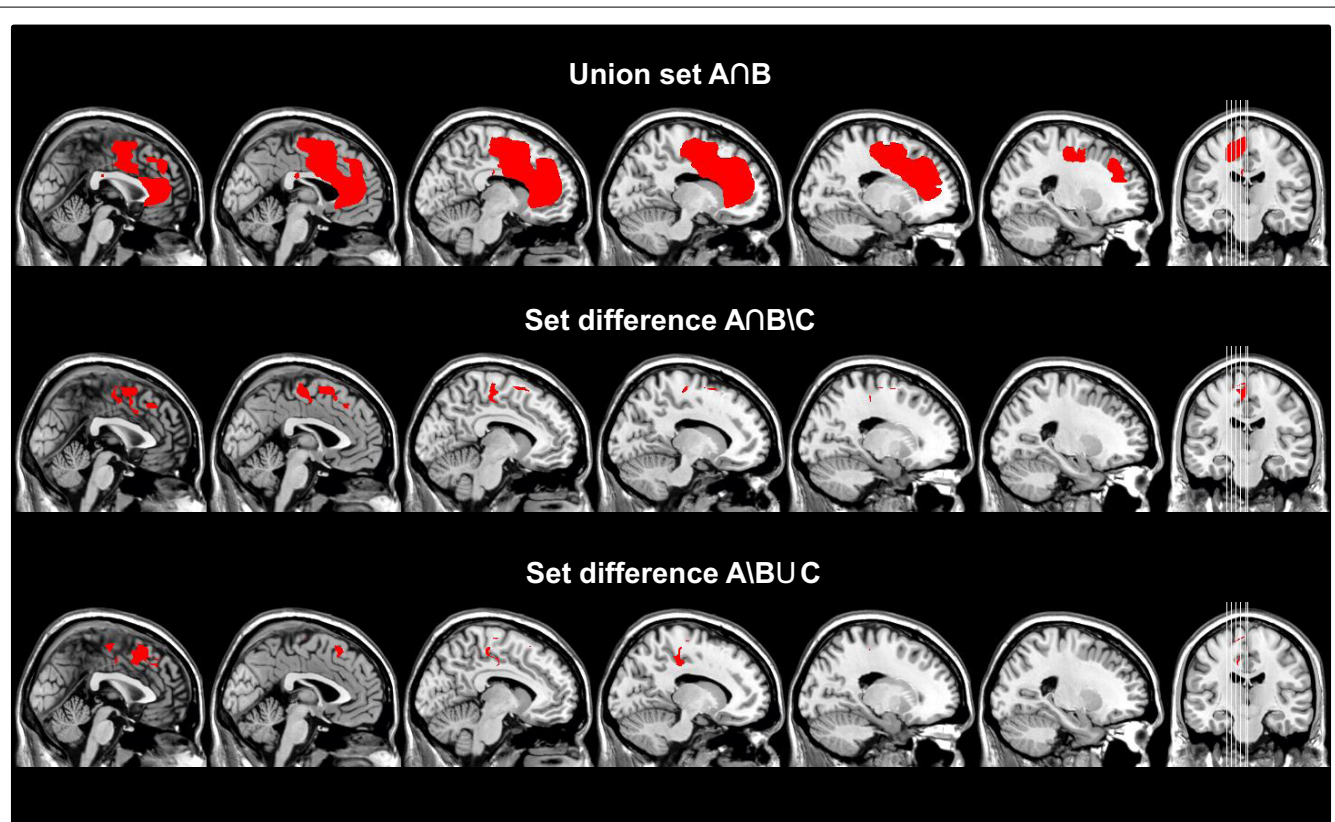


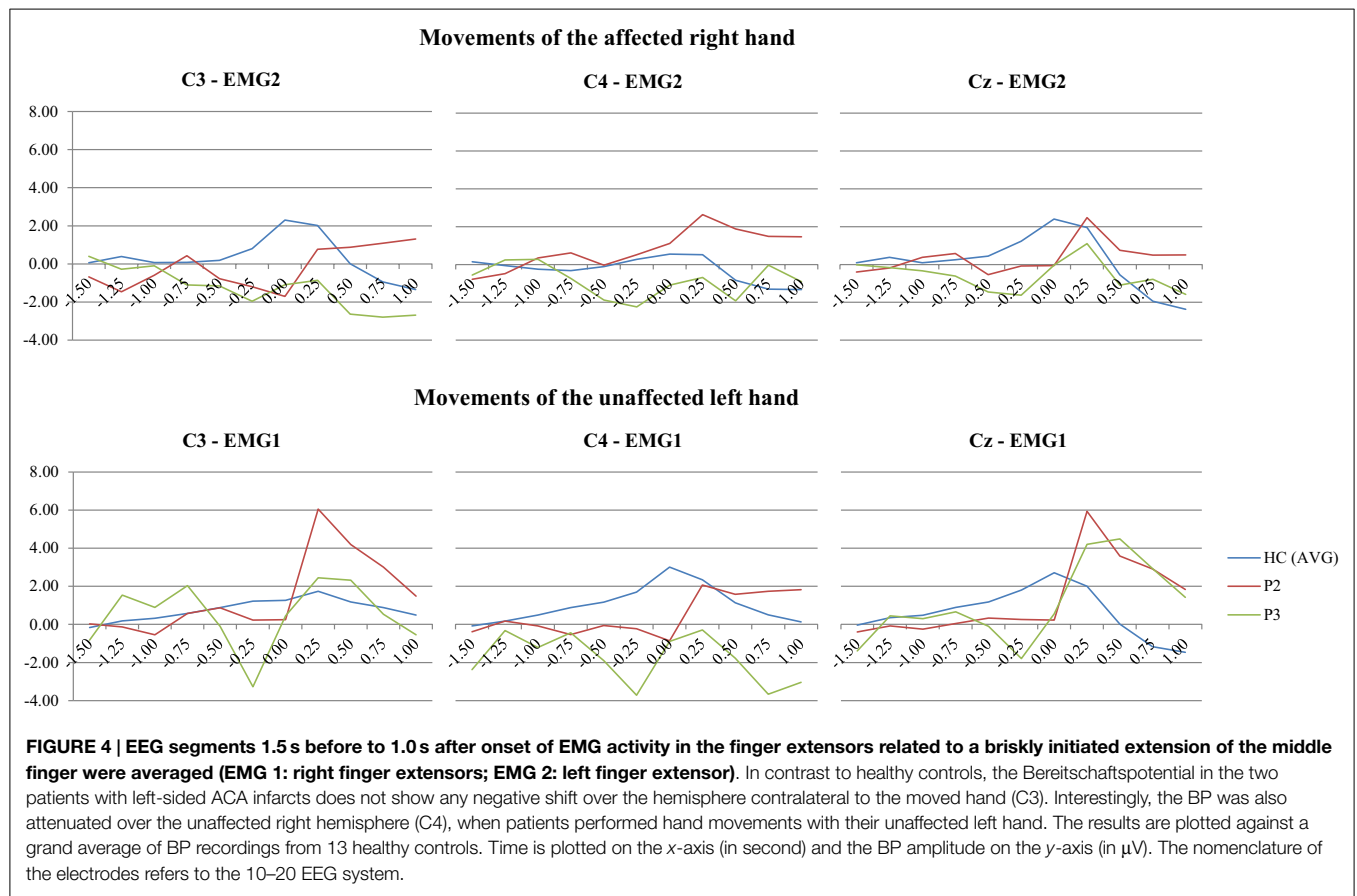
FIGURE 3 | Different sets ($A \cap B$, $A \cap B \setminus C$, $A \setminus B \cup C$) calculated from the respective summation maps after transforming them to binary maps are superimposed on sagittal slices of a standard T1 MRI Scan (MNI-coordinates: $x = -23, -18, -13, -8, -2, 0$). The union set of group A and B ($A \cap B$) and set difference ($A \cap B \setminus C$) are thought to reflect the anatomical substrates for disturbed motor control in general regardless if the signs are specific for an AHS or not, whereas the set difference $A \setminus (B \cup C)$ reveals the anatomical substrates for AHS-specific symptoms. Interestingly, the latter set difference involves mainly the SMA, whereas disturbed motor control involves the SMC in addition to other regions of the frontal and rostral parietal lobe.

A main finding of the present study is the predominant involvement of the pre-SMA in AHS-specific signs as shown by the approach with different set differences. This is a novel finding for ACA infarcts, but consistent with results from fMRI studies in healthy persons showing greater activations in rostral parts of the SMA after self-initiated movements (37). The pre-SMA, projects both to the lateral premotor cortex and the caudal parts of the SMA (38), although latter is not considered to play a major role in movement preparation as its projections descend directly through the pyramidal tract (39, 40). Gait apraxia was selected as a “reference”-clinical sign not associated with AHS and not affecting the upper extremities, but known to occur in lesions involving the medial frontal lobe. In line with this, gait apraxia was associated with lesions affecting the cingulate cortex in our study (21).

Previous studies of clinical-anatomical correlation in ACA stroke patients were biased mostly because of the approach with semi-quantitative analyses of predefined regions of interest. In the work of Chang and colleagues, AHS was associated with a combined involvement of the medial frontal lobe and the corpus callosum. An isolated or predominant affection of the cingulate cortex was found to result in an intermanual conflict, while medial frontal lesions were more likely to present with grasping behavior (10, 16). More recently, Sarva and colleagues published a systematic review of the literature on AHS (7). They

concordantly found that the SMC, cingulate cortex and corpus callosum were the most commonly affected structures in the “frontal” AHS variant. Predominant involvement of hemispheric structures more frequently led to involuntary grasping and groping behavior, whereas an intermanual conflict was the most frequent clinical sign in callosal lesions. Our findings, however, do not favor the same relevance of the corpus callosum for clinical signs of AHS as suggested by these authors.

There were some clinical signs, which have not yet been described as common signs in ACA strokes. Mirror movements are usually seen in early childhood due to mutations in the DCC and RAD51 genes (41), although they may sometimes also occur in patients with basal ganglia disorders and strokes, mainly of the corona radiata. However, they have rarely been described in association with ACA strokes (26, 42). Functional MRI revealed that mirror movements are paralleled by bilateral activation of M1 and the SMA (25). Mirror movements probably occur due to an insufficient interhemispheric inhibition of the motor cortex located ipsilateral to the moved limb by a network, which connects the SMC, dorsolateral PFC, and M1 (43). The unilateral tremor of the affected hand we observed in some patients also deserves further consideration. It occurred in all patients as a new clinical sign with a latency of a few weeks after stroke. To our best knowledge, there are hardly any comparable reports of



a hand tremor associated with ACA ischemia in the literature (25, 31). Stroke-associated tremor has mainly been reported in lesions of the thalamus, and the striatonigral, cerebello-thalamic or dentatorubrothalamic pathways (44). Clinically, the observed tremor resembles that of a dystonic tremor with a strong tendency to occur during action (45). In line with one previous report, the tremor was mostly seen just transiently (31). An association of the tremor with SMA and cingulate cortex lesions is of interest because an abnormal overactivity of these brain regions was found in an fMRI study in essential tremor (46). Our observations may thus suggest that an impaired function of the SMC or cingulate

cortex may play an important role in the generation or suppression of pathological oscillatory network activity.

Our findings underpin the crucial role of lesions involving the SMC and cingulate cortex for disturbed motor control after ACA infarcts. Error detection and conflict monitoring have previously been attributed to the anterior cingulate cortex (2). The SMC, in turn, is more important for the generation of self-initiated movements, generation of complex motor tasks and the suppression of stimulus-driven, though, purposeless movements (i.e., grasping) (1). In this context, the BP is also of interest since it presumably originates from the SMC and reflects cognitive motor control

prior to voluntary movements (3). So far, there are only two case reports of ACA strokes, which included BP recordings. In line with our findings, the BP following movements of the affected hand was also attenuated there (28–30, 47). Notably, the BP was also attenuated in our patients when they performed finger movements with their non-affected hand. This might indicate disturbed interhemispheric activation following a unilateral SMC lesion.

This analysis has several limitations. Due to its design as in parts retrospective case series, follow-ups were not standardized and patients were seen at different latencies after their strokes. Therefore, transient neurological signs may have been missed. Furthermore, this lack of standardized time intervals between the assessment in the acute stage and the follow-up assessments does not allow drawing definite conclusions to the clinical and functional outcome of these patients. A limitation of our clinical approach is the fact that it has not been validated elsewhere and there are no validated clinical scores for AHS symptoms in the literature. Therefore, we invented a semi-quantitative rating for our case series, which was proven here to have a very good IRR. Furthermore, the fact that just two patients underwent BP recordings does not allow to draw final conclusions on the BP in ACA strokes, since this potential is quite variable despite optimal recording settings (28). We acknowledge that a larger number of patients would also have increased the statistical power here. Moreover, our imaging results may have been flawed because of the different imaging methods used. A CT scan yields a different image of the brain in terms of contrast and distortion as an MRI scan. We attempted to overcome this concern making use of validated CT and MRI templates for spatial normalization (43). Nonetheless, we

decided to include the two ACA stroke patients with CT scans, because otherwise we would have abolished two clinically very interesting patients from our series. A theoretical issue is the definition of an adequate threshold to delineate damaged brain voxels for lesion analysis. In order to avoid false negative results in this small patient cohort, we went for a rather low threshold of more than 25% of individuals to explore the defined motor signs by voxel-based symptom lesion mapping (35). Furthermore, we determined lesion location as the basis of anatomical probability atlases, which do not account for individual variability of neuroanatomy.

Conclusion

In summary, AHS is primarily characterized by disturbed conscious awareness of intention and a deficient sense of agency for voluntary hand movement. This is reflected by the inability to carry out self-initiated movements while externally cued movements are neither suppressed nor perceived by the subjects. Common motor signs following ACA strokes are disturbed self-initiated movements, grasping and groping behavior, intermanual conflict, motor perseveration, mirror movements, and coarse tremor. Their occurrence is mainly associated with lesions of SMC, as well as the anterior and midcingulate cortex. The motor signs specifically related to AHS, i.e., disturbed self-initiated movements, grasping and intermanual conflict, are mainly related to lesions of the pre-SMA and MCC. To date, little is known about the clinical course and long-term outcome of these patients or about the best approach on how to rehabilitate these patients. Therefore, further studies in these patients are warranted.

References

- Nachev P, Kennard C, Husain M. Functional role of the supplementary and pre-supplementary motor areas. *Nat Rev Neurosci* (2008) 9(11):856–69. doi:10.1038/nrn2478
- Paus T. Primate anterior cingulate cortex: where motor control, drive and cognition interface. *Nat Rev Neurosci* (2001) 2(6):417–24. doi:10.1038/35077500
- Jahanshahi M, Jenkins IH, Brown RG, Marsden CD, Passingham RE, Brooks DJ. Self-initiated versus externally triggered movements. I. An investigation using measurement of regional cerebral blood flow with PET and movement-related potentials in normal and Parkinson's disease subjects. *Brain* (1995) 118(Pt 4):913–33. doi:10.1093/brain/118.4.913
- Shibasaki H, Hallett M. What is the Bereitschaftspotential? *Clin Neurophysiol* (2006) 117(11):2341–56. doi:10.1016/j.clinph.2006.04.025
- Haggard P. Conscious intention and motor cognition. *Trends Cogn Sci* (2005) 9(6):290–5. doi:10.1016/j.tics.2005.04.012
- Fried I, Katz A, McCarthy G, Sass KJ, Williamson P, Spencer SS, et al. Functional organization of human supplementary motor cortex studied by electrical stimulation. *J Neurosci* (1991) 11(11):3656–66.
- Sarva H, Deik A, Severt WL. Pathophysiology and treatment of alien hand syndrome. *Tremor Other Hyperkinet Mov (N Y)* (2014) 4:241. doi:10.7916/D8VX0F48
- Laplane D, Degos JD. Motor neglect. *J Neurol Neurosurg Psychiatry* (1983) 46(2):152–8. doi:10.1136/jnnp.46.2.152
- Nagaratnam N, Davies D, Chen E. Clinical effects of anterior cerebral artery infarction. *J Stroke Cerebrovasc Dis* (1998) 7(6):391–7. doi:10.1016/S1052-3057(98)80122-5
- Feinberg TE, Schindler RJ, Flanagan NG, Haber LD. Two alien hand syndromes. *Neurology* (1992) 42(1):19–24. doi:10.1212/WNL.42.1.19
- Goldstein K. Zur Lehre der motorischen Apraxie. *J Neurol Psychol* (1908) 11:169–87.
- Brion S, Jedynak CP. [Disorders of interhemispheric transfer (callosal disconnection). 3 Cases of tumor of the corpus callosum. The strange hand sign]. *Rev Neurol (Paris)* (1972) 126(4):257–66.
- Biran I, Chatterjee A. Alien hand syndrome. *Arch Neurol* (2004) 61(2):292–4. doi:10.1001/archneur.61.2.292
- Brainin M, Seiser A, Matz K. The mirror world of motor inhibition: the alien hand syndrome in chronic stroke. *J Neurol Neurosurg Psychiatry* (2008) 79(3):246–52. doi:10.1136/jnnp.2007.116046
- Dolado AM, Castrillo C, Urra DG, Varela de Seijas E. Alien hand sign or alien hand syndrome? *J Neurol Neurosurg Psychiatry* (1995) 59(1):100–1. doi:10.1136/jnnp.59.1.100
- Chan JL, Liu AB. Anatomical correlates of alien hand syndromes. *Neuropsychiatry Neuropsychol Behav Neurol* (1999) 12(3):149–55.
- Kang SY, Kim JS. Anterior cerebral artery infarction: stroke mechanism and clinical-imaging study in 100 patients. *Neurology* (2008) 70(24 Pt 2):2386–93. doi:10.1212/01.wnl.0000314686.94007.d0
- Rorden C, Karnath HO, Bonilha L. Improving lesion-symptom mapping. *J Cogn Neurosci* (2007) 19(7):1081–8. doi:10.1162/jocn.2007.19.7.1081
- Dimond SJ, Scammell RE, Brouwers EY, Weeks R. Functions of the centre section (trunk) of the corpus callosum in man. *Brain* (1977) 100(3):543–62. doi:10.1093/brain/100.3.543
- Aboitiz F, Carrasco X, Schroter C, Zaidel D, Zaidel E, Lavados M. The alien hand syndrome: classification of forms reported and discussion of a new condition. *Neurol Sci* (2003) 24(4):252–7. doi:10.1007/s10072-003-0149-4
- Della Sala S, Francescani A, Spinnler H. Gait apraxia after bilateral supplementary motor area lesion. *J Neurol Neurosurg Psychiatry* (2002) 72(1):77–85. doi:10.1136/jnnp.72.1.77
- Giovannetti T, Buxbaum LJ, Biran I, Chatterjee A. Reduced endogenous control in alien hand syndrome: evidence from naturalistic action. *Neuropsychologia* (2005) 43(1):75–88. doi:10.1016/j.neuropsychologia.2004.06.017

23. Hanakita J, Nishi S. Left alien hand sign and mirror writing after left anterior cerebral artery infarction. *Surg Neurol* (1991) 35(4):290–3. doi:10.1016/0090-3019(91)90007-V
24. Kikkert MA, Ribbers GM, Koudstaal PJ. Alien hand syndrome in stroke: a report of 2 cases and review of the literature. *Arch Phys Med Rehabil* (2006) 87(5):728–32. doi:10.1016/j.apmr.2006.02.002
25. Kim JS, Lee MC. Writing tremor after discrete cortical infarction. *Stroke* (1994) 25(11):2280–2. doi:10.1161/01.STR.25.11.2280
26. Lee MY, Choi JH, Park RJ, Kwon YH, Chang JS, Lee J, et al. Clinical characteristics and brain activation patterns of mirror movements in patients with corona radiata infarct. *Eur Neurol* (2010) 64(1):15–20. doi:10.1159/000313979
27. Levine DN, Rinn WE. Optic sensory ataxia and alien hand syndrome after posterior cerebral artery territory infarction. *Neurology* (1986) 36(8):1094–7. doi:10.1212/WNL.36.8.1094
28. McNabb AW, Carroll WM, Mastaglia FL. “Alien hand” and loss of bimanual coordination after dominant anterior cerebral artery territory infarction. *J Neurol Neurosurg Psychiatry* (1988) 51(2):218–22. doi:10.1136/jnnp.51.2.218
29. Giroud M, Dumas R. Clinical and topographical range of callosal infarction: a clinical and radiological correlation study. *J Neurol Neurosurg Psychiatry* (1995) 59(3):238–42. doi:10.1136/jnnp.59.3.238
30. Park YW, Kim CH, Kim MO, Jeong HJ, Jung HY. Alien hand syndrome in stroke – case report & neurophysiologic study. *Ann Rehabil Med* (2012) 36(4):556–60. doi:10.5535/arm.2012.36.4.556
31. Lopez Dominguez JM, Rojas-Marcos I, Sanz FG, Robledo SA. Frontal cortical infarction and contralateral postural and intentional tremor. *Neurologia* (2008) 23(1):62–4.
32. Adams HP Jr, Bendixen BH, Kappelle LJ, Biller J, Love BB, Gordon DL, et al. Classification of subtype of acute ischemic stroke. Definitions for use in a multicenter clinical trial. TOAST. Trial of Org 10172 in Acute Stroke Treatment. *Stroke* (1993) 24(1):35–41. doi:10.1161/01.STR.24.1.35
33. Nutt JG, Bloem BR, Giladi N, Hallett M, Horak FB, Nieuwboer A. Freezing of gait: moving forward on a mysterious clinical phenomenon. *Lancet Neurol* (2011) 10(8):734–44. doi:10.1016/S1474-4422(11)70143-0
34. Colebatch JG. Bereitschaftspotential and movement-related potentials: origin, significance, and application in disorders of human movement. *Mov Disord* (2007) 22(5):601–10. doi:10.1002/mds.21323
35. Abela E, Missimer J, Wiest R, Federspiel A, Hess C, Sturzenegger M, et al. Lesions to primary sensory and posterior parietal cortices impair recovery from hand paresis after stroke. *PLoS One* (2012) 7(2):e31275. doi:10.1371/journal.pone.0031275
36. Kim JH, Lee JM, Jo HJ, Kim SH, Lee JH, Kim ST, et al. Defining functional SMA and pre-SMA subregions in human MFC using resting state fMRI: functional connectivity-based parcellation method. *Neuroimage* (2010) 49(3):2375–86. doi:10.1016/j.neuroimage.2009.10.016
37. Jenkins IH, Jahanshahi M, Jueptner M, Passingham RE, Brooks DJ. Self-initiated versus externally triggered movements. II. The effect of movement predictability on regional cerebral blood flow. *Brain* (2000) 123(Pt 6):1216–28. doi:10.1093/brain/123.6.1216
38. Takada M, Nambu A, Hatanaka N, Tachibana Y, Miyachi S, Taira M, et al. Organization of prefrontal outflow toward frontal motor-related areas in macaque monkeys. *Eur J Neurosci* (2004) 19(12):3328–42. doi:10.1111/j.0953-816X.2004.03425.x
39. Muakkassa KF, Strick PL. Frontal lobe inputs to primate motor cortex: evidence for four somatotopically organized ‘premotor’ areas. *Brain Res* (1979) 177(1):176–82. doi:10.1016/0006-8993(79)90928-4
40. Dum RP, Strick PL. The origin of corticospinal projections from the premotor areas in the frontal lobe. *J Neurosci* (1991) 11(3):667–89.
41. Meneret A, Depienne C, Riant F, Trouillard O, Bouteiller D, Cincotta M, et al. Congenital mirror movements: mutational analysis of RAD51 and DCC in 26 cases. *Neurology* (2014) 82(22):1999–2002. doi:10.1212/WNL.0000000000000477
42. Cincotta M, Borgheresi A, Balestrieri F, Giovannelli F, Ragazzoni A, Vanni P, et al. Mechanisms underlying mirror movements in Parkinson’s disease: a transcranial magnetic stimulation study. *Mov Disord* (2006) 21(7):1019–25. doi:10.1002/mds.20850
43. Beaulieu V, Tremblay S, Theoret H. Interhemispheric control of unilateral movement. *Neural Plast* (2012) 2012:627816. doi:10.1155/2012/627816
44. Mehanna R, Jankovic J. Movement disorders in cerebrovascular disease. *Lancet Neurol* (2013) 12(6):597–608. doi:10.1016/S1474-4422(13)70057-7
45. Erro R, Rubio-Agusti I, Saifee TA, Cordivari C, Ganos C, Batla A, et al. Rest and other types of tremor in adult-onset primary dystonia. *J Neurol Neurosurg Psychiatry* (2014) 85(9):965–8. doi:10.1136/jnnp-2013-305876
46. Neely KA, Kurani AS, Shukla P, Planetta PJ, Wagle Shukla A, Goldman JG, et al. Functional brain activity relates to 0–3 and 3–8 Hz force oscillations in essential tremor. *Cereb Cortex* (2014). doi:10.1093/cercor/bhu142
47. Tanaka Y, Iwasa H, Yoshida M. Diagnostic dyspraxia: case report and movement-related potentials. *Neurology* (1990) 40(4):657–61. doi:10.1212/WNL.40.4.657

Conflict of Interest Statement: The authors declare that the research was conducted in the absence of any commercial or financial relationships that could be construed as a potential conflict of interest.

Copyright © 2015 Brugger, Galovic, Weder and Kägi. This is an open-access article distributed under the terms of the Creative Commons Attribution License (CC BY). The use, distribution or reproduction in other forums is permitted, provided the original author(s) or licensor are credited and that the original publication in this journal is cited, in accordance with accepted academic practice. No use, distribution or reproduction is permitted which does not comply with these terms.



Multi-modal imaging of neural correlates of motor speed performance in the trail making test

Julia A. Camilleri^{1,2*}, Andrew T. Reid¹, Veronika I. Müller^{1,2}, Christian Grefkes³, Katrin Amunts^{1,4} and Simon B. Eickhoff^{1,2}

¹ Research Centre Jülich, Institute of Neuroscience and Medicine (INM-1), Jülich, Germany, ² Institute of Clinical Neuroscience and Medical Psychology, Heinrich Heine University, Düsseldorf, Germany, ³ Department of Neurology, University Hospital Cologne, Cologne, Germany, ⁴ C. and O. Vogt Institute for Brain Research, Heinrich Heine University, Düsseldorf, Germany

OPEN ACCESS

Edited by:

Bruno J. Weder,
University of Bern, Switzerland

Reviewed by:

Olivier Godefroy,
Amiens University Hospital, France
Phil Clatworthy,
University of Bristol, UK

*Correspondence:

Julia A. Camilleri
j.camilleri@fz-juelich.de

Specialty section:

This article was submitted to Stroke,
a section of the
journal Frontiers in Neurology

Received: 15 May 2015

Accepted: 05 October 2015

Published: 27 October 2015

Citation:

Camilleri JA, Reid AT, Müller VI,
Grefkes C, Amunts K and Eickhoff SB
(2015) Multi-modal imaging of neural
correlates of motor speed
performance in the trail making test.
Front. Neurol. 6:219.
doi: 10.3389/fneur.2015.00219

The assessment of motor and executive functions following stroke or traumatic brain injury is a key aspect of impairment evaluation and used to guide further therapy. In clinical routine, such assessments are largely dominated by pen-and-paper tests. While these provide standardized, reliable, and ecologically valid measures of the individual level of functioning, rather little is yet known about their neurobiological underpinnings. Therefore, the aim of this study was to investigate brain regions and their associated networks that are related to upper extremity motor function, as quantified by the motor speed subtest of the trail making test (TMT-MS). Whole-brain voxel-based morphometry and whole-brain tract-based spatial statistics were used to investigate the association between TMT-MS performance with gray-matter volume (GMV) and white-matter integrity, respectively. While results demonstrated no relationship to local white-matter properties, we found a significant correlation between TMT-MS performance and GMV of the lower bank of the inferior frontal sulcus, a region associated with cognitive processing, as indicated by assessing its functional profile by the BrainMap database. Using this finding as a seed region, we further examined and compared networks as reflected by resting state connectivity, meta-analytic connectivity modeling, structural covariance, and probabilistic tractography. While differences between the different approaches were observed, all approaches converged on a network comprising regions that overlap with the multiple-demand network. Our data therefore indicate that performance may primarily depend on executive function, thus suggesting that motor speed in a more naturalistic setting should be more associated with executive rather than primary motor function. Moreover, results showed that while there were differences between the approaches, a convergence indicated that common networks can be revealed across highly divergent methods.

Keywords: trail-making test, motor speed, inferior frontal sulcus, voxel-based morphometry, resting state fMRI, meta-analytic connectivity modeling, structural covariance, probabilistic tractography

INTRODUCTION

Hand motor deficits are among the most common impairments following stroke (1). As a result, post-stroke assessment of motor functions is a key aspect of patient evaluation and is used to guide further therapy. In addition to fast but typically qualitative clinical assessments, this often involves neuropsychological tests of coordinated hand function. In practice, such assessments are still largely dominated by pen-and-paper tests. One example of such a simple pen-and-paper test is the motor speed subtest of the trail-making test (TMT-MS) from the Delis–Kaplan executive function system [D–KEFS; (2)]. This test measures the time that subjects take to manually trace a pre-specified trail. The TMT-MS requires the examinee to connect circles by following a dotted line, and aims to serve as a baseline measure of the motor component that should be shared by the other portions of the test. The results should thus provide information about the extent to which difficulty on the other TMT subtests probing higher, executive functions may be related to a motor deficit. However, the results of the TMT-MS cannot only be used as a baseline for other TMT subtests, but also provide information of drawing speed *per se*, and thus can be used by clinicians as an assessment of upper extremity motor function (2).

Pen-and-paper tests such as the TMT provide standardized and reliable valid measures of the individual level of functioning; however, rather little is yet known about their neurobiological underpinnings. Therefore, one aim of the current study is to investigate brain–behavior relationships with regard to upper extremity motor function, as quantified by the TMT-MS from the D–KEFS. Additionally, previous studies have demonstrated that while the brain can be subdivided into distinct modules based on functional and microstructural properties [reviewed in Ref. (3)], processes such as motor function are likely to involve the efficient integration of information across a number of such specialized regions. Due to this integrative nature of the brain, most higher mental functions are likely implemented as distributed networks (4), and it has therefore been suggested that an understanding of how a brain region subserves a specific task should require information regarding its interaction with other brain regions (3). Therefore, the current study additionally aims to investigate the networks associated with the regions we find to be related to TMT-MS performance.

A number of different approaches can be employed to investigate networks associated with a particular brain region. Task-free (seed-based) resting-state functional connectivity (RS-FC) refers to temporal correlations of a seed region with spatially distinct brain regions, when no task is presented (5, 6). Meta-analytic connectivity modeling (MACM) (7–9) investigates co-activation patterns between a seed region and the rest of the brain, by calculation of meta-analyses across many task-based fMRI experiments and paradigms stored in, e.g., the BrainMap database (10, 11). Structural covariance (SC) is based on the correlation patterns across a population of gray-matter characteristics such as volume or thickness (12, 13) that are thought to reflect shared mutational, genetic, and functional interaction effects of the regions involved (14, 15). While having conceptual differences, these three modalities all share

the goal of delineating regions that interact functionally with a particular seed region. By contrast, probabilistic tractography (PT) focuses on white-matter anatomical connectivity obtained from diffusion-weighted images (DWI) by producing a measure of the likelihood that two regions are structurally connected (16, 17). Previous studies have reported convergence between RS and MACM (18–20), between RS and SC (21, 22), RS and fiber tracking (23–26), and between RS, MACM, and SC (27, 28). However, striking differences among the different connectivity approaches have also been found (26, 27).

In this study, we first used whole-brain voxel-based morphometry [VBM; (29)] and whole-brain tract-based spatial statistics [TBSS; (30)] to investigate the association between TMT-MS performance with gray-matter volume (GMV) and white-matter integrity, respectively. Using the result of these initial analyses as the seed region of interest, we further examined and systematically compared networks obtained through RS-fMRI, MACM, SC, and PT. The aim of these analyses was twofold. First, we sought to explore the relationship of brain morphology to a simple measure of hand motor function. Second, we aimed to characterize both the divergence and convergence of four unique approaches to quantifying brain connectivity.

MATERIALS AND METHODS

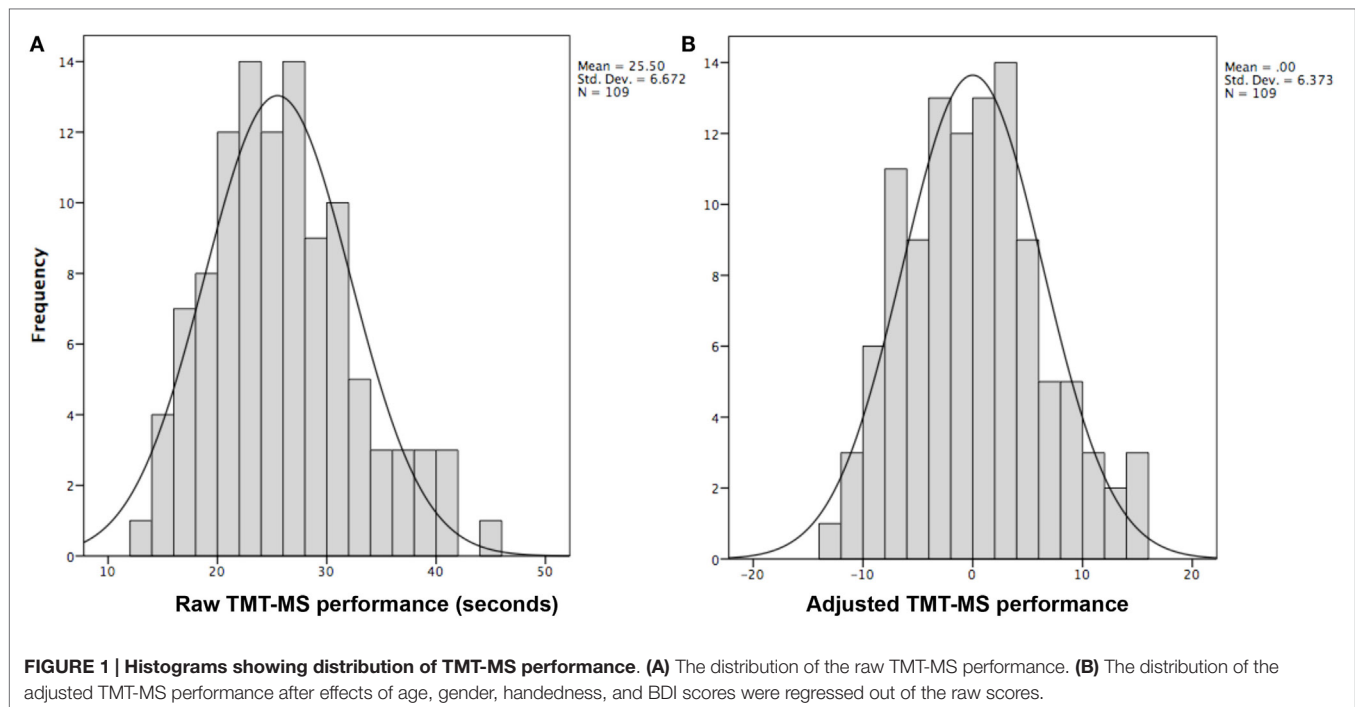
Subjects

Data from the Enhanced Nathan Kline Institute – Rockland Sample¹ (31) was used for all analyses except for meta-analytical connectivity modeling and functional characterization (where the BrainMap database was used). From this cohort, we used anatomical, RS, and DWI of subjects that had completed the TMT-MS, no current psychiatric diagnosis, a Beck depression inventory score (BDI) of less than 14 and did not exceed 3 SDs from the population mean. This resulted in a sample of 109 right-handed healthy volunteers between 18 and 75 years of age (mean age 40.39 ± 15.49 ; 37 males). First, effects of age, gender, handedness, and BDI score as known influences on hand motor speed (32, 33) were regressed out of the raw TMT-MS performance score (**Figure 1A**; **Table 1**). This resulted in an adjusted performance score, which indicated how much better or worse a subject performed than would be expected given these confounding factors (**Figure 1B**). The association of these adjusted scores with local GMV and white-matter integrity was then tested by carrying out whole-brain VBM and TBSS, respectively.

Delis–Kaplan Executive Function System: Trail-Making Test – Motor Speed

The Delis–Kaplan executive function system: trail-making test (D–KEFS TMT) consists of five different conditions (2). For the current study, we were exclusively interested in the TMT-MS, which requires participants to trace over a dotted line as quickly as possible while making sure that the line drawn touches every circle along the path. In particular, the participant is prompted to

¹http://fcon_1000.projects.nitrc.org/indi/enhanced



focus on speed rather than neatness but has to make sure that the line touches every circle along the path. If the line departs from the dotted line or is not correctly connected to the next circle, the participant is stopped immediately and redirected to the dotted line while keeping the stopwatch running. The scoring measure is the time (in seconds) that the participant needs to complete the task.

Relationship Between TMT-MS Performance and Gray-Matter Volume Whole-Brain VBM Analysis

The association between regional GMV and individual performance (adjusted for the potentially confounding effects of age, gender, handedness, and BDI), was investigated by performing a whole-brain VBM analysis. This analysis used the anatomical T1-weighted images of the 109 subjects described above. These scans were acquired in sagittal orientation on a Siemens TimTrio 3T scanner using an MP-RAGE sequence (TR = 1900 ms, TE = 2.52 ms, TI = 900 ms, flip angle = 9°, FOV = 250 mm, 176 slices, voxel size = 1 mm × 1 mm × 1 mm). Images were preprocessed using the VBM8 toolbox in SPM8 using standard settings, namely spatial normalization to register the individual images to ICBM-152 template space, and segmentation, wherein the different tissue types within the images are classified. The resulting normalized gray-matter segments, modulated only for the non-linear components of the deformations into standard space, were then smoothed using an 8 mm isotropic full-width-half-maximum (FWHM) kernel, and finally assessed for significant correlation between GMV and the adjusted TMT-MS performance scores. Age, gender, BDI scores, and Edinburgh handedness inventory (EHI) scores were used as covariates together with the adjusted

TMT-MS performance scores, leading to an analysis of partial correlations between GMV and TMT-MS. As we modulated the gray-matter probability maps by the non-linear components only to represent the absolute amount of tissue corrected for individual brain size, we did not include total brain volume as an additional covariate in the analysis. That is, given that the correction for inter-individual differences in brain volume was applied directly to the data it was not performed (a second time) as part of the statistical model. Statistical significance using non-parametric permutation inference was assessed at $p < 0.05$ [family-wise error (FWE) corrected for multiple comparisons].

Whole-Brain TBSS Analysis

A TBSS whole-brain analysis was performed to investigate the association between white-matter volume and adjusted TMT-MS performance. DWI from the same group of 109 volunteers acquired on a 3T TimTrio Siemens scanner (137 directions, $b = 1,500$ s/mm²) were used. Preprocessing was performed according to standard protocols using FSL². The DWI data were first corrected for head-motion and eddy-current effects of the diffusion gradients. The b0 images were averaged and skull-stripped using BET (34) to create the analysis mask. Within this mask, a simple diffusion-tensor model was estimated for each voxel. Finally, non-linear deformation fields between the diffusion space and the ICBM-152 reference space were computed using FSL's linear (FLIRT) (35, 36), and non-linear (FNIRT) image registration tools (37). These allow mapping between the individual (native) diffusion space and the ICBM-152 reference space; i.e., the same space

²www.fmrib.ox.ac.uk/fsl

TABLE 1 | Characteristics of the cohort.

Age	Gender	BDI	EHl	Age	Gender	BDI	EHl
26	Male	4	80	41	Male	1	70
20	Male	0	95	26	Female	7	75
53	Male	0	55	51	Female	5	75
48	Female	9	100	61	Female	0	80
62	Female	5	90	58	Male	5	80
18	Female	7	75	56	Female	0	65
54	Female	0	95	54	Female	4	95
18	Female	1	90	27	Male	5	60
21	Male	4	85	42	Female	9	70
62	Female	1	100	31	Female	7	100
53	Male	3	75	21	Female	1	100
22	Male	4	90	18	Male	3	90
62	Female	12	100	48	Female	3	85
54	Female	0	95	20	Female	5	55
24	Female	1	85	60	Female	1	100
44	Female	8	90	20	Female	1	90
57	Female	2	95	50	Female	2	90
44	Female	3	70	62	Male	7	70
51	Male	7	70	18	Male	2	85
63	Female	0	80	57	Female	1	100
26	Female	1	60	24	Female	0	95
59	Male	4	95	26	Female	0	80
30	Male	0	85	57	Female	5	85
50	Female	1	90	19	Male	2	70
26	Female	2	75	49	Male	0	60
18	Male	0	80	23	Female	2	85
24	Female	10	95	58	Female	5	55
64	Female	0	95	55	Male	4	80
47	Male	4	100	41	Female	5	100
38	Female	0	80	41	Female	0	100
23	Female	1	70	25	Female	2	75
42	Female	8	85	49	Female	0	90
59	Female	2	100	49	Female	1	100
26	Male	5	100	21	Female	6	75
18	Male	3	90	50	Male	1	85
19	Male	1	100	19	Male	3	65
27	Female	12	60	59	Male	3	85
20	Female	3	100	41	Male	0	80
56	Female	5	100	44	Male	13	100
18	Male	4	85	20	Female	13	85
30	Male	4	55	47	Male	5	90
58	Female	6	95	21	Male	2	55
52	Female	3	85	47	Female	7	55
38	Male	1	65	55	Female	1	90
64	Male	5	80	23	Female	13	100
41	Female	2	100	61	Male	1	80
49	Female	5	60	52	Female	0	100
57	Female	8	60	20	Male	10	60
40	Female	3	80	51	Female	0	65
48	Female	0	100	42	Female	0	100
36	Female	1	100	21	Female	0	80
20	Male	5	90	36	Female	8	100
60	Female	3	75	43	Female	9	85
59	Male	2	85	43	Female	5	95
52	Female	8	100				

to which also the VBM and RS (as described below) data are also registered. The FA images were hereby normalized into standard space and then merged to produce a mean FA image. This was in turn used to generate a skeleton representing all fiber tracts common to all subjects included in the study (30, 38). The maximal FA scores of each individual FA image were then projected onto

the mean FA skeleton. This projection aims to resolve any residual alignment problems after the initial non-linear registration (38). The resulting skeleton was then used to perform a multi-covariate analysis, using age, gender, BDI scores, EHI scores, and TMT-MS scores. Statistical significance using non-parametric permutation inference was again assessed at $p < 0.05$ multiple comparisons.

Seed Definition and Functional Characterization

The regions revealed by the initial VBM analysis were functionally characterized based on the behavioral domain meta-data from the BrainMap database³ (10, 11, 39), using both forward and reverse inference, as performed in previous studies (40, 41). Behavioral domains, which have been grouped for the purpose of the database, describe the cognitive processes probed by an experiment. Forward inference is the probability of observing activity in a brain region, given knowledge of the psychological process; whereas reverse inference is the probability of a psychological process being present, given knowledge of activation in a particular brain region. The results of both the forward and reverse inferences will be defined by the number and frequency of tasks in the database. In the forward inference approach, the functional profile was determined by identifying taxonomic labels for which the probability of finding activation in the respective region/set of regions was significantly higher than the overall (*a priori*) chance across the entire database. That is, we tested whether the conditional probability of activation given a particular label $P(\text{Activation}|\text{Task})$ was higher than the baseline probability of activating the region(s) in question *per se* $P(\text{Activation})$. Significance was established using a binomial test [$p < 0.05$, corrected for multiple comparisons using false discovery rate (FDR)]. In the reverse inference approach, the functional profile was determined by identifying the most likely behavioral domains, given activation in a particular region/set of regions. This likelihood $P(\text{Task}|\text{Activation})$ can be derived from $P(\text{Activation}|\text{Task})$ as well as $P(\text{Task})$ and $P(\text{Activation})$ using Bayes' rule. Significance (at $p < 0.05$, corrected for multiple comparisons using FDR) was then assessed by means of a chi-squared test.

Multi-Modal Connectivity Analyses

Multi-modal connectivity analyses were used to further characterize the results from the initial VBM analysis. In particular, we investigated; (1) RS-FC, inferred through correlations in the blood-oxygen-level-dependent (BOLD) signal obtained during a task-free, endogenously controlled state (5, 6); (2) MACM, revealing co-activation during the performance of external task demands (7, 8); (3) SC, identifying long-term coordination of brain morphology (15); and (4) probabilistic fiber tracking, providing information about anatomical connectivity by measuring the anisotropic diffusion of water in white-matter tracts (16, 17).

All the analyses were approved by the local ethics committee of the Heinrich Heine University Düsseldorf.

Task-Independent Functional Connectivity: Resting-State

A seed-based RS analysis was used to investigate the task-independent FC of the seed region (5, 6). RS-fMRI images of the 109 subjects described above were used. During the RS acquisition, subjects were instructed to not think about anything in particular but not to fall asleep. Images were acquired on a Siemens TimTrio 3T scanner using BOLD contrast [gradient-echo EPI pulse

sequence, TR = 1.4 s, TE = 30 ms, flip angle = 65°, voxel size = 2.0 mm × 2.0 mm × 2.0 mm, 64 slices (2.00 mm thickness)].

Data were processed using SPM8 (Wellcome Trust Centre for Neuroimaging, London⁴). The first four scans were excluded prior to further analyses and the remaining EPI images were then corrected for head movement by affine registration which involved the alignment to the initial volumes and then to the mean of all volumes. No slice time correction was applied. The mean EPI image for each subject was then spatially normalized to the ICBM-152 reference space by using the “unified segmentation” approach. (42). The resulting deformation was then applied to the individual EPI volumes. Furthermore, the images were smoothed with a 5-mm FWHM Gaussian kernel so as to improve the signal-to-noise ratio and to compensate for residual anatomic variations. The time-series of each voxel were processed as follows: spurious correlations were reduced by excluding variance that could be explained by the following nuisance variables: (i) the six motion parameters derived from the re-alignment of the image; (ii) their first derivatives; (iii) mean gray matter, white matter, and CSF signal. All nuisance variables entered the model as both first- and second-order terms. The data were then band-pass filtered preserving frequencies between 0.01 and 0.08 Hz. The time-course of the seed was extracted for every subject by computing the first eigenvariate of the time-series of all voxel within the seed. This seed time-course was then correlated with the time-series of all the other gray-matter voxels in the brain using linear (Pearson) correlation. The resulting correlation coefficients were transformed into Fisher's *z*-scores and tested for consistency across subjects by using a second-level ANOVA including age, gender, BDI scores, and EHI scores as covariates of no interest. Results were corrected for multiple comparisons using threshold-free cluster enhancement, a method that has been suggested to improve sensitivity and provide more interpretable output than cluster-based thresholding [TFCE; (43)], and FWE-correction at $p < 0.05$.

Task-Dependent Functional Connectivity: Meta-Analytic Connectivity Modeling

The whole-brain connectivity of the seed was characterized using a task-dependent approach by carrying out MACM. This method looks at FC as defined by task activation from previous fMRI studies and benefits from the fact that a large number of such studies are normally presented in a highly standardized format and stored in large-scale databases (9). Thus, MACM is based on the assessment of brain-wise co-activation patterns of a seed region across a large number of neuroimaging experiment results (7). All experiments that activate the particular seed region are first identified and then used in a quantitative meta-analysis to test for any convergence across all the activation foci reported in these experiments (9). Any significant convergence of reported foci in other brain regions as the seed was considered to indicate consistent co-activation with the seed. For this study, we used the BrainMap database to identify

³<http://www.brainmap.org>

⁴<http://www.fil.ion.ucl.ac.uk/spm/software/spm8/>

studies reporting neural activation within our seed region⁵ (10). A coordinate based meta-analysis was then used to identify consistent co-activations across the experiments identified by using activation likelihood estimation (ALE) (44–46). This algorithm treats the activation foci reported in the experiments as spatial probability distributions rather than single points, and aims at identifying areas that show convergence across experiments. The results were corrected using the same statistical criteria as for the RS imaging data, i.e., using TFCE (43) and FWE-correction at $p < 0.05$.

Structural Covariance

Structural covariance was used to investigate the pattern of cortical gray-matter morphology across the whole brain by measuring the correlations of GMV, obtained through VBM, between different regions. This method assumes that such morphometric correlations carry some information about the structural or functional connectivity between the regions involved (13–15, 21). SC analysis was performed using the GMV estimates obtained from the VBM pipeline, as described above. Following preprocessing of the anatomical images, we first computed the volume of the seed region by integrating the (non-linear) modulated voxel-wise gray-matter probabilities of all voxels of the seed, which was then used as our covariate of interest for the group analysis. A whole-brain general linear model (GLM) analysis was applied using the GMV of the seed, along with the same additional covariates (of no interest) as for the RS-FC analysis. The results were corrected using the same statistical criteria as for the other connectivity modalities, i.e., using TFCE (43) and FWE-correction at $p < 0.05$.

Probabilistic Tractography

Probabilistic tractography was used to investigate white-matter anatomical connectivity from our seed region to the rest of the brain. The PT analysis was performed based on the same DWI as used for the TBSS analysis using the Diffusion Toolbox FDT implemented in FSL (16, 47). Fiber orientation distributions in each voxel were estimated according to Behrens et al. (48), i.e., using the BEDPOSTX crossing fiber model. Linear and subsequent non-linear deformation fields between each subject's diffusion space and the MNI152 space as the location of the seeds and subsequent output were computed using the FLIRT and FNIRT tools, respectively. For PT, 100,000 samples were generated for each seed voxel and the number of probabilistic tracts reaching each location of a cortical gray matter. Importantly, we did not investigate the number of tracts reaching specific ROIs, but rather analyzed the number of tracts reaching each gray-matter voxel of the ICBM-152 template. The distance of each target (i.e., whole-brain gray matter) voxel from the seed voxel was computed using the ratio of the distance-corrected and non-corrected trace counts [cf. (49)]. This allowed us to address a limitation of structural connectivity profiles generated by PT, namely the fact that trace counts show a strong distance-dependent decay. That is, voxels close to the region of interest will inevitably feature higher connectivity values than even well-connected distant ones. These effects were adjusted

by referencing each voxel's trace count to the trace counts of all other gray-matter voxels in the same distance (with a 5-step, i.e., 2.5 mm, tolerance) along the fiber tracts [for a detailed description see Ref. (49)]. We thus replaced each trace count by a rank-based z-score indicating how likely streamlines passed a given voxel relative to the distribution of trace counts at that particular distance. The ensuing images were tested for consistency across subjects by using a second-level ANOVA. Results were corrected using the same statistical criteria as for the other connectivity modalities, i.e., using TFCE (43) and FWE-correction at $p < 0.05$.

Comparison of Connectivity Measures

The similarities and differences amongst all the different connectivity maps were compared and contrasted. The overlap between all the four thresholded connectivity maps (RS, MACM, SC, and PT) was computed using a minimum statistic conjunction (50), in order to identify *common connectivity* with the seed across the different modalities. This was done by computing the conjunction between the maps of the main effects for each of the modalities. An additional minimal conjunction analysis was also performed across the three modalities used to investigate gray-matter regions, namely, RS, MACM, and SC. Furthermore, we looked at *specifically present connectivity* for each of the modalities. *Specifically present connectivity* refers to regions that were connected with the seed in one modality but *not* in the other three [cf. (27)]. This was assessed by computing differences between the connectivity map of the first modality and those of the other three, respectively. Then a conjunction of these three different maps was performed. For example, the *specifically present connectivity* for MACM was assessed by computing the difference between the MACM map and the RS map in conjunction with the difference between the MACM map and the SC map and the difference between the MACM map and the PT map. Conversely, *specifically absent connectivity* was investigated by computing differences between one modality and the other three in order to identify regions that were present in the latter three modalities but not in the former. A conjunction of these different maps was then performed. For example, the *specifically absent connectivity* for MACM was assessed by computing the difference between the RS and MACM maps in conjunction with the difference between the SC and MACM maps and the difference between PT and MACM. All resulting maps were additionally thresholded with a cluster extent threshold of 100 voxels.

Finally, the resulting *common connectivity*, *specifically present connectivity* and *specifically absent connectivity* networks were functionally characterized based on the behavioral domain data from the BrainMap database as previously described for the seed region.

RESULTS

Relationships Between TMT-MS Performance and Brain Structure: Whole-Brain VBM and TBSS Analyses

The whole-brain VBM analysis revealed a significant negative correlation between the adjusted TMT-MS score and the GMV of a region in the lower bank of the left inferior frontal sulcus (IFS)

⁵<http://www.brainmap.org>

Figure 2A). Since the TMT-MS score refers to task completion time, this negative correlation indicates that better performance was associated with higher GMV in this region (**Figure 2B**).

The functional profile (based on the BrainMap database) of this region showed a significant association with cognition, specifically reasoning, at $p < 0.05$ (**Figure 3**).

The TBSS analysis of white-matter associations did not yield any significant results.

Connectivity of the IFS

Whole-brain connectivity of the region showing a significant association with TMT-MS performance was mapped using RS-FC, MACM, SC, and PT. Both similarities and differences amongst all the different connectivity maps were observed.

Converging Connectivity

Connectivity of the IFS seed, as revealed through RS-FC, MACM, SC, and PT analyses, included a number of distinct brain regions (**Figure 4**). Investigation of common regions interacting with

the IFS across the different connectivity modalities (calculated through a minimum statistical conjunction analysis across the four thresholded connectivity maps) revealed convergence in the left inferior frontal gyrus (IFG) extending into the left IFS. An additional cluster was observed in the right Brodmann Area 45 (**Figure 5A**; **Table 2**). Functional characterization of this network found across all four connectivity approaches indicated an association with processes related to language, including semantics, phonology, and speech. Additionally, associations with working memory and reasoning were also revealed (**Figure 5B**). On the other hand, a conjunction across the modalities used to investigate gray-matter regions (RS-FC, MACM, and SC) resulted in a broader convergence, including clusters in the IFG bilaterally extending into the precentral gyrus, together with clusters in the middle cingulate cortex, middle orbital gyrus, and insula lobe of the left hemisphere (**Figure 6**).

Specifically Present Connectivity for Each Modality

In the next step, we looked at the connectivity effects that were present in one modality but not in the other three (**Figure 7A**; **Table 3**).

For RS-FC, we found specific connectivity between the seed region and bilaterally in the inferior parietal lobule, IFG (pars opercularis and pars triangularis), middle frontal gyrus, inferior temporal gyrus, middle orbital gyrus, and supramarginal gyrus. Additionally, areas in the right IFG (p. orbitalis), cerebellum, superior orbital gyrus, middle occipital gyrus, and angular gyrus were also revealed by RS-FC. Moreover, specific RS-FC connectivity was found in areas of the left superior parietal lobule (**Figure 7A** in red). When functionally characterized using the BrainMap meta-data (**Figure 7B** in red) the components of this network were found to be mainly associated with cognitive functions, including working memory, attention, and action inhibition. In addition, fear was also found to be associated with this network.

Connectivity exclusively found using MACM was only observed in one region in the left hemisphere, namely in the insula lobe and adjacent IFG (p. triangularis), in an area slightly more posterior position to that found in RS-FC (**Figure 7A** in green). This region was found to be mainly associated with language functions, namely semantics, speech, and speech execution. Moreover, functions such as pain perception and music were also found to be related (**Figure 7B** in green).

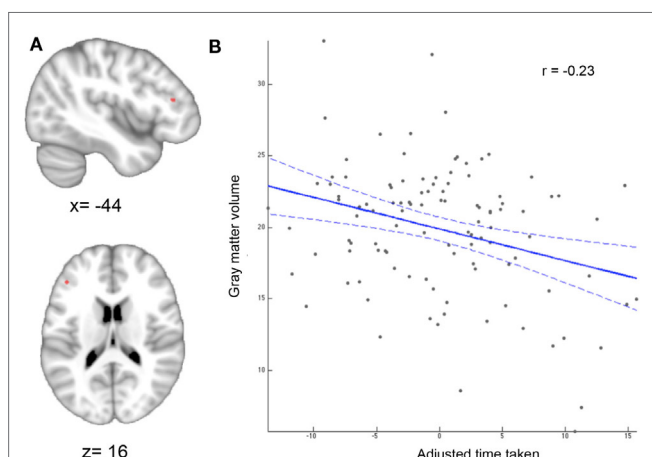


FIGURE 2 | Whole-brain VBM results. (A) Region showing significant correlation between gray-matter volume and adjusted time taken. Statistical significance using non-parametric permutation inference was assessed at $p < 0.05$ [family-wise error (few) corrected for multiple comparisons]. **(B)** Correlation between motor speed and gray-matter volume. The better (lower) the performance score the higher the gray-matter volume.

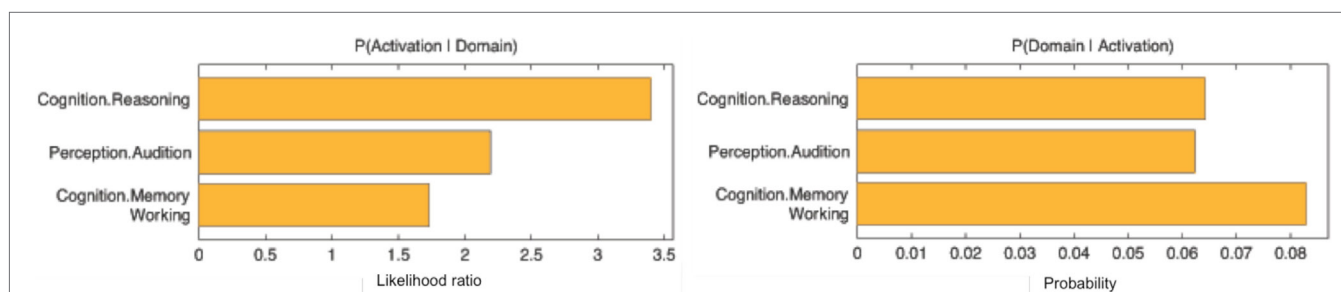


FIGURE 3 | Behavioral domains from the BrainMap database significantly associated with the seed, $p < 0.05$.

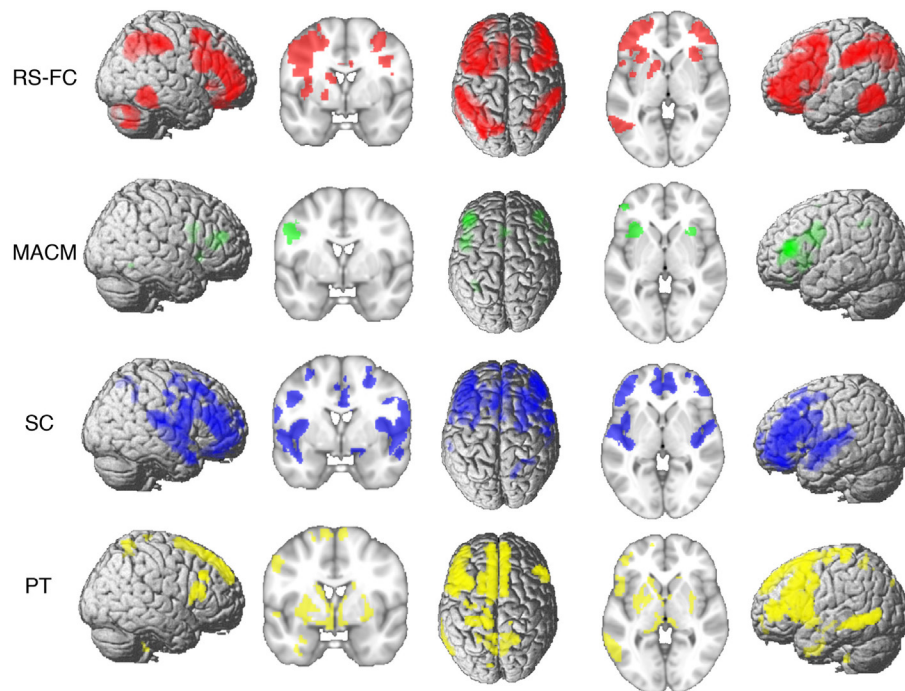


FIGURE 4 | Brain regions found to be significantly connected with the seed for each modality at $p < 0.05$, FWE corrected for multiple comparisons using threshold-free cluster enhancement (TFCE statistic).

Connectivity specific to SC was observed in the bilateral superior medial gyrus, temporal pole, superior temporal gyrus, Heschl's gyrus, rolandic operculum, supplementary motor area, superior and middle frontal gyri (more anterior to the effect found in RS-FC), IFG (p. orbitalis) (inferior to the area found in RS-FC on the right hemisphere) and middle orbital gyrus (bilaterally more anterior to the RS-FC effect). In the right hemisphere, specifically present SC connectivity included areas in the anterior cingulate cortex, insula lobe, middle temporal gyrus, supramarginal gyrus (more inferior to the area found in RS-FC), medial temporal pole, superior and inferior parietal lobules (the latter being more inferior to the area found in RS-FC), and superior orbital gyrus (more anterior to RS-FC specific connectivity in the same region). Additional connectivity was also observed in the left rectal gyrus, and left precentral gyrus (**Figure 7A** in blue). This network was found to be mainly functionally associated with functions related to emotion (fear, disgust, and sadness) and perception (audition and pain) (**Figure 7B** in blue).

The network specifically present for PT was found to be mainly functionally associated with functions related to emotion and pain. Additionally, functions such as action execution and action imagination were also found to be related (**Figures 7A,B** in yellow).

Specifically Absent Connectivity for Each Modality

Additionally, we looked at connectivity that was specifically absent in each modality, i.e., regions for which connectivity was absent in a particular modality but was observed in the other three (**Figure 8A**; **Table 4**). No regions were found to be specifically

absent for the RS-FC modality. By contrast, for MACM we found specifically absent connectivity with areas of the left middle and inferior frontal gyri (p. triangularis) (**Figure 8A** in green). These regions were found to be functionally associated with cognitive functions, namely working and explicit memory but also with phonology, semantics, and syntax (**Figure 8B** in green).

Conversely, for SC specifically absent connectivity was found for an area in the left precentral gyrus (**Figure 8A** in blue; **Table 4**). This region was in turn found to be mainly functionally associated with language-related functions (phonology, semantics, speech, and syntax) together with working memory (**Figure 8B** in blue).

Connectivity specifically absent for PT was also found to be functionally associated with language-related functions (phonology, semantics, and speech) together with working memory, reasoning, and attention (**Figures 8A,B** in yellow).

DISCUSSION

The aim of this study was to employ a multi-modal approach to investigate the regions and associated networks related to upper extremity motor function, as quantified by the TMT-MS. In a first step, we therefore correlated local GMV with performance in motor speed. This analysis revealed a significant correlation between TMT-MS performance and GMV in a small region in the IFS, which was functionally characterized as being involved in cognitive tasks. In turn, the TBSS analysis of local WM associations yielded no significant result. We then further investigated the connectivity of the left IFS seed using a multi-modal approach. Functional interactions with other gray-matter

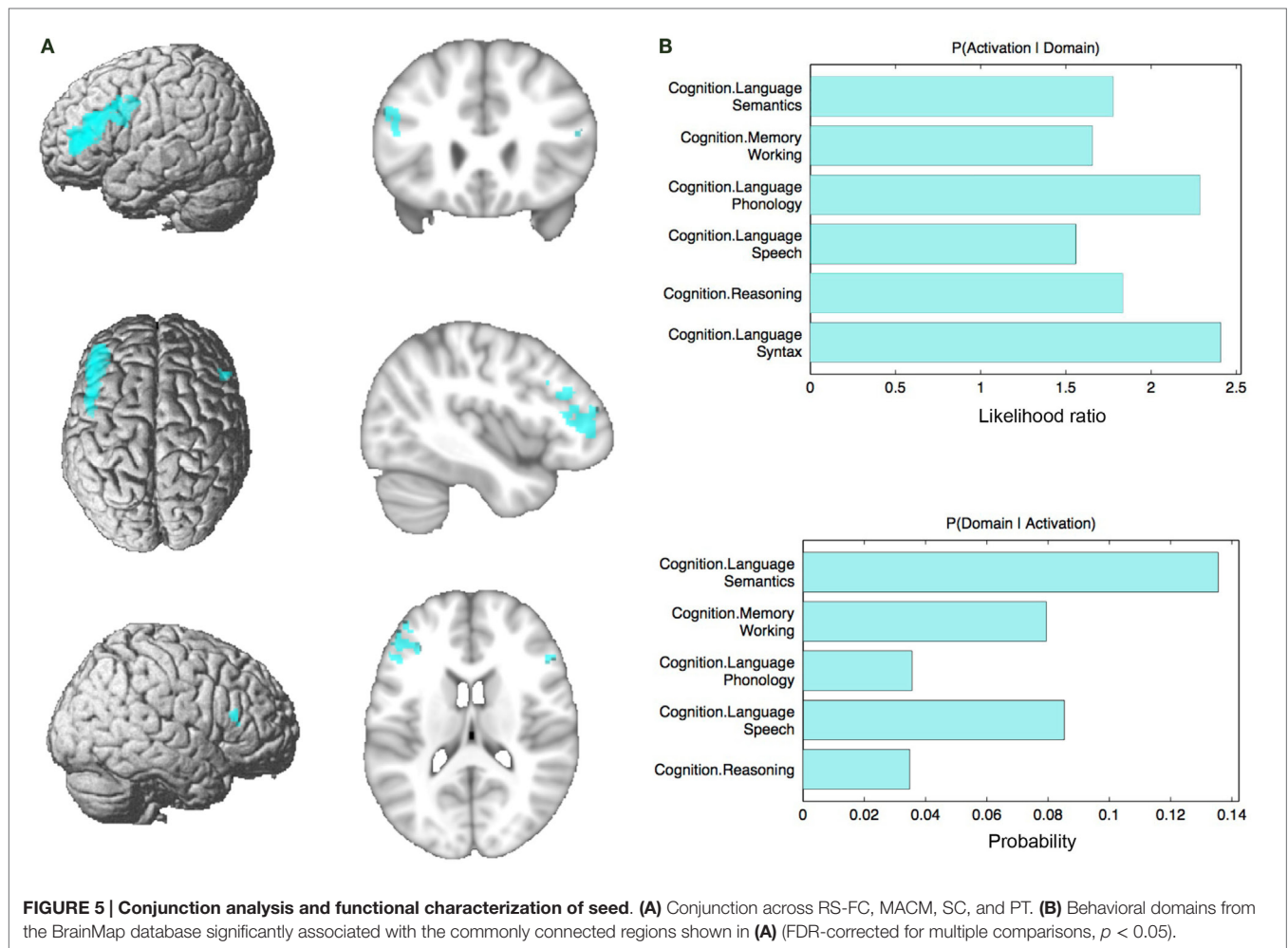


TABLE 2 | Converging connectivity of the IFS seed.

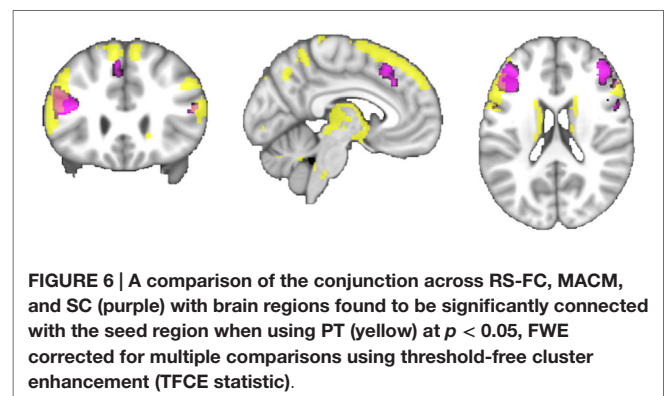
Region	x	y	z	Cytoarchitectonic assignment
Cluster 1 (780 voxels)				
L middle orbital gyrus	-46	46	-2	
Cluster 2 (1,235 voxels)				
R Inferior frontal gyrus (p. triangularis)	52	28	14	Area 45

x, y, and z coordinates refer to the peak voxel in MNI space. R, right; L, left.

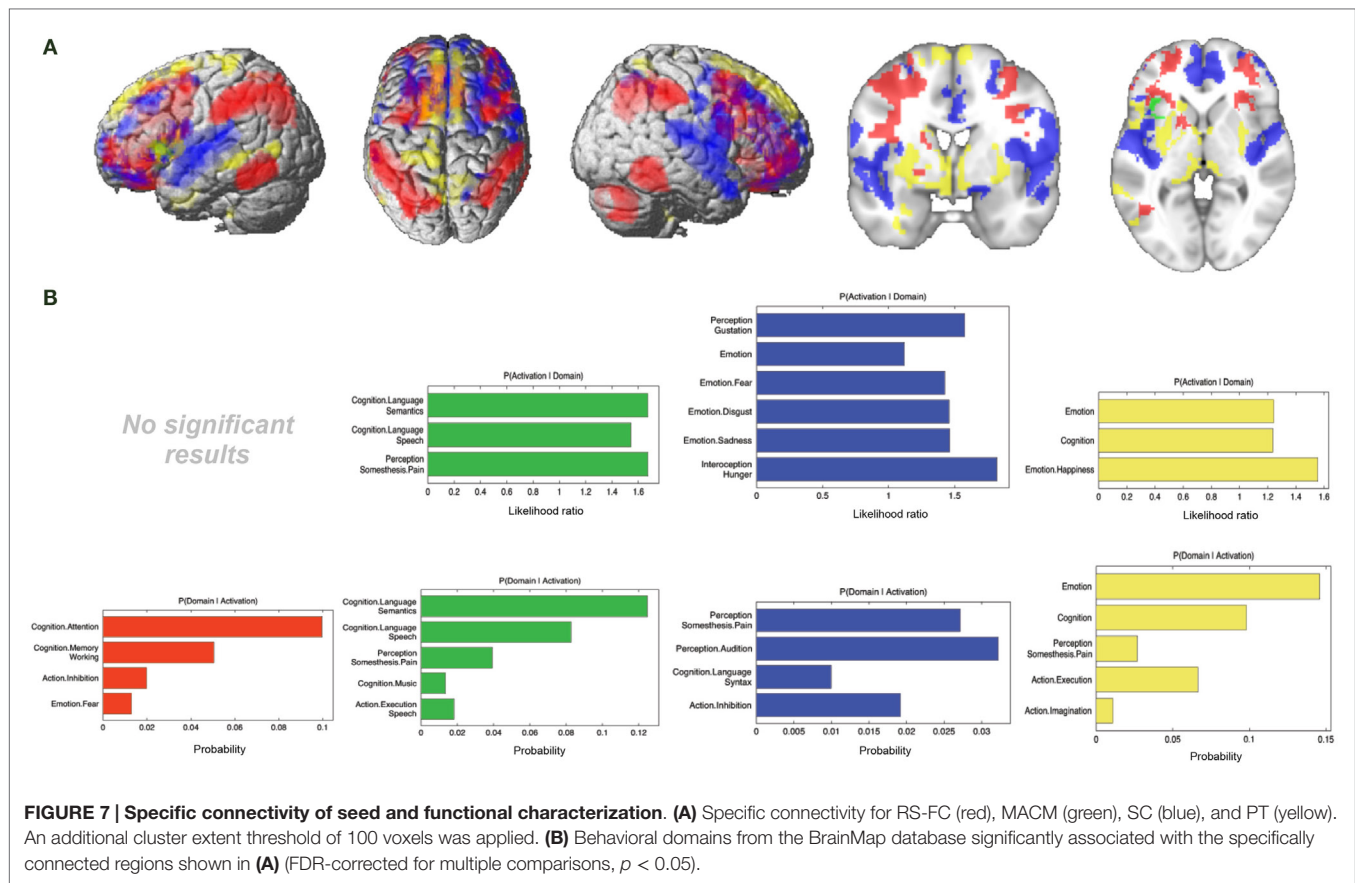
regions and white-matter structural connections were assessed using RS-FC, MACM, SC, and PT approaches. The networks that emerged revealed both similarities and differences between the different modalities. A conjunction analysis between the four connectivity approaches was used to delineate a core network. Further analyses were used to investigate connectivity patterns specific to each of the modalities.

Relationships Between TMT-MS Performance and Brain Structure

In this study, we found TMT-MS performance to be specifically related to the local brain volume of a region in the lower bank of the left IFS. That is, across subjects better performance (lower



completion time) was associated with higher GMV in this cluster. The left IFG, including IFS, has been formerly described as part of a multiple-demand system responsible for multiple kinds of cognitive demand, in which goals are achieved by assembling a series of sub-tasks, each separately defined and solved (51). An objective definition of this “multi-demand network” has recently been proposed by Müller et al. (52) based on a conjunction across three large-scale neuroimaging meta-analyses to identify regions consistently involved in sustained attention (53), working



memory (54), and inhibitory control (55). Importantly, the IFS location identified in the current study was found to be part of this multi-demand network, indicating that TMT-MS performance is related to brain structure in a region involved in executive rather than motor functions. This association between certain aspects of motor performance and cognitive or executive functions has already been suggested in earlier studies (56, 57).

At first glance, these results contradict the intention of the TMT-MS to measure motor speed, and to serve as a baseline measure for higher, executive aspects of the test (2). However, one may argue that since subjects are given specific instructions to follow a dotted line while making sure that the line drawn touches every circle along the path, the accurate completion of this task should in fact draw heavily on executive control processes. It may hence not surprise that performance in a task requiring a relatively high degree of executive motor control and attention is related to a structure that is part of the multi-demand network involved in executive functions (51). In turn, there was no significant association between performance and GMV in cortical or subcortical motor structures as may have been expected. In this context, it must be noted that adequate hand motor abilities are a necessary prerequisite for performing the TMT-MS test successfully; i.e., subjects have to be able to use their hand to draw the required lines. Hence, the reliance of TMT-MS completion on an intact cortical and subcortical motor system is obvious. What we found, however, is that performance (i.e., the speed at which the task is completed)

may seem to primarily depend on executive rather than more basic motor control processes. Does this contradict the assumption that the TMT-MS test is a baseline measure of motor speed? Not necessarily, but rather, given our findings, we would argue that motor speed in a more naturalistic setting should be more strongly associated with executive rather than primary motor function.

In congruence with the present results, previous studies have linked longer reaction times and motor slowing with sustained attention (58). However, lesion studies have associated slowing in motor processes with lesions in the right lateral frontal lobe (59, 60). Consequently, these results contrast with the findings of the present study. Additionally, the present results differ from those obtained using tasks that are commonly employed to investigate changes to the motor system following stroke; for instance, in functional neuroimaging studies using fist opening/closure paradigms (61, 62). Here, activation and interactions of the primary motor cortex as well as the lateral and medial pre-motor cortices are of essential importance. Similar regions were found in another functional neuroimaging study which used a finger tapping paradigm and focused on healthy subjects (63). In turn, activations involving the inferior frontal cortex and other regions of the executive, multi-demand network are not prominently seen. This implicates a potentially important distinction between neuroimaging assessments of stroke patients, in which more fundamental aspects of motor performance are usually tested, and paper-and-pencil tests that apparently, even when aimed at

TABLE 3 | Specifically present connectivity of IFS seed.

Region	x	y	z	Cytoarchitectonic assignment
RS-FC				
Cluster 1 (5322 voxels)				
L rectal gyrus	-4	24	-26	
Cluster 2 (4183 voxels)				
	-30	-72	20	
Cluster 3 (3958 voxels)				
	14	18	-28	
Cluster 4 (2318 voxels)				
	36	-64	24	
Cluster 5 (1630 voxels)				
R Cerebellum (Crus 2)	44	-66	-50	
Cluster 6 (1357 voxels)				
L inferior temporal gyrus	-52	-50	-26	
Cluster 7 (817 voxels)				
R inferior temporal gyrus	54	-50	-26	
MACM				
Cluster 1 (279 voxels)				
L insula lobe	-30	22	-10	
SC				
Cluster 1 (26511 voxels)				
R medial temporal pole	32	6	-33	
Cluster 2 (7299 voxels)				
	-39	3	-27	
Cluster 3 (2577 voxels)				
R superior frontal gyrus	21	33	30	
Cluster 4 (1710 voxels)				
L middle frontal gyrus	-40	51	10	
Cluster 5 (875 voxels)				
	-24	30	-23	
Cluster 6 (525 voxels)				
	28	-46	36	Area hIP1 (IPS)
Cluster 7 (341 voxels)				
L inferior frontal gyrus (p. Opercularis)	-57	15	7	Area 44
Cluster 8 (229 voxels)				
L SMA	-8	17	52	Area 6
Cluster 9 (153 voxels)				
L precentral gyrus	-33	-7	54	
Cluster 10 (122 voxels)				
L inferior frontal gyrus (p. Orbitalis)	-46	26	-5	
PT				
Cluster 1 (919 voxels)				
L superior medial gyrus	-8	54	28	
Cluster 2 (748 voxels)				
R superior medial gyrus	10	56	24	
Cluster 3 (387 voxels)				
L paracentral lobule	-10	-34	60	Area 4a
Cluster 4 (308 voxels)				
R precuneus	8	-66	40	Area 7A (SPL)
Cluster 5 (234 voxels)				
L inferior frontal gyrus (p. Orbitalis)	-48	22	-4	Area 45
Cluster 6 (232 voxels)				
L precuneus	-2	-72	36	Area 7P (SPL)
Cluster 7 (179 voxels)				
L middle temporal gyrus	-58	-28	-12	
Cluster 8 (111 voxels)				
	-4	-36	-48	
Cluster 9 (107 voxels)				
L middle occipital gyrus	-52	-70	-2	

x, y, and z coordinates refer to the peak voxel in MNI space. R, right; L, left.

testing basic motor speed, are more reflective of executive motor control. In summary, we would thus argue that the distinction between motor and “higher cognitive” tasks, which seems rather prevalent in (neuroimaging) stroke research, may be slightly misleading, as executive motor control functions may play a major role in the everyday impairments following stroke.

Core Network

Notably, all three FC approaches (RS-FC, MACM, and SC), together with locations revealed as structurally connected by PT, converged on a network comprising of the left inferior gyrus extending into the left IFS and an additional cluster in the right Brodmann Area 45. In combination with the observation of a fairly restrictive region associated with TMT-MS performance, these results suggest a core network of mostly regional connectivity that is in line with the current view on the role of the inferior frontal cortex in executive functioning (51).

Additionally, the right IFG, bilateral adjacent pre-motor cortices, and anterior insula were additionally found to converge when looking only at the FC approaches, namely, RS-FC, MACM, and SC (but not PT). Similar as the IFS seed, most of these clusters overlap with regions previously described to be part of the multiple-demand network (51, 52). In particular, the bilateral IFG, and left anterior insula as well as the MCC were the regions that overlapped with the multiple-demand network. Thus, we here show that, across different (functional) connectivity approaches the IFS shows robust interactions with regions associated with multiple cognitive demands. This is additionally supported by the functional characterization of the network robustly connected with the IFS across the different FC approaches, which show an association with multiple cognitive tasks. These observations thus continue to emphasize the important role of cognitive functions in the TMT-MS and thus suggest that this test might be tapping into executive rather than primary motor function.

Convergence and Differences Between Connectivity Measures

Convergence Among Modalities

Functional interactions can be probed by using different approaches, each having their own methodological features, and potentially also different biases even though the same statistical analyses and thresholds were used for each of the modalities. The use of the different modalities in the current study provided an opportunity to systematically compare all the different approaches. Despite the conceptual differences between the different modalities, a common network was revealed. When comparing the modalities RS-FC, MACM, and SC networks through a minimum statistic conjunction analysis, all three approaches converged on a core network that included adjacent parts of left IFG, its right-hemispheric homolog, right precentral gyrus, left middle cingulate cortex, middle orbital gyrus, and insular cortex. These results are in line with previous studies that used different seeds and therefore different networks, and also showed convergence between RS and MACM (18–20), between RS and SC (21, 22, 28), between RS and fiber tracking (23–26), and between RS, MACM, and SC (27, 64). As a result, it can be suggested that future studies could benefit from a multi-modal approach and

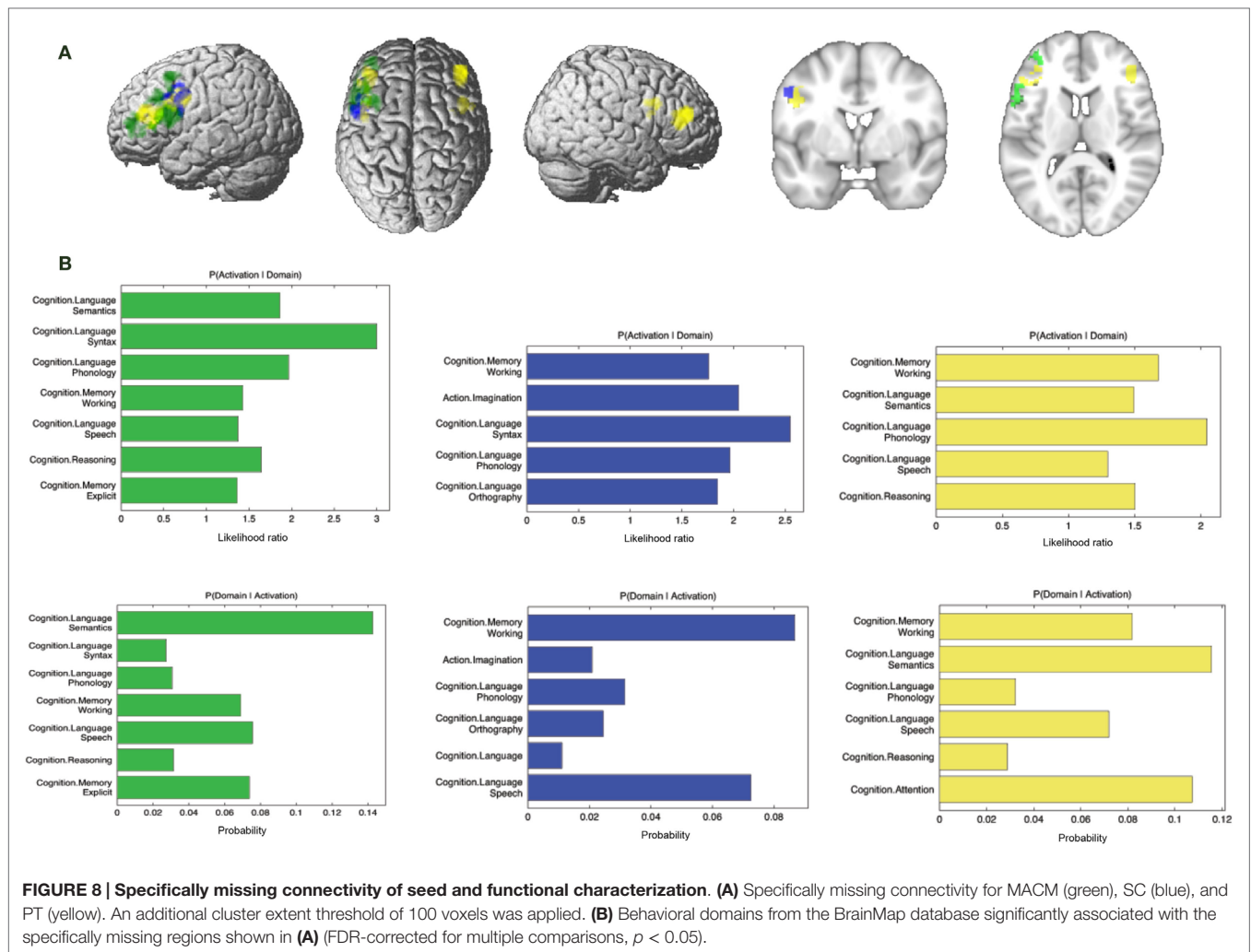


TABLE 4 | Specifically absent connectivity of IFS seed.

Region	x	y	z	Cytoarchitectonic assignment
MACM				
<i>Cluster 1 (735 voxels)</i>				
L inferior frontal gyrus (p. triangularis)	-42	40	-2	
L inferior frontal gyrus (p. triangularis)	-50	38	6	
L inferior frontal gyrus (p. triangularis)	-52	20	30	Area 45
<i>Cluster 2 (166 voxels)</i>				
L middle frontal gyrus	-44	12	38	Area 44
SC				
<i>Cluster 1 (205 voxels)</i>				
L precentral gyrus	-50	4	16	
PT				
<i>Cluster 1 (629 voxels)</i>				
L inferior frontal gyrus (p. triangularis)	-42	32	6	
<i>Cluster 2 (339 voxels)</i>				
R inferior frontal gyrus (p. triangularis)	46	34	6	Area 45
<i>Cluster 3 (119 voxels)</i>				
R precentral gyrus	54	6	18	Area 44

x, y, and z coordinates refer to the peak voxel in MNI space. R, right; L, left.

the consequent use and interpretation of the convergent network rather than focusing on a unimodal approach.

Furthermore, our resulting similarity between the SC and PT networks and the networks obtained from the other two modalities supports the idea that FC can be used to reflect structural connectivity and that SC of GMV can reflect functional networks in the brain (21, 22, 27). Consequently, our results together with previous findings provide evidence for the fact that SC is functional in nature.

Differences Among Modalities

Despite the convergence observed across all approaches, divergent connectivity patterns were also found when looking at contrasts of the different modalities. This is not surprising, given that the approaches use different data and methods in order to determine connectivity between a seed region and the rest of the brain. Previous studies have similarly reported striking differences between RS-FC and MACM connectivity approaches (20, 27). Clos et al. (27) and Jakobs et al. (20) have already argued that the differences that result from these two approaches may be the

result of the conceptual differences between the methods. While RS-FC is based on correlation of fMRI time-series measured in the absence of an external stimulus (5, 65), MACM delineates networks that are conjointly recruited by a broad range of tasks (3). That is, RS and MACM derive FC from different mental states, in the absence and presence of a task, respectively. As a result, spontaneous networks related to self-initiated behavior and thought processes that can be captured in the task-free state may be largely missed in MACM analyses (3).

In particular, RS-FC of our seed was specifically found in a number of regions that have been predominantly associated with executive functions, such as working memory, attention, action inhibition, and spatial cognition. Importantly, there were no regions that were present in SC, PT, and MACM, but absent in RS-FC as revealed by the specifically absent RS-FC. This indicates that RS-FC captures the broadest network. By contrast, specific connectivity observed for MACM was found to be mainly associated with language-related functions such as semantics and speech. In turn, specifically absent regions in MACM were found to be mainly associated with cognitive functions such as working memory and explicit memory as well as language-related functions. As already mentioned above, these diverging patterns, with RS-FC capturing a broader network than MACM is possibly due to the conceptual differences. Moreover, these two approaches also differ in the subject groups assessed. While a group of 109 subjects were recruited for the RS-FC analysis, the MACM analysis relied on a large amount of published neuroimaging studies from the BrainMap database (10), with the selection criteria being activation of our identified seed region. Thus, it is possible that this difference in subject groups may have also contributed to the difference in results obtained.

In contrast to the FC approaches mentioned above, specific SC connectivity was observed in regions found to be mainly associated with functions related to emotion (fear, disgust, and sadness) and perception (pain, gustation, audition, hunger, and somesthesia). Additional functions observed included action inhibition and cognition. On the other hand, functional characterization of areas that were found to be specifically absent for SC connectivity revealed an association with functions related to cognition and language such as working memory, phonology, orthography, syntax, and speech. Given these results, it can be noted that the specific SC network showed a prominent association with perception and emotional processing. The strong association with emotional processing in SC is particularly interesting since the functional characterization of the seed region and the conjunction network did not indicate such an involvement. Moreover, while the specific RS-FC network revealed regions that were predominately related to cognition and the MACM network revealed regions that were predominantly related to language, the SC network found such regions to be specifically missing. These differences may be largely due to the conceptual differences between the FC modalities described above and SC. The exact biological basis of SC is still rather unclear (27), but it has been hypothesized that SC networks arise from synchronized maturational change that could be mediated by axonal connections forming and reforming over the course of development (66). Therefore, early and reciprocal axonal connectivity between regions is expected to have a mutually trophic effect on regional growth in an individual brain

leading to covariance of regional volumes across subjects (14). That is, the correlation of anatomical structure between regions is the result of similarities in maturational trajectories (14). The specific connectivity pattern of the SC modality may thus be reflecting synchronized developmental patterns within a network of regions associated with perception and emotional processing. This could thus be the reason for particular regions to be present in the SC network and not in the MACM and RS-FC networks since the latter two modalities are more likely to highlight regions that are related to certain functions rather than long-term anatomical interactions. Additionally, SC is also likely to include other influences such as common genetic factors, developmental brain symmetry, neuromodulator distributions, and vascular territories (14, 15), which contribute to its more widespread distribution.

In congruence with the specific SC network, the PT network also showed a prominent association with perception and emotional processing while functional characterization of areas that were found to be specifically absent for PT connectivity revealed an association with functions related to cognition and language. These results further imply that the regions that were specifically associated with SC may reflect dominant long-term synchronized maturational patterns. However, despite the differences observed, it should be noted that the core network showed that the resulting SC network (also) revealed functional relations despite the fact that it was defined by anatomical covariance. SC may hence be regarded as a measure potentially bridging between structural and functional connectivity aspects. However, when comparing the PT to the other three networks, contrasting regions can be observed. This could be due to biases related to the use of conventional diffusion tensors. Such tensors can only capture the principal diffusion direction, and thus makes them prone to errors induced by crossing fibers (67). As a result, this could have limited the possible resulting convergence amongst the four modalities.

CONCLUSION

In summary, the present results demonstrate a significant correlation between TMT-MS performance and GMV in the lower bank of the IFS, which was functionally characterized as being involved in cognitive tasks. Additionally, all connectivity approaches used (RS-FC, MACM, SC, and PT) converged on a network comprising of regions that overlap with the multiple-demand network. Results therefore indicate that performance (i.e., the speed at which the task is completed) may primarily depend on executive function, thus suggesting that motor speed in a more naturalistic setting should be more strongly associated with executive rather than primary motor function. Moreover, the common connectivity resulting from the different modalities used verifies that common networks can be revealed across highly divergent methods.

ACKNOWLEDGMENTS

This study was supported by the Deutsche Forschungsgemeinschaft (DFG, EI 816/4-1, LA 3071/3-1; EI 816/6-1.), the National Institute of Mental Health (R01-MH074457), and the European Union Seventh Framework Programme (FP7/2007-2013) under grant agreement no. 604102 (Human Brain Project).

REFERENCES

- Raghavan P. The nature of hand motor impairment after stroke and its treatment. *Curr Treat Options Cardiovasc Med* (2007) **9**(3):221–8. doi:10.1007/s11936-007-0016-3
- Delis DC, Kaplan E, Kramer JH. *Delis-Kaplan Executive Function System (D-KEFS)*. San Antonio, TX: Psychological Corporation (2001).
- Eickhoff SB, Grefkes C. Approaches for the integrated analysis of structure, function and connectivity of the human brain. *Clin EEG Neurosci* (2011) **42**(2):107–21. doi:10.1177/155005941104200211
- Friston K. Functional integration and inference in the brain. *Prog Neurobiol* (2002) **68**(2):113–43. doi:10.1016/S0301-0082(02)00076-X
- Fox MD, Raichle ME. Spontaneous fluctuations in brain activity observed with functional magnetic resonance imaging. *Nat Rev Neurosci* (2007) **8**(9):700–11. doi:10.1038/nrn2201
- Smith SM, Vidaurre D, Beckmann CF, Glasser MF, Jenkinson M, Miller KL, et al. Functional connectomics from resting-state fMRI. *Trends Cogn Sci* (2013) **17**(12):666–82. doi:10.1016/j.tics.2013.09.016
- Eickhoff SB, Bzdok D, Laird AR, Roski C, Caspers S, Zilles K, et al. Co-activation patterns distinguish cortical modules, their connectivity and functional differentiation. *Neuroimage* (2011) **57**(3):938–49. doi:10.1016/j.neuroimage.2011.05.021
- Laird AR, Eickhoff SB, Rottschy C, Bzdok D, Ray KL, Fox PT. Networks of task co-activations. *Neuroimage* (2013) **80**:505–14. doi:10.1016/j.neuroimage.2013.04.073
- Fox PT, Lancaster JL, Laird AR, Eickhoff SB. Meta-analysis in human neuroimaging: computational modeling of large-scale databases. *Annu Rev Neurosci* (2014) **37**:409–34. doi:10.1146/annurev-neuro-062012-170320
- Laird AR, Eickhoff SB, Kurth F, Fox PM, Uecker AM, Turner JA, et al. ALE meta-analysis workflows via the brainmap database: progress towards a probabilistic functional brain atlas. *Front Neuroinform* (2009) **3**:23. doi:10.3389/neuro.11.023.2009
- Laird AR, Eickhoff SB, Fox PM, Uecker AM, Ray KL, Saenz JJ Jr, et al. The BrainMap strategy for standardization, sharing, and meta-analysis of neuroimaging data. *BMC Res Notes* (2011) **4**:349. doi:10.1186/1756-0500-4-349
- Albaugh MD, Ducharme S, Collins DL, Botteron KN, Althoff RR, Evans AC, et al. Evidence for a cerebral cortical thickness network anti-correlated with amygdalar volume in healthy youths: implications for the neural substrates of emotion regulation. *Neuroimage* (2013) **71**:42–9. doi:10.1016/j.neuroimage.2012.12.071
- Lerch JP, Worsley K, Shaw WP, Greenstein DK, Lenroot RK, Giedd J, et al. Mapping anatomical correlations across cerebral cortex (MACACC) using cortical thickness from MRI. *Neuroimage* (2006) **31**(3):993–1003. doi:10.1016/j.neuroimage.2006.01.042
- Alexander-Bloch A, Raznahan A, Bullmore E, Giedd J. The convergence of maturational change and structural covariance in human cortical networks. *J Neurosci* (2013) **33**(7):2889–99. doi:10.1523/JNEUROSCI.3554-12.2013
- Evans AC. Networks of anatomical covariance. *Neuroimage* (2013) **80**:489–504. doi:10.1016/j.neuroimage.2013.05.054
- Behrens T, Johansen-Berg H, Woolrich M, Smith S, Wheeler-Kingshott C, Boulby P, et al. Non-invasive mapping of connections between human thalamus and cortex using diffusion imaging. *Nat Neurosci* (2003) **6**(7):750–7. doi:10.1038/nn1075
- Parker GJ, Haroon HA, Wheeler-Kingshott CA. A framework for a streamline-based probabilistic index of connectivity (PICO) using a structural interpretation of MRI diffusion measurements. *J Magn Reson Imaging* (2003) **18**(2):242–54. doi:10.1002/jmri.10350
- Cauda F, Cavanna AE, D'Agata F, Sacco K, Duca S, Geminiani GC. Functional connectivity and coactivation of the nucleus accumbens: a combined functional connectivity and structure-based meta-analysis. *J Cogn Neurosci* (2011) **23**(10):2864–77. doi:10.1162/jocn.2011.21624
- Hoffstaedter F, Grefkes C, Caspers S, Roski C, Palomero-Gallagher N, Laird AR, et al. The role of anterior midcingulate cortex in cognitive motor control. *Hum Brain Mapp* (2014) **35**(6):2741–53. doi:10.1002/hbm.22363
- Jakobs O, Langner R, Caspers S, Roski C, Cieslik EC, Zilles K, et al. Across-study and within-subject functional connectivity of a right temporo-parietal junction subregion involved in stimulus-context integration. *Neuroimage* (2012) **60**(4):2389–98. doi:10.1016/j.neuroimage.2012.02.037
- He Y, Chen ZJ, Evans AC. Small-world anatomical networks in the human brain revealed by cortical thickness from MRI. *Cereb Cortex* (2007) **17**(10):2407–19. doi:10.1093/cercor/bhl149
- Seeley WW, Crawford RK, Zhou J, Miller BL, Greicius MD. Neurodegenerative diseases target large-scale human brain networks. *Neuron* (2009) **62**(1):42–52. doi:10.1016/j.neuron.2009.03.024
- Koch MA, Norris DG, Hund-Georgiadis M. An investigation of functional and anatomical connectivity using magnetic resonance imaging. *Neuroimage* (2002) **16**(1):241–50. doi:10.1006/nimg.2001.1052
- Greicius MD, Supekar K, Menon V, Dougherty RF. Resting-state functional connectivity reflects structural connectivity in the default mode network. *Cereb Cortex* (2009) **19**(1):72–8. doi:10.1093/cercor/bhn059
- van den Heuvel MP, Mandl RC, Kahn RS, Pol H, Hilleke E. Functionally linked resting-state networks reflect the underlying structural connectivity architecture of the human brain. *Hum Brain Mapp* (2009) **30**(10):3127–41. doi:10.1002/hbm.20737
- Damoiseaux JS, Greicius MD. Greater than the sum of its parts: a review of studies combining structural connectivity and resting-state functional connectivity. *Brain Struct Funct* (2009) **213**(6):525–33. doi:10.1007/s00429-009-0208-6
- Clos M, Rottschy C, Laird AR, Fox PT, Eickhoff SB. Comparison of structural covariance with functional connectivity approaches exemplified by an investigation of the left anterior insula. *Neuroimage* (2014) **99**:269–80. doi:10.1016/j.neuroimage.2014.05.030
- Reid AT, Bzdok D, Langner R, Fox PT, Laird AR, Amunts K, et al. Multimodal connectivity mapping of the human left anterior and posterior lateral prefrontal cortex. *Brain Struct Funct* (2015):1–17. doi:10.1007/s00429-015-1060-5
- Ashburner J, Friston KJ. Voxel-based morphometry – the methods. *Neuroimage* (2000) **11**(6):805–21. doi:10.1006/nimg.2000.0582
- Smith SM, Jenkinson M, Johansen-Berg H, Rueckert D, Nichols TE, Mackay CE, et al. Tract-based spatial statistics: voxelwise analysis of multi-subject diffusion data. *Neuroimage* (2006) **31**(4):1487–505. doi:10.1016/j.neuroimage.2006.02.024
- Nooner KB, Colcombe SJ, Tobe RH, Mennes M, Benedict MM, Moreno AL, et al. The NKI-rockland sample: a model for accelerating the pace of discovery science in psychiatry. *Front Neurosci* (2012) **6**:152. doi:10.3389/fnins.2012.00152
- Kauranen K, Vanharanta H. Influences of ageing, gender, and handedness on motor performance of upper and lower extremities. *Percept Mot Skills* (1996) **82**(2):515–25. doi:10.2466/pms.1996.82.2.515
- Lawrie SM, MacHale SM, Cavanagh JT, O'CARROLL RE, Goodwin GM. The difference in patterns of motor and cognitive function in chronic fatigue syndrome and severe depressive illness. *Psychol Med* (2000) **30**(02):433–42. doi:10.1017/S0033291799001816
- Fagiolo G, Waldman A, Hajnal J. A simple procedure to improve FMRIB software library brain extraction tool performance. *Br J Radiol* (2008) **81**(963):250–1. doi:10.1259/bjr/12956156
- Jenkinson M, Smith S. A global optimisation method for robust affine registration of brain images. *Med Image Anal* (2001) **5**(2):143–56. doi:10.1016/S1361-8415(01)00036-6
- Jenkinson M, Bannister P, Brady M, Smith S. Improved optimization for the robust and accurate linear registration and motion correction of brain images. *Neuroimage* (2002) **17**(2):825–41. doi:10.1006/nimg.2002.1132
- Andersson JL, Jenkinson M, Smith S. *Non-Linear Registration, Aka Spatial Normalisation FMRIB Technical Report*. Oxford: FMRIB Analysis Group of the University of Oxford (2007).
- Smith SM, Johansen-Berg H, Jenkinson M, Rueckert D, Nichols TE, Miller KL, et al. Acquisition and voxelwise analysis of multi-subject diffusion data with tract-based spatial statistics. *Nat Protoc* (2007) **2**(3):499–503. doi:10.1038/nprot.2007.45
- Fox PT, Lancaster JL. Mapping context and content: the BrainMap model. *Nat Rev Neurosci* (2002) **3**(4):319–21. doi:10.1038/nrn789
- Müller VI, Cieslik EC, Laird AR, Fox PT, Eickhoff SB. Dysregulated left inferior parietal activity in schizophrenia and depression: functional connectivity and characterization. *Front Hum Neurosci* (2013) **7**:268. doi:10.3389/fnhum.2013.00268
- Rottschy C, Caspers S, Roski C, Reetz K, Dogan I, Schulz J, et al. Differentiated parietal connectivity of frontal regions for “what” and “where” memory. *Brain Struct Funct* (2013) **218**(6):1551–67. doi:10.1007/s00429-012-0476-4

42. Ashburner J, Friston KJ. Unified segmentation. *Neuroimage* (2005) **26**(3):839–51. doi:10.1016/j.neuroimage.2005.02.018
43. Smith SM, Nichols TE. Threshold-free cluster enhancement: addressing problems of smoothing, threshold dependence and localisation in cluster inference. *Neuroimage* (2009) **44**(1):83–98. doi:10.1016/j.neuroimage.2008.03.061
44. Eickhoff SB, Laird AR, Grefkes C, Wang LE, Zilles K, Fox PT. Coordinate-based activation likelihood estimation meta-analysis of neuroimaging data: a random-effects approach based on empirical estimates of spatial uncertainty. *Hum Brain Mapp* (2009) **30**(9):2907–26. doi:10.1002/hbm.20718
45. Eickhoff SB, Bzdok D, Laird AR, Kurth F, Fox PT. Activation likelihood estimation meta-analysis revisited. *Neuroimage* (2012) **59**(3):2349–61. doi:10.1016/j.neuroimage.2011.09.017
46. Turkeltaub PE, Eickhoff SB, Laird AR, Fox M, Wiener M, Fox P. Minimizing within-experiment and within-group effects in activation likelihood estimation meta-analyses. *Hum Brain Mapp* (2012) **33**(1):1–13. doi:10.1002/hbm.21186
47. Smith SM, Jenkinson M, Woolrich MW, Beckmann CF, Behrens TE, Johansen-Berg H, et al. Advances in functional and structural MR image analysis and implementation as FSL. *Neuroimage* (2004) **23**:S208–19. doi:10.1016/j.neuroimage.2004.07.051
48. Behrens T, Berg HJ, Jbabdi S, Rushworth M, Woolrich M. Probabilistic diffusion tractography with multiple fibre orientations: what can we gain? *Neuroimage* (2007) **34**(1):144–55. doi:10.1016/j.neuroimage.2006.09.018
49. Caspers S, Eickhoff SB, Rick T, von Kapri A, Kuhlen T, Huang R, et al. Probabilistic fibre tract analysis of cytoarchitectonically defined human inferior parietal lobule areas reveals similarities to macaques. *Neuroimage* (2011) **58**(2):362–80. doi:10.1016/j.neuroimage.2011.06.027
50. Nichols T, Brett M, Andersson J, Wager T, Poline J. Valid conjunction inference with the minimum statistic. *Neuroimage* (2005) **25**(3):653–60. doi:10.1016/j.neuroimage.2004.12.005
51. Duncan J. The multiple-demand (MD) system of the primate brain: mental programs for intelligent behaviour. *Trends Cogn Sci* (2010) **14**(4):172–9. doi:10.1016/j.tics.2010.01.004
52. Müller VI, Langner R, Cieslik EC, Rottschy C, Eickhoff SB. Interindividual differences in cognitive flexibility: influence of gray matter volume, functional connectivity and trait impulsivity. *Brain Struct Funct* (2015) **220**(4):2401–14. doi:10.1007/s00429-014-0797-6
53. Langner R, Eickhoff SB. Sustaining attention to simple tasks: a meta-analytic review of the neural mechanisms of vigilant attention. *Psychol Bull* (2013) **139**(4):870. doi:10.1037/a0030694
54. Rottschy C, Langner R, Dogan I, Reetz K, Laird AR, Schulz JB, et al. Modelling neural correlates of working memory: a coordinate-based meta-analysis. *Neuroimage* (2012) **60**(1):830–46. doi:10.1016/j.neuroimage.2011.11.050
55. Cieslik EC, Mueller VI, Eickhoff CR, Langner R, Eickhoff SB. Three key regions for supervisory attentional control: evidence from neuroimaging meta-analyses. *Neurosci Biobehav Rev* (2015) **48**:22–34. doi:10.1016/j.neubiorev.2014.11.003
56. Diamond A. Close interrelation of motor development and cognitive development and of the cerebellum and prefrontal cortex. *Child Dev* (2000) **71**(1):44–56. doi:10.1111/1467-8624.00117
57. Rigoli D, Piek JP, Kane R, Oosterlaan J. An examination of the relationship between motor coordination and executive functions in adolescents. *Dev Med Child Neurol* (2012) **54**(11):1025–31. doi:10.1111/j.1469-8749.2012.04403.x
58. Godefroy O, Lhullier-Lamy C, Rousseaux M. SRT lengthening: role of an alertness deficit in frontal damaged patients. *Neuropsychologia* (2002) **40**(13):2234–41. doi:10.1016/S0028-3932(02)00109-4
59. Godefroy O, Spagnolo S, Roussel M, Boucart M. Stroke and action slowing: mechanisms, determinants and prognosis value. *Cerebrovasc Dis* (2010) **29**(5):508–14. doi:10.1159/000297968
60. Stuss DT, Alexander MP, Shallice T, Picton TW, Binns MA, Macdonald R, et al. Multiple frontal systems controlling response speed. *Neuropsychologia* (2005) **43**(3):396–417. doi:10.1016/j.neuropsychologia.2004.06.010
61. Grefkes C, Nowak DA, Eickhoff SB, Dafotakis M, Küst J, Karbe H, et al. Cortical connectivity after subcortical stroke assessed with functional magnetic resonance imaging. *Ann Neurol* (2008) **63**(2):236–46. doi:10.1002/ana.21228
62. Staines WR, McIlroy WE, Graham SJ, Black SE. Bilateral movement enhances ipsilesional cortical activity in acute stroke: a pilot functional MRI study. *Neurology* (2001) **56**(3):401–4. doi:10.1212/WNL.56.3.401
63. Roski C, Caspers S, Lux S, Hoffstaedter F, Bergs R, Amunts K, et al. Activation shift in elderly subjects across functional systems: an fMRI study. *Brain Struct Funct* (2014) **219**(2):707–18. doi:10.1007/s00429-013-0530-x
64. Hardwick RM, Lesage E, Eickhoff CR, Clos M, Fox P, Eickhoff SB. Multimodal connectivity of motor learning-related dorsal premotor cortex. *NeuroImage* (2015) **123**:114–28. doi:10.1016/j.neuroimage.2015.08.024
65. Deco G, Corbetta M. The dynamical balance of the brain at rest. *Neuroscientist* (2011) **17**(1):107–23. doi:10.1177/1073858409354384
66. Mechelli A, Friston KJ, Frackowiak RS, Price CJ. Structural covariance in the human cortex. *J Neurosci* (2005) **25**(36):8303–10. doi:10.1523/JNEUROSCI.0357-05.2005
67. Yoldemir B, Ng B, Abugharbieh R. Effects of tractography approach on consistency between anatomical and functional connectivity estimates. *Biomedical Imaging (ISBI), 2014 IEEE 11th International Symposium*. Beijing (2014). p. 250–53.

Conflict of Interest Statement: The authors declare that the research was conducted in the absence of any commercial or financial relationships that could be construed as a potential conflict of interest.

Copyright © 2015 Camilleri, Reid, Müller, Grefkes, Amunts and Eickhoff. This is an open-access article distributed under the terms of the Creative Commons Attribution License (CC BY). The use, distribution or reproduction in other forums is permitted, provided the original author(s) or licensor are credited and that the original publication in this journal is cited, in accordance with accepted academic practice. No use, distribution or reproduction is permitted which does not comply with these terms.

ADVANTAGES OF PUBLISHING IN FRONTIERS



FAST PUBLICATION

Average 90 days
from submission
to publication



COLLABORATIVE PEER-REVIEW

Designed to be rigorous –
yet also collaborative, fair and
constructive



RESEARCH NETWORK

Our network
increases readership
for your article



OPEN ACCESS

Articles are free to read,
for greatest visibility



TRANSPARENT

Editors and reviewers
acknowledged by name
on published articles



GLOBAL SPREAD

Six million monthly
page views worldwide



COPYRIGHT TO AUTHORS

No limit to
article distribution
and re-use



IMPACT METRICS

Advanced metrics
track your
article's impact



SUPPORT

By our Swiss-based
editorial team